NTM – THE NEW UBER-BUGS

EDITED BY: Veronique Dartois, Christine Sizemore and Thomas Dick
PUBLISHED IN: Frontiers in Microbiology

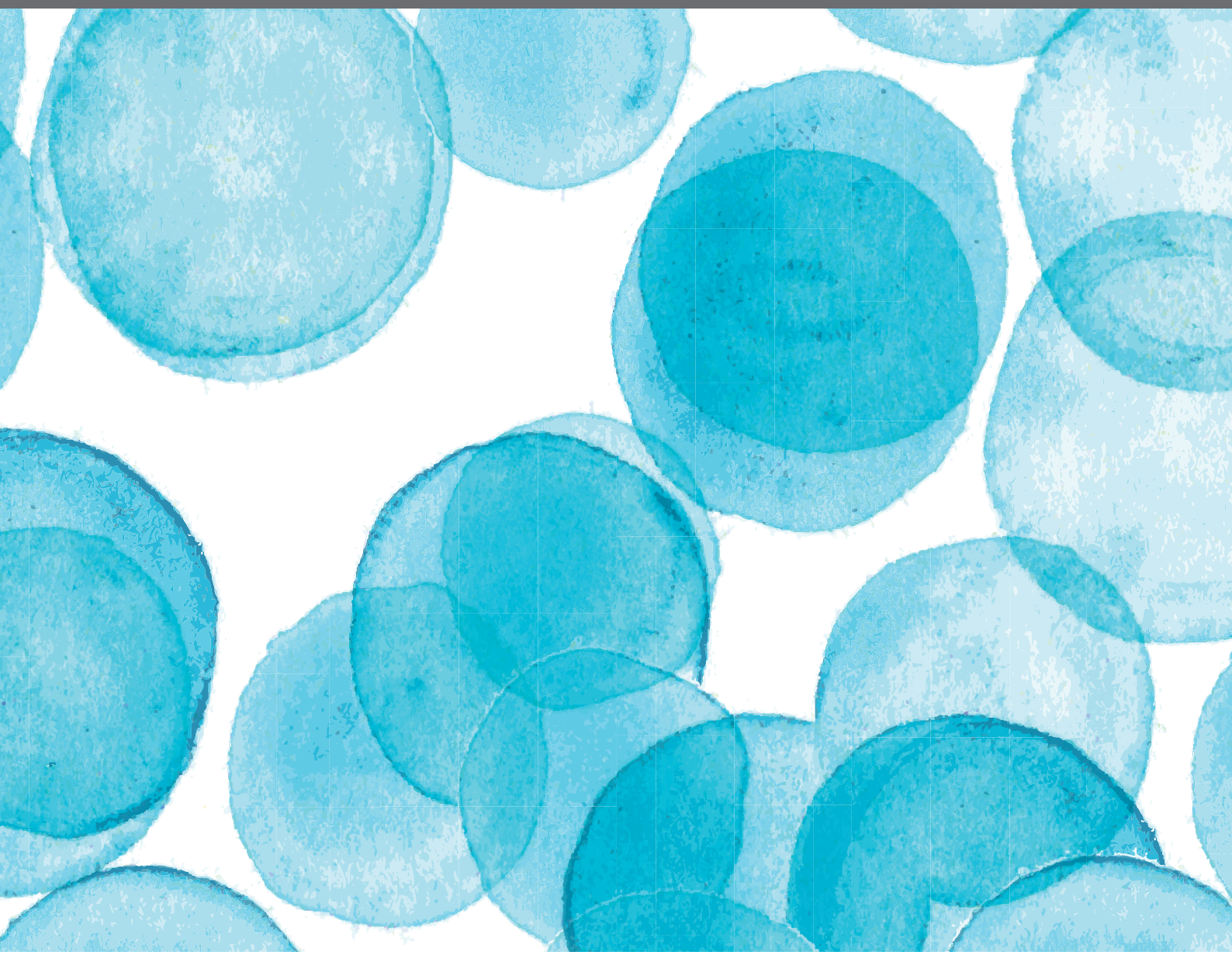

frontiers Research Topics

ISSN 1664-8714
ISBN 978-2-88963-012-7
DOI 10.3389/978-2-88963-012-7

About Frontiers

Frontiers is more than just an open-access publisher of scholarly articles: it is a pioneering approach to the world of academia, radically improving the way scholarly research is managed. The grand vision of Frontiers is a world where all people have an equal opportunity to seek, share and generate knowledge. Frontiers provides immediate and permanent online open access to all its publications, but this alone is not enough to realize our grand goals.

Frontiers Journal Series

The Frontiers Journal Series is a multi-tier and interdisciplinary set of open-access, online journals, promising a paradigm shift from the current review, selection and dissemination processes in academic publishing. All Frontiers journals are driven by researchers for researchers; therefore, they constitute a service to the scholarly community. At the same time, the Frontiers Journal Series operates on a revolutionary invention, the tiered publishing system, initially addressing specific communities of scholars, and gradually climbing up to broader public understanding, thus serving the interests of the lay society, too.

Dedication to Quality

Each Frontiers article is a landmark of the highest quality, thanks to genuinely collaborative interactions between authors and review editors, who include some of the world's best academicians. Research must be certified by peers before entering a stream of knowledge that may eventually reach the public - and shape society; therefore, Frontiers only applies the most rigorous and unbiased reviews.
Frontiers revolutionizes research publishing by freely delivering the most outstanding research, evaluated with no bias from both the academic and social point of view. By applying the most advanced information technologies, Frontiers is catapulting scholarly publishing into a new generation.

What are Frontiers Research Topics?

Frontiers Research Topics are very popular trademarks of the Frontiers Journals Series: they are collections of at least ten articles, all centered on a particular subject. With their unique mix of varied contributions from Original Research to Review Articles, Frontiers Research Topics unify the most influential researchers, the latest key findings and historical advances in a hot research area! Find out more on how to host your own Frontiers Research Topic or contribute to one as an author by contacting the Frontiers Editorial Office: researchtopics@frontiersin.org

NTM – THE NEW UBER-BUGS

Topic Editors:
Veronique Dartois, Center for Discovery and Innovation, Hackensack Meridian Health, United States
Christine Sizemore, National Institute of Allergy and Infectious Diseases, United States
Thomas Dick, Center for Discovery and Innovation, Hackensack Meridian Health, United States

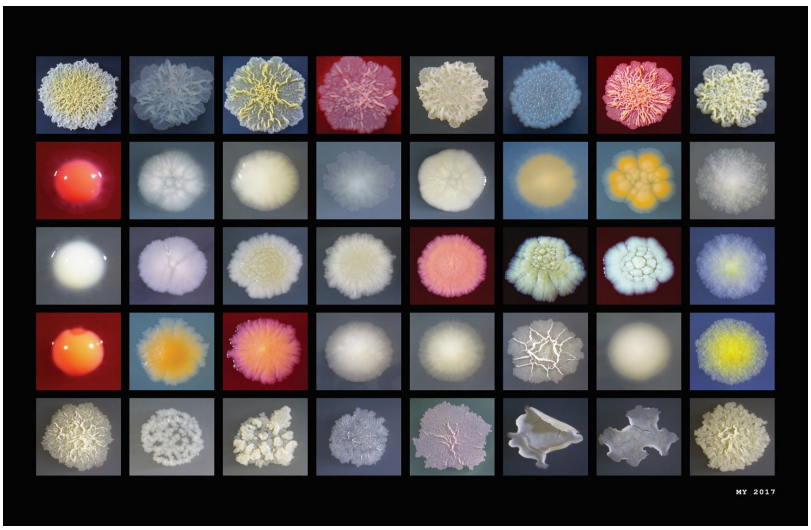

"Mycobacterium colonies" by Michelle Yee

Incidence of pulmonary disease caused by nontuberculous mycobacteria (NTM), such as Mycobacterium abscessus and M. avium, is increasing at an alarming rate, surpassing tuberculosis (TB) in many countries. Treatment durations are extremely long. With low sputum conversion rates, the outcomes are often disappointing. Thus, NTM disease resembles extremely drug resistant TB. There is an urgent need for increased research on this dreadful disease. For this book we brought together experts from a wide range of disciplines addressing current status, gaps and needs, and new developments in several NTM-relevant research areas. We start with the discussion of NTM disease presentations and clinical research. This is followed by contributions on epidemiology, antibiotic resistance mechanisms, drug discovery and development, bacteriology and targets, and new diagnostic tools. We would like to thank the 130 authors for sharing their work and insights. We hope that this collection of articles will stimulate discussions and research activities on the challenging lung disease caused by the diverse group of pathogens called NTM.

Citation: Dartois, V., Sizemore, C., Dick, T., eds. (2019). NTM – The New Uber-Bugs. Lausanne: Frontiers Media. doi: 10.3389/978-2-88963-012-7

Table of Contents

06 ***Editorial: NTM—The New Uber-Bugs***
Veronique Dartois, Christine Sizemore and Thomas Dick

DISEASE PRESENTATIONS AND CLINICAL RESEARCH

08 ***Host Variability in NTM Disease: Implications for Research Needs***
Colin Swenson, Christa S. Zerbe and Kevin Fennelly

20 ***Assessing Response to Therapy for Nontuberculous Mycobacterial Lung Disease: Quo Vadis?***
Christopher Vinnard, Alyssa Mezochow, Hannah Oakland, Ross Klingsberg, John Hansen-Flaschen and Keith Hamilton

EPIDEMIOLOGY

28 ***A Closer Look at the Genomic Variation of Geographically Diverse* Mycobacterium abscessus *Clones That Cause Human Infection and Disease***
Rebecca M. Davidson

35 ***Global Environmental Nontuberculous Mycobacteria and Their Contemporaneous Man-Made and Natural Niches***
Jennifer R. Honda, Ravleen Virdi and Edward D. Chan

46 **Mycobacterium abscessus*: Shapeshifter of the Mycobacterial World***
Keenan Ryan and Thomas F. Byrd

RESISTANCE MECHANISMS

56 ***The Role of Antibiotic-Target-Modifying and Antibiotic-Modifying Enzymes in* Mycobacterium abscessus *Drug Resistance***
Sakshi Luthra, Anna Rominski and Peter Sander

69 ***Mechanistic and Structural Insights Into the Unique TetR-Dependent Regulation of a Drug Efflux Pump in* Mycobacterium abscessus**
Matthias Richard, Ana Victoria Gutiérrez, Albertus J. Viljoen, Eric Ghigo, Mickael Blaise and Laurent Kremer

87 ***GlnR Activation Induces Peroxide Resistance in Mycobacterial Biofilms***
Yong Yang, Jacob P. Richards, Jennifer Gundrum and Anil K. Ojha

DRUG DISCOVERY AND DEVELOPMENT

100 ***Challenges of NTM Drug Development***
Joseph O. Falkinham

107 ***Amikacin Liposome Inhalation Suspension (ALIS) Penetrates Non-tuberculous Mycobacterial Biofilms and Enhances Amikacin Uptake Into Macrophages***
Jimin Zhang, Franziska Leifer, Sasha Rose, Dung Yu Chun, Jill Thaisz, Tracey Herr, Mary Nashed, Jayanthi Joseph, Walter R. Perkins and Keith DiPetrillo

119 ***Optimization and Lead Selection of Benzothiazole Amide Analogs Toward a Novel Antimycobacterial Agent***
Mary A. De Groote, Thale C. Jarvis, Christina Wong, James Graham, Teresa Hoang, Casey L. Young, Wendy Ribble, Joshua Day, Wei Li, Mary Jackson, Mercedes Gonzalez-Juarrero, Xicheng Sun and Urs A. Ochsner

129 **Mycobacterium abscessus *and ß-Lactams: Emerging Insights and Potential Opportunities***
Elizabeth Story-Roller, Emily C. Maggioncalda, Keira A. Cohen and Gyanu Lamichhane

139 ***Novel Screen to Assess Bactericidal Activity of Compounds Against Non-replicating* Mycobacterium abscessus**
Bryan J. Berube, Lina Castro, Dara Russell, Yulia Ovechkina and Tanya Parish

147 ***Tedizolid Activity Against Clinical* Mycobacterium abscessus *Complex Isolates—An* in vitro *Characterization Study***
Ying Wei Tang, Bernadette Cheng, Siang Fei Yeoh, Raymond T. P. Lin and Jeanette W. P. Teo

154 ***Therapy for* Mycobacterium kansasii *Infection: Beyond 2018***
Michelle S. DeStefano, Carolyn M. Shoen and Michael H. Cynamon

161 ***Teicoplanin – Tigecycline Combination Shows Synergy Against* Mycobacterium abscessus**
Dinah B. Aziz, Jeanette W. P. Teo, Véronique Dartois and Thomas Dick

169 **Mycobacterium avium *Infection in a C3HeB/FeJ Mouse Model***
Deepshikha Verma, Megan Stapleton, Jake Gadwa, Kridakorn Vongtongsalee, Alan R. Schenkel, Edward D. Chan and Diane Ordway

BACTERIOLOGY AND TARGETS

179 ***MmpL3 as a Target for the Treatment of Drug-Resistant Nontuberculous Mycobacterial Infections***
Wei Li, Amira Yazidi, Amitkumar N. Pandya, Pooja Hegde, Weiwei Tong, Vinicius Calado Nogueira de Moura, E. Jeffrey North, Jurgen Sygusch and Mary Jackson

188 ***Lsr2 is an Important Determinant of Intracellular Growth and Virulence in* Mycobacterium abscessus**
Vincent Le Moigne, Audrey Bernut, Mélanie Cortès, Albertus Viljoen, Christian Dupont, Alexandre Pawlik, Jean-Louis Gaillard, Fabienne Misguich, Frédéric Crémazy, Laurent Kremer and Jean-Louis Herrmann

199 ***Glycopeptidolipids, a Double-Edged Sword of the* Mycobacterium abscessus *Complex***
Ana Victoria Gutiérrez, Albertus Viljoen, Eric Ghigo, Jean-Louis Herrmann and Laurent Kremer

207 **Mycobacterium abscessus *subsp.* massiliense mycma_0076 *and* mycma_0077 *Genes Code for Ferritins That are Modulated by Iron Concentration***
Fábio M. Oliveira, Adeliane C. Da Costa, Victor O. Procopio, Wanius Garcia, Juscemácia N. Araújo, Roosevelt A. Da Silva, Ana Paula Junqueira-Kipnis and André Kipnis

DIAGNOSTIC TOOLS

223 ***Evaluation of a Novel MALDI Biotyper Algorithm to Distinguish* Mycobacterium intracellulare *From* Mycobacterium chimaera**

L. Elaine Epperson, Markus Timke, Nabeeh A. Hasan, Paul Godo, David Durbin, Niels K. Helstrom, Gongyi Shi, Markus Kostrzewa, Michael Strong and Max Salfinger

229 ***MALDI Spectra Database for Rapid Discrimination and Subtyping of* Mycobacterium kansasii**

Jayaseelan Murugaiyan, Astrid Lewin, Elisabeth Kamal, Zofia Bakuła, Jakko van Ingen, Vit Ulmann, Miren J. Unzaga Barañano, Joanna Humięcka, Aleksandra Safianowska, Uwe H. Roesler and Tomasz Jagielski

frontiers in Microbiology

EDITORIAL
published: 12 June 2019
doi: 10.3389/fmicb.2019.01299

Editorial: NTM—The New Uber-Bugs

Veronique Dartois[1], *Christine Sizemore*[2] *and Thomas Dick*[1]*

[1] Center for Discovery and Innovation, Hackensack Meridian Health, Nutley, NJ, United States, [2] Division of Microbiology and Infectious Diseases, National Institute of Allergy and Infectious Diseases, National Institutes of Health, Rockville, MD, United States

Keywords: non-tuberculous mycobacteria, environmental mycobacteria, lung disease, repositioning, from biology to solutions

Editorial on the Research Topic

NTM—The New Uber-Bugs

Pulmonary disease caused by non-tuberculous mycobacteria (NTM), relatives of *Mycobacterium tuberculosis*, is increasing at an alarming rate, surpassing tuberculosis (TB) in many countries. Patients suffering from chronic pulmonary diseases, including Cystic Fibrosis and Chronic Obstructive Pulmonary Disease, are particularly susceptible to NTM infections. These infections are difficult to diagnose and present significant challenges for treatment. The environmental reservoir of the infectious agents and an incomplete understanding of what makes individuals susceptible to infection complicates preventive approaches. Considering the rising incidence and likely underreporting of these infections, a clear understanding of the barriers to diagnosis, treatment and prevention, and focused research on the pathobiology and microbiology of NTMs and new methods to combat them is urgently needed.

Recognizing this emerging new health threat and the complex nature of these infections, the National Institute of Allergy and Infectious Diseases organized the first NTM-focused workshop "Advancing Translational Science for Pulmonary NTM Infections" in Rockville, MD, in September 2017. This workshop, bringing together scientists and physicians from the United States and abroad, identified gaps in fundamental biological and epidemiological research and mapped out possible approaches for targeted translational science to expedite improvements in detection and care (Daniel-Wayman et al., 2018). The gathering not only generated increased awareness of this new health issue, it also brought together research disciplines and investigators from across the world who previously had few opportunities to interact, and kick-started new collaborative research activities. Momentum created during this workshop also resulted in the Research Topic "NTM—The New Uber-Bugs."

NTM basic and translational research are still in their infancy with many questions remaining to understand the biological diversity of the infecting pathogens, their similarities and differences and how these affect pathobiology, transmission, and response to therapy. Furthermore, depending on where NTM infections occur globally, different species of NTM predominate, making rapid diagnostics that can speciate mycobacteria a necessity. This acute need to reduce the biological uncertainties around NTM pulmonary disease by increasing research efforts reminds of the state of knowledge TB research was facing two decades ago. Despite an initial research void in the TB field during the last quarter of the twentieth century, in part driven by the absence of molecular tools and animal models to study this difficult pathogen, significant progress has been achieved since the early 2000s. Knowledge and tools developed for the study of TB disease and approaches and technologies and platforms that have been applied to TB product development can be leveraged for NTM research.

OPEN ACCESS

Edited by:
Axel Cloeckaert, Institut National de la Recherche Agronomique (INRA), France

Reviewed by:
Philippe Lanotte, Université de Tours, France

***Correspondence:**
Thomas Dick
thomas.dick@HMH-CDI.org

Specialty section:
This article was submitted to Antimicrobials, Resistance and Chemotherapy, a section of the journal Frontiers in Microbiology

Received: *23 April 2019*
Accepted: *24 May 2019*
Published: *12 June 2019*

Citation:
Dartois V, Sizemore C and Dick T (2019) Editorial: NTM—The New Uber-Bugs. Front. Microbiol. 10:1299. doi: 10.3389/fmicb.2019.01299

For instance, chemical entities with activity against *Mycobacterium tuberculosis* that have been generated in TB screening campaigns can quickly also be tested against NTM and may facilitate repositioning and repurposing of chemical leads and create a complementary approach to de novo drug discovery. By exploiting strategies and tools developed for TB, together with increasing research and product development focused on high-priority NTM species, we believe that significant medical advances for NTM diseases will be achieved in the medium term.

The present Research Topic, "NTM—The New Uber-Bugs" compiles contemporary results and insights from a group of leading researchers into the high-priority research area of NTM infections. It also highlights that in order to truly understand the diverse nature of these infections and their impact on human health, more thorough trans-national collaborations and data sharing will be important. We would like to thank the reviewers for their many thoughtful and insightful comments, and the authors for their excellent contributions. We hope that this collection of manuscripts will stimulate much-needed discussions and research activities on the challenging lung disease caused by the diverse group of pathogens called non-tuberculous mycobacteria.

AUTHOR CONTRIBUTIONS

All authors listed have made a substantial, direct and intellectual contribution to the work, and approved it for publication.

FUNDING

TD holds a Toh Chin Chye Visiting Professorship at the Department of Microbiology and Immunology, Yong Loo Lin School of Medicine, National University of Singapore. His work is supported by the National Institute of Allergy and Infectious Diseases of the National Institutes of Health under Award Numbers R01AI132374 and 2R01AI106398-05 and by the Cystic Fibrosis Foundation under Award Number DICK17XX00. The content is solely the responsibility of the authors and does not necessarily represent the official views of the National Institutes of Health or the Cystic Fibrosis Foundation.

ACKNOWLEDGMENTS

We are grateful to all the authors and reviewers for their contributions to this Research Topic.

REFERENCES

Daniel-Wayman, S., Abate, G., Barber, D. L., Bermudez, L. E., Coler, R. N., Cynamon, M. H., et al. (2018). Advancing translational science for pulmonary nontuberculous mycobacterial infections. a road map for research. *Am. J. Respir. Crit. Care Med.* 199, 947–951. doi: 10.1164/rccm.201807-1273PP

Conflict of Interest Statement: The authors declare that the research was conducted in the absence of any commercial or financial relationships that could be construed as a potential conflict of interest.

frontiers in Microbiology

REVIEW
published: 03 December 2018
doi: 10.3389/fmicb.2018.02901

Host Variability in NTM Disease: Implications for Research Needs

Colin Swenson[1], Christa S. Zerbe[2] and Kevin Fennelly[3]*

[1] Division of Pulmonary, Allergy, Critical Care, and Sleep Medicine, Emory University, Atlanta, GA, United States, [2] Laboratory of Clinical Immunology and Microbiology, National Institute of Allergy and Infectious Diseases, National Institutes of Health, Bethesda, MD, United States, [3] Laboratory of Chronic Airway Infection, Pulmonary Branch, Division of Intramural Research, National Heart, Lung, and Blood Institute, National Institutes of Health, Bethesda, MD, United States

Non-tuberculous mycobacteria (NTM) are ubiquitous environmental organisms that may cause opportunistic infections in susceptible hosts. Lung infections in immunocompetent persons with structural lung disease are most common, while disseminated disease occurs primarily in immunocompromised individuals. Human disease caused by certain species, such as *Mycobacterium avium* complex, *Mycobacterium abscessus*, and *Mycobacterium kansasii,* is increasing in incidence and varies by geographic distribution. The spectrum of NTM disease varies widely in presentation and clinical outcome, but certain patterns can be organized into clinical phenotypes. Treatment options are limited, lengthy, and often toxic. The purpose of this case-based review is to provide non-clinician scientists with a better understanding of human NTM disease with an aim to stimulate more research and development.

Keywords: non-tuberculous mycobacteria, pulmonary, bronchiectasis, disseminated, COPD, cystic fibrosis, osteomyelitis

OPEN ACCESS

Edited by:
Thomas Dick,
Rutgers, The State University of New Jersey, United States

Reviewed by:
Jennifer R. Honda,
National Jewish Health, United States
Mary Ann Degroote,
SomaLogic, United States

****Correspondence:***
Colin Swenson
colin.swenson@emory.edu

Specialty section:
This article was submitted to Antimicrobials, Resistance and Chemotherapy, a section of the journal Frontiers in Microbiology

Received: *06 August 2018*
Accepted: *12 November 2018*
Published: *03 December 2018*

Citation:
Swenson C, Zerbe CS and Fennelly K (2018) Host Variability in NTM Disease: Implications for Research Needs. Front. Microbiol. 9:2901. doi: 10.3389/fmicb.2018.02901

> "It is more important to know what sort of person has a disease than to know what sort of disease a person has."
>
> – Hippocrates, Greek Physician, 460–370 B.C.

INTRODUCTION

Non-tuberculous mycobacteria (NTM) are ubiquitous environmental organisms that are frequently isolated from soil and water, as well as other environmental sources. NTM are acid-fast bacilli (AFB) that are clinically categorized as either rapid growers (RG), taking fewer than 7 days to grow on culture media, or slow growers (SG), taking more than 7 days (**Table 1**). Certain species are well known causes of human disease, most commonly *Mycobacterium avium* complex (MAC), which includes the species *M. avium*, *M. intracellulare*, and *M. chimaera*, and the *M. abscessus* complex (MABSC), which includes the subspecies *abscessus*, *massiliense*, and *bolletii*. Considered opportunistic pathogens, NTM organisms may occasionally be isolated from the sputa samples of healthy individuals, but there is a higher prevalence of NTM infection among patients with cystic fibrosis and non-cystic fibrosis bronchiectasis, as well as chronic obstructive pulmonary disease (COPD) (Adjemian et al., 2012; Fleshner et al., 2016). While all MAC species may be isolated from water and soil sources, *M. avium* is more commonly isolated from fresh water sources, and *M. intracellulare* is associated with garden soils (Falkinham, 2015). This predilection has been proposed as an explanation for the epidemiologic clusters observed in regions with abundant surface water and loamy soil.

TABLE 1 | Clinically important mycobacterial species organized by growth time.

Slow growing mycobacteria	Rapid growing mycobacteria
*M. avium complex**	*M. abscessus complex***
M. kansasii	*M. fortuitum*
M. xenopi	*M. chelonae*
M. szulgai	*M. mucogenicum*
M. simiae	

*Slow growing organisms take greater than 7 days to culture. Rapid growing organisms take fewer than 7 days to culture. *Includes M. avium, M. intracellulare, and M. chimaera. **Includes M. abscessus, M. massiliense, and M. bolletii.*

While NTM species may rarely cause pulmonary infections in normal hosts, those with structural lung disease, such as bronchiectasis and emphysema, are at increased risk. The hallmark of the disease is granulomatous inflammation of the airways, which, over time, may lead to worsening bronchiectasis and cavitary lung disease (Fujita et al., 1999). Among patients with pulmonary NTM infections, distinct phenotypes have been described based primarily on the underlying lung disease. These phenotypes have characteristic presentations on lung imaging (**Table 2**).

Although once considered rare diseases, human infections with NTM appear to be increasing in North America and Europe, and they are increasingly recognized in areas of the world considered endemic for tuberculosis (TB), including Africa, South America and India (Adjemian et al., 2012). Human lung disease caused by NTM was first recognized in the 1950s as the incidence of TB was decreasing (Timpe and Runyon, 1954). Given the similarities of clinical microbiology and of the drugs used to treat TB, the care of patients with NTM disease has often been provided by clinicians and hospitals initially established to manage TB. The HIV/AIDS epidemic introduced many physicians and scientists to disseminated infections with MAC, which has waned in incidence along with other opportunistic infections due to the development and widespread use of highly active antiretroviral therapy. Most disseminated NTM infections occur in immunocompromised patients. Similar to TB, pulmonary NTM disease accounts for approximately 85% of cases and disseminated NTM disease for about 15% (Jones et al., 2018). The major types of human NTM disease are summarized in **Table 3**.

The primary purpose of this review is to introduce microbiologists and other scientists who are not clinicians to the wide variety of clinical presentations among humans infected with NTM. Given the variable responses observed to infections with the same pathogen among various inbred strains of mice and other experimental animal models, it should not be surprising that the 'human host' is not just one host, but rather many. However, in spite of the enormous genetic variability among humans, there are similarities in presentations of NTM disease among various human 'phenotypes.' We will present representative cases, most of which are actual cases that we have seen, followed by a discussion of that category of disease and figures of imaging studies. We hope that a better understanding of the various human diseases caused by NTM can help inspire our non-clinical colleagues to develop better diagnostic tests, drug therapies and vaccines and other preventive interventions.

FIGURE 1 | Axial CT chest image demonstrating bronchiectasis and mucoid impaction in the right middle lobe. The tree-in-bud nodularity in the left lung (yellow arrow).

PROTECTION OF RESEARCH PARTICIPANTS

Written consent was obtained from each patient presented in this article. He or she explicitly consented to the inclusion of background and clinical data, as well as radiographic images.

NON-CYSTIC FIBROSIS BRONCHIECTASIS (NCFB)

Case

A 67-year-old female lifelong non-smoker with a history of scoliosis and early osteoporosis developed a non-productive cough for 6 months, an unintentional weight loss, and daytime fatigue. She had experienced a seven-pound weight loss over 6 months, to a body mass index (BMI) of 17.5 kg/m^2 (normal: 19–24 kg/m^2). An avid swimmer and jogger, she had also noticed a gradual decline in her stamina, with an increase in shortness of breath with moderate exercise. Her primary care provider ordered a chest radiograph, which showed possible right middle lobe pneumonia. She was prescribed 10 days of levofloxacin, which did not improve her respiratory symptoms. She developed severe diarrhea, and on the seventh day of levofloxacin, her husband took her to the emergency department, where she was admitted for dehydration secondary to *Clostridium difficile* colitis. Because the cough had not improved with antibiotics, a CT of the chest was performed, showing right middle lobe and lingula bronchiectasis, nodularity, and mucus impaction (**Figure 1**). She was placed on airborne isolation for possible pulmonary tuberculosis. MTB PCR probe was negative on an

TABLE 2 | Radiographic presentations of pulmonary NTM diseases.

Radiographic appearance	Representative underlying disease
Fibrocavitary	Chronic obstructive pulmonary disease (COPD)
Nodular bronchiectasis	Idiopathic bronchiectasis in thin older women
Upper lobe bronchiectasis	Cystic fibrosis in children and young adults
Lower lobe bronchiectasis and chronic sinusitis	Primary ciliary dyskinesia in children, young adults
Lower lobe bronchiectasis	Chronic GERD and aspiration in older adult
Upper/mid-lung fine nodules	Hypersensitivity pneumonitis: 'hot-tub lung'

induced sputum sample, so she was taken for bronchoscopy with lavage. These samples were smear positive for AFB, and 10 days later, grew *M. avium*. She was discharged from the hospital on a combination of ethambutol, rifampin, and azithromycin three times weekly, and after 3 months of treatment, her cough resolved and she began to gain weight. Repeat CT imaging at 6 months demonstrated fewer lung nodules, with less mucus impaction.

Discussion

The nodular-bronchiectatic phenotype of pulmonary NTM disease is also known as "Lady Windermere Syndrome," in reference to the character from Oscar Wilde's 1892 play entitled "Lady Windermere's Fan" (Reich and Johnson, 1992). While the term has had wide adoption in the medical literature, it is, in fact, a malapropism, since the character for which the syndrome is named is a young woman without respiratory symptoms of any kind. Further, the authors who originally named this syndrome believed that the infection resulted from women chronically suppressing their cough, leading to mucus inspissation in the longer airways of the right middle lobe and lingula. This hypothesis has more recently been challenged, since a hallmark of the nodular-bronchiectatic phenotype is chronic cough and sputum production (Olivier, 2016; Tsai et al., 2017). Reflex cough responses in elderly women with stable pulmonary NTM disease appear similar to age-matched controls, except for a mildly decreased urge-to-cough, arguing against cough suppression (Tsai et al., 2017).

Individuals with this phenotype are typically female, elderly, are tall with thin body habitus, have pectus excavatum, scoliosis, and a non-smoking history (Kim et al., 2008; Park et al., 2009; Lee et al., 2013). Radiographically, the right middle lobe and lingula are most often affected, though any area of the lung may be affected (**Figure 1**). Typically, the radiographic pattern is described as "tree-in-bud," indicating bronchiolar inflammation and mucus impaction. Coinfection with more than one species of *Mycobacterium*, or with Gram-negative bacteria, characterizes later, more advanced disease.

Symptomatically, patients with the nodular-bronchiectatic phenotype typically complain of chronic cough, which may or may not be productive, and may or may not be associated with hemoptysis, persistent fatigue, night sweats, and unintentional weight loss. The infection may be mistaken for active pulmonary tuberculosis, leading to airborne isolation and prolonged hospitalization, as happened with our patient. Treatment is typically a prolonged combination regimen of a rifamycin, most often rifampin, ethambutol, and a macrolide, typically azithromycin or clarithromycin. The frequency of dosing

TABLE 3 | Types of NTM disease based on underlying pathophysiology.

Type of NTM disease	Underlying pathophysiology
Pulmonary	
COPD	Protease-antiprotease imbalance
Cystic fibrosis (CF) bronchiectasis	CFTR abnormalities: abnormal airway surface fluid
Non-CF bronchiectasis: child/young adult	Primary ciliary dyskinesia: abnormal mucociliary clearance
Non-CF bronchiectasis	Idiopathic; Chronic aspiration; Chest wall abnormalities: scoliosis, pectus excavatum, etc. Primary immunodeficiencies, e.g., CVID Connective tissue diseases, e.g., RA, Sjogren's syndrome
Hypersensitivity pneumonitis	Exposures to aerosolized NTM; immunological
Cervical lymphadenitis	Children via oropharyngeal mucosa inoculation
Skin and soft tissue infections	Direct inoculation; surgical wound infections
Osteoarticular infections	Trauma
Disseminated infection	HIV/AIDS; Contaminated heart-lung machine in cardiac surgery; Immunological deficiencies in the Th1 pathway: *Interferon gamma receptor; Interleukin-12 receptor; Signal transducer and activator of transcription 1 (STAT1); Interferon regulatory factor 8; GATA2 (MonoMAC syndrome); Interferon-stimulated gene 15; Nuclear factor-kappa-B essential modulator (NEMO); X-linked chronic granulomatous disease*

FIGURE 2 | Left: chest radiograph demonstrating cystic bronchiectasis. Right: CT image of chest showing a left upper lobe infiltrate on a background of cystic bronchiectasis (yellow arrow).

depends on the extent of radiographic disease: mild nodular-bronchiectatic disease may be treated with a thrice-weekly regimen, while more severe bronchiectasis requires a daily regimen. In the most severe cases, particularly those with cystic bronchiectasis and cavitary lung disease, a concurrent thrice-weekly parenteral aminoglycoside, such as amikacin, may be necessary (Griffith et al., 2007). As with the *M. abscessus* group, surgical resection in localized or cavitary disease is an option where medical treatment has failed to eradicate infection. Since individuals with the nodular-bronchiectatic phenotype are typically elderly and frail, the risks of surgical resection may outweigh potential benefits, in which case a chronic suppressive strategy with antibiotics is a reasonable alternative.

Complete clearance of MAC infection is variable, and often depends on the severity of disease. Further limiting the successful clearance of MAC infection is the low rate of clinician adherence to the 2007 ATS/IDSA treatment guidelines (Adjemian et al., 2014a,b). With the guidelines-based treatment approach, more than 60% of patients with nodular-bronchiectatic disease will have treatment success (Wallace et al., 2014; Diel et al., 2018). These patients continue to be susceptible to reinfection, however, often with entirely new strains or subspecies. Overall, the recurrence of pulmonary MAC infection approaches 40%, with the highest rates of recurrence among the nodular-bronchiectatic cohort (Lee et al., 2015; Boyle et al., 2016). The rate of relapsed disease, where the same clinical isolate is again isolated within 12 months of supposed cure, is unknown. While environmental exposure has been proposed as a source of infection, it is unclear what role remediation and exposure avoidance have on preventing reinfection.

CYSTIC FIBROSIS LUNG DISEASE (CF)

Case

A 21-year-old man with CF presented to the outpatient clinic with worsening dyspnea, weight loss, fever, and hemoptysis over approximately 2 months. He had last been in clinic 3 months prior when he had reported feeling well. Induced sputum sample during that clinic visit grew scant mucoid fluoroquinolone-resistant *Pseudomonas aeruginosa*. Mycobacterial cultures were negative at that time, and his forced expiratory volume (FEV_1: typically the best overall measure of lung function) was stable at 2.5 L (normal for patient's age: 4.5 L). His BMI was chronically low at 17.8 kg/m2 (normal: 19–24 kg/m^2). At the current clinic visit, his FEV_1 had declined to 2.1 L, and his sputum sample was a dark gray streaked with blood. Because his resting pulse oximetry reading was consistently in the upper-80% range, he was directly admitted to hospital, where sputum sample was smear positive for AFB. *M. tuberculosis* PCR probe was negative. Chest radiograph on admission demonstrated upper and mid-lung zone cystic bronchiectasis with a new possible left upper lobe infiltrate (**Figure 2**, left). CT of chest confirmed the development of a left upper lobe infiltrate, with new tree-in-bud attenuation (**Figure 2**, right). The sputum culture grew *M. abscessus* 5 days after admission.

Discussion

Patients with CF have a higher prevalence of NTM disease than the general population. Pathogenic NTM species are isolated from approximately 1 in 5 patients with CF, and the incidence appears to be increasing by 5% per year, depending on geographic location (Adjemian et al., 2014a, 2018). Among the NTM species affecting this patient population, approximately 60% of isolates are MAC, while almost 40% are MABSC. MABSC is comprised of three subspecies: *M. abscessus*, *M. bolletii*, and *M. massiliense*, all of which are rapidly growing organisms. MABSC is a notoriously difficult infection to treat, owing in part to the *erm*(41) gene, which confers inducible macrolide resistance (Adjemian et al., 2018). The subspecies *M. massiliense* is an exception, however, since it lacks a functional *erm*(41) gene, and is therefore more easily eradicated (Kim et al., 2010; Roux et al., 2015). Patients with CF who develop MABSC infection typically have a lower BMI and, paradoxically, a higher FEV_1 than those without MABSC infection (Adjemian et al., 2018).

Infection with MABSC is considered a relative contraindication to lung transplantation, since MABSC infection may prove fatal in the post-transplant period, when recipients are on maximal immunosuppressive therapy (Chalermskulrat et al., 2006; Gilljam et al., 2010). Because subjects with CF have progressive lung disease, lung transplantation is often a consideration at the later stages of disease. Our patient was concurrently followed by the lung transplant clinic, though he had never been listed. His sputum isolate was ultimately identified as subspecies *M. massiliense*, and he was successfully treated with a regimen consisting of azithromycin, amikacin, and cefoxitin. Sputum samples at 3, 6, and 9 months were negative for NTM species. His hemoptysis resolved, and he did not require supplemental oxygen at his three-month follow-up appointment.

CHRONIC OBSTRUCTIVE LUNG DISEASE (COPD)

Case

A 55-year-old man with a history of COPD associated with smoking developed a chronic cough productive of sputum, malaise, and night sweats. The social history was remarkable

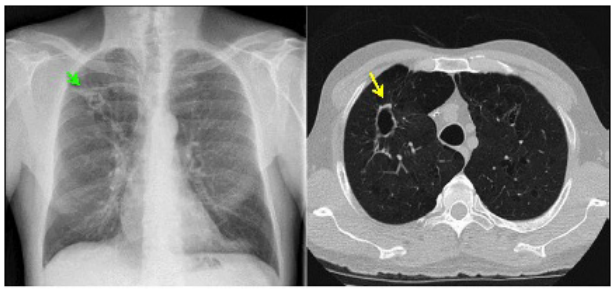

FIGURE 3 | Left: chest radiograph demonstrating a right upper lobe cavitary lesion on a background of emphysema (green arrow). Right: axial CT image demonstrating the same cavitary lesion in the right lung (yellow arrow). Reprinted with permission of the American Thoracic Society. Copyright© 2018 American Thoracic Society. Fennelly et al. (2016) is an official journal of the American Thoracic Society.

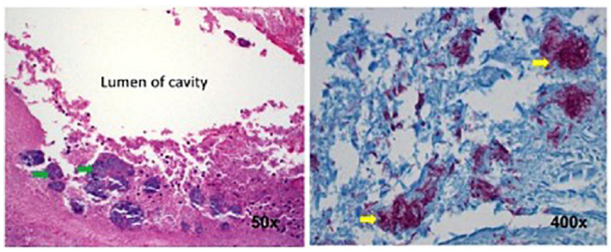

FIGURE 4 | Histopathology of the surgical specimen (using hematoxylin and eosin stains) demonstrating aggregates of bacteria (left, green arrows) along the inner wall of the lung cavity, with many AFB seen at higher power using Ziehl Nissen stain (right, yellow arrows). Reprinted with permission of the American Thoracic Society. Copyright© 2018 American Thoracic Society. Fennelly et al. (2016) is an official journal of the American Thoracic Society.

for use of a hot tub at his home. Sputum microbiology was notable for 3+ AFB on smear and three cultures grew *M. abscessus*, susceptible to amikacin and linezolid, and intermediate to clarithromycin (without *erm* gene testing) and cefoxitin. Pulmonary function testing showed airflow obstruction and a low diffusing capacity, and imaging demonstrated a right upper lobe cavity and emphysematous changes, consistent with COPD (**Figure 3**). He and his wife had just retired and sold their home in northern Florida. They were en route to vacation in the American West in their recreational vehicle (RV), hoping to receive some oral antibiotics and be on their way. His symptoms responded well to treatment with intravenous amikacin once daily and intravenous imipenem-cilastatin twice daily and azithromycin (home health nursing visited him in a state forest campground where they lived in their RV during his treatment). However, 4 months after treatment he was admitted to the hospital with new shortness of breath, fevers, and with ground-glass opacities, consistent with parenchymal inflammation, in the posterior aspects of both upper lobes. Bronchoalveolar lavage (BAL) grew only *M. abscessus*, and the BAL cell count was markedly lymphocytic. This pattern was consistent with an allergic alveolitis due to a spill of the cavity, so

FIGURE 5 | Left: chest radiograph showing right upper lobe consolidation with central cavitary changes (green arrow) in a woman with COPD and pulmonary NTM disease. Right: chest radiograph of same subject demonstrating marked progression of pulmonary NTM disease, including likely spillage of the previous right upper lobe cavitary lesion.

he was treated with oral corticosteroids and his antimycobacterial regimen intensified by the addition of linezolid once daily. As the cavity was the major site of disease and his lung function was only mildly decreased, he was referred for surgical resection of the right upper lobe. The histopathology of the cavity was remarkable for aggregates of AFB along the inner wall of the cavity (**Figure 4**). *M. abscessus* grew from a culture of the resected lung cavity within 3 days. Scanning electron microscopy of the inner wall of the resected cavity demonstrated bacilli embedded within a matrix. There were 3.83×10^7 colony forming units (CFU) of total bacteria in a 0.5 g sample from the lung cavity; 7.17×10^5 CFU were in biofilm. The bacterial composition was 97.7% mycobacterial using 16s ribosomal RNA sequencing (Fennelly et al., 2016). The patient's symptoms and imaging improved post-operatively, and all sputa specimens were negative on culture in the subsequent 10 months of his tour of the West.

Discussion

Patients with COPD often have emphysema that is typically more prominent in the upper lobes. The 'blebs' or holes within the lung parenchyma are presumably infected by NTM. The mode of infection is not well understood, but we suspect that it was likely due to inhalation in this case. We see a similar pattern of *Aspergillus fumigatus* infecting the upper lobes of COPD patients, and *Aspergillus* in the most ubiquitous airborne mold. As TB often presents with upper lobe cavities, COPD patients with AFB in their sputum are often initially placed in respiratory isolation as TB suspects unless a rapidly done molecular diagnostic can confirm that the AFB are not *M. tuberculosis*.

Pulmonary NTM infections in COPD patients have a low cure rate, generally considered to be about 50% compared to about 75% in patients with idiopathic bronchiectasis (Jones et al., 2018). Whether or not this lower cure rate is due to the presence of cavities is unknown. Surgical resection of a cavity can be curative, as in this case. Unfortunately, many patients with cavitary disease have lung function that it so diminished that they cannot tolerate surgery. Surgical resection may also be contraindicated if there is extensive bilateral disease.

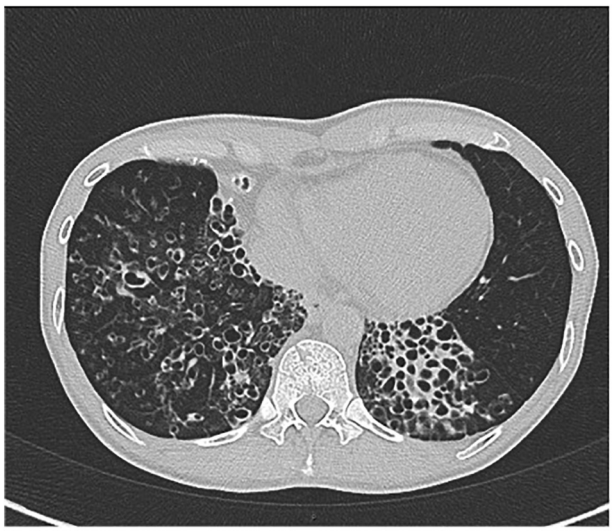

FIGURE 6 | CT chest image showing cystic bronchiectasis in the right and left lower lobes.

However, medical treatment can have a role in preventing further progression of disease, possibly by suppressing bacterial growth within cavities or by protecting healthy lung tissue by eradicating small amounts of bacteria that are spread from diseased areas. **Figure 5** shows the chest radiographs of a woman with COPD who had cavitary pulmonary MAC disease (**Figure 5**, Left). Although her sputum remained AFB smear- and culture-positive during her course of treatment, her symptoms had improved and there was no further radiographic evidence of disease progression. Unfortunately, she stopped all her medications when she was given a diagnosis cervical cancer and became depressed, and she was lost to follow-up. Approximately 6 months later she was admitted to the intensive care unit, and a repeat chest radiograph showed dramatic progression of disease (**Figure 5**, Right). The right upper lobe cavity appeared to have extended and spilled, destroying her entire right lung and significantly involving the left. She died 2 weeks later. COPD appears to be the most important underlying condition leading to mortality in patients with pulmonary NTM infections (Hayashi et al., 2012; Ito et al., 2012; Mirsaeidi et al., 2014; Gommans et al., 2015; Jones et al., 2018), although fibrocavitary disease without COPD is also associated with increased mortality (Fleshner et al., 2016).

PRIMARY CILIARY DYSKINESIA (PCD)

Case

A 53 year old woman is followed for bronchiectasis, sinusitis and chronic lung infections with MAC and *P. aeruginosa*. She had no respiratory distress as an infant, but she began to develop recurrent sinus infection and a productive cough around age four. At the age of 18 she was diagnosed with bronchiectasis. She had been evaluated for CF with sweat chloride tests were negative on three occasions. She has two children, and no other family members have respiratory disease. On exam now, she is thin with a body-mass index of 17.9 (normal: 19–24 kg/m^2). On lung exam she has scattered wheezes and rales in the bases. She inhales nebulized hypertonic saline twice daily and engages in aerobic exercise daily for airway clearance.

Imaging of her sinuses shows chronic sinusitis, with air-fluid levels in both maxillary sinuses and opacified ethmoid and frontal sinuses, in spite of evidence of prior surgeries. Computed tomography (CT) of the chest is remarkable for severe bronchiectasis, predominantly in both lower lobes (**Figure 6**).

At the age of 37, she was first diagnosed with pulmonary MAC infection after presenting with worsening cough. She improved on treatment with clarithromycin, ethambutol and rifampin for 9 months. However, her cough returned several months after treatment was stopped, and she was restarted on the same treatment except with azithromycin instead of clarithromycin. Unfortunately, she noticed difficulties discriminating red and green colors and was diagnosed with optic neuritis secondary to ethambutol but this resolved after discontinuation of the drug. She was treated with inhaled amikacin but it was stopped due to severe hoarseness. Linezolid was recently added but the discontinued after she developed numbness and tingling in her fingers and toes consistent with peripheral neuropathy.

At the age of 47, the diagnosis of PCD was confirmed by low nasal nitric oxide of 15 nL/min and genetic analysis demonstrating two disease-causing mutations in *DNAH11*. Electron microscopy showed no structural changes of the cilia as seen in classic PCD.

P. aeruginosa was first cultured from her sputum in early 2017, but she was feeling relatively well. She received three courses of oral ciprofloxacin without eradication. In the fall of 2017, she complained of more cough and sputum production. She was treated with cefepime and tobramycin by the intravenous route for 2 weeks to treat a bronchiectasis exacerbation due to *P. aeruginosa*. She had baseline mild tinnitus that did not change. A follow-up audiological evaluation 1 month later showed the development of mild to moderate high frequency sensorineural hearing loss bilaterally, although the patient did not perceive hearing loss. Follow-up audiological evaluations after another month and then 6 months later showed no improvement in the hearing acuity, but it remained stable. Unfortunately, her *Pseudomonas* infection now appears chronic. She is feeling relatively well on suppressive therapy with inhaled aztreonam.

Discussion

PCD, or immotile cilia syndrome, is an autosomal recessive disorder of motile cilia dysfunction resulting in impairment of mucociliary clearance. It is heterogenous, with over 30 genetic variants described to date and a wide range of clinical manifestations. Unlike the patient above, approximately 80% of newborns have neonatal respiratory distress. About one-half of PCD patients have 'laterality defects' such as situs inversus, in which the organs are on the opposite side of the body due to defects in the embryonic nodal cilia. In children, CF and PCD may both present with respiratory infections and distress. In CF, the problem is due to alterations of the airway surface fluid,

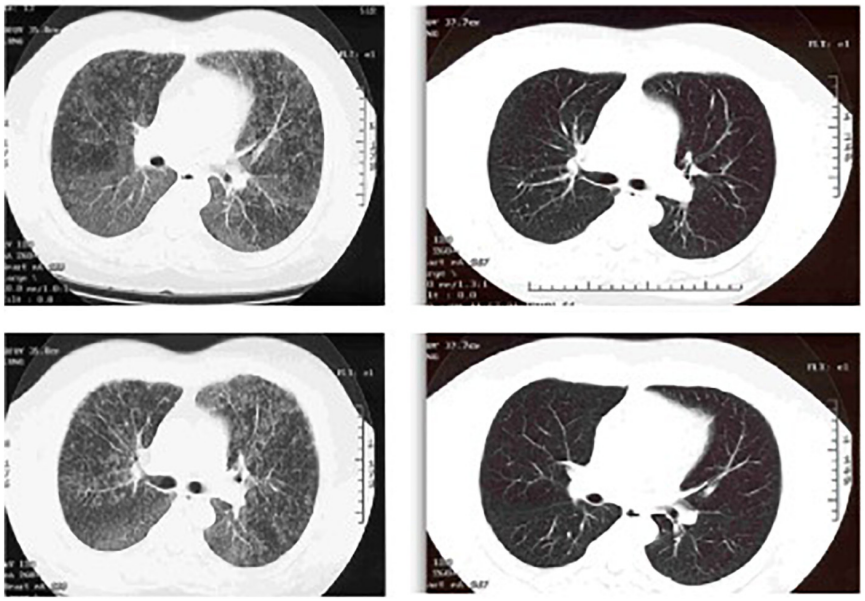

FIGURE 7 | Left: CT chest showing diffuse ground glass centrilobular nodules and mosaic attenuation. Right: post-treatment images demonstrating resolution of the prior findings.

whereas in PCD the problem is with poor movement of the fluid due to the dysfunctional cilia. Both result in bronchiectasis (dilated, chronically inflamed bronchi), but the location tends to be in the upper lobes in CF and in the lower lobes in PCD. Nearly all PCD patients have rhinosinusitis. Infertility is a possibility, but not universal as in this case. The median age of diagnosis in childhood is about 5 years of age, but the age of diagnosis in adults is widely variable. Diagnosis has traditionally been difficult due to variable availability and accuracy of tests such as transmission emission microscopy to evaluate 'classic' ciliary ultrastructural defects and nasal nitric oxide measurements. However, the increased availability of genetic testing has been a significant advance. A recent clinical practice guideline provides a very helpful diagnostic algorithm (Shapiro et al., 2018).

Most PCD patients live an active life and have a normal lifespan, although lung infections can interfere with their normal social functions. The rate of decline in their lung function is slower than in CF. The rates of NTM infections among patients with PCD is not known. In a recent registry study, PCD patients were less likely to have NTM infections than those with bronchiectasis associated with gastroesophageal reflux disease (GERD).

This case highlights problems of drug toxicity experienced by most patients with NTM lung diseases, who are also frequently co-infected with Gram-negative bacteria or fungal pathogens. In review, this patient has had adverse reactions to ethambutol (optic neuritis), inhaled amikacin (laryngitis), linezolid (peripheral neuropathy), and intravenous tobramycin (ototoxicity). Due to the multiple adverse reactions, her chronic MAC infection now can be treated only with azithromycin and rifampin, a suboptimal regimen for cure, which is probably unlikely to occur due to the severity of her bronchiectasis. The goal of therapy for both the MAC and the *Pseudomonas* is now suppression of bacterial growth to prevent exacerbations and further lung destruction. Such adverse reactions to drugs limit the armamentarium available to physicians to treat patients, and contribute to the urgent need for additional antibacterial drugs.

HYPERSENSITIVITY PNEUMONITIS (HP)

Case

One of us (KF) was consulted on the case of a 52 year-old pulp mill worker for evaluation of possible underlying occupational lung disease. He had been referred to the infectious disease service after a surgical lung biopsy at an outside hospital showed non-caseating granulomas and AFB. The lung tissue culture had grown MAC. The patient had noted progressive shortness of breath. On physical examination, the patient had a very rapid breathing rate in spite of being on supplemental oxygen by nasal cannula with a reservoir device at 15 l/min. There were inspiratory crackles on lung exam. The lung imaging was remarkable for diffuse 'mosaic attenuation' and fine nodules (**Figure 7**) which was not consistent with what is usually seen in MAC infections. It was originally suspected that he might have HP due to airborne molds within the pulp mill. However, the history revealed that he had not worked inside the pulp mill for several years due to a severe back injury. He worked in a control room in another building at a distance from the plant. To manage his back pain, the patient had the habit of soaking in a hot tub for 30 min in the morning after awakening and then again in the evening when he returned from work. The hot tub was in a room just outside his bedroom. He was too short of breath to be able to do pulmonary function testing. We considered performing

a bronchoscopy to obtain BAL fluid for cell counts, but we realized that both HP and mycobacterial infection would be predominantly lymphocytic. Given his tenuous respiratory status and his tissue diagnosis, the risk of the procedure far outweighed any benefit. He was treated with both systemic corticosteroids for the HP and with azithromycin, rifampin and ethambutol for the MAC infection. He began to improve within a few days in the hospital, and was discharged home with the advice to drain the hot tub after obtaining a water sample for culture. He sent the water to the local state public health laboratory and received a report that it grew MAC. Unfortunately, when we called to request the isolate to determine if it was identical to the clinical one, the laboratory in a southeastern state had already discarded it because they were overwhelmed with such cultures. When we saw him 18 months after his removal from exposure and initiation of treatment, his symptoms, exam, imaging and pulmonary function tests were completely normal.

Discussion

This was a classic case of 'hot tub lung' due to inhalation of NTM. This form of HP was first described in case reports in 1997, and multiple cases have now been reported in the literature. In a retrospective case series of 21 patients at a referral center, all patients presented with shortness of breath and cough and about half were hypoxemic. MAC was isolated from both the hot tub water and the respiratory secretions or tissue in all cases (Hanak et al., 2006). All improved with avoidance of exposure, and there was a mix of additional corticosteroid and antimycobacterial therapy, but five (24%) received neither. Thus, avoidance of exposure appears to be the most important element. However, in patients with severe illness like our case, more aggressive treatment is warranted. Some of the more interesting case reports have involved multiple immunocompetent family members developing HP due to MAC and possibly other NTM (Mangione et al., 2001; Kitahara et al., 2016).

An occupational respiratory illness associated with NTM that emerged in the last decade is HP associated with metal-working fluids in both the United States and the United Kingdom (Dawkins et al., 2006). These fluids were found to be contaminated with a rapidly growing *Mycobacterium* now known as *M. immunogenum* (Wallace et al., 2002).

Mycobacterium chelonae was isolated from a bassoon played by a professional musician diagnosed with HP, but molds were also isolated and no NTM or molds were isolated from the BAL from the patient (Moller et al., 2017). Thus, the association may not be causal. NTM contamination in a water-damaged building was recently associated with asthma symptoms (Park et al., 2017). Environmental sampling for NTM is not commonly done in indoor environments, suggesting a need for further research about environmental exposures to airborne NTM.

DISSEMINATED DISEASE

Case

A 49-year-old denied any infections or hospitalizations in his childhood. As a young adult he had histoplasmosis lymphadenitis and was treated successfully. He did well until 47 years of age when he presented to a hospital complaining of diarrhea after having several year history of GERD, intermittent nausea and emesis. Colonoscopy was performed and pathology showed Periodic Acid Schiff stain (PAS) positivity, so empiric treatment for Whipple's disease, a rare systemic infection caused by the bacterium *Tropheryma whipplei*, was initiated. One month later, he presented to a large tertiary hospital with mycobacteremia, hypotension and sepsis. He was diagnosed with idiopathic CD4 lymphopenia and disseminated MAC. He suffered multiple cerebral embolic events, had a tracheostomy placed, underwent PEG placement and suffered extensive end-organ damage from long term aminoglycoside therapy. His GI disease was indicative of his overall burden of disease. He was referred to the NIH after the diagnoses of two variants (IL12Rβ1 c.512 A > C, p.Q171P; and IL12Rβ1 c. 1442A > G, p.Y481C) were found in IL-12 receptor 1. He required years of intensive multidrug therapy in addition to immune therapies including exogenous interferon gamma.

Discussion

Genetic susceptibility to disseminated mycobacterial infection is well described and should be considered in anyone who presents with disseminated disease without HIV infection (Wu and Holland, 2015). Even diseases that are often diagnosed in childhood can present with disseminated infection in adulthood when their mutation results in a less severe phenotype (Hsu et al., 2018). Host control depends on the interleukin 12-interferon pathway that connects myeloid and lymphoid cells. The genetic susceptibilities, if inherited, can be elucidated by a careful family medical history. Autosomal dominant patterns of inheritance include: IFNR1/R2, STAT1, IRF8, GATA2, IL12Rβ1/R2 X-linked: NEMO. Autosomal recessive patterns of inheritance typically present early in life and would not have been considered in this age patient. Non-HIV Acquired immunodeficiency such as autoantibodies to interferon gamma (IFN) would have been another consideration in this patient and one that is important to consider in adults with disseminated infection. However, in the United States, women have been identified more frequently than men, and have mainly been described in the East Asian population.

IL-12Rβ1 encodes the 1 chain of IL-12 and IL-23 receptors and activation of pSTAT4 and is important in the subsequent signaling of IFN and activation of macrophage intracellular killing. IL-12Rβ1 has been reported in more than 200 patients worldwide (de Beaucoudrey et al., 2010). Typically, they will present after BCG vaccination in countries where TB is endemic. However, in the United States, these patients may present later in life, as our patient presented. This case of a primary immune deficiency that phenotypically presented in adulthood highlights the importance of evaluating genetic disorders that may predispose individuals to disseminated infection with a low virulent organism in the absence of known risk factors.

Case

A 32-year-old Filipina woman presented to her primary care provider with fevers, neck and back pain, and cervical

lymphadenopathy. She was diagnosed with community-acquired pneumonia, and treated with azithromycin and oral corticosteroids as well as a subsequent course of doxycycline with more oral corticosteroids. While her pain improved on the corticosteroids, she started having night sweats off of prednisone. An eventual CT of her neck showed destruction of her C3 vertebra, and lymphadenopathy. A PET/CT showed uptake in activity in lymph nodes, femurs, left acetabulum, left pubic ramus, sacrum, right ischium, both iliac bones, ribs, and clavicles. She underwent C3 corpectomy with fusion; followed by right femoral curettage 1 month later. When AFB+ organisms were seen, an interferon gamma release assay (IGRA) was indeterminate. Cultures grew MAC. Three months after the first surgery, she continued to have pain and underwent debridement of an epidural abscess in T8, involving a laminectomy, foraminectomy and hardware placement of screws at T6, T7, T10, and T11. Her disease continued to worsen despite optimal multi-drug therapy. Subsequent testing at the National Institutes of Health (NIH) showed very high titer autoantibodies to Interferon gamma. She was referred to the NIH and continued on multi-drug antibiotic therapy and given rituximab with improvement in her disease. Unfortunately, when her B-cells returned after 2 years, her disease recurred and she remains on therapy for her infection and is getting repeat rituximab infusions for the IFN autoantibodies.

Discussion

Autoantibodies to IFN were first reported by Doffinger et al. (2004). An adult-onset immunodeficiency due to these autoantibodies in Thailand and Taiwan was described in 2012 in a population of HIV negative patients presenting with opportunistic infections (Browne et al., 2012). They have since been described in patients with thymic neoplasia (Burbelo et al., 2010). An indeterminate IGRA test is characteristic in these patients, as sera from them will block positive controls for this commercial test and will therefore be reported as indeterminate. *In vitro*, the pSTAT1 activation is negative when patient sera is tested in the presence of normal PBMCs. Especially in Asians, one should consider autoantibodies to IFN when encountering an adult with disseminated NTM, particularly when there is no family history of disease.

VERTEBRAL OSTEOMYELITIS

Case

A 16-year-old girl was evaluated for progressive mid-thoracic back pain. She reported the onset after abatement of symptoms of a flu-like illness with fever, nasal congestion, sore throat and non-productive cough and muscle aches. She was a competitive roller-skater, and she had experienced multiple falls in the prior year. She recalled multiple ecchymoses and abrasions due to these falls. She had no history of unusual infections earlier in her life, and there was no suggestion of immunodeficiency in her laboratory data. The C-reactive protein (a non-specific marker of systemic inflammation) was minimally elevated at 1.3 mg/dL. Her examination was normal with no neurological deficits. A CT scan of her lungs was normal. A radionuclide bone scan demonstrated increased uptake in the vertebral body of T9, and magnetic resonance imaging (MRI) showed a soft tissue mass anterior to the vertebral bodies of T8, T9, and T10. Thoracoscopic biopsy of the T9 vertebral body demonstrated necrotizing granulomas of the bone; special stains for bacteria, mycobacteria and fungi were negative (**Figure 8**). She was treated initially for both *M. tuberculosis* and NTM with isoniazid, rifampin, ethambutol and clarithromycin. After the culture grew only *M. abscessus*, she was treated with only clarithromycin; the other drugs for tuberculosis were discontinued. A follow-up MRI showed resolution of the edema and overall improvement at 4 months. The clarithromycin was discontinued after 6 months, and she was well with a normal C-reactive protein 3 months later. She was advised to discontinue roller-skating and other potentially traumatic activities and to be closely monitored for relapse.

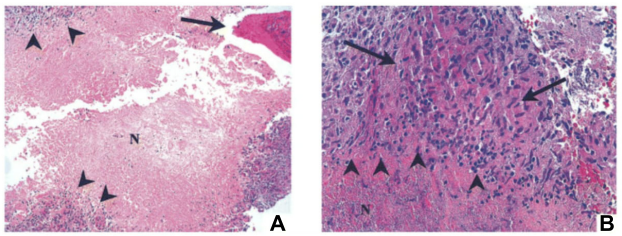

FIGURE 8 | Bone biopsy specimen (T9 vertebra) of patient 1 showing necrotizing granulomas. **(A)** Area of necrotic bone is shown (arrow; hematoxylin and eosin stain; original magnification, ×100). Surrounding the area of caseous necrosis (N) is a rim of granulomatous tissue reaction (arrowheads). **(B)** At higher magnification (hematoxylin and eosin stain; magnification, ×400), the granulomas are principally composed of macrophages (area between the arrows) and lymphocytes (arrowheads). Acid-fast and fungal stains showed negative results, but culture was positive for *Mycobacterium abscessus*. Reprinted with permission of Oxford University Press; Chan et al. (2001).

Discussion

Although most cases of disseminated NTM disease suggest the presence of an immunodeficiency, NTM infections can occasionally occur at distant sites from the lung in special situations. Obviously these organisms can gain access to bone or other internal structures during penetrating trauma. However, this case was associated with blunt trauma and so illustrates the principle of 'locus minoris resistentiae,' i.e., a place of less resistance, in this case to microbes. This unusual case was previously published along with two similar cases in 2001 (Chan et al., 2001). In retrospect, such a case now would probably be treated not only with a macrolide like clarithromycin, but also with at least one intravenous medication such as amikacin. The isolate in this case was most likely a *M. massiliense* subspecies that was susceptible to clarithromycin. Interestingly, shorter courses of therapy than are used for pulmonary disease are acceptable for bone infections.

NOSOCOMIAL INFECTIONS WITH *Mycobacterium chimaera* AFTER CARDIAC SURGERY

Case

A 64-year-old man had cardiac surgery for a mitral valve porcine mitral valve replacement and a new prosthetic aortic valve in March of 2012. His postoperative course was uneventful until 5 months after the surgery when he developed persistent fevers between 103 and 104 degrees Fahrenheit. Blood cultures were negative, and transthoracic and transesophageal echocardiograms were normal. He was treated empirically with both oral and intravenous antibiotics for culture negative endocarditis in the setting of his recent surgery. In December 2012 (9 months after surgery) blood cultures drawn 30 days prior grew *M. chimaera (*a species in the *M. avium* complex*)*. Despite optimal medical management with intravenous and oral multi-drug therapy, he remained persistently bacteremic for 2 years. Unfortunately, despite multi-drug therapy and close medical follow-up, the patient died of his persistent bacteremia.

Discussion

A prolonged outbreak of *M. chimaera* infections after open-chest cardiac surgery was first reported by Swiss investigators in 2015. After the recognition of a cluster of cases of disseminated *M. chimaera* after cardiac surgery at the same hospital as our patient's, the US Centers for Disease Control and Prevention (CDC) and the Pennsylvania Department of Health investigated the outbreak. They found that the heater-cooler devices (HCDs) used to maintain the patients' body temperature during extracorporeal circulation (also known as cardiac bypass) were contaminated with *M. chimaera*, confirming similar findings by the Swiss investigators (Perkins et al., 2016). The isolates obtained from HCDs from three different European countries were nearly identical to those from the manufacturing site in another study. The results of these investigations strongly suggested a point-source contamination in the manufacturing of a specific HCD. There is a growing body of literature on this problem, and investigations are on-going.

Whole exome sequencing revealed that our patient had a mutation of interferon regulatory factor 8 (IRF8), which regulates expression of interferon-alpha and interferon beta genes. IRF8 is critically important in immune responses to intracellular pathogens, especially mycobacteria, involving the production of interleukin-12 in response to interferon-gamma (Hambleton et al., 2011). This mutation likely contributed to his susceptibility and death due to this infection.

CONCLUSION

The cases presented in this paper demonstrate that NTM infections vary widely in presentation, treatment, and clinical outcome. While ubiquitous in the environment, NTM species tend to infect certain vulnerable patient populations, and these infections can often be organized into clinical phenotypes. While many NTM species have low pathogenicity, some opportunistic pathogens are important causes of human disease. Infection with these organisms, including MAC, MABSC, *M. kansasii*, *M. xenopi*, and others, are increasing in incidence and geographic distribution. Most human disease is pulmonary, primarily affecting immunocompetent patients with underlying structural lung disease such as bronchiectasis or COPD. Disseminated disease is usually more life-threatening, and primarily occurs in immunocompromised individuals. Among those most severely affected by disseminated disease are children with specific primary immunodeficiencies, and those with acquired T cell immunodeficiency due to anti-cytokine antibodies or iatrogenic administration of immunosuppressive medications, particularly tumor-necrosis factor alpha antagonists.

We hope that the host variability in NTM disease presented in this paper serves to stimulate and inspire basic and translational scientists to consider a similar variety of innovative interventions. For example, the poor response to treatment and increased mortality seen in fibrocavitary lung disease might be improved by drugs targeting biofilm dispersion (COPD Case). Inhaled liposomal amikacin was recently approved for pulmonary MAC disease in the United States, and translational studies on its role in biofilm infections may be a next step. Elucidation of the pathogenesis of non-CF bronchiectasis in tall, thin women may enable us to 1 day prevent the development of the disease. Candidate areas of research for the nodular-bronchiectasis MAC phenotype include leptin and ghrelin hormone influences on the immune response, cellular senescence, and the aging lung. In CF, research is needed on potential airborne transmission of *M. abscessus*, biofilm formation in the airways by *M. abscessus*, the effect of new CFTR modulator drugs on mycobacterial infection, among others. In PCD, it is possible that drugs improving the function of cilia may have a role in preventing NTM infections, and perhaps gene mutations could be corrected in the future. HP could be prevented by improved water disinfection techniques, and disseminated disease acquired during cardiac bypass could also be prevented by improved disinfection of heart-lung machines. Disseminated diseases associated with immunodeficiencies could be prevented by better immunomodulatory drugs that could correct such defects. Obviously, most patients would benefit from simpler, shorter and more effective drug treatment regimens against the mycobacteria, and the role of inhaled liposomal amikacin in such regimens continues to be defined.

The cases that we have presented illustrate the broad spectrum of NTM disease. We hope that these clinical vignettes have provided non-clinical scientists with a better understanding of human NTM diseases.

AUTHOR CONTRIBUTIONS

All authors contributed sections to the manuscript, and all reviewed and contributed to revisions.

REFERENCES

Adjemian, J., Olivier, K. N., and Prevots, D. R. (2014a). Nontuberculous mycobacteria among patients with cystic fibrosis in the United States: screening practices and environmental risk. *Am. J. Respir. Crit. Care Med.* 190, 581–586. doi: 10.1164/rccm.201405-0884OC

Adjemian, J., Olivier, K. N., and Prevots, D. R. (2018). Epidemiology of pulmonary Nontuberculous Mycobacterial sputum positivity in patients with cystic fibrosis in the United States, 2010-2014. *Ann. Am. Thorac. Soc.* 15, 817–826. doi: 10.1513/AnnalsATS.201709-727OC

Adjemian, J., Prevots, D. R., Gallagher, J., Heap, K., Gupta, R., and Griffith, D. (2014b). Lack of adherence to evidence-based treatment guidelines for nontuberculous mycobacterial lung disease. *Ann. Am. Thorac. Soc.* 11, 9–16. doi: 10.1513/AnnalsATS.201304-085OC

Adjemian, J., Seitz, A. E., Holland, S. M., and Prevots, D. R. (2012). Prevalence of nontuberculous mycobacterial lung disease in U.S. Medicare beneficiaries. *Am. J. Respir. Crit. Care Med.* 185, 881–886. doi: 10.1164/rccm.201111-2016OC

Boyle, D. P., Zembower, T. R., and Qi, C. (2016). Relapse versus Reinfection of *Mycobacterium avium complex* Pulmonary disease. Patient characteristics and macrolide susceptibility. *Ann. Am. Thorac. Soc.* 13, 1956–1961. doi: 10.1513/AnnalsATS.201605-344BC

Browne, S. K., Burbelo, P. D., Chetchotisakd, P., Suputtamongkol, Y., Kiertiburanakul, S., Shaw, P. A., et al. (2012). Mo, Iadarola, M., and Holland, S. M.: adult-onset immunodeficiency in Thailand and Taiwan. *N. Engl. J. Med.* 367, 725–734. doi: 10.1056/NEJMoa1111160

Burbelo, P. D., Browne, S. K., Sampaio, E. P., Giaccone, G., Zaman, R., Kristosturyan, E., et al. (2010). Iadarola and Holland, S. M.: anti-cytokine autoantibodies are associated with opportunistic infection in patients with thymic neoplasia. *Blood* 116, 4848–4858. doi: 10.1182/blood-2010-05-286161

Chalermskulrat, W., Sood, N., Neuringer, I. P., Hecker, T. M., Chang, L., Rivera, M. P., et al. (2006). Non-tuberculous mycobacteria in end stage cystic fibrosis: implications for lung transplantation. *Thorax* 61, 507–513. doi: 10.1136/thx.2005.049247

Chan, E. D., Kong, P. M., Fennelly, K., Dwyer, A. P., and Iseman, M. D. (2001). Vertebral osteomyelitis due to infection with nontuberculous Mycobacterium species after blunt trauma to the back: 3 examples of the principle of locus minoris resistentiae. *Clin. Infect. Dis.* 32, 1506–1510. doi: 10.1086/320155

Dawkins, P., Robertson, A., Robertson, W., Moore, V., Reynolds, J., Langman, G., et al. (2006). An outbreak of extrinsic alveolitis at a car engine plant. *Occup. Med.* 56, 559–565. doi: 10.1093/occmed/kql110

de Beaucoudrey, L., Samarina, A., Bustamante, J., Cobat, A., Boisson-Dupuis, S., Feinberg, J., et al. (2010). Revisiting human IL-12Rbeta1 deficiency: a survey of 141 patients from 30 countries. *Medicine* 89, 381–402. doi: 10.1097/MD.0b013e3181fdd832

Diel, R., Nienhaus, A., Ringshausen, F. C., Richter, E., Welte, T., Rabe, K. F., et al. (2018). Microbiologic outcome of interventions against *Mycobacterium avium complex* Pulmonary disease: a systematic review. *Chest* 153, 888–921. doi: 10.1016/j.chest.2018.01.024

Doffinger, R., Helbert, M. R., Barcenas-Morales, G., Yang, K., Dupuis, S., Ceron-Gutierrez, L., et al. (2004). Autoantibodies to interferon-gamma in a patient with selective susceptibility to mycobacterial infection and organ-specific autoimmunity. *Clin. Infect. Dis.* 38, e10–e14. doi: 10.1086/380453

Falkinham, J. O. III (2015). Environmental sources of nontuberculous mycobacteria. *Clin. Chest. Med.* 36, 35–41. doi: 10.1016/j.ccm.2014.10.003

Fennelly, K. P., Ojano-Dirain, C., Yang, Q., Liu, L., Lu, L., Progulske-Fox, A., et al. (2016). Biofilm formation by *Mycobacterium abscessus* in a Lung cavity. *Am. J. Respir. Crit. Care Med.* 193, 692–693. doi: 10.1164/rccm.201508-1586IM

Fleshner, M., Olivier, K. N., Shaw, P. A., Adjemian, J., Strollo, S., Claypool, R. J., et al. (2016). Mortality among patients with pulmonary non-tuberculous mycobacteria disease. *Int. J. Tuberc. Lung Dis.* 20, 582–587. doi: 10.5588/ijtld.15.0807

Fujita, J., Ohtsuki, Y., Suemitsu, I., Shigeto, E., Yamadori, I., Obayashi, Y., et al. (1999). Pathological and radiological changes in resected lung specimens in *Mycobacterium avium* intracellulare complex disease. *Eur. Respir. J.* 13, 535–540. doi: 10.1183/09031936.99.13353599

Gilljam, M., Schersten, H., Silverborn, M., Jonsson, B., and Ericsson Hollsing, A. (2010). Lung transplantation in patients with cystic fibrosis and *Mycobacterium abscessus* infection. *J. Cyst. Fibros* 9, 272–276. doi: 10.1016/j.jcf.2010.03.008

Gommans, E. P., Even, P., Linssen, C. F., van Dessel, H., van Haren, E., de Vries, G. J., et al. (2015). Risk factors for mortality in patients with pulmonary infections with non-tuberculous mycobacteria: a retrospective cohort study. *Respir. Med.* 109, 137–145. doi: 10.1016/j.rmed.2014.10.013

Griffith, D. E., Aksamit, T., Brown, B. A., Catanzaro-Elliott, A., Daley, C., Gordin, F., et al. (2007). American thoracic and A. Infectious Disease Society of: an official ATS/IDSA statement: diagnosis, treatment, and prevention of nontuberculous mycobacterial diseases. *Am. J. Respir. Crit. Care Med.* 175, 367–416. doi: 10.1164/rccm.200604-571ST

Hambleton, S., Salem, S., Bustamante, J., Bigley, V., Boisson-Dupuis, S., Azevedo, J., et al. (2011). Casanova and gros, P.: IRF8 mutations and human dendritic-cell immunodeficiency. *N. Engl. J. Med.* 365, 127–138. doi: 10.1056/NEJMoa1100066

Hanak, V., Kalra, S., Aksamit, T. R., Hartman, T. E., Tazelaar, H. D., and Ryu, J. H. (2006). Hot tub lung: presenting features and clinical course of 21 patients. *Respir. Med.* 100, 610–615. doi: 10.1016/j.rmed.2005.08.005

Hayashi, M., Takayanagi, N., Kanauchi, T., Miyahara, Y., Yanagisawa, T., and Sugita, Y. (2012). Prognostic factors of 634 HIV-negative patients with *Mycobacterium avium complex* lung disease. *Am. J. Respir. Crit. Care Med.* 185, 575–583. doi: 10.1164/rccm.201107-1203OC

Hsu, D. C., Breglio, K. F., Pei, L., Wong, C. S., Andrade, B. B., Sheikh, V., et al. (2018). Emergence of polyfunctional cytotoxic CD4+ T Cells in *Mycobacterium avium* immune reconstitution inflammatory syndrome in human immunodeficiency virus-infected patients. *Clin. Infect. Dis.* 67, 437–446. doi: 10.1093/cid/ciy016

Ito, Y., Hirai, T., Maekawa, K., Fujita, K., Imai, S., Tatsumi, S., et al. (2012). Predictors of 5-year mortality in pulmonary *Mycobacterium avium*-intracellulare complex disease. *Int. J. Tuberc. Lung Dis.* 16, 408–414. doi: 10.5588/ijtld.11.0148

Jones, M. M., Winthrop, K. L., Nelson, S. D., Duvall, S. L., Patterson, O. V., Nechodom, K. E., et al. (2018). Epidemiology of nontuberculous mycobacterial infections in the U.S. Veterans Health Administration. *PLoS One* 13:e0197976. doi: 10.1371/journal.pone.0197976

Kim, H. Y., Kim, B. J., Kook, Y., Yun, Y. J., Shin, J. H., Kim, B. J., et al. (2010). *Mycobacterium massiliense* is differentiated from *Mycobacterium abscessus* and *Mycobacterium bolletii* by erythromycin ribosome methyltransferase gene (erm) and clarithromycin susceptibility patterns. *Microbiol. Immunol.* 54, 347–353. doi: 10.1111/j.1348-0421.2010.00221.x

Kim, R. D., Greenberg, D. E., Ehrmantraut, M. E., Guide, S. V., Ding, L., Shea, Y., et al. (2008). Pulmonary nontuberculous mycobacterial disease: prospective study of a distinct preexisting syndrome. *Am. J. Respir. Crit. Care Med.* 178, 1066–1074. doi: 10.1164/rccm.200805-686OC

Kitahara, Y., Araki, Y., and Nakano, K. (2016). A case of familial hot tub lung. *Respir. Med. Case Rep.* 17, 71–74. doi: 10.1016/j.rmcr.2016.02.001

Lee, B. Y., Kim, S., Hong, Y., Lee, S. D., Kim, W. S., Kim, D. S., et al. (2015). Risk factors for recurrence after successful treatment of *Mycobacterium avium complex* lung disease. *Antimicrob. Agents Chemother.* 59, 2972–2977. doi: 10.1128/AAC.04577-14

Lee, R., Lee, J., Choi, S. M., Seong, M. W., Kim, S. A., Kim, M., et al. (2013). Phenotypic, immunologic, and clinical characteristics of patients with nontuberculous mycobacterial lung disease in Korea. *BMC Infect. Dis.* 13:558. doi: 10.1186/1471-2334-13-558

Mangione, E. J., Huitt, G., Lenaway, D., Beebe, J., Bailey, A., Figoski, M., et al. (2001). Nontuberculous mycobacterial disease following hot tub exposure. *Emerg. Infect. Dis.* 7, 1039–1042. doi: 10.3201/eid0706.010623

Mirsaeidi, M., Machado, R. F., Garcia, J. G., and Schraufnagel, D. E. (2014). Nontuberculous mycobacterial disease mortality in the United States, 1999-2010: a population-based comparative study. *PLoS One* 9:e91879. doi: 10.1371/journal.pone.0091879

Moller, J., Hyldgaard, C., Kronborg-White, S. B., Rasmussen, F., and Bendstrup, E. (2017). Hypersensitivity pneumonitis among wind musicians - an overlooked disease? *Eur. Clin. Respir. J.* 4:1351268. doi: 10.1080/20018525.2017.1351268

Olivier, K. N. (2016). Lady windermere dissected: more form than fastidious. *Ann. Am. Thorac. Soc.* 13, 1674–1676. doi: 10.1513/AnnalsATS.201607-521ED

Park, H. Y., Suh, G. Y., Chung, M. P., Kim, H., Kwon, O. J., Chung, M. J., et al. (2009). Comparison of clinical and radiographic characteristics between nodular bronchiectatic form of nontuberculous mycobacterial lung disease and

diffuse panbronchiolitis. *J. Korean Med. Sci.* 24, 427–432. doi: 10.3346/jkms.2009.24.3.427

Park, J. H., Cox-Ganser, J. M., White, S. K., Laney, A. S., Caulfield, S. M., Turner, W. A., et al. (2017). Bacteria in a water-damaged building: associations of actinomycetes and non-tuberculous mycobacteria with respiratory health in occupants. *Indoor Air* 27, 24–33. doi: 10.1111/ina.1227838

Perkins, K. M., Lawsin, A., Hasan, N. A., Strong, M., Halpin, A. L., Rodger, R. R., et al. (2016). Perz: notes from the Field: *Mycobacterium chimaera* contamination of heater-cooler devices used in cardiac surgery - United States. *Morb. Mortal. Wkly. Rep.* 65, 1117–1118. doi: 10.15585/mmwr.mm6540a6

Reich, J. M., and Johnson, R. E. (1992). *Mycobacterium avium complex* pulmonary disease presenting as an isolated lingular or middle lobe pattern. The lady windermere syndrome. *Chest* 101, 1605–1609. doi: 10.1378/chest.101.6.1605

Roux, L., Catherinot, E., Soismier, N., Heym, B., Bellis, G., Lemonnier, L., et al. (2015). Comparing *Mycobacterium massiliense* and *Mycobacterium abscessus* lung infections in cystic fibrosis patients. *J. Cyst. Fibros* 14, 63–69. doi: 10.1016/j.jcf.2014.07.004

Shapiro, J., Davis, S. D., Polineni, D., Manion, M., Rosenfeld, M., Dell, S. D., et al. (2018). Lavergne and P. American thoracic society assembly on: diagnosis of primary ciliary dyskinesia. An official american thoracic society clinical practice guideline. *Am. J. Respir. Crit. Care Med.* 197, e24–e39. doi: 10.1164/rccm.201805-0819ST

Timpe, A., and Runyon, E. H. (1954). The relationship of atypical acid-fast bacteria to human disease; a preliminary report. *J. Lab. Clin. Med.* 44, 202–209.

Tsai, H. W., Fennelly, K., Wheeler-Hegland, K., Adams, S., Condrey, J., Hosford, J. L., et al. (2017). Cough physiology in elderly women with nontuberculous mycobacterial lung infections. *J. Appl. Physiol.* 122, 1262–1266. doi: 10.1152/japplphysiol.00939.2016

Wallace, R. J. Jr., Zhang, Y., Wilson, R. W., Mann, L., and Rossmoore, H. (2002). Presence of a single genotype of the newly described species *Mycobacterium immunogenum* in industrial metalworking fluids associated with hypersensitivity pneumonitis. *Appl. Environ. Microbiol.* 68, 5580–5584. doi: 10.1128/AEM.68.11.5580-5584.2002

Wallace, R. J. Jr., Brown-Elliott, B. A., McNulty, S., Philley, J. V., Killingley, J., Wilson, R. W., et al. (2014). Macrolide/Azalide therapy for nodular/bronchiectatic *Mycobacterium avium complex* lung disease. *Chest* 146, 276–282. doi: 10.1378/chest.13-2538

Wu, U. I., and Holland, S. M. (2015). Host susceptibility to non-tuberculous mycobacterial infections. *Lancet Infect. Dis.* 15, 968–980. doi: 10.1016/S1473-3099(15)00089-4

Conflict of Interest Statement: The authors declare that the research was conducted in the absence of any commercial or financial relationships that could be construed as a potential conflict of interest.

frontiers in Microbiology

MINI REVIEW
published: 20 November 2018
doi: 10.3389/fmicb.2018.02813

Assessing Response to Therapy for Nontuberculous Mycobacterial Lung Disease: Quo Vadis?

Christopher Vinnard[1], Alyssa Mezochow[2], Hannah Oakland[3], Ross Klingsberg[3], John Hansen-Flaschen[2] and Keith Hamilton[2]*

[1] Public Health Research Institute, New Jersey Medical School, Newark, NJ, United States, [2] Perelman School of Medicine, University of Pennsylvania, Philadelphia, PA, United States, [3] Department of Medicine, Tulane University School of Medicine, New Orleans, LA, United States

Assessing progression of disease or response to treatment remains a major challenge in the clinical management of nontuberculous mycobacterial (NTM) infections of the lungs. Serial assessments of validated measures of treatment response address whether the current therapeutic approach is on track toward clinical cure, which remains a fundamental question for clinicians and patients during the course of NTM disease treatment. The 2015 NTM Research Consortium Workshop, which included a patient advisory panel, identified treatment response biomarkers as a priority area for investigation. Limited progress in addressing this challenge also hampers drug development efforts. The Biomarker Qualification Program at the FDA supports the use of a validated treatment response biomarker across multiple drug development programs. Current approaches in clinical practice include microbiologic and radiographic monitoring, along with symptomatic and quality-of-life assessments. Blood-based monitoring, including assessments of humoral and cell-mediated NTM-driven immune responses, remain under investigation. Alignment of data collection schemes in prospective multicenter studies, including the support of biosample repositories, will support identification of treatment response biomarkers under standard-of-care and investigational therapeutic strategies. In this review, we outline the role of treatment monitoring biomarkers in both clinical practice and drug development frameworks.

Keywords: nontuberculous mycobactena, biomarker (development), response, therapeutics, clinical trial, radiography, quantitative culture

OPEN ACCESS

Edited by:
Rustam Aminov, University of Aberdeen, United Kingdom

Reviewed by:
David E. Griffith, The University of Texas Health Science Center at Tyler, United States
Debra Hanna, Bill & Melinda Gates Foundation, United States

****Correspondence:***
Christopher Vinnard
christopher.vinnard@njms.rutgers.edu

Specialty section:
This article was submitted to Antimicrobials, Resistance and Chemotherapy, a section of the journal Frontiers in Microbiology

Received: *02 July 2018*
Accepted: *01 November 2018*
Published: *20 November 2018*

Citation:
Vinnard C, Mezochow A, Oakland H, Klingsberg R, Hansen-Flaschen J and Hamilton K (2018) Assessing Response to Therapy for Nontuberculous Mycobacterial Lung Disease: Quo Vadis?. Front. Microbiol. 9:2813. doi: 10.3389/fmicb.2018.02813

Nontuberculous mycobacteria (NTM) are ubiquitous environmental organisms capable of causing significant morbidity (Yeung et al., 2016) and mortality (Vinnard et al., 2016; Diel et al., 2018), predominantly in the form of chronic lung disease (Wassilew et al., 2016). Profound knowledge gaps regarding the diagnosis of NTM lung infections (Griffith et al., 2007) include distinguishing NTM colonization from infection (van Ingen, 2015), identification of patients most likely to benefit from treatment (Mirsaeidi et al., 2014), selection of an optimal initial drug regimen (Philley and Griffith, 2015), and classification of treatment endpoints. As an explanation for these knowledge gaps, the formal study of NTM lung disease is relatively recent compared to tuberculosis, and basic understanding of NTM lung disease pathophysiology has only recently emerged.

In this review, we address uncertainties regarding the clinical "waypoints" of NTM treatment. Intermediate and definitive markers of treatment response provide crucial feedback to NTM patients, their clinicians, and developers of novel therapies. We outline the role of

treatment monitoring biomarkers in both clinical practice and drug development. We summarize the existing knowledge base regarding biomarkers of treatment response for NTM disease and we identify areas for ongoing and potential future investigation.

THE UTILITY OF A TREATMENT RESPONSE BIOMARKERS IN CLINICAL CARE AND DRUG DEVELOPMENT

In his seminal framework for defining surrogate endpoints in clinical trials, Ross Prentice proposed that a valid surrogate endpoint must "capture" the underlying relationship between the intervention and the clinical endpoint, allowing for comparison of intervention groups based on the surrogate rather than the definitive clinical endpoint at any time during the follow-up period (Prentice, 1989). By comparison, the concept of a treatment monitoring biomarker is less restrictive than a surrogate endpoint. The Institute of Medicine defines a biomarker as "a characteristic that is objectively measured and evaluated as an indicator of normal biologic processes, pathogenic processes, or biologic responses to a therapeutic intervention" (Institute of Medicine (US) Committee on Qualification of Biomarkers and Surrogate Endpoints in Chronic Disease, 2010).

The BEST (Biomarkers, EndpointS, and other Tools) Resource, published by the FDA-NIH Biomarker Working Group, provides descriptions and examples of disease monitoring biomarkers, which are "assessed serially over time to measure presence, status, or extent of disease or medical condition, or to provide evidence of an intervention effect or exposure, including exposure to a medical product or environmental agent" (Cagney et al., 2017).

Thus, the interpretation of a monitoring biomarker is not based on a snapshot level, as with a baseline clinical predictor of response to therapy, but rather on changes in values during serial measurements. As examples, quantification of HIV RNA in blood serves as a monitoring biomarker for the clinical efficacy of antiretroviral therapy, and the amount of air that an individual can forcefully exhale in one second (FEV1) reflects response to chronic obstructive pulmonary disease management. Ideally, a treatment monitoring biomarker could be readily adopted into existing procedures that support routine use in clinical settings (Nahid et al., 2011).

The therapeutic approach to NTM lung disease lacks the evidence base of tuberculosis, where standard-of-care combination drug regimens are based on randomized clinical trials that enrolled tens of thousands of tuberculosis patients. Unlike tuberculosis, the NTM lung disease research agenda has not been propelled by public health pressure or urgency. Consequently, much of the clinical approach to NTM disease rests on a foundation of observational data and expert opinion, supported by only a few randomized clinical trials (Research Committee of the British Thoracic Society, 2001). In general, this evidence base has demonstrated that antimycobacterial therapies are less effective for NTM lung disease than tuberculosis (Griffith et al., 2007). The 2015 NTM Research Consortium Workshop, which included a patient advisory panel, identified treatment response biomarkers as a priority area for investigation (Henkle et al., 2016). One or more treatment response biomarkers would help to answer a fundamental question for clinicians and patients during the course of NTM disease treatment: is the current therapeutic approach on track toward a clinical cure?

This question has a particular significance for NTM disease given the complexity of treatment and the frequency of drug-related adverse events. Interval monitoring of treatment response would support clinical decision-making with regards to the intensification or de-escalation of therapies. When an initial period of intravenous therapy is used, for example with disease caused by *M. abscessus* complex, the optimal time point for transitioning to an all-oral regimen is uncertain. Surgical interventions may be the most appropriate approach for a subset of patients with severe *M. abscessus* complex lung disease, but potentially could be deferred in a subset of patients that are responsive to medical management (Jarand et al., 2011). Such decision nodes provide a potential point of application for a treatment monitoring biomarker. Monitoring biomarker response early in treatment could also inform clinical decision-making in advance of drug susceptibility testing (DST) results, which have a delay of several weeks and lack correlation between *in vitro* susceptibility and clinical outcomes for many antibiotics.

Aside from their value in clinical management decisions, treatment monitoring biomarkers support drug development efforts. According to guidelines established by the Food and Drug Administration (FDA), the use of a biomarker in the context of drug development relies on "qualification" that specifies its contextual use and interpretation. The Biomarker Qualification Program at the FDA provides a pathway for a particular biomarker to become accepted into the regulatory framework independent of approval of a specific drug (Amur et al., 2015). This program was recently updated in response to the 21st Century Cures Act, establishing formal qualification plans for biomarkers and other drug development tools. As an example, the Critical Path Institute (Tuscon, AZ, United States) is evaluating sputum levels of lipoarabinomannan, a component of the mycobacterial cell wall, as a non-culture based measure of tuberculosis treatment response, which could be incorporated into adaptive clinical trial designs (FDA, 2018a). Similarly, a qualified biomarker of treatment response for NTM disease would support drug development efforts across multiple programs, a notable advantage given the likelihood that combination antimicrobial therapies will remain essential to future drug regimens.

CURRENT APPROACHES TO MONITORING TREATMENT RESPONSE TO NTM DISEASE

Microbiologic Monitoring

Presently, culture of serial sputum samples serves as the primary biomarker for monitoring the response to treatment

of mycobacterial lung infections. In 2016, an expert panel composed of NTM clinicians reached consensus definitions for several endpoints related to the treatment of NTM lung disease, including cure, relapse, and re-infection (van Ingen et al., 2018). Serial culturing of sputum and deep respiratory samples during treatment of NTM lung disease provides the basis for definition of microbiologic cure, which is defined as 3 negative sputum cultures collected at least 4 weeks apart.

Interval microbiologic data may also provide insight into the effectiveness of therapy when the microbiologic cure endpoint has not yet been reached. Mycobacterial cultures from respiratory specimens can be classified semiquantitatively according to growth characteristics in liquid and solid media (Griffith et al., 2015; **Table 1**). Using this scoring system, Griffith et al. (2015) analyzed semiquantitative sputum culture scores on 180 patients with lung disease caused by *M. avium* complex (MAC), grouping patients into converters and non-converters based on sputum culture status after 12 months of treatment. Although baseline semi quantitative culture scores were not significantly different between converters and non-converters, the change in semi quantitative culture scores after 2 months of MAC-directed treatment was highly predictive of sputum culture conversion, with each 1-point decline in the scoring scale associated with a 20% increase in the likelihood of achieving conversion at 12 months. Importantly, early microbiologic response also correlated with symptomatic and radiographic improvements, suggesting that semi quantitative culture data can be explored as a surrogate endpoint in drug development. One limitation of this approach may be that some NTM lung disease patients do not expectorate sputum (Huang et al., 1999), although proper application of sputum induction technique considerably improves microbiologic yield (Guiot et al., 2017).

Interval treatment response monitoring based on microbiologic data is supported by recently published NTM lung disease treatment guidelines. The British Thoracic Society recommends obtaining interval sputum cultures every 4–12 weeks during treatment to assess microbiologic response (Haworth et al., 2017). Similarly, consensus recommendations provided by the US Cystic Fibrosis Foundation and the European Cystic Fibrosis Society for the management of NTM lung disease include interval monitoring of sputum culture every 4–8 weeks during treatment (Floto et al., 2016). An update from the American Thoracic Society/Infectious Disease Society of America regarding management of NTM lung disease is currently in preparation. Unlike tuberculosis, there are no data supporting non-culture based microbiologic monitoring during NTM lung disease treatment.

TABLE 1 | A Semiquantitative Mycobacterial Culture Scoring System (Griffith et al., 2015).

Semi quantitative Culture Scores	Growth Scale	Growth in Broth	Growth on an Agar Plate	Countable Colonies on an Agar Plate
0	Negative	–	–	0
1	Positive broth only	+	–	0
2	1+	+	+	≤50
3	2+	+	+	50–99
4	2+	+	+	100–199
5	3+	+	+	200–299
6	4+	+	+	≥300

Radiographic Monitoring

Radiographic imaging studies have long served an essential role, not only in diagnosing NTM lung infection and determining the extent of disease, but also in assessing response to treatment (Griffith et al., 2007). A simple chest radiograph scoring system with 3 tiers (improved, no change, or worsened in comparison with the preceding examination) was predictive of sputum culture conversion among MAC lung disease patients, with repeated routine chest radiography performed a mean of 59 days after the baseline (pre-treatment) examination (Griffith et al., 2015). Computed tomographic (CT) imaging considerably improves assessment and comparison of NTM disease extent compared to chest radiographs. Indeed, several scoring criteria for CT imaging studies have been developed and evaluated for this purpose (Kim et al., 2012; Lee et al., 2013).

Untreated patients with NTM lung disease demonstrate progression of CT findings on serial studies that inform decisions to initiate treatment, particularly with the nodular bronchiectatic form of MAC lung disease (Park et al., 2017). Similar to microbiologic endpoints, radiographic improvement at the conclusion of therapy can characterize successful treatment of NTM lung disease. However, less is known regarding the contribution of early radiographic changes as a marker of treatment response. Moreover, interval radiographic findings during treatment of NTM lung disease may be confounded by the extent of underlying lung disease and by the presence of concomitant infection or colonization of airways (Park et al., 2016; Cohen-Cymberknoh et al., 2017). Other limitations of serial CT imaging for monitoring treatment response include the difficulty with classification of NTM lung disease patients with fibrocavitary disease (an alternate form of MAC lung disease), or structural lung changes due to additional treatment modalities (such as surgical resection or radiation fibrosis) (Lee et al., 2013).

Patients with active chronic lung diseases are exposed to significant radiation when monitored by chest CT imaging. Because proton magnetic resonance imaging (MRI) does not use ionizing radiation this imaging modality has been studied for assessment of cystic fibrosis and sarcoidosis, performing comparably to chest CT in identifying various pathologic patterns of the disease in lung parenchyma. Chung and associates have proposed that MRI may emerge as a viable alternative to CT imaging for assessing the distribution and extent of NTM lung infection (Chung et al., 2016). In an exploratory study of 25 patients known to have lung infection with MAC, they found excellent agreement between noncontrast MRI and CT imaging for detection of nodules and cavities, but only limited agreement for detection of bronchial mucous plugging (Chung et al., 2016;

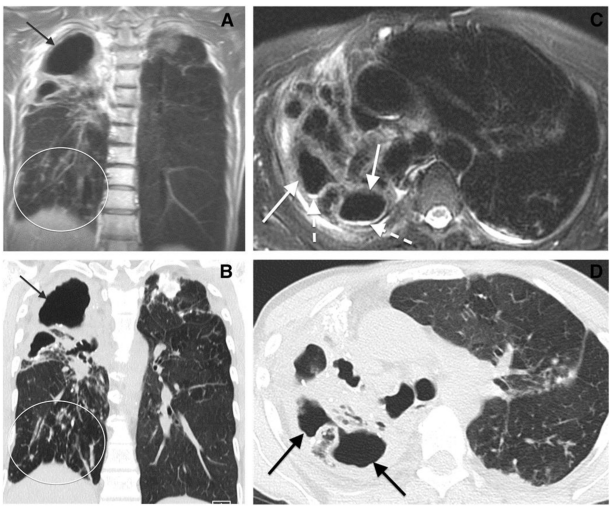

FIGURE 1 | Comparison of chest MR to CT imaging for assessment of *Mycobacterium avium* complex lung infection. Cavitary Mycobacterium avium complex (MAC) pneumonia in a 64-year-old woman. **(A)** Coronal MR and **(B)** coronal computed tomographic (CT) images show cavitary disease (arrows) and traction bronchiectasis in the right upper lobe. Subcentimeter nodules (oval) are present in the right lower lobe. **(C)** Axial MR and **(D)** CT images of the upper lungs show cavitary disease (solid arrows) and traction bronchiectasis in the right upper lobe. Reproduced with permission from Chung et al. (2016).

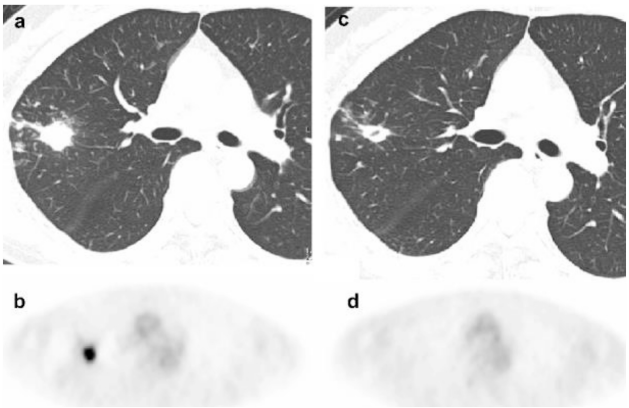

FIGURE 2 | ^{18}F-FDG PET imaging before and after treatment of mycobacterium avium complex lung infection. Thoracic images obtained from a patient with mycobacterium avium complex lung infection before and after treatment. **(a)** An axial CT image shows an untreated nodule **(b)** ^{18}F-FDG PET image reveals intense accumulation in the nodule (SUV 7.5) in the untreated nodule. **(c)** A CT image shows persistence of the nodule with interim cavitation after treatment. **(d)** ^{18}F-FDG PET image shows complete absence of FDG accumulation in the nodule after treatment. Reproduced with permission from Demura et al. (2009).

Figure 1). The authors postulated that further improvement in special discrimination of NTM lung infection may be achievable by application of maximum intensity projection reconstruction and contrast enhancement. To our knowledge, no published studies have reported on the usefulness of MRI for serial assessment of NTM lung infection.

Interval examination with ^{18}F-fluorodeoxyglucose positron-emission tomography [^{18}F-FDG PET] is a routine component of monitoring response to chemotherapy for lung cancer, based on the detection of increased glucose metabolism that is characteristic of malignant lesions. More recently, the use of PET modalities has been examined for diagnosis and treatment monitoring of tuberculosis, detecting the increase in glucose metabolism associated with the host inflammatory response (Vorster et al., 2014). Nodular MAC lung disease may show a similar pattern of increased glucose metabolism on PET/CT imaging, raising the possibility of interval monitoring during treatment. Among 6 patients with MAC lung disease assessed with ^{18}F-FDG PET studies before and after MAC-directed treatment, all patients demonstrated a decline in ^{18}F-FDG uptake after treatment, even in the absence of significant improvement in high-resolution CT images (Demura et al., 2009; **Figure 2**).

Symptomatic Improvement and Quality-of-Life Monitoring

The concept of clinical cure of NTM disease is tied to symptomatic improvement at the conclusion of treatment, which may not reach complete resolution of symptoms due to underlying structural lung disease (van Ingen et al., 2018). A number of studies have measured baseline quality-of-life indicators among NTM lung disease patients using various assessment tools, including the St. George Respiratory Questionnaire (SGRQ) (Mehta and Marras, 2011), the EuroQOL Five Dimensions (Hong et al., 2014), and the Medical Outcomes Short-Form-36 Questionnaire (SF-36) (Mehta and Marras, 2011; Asakura et al., 2015). However, there are a paucity of data regarding the formal assessment of quality-of-life during NTM treatment as an interval marker of clinical response, a notable knowledge deficit given the importance of patient reported outcomes in the context of drug development efforts. Importantly, under the 21st Century Cures Act, the FDA has updated the regulatory framework for evaluating these types of patient-reported outcomes in the Clinical Outcome Assessment Qualification Program, which operates in parallel with the Biomarker Qualification Program to support the evaluation of drug development tools for a disease area (FDA, 2018b).

Czaja et al. (2016) studied 47 patients with MAC lung disease, assessing quality-of-life at regular intervals during treatment with the SGRQ, and observing a significant improvement as early as 3 months from the treatment initiation. Notably, improvements in quality-of-life assessments were not related to improvements in CT imaging, perhaps a reflection of the limitations of CT imaging as discussed above, along with the greater degree of overall disease status and complexity that can be captured by quality-of-life assessments. A cross-sectional study of MAC complex lung disease patients, based on the SF-36, found that quality-of-life scores were lower among currently treated patients compared to previously- or never-treated patients, but repeated assessments during treatment were not performed (Asakura et al., 2015). While one

interpretation of these findings would be that current MAC treatment modalities negatively affect quality-of-life, an alternate explanation would be that patients are selected for MAC treatment based on current symptoms, as reflected in quality-of-life scores.

Blood-Based Monitoring

Both humoral and cell-mediated NTM-driven immune responses have been examined as potential sources of treatment monitoring biomarkers. As an alternative to sputum-based biologic sampling, blood-based monitoring may offer several advantages. Unlike sputum, blood is readily available throughout the treatment course, and continuously distributed biomarkers in blood would support precise comparisons with baseline levels without relying on hierarchical scoring systems (as used for radiographic findings or microbiology results). Furthermore, patients undergoing treatment for extra-pulmonary forms of NTM disease could potentially benefit from a validated blood-based biomarker of treatment response, for example during treatment of deep tissue infections such as osteomyelitis, where clinical response is less apparent on physical examination. Immune-based biomarkers of treatment response may also shed insight into the immunologic correlates of protection against disease in at-risk patient populations.

The Capilia MAC Ab ELISA kit (TAUNS, Shizuoka, Japan) developed for the diagnosis of MAC lung disease, measures serum levels of IgA antibodies against glycopeptidolipid (GPL), a major component of the MAC cell wall (Shibata et al., 2016). Serum anti-GPL IgA levels have been proposed as potential biomarkers of treatment response (Jhun et al., 2017; Kitada et al., 2017), although clinical evidence is limited to studies where serum anti-GPL IgA levels were compared before and after treatment, rather than at earlier timepoints during treatment.

Kitada et al. (2005) followed 27 patients with pulmonary MAC disease, obtaining serum samples before and after anti-MAC therapy. Among patients achieving clinical cure, a reduction in anti-GPL IgA levels was observed, while no difference was observed among 13 patients with treatment failure. Interestingly, a single patient with medical treatment failure then underwent surgical lobectomy, and subsequently demonstrated a fall in serum anti-GPL IgA levels, corresponding to conversion of sputum cultures. In a subsequent study that included 34 patients with MAC lung disease, serum anti-GPL IgA post-treatment declined from pre-treatment values among 19 patients who achieved sputum culture conversion, but not among 7 patients who either had disease recurrence or 8 patients who failed to achieve conversion (Kitada et al., 2017).

Jhun et al. (2017) evaluated serial changes in serum anti-GPL IgA levels during treatment of MAC lung disease at baseline, 3 months, and 6 months of treatment. Across all 57 patients, a decrease in serum anti-GPL IgA levels was observed. In contrast to the earlier findings discussed above (Czaja et al., 2016), patients with unfavorable treatment responses also had significant declines in anti-GPL IgA levels, although baseline levels were higher among patients who eventually developed treatment failure, perhaps reflecting a greater initial disease burden.

Cell-mediated immune responses, rather than antibody responses, could provide an alternate approach for immunologic monitoring of treatment response. Kim et al. (2014) enrolled 42 patients with MAC lung disease and measured serum concentrations of 36 different type I cytokine-associated molecules before and after 12 months of treatment. Declining levels of IL-17 and IL-23 during follow-up were associated with treatment failure, suggesting that continued impairment of the IL-17 pathway reflects ongoing disease processes. These findings are consistent with earlier work demonstrating that low IL-17 levels are a risk factor for developing MAC lung disease (Lim et al., 2010). Depending on the temporal dynamics of serum cytokines in the IL-17 pathway earlier in treatment, the measurement of one or more molecules on this pathway could be of interest as a potential monitoring biomarker.

Carbohydrate antigen 19-9 (CA 19-9) is a treatment monitoring biomarker for several forms of cancer. Elevated blood levels of CA 19-9 are also seen in various forms of chronic lung disease, including bronchiectasis. Recently, CA 19-9 was examined as biomarker of treatment response among 24 patients with NTM lung disease in South Korea (Hong et al., 2016). Among 17 patients with treatment response (defined as symptomatic improvement and sputum culture conversion within 12 months of therapy), CA 19-9 levels significant declined, while no difference was observed among the 7 patients without clinical response. Larger cohort studies with serial measurements of CA 19-9 earlier in treatment may be of interest.

Pulmonary Function Monitoring

Measurement of forced expiratory volume is a prognostic indicator for several chronic respiratory diseases, including COPD and cystic fibrosis, and the FEV1 is a qualified biomarker for COPD drug development efforts. The utility of pulmonary function monitoring as a general biomarker of treatment response for NTM lung disease will likely be limited by the tremendous heterogeneity in underlying chronic lung diseases and NTM disease presentations (for example, nodular bronchiectatic vs. fibrocavitary disease). In a single center study of 37 cystic fibrosis patients with pulmonary *M. abscessus* infection, early improvements in FEV1 after treatment initiation (either 30 or 60 days) were not associated with long-term microbiologic outcomes or sustained improvements in pulmonary function (DaCosta et al., 2017).

FUTURE DIRECTIONS

Clinical research centers specializing in the treatment of NTM lung disease will benefit from alignment of prospective data collection schemes that include specimen repositories for blood (both plasma and peripheral blood mononuclear cells), sputum,

and urine. The Bronchiectasis and NTM Research Registry, originally designed to enroll patients with bronchiectasis without underlying cystic fibrosis, supports serial banking of blood and deep respiratory specimens (Aksamit et al., 2017). This framework could provide the basis for investigating some of the potential microbiologic and serum and biomarkers discussed above. Future advances in MRI and PET imaging and in quantitative comparison of serial imaging studies may accelerate future research on changes in anatomic extent and metabolic activity of NTM infections in response to treatment.

Complementary prospective, observational studies would support comprehensive phenotyping of NTM disease patients with serial assessments of novel biomarkers of disease status and treatment response, and potentially could compare treatment monitoring biomarkers between patients treated for pulmonary and extra-pulmonary NTM disease. Prospective studies of novel monitoring biomarkers should also consider the potential for ongoing environmental re-exposure to NTM pathogens leading to re-infection, as can occur with contaminated household water sources (Lande et al., 2018) or nosocomial infections (Baker et al., 2017). Finally, much of the treatment response work thus far has focused on NTM lung disease has centered on MAC, and multicenter enrollment strategies may be essential to study response biomarkers for non-MAC lung disease, in particular lung disease caused by *M. abscessus* complex. These types of large scale, multicenter studies will also be essential to the prospective evaluation of novel treatment regimens for NTM lung disease. Multiple enrollment sites will be required to provide the statistical power for comparing alternative therapeutic strategies, given the smaller number of NTM lung disease patients compared with tuberculosis on a global scale. Furthermore, clinical studies supported by the National Institutes of Health (Sigal et al., 2017) and the Bill & Melinda Gates Foundation (Chen et al., 2017) have demonstrated the feasibility of integrating biomarker assessment into clinical trial design.

SUMMARY

"Quo vadis" ("whither goest thou?") remains a central question for NTM patients and their physicians. It is uncertain whether a single biomarker of clinical response will sufficiently capture the complexity of NTM disease presentations in a heterogeneous patient population, or whether the current "all of the above" strategy can be improved with refinement of microbiologic, radiographic, and quality-of-life assessments. Should a composite biomarker be developed under the FDA Biomarker Qualification program, it would require a "Context of Use" defining the specific algorithm for combining these individual components into a single treatment response measure. Ongoing research efforts for NTM disease should support the evaluation of biomarkers of response to treatment in parallel with studies of novel therapeutics and mechanisms of disease. Patients, clinicians, and investigators will benefit from the knowledge that the road they travel leads toward clinical cure.

AUTHOR CONTRIBUTIONS

AM, CV, JH-F, and KH performed the literature review. CV wrote the initial draft. AM, HO, RK, JH-F, and KH critically appraised and revised.

FUNDING

CV was supported by NIH (K23AI10263).

REFERENCES

Aksamit, T. R., O'Donnell, A. E., Barker, A., Olivier, K. N., Winthrop, K. L., Daniels, M. L. A., et al. (2017). Adult patients with bronchiectasis: a first look at the US bronchiectasis research registry. *Chest* 151, 982–992. doi: 10.1016/j.chest.2016.10.055

Amur, S., LaVange, L., Zineh, I., Buckman-Garner, S., and Woodcock, J. (2015). Biomarker qualification: toward a multiple stakeholder framework for biomarker development, regulatory acceptance, and utilization. *Clin. Pharmacol. Ther.* 98, 34–46. doi: 10.1002/cpt.136

Asakura, T., Funatsu, Y., Ishii, M., Namkoong, H., Yagi, K., Suzuki, S., et al. (2015). Health-related quality of life is inversely correlated with C-reactive protein and age in *Mycobacterium avium complex* lung disease: a cross-sectional analysis of 235 patients. *Respir. Res.* 16:145. doi: 10.1186/s12931-015-0304-5

Baker, A. W., Lewis, S. S., Alexander, B. D., Chen, L. F., Wallace, R. J. Jr., Brown-Elliott, B. A., et al. (2017). Two-phase hospital-associated outbreak of *Mycobacterium abscessus*: investigation and mitigation. *Clin. Infect. Dis.* 64, 902–911. doi: 10.1093/cid/ciw877

Cagney, D. N., Sul, J., Huang, R. Y., Ligon, K. L., Wen, P. Y., and Alexander, B. M. (2017). The FDA NIH biomarkers, EndpointS, and other tools (BEST) resource in neuro-oncology. *Neuro Oncol.* 20, 1162–1172. doi: 10.1093/neuonc/nox242

Chen, R. Y., Via, L. E., Dodd, L. E., Walzl, G., Malherbe, S. T., Loxton, A. G., et al. (2017). Using biomarkers to predict TB treatment duration (Predict TB): a prospective, randomized, noninferiority, treatment shortening clinical trial. *Gates Open Res.* 1:9. doi: 10.12688/gatesopenres.12750.1

Chung, J. H., Huitt, G., Yagihashi, K., Hobbs, S. B., Faino, A. V., Bolster, B. D. Jr., et al. (2016). Proton magnetic resonance imaging for initial assessment of isolated *Mycobacterium avium Complex* Pneumonia. *Ann. Am. Thorac. Soc.* 13, 49–57. doi: 10.1513/AnnalsATS.201505-282OC

Cohen-Cymberknoh, M., Weigert, N., Gileles-Hillel, A., Breuer, O., Simanovsky, N., Boon, M., et al. (2017). Clinical impact of *Pseudomonas aeruginosa* colonization in patients with primary ciliary Dyskinesia. *Respir. Med.* 131, 241–246. doi: 10.1016/j.rmed.2017.08.028

Czaja, C. A., Levin, A. R., Cox, C. W., Vargas, D., Daley, C. L., and Cott, G. R. (2016). Improvement in quality of life after therapy for *Mycobacterium abscessus* group lung infection. A prospective cohort study. *Ann. Am. Thorac. Soc.* 13, 40–48. doi: 10.1513/AnnalsATS.201508-529OC

DaCosta, A., Jordan, C. L., Giddings, O., Lin, F. C., Gilligan, P., and Esther, C. R. Jr. (2017). Outcomes associated with antibiotic regimens for treatment of *Mycobacterium abscessus* in cystic fibrosis patients. *J. Cyst. Fibros.* 16, 483–487. doi: 10.1016/j.jcf.2017.04.013

Demura, Y., Tsuchida, T., Uesaka, D., Umeda, Y., Morikawa, M., Ameshima, S., et al. (2009). Usefulness of 18F-fluorodeoxyglucose positron emission tomography for diagnosing disease activity and monitoring therapeutic

response in patients with pulmonary mycobacteriosis. *Eur. J. Nucl. Med. Mol. Imaging* 36, 632–639. doi: 10.1007/s00259-008-1009-5

Diel, R., Lipman, M., and Hoefsloot, W. (2018). High mortality in patients with *Mycobacterium avium complex* lung disease: a systematic review. *BMC Infect. Dis.* 18:206. doi: 10.1186/s12879-018-3113-x

FDA (2018a). Available at: https://www.fda.gov/Drugs/DevelopmentApprovalProcess/DrugDevelopmentToolsQualificationProgram/BiomarkerQualificationProgram/ucm535881.htm [accessed September 4, 2018].

FDA (2018b). Available at: https://www.fda.gov/Drugs/DevelopmentApprovalProcess/DrugDevelopmentToolsQualificationProgram/ucm284077.htm [accessed September 4, 2018].

Floto, R. A., Olivier, K. N., Saiman, L., Daley, C. L., Herrmann, J. L., Nick, J. A., et al. (2016). US cystic fibrosis foundation and european cystic fibrosis society consensus recommendations for the management of Non-tuberculous mycobacteria in individuals with cystic fibrosis: executive summary. *Thorax* 71, 88–90. doi: 10.1136/thoraxjnl-2015-207983

Griffith, D. E., Adjemian, J., Brown-Elliott, B. A., Philley, J. V., Prevots, D. R., Gaston, C., et al. (2015). Semiquantitative culture analysis during therapy for *Mycobacterium avium complex* lung disease. *Am. J. Respir. Crit. Care Med.* 192, 754–760. doi: 10.1164/rccm.201503-0444OC

Griffith, D. E., Aksamit, T., Brown-Elliott, B. A., Catanzaro, A., Daley, C., Gordin, F., et al. (2007). An official ATS/IDSA statement: diagnosis, treatment, and prevention of Nontuberculous mycobacterial diseases. *Am. J. Respir. Crit. Care Med.* 175, 367–416. doi: 10.1164/rccm.200604-571ST

Guiot, J., Demarche, S., Henket, M., Paulus, V., Graff, S., Schleich, F., et al. (2017). Methodology for sputum induction and laboratory processing. *J. Vis. Exp.* 130:e56612. doi: 10.3791/56612

Haworth, C. S., Banks, J., Capstick, T., Fisher, A. J., Gorsuch, T., Laurenson, I. F., et al. (2017). British Thoracic Society guidelines for the management of non-tuberculous mycobacterial pulmonary disease (NTM-PD). *Thorax* 72, ii1–ii64. doi: 10.1136/thoraxjnl-2017-210929

Henkle, E., Aksamit, T., Barker, A., Daley, C. L., Griffith, D., Leitman, P., et al. (2016). Patient-centered research priorities for pulmonary Nontuberculous Mycobacteria (NTM) infection. An NTM research Consortium Workshop Report. *Ann. Am. Thorac. Soc.* 13, S379–S384. doi: 10.1513/AnnalsATS.201605-387WS

Hong, J. Y., Jang, S. H., Kim, S. Y., Chung, K. S., Song, J. H., Park, M. S., et al. (2016). Elevated serum CA 19-9 levels in patients with pulmonary Nontuberculous mycobacterial disease. *Braz. J. Infect. Dis.* 20, 26–32. doi: 10.1016/j.bjid.2015.09.005

Hong, J. Y., Lee, S. A., Kim, S. Y., Chung, K. S., Moon, S. W., Kim, E. Y., et al. (2014). Factors associated with quality of life measured by EQ-5D in patients with Nontuberculous mycobacterial pulmonary disease. *Qual. Life Res.* 23, 2735–2741. doi: 10.1007/s11136-014-0727-3

Huang, J. H., Kao, P. N., Adi, V., and Ruoss, S. J. (1999). *Mycobacterium avium*-intracellulare pulmonary infection in HIV-negative patients without preexisting lung disease: diagnostic and management limitations. *Chest* 115, 1033–1040. doi: 10.1378/chest.115.4.1033

Institute of Medicine (US) Committee on Qualification of Biomarkers and Surrogate Endpoints in Chronic Disease (2010). *Evaluation of Biomarkers and Surrogate Endpoints in Chronic Disease*. Washington, DC: National Academies Press. doi: 10.1093/cid/ciq237

Jarand, J., Levin, A., Zhang, L., Huitt, G., Mitchell, J. D., and Daley, C. L. (2011). Clinical and microbiologic outcomes in patients receiving treatment for *Mycobacterium abscessus* pulmonary disease. *Clin. Infect. Dis.* 52, 565–571. doi: 10.1093/cid/ciq237

Jhun, B. W., Kim, S. Y., Park, H. Y., Jeon, K., Shin, S. J., and Koh, W. J. (2017). Changes in serum IgA antibody levels against the Glycopeptidolipid core antigen during antibiotic treatment of *Mycobacterium avium Complex* Lung disease. *Jpn. J. Infect. Dis.* 70, 582–585. doi: 10.7883/yoken.JJID.2016.523

Kim, H. S., Lee, K. S., Koh, W. J., Jeon, K., Lee, E. J., Kang, H., et al. (2012). Serial CT findings of *Mycobacterium massiliense* pulmonary disease compared with *Mycobacterium abscessus* disease after treatment with antibiotic therapy. *Radiology* 263, 260–270. doi: 10.1148/radiol.12111374

Kim, S. Y., Koh, W. J., Park, H. Y., Jeon, K., Kwon, O. J., Cho, S. N., et al. (2014). Changes in serum immunomolecules during antibiotic therapy for *Mycobacterium avium complex* lung disease. *Clin. Exp. Immunol.* 176, 93–101. doi: 10.1111/cei.12253

Kitada, S., Maekura, R., Toyoshima, N., Naka, T., Fujiwara, N., Kobayashi, M., et al. (2005). Use of glycopeptidolipid core antigen for serodiagnosis of *mycobacterium avium complex* pulmonary disease in immunocompetent patients. *Clin. Diagn. Lab. Immunol.* 12, 44–51. doi: 10.1128/CDLI.12.1.44-51.2005

Kitada, S., Maekura, R., Yoshimura, K., Miki, K., Miki, M., Oshitani, Y., et al. (2017). Levels of antibody against Glycopeptidolipid Core as a marker for monitoring treatment response in *Mycobacterium avium Complex* Pulmonary disease: a prospective cohort study. *J. Clin. Microbiol.* 55, 884–892. doi: 10.1128/JCM.02010-16

Lande, L., George, J., and Plush, T. (2018). *Mycobacterium avium complex* pulmonary disease: new epidemiology and management concepts. *Curr. Opin. Infect. Dis.* 31, 199–207. doi: 10.1097/QCO.0000000000000437

Lee, G., Kim, H. S., Lee, K. S., Koh, W. J., Jeon, K., Jeong, B. H., et al. (2013). Serial CT findings of nodular bronchiectatic *Mycobacterium avium complex* pulmonary disease with antibiotic treatment. *AJR Am. J. Roentgenol.* 201, 764–772. doi: 10.2214/AJR.12.9897

Lim, A., Allison, C., Price, P., and Waterer, G. (2010). Susceptibility to pulmonary disease due to *Mycobacterium avium*-intracellulare complex may reflect low IL-17 and high IL-10 responses rather than Th1 deficiency. *Clin. Immunol.* 137, 296–302. doi: 10.1016/j.clim.2010.07.011

Mehta, M., and Marras, T. K. (2011). Impaired health-related quality of life in pulmonary nontuberculous mycobacterial disease. *Respir. Med.* 105, 1718–1725. doi: 10.1016/j.rmed.2011.08.004

Mirsaeidi, M., Farshidpour, M., Ebrahimi, G., Aliberti, S., and Falkinham, J. O. III (2014). Management of nontuberculous mycobacterial infection in the elderly. *Eur. J. Intern. Med.* 25, 356–363. doi: 10.1016/j.ejim.2014.03.008

Nahid, P., Saukkonen, J., Mac, Kenzie WR, Johnson, J. L., Phillips, P. P., Andersen, J., et al. (2011). CDC/NIH Workshop. Tuberculosis biomarker and surrogate endpoint research roadmap. *Am. J. Respir. Crit. Care Med.* 184, 972–979. doi: 10.1164/rccm.201105-0827WS

Park, J., Kim, S., Lee, Y. J., Park, J. S., Cho, Y. J., Yoon, H. I., et al. (2016). Factors associated with radiologic progression of non-cystic fibrosis bronchiectasis during long-term follow-up. *Respirology* 21, 1049–1054. doi: 10.1111/resp.12768

Park, T. Y., Chong, S., Jung, J. W., Park, I. W., Choi, B. W., Lim, C., et al. (2017). Natural course of the nodular bronchiectatic form of *Mycobacterium Avium complex* lung disease: long-term radiologic change without treatment. *PLoS One* 12:e0185774. doi: 10.1371/journal.pone.0185774

Philley, J. V., and Griffith, D. E. (2015). Treatment of slowly growing mycobacteria. *Clin. Chest Med.* 36, 79–90. doi: 10.1016/j.ccm.2014.10.005

Prentice, R. L. (1989). Surrogate endpoints in clinical trials: definition and operational criteria. *Stat. Med.* 8, 431–440. doi: 10.1002/sim.4780080407

Research Committee of the British Thoracic Society. (2001). First randomised trial of treatments for pulmonary disease caused by *M. avium intracellulare*, *M. malmoense*, and *M. xenopi* in HIV negative patients: rifampicin, ethambutol and isoniazid versus rifampicin and ethambutol. *Thorax* 56, 167–172.

Shibata, Y., Horita, N., Yamamoto, M., Tsukahara, T., Nagakura, H., Tashiro, K., et al. (2016). Diagnostic test accuracy of anti-glycopeptidolipid-core IgA antibodies for *Mycobacterium avium complex* pulmonary disease: systematic review and meta-analysis. *Sci. Rep.* 6:29325. doi: 10.1038/srep29325

Sigal, G. B., Segal, M. R., Mathew, A., Jarlsberg, L., Wang, M., Barbero, S., et al. (2017). Biomarkers of tuberculosis severity and treatment effect: a directed screen of 70 host markers in a randomized trial. *EBioMedicine* 25, 112–121. doi: 10.1016/j.ebiom.2017.10.018

van Ingen, J. (2015). Microbiological diagnosis of nontuberculous mycobacterial pulmonary disease. *Clin. Chest Med.* 36, 43–54. doi: 10.1016/j.ccm.2014.11.005

van Ingen, J., Aksamit, T., Andrejak, C., Böttger, E. C., Cambau, E., Daley, C. L., et al. (2018). Treatment outcome definitions in nontuberculous mycobacterial pulmonary disease: an NTM-NET consensus statement. *Eur. Respir. J.* 51:1800170. doi: 10.1183/13993003.00170-2018

Vinnard, C., Longworth, S., Mezochow, A., Patrawalla, A., Kreiswirth, B. N., and Hamilton, K. (2016). Deaths related to nontuberculous mycobacterial infections in the United States, 1999-2014. *Ann. Am. Thorac. Soc.* 13, 1951–1955. doi: 10.1513/AnnalsATS.201606-474BC

Vorster, M., Sathekge, M. M., and Bomanji, J. (2014). Advances in imaging of tuberculosis: the role of (1)(8)F-FDG PET and PET/CT. *Curr. Opin. Pulm. Med.* 20, 287–293. doi: 10.1097/MCP.0000000000000043

Wassilew, N., Hoffmann, H., Andrejak, C., and Lange, C. (2016). Pulmonary disease caused by Non-Tuberculous Mycobacteria. *Respiration* 91, 386–402. doi: 10.1159/000445906

Yeung, M. W., Khoo, E., Brode, S. K., Jamieson, F. B., Kamiya, H., Kwong, J. C., et al. (2016). Health-related quality of life, comorbidities and mortality in pulmonary nontuberculous mycobacterial infections: a systematic review. *Respirology* 21, 1015–1025. doi: 10.1111/resp.12767

Conflict of Interest Statement: The authors declare that the research was conducted in the absence of any commercial or financial relationships that could be construed as a potential conflict of interest.

frontiers in Microbiology

MINI REVIEW
published: 05 December 2018
doi: 10.3389/fmicb.2018.02988

A Closer Look at the Genomic Variation of Geographically Diverse *Mycobacterium abscessus* Clones That Cause Human Infection and Disease

*Rebecca M. Davidson**

Center for Genes, Environment and Health, National Jewish Health, Denver, CO, United States

OPEN ACCESS

Edited by:
Veronique Anne Dartois, Rutgers, The State University of New Jersey, United States

Reviewed by:
Joseph Oliver Falkinham, Virginia Tech, United States
Rachel Thomson, The University of Queensland, Australia

***Correspondence:**
Rebecca M. Davidson
DavidsonR@NJHealth.org

Specialty section:
This article was submitted to Antimicrobials, Resistance and Chemotherapy, a section of the journal Frontiers in Microbiology

Received: *15 August 2018*
Accepted: *19 November 2018*
Published: *05 December 2018*

Citation:
Davidson RM (2018) A Closer Look at the Genomic Variation of Geographically Diverse Mycobacterium abscessus Clones That Cause Human Infection and Disease. Front. Microbiol. 9:2988. doi: 10.3389/fmicb.2018.02988

Mycobacterium abscessus is a multidrug resistant bacterium that causes pulmonary and extrapulmonary disease. The reported prevalence of pulmonary *M. abscessus* infections appears to be increasing in the United States (US) and around the world. In the last five years, multiple studies have utilized whole genome sequencing to investigate the genetic epidemiology of two clinically relevant subspecies, *M. abscessus* subsp. *abscessus* (MAB) and *M. abscessus* subsp. *massiliense* (MMAS). Phylogenomic comparisons of clinical isolates revealed that substantial proportions of patients have MAB and MMAS isolates that belong to genetically similar clusters also known as 'dominant clones'. Unlike the genetic lineages of *Mycobacterium tuberculosis* that tend to be geographically clustered, the MAB and MMAS clones have been found in clinical populations from the US, Europe, Australia and South America. Moreover, the clones have been associated with worse clinical outcomes and show increased pathogenicity in macrophage and mouse models. While some have suggested that they may have spread locally and then globally through 'indirect transmission' within cystic fibrosis (CF) clinics, isolates of these clones have also been associated with sporadic pulmonary infections in non-CF patients and unrelated hospital-acquired soft tissue infections. *M. abscessus* has long been thought to be acquired from the environment, but the prevalence, exposure risk and environmental reservoirs of the dominant clones are currently not known. This review summarizes the genomic studies of *M. abscessus* and synthesizes the current knowledge surrounding the geographically diverse dominant clones identified from patient samples. Furthermore, it discusses the limitations of core genome comparisons for studying these genetically similar isolates and explores the breadth of accessory genome variation that has been observed to date. The combination of both core and accessory genome variation among these isolates may be the key to elucidating the origin, spread and evolution of these frequent genotypes.

Keywords: nontuberculous mycobacteria (NTM), genome evolution, pulmonary infection, core genome, accessory genome, *Mycobacterium abscessus*

INTRODUCTION

Nontuberculous mycobacteria (NTM) include slowly and rapidly growing species in the genus *Mycobacterium* that are opportunistic pathogens in humans. A common clinical presentation is pulmonary infection, which occurs in susceptible individuals such as those with cystic fibrosis (CF), COPD, and adults with certain morphological phenotypes (Cassidy et al., 2009; Daley and Griffith, 2010; Winthrop et al., 2010; Martiniano et al., 2017). Another presentation is extrapulmonary NTM infection that can result from environmental exposures or healthcare-associated outbreaks (Lai et al., 1998; Duarte et al., 2009; Li et al., 2017). One of the most clinically challenging NTM that causes human disease is the rapidly growing species, *Mycobacterium abscessus* (*M. abscessus*), which is classified into three subspecies: *M. abscessus* subsp. *abscessus* (MAB), *M. abscessus* subsp. *massiliense* (MMAS) and *M. abscessus* subsp. *bolletii* (MBOL). MAB is the most frequently observed subspecies in clinical populations followed by MMAS, and MBOL is relatively rare (Bryant et al., 2016). Epidemiological studies in the United States (US) show an increase in pulmonary NTM infections (including *M. abscessus*) in CF populations (Olivier et al., 2003; Adjemian et al., 2018) and patients over 60 years old (Prevots et al., 2010). *M. abscessus* is also one of the most prevalent species associated with NTM infections in Europe (Roux et al., 2009; Hoefsloot et al., 2013). *M. abscessus* infections are of particular concern due to the bacteria's innate resistance to a range of antibiotics often resulting in lengthy treatment courses and poor clinical outcomes (Jarand et al., 2011; Koh et al., 2011).

An interesting aspect of *M. abscessus* infections is that little is known about exposure risks and modes of transmission associated with pulmonary infections. The prevailing wisdom is that NTMare acquired from the environment, as they inhabit plumbing and water systems (Feazel et al., 2009; Falkinham, 2011; Ovrutsky et al., 2013; Honda et al., 2016; Zhao et al., 2017), as well as aquatic environments and soil (Primm et al., 2004; De Groote et al., 2006). These surveys have predominantly detected slowly growing NTM species, however, underscoring the potential for *M. abscessus* to occupy different and possibly yet to be identified niches within the environment. Studies of *M. abscessus* outbreaks and pseudo-outbreaks have found the offending bacteria in contaminated laboratories (Lai et al., 1998), clinic disinfectants (Tiwari et al., 2003) and hospital water sources (Baker et al., 2017), and some epidemic strains show disinfectant resistance (Duarte et al., 2009; Leao et al., 2010). Environmental surveys of NTM in household environments pinpoint the ecological niche of *M. abscessus* as indoor water and plumbing biofilms (Thomson et al., 2013a; Honda et al., 2016), *M. abscessus* also exhibits long-term survival on fomite particles (Malcolm et al., 2017). Epidemiological studies, however, have not found clear links between household exposure risks and acquisition of NTM (Prevots et al., 2014). Only two studies from Australia have demonstrated genetic links between pulmonary patient isolates of *M. abscessus* and environmental isolates from household water sources (Thomson et al., 2013a,b), though the directionality of infection has not been confirmed. Finally, attempts to isolate *M. abscessus* from environmental sources in the context of suspected outbreaks within CF centers have been unsuccessful.

The first case of person-to-person transmission of any NTM species was proposed among five CF patients with MMAS cared for at a US CF Center, raising concerns about adequacy of infection control and risks associated with patient exposure during CF care (Aitken et al., 2012). This coincided with using whole genome sequencing (WGS) to characterize genomic diversity and perform genetic strain matching. Since then, several studies have used WGS to examine genetic diversity of pulmonary *M. abscessus* isolates from patients in a US referral hospital (Davidson et al., 2014), suspected outbreaks of pulmonary infections in CF centers (Bryant et al., 2013; Tettelin et al., 2014; Harris et al., 2015; Tortoli et al., 2017); a nationwide epidemic of soft tissue infections in Brazil (Davidson et al., 2013a; Everall et al., 2017) and a global population study of CF-associated pulmonary isolates from multiple CF centers in three continents (Bryant et al., 2016). One of the most intriguing observations from these studies was that a large proportion of MAB and MMAS clinical isolates grouped into "dominant clones", which have high genetic similarity, but are not identical. Moreover, these clones have been found in nearly every WGS study regardless of worldwide location. This finding led to speculation that the clones may have both spread locally within CF clinics, likely through 'indirect transmission' of contaminated clinical environments, and then globally between CF centers (Bryant et al., 2016). However, detection of these clones sporadically from non-CF patients (Davidson et al., 2014) and in cases of extrapulmonary infections (Ripoll et al., 2009; Everall et al., 2017), combined with their unknown prevalence in the environment, challenge this hypothesis.

This review will take a closer look at the genomic studies of *M. abscessus* (subspecies MAB and MMAS) and summarize observations of the dominant clones (**Table 1**). It will address the limitations of core genome phylogenomic analysis for genetic matching, and explore how accessory genome variation may be the key to revealing the relationships among clonal isolates from disparate geographic regions and infection types. Genomic studies of *M. abscessus* will undoubtedly be needed in the future to further study the evolution and spread of the dominant clones in both environmental and clinical settings.

GENOTYPING METHODS FOR *M. abscessus*

Several molecular techniques have been used to identify and classify *M. abscessus* isolates. Early studies relied on single gene sequencing or multi-locus sequence typing (MLST) using genes such as *rpoB* (Adekambi et al., 2006), *hsp65*, *secA* and the internal transcribed spacer (Adekambi et al., 2003; Adekambi and Drancourt, 2004; Zelazny et al., 2009), to classify isolates to the subspecies level. To further evaluate whether strains were "genetically matched" in the context of potential outbreaks, pulsed field gel electrophoresis (PFGE), randomly amplified polymorphic DNA polymerase chain reaction (RAPD-PCR) and repetitive sequence polymerase chain reaction (rep-PCR)

TABLE 1 | Isolates of the *M. abscessus* dominant clones that have been identified by WGS.

Subspecies	Infection type	Location of Study	Representative Strain(s)	Publication(s)
M. abscessus subsp. *massiliense* (MMAS)	CF pulmonary	Papworth Hospital, Cambridge, United Kingdom	patients 2, 8, 12,14,17, 19, 20, 22, 28, 29, 30	Bryant et al., 2013
	CF pulmonary	Seattle, WA, United States	Index case: 2B-0107 MAB_082312_2258 MAB_091912_2446	Aitken et al., 2012; Tettelin et al., 2014
	post surgical soft tissue	Rio de Janeiro, Brazil	CRM-0020	Duarte et al., 2009; Davidson et al., 2013a,b
	pediatric CF pulmonary	Great Ormond Street Hospital, London, United Kingdom	patient 7	Harris et al., 2015
	CF pulmonary	United States, United Kingdom, Ireland, Sweden, Netherlands, Denmark, Ireland and Australia	UNC666 (United States), SMRL275 (United Kingdom), DEN524 (Denmark), AUS755 (Australia), SVH899 (Ireland)	Bryant et al., 2016
	post surgical soft tissue	Para, Brazil	BRA_PA_42	Everall et al., 2017
M. abscessus subsp. *abscessus* (MAB)	post surgical soft tissue	Missouri, United States	type strain ATCC19977^T	Moore and Frerichs, 1953; Ripoll et al., 2009
	CF and non-CF pulmonary	Colorado, United States	NJH1-6, NJH9-10	Davidson et al., 2014
	pediatric CF pulmonary	Great Ormond Street Hospital, London, United Kingdom	patients 3, 18, 19, 22	Harris et al., 2015
	CF pulmonary	United States, United Kingdom, Ireland, Sweden, Netherlands, Denmark, Ireland and Australia	UNC617 (United States), SMRL461 (United Kingdom), DEN541 (Denmark), AUS774 (Australia)	Bryant et al., 2016
	CF pulmonary	Italy	patients CP, CR, GL, BE, GM	Tortoli et al., 2017

(Healy et al., 2005) have been used. The highest resolution method for genetic matching is whole genome sequencing (WGS) as millions of genomic positions and thousands of loci can be compared, vs. a limited number of loci (usually less than 100) with the previous methods.

In 2009, a complete reference genome at 5.03 megabases (Mb) was published for the MAB type strain, ATCC19977^T (Ripoll et al., 2009) followed by genomes for the type strains of MMAS at 4.8 Mb (CCUG48898^T) (Tettelin et al., 2012) and MBOL at 5.0 Mb (BD^T) (Choi et al., 2012). This ushered in a new era in population genomic studies. Since 2013, several groups have utilized WGS to examine *M. abscessus* subspecies at the population level, comparing patient isolates within a single clinic (Bryant et al., 2013; Davidson et al., 2014; Harris et al., 2015) and on a larger scale, between CF clinics in one or more countries (Bryant et al., 2016; Tortoli et al., 2017).

GENOME STRUCTURE OF *M. abscessus*

To understand the nuances in interpreting comparative genomics analyses, we should consider the structure of bacterial genomes, which are classified into two components. The ***core genome*** is defined as the genomic regions or genes that are shared by all isolates within a population (at the genus, species or subspecies level) (Medini et al., 2005). These include "housekeeping genes" that are necessary for survival and which evolve at relatively predictable rates. Variation in the core genome is measured by the single nucleotide polymorphisms (SNP) found in the shared regions. Depending on the species, as much as 65% or more of the genomic space can be analyzed in this way. The ***accessory genome*** includes genetic material that is shared by one or more, but not all, isolates in a population. This includes regions that are acquired by horizontal gene transfer (HGT) such as genomic islands, transposases, mycobacteriophages, and plasmids, which have the potential to change bacterial phenotypes through acquisition of antimicrobial resistance genes and entire gene cassettes that code for novel metabolic processes (Juhas et al., 2009; Sassi and Drancourt, 2014; Garcia et al., 2015; Gray and Derbyshire, 2018). Accessory genome features, such as genes, groups of genes and plasmids, are measured in an isolate population as presence or absence.

The sum of the core genes plus accessory genes in an isolate population is called the ***pan genome***. A pan genome study of 40 *M. abscessus* genomes from all three subspecies revealed a core genome of 3,345 genes, which is about 68% of a typical MAB or MBOL genome and 71% of a typical MMAS genome (Choo et al., 2014). This means that approximately 30% of the *M. abscessus* genome is made up of accessory genes that are present in only a subset of isolates or are strain-specific. The accessory genome of *M. abscessus* is known to include prophages, plasmids and genomic islands transferred by HGT from other bacterial genera (Ripoll et al., 2009; Leao et al., 2013; Davidson et al., 2014; Gray and Derbyshire, 2018) consistent with an environmental bacterium exposed to a diverse microbiome. Population genomic studies can use both core and accessory genome data in their genetic matching analyses, but it is common to find studies using only core genome comparisons as these

have the most well-defined and reproducible computational methods. The accessory genome, however, can provide additional discrimination among closely related isolates.

GENOMICS STUDIES OF *M. abscessus* FROM CF POPULATIONS

Following the first published case of inter-patient transmission of MMAS isolates among CF patients in the US (Aitken et al., 2012), multiple European studies used core genome analysis to look for evidence of person-to-person transmission in their CF clinics (reviewed in detail in Martiniano et al., 2017). A retrospective analysis of 168 *M. abscessus* isolates from 31 adult CF patients at the Papworth hospital in the United Kingdom (UK) (Bryant et al., 2013) revealed two genetic clusters of MMAS with high genetic similarity. This study was the first to define a quantitative SNP threshold indicating probable transmission between patient isolates as less than 25 SNPs. The use of this SNP threshold for isolates from different patients coupled with social network analysis showed that while the patients lived in different geographic areas, they had multiple opportunities for cross-infection through overlapping clinic visits. Moreover, the potentially transmissible isolates shared the same SNP in the 16S rRNA that confers amikacin resistance, including isolates from patients that had not previously used nebulized aminoglycosides. The authors were unable to identify a local environmental source of MMAS inoculum, and thus surmised that person-to-person transmission did occur within their hospital. The absence of isolation in the environment, however, could also reflect insufficient culturing methods or non-exhaustive sampling. Another study at the Great Ormond Street Hospital in the United Kingdom used a similar experimental design to assess the potential for cross-infection among 20 pediatric CF patients (Harris et al., 2015). Core genome analysis of 27 *M. abscessus* isolates revealed genetic clusters of both MAB and MMAS. The authors used the suggested threshold of less than 25 SNPs between patient isolates as defined in the Papworth study (Bryant et al., 2013) and identified four patients involved in suspected transmission events, but they did not find intersecting clinic visits between any of the patients. Finally, an Italian study analyzed 162 *M. abscessus* isolates from 48 patients attending CF centers in "four geographically distinct regions in Italy" (Tortoli et al., 2017). Using a conservative threshold of less than 30 SNPs between patient isolates, they found isolate clusters of MAB, MMAS and MBOL, and identified and seven "possible transmission episodes" among patients. In three potential episodes including two clusters of MMAS and one cluster of MBOL, two patients were found to have attended the same clinic within the same timeframe. The authors concluded that the lack of major outbreaks over the 12-year study period signified minimal risk of inter-human transmission in their CF centers. In summary, the occurrence and frequency of cross-infection between CF patients in the clinic remains controversial and further studies will be needed. It would also be useful to compare and contrast infection control strategies in this context.

In 2016, a large-scale study utilized WGS and core genome analyses to examine the global population structure of 1,080 *M. abscessus* isolates from 510 CF patients sampled at clinics across multiple European countries, the US and Australia (Bryant et al., 2016). The study identified predominant clusters of genotypes that they coined "dominant circulating clones" as well as several other genetically diverse genotypes. The dominant clones are defined as phylogenetically clustered isolates found in a high proportion of patients. The study identified a primary dominant clone of MAB (known as Abscessus Cluster 1) and a dominant clone of MMAS (known as Massiliense Cluster 1) that corresponds to the "transmissible clone" from the previous Papworth study (Bryant et al., 2013). Collectively, clustered isolates had a higher proportion of drug resistance mutations to amikacin and clarithromycin and were more likely to be associated with chronic infections compared with unclustered isolates. Moreover, the clones had increased phagocytic uptake and intracellular survival in macrophages, and significantly greater bacterial burden and granulomatous inflammation in SCID mice suggesting differences in virulence compared with unclustered isolates.

DOMINANT CLONE OF *M. abscessus* subsp. *massiliense*

Three "transmissible" MMAS isolates from the CF clinic outbreak in Seattle, Washington (Aitken et al., 2012) were sequenced in 2014, and the genomes were compared with other publically available genomes (Tettelin et al., 2014). Intriguingly, the Seattle MMAS isolates were highly similar to the transmissible MMAS clones from the Papworth, United Kingdom CF clinic study (Bryant et al., 2013) and an epidemic MMAS strain from Rio de Janiero, Brazil (CRM-0020) (Davidson et al., 2013a,b). Core genome diversity among the geographically disparate isolates was only 11 to 86 SNPs, and the accessory genome variation included a 11.5 kb genomic island that was unique to the Papworth strains and three genomic regions (totaling 95 kb) and a 44 kb IncP-1β plasmids that were unique to the Brazilian strain. Then, two years later, it was revealed that this potentially "transmissible clone" was the most prevalent MMAS (Massiliense Cluster 1) in the global population study of CF-NTM isolates and was present in all the countries sampled including the United States, United Kingdom, Ireland, Sweden, Netherlands, Denmark, Ireland and Australia (Bryant et al., 2016).

The Brazilian clone (also called BRA100) with high genetic similarity to the pulmonary CF strains was responsible for an epidemic of soft tissue infections from 2004–2009 (Duarte et al., 2009; Leao et al., 2010). The series of infections that spread through multiple states were attributed to contaminated surgical equipment that that had been cleaned with glutaraldehyde, which ultimately selected for a disinfectant resistant clone. A follow up population genomics study of 188 epidemic strains from nine Brazilian states revealed that the isolates had one or two different plasmids (pMAB01 and pMAB02) that were absent from

the corresponding pulmonary CF isolates (Everall et al., 2017). Divergence dating analysis estimated that the Brazilian lineage emerged in 2003 suggesting a recent introduction, however, it is unknown if BRA100 exists locally in the environment of Brazil. The two plasmids from the Brazilian isolates have been fully sequenced (Leao et al., 2013; Everall et al., 2017), but the mechanism of glutaraldehyde resistance is still not known.

DOMINANT CLONE OF *M. abscessus* subsp. *abscessus*

The dominant clone of MAB identified in the global NTM population study (Abscessus Cluster 1) was found in CF patients from all of the countries and continents sampled (Bryant et al., 2016). Interestingly, this clone is highly genetically similar to the MAB type strain, ATCC19977^T, that was initially isolated in the early 1950's from a midwestern US patient with "an acid-fast infection of the knee" and "subcutaneous abscess-like lesions of the gluteal region" (Moore and Frerichs, 1953). This clone was present in pulmonary isolate clusters found in the CF study in Great Ormand Hospital in the United Kingdom (Harris et al., 2015), the *M. abscessus* study from four Italian CF centers (Tortoli et al., 2017), and in a study of pulmonary isolates from CF and non-CF patients in a US referral hospital in Colorado (Davidson et al., 2014).

The MAB dominant clone isolates appear highly similar by core genome SNP analyses, but they also show significant variation in their accessory genomes. For example, the type strain (ATCC19977^T) reference genome includes a 23.3 Kb plasmid with a mercury resistance operon (Ripoll et al., 2009). In the Colorado WGS study with nine clustered pulmonary isolates of the MAB dominant clone, only one (1/9 = 11%) contained the full plasmid, and up to 8.3% of the reference ATCC19977^T genome was absent in these isolates including a prophage region and multiple transposase-related genomic islands (Davidson et al., 2014). This study also showed that the nine isolates clustered geographically when comparing the presence or absence of genomic islands suggesting that the accessory genome may be subject to local, environmental-specific adaptations.

CONCLUSION AND PERSPECTIVES

The dominant clones of *M. abscessus* (including MMAS and MAB) have been observed several times over the years associated with a range of disease etiologies (**Table 1**), Recently, WGS and population genomics has revealed the extent of genomic variation in the core genome with less than 100 variable SNP positions, while the accessory genome can include presence or absence of large plasmids and genomic islands. The widespread geographic diversity of the dominant clones is intriguing, and it is currently not known if they have spread globally via inter-continental transmission or if they inhabitant local environments and just happen to be the most effective genotypes for human infection. A large scale genomic study of randomly sampled environmental NTM isolates would reveal the niches of *M. abscessus* dominant clones in nature and the true risk of environmental exposure to susceptible patient populations (Strong and Davidson, 2017). Such environmental studies are time consuming and costly, and appropriate funding mechanisms will need to be identified. Future genomic studies of *M. abscessus* will benefit from analyzing diversity in both the core and accessory genes to reveal local adaptations, identify potential mechanisms of virulence and monitor the evolution and mutation rates of these clinically important genotypes.

AUTHOR CONTRIBUTIONS

RD conceived of topic and wrote the manuscript.

FUNDING

RD acknowledges the NIH/NIAID (award no. 5K01AI125 726-02).

REFERENCES

Adekambi, T., Berger, P., Raoult, D., and Drancourt, M. (2006). rpoB gene sequence-based characterization of emerging non-tuberculous mycobacteria with descriptions of *Mycobacterium bolletii* sp. nov., *Mycobacterium phocaicum* sp. nov. and *Mycobacterium aubagnense* sp. nov. *Int. J. Syst. Evol. Microbiol.* 56(Pt 1), 133–143. doi: 10.1099/ijs.0.63969-0

Adekambi, T., Colson, P., and Drancourt, M. (2003). rpoB-based identification of nonpigmented and late-pigmenting rapidly growing mycobacteria. *J. Clin. Microbiol.* 41, 5699–5708. doi: 10.1128/JCM.41.12.5699-5708.2003

Adekambi, T., and Drancourt, M. (2004). Dissection of phylogenetic relationships among 19 rapidly growing Mycobacterium species by 16S rRNA, hsp65, sodA, recA and rpoB gene sequencing. *Int. J. Syst. Evol. Microbiol.* 54(Pt 6), 2095–2105. doi: 10.1099/ijs.0.63094-0

Adjemian, J., Olivier, K. N., and Prevots, D. R. (2018). Epidemiology of pulmonary nontuberculous mycobacterial sputum positivity in patients with cystic fibrosis in the United States, 2010-2014. *Ann. Am. Thorac. Soc.* 15, 817–826. doi: 10.1513/AnnalsATS.201709-727OC

Aitken, M. L., Limaye, A., Pottinger, P., Whimbey, E., Goss, C. H., Tonelli, M. R., et al. (2012). Respiratory outbreak of *Mycobacterium abscessus* subspecies massiliense in a lung transplant and cystic fibrosis center. *Am. J. Respir. Crit. Care Med.* 185, 231–232. doi: 10.1164/ajrccm.185.2.231

Baker, A. W., Lewis, S. S., Alexander, B. D., Chen, L. F., Wallace, R. J. Jr., Brown-Elliott, B. A., et al. (2017). Two-phase hospital-associated outbreak of *Mycobacterium abscessus*: investigation and mitigation. *Clin. Infect. Dis.* 64, 902–911. doi: 10.1093/cid/ciw877

Bryant, J. M., Grogono, D. M., Greaves, D., Foweraker, J., Roddick, I., Inns, T., et al. (2013). Whole-genome sequencing to identify transmission of *Mycobacterium abscessus* between patients with cystic fibrosis: a retrospective cohort study. *Lancet* 381, 1551–1560. doi: 10.1016/S0140-6736(13)60632-7

Bryant, J. M., Grogono, D. M., Rodriguez-Rincon, D., Everall, I., Brown, K. P., Moreno, P., et al. (2016). Emergence and spread of a human-transmissible multidrug-resistant nontuberculous mycobacterium. *Science* 354, 751–757. doi: 10.1126/science.aaf8156

Cassidy, P. M., Hedberg, K., Saulson, A., McNelly, E., and Winthrop, K. L. (2009). Nontuberculous mycobacterial disease prevalence and risk factors: a changing epidemiology. *Clin. Infect. Dis.* 49, e124–e129. doi: 10.1086/648443

Choi, G. E., Cho, Y. J., Koh, W. J., Chun, J., Cho, S. N., and Shin, S. J. (2012). Draft genome sequence of *Mycobacterium abscessus* subsp. *bolletii* BD(T). *J. Bacteriol.* 194, 2756–2757. doi: 10.1128/JB.00354-12

Choo, S. W., Wee, W. Y., Ngeow, Y. F., Mitchell, W., Tan, J. L., Wong, G. J., et al. (2014). Genomic reconnaissance of clinical isolates of emerging human pathogen *Mycobacterium abscessus* reveals high evolutionary potential. *Sci. Rep.* 4:4061. doi: 10.1038/srep04061

Daley, C. L., and Griffith, D. E. (2010). Pulmonary non-tuberculous mycobacterial infections. *Int. J. Tuberc. Lung Dis.* 14, 665–671.

Davidson, R. M., Hasan, N. A., de Moura, V. C., Duarte, R. S., Jackson, M., and Strong, M. (2013a). Phylogenomics of Brazilian epidemic isolates of *Mycobacterium abscessus* subsp. *bolletii* reveals relationships of global outbreak strains. *Infect. Genet. Evol.* 20, 292–297. doi: 10.1016/j.meegid.2013.09.012

Davidson, R. M., Reynolds, P. R., Farias-Hesson, E., Duarte, R. S., Jackson, M., and Strong, M. (2013b). Genome sequence of an epidemic isolate of *Mycobacterium abscessus* subsp. *bolletii* from Rio de Janeiro. *Brazil. Genome Announc.* 1:e00617-13. doi: 10.1128/genomeA.00617-13

Davidson, R. M., Hasan, N. A., Reynolds, P. R., Totten, S., Garcia, B., Levin, A., et al. (2014). Genome sequencing of *Mycobacterium abscessus* isolates from patients in the United States and comparisons to globally diverse clinical strains. *J. Clin. Microbiol.* 52, 3573–3582. doi: 10.1128/JCM.01144-14

De Groote, M. A., Pace, N. R., Fulton, K., and Falkinham, J. O. (2006). Relationships between *Mycobacterium* isolates from patients with pulmonary mycobacterial infection and potting soils. *Appl. Environ. Microbiol.* 72, 7602–7606. doi: 10.1128/AEM.00930-06

Duarte, R. S., Lourenco, M. C., Fonseca Lde, S., Leao, S. C., Amorim Ede, L., Rocha, I. L., et al. (2009). Epidemic of postsurgical infections caused by *Mycobacterium massiliense*. *J. Clin. Microbiol.* 47, 2149–2155. doi: 10.1128/JCM.00027-09

Everall, I., Nogueira, C. L., Bryant, J. M., Sanchez-Buso, L., Chimara, E., Duarte, R. D. S., et al. (2017). Genomic epidemiology of a national outbreak of post-surgical *Mycobacterium abscessus* wound infections in Brazil. *Microb. Genom.* 3:e000111. doi: 10.1099/mgen.0.000111

Falkinham, J. O. III (2011). Nontuberculous mycobacteria from household plumbing of patients with nontuberculous mycobacteria disease. *Emerg. Infect. Dis.* 17, 419–424. doi: 10.3201/eid1703.101510

Feazel, L. M., Baumgartner, L. K., Peterson, K. L., Frank, D. N., Harris, J. K., and Pace, N. R. (2009). Opportunistic pathogens enriched in showerhead biofilms. *Proc. Natl. Acad. Sci. U.S.A.* 106, 16393–16399. doi: 10.1073/pnas.0908446106

Garcia, B. J., Datta, G., Davidson, R. M., and Strong, M. (2015). MycoBASE: expanding the functional annotation coverage of mycobacterial genomes. *BMC Genomics* 16:1102. doi: 10.1186/s12864-015-2311-9

Gray, T. A., and Derbyshire, K. M. (2018). Blending genomes: distributive conjugal transfer in mycobacteria, a sexier form of HGT. *Mol. Microbiol.* 108, 601–613. doi: 10.1111/mmi.13971

Harris, K. A., Underwood, A., Kenna, D. T., Brooks, A., Kavaliunaite, E., Kapatai, G., et al. (2015). Whole-genome sequencing and epidemiological analysis do not provide evidence for cross-transmission of *Mycobacterium abscessus* in a cohort of pediatric cystic fibrosis patients. *Clin. Infect. Dis.* 60, 1007–1016. doi: 10.1093/cid/ciu967

Healy, M., Huong, J., Bittner, T., Lising, M., Frye, S., Raza, S., et al. (2005). Microbial DNA typing by automated repetitive-sequence-based PCR. *J. Clin. Microbiol.* 43, 199–207. doi: 10.1128/JCM.43.1.199-207.2005

Hoefsloot, W., van Ingen, J., Andrejak, C., Angeby, K., Bauriaud, R., Bemer, P., et al. (2013). The geographic diversity of nontuberculous mycobacteria isolated from pulmonary samples: an NTM-NET collaborative study. *Eur. Respir. J.* 42, 1604–1613. doi: 10.1183/09031936.00149212

Honda, J. R., Hasan, N. A., Davidson, R. M., Williams, M. D., Epperson, L. E., Reynolds, P. R., et al. (2016). Environmental nontuberculous Mycobacteria in the Hawaiian Islands. *PLoS Negl. Trop. Dis.* 10:e0005068. doi: 10.1371/journal.pntd.0005068

Jarand, J., Levin, A., Zhang, L., Huitt, G., Mitchell, J. D., and Daley, C. L. (2011). Clinical and microbiologic outcomes in patients receiving treatment for *Mycobacterium abscessus* pulmonary disease. *Clin. Infect. Dis.* 52, 565–571. doi: 10.1093/cid/ciq237

Juhas, M., van der Meer, J. R., Gaillard, M., Harding, R. M., Hood, D. W., and Crook, D. W. (2009). Genomic islands: tools of bacterial horizontal gene transfer and evolution. *FEMS Microbiol. Rev.* 33, 376–393. doi: 10.1111/j.1574-6976.2008.00136.x

Koh, W. J., Jeon, K., Lee, N. Y., Kim, B. J., Kook, Y. H., Lee, S. H., et al. (2011). Clinical significance of differentiation of *Mycobacterium massiliense* from *Mycobacterium abscessus*. *Am. J. Respir. Crit. Care Med.* 183, 405–410. doi: 10.1164/rccm.201003-0395OC

Lai, K. K., Brown, B. A., Westerling, J. A., Fontecchio, S. A., Zhang, Y., and Wallace, R. J. Jr. (1998). Long-term laboratory contamination by *Mycobacterium abscessus* resulting in two pseudo-outbreaks: recognition with use of random amplified polymorphic DNA (RAPD) polymerase chain reaction. *Clin. Infect. Dis.* 27, 169–175. doi: 10.1086/514635

Leao, S. C., Matsumoto, C. K., Carneiro, A., Ramos, R. T., Nogueira, C. L., Lima, J. D., et al. (2013). The detection and sequencing of a broad-host-range conjugative IncP-1beta plasmid in an epidemic strain of *Mycobacterium abscessus* subsp. *bolletii*. *PLoS One* 8:e60746. doi: 10.1371/journal.pone.0060746

Leao, S. C., Viana-Niero, C., Matsumoto, C. K., Lima, K. V., Lopes, M. L., Palaci, M., et al. (2010). Epidemic of surgical-site infections by a single clone of rapidly growing mycobacteria in Brazil. *Future Microbiol.* 5, 971–980. doi: 10.2217/fmb.10.49

Li, T., Abebe, L. S., Cronk, R., and Bartram, J. (2017). A systematic review of waterborne infections from nontuberculous mycobacteria in health care facility water systems. *Int. J. Hyg. Environ. Health* 220, 611–620. doi: 10.1016/j.ijheh.2016.12.002

Malcolm, K. C., Caceres, S. M., Honda, J. R., Davidson, R. M., Epperson, L. E., Strong, M., et al. (2017). *Mycobacterium abscessus* displays fitness for fomite transmission. *Appl. Environ. Microbiol.* 83:e00562-17. doi: 10.1128/AEM.00562-17

Martiniano, S. L., Davidson, R. M., and Nick, J. A. (2017). Nontuberculous mycobacteria in cystic fibrosis: updates and the path forward. *Pediatr. Pulmonol.* 52, S29–S36. doi: 10.1002/ppul.23825

Medini, D., Donati, C., Tettelin, H., Masignani, V., and Rappuoli, R. (2005). The microbial pan-genome. *Curr. Opin. Genet. Dev.* 15, 589–594. doi: 10.1016/j.gde.2005.09.006

Moore, M., and Frerichs, J. B. (1953). An unusual acid-fast infection of the knee with subcutaneous, abscess-like lesions of the gluteal region; report of a case with a study of the organism, *Mycobacterium abscessus*, n. sp. *J. Invest. Dermatol.* 20, 133–169. doi: 10.1038/jid.1953.18

Olivier, K. N., Weber, D. J., Wallace, R. J. Jr., Faiz, A. R., Lee, J. H., Zhang, Y., et al. (2003). Nontuberculous mycobacteria. I: multicenter prevalence study in cystic fibrosis. *Am. J. Respir. Crit. Care Med.* 167, 828–834. doi: 10.1164/rccm.200207-678OC

Ovrutsky, A. R., Chan, E. D., Kartalija, M., Bai, X., Jackson, M., Gibbs, S., et al. (2013). Cooccurrence of free-living amoebae and nontuberculous Mycobacteria in hospital water networks, and preferential growth of *Mycobacterium avium* in *Acanthamoeba lenticulata*. *Appl. Environ. Microbiol.* 79, 3185–3192. doi: 10.1128/AEM.03823-12

Prevots, D. R., Adjemian, J., Fernandez, A. G., Knowles, M. R., and Olivier, K. N. (2014). Environmental risks for nontuberculous mycobacteria. Individual exposures and climatic factors in the cystic fibrosis population. *Ann. Am. Thorac. Soc.* 11, 1032–1038. doi: 10.1513/AnnalsATS.201404-184OC

Prevots, D. R., Shaw, P. A., Strickland, D., Jackson, L. A., Raebel, M. A., Blosky, M., et al. (2010). Nontuberculous mycobacterial lung disease prevalence at four integrated health care delivery systems. *Am. J. Respir. Crit. Care Med.* 182, 970–976. doi: 10.1164/rccm.201002-0310OC

Primm, T. P., Lucero, C. A., and Falkinham, J. O. (2004). Health impacts of environmental mycobacteria. *Clin. Microbiol. Rev.* 17, 98–106. doi: 10.1128/CMR.17.1.98-106.2004

Ripoll, F., Pasek, S., Schenowitz, C., Dossat, C., Barbe, V., Rottman, M., et al. (2009). Non mycobacterial virulence genes in the genome of the emerging pathogen *Mycobacterium abscessus*. *PLoS One* 4:e5660. doi: 10.1371/journal.pone.0005660

Roux, A. L., Catherinot, E., Ripoll, F., Soismier, N., Macheras, E., Ravilly, S., et al. (2009). Multicenter study of prevalence of nontuberculous mycobacteria in patients with cystic fibrosis in France. *J. Clin. Microbiol.* 47, 4124–4128. doi: 10.1128/JCM.01257-09

Sassi, M., and Drancourt, M. (2014). Genome analysis reveals three genomospecies in *Mycobacterium abscessus*. *BMC Genomics* 15:359. doi: 10.1186/1471-2164-15-359

Strong, M., and Davidson, R. M. (2017). Microbiology: Bacterial transmission tactics. *Nature* 543, 495–496. doi: 10.1038/543495a

Tettelin, H., Davidson, R. M., Agrawal, S., Aitken, M. L., Shallom, S., Hasan, N. A., et al. (2014). High-level relatedness among *Mycobacterium abscessus* subsp. *massiliense* strains from widely separated outbreaks. *Emerg. Infect. Dis.* 20, 364–371. doi: 10.3201/eid2003.131106

Tettelin, H., Sampaio, E. P., Daugherty, S. C., Hine, E., Riley, D. R., Sadzewicz, L., et al. (2012). Genomic insights into the emerging human pathogen *Mycobacterium massiliense*. *J. Bacteriol.* 194:5450. doi: 10.1128/JB.01200-12

Thomson, R., Tolson, C., Carter, R., Coulter, C., Huygens, F., and Hargreaves, M. (2013a). Isolation of nontuberculous mycobacteria (NTM) from household water and shower aerosols in patients with pulmonary disease caused by NTM. *J. Clin. Microbiol.* 51, 3006–3011. doi: 10.1128/JCM.00899-13

Thomson, R., Tolson, C., Sidjabat, H., Huygens, F., and Hargreaves, M. (2013b). Mycobacterium abscessus isolated from municipal water - a potential source of human infection. *BMC Infect. Dis.* 13:241. doi: 10.1186/1471-2334-13-241

Tiwari, T. S., Ray, B., Jost, K. C. Jr., Rathod, M. K., Zhang, Y., Brown-Elliott, B. A., et al. (2003). Forty years of disinfectant failure: outbreak of postinjection *Mycobacterium abscessus* infection caused by contamination of benzalkonium chloride. *Clin. Infect. Dis.* 36, 954–962. doi: 10.1086/368192

Tortoli, E., Kohl, T. A., Trovato, A., Baldan, R., Campana, S., Cariani, L., et al. (2017). *Mycobacterium abscessus* in patients with cystic fibrosis: low impact of inter-human transmission in Italy. *Eur. Respir. J.* 50:1602525. doi: 10.1183/13993003.02525-2016

Winthrop, K. L., McNelley, E., Kendall, B., Marshall-Olson, A., Morris, C., Cassidy, M., et al. (2010). Pulmonary nontuberculous mycobacterial disease prevalence and clinical features: an emerging public health disease. *Am. J. Respir. Crit. Care Med.* 182, 977–982. doi: 10.1164/rccm.201003-0503OC

Zelazny, A. M., Root, J. M., Shea, Y. R., Colombo, R. E., Shamputa, I. C., Stock, F., et al. (2009). Cohort study of molecular identification and typing of *Mycobacterium abscessus*, *Mycobacterium massiliense*, and *Mycobacterium bolletii*. *J. Clin. Microbiol.* 47, 1985–1995. doi: 10.1128/JCM.01688-08

Zhao, X., Epperson, L. E., Hasan, N. A., Honda, J. R., Chan, E. D., Strong, M., et al. (2017). Complete genome sequence of *Mycobacterium avium* subsp. *hominissuis* Strain H87 isolated from an indoor water sample. *Genome Announc.* 5:e00189-17. doi: 10.1128/genomeA.00189-17

Conflict of Interest Statement: The author declares that the research was conducted in the absence of any commercial or financial relationships that could be construed as a potential conflict of interest.

frontiers in Microbiology

REVIEW
published: 30 August 2018
doi: 10.3389/fmicb.2018.02029

Global Environmental Nontuberculous Mycobacteria and Their Contemporaneous Man-Made and Natural Niches

Jennifer R. Honda[1], Ravleen Virdi[1] and Edward D. Chan[2,3,4]*

[1] Department of Biomedical Research and the Center for Genes, Environment, and Health, National Jewish Health, Denver, CO, United States, [2] Medicine and Academic Affairs, National Jewish Health, Denver, CO, United States, [3] Division of Pulmonary Sciences and Critical Care Medicine, University of Colorado Denver, Aurora, CO, United States, [4] Department of Medicine, Denver Veterans Affairs Medical Center, Denver, CO, United States

Seminal microbiological work of environmental nontuberculous mycobacteria (NTM) includes the discovery that NTM inhabit water distribution systems and soil, and that the species of NTM found are geographically diverse. It is likely that patients acquire their infections from repeated exposures to their environments, based on the well-accepted paradigm that water and soil bioaerosols – enriched for NTM – can be inhaled into the lungs. Support comes from reports demonstrating NTM isolated from the lungs of patients are genetically identical to NTM found in their environment. Well documented sources of NTM include peat-rich soils, natural waters, drinking water, hot water heaters, refrigerator taps, catheters, and environmental amoeba. However, NTM have also been recovered in biofilms from ice machines, heated nebulizers, and heater-cooler units, as well as seat dust from theaters, vacuum cleaners, and cobwebs. New studies on the horizon aim to significantly expand the current knowledge of environmental NTM niches in order to improve our current understanding of the specific ecological factors driving the emergence of NTM lung disease. Specifically, the Hawaiian Island environment is currently being studied as a model to identify other point sources of exposure as it is the U.S. state with the highest number of NTM lung disease cases. Because of its geographic isolation and unique ecosystem, the Hawaiian environment is being probed for correlative factors that may promote environmental NTM colonization.

Keywords: nontuberculous mycobacteria, environments, man-made, natural, Hawaii

OPEN ACCESS

Edited by:
Thomas Dick, Rutgers, The State University of New Jersey, Newark, United States

Reviewed by:
Joseph Oliver Falkinham, Virginia Tech, United States
Giovanni Delogu, Università Cattolica del Sacro Cuore, Italy

****Correspondence:***
Jennifer R. Honda
hondaj@njhealth.org

Specialty section:
This article was submitted to Antimicrobials, Resistance and Chemotherapy, a section of the journal Frontiers in Microbiology

Received: *26 June 2018*
Accepted: *10 August 2018*
Published: *30 August 2018*

Citation:
Honda JR, Virdi R and Chan ED (2018) Global Environmental Nontuberculous Mycobacteria and Their Contemporaneous Man-Made and Natural Niches. Front. Microbiol. 9:2029. doi: 10.3389/fmicb.2018.02029

BACKGROUND

Nontuberculous mycobacteria (NTM) and their environments are intricately bound. NTM share these environments with humans and domesticated animals and repeated exposure is a well-accepted mode of acquiring these infections. While most casual NTM exposures do not results in disease, those with anatomic lung abnormalities of bronchiectasis and emphysema are particularly predisposed to develop NTM lung disease (NTM-LD). However, in individuals without obvious pre-existing risk factors, it is likely that multiple risk factors – some genetic or other acquired factors – may collude to increase their vulnerability. While there have been case reports and small case series linking genetically identical NTM in patients to their home environment, the

specific factors facilitating their acquisition remains poorly characterized. These factors encompass (i) varied sources of infection, (ii) modes of aquisition, and (iii) other physical aspects of the environment such as temperature, humidity, air exchange, surface types, and turbulence created by wind and natural disasters, and (iv) human behaviors, the combination of which are likely to be relatively unique among affected individuals (Honda et al., 2015; Nishiuchi et al., 2017).

Herein, we discuss the traditional environmental niches associated with NTM organisms, but also review the lesser-recognized environmental locales that NTM colonize including non-traditional niches and non-human hosts. We also summarize previous studies that link ecological factors with risk for infection and epidemiological information. Finally, we introduce new, ongoing work to study the particular environmental drivers of NTM emergence in Hawai'i, a geographic location deemed a major hot spot for NTM-LD.

NTM ORIGINS?

The interaction of humans with their natural and built environments along with changes humans make to their environment (*e.g.*, installation of mechanical devices that change environmental temperature and humidity, or others), and differences in the robustness of human health may impact the emergence of infectious diseases. The origins of NTM-LD remain a mystery, but may be intrinsically linked to human interaction with their environments. As soon as early humans learned to prepare small, controlled fires, the light and heat produced gathered people together for social interactions, vastly improved food preparation, and helped communities defend against invasion – activities that significantly lengthened human survival (Chisholm et al., 2016). Because NTM are found in the environment, it is plausible that these bacteria were historically aerosolized from soil with increased fire-making, infecting human lungs already impacted by long-term exposure to campfire smoke. Nonetheless, there is no evidence to show that the number of NTM-LD cases increase after camping or large scale environmental fires. For now, the origins of lung disease caused by NTM organisms remains an area of investigation.

GLOBAL GEOGRAPHY AND NTM

The ability of NTM to cause LD and its clinical relevance varies globally. Geographic distribution of NTM species provides information regarding geographic-specific drivers of exposure such as climate, environment, and host factors associated with NTM-LD that would be specific to a global region (Falkinham, 1996; Griffith et al., 2007).

Mycobacterium avium complex (MAC) is the most frequently isolated group of NTM species worldwide and the most common organism associated with NTM-LD. MAC consists of various species of slow-growing mycobacteria (SGM) including *M. avium, M. intracellulare*, *M. chimaera*, *M. colombiense*, *M. marseillense*, *M. arosiense*, *M. timonense, M. bouchedurhonense*, and *M. ituriense*. Subspecies of *M. avium* include *avium, silvaticum, hominissuis*, and *paratuberculosis* (Hoefsloot et al., 2013; Johnson and Odell, 2014). Currently, the lowest number of MAC isolates in the world are seen in South America, but this may be because there is little NTM information available from this region (Hoefsloot et al., 2013; Halstrom et al., 2015; Stout et al., 2016). High incidence of NTM-LD due to MAC, *M. kansasii*, *M. gordonae,* and *M. malmoense* are observed in Europe, North America and Australia.

Rapid-growing mycobacteria (RGM) including the *Mycobacterium abscessus* and *Mycobacterium fortuitum* groups also contribute to a large proportion of NTM-LD cases globally. The *Mycobacterium abscessus* group is comprised of three subspecies: *M. abscessus* subsp. *abscessus*, *M. abscessus* subsp. *massiliense*, and *M. abscessus* subsp. *bolletii*. In the United States (U.S.), *M. abscessus* complex infections are secondary only to MAC infections, comprising 3-13% of all NTM-LD cases (Lee et al., 2015). The *M. abscessus* group is also commonly observed in patients in East Asia; in Taiwan 17.2% of all clinical NTM isolates belong to the *M. abscessus* group (Lai et al., 2010). The *M. fortuitum* group comprises *M. fortuitum*, *M. peregrinum*, *M. senegalense*, *M. alvei*, *M. houstonense*, *M. neworleansense*, *M. boenickei*, *M. septicum*, and *M. porcinum* (Adekambi and Drancourt, 2004; Schinsky et al., 2004). Besides LD, *M. fortuitum* cause soft tissue, skeletal, catheter-related, and disseminated infections in immunocompromised patients (Brown-Elliott and Wallace, 2002).

United States

The most commonly occurring NTM species in many parts of U.S. are MAC and *M. kansasii* (Hoefsloot et al., 2013). Nearly 80% of all NTM-LD in the U.S. is due to a species of MAC, followed *by M, kansasii* - the second most common NTM associated with LD (Falkinham, 1996; Griffith et al., 2007). The U.S. states with the highest overall risk for NTM-LD include Hawai'i, California, New York, Louisiana, Pennsylvania, Florida, Oklahoma and Wisconsin (Adjemian et al., 2012a). *M. abscessus* is the most commonly recovered RGM from southeastern parts of U.S. (Halstrom et al., 2015; Stout et al., 2016). For unknown reasons, NTM-LD cases are lowest in North Dakota, South Dakota, Minnesota, Michigan, New Mexico, and West Virgina (Adjemian et al., 2012a).

Europe and United Kingdom

Higher isolation rates of MAC (44%) are seen in northern Europe as compared to southern Europe (31%) with *M. avium* as the most prevalent species. *M. kansasii* is the predominant NTM species to cause LD in London, United Kingdom. and *M. lentiflavum* is most frequently isolated from clinical samples in Crete, Greece (Neonakis et al., 2007; Wassilew et al., 2016). Slovakia, Poland, and the United Kingdom have the highest amount of *M. kansasii* isolates in Europe (Hoefsloot et al., 2013; Wassilew et al., 2016). In contrast, higher isolation rates for *M. xenopi* are observed in southern Europe (21%) as compared to northern Europe (6%), but are most commonly isolated in Hungary (46%) (Hoefsloot et al., 2013; Wassilew et al., 2016). RGM are more commonly seen in the United Kingdom and

Greece as compared to the rest of Europe (Hoefsloot et al., 2013). While not considered to be a pathogen, *M. gordonae* is most commonly recovered from environmental sources in Canada and Europe (Hoefsloot et al., 2013; Halstrom et al., 2015; Stout et al., 2016).

Asia

A recent study in China observed that an increase in latitude was associated with higher isolation rates of MAC species (predominantly *M. intracellulare*) whereas the number of RGM (most commonly *M. chelonae*) increased with a decrease in latitude (Yu et al., 2016). A similar trend is observed in Taiwan, with higher cases of NTM due to MAC recovered in the north and RGM like *M. abscessus* in the south (Huang et al., 2017). *M. scrofulaceum* and *M. szulgai* are also intermittently found in respiratory specimens from Asia (Simons et al., 2011). Overall, elderly women are disproportionately affected by NTM-LD, but in Saudi Arabia and most of the Persian Gulf countries, elderly men are found to be more affected (perhaps due to a lifetime of extended outdoor exposure) with MAC and *M. abscessus* being the main causative agents (Al-Ghafli and Al-Hajoj, 2017). MAC, *M. simiae,* and *M. marinum* are most commonly observed in NTM-LD individuals in Oman (Al-Ghafli and Al-Hajoj, 2017). In Western Asia, *M. fortuitum* and *M. flavescens* are the most prevalent RGM and SGM organisms, respectively with much higher frequency of NTM in northern Iran (73.2%) (Khaledi et al., 2016). In India, *M. abscessus, M. fortuitum,* and *M. intracellulare* are most commonly isolated from clinical samples (Desikan et al., 2017). *M. abscessus* are more widespread in Singapore and Okinawa (Hoefsloot et al., 2013).

Australia

Similar to the aforementioned geographic areas, LD caused by NTM are also increasingly observed in Australia (Thomson, 2010). MAC is the most commonly isolated NTM in Queensland with *M. intracellulare* comprising nearly 80% of the MAC isolates (Hoefsloot et al., 2013). RGM are the second most common cause of NTM-LD with *M. abscessus* the most commonly recovered from southern Australia (Hoefsloot et al., 2013; Wassilew et al., 2016). Unlike many other regions of the world, NTM are notifiable infections under the Queensland Public Health Act, 2005 which has facilitated the surveillance of potentially highly virulent and transmissible NTM strains (Thomson et al., 2017).

Africa

Information regarding the causative agents of NTM-LD in Africa are limited and is likely due to the overwhelming burden of tuberculosis in the regions. However, *M. abscessus, M. avium, M. fortuitum,* and *M. nebraskense* are recognized as the most frequently isolated NTM species from clinical samples in Zambia (Monde et al., 2018). *M. gordonae* has been recently found to be highly prevalent in water reservoirs like borehole wells, rivers dams, and tap water (Monde et al., 2018).

FACTORS THAT HELP SUSTAIN NTM IN THE ENVIRONMENT

NTM are slow-growing compared to other types of bacteria, with the ability to form biofilms, resist high temperatures, and grow in marginal environments with low nutrient and oxygen content (Kirschner et al., 1992; Falkinham, 2009). However, cell surface hydrophobicity is the major driver sustaining NTM in the biofilms of both natural waters and man-made drinking water distribution systems, hospitals, and household plumbing. Due to their repulsion to water, NTM are found in aerosolized particles present above natural water bodies, showerheads, humidifiers, hot tubs and spas as well as in biofilms that form in these places (Falkinham, 2013). Environmental factors such as high humidity levels and high evapotranspiration (movement of water from land to the atmosphere) rates are known to be associated with an increased risk of NTM infection in susceptible individuals (Adjemian et al., 2012a). This is particularly translatable to the recovery of NTM during different seasons. For example, the species of NTM isolated from municipal water distribution systems in Brisbane, Australia differed in the samples collected in summer as compared to those collected in the winter months with higher numbers of *M. gordonae, M. kansasii, M. abscessus, M. mucogenicum,* and MAC isolated in the winter (Thomson R. M. et al., 2013).

Other environmental factors have a profound impact of NTM viability. For example, NTM have been isolated from water bodies with moderate salinity (1–2% NaCl) like estuaries (Chesapeake Bay) (Kirschner et al., 1992; Falkinham, 2009). But in a separate study, reduced numbers of NTM isolates were observed when water salinity exceeded 2% (Gruft et al., 1981). NTM also favor environments with acidic pH. Humic and fulvic acids and acidic brown water swamps along the southeastern coast of the U.S. support high numbers of MAC (Falkinham, 2009, 2013). Pine forest (boreal rich) and peat rich soils, brackish marshes, and drainage water are also rich in NTM (Kirschner et al., 1992; Falkinham, 2009). Minerals widely found in clay soils such as kaolin and dust have also been demonstrated to facilitate the growth of *M. abscessus* (Malcolm et al., 2017).

TYPICAL ENVIRONMENTAL HABITATS OF NTM

M. avium, *M. fortuitum*, *M. chelonae*, *M. kansasii*, *M. gordonae,* and *M. xenopi* are the NTM species most commonly found in water distribution systems, water bodies including lakes, rivers and streams as well as soil and dust (Falkinham, 2009; Ulmann et al., 2015). Falkinham et al. (2008) was the first to demonstrate that the *M. avium* isolated from a patient with NTM-LD had a clonal relationship with the *M. avium* isolated from her home showerhead biofilm. Falkinham also first reported identical NTM DNA fingerprints from patients' sputa and matched shower water isolates, shedding light on the paradigm that inhalation of aerosols while showering is a likely mode of NTM acquisition (Falkinham, 2011). Similar

reports are observed from Japan where MAC isolates recovered from bathtub inlets and showerheads showed identical pulse-field gel electrophoresis profiles when compared to their respective clinical isolates (Nishiuchi et al., 2009; Ichijo et al., 2014). Thus, showerhead biofilms remain one of the most frequently sampled environmental sources used to describe the presence of NTM globally. In an interesting turn of events, early methods such as hybridization probes and multiplex 16S rRNA gene PCR methodologies identified *M. intracellulare* in households and potable water (Tichenor et al., 2012; Whiley et al., 2012). However, Falkinham et al. (2008) and Wallace et al. (2013) reanalyzed environmental household water and biofilm isolates originally identified as *M. intracellulare* by sequencing the 280 bp 16S to 23S internal transcribed spacer region and discovered that these isolates were instead *M. chimaera* (Thomson, 2010; Falkinham, 2011; Koh W. J. et al., 2012; Tichenor et al., 2012). Using the same sequencing method, isolates originally called *M. avium* were confirmed as *M. avium*. Thus, *M. chimaera* is now widely recognized in water biofilms, while *M. intracellulare* is found to be absent from them. A clue to their sources may come from a study conducted in American Samoa where *M. intracellulare* was identified in roof-harvested rainwater (Kirs et al., 2017) and soil (Honda et al., 2016).

NTM found in households are likely piped into home plumbing systems from public utility sources where biofilms are commonly formed. However, NTM are also known inhabitants of natural freshwater ecosystems. Of two recreational lakes, RGM were the dominant NTM, but a diversity of other mycobacteria were found in high density in the water column, air-water interface, sediment, and in association with benthic algae growing on plants and fine sediment using quantitative real-time PCR and the MiSeq Illumina platform (Roguet et al., 2016). Yet, NTM remain seldomly recovered from well and groundwaters (Martin et al., 1987).

Nosocomial NTM lung infections have been reported in the literature. MAC species have been detected in hospital potable hot water distribution systems, hospital tap water used for dialysis, and in water used to prepare medical solutions, highlighting their propensity to stick to piped surfaces (Bolan et al., 1985; Safranek et al., 1987; Hector et al., 1992). After a significant increase in NTM-positive sputa was observed from patients referred to respiratory wards in Rome, an infection control investigation revealed a massive presence of NTM in the hospital water network (D'Antonio et al., 2016). In another study, 83% of U.S. dialyses centers examined showed NTM in municipal water supplies (Carson et al., 1988). More recently, global outbreaks of *M. chimaera* associated with heater-cooler units used during open-heart surgery have provided unique challenges for the medical community (Sax et al., 2015; Schreiber et al., 2016; Marra et al., 2017). Investigations point to model-specific designs in air flow direction, location of cooling ventilators, and the continuous cooling of unit water tanks significantly increased the risk of disseminating colonized *M. chimaera* into the air of operating rooms (Kuehl et al., 2018). Of the first thirty cases affected by this outbreak in the United Kingdom, 60% (18/30) died at a median of 30 months after initial surgery (Scriven et al., 2018). Poor disinfection and resistance to glutaraldehydes have been highlighted in pseudo-outbreaks of *M. abscessus* subsp. *bolletii* in bronchoscopes, endoscopes, and disinfection units (Guimaraes et al., 2016). In other areas of the hospital, patient accessible ice machines have been shown to be laden with NTM, particularly *M. paraffinicum* and *M. fortuitum* (Gebo et al., 2002; Wang et al., 2009).

M. fortuitum skin infections have been associated with pedicure-associated whirlpool footbaths in California and Georgia nail salons (Winthrop et al., 2004). Skin infections due to other NTM such as *M. chelonae* have been linked to contaminated water used for diluting tattoo ink and to unsterilized instrumentation (Mudedla et al., 2015). Dental unit water lines have also been shown to harbor a variety of environmental NTM species (Schulze-Robbecke et al., 1995), but remain as unproven sources of NTM lung infection. MAC-associated hypersensitivity pneumonitis (HP) has been linked to exposure to warm, bubbly water found in rarely cleaned hot tubs and spa baths (Embil et al., 1997; Sugita et al., 2000; Rickman et al., 2002). However, MAC has also been isolated from cold water sources including swimming pool water. In fact, lifeguards with long-term exposure to indoor swimming pool aerosols are susceptible to work-associated exposures and are at increased risk for MAC-associated HP (Rose et al., 1998; Koschel et al., 2006). Besides tap water, a Dutch group found NTM in swimming pools and whirlpool water (Havelaar et al., 1985). NTM-associated HP has also been linked to occupational exposures to aerosols produced through manipulation of metalworking fluids (Bernstein et al., 1995; Wilson et al., 2001).

Soil is also a widely recognized environmental niche for NTM. NTM patients' potting soils yielded NTM that were identical by DNA fingerprinting to the NTM isolates from the same patients' lungs (Ichiyama et al., 1988; De Groote et al., 2006). Moreover, *M. avium* subsp. *hominissuis* (MAH) was predominant in soil and dust, but not identified in German water and biofilm samples by culture (Lahiri et al., 2014). A study in Iran found that 6-15% of soil samples compared to 10–27% of water samples collected from the suburbs of Tehran had NTM isolated by culture with *M. farcinogens* and *M. fortuitum* being the most common species (Velayati et al., 2014). Furthermore, the risk for acquiring NTM is significantly higher in communities engaged in occupations that generate aerosols and are exposed to soil for a longer time (*e.g.,* agriculture, mining, landscaping, and tunnel work) as compared to communities that have a limited exposure to soil (Hamada et al., 2016). In West Harima, Japan, NTM-LD was associated with natural resource activities, construction, mining, and soil exposure (Hamada et al., 2016). In a separate study, *M. chelonae, M. fortuitum,* and *M. kansasii* were identified in 85% of the alpine and subalpine soil, peat, humus, porous ricks, mosses, and wood examined suggesting NTM thrive in mountain ranges and elevations (Thorel et al., 2004). Rare and unique NTM species have also been described in polluted soils of Hawai'i where they functioned as polycyclic aromatic hydrocarbon pollutant-degrading organisms (Hennessee et al., 2009).

NTM IN THE KITCHEN

NTM have been reported in kitchen sink biofilms as well as household refrigerator taps and home ice machines (Ichijo et al., 2014). MAC organisms have been found to colonize point-of-use filters used to filter tap water including carbon filers impregnated with silver (Rodgers et al., 1999; Hamilton et al., 2017). Due to the appearance of disseminated *M. avium* infections during the height of the HIV-AIDS epidemic, two studies tested for the presence of NTM in foods consumed by HIV-infected patients. PCR typing revealed 29 different mycobacterial isolates in 21% (25/121) of food samples tested; 41% of the 29 samples (n = 12) were *M. avium* (Yoder et al., 1999). One of the clinical *M. avium* isolates was identical to a food isolate, suggesting food as a potential source of *M. avium* infections. In the second study, water, food and soil samples from 290 homes of HIV-infected patients were tested for mycobacteria using DNA probes, serotyping, and multi-locus enzyme electrophoresis and compared to clinical isolates (Yajko et al., 1995). Soil, rather than water sources, were found to harbor more *M. avium*. While not considered a food-borne illness, *M. avium* subspecies DNA was also identified in raw meats (Lorencova et al., 2014). In contrast, smoked fish products did not show NTM, but 12% of samples collected from pond fish (4%), retail sold fish (61%), and frozen fish (91%) contained NTM DNA (Lorencova et al., 2013). Although unproven, the acid-resistant NTM organisms may remain viable in the stomach where food is consumed and digested. Evidence suggests patients with the nodular bronchiectatic form of NTM-LD have a high prevalence of increased esophageal acid exposure and gastroesophageal reflux disease was found to be significantly associated with RGM organisms (Winthrop et al., 2010; Koh E. et al., 2012).

NTM IN NON-CANONICAL ENVIRONMENTS

Besides their well-known habitation in the numerous sources detailed above, rare NTM species (*e.g.*, *M. algericum, M. arabiense, M. heraklionense*) have been cultured and identified from primary sludge samples of water treatment plants even after decontamination (Makovcova et al., 2015). *M. avium, M. gordonae*, and *M. flavescens* have been also been identified in non-traditional water sources including untreated, drinking well water in rural areas of Montana as well as in treated municipal wastewater from arid regions (Richards et al., 2015; Amha et al., 2017). Qualitative assessments were used to determine the risk of MAC exposure in Queensland, Australia, an area that utilizes rainwater catchment systems. Untreated rainwater is commonly used for showering, car washing, toilet flushing, and food preparation (Hamilton et al., 2017). But in this study, rainwater used for drinking presented the greatest risk for MAC infection; yet the species of MAC responsible was not reported. In most cases, disinfection methods to remove potential pathogens from these water sources is a decision left up to the household and can range from no disinfection methods to point-of-use filters, UV irradiation, solar disinfection, chlorine or a combination of them. More work is needed in these areas to determine the impact of using different disinfection methods to reduce exposures in NTM patients who use these water source types.

NTM have also been detected, albeit, rarely in cobwebs above hen nests, soil fertilized with chicken droppings, and moss but more commonly in dust from vacuum cleaners, and air conditioners (Nishiuchi et al., 2009; Kaevska et al., 2011). Of particular significance to smokers is the recovery and identification of *M. avium* from cigarettes (Eaton et al., 1995). While not directly shown to cause LD, MAC has been identified from clothing washed during laundry cycles suggesting laundry water maybe an unintentional source of household NTM (Yajko et al., 1993). Finally, *M. avium* was detected in samples of condensation water formed from the coagulation of steam in three different rooms inside the Russian space station, Mir (Kawamura et al., 2001).

THE "ENVIRONMENTAL MACROPHAGE" AND NTM

Amoeba are free-living, freshwater associated protozoans that are ubiquitously found in water systems often cohabited by NTM. Many species of amoeba phagocytose free-living bacteria and feed on them; however, some NTM are able to resist and evade degradation. In particular, most species of MAC, including *M. avium*, *M. intracellulare*, *M. chimaera*, *M. colombiense*, *M. arosiense*, *M. marseillense*, *M. timonense,* and *M. bouchedurhonense* reside within free-living *Acanthamoeba polyphaga* and their exocysts as well as *A. castellanii* found in potable water (Cirillo et al., 1997; Taylor et al., 2009; Ben Salah and Drancourt, 2010). Delafont et al. (2014) demonstrated amoeba-mycobacteria associations in drinking water networks in a year-long sampling study. Nearly 88% of amoeba including the genera *Acanthamoeba, Vermamoeba, Echinamoeba*, and *Protacanthamoeba* recovered from drinking water were found to contain *M. llatzerense* and *M. chelonae* (Delafont et al., 2014). NTM cultured in amoeba also show increased resistance to antibiotics and enhanced virulence compared to NTM grown in chickens and mice (Cirillo et al., 1997; Falkinham et al., 2001).

EVIDENCE FOR ANIMAL AND INSECT RESERVOIRS FOR NTM ASSOCIATED WITH EXTRAPULMONARY INFECTIONS

NTM infections in mammals occur sporadically and are rarely transmissible between animals and seldomly considered *bone fide* zoonotic diseases. Except under particular scenarios, NTM infections are also generally not transmissible from human to human (Bryant et al., 2016). Nonetheless, NTM have been known to infect animals such as chickens and quails (Meissner and Anz, 1977; Morita et al., 1999). Drug-susceptible *M. fortuitum* and *M. abscessus* were identified in a cutaneous lesion on the snout and nostrils of a captive *Trichechus inunguis* (manatee) in the Amazon (Reisfeld et al., 2018). In captive non-domesticated hoofed animals and in immunosuppressed dogs and cats,

M. avium has been reported as disseminated disease (Thorel et al., 2004). With the potential for cross species infection or transmission in the Serengeti, tissues from wildlife species and indigenous cattle were probed for mycobacteria, revealing *M. intracellulare* as the most frequently isolated species, followed by *M. lentiflavum, M. fortuitum*, and *M. chelonae/abscessus*. MAC organisms were also detected in animal feces and huts from pastoral Uganda (Kankya et al., 2011). Because *M. avium* isolates from pigs showed shared genetic characteristics to *M. avium* isolated from humans, pigs have been theorized as potential sources of infection (Bono et al., 1995). Among 1,249 mandibular lymph node samples collected from the wild boar, *Sus scrofa*, between 2007 and 2011 in Spain, *M. chelonae* and *M. avium* represented 61 and 11% of the NTM isolates (Garcia-Jimenez et al., 2015). In a separate study, a low degree of similarity between MAH isolates from Japanese patients and local pigs was found, while there was a high degree of similarity between European patient and pig isolates, suggesting geographic distinctions (Iwamoto et al., 2012).

NTM infections are among the most common chronic disease of aquatic animals (Gcebe et al., 2018). After their original discovery in 1897, NTM organisms continue to cause disease in sea bass, mullets, and amberjacks that live in temperate zones (Lescenko et al., 2003). The most common NTM pathogens of fish include *M. chelonae* (sea horses), *M. avium,* and *M. fortuitum*. *M. marinum* remains the most typical NTM found in aquatic environments and often coinhabit on shrimp, frogs, eels, oysters, and shellfish (Piersimoni and Scarparo, 2009). *M. marinum* is one of the only known species of NTM that grow in waters with high salt concentrations (>3% NaCl) (Kirschner et al., 1992; Falkinham, 2009). In some cases, *M. marinum* cause extrapulmonary infections and cutaneous "fish tank granulomas" in humans. Controlling NTM infections in the aquaculture setting is difficult, relying only on destruction of the infected stocks in the absence of effective treatments (Gcebe et al., 2018). *Carassius auratus* (goldfish) have been evaluated as a novel *in vivo* model to study the pathogenesis of *M. marinum*. After intraperitoneal administration of 10^2 and 10^9 CFU of *M. marinum* organisms, an acute and chronic infection was respectively observed with high recovery of NTM from inoculated animals (Talaat et al., 1999).

Although seldom reported, reptiles and insects can potentially carry pathogenic NTM. *M. chelonae* was originally isolated from the lungs of sea turtles in 1903 (Männikkö, 2011), *M. intracellulare* has been identified in a rusty monitor reptile with lung nodules (Friend and Russell, 1979), and *M. szulgai* has been isolated from a crocodile showing tuberculosis-like lung lesions (Gcebe et al., 2018). In a separate case, *M. gordonae, M. avium*, and *M. kansasii* were isolated off cockroaches from a South Taiwan hospital (Pai et al., 2003).

Mycobacterium ulcerans can infect skin and subcutaneous tissues developing into non-ulcerated nodules or lesions. Although *M. ulcerans* has not yet been cultured from the environment, its DNA has been detected in low levels in suspended solids/water residues and soil. High concentrations of *M. ulcerans* DNA are observed in the feces of Australian ringtails and brushtails possums residing in locations where human cases were reported. These findings suggest possums are naturally infected and are potential environmental reservoirs (Fyfe et al., 2010).

STUDIES LINKING NTM ECOLOGY WITH AVAILABLE EPIDEMIOLOGICAL DATA

To understand the environmental risk factors for infection, most studies described above have either probed for the occurrence of NTM in various environmental sources or in pulmonary samples from various geographic areas. Yet, the number of studies that have overlaid and integrated ecological and geographic information with epidemiological information of NTM-LD risk are scant. However, an exciting recent study has enhanced our understanding of how ecology relates to risk for NTM infection. In Colorado, soil acidity, low manganese concentrations, and silt were significantly associated with increased disease risk for NTM (Lipner et al., 2017). This same study also identified high-risk clusters of NTM-LD and high-risk watershed locations in the same geographic region using spatial scanning methods. Another study from Queensland, Australia (2001–2010) investigated the associations between climate, soil characteristics, land use, demographic, and socio-economic variables with spatial patterns of NTM infection (Chou et al., 2014). High risk clusters of *M. kansasii, M. intracellulare*, and *M. abscesses* infections were found to be associated with areas of high agricultural, mining, and tourism activity.

Higher rates of NTM lung infections have been associated with oceanic coastlines, accounting for 70% of annual NTM cases in the U.S. (Strollo et al., 2015). Statistically significant increases in NTM identification have been reported in the U.S. Affiliated Pacific Islands (USAPI) including American Samoa, Guam, Northern Marina Islands, Palau, Marshall Islands, and the Federated States of Micronesia (Lin et al., 2018). After analyzing respiratory cultures submitted for species identification between 2007 and 2011 at a clinical reference laboratory, the overall period prevalence of NTM isolation in this study was 106 cases/100,000 persons. The authors acknowledge that the prevalence of NTM isolation varied by island nation and may be related to urbanization. The lowest period prevalence of NTM isolation (22 cases/100,000 persons) was reported in American Samoa with 87.2% of patients living in high urban areas. The highest period prevalence (164/100,000 cases) was observed in respiratory samples from the Federated States of Micronesia which also showed the lowest percentage of urban dwellers (22.4%).

Of interest, the first nationwide population-based analysis on the prevalence of NTM-LD found that Hawai'i had the highest period prevalence (1997–2007) of any U.S. state with 396 cases/100,000 persons among persons > 65 years-old (Adjemian et al., 2012b), a rate that is four times greater than the national average. Using national Medicare claims, U.S. Census data, as well as U.S. Geological and Forest Services environmental and climatic data, high and low risk U.S. counties were identified (Adjemian et al., 2012a). High-risk regions for NTM were noted in particular geographic areas of

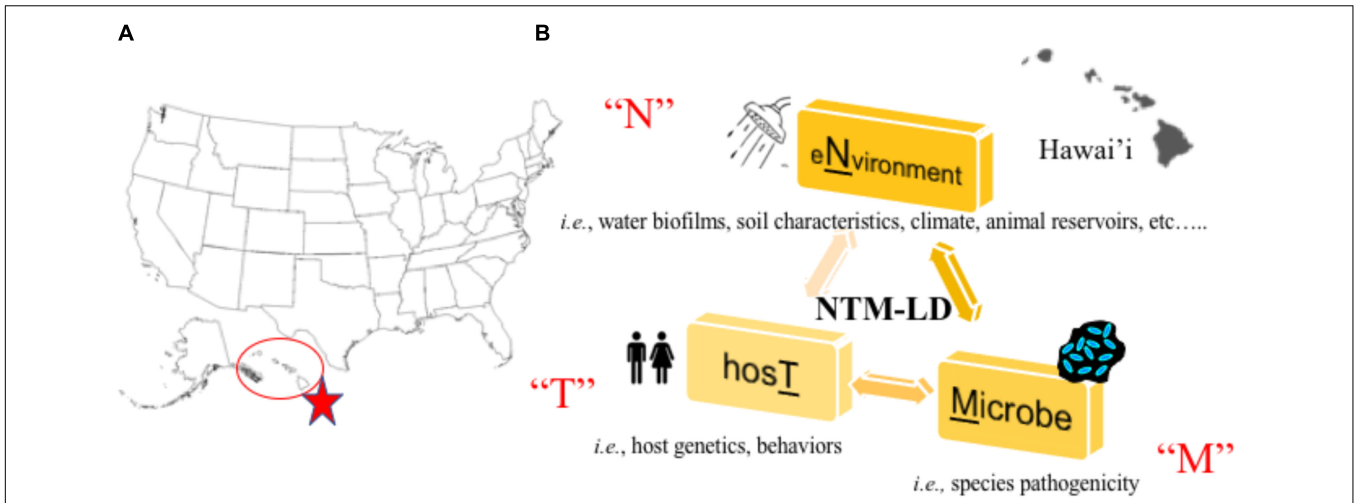

FIGURE 1 | (A) Hawai'i is a hot spot for NTM lung disease in the United States (Rudis, 2018). **(B)** Our research program aims to study the "N-T-M" specific factors that contribute to lung disease by studying the environmental, host, and microbial factors that facilitate NTM lung disease emergence in Hawai'i.

Hawai'i. Higher daily evapotranspiration levels, higher number of surfaces covered by water, higher soil copper and sodium, and lower manganese levels were characteristics of high risk areas. More ominous, Hawai'i also shows the highest, national age-adjusted mortality rates from NTM-LD (Mirsaeidi et al., 2014).

In a recent large-scale study, researchers partnered with a network of citizen scientists to collect showerhead biofilm samples from 606 households across 49 of 50 U.S. states to simultaneously superimpose the identities of showerhead microbes over geographic areas where NTM-LD is most prevalent (Gebert et al., 2018). Multiple concluding findings were reported that reinforce known paradigms. First, *Mycobacteria* was the most abundant group of bacteria identified in showerhead biofilms by *16S* rRNA gene sequencing, corroborating prior studies (Feazel et al., 2009; Thomson R. et al., 2013). Next, the most frequently identified NTM species by *hsp65* gene sequencing were MAC, *M. abscessus,* and the *M. fortuitum* complex which are also the most problematic NTM for patients. As already observed (Garcia et al., 2013; Ovrutsky et al., 2013), mycobacteria often co-occurred with free-living amoeba. Second, similar to other studies (Feazel et al., 2009), homes using municipal treated water showed twice more mycobacteria than homes using water from wells and the former contained higher chlorine and iron concentrations. Third, by overlapping these data with previously reported epidemiological information, this study is the first to show showerhead-associated mycobacteria with the potential to cause pathogenic LD are indeed found in U.S. households in regions with the highest number of NTM-LD cases including Florida, southern California, and northeast states. It is clear mycobacterial lineages showed distinct geographic distributions. Finally, supporting prior work, this study confirms Hawai'i as the state with the most abundant mycobacterial showerhead biofilms and show these are predominated by MAC and *M. abscessus* organisms. Undoubtedly, Hawai'i is a U.S. hot spot for NTM-LD (**Figure 1A**) and the islands' unique characteristics may contribute to greater exposures.

MOVEMENT TO COLLECTIVELY UNDERSTAND NTM ECOLOGY, EPIDEMIOLOGY, AND ORGANISM VIRULENCE IN THE HAWAIIAN ISLAND ENVIRONMENT

We have previously shown increased prevalence of NTM infection in Hawai'i using patient laboratory data from a representative population of in-state residents enrolled in a closed healthcare system (Adjemian et al., 2017). Indeed, the most frequently isolated species was MAC, followed by *M. fortuitum* that was more common among Vietnamese and Korean patients, while *M. abscessus* was more associated with Japanese and Filipino patients. In this study, Native Hawaiian/Other Pacific Islander populations were less likely to have NTM infection than other racial/ethnic groups examined. A logical hypothesis is that native populations inhabited the islands for a longer period of time, evolving and developing resistance to infection.

We have also previously demonstrated not only the overwhelming presence of MAC in both clinical samples in respiratory specimens from Hawai'i, but also in water biofilm samples collected from households in Hawai'i (Honda et al., 2016). Using partial *rpoB* gene sequencing, *M. avium* was not identified in any of the samples examined, providing a contrast to previous studies from the continental U.S. *M. intracellulare* was found in 27% (4/15) SGM respiratory specimens examined and a soil sample. While absent from soil, *M. chelonae* was significantly more common in kitchen sink biofilms (9/35, 35%) compared to bathroom sink biofilms (3/34, 9%) and *M. abscessus* was found equally in kitchen (5/34, 15%) and bathroom sink (4/30, 13%) biofilms. *M. porcinum* was also frequently recovered

from showerhead biofilm samples, a species normally associated with swine, but also a cause of human infections (Wallace et al., 2004; Brown-Elliott et al., 2011; Perez-Martinez et al., 2013). This observation may be particularly important in Hawai'i, which has a sizeable feral pig population (Hess et al., 2006). Importantly, we identified *M. chimaera* as the predominant species of MAC in these islands; in fact, *M. chimaera* was recovered from 56% of the 75 environmental samples tested and 67% of ten clinical isolates tested (Honda et al., 2016). By comparison, of 8,800 isolates analyzed using *rpoB* gene sequencing in 26 months at National Jewish Health, only 6% were *M. chimaera* (Dr. Max Salfinger, National Jewish Health, personal communication). Taken together, *M. chimaera* is emerging as a major NTM species of interest in Hawai'i, underscoring the need for further studies to define the drivers for NTM emergence there and in other Pacific Islands.

In new and on-going work to understand the Hawai'i specific environmental, host, and NTM factors that contribute to NTM-LD emergence (**Figure 1B**), we are synergizing environmental and human behavioral/genetic findings with microbiological and NTM genomic data in dynamic statistical, spatial/temporal models to uncover not only disease drivers, but also potential points of intervention to prevent future infections. Isolates collected through this work will also be applied in future studies of NTM virulence. To accomplish this, a complementary team has been formed including a NTM microbiologist born and raised in Hawai'i with significant ties to the local community, a mycobacterial pulmonologist, epidemiologist, earth geochemist, climatologist, microbial ecologist, volcanic scientists, ecological modelers, local clinicians, and a team of microbial genomic and computational scientists as well as Hawai'i residents, high school/college students, their mentors, and local pig hunters.

FUTURE DIRECTIONS

Future studies should investigate the: (i) factors that drive the relative absence of NTM from seawater, but association with higher humidity and associated biofilms collected from different areas of the world, (ii) NTM prevalence and diversity in areas of the world with endemic tuberculosis, (iii) role of animal and protozoal reservoirs in the maintenance and spread of environmental NTM, and (iv) contributions of temperature, evapotranspiration, and air pollution including climatic determinants of disease. In the meantime, we spotlight the NTM crisis in Hawai'i as a useful model system to understand NTM transmission and disease dynamics. New information gathered from this work will then be used and applied to study NTM-LD in other areas of the world where NTM-LD is prevalent and emergent.

AUTHOR CONTRIBUTIONS

JH conceived the project. JH, RV, and EC wrote and edited the manuscript.

ACKNOWLEDGMENTS

JH would like to thank the Shoot for the Cure and Padosi Foundations. The authors also acknowledge Drs. Michael Strong, Stephen Nelson, James Crooks, Krishna Pacifici and Stacey Honda as co-PI and collaborators on our work supported by the National Science Foundation, Ecology, Evolution, and Infectious Disease Program, Award # 1743587. Assistance to create the U.S. map shown in this manuscript provided by James Crooks.

REFERENCES

Adekambi, T., and Drancourt, M. (2004). Dissection of phylogenetic relationships among 19 rapidly growing *Mycobacterium* species by 16S rRNA, hsp65, sodA, recA and rpoB gene sequencing. *Int. J. Syst. Evol. Microbiol.* 54, 2095–2105.

Adjemian, J., Frankland, T. B., Daida, Y. G., Honda, J. R., Olivier, K. N., Zelazny, A., et al. (2017). Epidemiology of nontuberculous mycobacterial lung disease and tuberculosis, Hawaii, USA. *Emerg. Infect. Dis.* 23, 439–447.

Adjemian, J., Olivier, K. N., Seitz, A. E., Falkinham, J. O. III, Holland, S. M., and Prevots, D. R. (2012a). Spatial clusters of nontuberculous mycobacterial lung disease in the United States. *Am. J. Respir. Crit. Care Med.* 186, 553–558.

Adjemian, J., Olivier, K. N., Seitz, A. E., Holland, S. M., and Prevots, D. R. (2012b). Prevalence of nontuberculous mycobacterial lung disease in U.S. *Medicare beneficiaries. Am. J. Respir. Crit. Care Med.* 185, 881–886.

Al-Ghafli, H., and Al-Hajoj, S. (2017). Nontuberculous mycobacteria in saudi arabia and gulf countries: a review. *Can. Respir. J.* 2017:5035932.

Amha, Y. M., Anwar, M. Z., Kumaraswamy, R., Henschel, A., and Ahmad, F. (2017). Mycobacteria in municipal wastewater treatment and reuse: microbial diversity for screening the occurrence of clinically and environmentally relevant species in arid regions. *Environ. Sci. Technol.* 51, 3048–3056.

Ben Salah, I., and Drancourt, M. (2010). Surviving within the amoebal exocyst: the *Mycobacterium avium* complex paradigm. *BMC Microbiol.* 10:99. doi: 10.1186/1471-2180-10-99

Bernstein, D. I., Lummus, Z. L., Santilli, G., Siskosky, J., and Bernstein, I. L. (1995). Machine operator's lung. A hypersensitivity pneumonitis disorder associated with exposure to metalworking fluid aerosols. *Chest* 108, 636–641.

Bolan, G., Reingold, A. L., Carson, L. A., Silcox, V. A., Woodley, C. L., Hayes, P. S., et al. (1985). Infections with *Mycobacterium chelonei* in patients receiving dialysis and using processed hemodialyzers. *J. Infect. Dis.* 152, 1013–1019.

Bono, M., Jemmi, T., Bernasconi, C., Burki, D., Telenti, A., and Bodmer, T. (1995). Genotypic characterization of *Mycobacterium avium* strains recovered from animals and their comparison to human strains. *Appl. Environ. Microbiol.* 61, 371–373.

Brown-Elliott, B. A., and Wallace, R. J. Jr. (2002). Clinical and taxonomic status of pathogenic nonpigmented or late-pigmenting rapidly growing mycobacteria. *Clin. Microbiol. Rev.* 15, 716–746.

Brown-Elliott, B. A., Wallace, R. J. Jr., Tichindelean, C., Sarria, J. C., Mcnulty, S., Vasireddy, R., et al. (2011). Five-year outbreak of community- and hospital-acquired *Mycobacterium porcinum* infections related to public water supplies. *J. Clin. Microbiol.* 49, 4231–4238.

Bryant, J. M., Grogono, D. M., Rodriguez-Rincon, D., Everall, I., Brown, K. P., Moreno, P., et al. (2016). Emergence and spread of a human-transmissible multidrug-resistant nontuberculous *Mycobacterium*. *Science* 354, 751–757.

Carson, L. A., Bland, L. A., Cusick, L. B., Favero, M. S., Bolan, G. A., Reingold, A. L., et al. (1988). Prevalence of nontuberculous mycobacteria in water supplies of hemodialysis centers. *Appl. Environ. Microbiol.* 54, 3122–3125.

Chisholm, R. H., Trauer, J. M., Curnoe, D., and Tanaka, M. M. (2016). Controlled fire use in early humans might have triggered the evolutionary emergence of tuberculosis. *Proc. Natl. Acad. Sci. U.S.A.* 113, 9051–9056.

Chou, M. P., Clements, A. C., and Thomson, R. M. (2014). A spatial epidemiological analysis of nontuberculous mycobacterial infections in Queensland, Australia. *BMC Infect. Dis.* 14: 279. doi: 10.1186/1471-2334-14-279

Cirillo, J. D., Falkow, S., Tompkins, L. S., and Bermudez, L. E. (1997). Interaction of *Mycobacterium avium* with environmental amoebae enhances virulence. *Infect. Immun.* 65, 3759–3767.

D'Antonio, S., Rogliani, P., Paone, G., Altieri, A., Alma, M. G., Cazzola, M., et al. (2016). An unusual outbreak of nontuberculous mycobacteria in hospital respiratory wards: association with nontuberculous mycobacterial colonization of hospital water supply network. *Int. J. Mycobacteriol.* 5, 244–247.

De Groote, M. A., Pace, N. R., Fulton, K., and Falkinham, J. O. (2006). Relationships between *Mycobacterium* isolated from patients with pulmonary mycobacterial infection and potting soils. *Appl. Environ. Microbiol.* 72, 7602–7606.

Delafont, V., Mougari, F., Cambau, E., Joyeux, M., Bouchon, D., Hechard, Y., et al. (2014). First evidence of amoebae-mycobacteria association in drinking water network. *Environ. Sci. Technol.* 48, 11872–11882.

Desikan, P., Tiwari, K., Panwalkar, N., Khaliq, S., Chourey, M., Varathe, R., et al. (2017). Public health relevance of Non-tuberculous mycobacteria among AFB positive sputa. *Germs* 7, 10–18.

Eaton, T., Falkinham, J. O. III, and Von Reyn, C. F. (1995). Recovery of *Mycobacterium avium* from cigarettes. *J. Clin. Microbiol.* 33, 2757–2758.

Embil, J., Warren, P., Yakrus, M., Stark, R., Corne, S., Forrest, D., et al. (1997). Pulmonary illness associated with exposure to *Mycobacterium-avium* complex in hot tub water, hypersensitivity pneumonitis or infection? *Chest* 111, 813–816.

Falkinham, J. O. III, Iseman, M. D., De Haas, P., and Van Soolingen, D. (2008). *Mycobacterium avium* in a shower linked to pulmonary disease. *J. Water Health* 6, 209–213.

Falkinham, J. O., Norton, C. D., and Lechevallier, M. W. (2001). Factors influencing numbers of *Mycobacterium avium*, *Mycobacterium intracellulare*, and other mycobacteria in drinking water distribution systems. *Appl. Environ. Microbiol.* 67, 1225–1231.

Falkinham, J. O. III. (1996). Epidemiology of infection by nontuberculous mycobacteria. *Clin. Microbiol. Rev.* 9, 177–215.

Falkinham, J. O. III. (2009). Surrounded by mycobacteria: nontuberculous mycobacteria in the human environment. *J. Appl. Microbiol.* 107, 356–367.

Falkinham, J. O. III. (2011). Nontuberculous mycobacteria from household plumbing of patients with nontuberculous mycobacteria disease. *Emerg. Infect. Dis.* 17, 419–424.

Falkinham, J. O. III. (2013). Ecology of nontuberculous mycobacteria-where do human infections come from? *Semin. Respir. Crit. Care Med.* 34, 95–102.

Feazel, L. M., Baumgartner, L. K., Peterson, K. L., Frank, D. N., Harris, J. K., and Pace, N. R. (2009). Opportunistic pathogens enriched in showerhead biofilms. *Proc. Natl. Acad. Sci. U.S.A.* 106, 16393–16399.

Friend, S. C., and Russell, E. G. (1979). *Mycobacterium intracellulare* infection in a water monitor. *J. Wild. Dis.* 15, 229–233.

Fyfe, J. A., Lavender, C. J., Handasyde, K. A., Legione, A. R., O'brien, C. R., Stinear, T. P., et al. (2010). A major role for mammals in the ecology of *Mycobacterium ulcerans*. *PLoS Negl. Trop Dis.* 4:e791. doi: 10.1371/journal.pntd.0000791

Garcia, A., Goni, P., Cieloszyk, J., Fernandez, M. T., Calvo-Begueria, L., Rubio, E., et al. (2013). Identification of free-living amoebae and amoeba-associated bacteria from reservoirs and water treatment plants by molecular techniques. *Environ. Sci. Technol.* 47, 3132–3140.

Garcia-Jimenez, W. L., Benitez-Medina, J. M., Martinez, R., Carranza, J., Cerrato, R., Garcia-Sanchez, A., et al. (2015). Non-tuberculous mycobacteria in wild boar (*Sus scrofa*) from Southern Spain: epidemiological, clinical and diagnostic concerns. *Transbound. Emerg. Dis.* 62, 72–80.

Gcebe, N., Michel, A. L., and Hlokwe, T. M. (2018). Non-tuberculous *Mycobacterium* species causing mycobacteriosis in farmed aquatic animals of South Africa. *BMC Microbiol.* 18:32. doi: 10.1186/s12866-018-1177-9

Gebert, M., Delgado-Baquerizo, M., Oliverio, A., Webster, T., Nichols, L., Honda, J., et al. (2018). Ecological analyses of mycobacteria in showerhead biofilms and their relevance to human health. *bioRxiv* [Preprint]. doi: 10.1101/366088

Gebo, K. A., Srinivasan, A., Perl, T. M., Ross, T., Groth, A., and Merz, W. G. (2002). Pseudo-outbreak of *Mycobacterium fortuitum* on a human immunodeficiency virus ward: transient respiratory tract colonization from a contaminated ice machine. *Clin. Infect. Dis.* 35, 32–38.

Griffith, D. E., Aksamit, T., Brown-Elliott, B. A., Catanzaro, A., Daley, C., Gordin, F., et al. (2007). An official ATS/IDSA statement: diagnosis, treatment, and prevention of nontuberculous mycobacterial diseases. *Am. J. Respir. Crit. Care Med.* 175, 367–416.

Gruft, H., Falkinham, J. O. III, and Parker, B. C. (1981). Recent experience in the epidemiology of disease caused by atypical mycobacteria. *Rev. Infect Dis.* 3, 990–996.

Guimaraes, T., Chimara, E., Do Prado, G. V., Ferrazoli, L., Carvalho, N. G., Simeao, F. C., et al. (2016). Pseudooutbreak of rapidly growing mycobacteria due to *Mycobacterium abscessus* subsp bolletii in a digestive and respiratory endoscopy unit caused by the same clone as that of a countrywide outbreak. *Am. J. Infect. Control.* 44, e221–e226.

Halstrom, S., Price, P., and Thomson, R. (2015). Review: environmental mycobacteria as a cause of human infection. *Int. J. Mycobacteriol.* 4, 81–91.

Hamada, S., Ito, Y., Hirai, T., Murase, K., Tsuji, T., Fujita, K., et al. (2016). Impact of industrial structure and soil exposure on the regional variations in pulmonary nontuberculous mycobacterial disease prevalence. *Int. J. Mycobacteriol.* 5, 170–176.

Hamilton, K. A., Ahmed, W., Toze, S., and Haas, C. N. (2017). Human health risks for *Legionella* and *Mycobacterium avium* complex (MAC) from potable and non-potable uses of roof-harvested rainwater. *Water Res.* 119, 288–303.

Havelaar, A. H., Berwald, L. G., Groothuis, D. G., and Baas, J. G. (1985). Mycobacteria in semi-public swimming-pools and whirlpools. *Zentralbl. Bakteriol. Mikrobiol. Hyg. B* 180, 505–514.

Hector, J. S., Pang, Y., Mazurek, G. H., Zhang, Y., Brown, B. A., Wallace, R. J., et al. (1992). Large restriction fragment patterns of genomic *Mycobacterium fortuitum* DNA as strain-specific markers and their use in epidemiologic investigation of four nosocomial outbreaks. *J. Clin. Microbiol.* 30, 1250–1255.

Hennessee, C. T., Seo, J. S., Alvarez, A. M., and Li, Q. X. (2009). Polycyclic aromatic hydrocarbon-degrading species isolated from Hawaiian soils: *Mycobacterium crocinum* sp. nov., *Mycobacterium pallens* sp. nov., *Mycobacterium rutilum* sp. nov., *Mycobacterium rufum* sp. nov. and *Mycobacterium aromaticivorans* sp. nov. *Int. J. Syst. Evol. Microbiol.* 59, 378–387.

Hess, S. C., Jeffrey, J. J., Ball, D. L., and Babich, L. (2006). Efficacy of feral pig removals at Hakalau forest national wildlife refuge. *Hawai'i Trans. Western Sec. Wildlife Soc.* 42, 53–67.

Hoefsloot, W., Van Ingen, J., Andrejak, C., Angeby, K., Bauriaud, R., Bemer, P., et al. (2013). The geographic diversity of nontuberculous mycobacteria isolated from pulmonary samples: an NTM-NET collaborative study. *Eur. Respir. J.* 42, 1604–1613.

Honda, J. R., Bernhard, J. N., and Chan, E. D. (2015). Natural disasters and nontuberculous mycobacteria: a recipe for increased disease? *Chest* 147, 304–308.

Honda, J. R., Hasan, N. A., Davidson, R. M., Williams, M. D., Epperson, L. E., Reynolds, P. R., et al. (2016). Environmental nontuberculous mycobacteria in the hawaiian islands. *PLoS Negl. Trop. Dis.* 10:e0005068. doi: 10.1371/journal.pntd.0005068

Huang, H. L., Cheng, M. H., Lu, P. L., Shu, C. C., Wang, J. Y., Wang, J. T., et al. (2017). Epidemiology and predictors of NTM pulmonary infection in taiwan – A retrospective, five-year multicenter study. *Sci. Rep.* 7:16300.

Ichijo, T., Izumi, Y., Nakamoto, S., Yamaguchi, N., and Nasu, M. (2014). Distribution and respiratory activity of mycobacteria in household water system of healthy volunteers in Japan. *PLoS One* 9:e110554. doi: 10.1371/journal.pone.0110554

Ichiyama, S., Shimokata, K., and Tsukamura, M. (1988). The isolation of *Mycobacterium avium* complex from soil, water, and dusts. *Microbiol. Immunol.* 32, 733–739.

Iwamoto, T., Nakajima, C., Nishiuchi, Y., Kato, T., Yoshida, S., Nakanishi, N., et al. (2012). Genetic diversity of *Mycobacterium avium* subsp. hominissuis strains isolated from humans, pigs, and human living environment. *Infect. Genet. Evol.* 12, 846–852.

Johnson, M. M., and Odell, J. A. (2014). Nontuberculous mycobacterial pulmonary infections. *J. Thorac. Dis.* 6, 210–220.

Kaevska, M., Slana, I., Kralik, P., Reischl, U., Orosova, J., Holcikova, A., et al. (2011). "*Mycobacterium avium* subsp. hominissuis" in neck lymph nodes of children and their environment examined by culture and triplex quantitative real-time PCR. *J. Clin. Microbiol.* 49, 167–172.

Kankya, C., Muwonge, A., Djonne, B., Munyeme, M., Opuda-Asibo, J., Skjerve, E., et al. (2011). Isolation of Non-tuberculous mycobacteria from pastoral

ecosystems of Uganda: public health significance. *BMC Public Health* 11:320. doi: 10.1186/1471-2458-11-320

Kawamura, Y., Li, Y., Liu, H., Huang, X., Li, Z., and Ezaki, T. (2001). Bacterial population in Russian space station "Mir". *Microbiol. Immunol.* 45, 819–828.

Khaledi, A., Bahador, A., Esmaeili, D., Tafazoli, A., Ghazvini, K., and Mansury, D. (2016). Prevalence of nontuberculous mycobacteria isolated from environmental samples in Iran: a meta-analysis. *J. Res. Med. Sci.* 21:58.

Kirs, M., Moravcik, P., Gyawali, P., Hamilton, K., Kisand, V., Gurr, I., et al. (2017). Rainwater harvesting in american samoa: current practices and indicative health risks. *Environ. Sci. Pollut. Res. Int.* 24, 12384–12392.

Kirschner, R. A. Jr., Parker, B. C., and Falkinham, J. O. III. (1992). Epidemiology of infection by nontuberculous mycobacteria. *Mycobacterium avium*, *Mycobacterium intracellulare*, and *Mycobacterium scrofulaceum* in acid, brown-water swamps of the southeastern United States and their association with environmental variables. *Am. Rev. Respir. Dis.* 145, 271–275.

Koh, E., Iizasa, T., Yamaji, H., Sekine, Y., Hiroshima, K., Yoshino, I., et al. (2012). Significance of the correlation between the expression of interleukin 6 and clinical features in patients with non-small cell lung cancer. *Int. J. Surg. Pathol.* 20, 233–239.

Koh, W. J., Jeong, B. H., Jeon, K., Lee, N. Y., Lee, K. S., Woo, S. Y., et al. (2012). Clinical significance of the differentiation between *Mycobacterium avium* and *Mycobacterium intracellulare* in *M. avium* complex lung disease. *Chest* 142, 1482–1488.

Koschel, D., Pietrzyk, C., Sennekamp, J., and Muller-Wening, D. (2006). [Swimming pool lung – Extrinsic allergic alveolitis or mycobacterial disease?]. *Pneumologie* 60, 285–289.

Kuehl, R., Banderet, F., Egli, A., Keller, P. M., Frei, R., Dobele, T., et al. (2018). Different types of heater-cooler units and their risk of transmission of *Mycobacterium chimaera* during open-heart surgery: clues from device design. *Infect. Control. Hosp. Epidemiol.* 39, 834–840.

Lahiri, A., Kneisel, J., Kloster, I., Kamal, E., and Lewin, A. (2014). Abundance of *Mycobacterium avium* ssp. hominissuis in soil and dust in Germany – Implications for the infection route. *Lett. Appl. Microbiol.* 59, 65–70.

Lai, C. C., Tan, C. K., Chou, C. H., Hsu, H. L., Liao, C. H., Huang, Y. T., et al. (2010). Increasing incidence of nontuberculous mycobacteria, Taiwan, 2000-2008. *Emerg. Infect. Dis.* 16, 294–296.

Lee, M. R., Sheng, W. H., Hung, C. C., Yu, C. J., Lee, L. N., and Hsueh, P. R. (2015). *Mycobacterium abscessus* complex infections in humans. *Emerg. Infect. Dis.* 21, 1638–1646.

Lescenko, P., Matlova, L., Dvorska, L., Bartos, M., Vavra, O., Navratil, L., et al. (2003). Mycobacterial infection in aquarium fish. *Vet. Med. – Czech* 48, 71–78.

Lin, C., Russell, C., Soll, B., Chow, D., Bamrah, S., Brostrom, R., et al. (2018). Increasing prevalence of nontuberculous mycobacteria in respiratory specimens from US-Affiliated Pacific island jurisdictions(1). *Emerg. Infect. Dis.* 24, 485–491.

Lipner, E. M., Knox, D., French, J., Rudman, J., Strong, M., and Crooks, J. L. (2017). A geospatial epidemiologic analysis of nontuberculous mycobacterial infection: an ecological study in colorado. *Ann. Am. Thorac. Soc.* 14, 1523–1532.

Lorencova, A., Klanicova, B., Makovcova, J., Slana, I., Vojkovska, H., Babak, V., et al. (2013). Nontuberculous mycobacteria in freshwater fish and fish products intended for human consumption. *Foodborne Pathog. Dis.* 10, 573–576.

Lorencova, A., Vasickova, P., Makovcova, J., and Slana, I. (2014). Presence of *Mycobacterium avium* subspecies and hepatitis E virus in raw meat products. *J. Food Prot.* 77, 335–338.

Makovcova, J., Babak, V., Slany, M., and Slana, I. (2015). Comparison of methods for the isolation of mycobacteria from water treatment plant sludge. *Antonie Van Leeuwenhoek* 107, 1165–1179.

Malcolm, K. C., Caceres, S. M., Honda, J. R., Davidson, R. M., Epperson, L. E., Strong, M., et al. (2017). *Mycobacterium abscessus* displays fitness for fomite transmission. *Appl. Environ. Microbiol.* 83:e00562-17.

Männikkö, N. (2011). Etymologia: *Mycobacterium chelonae*. *Emerg. Infect. Dis.* 17:1712.

Marra, A. R., Diekema, D. J., and Edmond, M. B. (2017). *Mycobacterium chimaera* infections associated with contaminated heater-cooler devices for cardiac surgery: outbreak management. *Clin. Infect. Dis.* 65, 669–674.

Martin, E. C., Parker, B. C., and Falkinham, J. O. III (1987). Epidemiology of infection by nontuberculous mycobacteria. VII. Absence of mycobacteria in southeastern groundwaters. *Am. Rev. Respir. Dis.* 136, 344–348.

Meissner, G., and Anz, W. (1977). Sources of *Mycobacterium avium* complex infection resulting in human diseases. *Am. Rev. Respir. Dis.* 116, 1057–1064.

Mirsaeidi, M., Machado, R. F., Garcia, J. G., and Schraufnagel, D. E. (2014). Nontuberculous mycobacterial disease mortality in the United States, 1999-2010: a population-based comparative study. *PLoS One* 9:e91879. doi: 10.1371/journal.pone.0091879

Monde, N., Munyeme, M., Muwonge, A., Muma, J. B., and Malama, S. (2018). Characterization of Non-tuberculous *Mycobacterium* from humans and water in an Agropastoral area in Zambia. *BMC Infect. Dis.* 18:20. doi: 10.1186/s12879-017-2939-y

Morita, Y., Maruyama, S., Hashizaki, F., and Katsube, Y. (1999). Pathogenicity of *Mycobacterium avium* complex serovar 9 isolated from painted quail (Excalfactoria chinensis). *J. Vet. Med. Sci.* 61, 1309–1312.

Mudedla, S., Avendano, E. E., and Raman, G. (2015). Non-tuberculous *Mycobacterium* skin infections after tattooing in healthy individuals: a systematic review of case reports. *Dermatol. Online J.* 21:13030/qt8mr3r4f0.

Neonakis, I. K., Gitti, Z., Kourbeti, I. S., Michelaki, H., Baritaki, M., Alevraki, G., et al. (2007). Mycobacterial species diversity at a general hospital on the island of Crete: first detection of *Mycobacterium lentiflavum* in Greece. *Scand. J. Infect. Dis.* 39, 875–879.

Nishiuchi, Y., Iwamoto, T., and Maruyama, F. (2017). Infection sources of a common Non-tuberculous mycobacterial pathogen, *Mycobacterium avium complex*. *Front. Med. (Lausanne)* 4:27. doi: 10.3389/fmed.2017.00027

Nishiuchi, Y., Tamura, A., Kitada, S., Taguri, T., Matsumoto, S., Tateishi, Y., et al. (2009). *Mycobacterium avium* complex organisms predominantly colonize in the bathtub inlets of patients' bathrooms. *Jpn. J. Infect. Dis.* 62, 182–186.

Ovrutsky, A. R., Chan, E. D., Kartalija, M., Bai, X., Jackson, M., Gibbs, S., et al. (2013). Cooccurrence of free-living amoebae and nontuberculous mycobacteria in hospital water networks, and preferential growth of *Mycobacterium avium* in *Acanthamoeba lenticulata*. *Appl. Environ. Microbiol.* 79, 3185–3192.

Pai, H. H., Chen, W. C., and Peng, C. F. (2003). Isolation of Non-tuberculous mycobacteria from hospital cockroaches (*Periplaneta americana*). *J. Hosp. Infect.* 53, 224–228.

Perez-Martinez, I., Aguilar-Ayala, D. A., Fernandez-Rendon, E., Carrillo-Sanchez, A. K., Helguera-Repetto, A. C., Rivera-Gutierrez, S., et al. (2013). Occurrence of potentially pathogenic nontuberculous mycobacteria in Mexican household potable water: a pilot study. *BMC Res. Notes* 6:531. doi: 10.1186/1756-0500-6-531

Piersimoni, C., and Scarparo, C. (2009). Extrapulmonary infections associated with nontuberculous mycobacteria in immunocompetent persons. *Emerg. Infect. Dis.* 15, 1351–1358; quiz 1544.

Reisfeld, L., Ikuta, C. Y., Ippolito, L., Silvatti, B., Ferreira Neto, J. S., Catao-Dias, J. L., et al. (2018). Cutaneous mycobacteriosis in a captive Amazonian manatee *Trichechus inunguis*. *Dis. Aquat. Organ.* 127, 231–236.

Richards, C. L., Broadaway, S. C., Eggers, M. J., Doyle, J., Pyle, B. H., Camper, A. K., et al. (2015). Detection of pathogenic and non-pathogenic bacteria in drinking water and associated biofilms on the crow reservation, Montana, USA. *Microb. Ecol.* 76, 52–63.

Rickman, O. B., Ryu, J. H., Fidler, M. E., and Kalra, S. (2002). Hypersensitivity pneumonitis associated with *Mycobacterium avium* complex and hot tub use. *Mayo Clin. Proc.* 77, 1233–1237.

Rodgers, M. R., Blackstone, B. J., Reyes, A. L., and Covert, T. C. (1999). Colonisation of point of use water filters by silver resistant Non-tuberculous mycobacteria. *J. Clin. Pathol.* 52:629.

Roguet, A., Therial, C., Saad, M., Boudahmane, L., Moulin, L., and Lucas, F. S. (2016). High mycobacterial diversity in recreational lakes. *Antonie Van Leeuwenhoek* 109, 619–631.

Rose, C. S., Martyny, J. W., Newman, L. S., Milton, D. K., King, T. E. Jr., et al. (1998). "Lifeguard lung": endemic granulomatous pneumonitis in an indoor swimming pool. *Am. J. Public Health* 88, 1795–1800.

Rudis, B. (2018). *albersusa: Tools, Shapefiles and Data to Work with an 'AlbersUSA' Composite Projection. R package version 0.3.1.* Avialable at: https://github.com/hrbrmstr/albersusa

Safranek, T. J., Jarvis, W. R., Carson, L. A., Cusick, L. B., Bland, L. A., Swenson, J. M., et al. (1987). *Mycobacterium chelonae* wound infections after plastic surgery employing contaminated gentian violet skin-marking solution. *N. Engl. J. Med.* 317, 197–201.

Sax, H., Bloemberg, G., Hasse, B., Sommerstein, R., Kohler, P., Achermann, Y., et al. (2015). Prolonged outbreak of *Mycobacterium chimaera* infection after open-chest heart surgery. *Clin. Infect Dis.* 61, 67–75.

Schinsky, M. F., Morey, R. E., Steigerwalt, A. G., Douglas, M. P., Wilson, R. W., Floyd, M. M., et al. (2004). Taxonomic variation in the *Mycobacterium fortuitum* third biovariant complex: description of *Mycobacterium boenickei* sp. nov. *Mycobacterium houstonense sp. nov., Mycobacterium neworleansense sp. nov. and Mycobacterium brisbanense sp. nov.* and recognition of *Mycobacterium porcinum* from human clinical isolates. *Int. J. Syst. Evol. Microbiol.* 54, 1653–1667.

Schreiber, P. W., Kuster, S. P., Hasse, B., Bayard, C., Ruegg, C., Kohler, P., et al. (2016). Reemergence of *Mycobacterium chimaera* in heater-cooler units despite intensified cleaning and disinfection protocol. *Emerg. Infect. Dis.* 22, 1830–1833.

Schulze-Robbecke, R., Feldmann, C., Fischeder, R., Janning, B., Exner, M., and Wahl, G. (1995). Dental units: an environmental study of sources of potentially pathogenic mycobacteria. *Tuber Lung. Dis.* 76, 318–323.

Scriven, J. E., Scobie, A., Verlander, N. Q., Houston, A., Collyns, T., Cajic, V., et al. (2018). *Mycobacterium chimaera* infection following cardiac surgery in the United Kingdom: clinical features and outcome of the first 30 cases. *Clin. Microbiol. Infect.* [Epub ahead of print].

Simons, S., Van Ingen, J., Hsueh, P. R., Van Hung, N., Dekhuijzen, P. N., Boeree, M. J., et al. (2011). Nontuberculous mycobacteria in respiratory tract infections, eastern Asia. *Emerg. Infect. Dis.* 17, 343–349.

Stout, J. E., Koh, W. J., and Yew, W. W. (2016). Update on pulmonary disease due to Non-tuberculous mycobacteria. *Int. J. Infect. Dis.* 45, 123–134.

Strollo, S. E., Adjemian, J., Adjemian, M. K., and Prevots, D. R. (2015). The burden of pulmonary nontuberculous mycobacterial disease in the United States. *Ann. Am. Thorac. Soc.* 12, 1458–1464.

Sugita, Y., Ishii, N., Katsuno, M., Yamada, R., and Nakajima, H. (2000). Familial cluster of cutaneous *Mycobacterium avium* infection resulting from use of a circulating, constantly heated bath water system. *Br. J. Dermatol.* 142, 789–793.

Talaat, A. M., Trucksis, M., Kane, A. S., and Reimschuessel, R. (1999). Pathogenicity of *Mycobacterium fortuitum* and *Mycobacterium smegmatis* to goldfish, *Carassius auratus*. *Vet. Microbiol.* 66, 151–164.

Taylor, M., Ross, K., and Bentham, R. (2009). Legionella, protozoa, and biofilms: interactions within complex microbial systems. *Microb. Ecol.* 58, 538–547.

Thomson, R., Donnan, E., and Konstantinos, A. (2017). Notification of nontuberculous mycobacteria: an australian perspective. *Ann. Am. Thorac. Soc.* 14, 318–323.

Thomson, R., Tolson, C., Carter, R., Coulter, C., Huygens, F., and Hargreaves, M. (2013). Isolation of nontuberculous mycobacteria (NTM) from household water and shower aerosols in patients with pulmonary disease caused by NTM. *J. Clin. Microbiol.* 51, 3006–3011.

Thomson, R. M. (2010). Changing epidemiology of pulmonary nontuberculous mycobacteria infections. *Emerg. Infect. Dis.* 16, 1576–1583.

Thomson, R. M., Carter, R., Tolson, C., Coulter, C., Huygens, F., and Hargreaves, M. (2013). Factors associated with the isolation of nontuberculous mycobacteria (NTM) from a large municipal water system in Brisbane, Australia. *BMC Microbiol.* 13:89. doi: 10.1186/1471-2180-13-89

Thorel, M. F., Falkinham, J. O. III, and Moreau, R. G. (2004). Environmental mycobacteria from alpine and subalpine habitats. *FEMS Microbiol. Ecol.* 49, 343–347.

Tichenor, W. S., Thurlow, J., Mcnulty, S., Brown-Elliott, B. A., Wallace, R. J. Jr., and Falkinham, J. O. III. (2012). Nontuberculous mycobacteria in household plumbing as possible cause of chronic rhinosinusitis. *Emerg. Infect. Dis.* 18, 1612–1617.

Ulmann, V., Kracalikova, A., and Dziedzinska, R. (2015). Mycobacteria in water used for personal hygiene in heavy industry and collieries: a potential risk for employees. *Int. J. Environ. Res. Public Health* 12, 2870–2877.

Velayati, A. A., Farnia, P., Mozafari, M., Malekshahian, D., Seif, S., Rahideh, S., et al. (2014). Molecular epidemiology of nontuberculous mycobacteria isolates from clinical and environmental sources of a metropolitan city. *PLoS One* 9:e114428. doi: 10.1371/journal.pone.0114428

Wallace, R. J. Jr., Brown-Elliott, B. A., Wilson, R. W., Mann, L., Hall, L., Zhang, Y., et al. (2004). Clinical and laboratory features of *Mycobacterium porcinum*. *J. Clin. Microbiol.* 42, 5689–5697.

Wallace, R. J. Jr., Iakhiaeva, E., Williams, M. D., Brown-Elliott, B. A., Vasireddy, S., et al. (2013). Absence of *Mycobacterium intracellulare* and the presence of *Mycobacterium chimaera* in household water and biofilm samples of patients in the U.S. With *Mycobacterium avium* complex respiratory disease. *J. Clin. Microbiol.* 51, 1747–1752.

Wang, S. H., Pancholi, P., Stevenson, K., Yakrus, M. A., Butler, W. R., Schlesinger, L. S., et al. (2009). Pseudo-outbreak of "*Mycobacterium paraffinicum*" infection and/or colonization in a tertiary care medical center. *Infect. Control Hosp. Epidemiol.* 30, 848–853.

Wassilew, N., Hoffmann, H., Andrejak, C., and Lange, C. (2016). Pulmonary disease caused by Non-tuberculous mycobacteria. *Respiration* 91, 386–402.

Whiley, H., Keegan, A., Giglio, S., and Bentham, R. (2012). *Mycobacterium avium* complex–the role of potable water in disease transmission. *J. Appl. Microbiol.* 113, 223–232.

Wilson, R. W., Steingrube, V. A., Bottger, E. C., Springer, B., Brown-Elliott, B. A., Vincent, V., et al. (2001). *Mycobacterium immunogenum* sp. nov., a novel species related to *Mycobacterium abscessus* and associated with clinical disease, pseudo-outbreaks and contaminated metalworking fluids: an international cooperative study on mycobacterial taxonomy. *Int. J. Syst. Evol. Microbiol.* 51, 1751–1764.

Winthrop, K. L., Albridge, K., South, D., Albrecht, P., Abrams, M., Samuel, M. C., et al. (2004). The clinical management and outcome of nail salon-acquired *Mycobacterium fortuitum* skin infection. *Clin. Infect. Dis.* 38, 38–44.

Winthrop, K. L., Mcnelley, E., Kendall, B., Marshall-Olson, A., Morris, C., Cassidy, M., et al. (2010). Pulmonary nontuberculous mycobacterial disease prevalence and clinical features: an emerging public health disease. *Am. J. Respir. Crit. Care Med.* 182, 977–982.

Yajko, D. M., Chin, D. P., Gonzalez, P. C., Nassos, P. S., Hopewell, P. C., Reingold, A. L., et al. (1995). *Mycobacterium avium* complex in water, food, and soil samples collected from the environment of HIV-infected individuals. *J. Acquir. Immune Defic. Syndr. Hum. Retrovirol.* 9, 176–182.

Yajko, D. M., Nassos, P. S., Sanders, C. A., Gonzalez, P. C., Reingold, A. L., Horsburgh, C. R., et al. (1993). Comparison of four decontamination methods for recovery of *Mycobacterium avium* complex from stools. *J. Clin. Microbiol.* 31, 302–306.

Yoder, S., Argueta, C., Holtzman, A., Aronson, T., Berlin, O. G., Tomasek, P., et al. (1999). PCR comparison of *Mycobacterium avium* isolates obtained from patients and foods. *Appl. Environ. Microbiol.* 65, 2650–2653.

Yu, X., Liu, P., Liu, G., Zhao, L., Hu, Y., Wei, G., et al. (2016). The prevalence of Non-tuberculous mycobacterial infections in mainland China: systematic review and meta-analysis. *J. Infect.* 73, 558–567.

Conflict of Interest Statement: The authors declare that the research was conducted in the absence of any commercial or financial relationships that could be construed as a potential conflict of interest.

frontiers in Microbiology

REVIEW
published: 01 November 2018
doi: 10.3389/fmicb.2018.02642

Mycobacterium abscessus: Shapeshifter of the Mycobacterial World

Keenan Ryan[1] *and Thomas F. Byrd*[2]*

[1] Department of Pharmacy, University of New Mexico Hospital, Albuquerque, NM, United States, [2] Department of Medicine, The University of New Mexico School of Medicine, Albuquerque, NM, United States

In this review we will focus on unique aspects of *Mycobacterium abscessus* (*MABS*) which we feel earn it the designation of "shapeshifter of the mycobacterial world." We will review its emergence as a distinct species, the recognition and description of *MABS* subspecies which are only now being clearly defined in terms of pathogenicity, its ability to exist in different forms favoring a saprophytic lifestyle or one more suitable to invasion of mammalian hosts, as well as current challenges in terms of antimicrobial therapy and future directions for research. One can see in the various phases of *MABS*, a species transitioning from a free living saprophyte to a host-adapted pathogen.

Keywords: glycopeptidolipid, toll-like receptor 2, cystic fibrosis, bronchiectasis, serpentine cording, fibroblasts

OPEN ACCESS

Edited by:
Thomas Dick, Rutgers, The State University of New Jersey, United States

Reviewed by:
Michael Henry Cynamon, Syracuse VA Medical Center, United States
Joon Liang Tan, Multimedia University, Malaysia
Albertus Johannes Viljoen, IRIM, France

***Correspondence:**
Thomas F. Byrd
tbyrd@salud.unm.edu

Specialty section:
This article was submitted to Antimicrobials, Resistance and Chemotherapy, a section of the journal Frontiers in Microbiology

Received: *11 July 2018*
Accepted: *16 October 2018*
Published: *01 November 2018*

Citation:
Ryan K and Byrd TF (2018) Mycobacterium abscessus: Shapeshifter of the Mycobacterial World. Front. Microbiol. 9:2642. doi: 10.3389/fmicb.2018.02642

EVOLVING NOMENCLATURE

Mycobacterium abscessus (*MABS*), a rapidly growing non-tuberculous mycobacterium (NTM) (Howard and Byrd, 2000) is an emerging pathogen worldwide. Perhaps the earliest case of *MABS* was reported in 1951 and described infection which occurred in the setting of traumatic knee injury. This infection was characterized by "subcutaneous, abscess-like lesions with a peripherally tuberculoid structure." The unique characteristics of this mycobacterium prompted the investigators to propose it as a new species, *Mycobacterium abscessus* (Moore and Frerichs, 1953). In more recent times, *MABS* was considered a subspecies of *Mycobacterium chelonae* until 1992 when genetic analysis demonstrated that it was a distinct species and it was elevated to species status as *MABS* (Kusunoki and Ezaki, 1992). This resulted in the realization that most prior reports of *M. chelonae* lung infection were likely a mischaracterization of actual *MABS* lung infection as it is now recognized that pulmonary infection is a common clinical manifestation of *MABS* whereas it is rarely caused by *M. chelonae*. In recent years, *MABS* has been further characterized into three distinct subspecies; *MABS* subspecies *abscessus*, *MABS* subspecies *bolletii* and *MABS* subspecies *massiliense* (Adekambi et al., 2017). They differ in terms of drug susceptibility, and may have differences related to transmissibility as well which will be discussed (Tan et al., 2017). Genomic analysis of *MABS* reveals evidence of horizontal gene transfer (Howard et al., 2002). In addition to genes associated with mycobacterial virulence, genes with similar function to those found in *Pseudomonas aeruginosa* and *Burkholderia cepacia*, pathogens commonly found in the lungs of cystic fibrosis (CF) patients, have also been identified (Ripoll et al., 2009). Thus *MABS* can be thought of as a pathogen uniquely adapted to different niches within the host lung environment.

EPIDEMIOLOGY AND EMERGENCE AS A PATHOGEN

The incidence of NTM infection is increasing in the United States (Prevots et al., 2010) and worldwide (Prevots and Marras, 2015). Pulmonary infection is the most common clinical

presentation, however, extrapulmonary infection either due to direct inoculation into the skin or due to disseminated disease, often in association with disease modifying anti-TNFα therapy, is also being recognized with increased frequency (Winthrop et al., 2009). In the United States, *Mycobacterium avium* complex (*MAC*) is the most common NTM clinical pulmonary isolate followed by *MABS* (Prevots and Marras, 2015). It has also been reported that there are geographic differences in the types of NTM isolates in the United States. *MAC* is the most frequent and predominant isolate in the South and Northeast with proportionally higher rates of isolation of *MABS*, *M. chelonae*, *M. fortuitum*, and *M. kansasii* in the Western United States (Spaulding et al., 2017). It is noteworthy that in parts of Asia *MABS* is the predominant pulmonary NTM pathogen (Umrao et al., 2016; Nagano et al., 2017; Lim et al., 2018). Furthermore, limited epidemiologic data suggests that there may be a relative genetic susceptibility to *MABS* infection in certain Asian populations (Adjemian et al., 2017).

Perhaps what is most disconcerting about *MABS* from an epidemiologic standpoint is its unique ability among NTM to cause outbreaks of infection over wide geographic regions without linkage to a single or specific point source. The best described instance of this relates to a study of post-surgical wound infections with *MABS* subspecies *massiliense* in Brazil. Using genomic analysis it was found that a recently emergent single clone caused multiple outbreaks of post-surgical wound infections. The organism spread throughout Brazil and persisted in hospital environments. Evidence was also provided that there is a loss of genetic material from this lineage raising the possibility that it is undergoing reductive evolution as it adapts to its new niche in the hospital environment (Everall et al., 2017). It is noteworthy that this isolate is genetically related to another *MABS* subspecies *massillense* clone that has been reported to be circulating among CF treatment centers throughout the world. There is evidence that acquisition of this strain by CF patients may be associated with worse clinical outcomes. Data from cell culture and animal infection experiments provide evidence that this clone may be more virulent in comparison to unclustered *MABS* subspecies *abscessus* isolates. Review of this data shows that although the observed differences are statistically significant, they are small (Bryant et al., 2016), and whether they have clinical relevance in terms of virulence remains unclear. Nonetheless these studies raise the disconcerting possibility that evolutionary changes affecting transmissibility and adaptation to mammalian hosts could lead to further spread of *MABS* into the susceptible general population of patients with abnormal lung airways and/or states of immunosuppression (Winthrop et al., 2009). The possible mechanisms responsible for spread of *MABS* include fomites, aerosolized airway secretions and contaminated hospital and municipal tap water (Baker et al., 2017; Donohue, 2018). One study has reported an association between warm humid climates and high atmospheric vapor pressure with the prevalence of NTM infection (Prevots and Marras, 2015). This raises the question of whether climate change is contributing to the rising incidence of NTM infection.

CLINICAL INFECTION

The clinical spectrum of *MABS* and other rapidly growing mycobacteria has been well-described and broadly categorized as pulmonary and extrapulmonary disease (Howard and Byrd, 2000). *MABS* extrapulmonary infection can involve a variety of sites, most commonly the skin. It can occur via dissemination in immunosuppressed patients (Scholze et al., 2005), often from an occult source, or from direct inoculation, either iatrogenically [for example, contaminated acupuncture needles, injection solutions, and surgical procedures (Ryu et al., 2005; Yuan et al., 2009; Schnabel et al., 2016)], or as a result of wound contamination in the setting of trauma (Petrini et al., 2006). Infection of many anatomic sites has been reported including the eye, bone, joint, and central nervous system (Chu et al., 2015; Fukui et al., 2015; Baidya et al., 2016; Jeong et al., 2017). Extrapulmonary infection is generally responsive to treatment with antibiotics to which the isolate is susceptible with adjunctive surgical debridement where indicated.

MABS was first recognized as a cause of chronic pulmonary infection in 1993. The majority of pulmonary infections occur in older adults often with no history of cigarette smoking who are otherwise healthy, but who have underlying lung airway abnormalities (Griffith et al., 1993). The clinical presentation is indistinguishable from lung infection caused by *MAC*. Unlike *MAC*, however, effective antibiotic treatment options are limited with many patients requiring a combination of medical and surgical intervention for cure (Jarand et al., 2011). In patients with CF, *MABS* pulmonary infection is an important cause of morbidity and mortality, and is a relative contraindication to lung transplantation (Dorgan and Hadjiliadis, 2014). It is important to note that immune dysregulation as a result of mutations in the *CF Transmembrane Conductance Regulator gene* (*CFTR*) contributes to the inflammatory phenotype in CF lung disease, and may result in a pathogenic process that differs from that seen in otherwise healthy individuals who have *MABS* infection and abnormal lung airways (Rieber et al., 2014). One clinically apparent difference is that *MABS* chronic colonization of the lung by smooth variants as well as by rough invasive variants is a cause of morbidity in CF patients (Bryant et al., 2016). In otherwise healthy patients with abnormal lung airways *MABS* colonization is more likely to be transient.

A common characteristic of patients with *MABS* pulmonary infection is bronchiectasis. An obvious question is whether bronchiectasis is the end result of infection with *MABS* or a predisposing factor for *MABS* infection? An experiment of nature provides evidence that bronchiectasis *per se* predisposes to NTM infection in the absence of preceding inflammation. Patients with the genetic disorder known as primary ciliary dyskinesia have a loss of normal ciliary structure and function leading to development of bronchiectasis which may occur in the absence of antecedent inflammation. These individuals are prone to recurrent oto-sino-pulmonary infections. In addition to lung infection with pyogenic bacteria such as *P. aeruginosa* and *Staphylococcus aureus*, these patients are also susceptible to colonization and invasive infection with *MABS* and *MAC* (Noone et al., 2004). The other lung airway disease which

predisposes to colonization and infection with NTM such as *MABS* and *MAC* is chronic obstructive pulmonary disease (COPD) (Billinger, 2009). Large upper lobe bullous cavities in the lung are a predisposing factor to NTM infection in these patients. It is also noteworthy that bronchiectasis is also present in a high percentage of patients diagnosed with COPD (Patel et al., 2004; Martinez-Garcia et al., 2013) suggesting that the presence of bronchiectasis may be an important factor in *MABS* and *MAC* disease pathogenesis in these patients as well.

PATHOGENESIS: THE IMPORTANCE OF ROUGH AND SMOOTH COLONY PHENOTYPES

Microdroplet nuclei aerosolized after an individual with pulmonary tuberculosis coughs, with subsequent inhalation by an uninfected host, is the mode of person to person spread of *M. tuberculosis*. In contrast, epidemiologic studies have not demonstrated this to be an efficient mechanism for acquisition of pulmonary *MABS* infection although there is experimental evidence that long lived infected aerosols generated by a coughing patient may contain respiratable bacteria (Bryant et al., 2016). Respiratable bacteria could also result from other sources of aerosols contaminated with *MABS*, for example colonized showerheads. Fomites have also been implicated in transmission of an outbreak strain (Bryant et al., 2016). It would seem unlikely that bacteria adherent to a fomite could be easily re-aerosolized. This mechanism of transmission could involve contact transfer from the fomite to the mouth with subsequent colonization of the oropharynx. Microaspiration of bacteria into the lung would lead to colonization of the lung airways and/or invasive lung infection (Thomson et al., 2007).

We first described rough and smooth colony phenotypes of *MABS* which arose from a single parental strain, and demonstrated that the rough variant persists in the lungs of SCID mice, replicates in macrophages, and forms corded, invasive microcolonies in fibroblast monolayers. The smooth variant demonstrated none of these characteristics (Byrd and Lyons, 1999). We then identified glycopeptidolipid (GPL) in the cell wall of the smooth variant as being responsible for the smooth colony phenotype and for the ability of the smooth strain to exhibit sliding motility and biofilm formation (Howard et al., 2006; Nessar et al., 2011). Importantly, we demonstrated that a mutant which lacks GPL and exhibits the rough phenotype can spontaneously arise from the smooth phenotype and regain virulence characteristics (Howard et al., 2006). We showed by light and electron microscopy (Byrd and Lyons, 1999; Howard et al., 2006), and in a later publication using scanning electron microscopy (Sanchez-Chardi et al., 2011), that the rough phenotype exhibits cording, a property associated with virulence in *M. tuberculosis*. These observations were replicated by others, and the ability of spontaneous rough mutants to arise in infected mice from initial infecting *MABS* smooth variants was subsequently demonstrated (Catherinot et al., 2007; De Groote et al., 2014). The clinical relevance of these observations is supported by studies indicating that the majority of clinical isolates from individuals with chronic lung disease exhibit the rough phenotype whereas environmental contaminants and isolates from wounds exhibit the smooth phenotype (Jonsson et al., 2007). A study which longitudinally characterized *MABS* isolates from ten CF and three non-CF patients over a 10 year period found that a switch from smooth to rough colony morphology was observed in 6 of the patients during the course of long-term infection and was associated with increased severity of clinical symptoms (Kreutzfeldt et al., 2013). In addition, it has been documented that deterioration of lung function in a *MABS*-infected CF patient was associated with conversion of a sputum isolates from the smooth phenotype to an isogenic rough phenotype (Catherinot et al., 2009). These observations are consistent with our hypothesis that *MABS* initially gains entry to the lung as a GPL-expressing smooth variant which colonizes abnormal lung airways, and that spontaneous loss of GPL expression leads to a virulent phenotype capable of causing inflammation and invasive lung disease (Howard et al., 2006; Rhoades et al., 2009). In support of this pathogenic mechanism, we have provided evidence that *MABS* GPL is immunologically inert and that loss of GPL unmasks underlying *MABS* cell wall molecules such phosphatidyl-myo-inositol mannosides (PIMs) which are recognized by toll like receptor 2 (TLR2) on macrophages and epithelial cells thereby initiating an inflammatory response. Establishment of a smooth strain in the lungs of individuals with normal lung airways is likely prevented by the normal lung mucociliary clearance mechanism. This prevents establishment of lung airway biofilm from which invasive rough variants which have lost GPL can emerge. In patients with abnormal lung airways and diminished mucociliary clearance, *MABS* smooth variants have been demonstrated to establish biofilm in lung airways (Qvist et al., 2015). In CF patients, heavy colonization of lung airways with smooth variants in the absence of lung invasion is also likely to contribute to morbidity. Evidence indicates that genetic mutation involving a gene coding for one of the MmpL proteins involved in the biosynthesis of the *MABS* cell envelope is responsible for the smooth to rough transition in one *MABS* strain (Bernut et al., 2016b). However, we have presented evidence that in some strains of *MABS,* expression of GPL is temperature dependent and reversible, with expression at lower temperatures and loss of expression at higher temperatures (Rhoades et al., 2009). This suggests that alternative mechanisms regulating GPL production in the smooth to rough transition are operating. In addition, temperature-dependent transitioning of the smooth to rough phenotype could be a mechanism whereby a GPL expressing environmental strain gains access to abnormal lung airways where higher internal core temperature of the lungs would result in loss of GPL and emergence of the rough virulent phenotype. Our current model of *MABS* pathogenesis is summarized in **Figure 1**.

With the exception of *MABS* rough strains from chronically infected CF patients contaminating the hospital/surgical or CF clinic environment, the majority of environmental strains have the smooth colony phenotype (Jonsson et al., 2007; Baker et al., 2017). Direct acquisition of a *MABS* rough variant into abnormal lung airways as might occur in a contaminated clinical

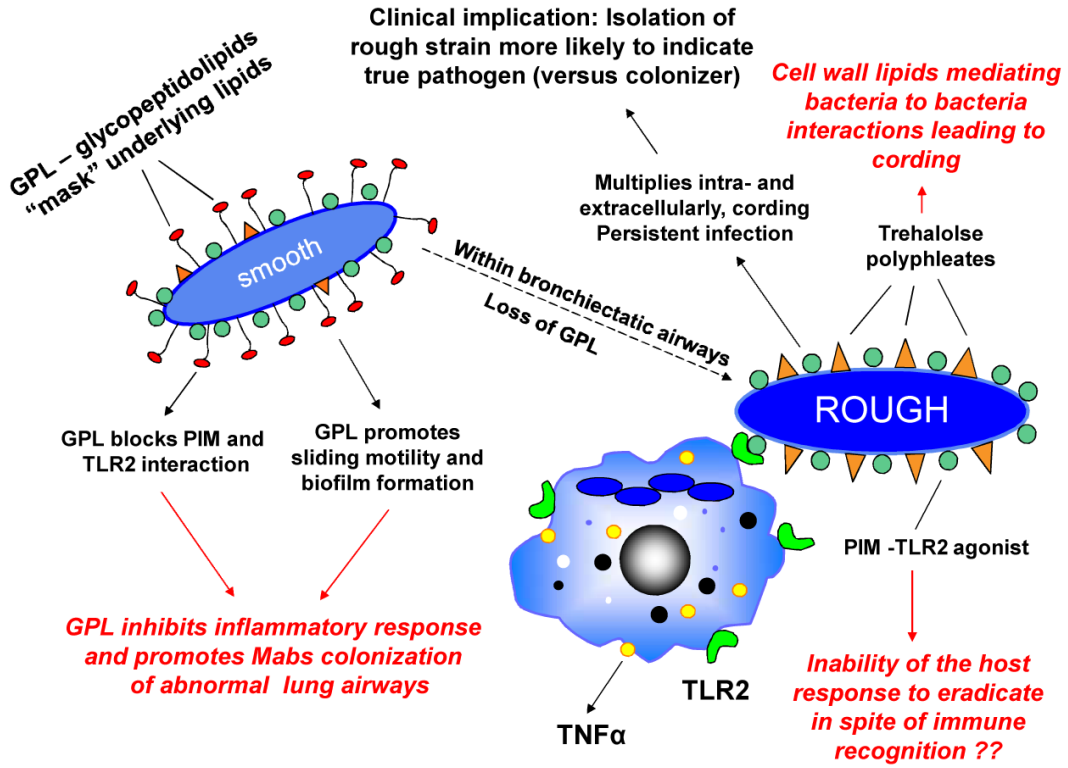

FIGURE 1 | Environmental *Mycobacterium abscessus* (*MABS*) isolates have the smooth colony morphotype and express glycopeptidolipid (GPL). GPL in the outermost aspect of the cell wall "masks" underlying glycosylated lipoproteins such as phosphatidyl-myo-inositol mannosides (PIMs) involved in immune recognition and blocks the bacterial cell–cell interaction of lipids such trehalose polyphleates which may play a role in clumping and cord formation. By preventing *MABS* from being recognized by innate immune surveillance mechanisms and promoting biofilm formation, GPL facilitates colonization of bronchiectatic lung airways. After colonization, spontaneous or temperature sensitive loss of GPL is associated with "unmasking" of these molecules. This leads to recognition by TLR2 on macrophages and respiratory epithelial cells resulting in release of the proinflammatory cytokines TNFα (from macrophages) and IL-8 (from respiratory epithelial cells). Rough variants acquire a virulent phenotype characterized by the ability to grow in serpentine cords and cause macrophage apoptosis leading to rapid cell–cell spread and propagation of infection. Isolation of *MABS* rough variants from the sputum is associated with progressive lung infection.

environment would likely result in a less indolent infection due to the greater virulence of rough variants and stimulation of a robust innate immune response.

COMPARISON TO OTHER CLINICALLY SIGNIFICANT NTM

Other clinically significant NTM may express some form of GPL or exhibit cording, but there are few examples of other NTM which can transition between both phenotypes with such a clear correlation between colonization and invasion. For example, *MAC* expresses serovar-specific GPLs that differ from the non-specific core GPL found in *MABS* through modification by addition of oligosaccharides (Brennan et al., 1981). In contrast to *MABS* GPL, these molecules are immunogenic and are associated with *MAC* virulence (Barrow et al., 1995; Sweet and Schorey, 2006). *M. kansasii* variants may have a smooth colony phenotype associated with expression of characteristic lipids distinct from GPLs (Nataraj et al., 2015). Both *MAC* and *M. kansasii* form microscopic bacterial aggregates in broth culture, but do not exhibit the serpentine cording found in *M. tuberculosis* and *MABS* that is associated with mycobacterial virulence (Tu et al., 2003). In contrast, *M. marinum* does not express GPLs, but does exhibit serpentine cording (Hall-Stoodley et al., 2006). Thus, *MABS* may be viewed as a pathogen which has a unique ability to shift from a ubiquitous environmental saprophyte to an invasive human pathogen – this transformation is apparent upon inspection of the shape of its bacterial colonies growing on nutrient agar.

THE PARADOX OF LOW VIRULENCE AND INEFFECTIVE HOST RESPONSE

Perhaps the most puzzling aspect of *MABS* pulmonary infection is that it rarely occurs in immunocompetent individuals with normal lung airways in spite of the ability of this pathogen to invade and replicate in mononuclear phagocytes and non-professional phagocytes (Byrd and Lyons, 1999). Determining the reason(s) why has been impeded by the lack of a suitable mouse model that mimics human lung bronchiectasis. For example, mice with in which the *CFTR* gene has been disrupted have organ specific pathology which is mild in the lung (Clarke et al., 1994).

A non-CF mouse model utilizes GM-CSF knock out mice in which a chronic lung infection can be established. In this model, colony forming units in mouse lung persist and gradually decline over a month but then begin to increase at 2 months – at that time the mice have begun to develop bronchiectasis. The limitations of this model are that the mice are immunocompromised, and that bronchiectasis develops late in the course of infection (De Groote et al., 2014). In spite of the current lack of an ideal model, a pattern of bacterial – host interaction is beginning to emerge based on clinical and experimental evidence to date.

At the cellular level, important differences have been reported regarding the intracellular life cycle of *MABS* smooth and rough variants. Since both variants replicate in tissue culture medium assessing growth in macrophages requires extensive washing after infection, incubation with amikacin to kill extracellular bacteria and then removal of amikacin followed by lysis of macrophages and plating lysates for bacterial CFU. Using this model, rough variants replicate intracellularly resulting in lysis of cell monolayers whereas smooth variants persist and/or decline within cells, but do not destroy cell monolayers in the time frames studied in these experiments (Byrd and Lyons, 1999; Howard et al., 2006; Greendyke and Byrd, 2008; Nessar et al., 2011). Recent studies have demonstrated differences in intracellular behavior comparing smooth and rough variants which may account for these findings. Smooth variants have been found to reside in phagosomes in which they are surrounded by electron translucent zone representing cell wall GPL. They are typically present as a single organism which is likely due to the fact that they are easily dispersed into single cell suspensions prior to infecting cells. In contrast, rough variants clump in a manner similar to *M. tuberculosis* and are difficult to get into single cells suspension, thus they are usually present as two or more bacteria per phagosome (Byrd and Lyons, 1999; Roux et al., 2016). Consistent with the lack of destruction of macrophage monolayers infected with smooth variants (Nessar et al., 2011) is the finding that smooth variants are poor inducers of apoptosis and autophagy in contrast to rough variants which end up in phagolysosomes but nonetheless replicate intracellularly and induce apoptosis (Roux et al., 2016). In fact, uptake of large clumps of *MABS* rough variants leads to rapid dissolution of macrophages and emergence of *MABS* cords (Brambilla et al., 2016). There is evidence that smooth variants cause disruption of the phagosomal membrane allowing for direct cytosolic contact (Roux et al., 2016). Thus, as a mechanism of apoptosis inhibition, polar GPLs found on the surface of *MABS* smooth variants (Lopez-Marin et al., 1994; Howard et al., 2006) have access to cytosolic contents and have been demonstrated to interact with mitochondrial cyclophilin D, a component of the mitochondrial permeability transition pore (MPTP) to stabilize the pore and inhibit apoptosis (Whang et al., 2017).

MABS has an ESX-4 type VII secretion system encoded for by five genes. A gene in this locus, *eccB4* was found to be necessary for low level replication (approximately 0.5 log over 5 days), but not persistence, of the smooth *MABS subspecies massiliense* 43S strain in *Acanthamoeba castellani* and J774.2 mouse macrophages. This gene was also found to be necessary for prevention of phagosome acidification and for causing phagosome rupture (Laencina et al., 2018). Other studies have found that under stringent conditions to prevent extracellular replication in tissue culture media, colony forming units of *MABS* smooth variants in human monocyte-derived macrophage monolayers have limited replicative capacity over a 5 day period and do not persist in the lungs of infected SCID mice (Byrd and Lyons, 1999; Howard et al., 2006). These latter findings raise the question of the significance of the slight loss of replicative ability in the *eccB4* deletion mutant. The question of the effect of expression of the genes of the ESX-4 type VII type secretion system by the more virulent rough *MABS* phenotype is unexplored although as noted, another study did not report phagosome disruption but rather trafficking of rough variants through the autophagic pathway ending up in phagolysosomes where they replicate and rapidly induce apoptosis (Roux et al., 2016). It remains unclear why rough variants, which are able to arise from the smooth variant used in this study (Ripoll et al., 2009), would not also rupture the phagosome. Finally, as would be expected for an intracellular pathogen establishing cytosolic contact and activating the inflammasome, this study found that IL1β release was increased by cells infected with wild type bacteria. There was a significant decrease in IL1β release from cells infected with the *eccB4* deletion mutant. Since inflammasome activation results in cell death via pyroptosis (Sharma and Kanneganti, 2016), and human macrophage monolayers infected with *MABS* smooth variants typically remain intact and viable throughout the course of infection, this discrepancy remains unexplained. It may be that GPL-mediated inhibition of macrophage apoptosis counteracts the effect of inflammasome activation (Whang et al., 2017).

One important function of GPL is that it prevents bacteria to bacteria interaction of underlying surface molecules such as trehalose polyphleates which may play a role in the cording exhibited by rough variants (Llorens-Fons et al., 2017). With loss of GPL, rough variants taken up by macrophages rapidly induce apoptosis (Roux et al., 2016) and demonstrate rapid cell–cell spread via serpentine cord formation (Byrd and Lyons, 1999). The fact that serpentine cording is an important virulence determinant of rough *MABS* strains was demonstrated using a rough deletion mutant lacking a gene coding for a dehydratase necessary for cord formation. This mutant was found to be markedly attenuated for virulence in the zebrafish model (Halloum et al., 2016). A comparison of the behavior of *MABS* rough and smooth variants to the virulent *M. tuberculosis* strains H37Rv/Erdman, and the avirulent strain H37Ra shows similar behavior in a fibroblast microcolony assay which we described (Byrd et al., 1998; Byrd and Lyons, 1999). The differences relate to the addition of extracellular acting aminoglycoside antibiotics. Both the *MABS* rough variant and H37Rv/Erdman demonstrate elongated, corded microcolonies within the plane of the agar-overlaid monolayers, while the *MABS* smooth variant and H37Ra demonstrate significantly smaller, rounded microcolony morphology. Importantly, the addition of streptomycin does not prevent formation of H37Rv/Erdman microcolonies, presumably due to a mechanism of direct cell–cell spread wherein *M. tuberculosis* avoids exposure to the extracellular environment. In contrast, addition of amikacin to

fibroblast monolayers infected with the *MABS* rough variant prevents the formation of corded microcolonies. This suggests that *M. tuberculosis* is host adapted to favor replication within the intracellular environment while *MABS* may be viewed as an environmental saprophyte that has not quite made the transition to an intracellular lifestyle.

In spite of the ability to replicate extracellularly and form microabscesses in the zebrafish model of infection, *MABS* pulmonary infection does not occur in immunocompetent humans (or mice) with normal lung airways. Why this is so is a central question in terms of *MABS* pathogenesis. TLR2 has been found to be important in innate immune recognition and signaling in response to *MABS*. PIMs exposed on the surface of rough variants interact directly with TLR2 on human macrophages and epithelial cells to promote release of TNFα and IL-8, respectively, whereas PIMs are "masked" by GPL on the surface of smooth variants which are not recognized by TLR2 (Rhoades et al., 2009; Davidson et al., 2011). Both TNFα and IL-8 have both been found to be important for control of infection by *MABS* rough variants in the zebrafish model of infection (Bernut et al., 2016a). On the other hand, human neutrophils have been found to be less effective at killing *MABS* than killing *S. aureus*, and dead and dying neutrophils have been found to enhance biofilm formation by smooth variants (Malcolm et al., 2013). Thus in abnormal lung airways with impaired mucociliary clearance and *MABS* smooth variant biofilm formation, ongoing inflammation with IL-8 mediated neutrophil recruitment may promote biofilm persistence. This may have particular relevance in patients with CF who are often co-infected with multiple pulmonary pathogens and in whom chronic lung airway inflammation dominated by the presence of neutrophils is felt to be central to disease pathogenesis (Cantin et al., 2015). Another aspect of the innate immune response relates to single nucleotide polymorphisms (SNPs) that alter host responses to infectious agents. TLR2 signaling in response to mycobacterial lipopeptides depends upon formation of TLR2/TLR1 heterodimers at the cell surface. SNPs that alter the function of either TLR2 and/or TLR1 may thus affect innate immune responses to mycobacteria. We have reported that a well described SNP, TLR1 SNP I602S, is present in the respiratory epithelial cell line CFBE41o-, which was derived from the bronchus of a patient with CF and immortalized with SV40. This cell line is hyporesponsive to TLR2/TLR1 receptor agonist and the rough *MABS* 390R strain. This SNP is likely to be present in the CF patient population (Kempaiah et al., 2013). Paradoxically the presence of this SNP is protective against infection with *Mycobacterium leprae* (Johnson et al., 2007). An unanswered question is how the presence of this SNP affects susceptibility to NTM infection in both CF and non-CF patients.

In terms of the cell-mediated immune response, as would be predicted, anti-TNFα inhibitor therapy has been associated with disseminated NTM infection, including *MABS* (Winthrop et al., 2009). Th1 CD4+ T cell responses are also important for control of infection with NTM. It is established that patients with advanced HIV and low CD4+ T cell counts are susceptible to infection with *MAC*, and cases of disseminated *MABS* infection have been reported in these patients as well (Tan et al., 2010). The importance of IFNγ in control of *MABS* infection is highlighted in a recent case-control study from Thailand in which *MABS* was found to be the most common NTM clinical isolate, and the presence of anti-IFNγ autoantibody was strongly associated with disseminated infection (Phoompoung et al., 2017). Since defects in cell-mediated immunity have not been identified in the majority of non-CF patients with chronic *MABS* lung infection, it remains unclear why patients with underlying lung airway abnormalities such as bronchiectasis are uniquely susceptible to infection, and why an effective cell-mediated immune response does not develop in response to pulmonary infection.

A LIMITED ANTIMICROBIAL ARMAMENTARIUM

In spite of its low virulence compared to pathogens such as *M. tuberculosis*, *MABS* infection of the lung is the most difficult NTM to treat, resembling multi-drug resistant tuberculosis. Numerous resistance mechanisms in *MABS* have been identified that limit the number of available antibiotics in comparison to infections caused by other NTM (Brown-Elliott et al., 2012; Nessar et al., 2012; Luthra et al., 2018). Of the limited antibiotics used to treat *MABS* infection most are bacteriostatic and not bactericidal for both intra- and extracellular bacteria *in vitro* (Greendyke and Byrd, 2008; Maurer et al., 2014). *MABS* biofilm formation has been described for GPL-expressing smooth variants, and biofilm consisting primarily of smooth variants has been found in the lung airways of explanted lungs from CF patients prior to lung transplantation (Qvist et al., 2015). Under certain *in vitro* culture conditions *MABS* rough variants grow as biofilms as well (Clary et al., 2018). Biofilms formed by both smooth and rough *MABS* variants are relatively resistant to antibiotics when compared to planktonic bacteria (Greendyke and Byrd, 2008; Clary et al., 2018). The bacteriostatic activity of currently used antibiotics against intracellular *MABS*, and the relative antibiotic resistance of *MABS* biofilms in abnormal lung airways make eradication of *MABS* from the lung extremely difficult.

Of the antibiotics used to treat *MABS* infection, macrolides are felt to be the cornerstone of therapy. Importantly, there are differences in macrolide susceptibility among the different *MABS* subspecies based on the presence and functional status of the *erythromycin ribosomal methylation gene 41* (*erm41*). The *erm41* gene encodes for an enzyme that confers intrinsic, inducible resistance in *MABS* (Nash et al., 2009). In *MABS* strains with a functional *erm41* gene, clarithromycin may initially appear to be active; however, resistance may develop in the time frame of 3–14 days, the Clinical and Laboratory Standard Institute (CLSI) recommendation for length of incubation (Nash et al., 2009; Koh et al., 2011; CLSI, 2011). PCR is now being used to identify *MABS* subspecies and *erm41* gene status (Shallom et al., 2015).

Broth microdilution with determination of minimum inhibitory concentration (MIC) is recommended as the gold standard for NTM antibiotic susceptibility testing. Due to the relative rarity of *MABS* infections in the past, correlating *in vitro* modeling and susceptibility testing with effective clinical

response has been limited. In fact, tigecycline, a glycine antibiotic commonly used in treatment of *MABS* infection, currently lacks MIC interpretation from CLSI (Brown-Elliott et al., 2012). When *MABS* infection involves sites such as the CNS and bone, it is important to consider pharmacokinetic properties to maximize antibiotics exposure at the target site (Landersdorfer et al., 2009; Nau et al., 2010). Dosing regimens should be individualized to maximize drug exposure at the target site while limiting potential side-effects. The use of inhaled aminoglycosides for pulmonary *MABS* infection is one strategy to maximize the concentration at the active site while decreasing the likelihood of side-effects. Several small trials of inhaled amikacin for the treatment of NTM, specifically *MABS* and *MAC*, have had positive results including negative culture conversion and improvement seen on lung imaging (Olivier et al., 2014; Yagi et al., 2017). Even though serum concentrations are lower with inhaled amikacin it is not completely without risk. In one study, ototoxicity occurred at a relatively high rate (Olivier et al., 2014). Inhaled liposomal amikacin may be a further advancement in localized therapy for *MABS*. The liposome capsule penetrates biofilms and is also taken up by macrophages within the lung, thus delivering amikacin directly to the site of infection (Zhang et al., 2018). It should be noted that a Phase 2 trial of inhaled liposomal amikacin in addition to standard therapy failed to meet its primary endpoint for both *MABS* and *MAC* but did show improvement in culture clearance and 6-minute walk test (Olivier et al., 2017). Inhaled liposomal amikacin has recently been approved in the United States for the treatment of refractory *MAC* following a Phase 3 trial that demonstrated an increase in sputum clearance at 6 months (Griffith et al., 2018). More data about the use specifically in *MABS* is still needed. It is apparent that development of new drugs specifically targeting *MABS* infection should be a high priority and drug discovery efforts are underway utilizing novel high throughput screening platforms (Gupta et al., 2017). There are currently two new antibiotics designed and approved for alternative infectious indications which may add to the *MABS* antimicrobial armamentarium and are worth mentioning. The first antibiotic is an FDA-approved agent named tedizolid. Compared to the related antibiotic linezolid which is generally active against *MABS*, tedizolid has a higher ribosomal binding affinity that allows for lower effective serum concentration and once daily dosing (Burdette and Trotman, 2015). *In vitro* testing of NTM isolates shows promise as MIC values are 1–8 times lower than that of linezolid (Brown-Elliott and Wallace, 2017). Importantly, tedizolid has a lower incidence of side-effects and drug interactions as compared to linezolid (Burdette and Trotman, 2015). There is little data on long-term use of tedizolid that has been reported, but overall it appears to be well tolerated (Nigo et al., 2018). The second antibiotic is avibactam, a non-β-lactam β-lactamase inhibitor commercially available as a coformulation with ceftazidime, which can inactivate the *MABS* β-lactmase Bla_{mab}. When avibactam is combined with β-lactams, this combination may have enhanced activity for the treatment of *MABS* infection (Kaushik et al., 2017; Le Run et al., 2018).

FUTURE DIRECTIONS

Mycobacterium abscessus (*MABS*) has emerged as a significant infectious disease threat and warrants the designation of "shapeshifter of the mycobacterial world." Its ability to exist as a GPL-expressing environmental saprophyte forming biofilms along with the ability to "unmask" itself within the human host and display virulence properties such as serpentine cording is unprecedented for a bacterial pathogen. The ability of evolving clones to spread among clinical environments foreshadows an increasing incidence of nosocomial infections. The fact that many strains are multidrug resistant and that the *MABS* subspecies differ in terms of their inherent antimicrobial susceptibility creates an enormous challenge, particularly since patients often require months of therapy to achieve cure. There is an urgent need for better models that mimic human pulmonary infection to better understand disease pathogenesis and test new compounds for antimicrobial activity.

AUTHOR CONTRIBUTIONS

KR contributed ideas and expertise, and drafted the section related to antimicrobial therapy. TFB conceived and wrote the final manuscript.

FUNDING

Ongoing work in the TFB laboratory is supported by the National Institutes of Health (NIH) grant AI137633.

REFERENCES

Adekambi, T., Sassi, M., van Ingen, J., and Drancourt, M. (2017). Reinstating *Mycobacterium massiliense* and *Mycobacterium bolletii* as species of the *Mycobacterium abscessus* complex. *Int. J. Syst. Evol. Microbiol.* 67, 2726–2730. doi: 10.1099/ijsem.0.002011

Adjemian, J., Frankland, T. B., Daida, Y. G., Honda, J. R., Olivier, K. N., Zelazny, A., et al. (2017). Epidemiology of nontuberculous mycobacterial lung disease and tuberculosis, Hawaii, USA. *Emerg. Infect. Dis.* 23, 439–447. doi: 10.3201/eid2303.161827

Baidya, A., Tripathi, M., Pandey, P., and Singh, U. B. (2016). *Mycobacterium abscessus* as a cause of chronic meningitis: a rare clinical entity. *Am. J. Med. Sci.* 351, 437–439. doi: 10.1016/j.amjms.2016.02.009

Baker, A. W., Lewis, S. S., Alexander, B. D., Chen, L. F., Wallace, R. J. Jr., et al. (2017). Two-phase hospital-associated outbreak of *Mycobacterium abscessus*: investigation and Mitigation. *Clin. Infect. Dis.* 64, 902–911. doi: 10.1093/cid/ciw877

Barrow, W. W., Davis, T. L., Wright, E. L., Labrousse, V., Bachelet, M., and Rastogi, N. (1995). Immunomodulatory spectrum of lipids associated with *Mycobacterium avium* serovar 8. *Infect. Immun.* 63, 126–133.

Bernut, A., Nguyen-Chi, M., Halloum, I., Herrmann, J. L., Lutfalla, G., and Kremer, L. (2016a). *Mycobacterium abscessus*-induced granuloma formation is strictly dependent on tnf signaling and neutrophil trafficking. *PLoS Pathog.* 12:e1005986. doi: 10.1371/journal.ppat.1005986

Bernut, A., Viljoen, A., Dupont, C., Sapriel, G., Blaise, M., Bouchier, C., et al. (2016b). Insights into the smooth-to-rough transitioning in *Mycobacterium*

bolletii unravels a functional Tyr residue conserved in all mycobacterial MmpL family members. *Mol. Microbiol.* 99, 866–883. doi: 10.1111/mmi.13283

Billinger, M. E. (2009). Nontuberculous *Mycobacteria*-associated lung disease, United States in Hospitalized Persons, 1998–2005. *Emerg. Infect. Dis.* 15, 1562–1569. doi: 10.3201/eid1510.090196

Brambilla, C., Llorens-Fons, M., Julian, E., Noguera-Ortega, E., Tomas-Martinez, C., Perez-Trujillo, M., et al. (2016). *Mycobacteria* clumping increase their capacity to damage macrophages. *Front. Microbiol.* 7:1562. doi: 10.3389/fmicb.2016.01562

Brennan, P. J., Aspinall, G. O., and Shin, J. E. (1981). Structure of the specific oligosaccharides from the glycopeptidolipid antigens of serovars in the *Mycobacterium avium-Mycobacterium intracellulare-Mycobacterium scrofulaceum* complex. *J. Biol. Chem.* 256, 6817–6822.

Brown-Elliott, B. A., Nash, K. A., and Wallace, R. J. Jr. (2012). Antimicrobial susceptibility testing, drug resistance mechanisms, and therapy of infections with nontuberculous mycobacteria. *Clin. Microbiol. Rev.* 25, 545–582. doi: 10.1128/CMR.05030-11

Brown-Elliott, B. A., and Wallace, R. J. Jr. (2017). In vitro susceptibility testing of tedizolid against nontuberculous mycobacteria. *J. Clin. Microbiol.* 55, 1747–1754. doi: 10.1128/JCM.00274-17

Bryant, J. M., Grogono, D. M., Rodriguez-Rincon, D., Everall, I., Brown, K. P., Moreno, P., et al. (2016). Emergence and spread of a human-transmissible multidrug-resistant nontuberculous mycobacterium. *Science* 354, 751–757. doi: 10.1126/science.aaf8156

Burdette, S. D., and Trotman, R. (2015). Tedizolid: the first once-daily oxazolidinone class antibiotic. *Clin. Infect. Dis.* 61, 1315–1321. doi: 10.1093/cid/civ501

Byrd, T. F., Green, G. M., Fowlston, S. E., and Lyons, C. R. (1998). Differential growth characteristics and streptomycin susceptibility of virulent and avirulent *Mycobacterium tuberculosis* strains in a novel fibroblast-mycobacterium microcolony assay. *Infect. Immun.* 66, 5132–5139.

Byrd, T. F., and Lyons, C. R. (1999). Preliminary characterization of a *Mycobacterium abscessus* mutant in human and murine models of infection. *Infect. Immun.* 67, 4700–4707.

Cantin, A. M., Hartl, D., Konstan, M. W., and Chmiel, J. F. (2015). Inflammation in cystic fibrosis lung disease: pathogenesis and therapy. *J. Cyst. Fibros* 14, 419–430. doi: 10.1016/j.jcf.2015.03.003

Catherinot, E., Clarissou, J., Etienne, G., Ripoll, F., Emile, J. F., Daffe, M., et al. (2007). Hypervirulence of a rough variant of the *Mycobacterium abscessus* type strain. *Infect. Immun.* 75, 1055–1058. doi: 10.1128/IAI.00835-06

Catherinot, E., Roux, A. L., Macheras, E., Hubert, D., Matmar, M., Dannhoffer, L., et al. (2009). Acute respiratory failure involving an R variant of *Mycobacterium abscessus*. *J. Clin. Microbiol.* 47, 271–274. doi: 10.1128/JCM.01478-08

Chu, H. S., Chang, S. C., Shen, E. P., and Hu, F. R. (2015). Nontuberculous mycobacterial ocular infections–comparing the clinical and microbiological characteristics between *Mycobacterium abscessus* and *Mycobacterium massiliense*. *PLoS One* 10:e0116236. doi: 10.1371/journal.pone.0116236

Clarke, L. L., Grubb, B. R., Yankaskas, J. R., Cotton, C. U., McKenzie, A., and Boucher, R. C. (1994). Relationship of a non-cystic fibrosis transmembrane conductance regulator-mediated chloride conductance to organ-level disease in Cftr(–/–) mice. *Proc. Natl. Acad. Sci. U.S.A.* 91, 479–483. doi: 10.1073/pnas.91.2.479

Clary, G., Sasindran, S. J., Nesbitt, N., Mason, L., Cole, S., Azad, A., et al. (2018). *Mycobacterium abscessus* smooth and rough morphotypes form antimicrobial-tolerant biofilm phenotypes but are killed by acetic acid. *Antimicrob. Agents Chemother.* 62:e01782-17. doi: 10.1128/AAC.01782-17

CLSI (2011). *Susceptibility Testing of Mycobacteria, Nocardiae and Other Aerobic Actinomycetes*. Wayne, PA: Clinical and Laboratory Standards Institute (CLSI).

Davidson, L. B., Nessar, R., Kempaiah, P., Perkins, D. J., and Byrd, T. F. (2011). *Mycobacterium abscessus* glycopeptidolipid prevents respiratory epithelial TLR2 signaling as measured by HβD2 gene expression and IL-8 Release. *PLoS One* 6:e29148. doi: 10.1371/journal.pone.0029148

De Groote, M. A., Johnson, L., Podell, B., Brooks, E., Basaraba, R., and Gonzalez-Juarrero, M. (2014). GM-CSF knockout mice for preclinical testing of agents with antimicrobial activity against *Mycobacterium abscessus*. *J. Antimicrob. Chemother.* 69, 1057–1064. doi: 10.1093/jac/dkt451

Donohue, M. J. (2018). Increasing nontuberculous mycobacteria reporting rates and species diversity identified in clinical laboratory reports. *BMC Infect. Dis.* 18:163. doi: 10.1186/s12879-018-3043-7

Dorgan, D. J., and Hadjiliadis, D. (2014). Lung transplantation in patients with cystic fibrosis: special focus to infection and comorbidities. *Exp. Rev. Respirat. Med.* 8, 315–326. doi: 10.1586/17476348.2014.899906

Everall, I., Nogueira, C. L., Bryant, J. M., Sanchez-Buso, L., Chimara, E., Duarte, R. D. S., et al. (2017). Genomic epidemiology of a national outbreak of post-surgical *Mycobacterium abscessus* wound infections in Brazil. *Microb. Genome* 3:e000111. doi: 10.1099/mgen.0.000111

Fukui, S., Sekiya, N., Takizawa, Y., Morioka, H., Kato, H., Aono, A., et al. (2015). Disseminated *Mycobacterium abscessus* infection following septic arthritis: a case report and review of the literature. *Medicine (Baltimore)* 94:e861. doi: 10.1097/MD.0000000000000861

Greendyke, R., and Byrd, T. F. (2008). Differential antibiotic susceptibility of *Mycobacterium abscessus* variants in biofilms and macrophages compared to that of planktonic bacteria. *Antimicrob. Agents Chemother.* 52, 2019–2026. doi: 10.1128/AAC.00986-07

Griffith, D. E., Eagle, G., Thomson, R., Aksamit, T. R., Hasegawa, N., Morimoto, K., et al. (2018). Amikacin liposome inhalation suspension for treatment-refractory lung disease caused by *Mycobacterium avium* complex (CONVERT): a prospective, open-label, randomized study. *Am. J. Respir Crit. Care Med.* doi: 10.1164/rccm.201807-1318OC [Epub ahead of print].

Griffith, D. E., Girard, W., and Wallace, R. J. Jr. (1993). Clinical features of pulmonary disease caused by rapidly growing mycobacteria. An analysis of 154 patients. *Am. Rev. Respir. Dis.* 147, 1271–1278. doi: 10.1164/ajrccm/147.5.1271

Gupta, R., Netherton, M., Byrd, T. F., and Rohde, K. H. (2017). Reporter-based assays for high-throughput drug screening against *Mycobacterium abscessus*. *Front. Microbiol.* 8:2204. doi: 10.3389/fmicb.2017.02204

Halloum, I., Carrere-Kremer, S., Blaise, M., Viljoen, A., Bernut, A., Le Moigne, V., et al. (2016). Deletion of a dehydratase important for intracellular growth and cording renders rough *Mycobacterium abscessus* avirulent. *Proc. Natl. Acad. Sci. U.S.A.* 113, E4228–E4237. doi: 10.1073/pnas.1605477113

Hall-Stoodley, L., Brun, O. S., Polshyna, G., and Barker, L. P. (2006). *Mycobacterium marinum* biofilm formation reveals cording morphology. *FEMS Microbiol. Lett.* 257, 43–49. doi: 10.1111/j.1574-6968.2006.00143.x

Howard, S. T., and Byrd, T. F. (2000). The rapidly growing mycobacteria: saprophytes and parasites. *Microbes Infect. Institut. Pasteur.* 2, 1845–1853. doi: 10.1016/S1286-4579(00)01338-1

Howard, S. T., Byrd, T. F., and Lyons, C. R. (2002). A polymorphic region in *Mycobacterium abscessus* contains a novel insertion sequence element. *Microbiology* 148(Pt 10), 2987–2996. doi: 10.1099/00221287-148-10-2987

Howard, S. T., Rhoades, E., Recht, J., Pang, X., Alsup, A., Kolter, R., et al. (2006). Spontaneous reversion of *Mycobacterium abscessus* from a smooth to a rough morphotype is associated with reduced expression of glycopeptidolipid and reacquisition of an invasive phenotype. *Microbiology* 152(Pt 6), 1581–1590. doi: 10.1099/mic.0.28625-0

Jarand, J., Levin, A., Zhang, L., Huitt, G., Mitchell, J. D., and Daley, C. L. (2011). Clinical and microbiologic outcomes in patients receiving treatment for *Mycobacterium abscessus* pulmonary disease. *Clin. Infect. Dis.* 52, 565–571. doi: 10.1093/cid/ciq237

Jeong, S. H., Kim, S. Y., Huh, H. J., Ki, C. S., Lee, N. Y., Kang, C. I., et al. (2017). Mycobacteriological characteristics and treatment outcomes in extrapulmonary *Mycobacterium abscessus* complex infections. *Int. J. Infect. Dis.* 60, 49–56. doi: 10.1016/j.ijid.2017.05.007

Johnson, C. M., Lyle, E., Omueti, K. O., Stepensky, V. A., Yegin, O., Alpsoy, E., et al. (2007). Cutting edge: a common polymorphism impairs cell surface trafficking and functional responses of TLR1 but protects against leprosy. *J. Immunol.* 178, 7520–7524. doi: 10.4049/jimmunol.178.12.7520

Jonsson, B. E., Gilljam, M., Lindblad, A., Ridell, M., Wold, A. E., and Welinder-Olsson, C. (2007). Molecular epidemiology of *Mycobacterium abscessus*, with focus on cystic fibrosis. *J. Clin. Microbiol.* 45, 1497–1504. doi: 10.1128/JCM.02592-06

Kaushik, A., Gupta, C., Fisher, S., Story-Roller, E., Galanis, C., Parrish, N., et al. (2017). Combinations of avibactam and carbapenems exhibit enhanced potencies against drug-resistant *Mycobacterium abscessus*. *Future Microbiol.* 12, 473–480. doi: 10.2217/fmb-2016-0234

Kempaiah, P., Davidson, L. B., Perkins, D. J., and Byrd, T. F. (2013). Cystic fibrosis CFBE41o- cells contain TLR1 SNP I602S and fail to respond to *Mycobacterium abscessus*. *J. Cyst. Fibr.* 12, 773–779. doi: 10.1016/j.jcf.2013.01.001

Koh, W. J., Jeon, K., Lee, N. Y., Kim, B. J., Kook, Y. H., Lee, S. H., et al. (2011). Clinical significance of differentiation of *Mycobacterium massiliense* from *Mycobacterium abscessus*. *Am. J. Respir. Crit. Care Med.* 183, 405–410. doi: 10.1164/rccm.201003-0395OC

Kreutzfeldt, K. M., McAdam, P. R., Claxton, P., Holmes, A., Seagar, A. L., Laurenson, I. F., et al. (2013). Molecular longitudinal tracking of *Mycobacterium abscessus* spp. during chronic infection of the human lung. *PLoS One* 8:e63237. doi: 10.1371/journal.pone.0063237

Kusunoki, S., and Ezaki, T. (1992). Proposal of *Mycobacterium peregrinum* sp. nov., nom. rev., and elevation of *Mycobacterium chelonae* subsp. abscessus (Kubica et al.) to species status: *Mycobacterium abscessus* comb. nov. *Int. J. Syst. Bacteriol.* 42, 240–245. doi: 10.1099/00207713-42-2-240

Laencina, L., Dubois, V., Le Moigne, V., Viljoen, A., Majlessi, L., Pritchard, J., et al. (2018). Identification of genes required for *Mycobacterium abscessus* growth in vivo with a prominent role of the ESX-4 locus. *Proc. Natl. Acad. Sci. U.S.A.* 115, E1002–E1011. doi: 10.1073/pnas.1713195115

Landersdorfer, C. B., Bulitta, J. B., Kinzig, M., Holzgrabe, U., and Sorgel, F. (2009). Penetration of antibacterials into bone: pharmacokinetic, pharmacodynamic and bioanalytical considerations. *Clin. Pharmacokinet.* 48, 89–124. doi: 10.2165/0003088-200948020-00002

Le Run, E., Arthur, M., and Mainardi, J. L. (2018). In vitro and intracellular activity of imipenem combined to rifabutin and avibactam against *Mycobacterium abscessus*. *Antimicrob Agents Chemother.* 62:e00623-18. doi: 10.1128/AAC.00623-18

Lim, A. Y. H., Chotirmall, S. H., Fok, E. T. K., Verma, A., De, P. P., Goh, S. K., et al. (2018). Profiling non-tuberculous mycobacteria in an Asian setting: characteristics and clinical outcomes of hospitalized patients in Singapore. *BMC Pulm Med* 18:85. doi: 10.1186/s12890-018-0637-1

Llorens-Fons, M., Perez-Trujillo, M., Julian, E., Brambilla, C., Alcaide, F., Byrd, T. F., et al. (2017). Trehalose polyphleates, external cell wall lipids in *Mycobacterium abscessus*, are associated with the formation of clumps with cording morphology, which have been associated with virulence. *Front. Microbiol.* 8:1402. doi: 10.3389/fmicb.2017.01402

Lopez-Marin, L. M., Gautier, N., Laneelle, M. A., Silve, G., and Daffe, M. (1994). Structures of the glycopeptidolipid antigens of *Mycobacterium abscessus* and *Mycobacterium chelonae* and possible chemical basis of the serological cross-reactions in the *Mycobacterium fortuitum* complex. *Microbiology* 140, 1109–1118. doi: 10.1099/13500872-140-5-1109

Luthra, S., Rominski, A., and Sander, P. (2018). The role of antibiotic-target-modifying and antibiotic-modifying enzymes in *Mycobacterium abscessus* drug resistance. *Front. Microbiol.* 9:2179. doi: 10.3389/fmicb.2018.02179

Malcolm, K. C., Nichols, E. M., Caceres, S. M., Kret, J. E., Martiniano, S. L., Sagel, S. D., et al. (2013). *Mycobacterium abscessus* induces a limited pattern of neutrophil activation that promotes pathogen survival. *PLoS One* 8:e57402. doi: 10.1371/journal.pone.0057402

Martinez-Garcia, M. A., de la Rosa Carrillo, D., Soler-Cataluna, J. J., Donat-Sanz, Y., Serra, P. C., Lerma, M. A., et al. (2013). Prognostic value of bronchiectasis in patients with moderate-to-severe chronic obstructive pulmonary disease. *Am. J. Respir. Crit. Care Med.* 187, 823–831. doi: 10.1164/rccm.201208-1518OC

Maurer, F. P., Bruderer, V. L., Ritter, C., Castelberg, C., Bloemberg, G. V., and Bottger, E. C. (2014). Lack of antimicrobial bactericidal activity in *Mycobacterium abscessus*. *Antimicrob. Agents Chemother.* 58, 3828–3836. doi: 10.1128/AAC.02448-14

Moore, M., and Frerichs, J. B. (1953). An unusual acid-fast infection of the knee with subcutaneous, abscess-like lesions of the gluteal region; report of a case with a study of the organism, *Mycobacterium abscessus*, n. sp. *J. Invest Dermatol.* 20, 133–169. doi: 10.1038/jid.1953.18

Nagano, H., Kinjo, T., Nei, Y., Yamashiro, S., Fujita, J., and Kishaba, T. (2017). Causative species of nontuberculous mycobacterial lung disease and comparative investigation on clinical features of *Mycobacterium abscessus* complex disease: a retrospective analysis for two major hospitals in a subtropical region of Japan. *PLoS One* 12:e0186826. doi: 10.1371/journal.pone.0186826

Nash, K. A., Brown-Elliott, B. A., and Wallace, R. J. Jr. (2009). A novel gene, erm(41), confers inducible macrolide resistance to clinical isolates of *Mycobacterium abscessus* but is absent from *Mycobacterium chelonae*. *Antimicrob. Agents Chemother.* 53, 1367–1376. doi: 10.1128/AAC.01275-08

Nataraj, V., Pang, P. C., Haslam, S. M., Veerapen, N., Minnikin, D. E., Dell, A., et al. (2015). MKAN27435 is required for the biosynthesis of higher subclasses of lipooligosaccharides in *Mycobacterium kansasii*. *PLoS One* 10:e0122804. doi: 10.1371/journal.pone.0122804

Nau, R., Sorgel, F., and Eiffert, H. (2010). Penetration of drugs through the blood-cerebrospinal fluid/blood-brain barrier for treatment of central nervous system infections. *Clin. Microbiol. Rev.* 23, 858–883. doi: 10.1128/CMR.00007-10

Nessar, R., Cambau, E., Reyrat, J. M., Murray, A., and Gicquel, B. (2012). *Mycobacterium abscessus*: a new antibiotic nightmare. *J. Antimicrob. Chemother.* 67, 810–818. doi: 10.1093/jac/dkr578

Nessar, R., Reyrat, J. M., Davidson, L. B., and Byrd, T. F. (2011). Deletion of the mmpL4b gene in the *Mycobacterium abscessus* glycopeptidolipid biosynthetic pathway results in loss of surface colonization capability, but enhanced ability to replicate in human macrophages and stimulate their innate immune response. *Microbiology* 157(Pt 4), 1187–1195. doi: 10.1099/mic.0.046557-0

Nigo, M., Luce, A. M., and Arias, C. A. (2018). Long-term use of tedizolid as suppressive therapy for recurrent methicillin-resistant *Staphylococcus aureus* graft infection. *Clin. Infect. Dis.* 66, 1975–1976. doi: 10.1093/cid/ciy041

Noone, P. G., Leigh, M. W., Sannuti, A., Minnix, S. L., Carson, J. L., Hazucha, M., et al. (2004). Primary ciliary dyskinesia: diagnostic and phenotypic features. *Am. J. Respir. Crit. Care Med.* 169, 459–467. doi: 10.1164/rccm.200303-365OC

Olivier, K. N., Griffith, D. E., Eagle, G., McGinnis, J. P. II, Micioni, L., Liu, K., et al. (2017). Randomized trial of liposomal amikacin for inhalation in nontuberculous mycobacterial lung disease. *Am. J. Respir. Crit. Care Med.* 195, 814–823. doi: 10.1164/rccm.201604-0700OC

Olivier, K. N., Shaw, P. A., Glaser, T. S., Bhattacharyya, D., Fleshner, M., Brewer, C. C., et al. (2014). Inhaled amikacin for treatment of refractory pulmonary nontuberculous mycobacterial disease. *Ann. Am. Thorac. Soc.* 11, 30–35. doi: 10.1513/AnnalsATS.201307-231OC

Patel, I. S., Vlahos, I., Wilkinson, T. M., Lloyd-Owen, S. J., Donaldson, G. C., Wilks, M., et al. (2004). Bronchiectasis, exacerbation indices, and inflammation in chronic obstructive pulmonary disease. *Am. J. Respir. Crit. Care Med.* 170, 400–407. doi: 10.1164/rccm.200305-648OC

Petrini, B., Farnebo, F., Hedblad, M. A., and Appelgren, P. (2006). Concomitant late soft tissue infections by *Cladophialophora bantiana* and *Mycobacterium abscessus* following tsunami injuries. *Med. Mycol.* 44, 189–192. doi: 10.1080/13693780500294949

Phoompoung, P., Ankasekwinai, N., Pithukpakorn, M., Foongladda, S., Umrod, P., Suktitipat, B., et al. (2017). Factors associated with acquired Anti IFN- gamma autoantibody in patients with nontuberculous mycobacterial infection. *PLoS One* 12:e0176342. doi: 10.1371/journal.pone.0176342

Prevots, D. R., and Marras, T. K. (2015). Epidemiology of human pulmonary infection with nontuberculous mycobacteria: a review. *Clin. Chest. Med.* 36, 13–34. doi: 10.1016/j.ccm.2014.10.002

Prevots, D. R., Shaw, P. A., Strickland, D., Jackson, L. A., Raebel, M. A., Blosky, M. A., et al. (2010). Nontuberculous mycobacterial lung disease prevalence at four integrated health care delivery systems. *Am. J. Respir. Crit. Care Med.* 182, 970–976. doi: 10.1164/rccm.201002-0310OC

Qvist, T., Eickhardt, S., Kragh, K. N., Andersen, C. B., Iversen, M., Hoiby, N., et al. (2015). Chronic pulmonary disease with *Mycobacterium abscessus* complex is a biofilm infection. *Eur. Respir. J.* 46, 1823–1826. doi: 10.1183/13993003.01102-2015

Rhoades, E. R., Archambault, A. S., Greendyke, R., Hsu, F. F., Streeter, C., and Byrd, T. F. (2009). *Mycobacterium abscessus* glycopeptidolipids mask underlying cell wall phosphatidyl-myo-inositol mannosides blocking induction of human macrophage TNF- by preventing interaction with TLR2. *J. Immunol.* 183, 1997–2007. doi: 10.4049/jimmunol.0802181

Rieber, N., Hector, A., Carevic, M., and Hartl, D. (2014). Current concepts of immune dysregulation in cystic fibrosis. *Int. J. Biochem. Cell Biol.* 52, 108–112. doi: 10.1016/j.biocel.2014.01.017

Ripoll, F., Pasek, S., Schenowitz, C., Dossat, C., Barbe, V., Rottman, M., et al. (2009). Non mycobacterial virulence genes in the genome of the emerging pathogen *Mycobacterium abscessus*. *PLoS One* 4:e5660. doi: 10.1371/journal.pone.0005660

Roux, A. L., Viljoen, A., Bah, A., Simeone, R., Bernut, A., Laencina, L., et al. (2016). The distinct fate of smooth and rough Mycobacterium

abscessus variants inside macrophages. *Open Biol.* 6:160185. doi: 10.1098/rsob.160185

Ryu, H. J., Kim, W. J., Oh, C. H., and Song, H. J. (2005). Iatrogenic *Mycobacterium abscessus* infection associated with acupuncture: clinical manifestations and its treatment. *Int. J. Dermatol.* 44, 846–850. doi: 10.1111/j.1365-4632.2005.02241.x

Sanchez-Chardi, A., Olivares, F., Byrd, T. F., Julian, E., Brambilla, C., and Luquin, M. (2011). Demonstration of cord formation by rough *Mycobacterium abscessus* variants: implications for the clinical microbiology laboratory. *J. Clin. Microbiol.* 49, 2293–2295. doi: 10.1128/JCM.02322-10

Schnabel, D., Esposito, D. H., Gaines, J., Ridpath, A., Barry, M. A., Feldman, K. A., et al. (2016). Multistate US outbreak of rapidly growing mycobacterial infections associated with medical tourism to the dominican republic, 2013-2014(1). *Emerg. Infect. Dis.* 22, 1340–1347. doi: 10.3201/eid2208.151938

Scholze, A., Loddenkemper, C., Grunbaum, M., Moosmayer, I., Offermann, G., and Tepel, M. (2005). Cutaneous *Mycobacterium abscessus* infection after kidney transplantation. *Nephrol. Dial. Transplant.* 20, 1764–1765. doi: 10.1093/ndt/gfh736

Shallom, S. J., Moura, N. S., Olivier, K. N., Sampaio, E. P., Holland, S. M., and Zelazny, A. M. (2015). New real-time PCR assays for detection of inducible and acquired clarithromycin resistance in the *Mycobacterium abscessus* group. *J. Clin. Microbiol.* 53, 3430–3437. doi: 10.1128/JCM.01714-15

Sharma, D., and Kanneganti, T. D. (2016). The cell biology of inflammasomes: mechanisms of inflammasome activation and regulation. *J. Cell Biol.* 213, 617–629. doi: 10.1083/jcb.201602089

Spaulding, A. B., Lai, Y. L., Zelazny, A. M., Olivier, K. N., Kadri, S. S., Prevots, D. R., et al. (2017). Geographic distribution of nontuberculous mycobacterial species identified among clinical isolates in the united states, 2009-2013. *Ann. Am. Thorac. Soc.* 14, 1655–1661. doi: 10.1513/AnnalsATS.201611-860OC

Sweet, L., and Schorey, J. S. (2006). Glycopeptidolipids from *Mycobacterium avium* promote macrophage activation in a TLR2- and MyD88-dependent manner. *J. Leukoc. Biol.* 80, 415–423. doi: 10.1189/jlb.1205702

Tan, C. K., Lai, C. C., Liao, C. H., Chou, C. H., Hsu, H. L., Huang, Y. T., et al. (2010). Mycobacterial bacteraemia in patients infected and not infected with human immunodeficiency virus, Taiwan. *Clin. Microbiol. Infect.* 16, 627–630. doi: 10.1111/j.1469-0691.2009.02939.x

Tan, J. L., Ng, K. P., Ong, C. S., and Ngeow, Y. F. (2017). Genomic comparisons reveal microevolutionary differences in *Mycobacterium abscessus* subspecies. *Front. Microbiol.* 8:2042. doi: 10.3389/fmicb.2017.02042

Thomson, R. M., Armstrong, J. G., and Looke, D. F. (2007). Gastroesophageal reflux disease, acid suppression, and *Mycobacterium avium* complex pulmonary disease. *Chest* 131, 1166–1172. doi: 10.1378/chest.06-1906

Tu, H. Z., Chang, S. H., Huaug, T. S., Huaug, W. K., Liu, Y. C., and Lee, S. S. (2003). Microscopic morphology in smears prepared from MGIT broth medium for rapid presumptive identification of *Mycobacterium tuberculosis* complex, *Mycobacterium avium* complex and *Mycobacterium kansasii*. *Ann. Clin. Lab. Sci.* 33, 179–183.

Umrao, J., Singh, D., Zia, A., Saxena, S., Sarsaiya, S., Singh, S., et al. (2016). Prevalence and species spectrum of both pulmonary and extrapulmonary nontuberculous mycobacteria isolates at a tertiary care center. *Int. J. Mycobacteriol.* 5, 288–293. doi: 10.1016/j.ijmyco.2016.06.008

Whang, J., Back, Y. W., Lee, K. I., Fujiwara, N., Paik, S., Choi, C. H., et al. (2017). *Mycobacterium abscessus* glycopeptidolipids inhibit macrophage apoptosis and bacterial spreading by targeting mitochondrial cyclophilin D. *Cell Death Dis.* 8:e3012. doi: 10.1038/cddis.2017.420

Winthrop, K. L., Chang, E., Yamashita, S., Iademarco, M. F., and LoBue, P. A. (2009). Nontuberculous mycobacteria infections and anti-tumor necrosis factor-alpha therapy. *Emerg. Infect. Dis.* 15, 1556–1561. doi: 10.3201/eid1510.090310

Yagi, K., Ishii, M., Namkoong, H., Asami, T., Iketani, O., Asakura, T., et al. (2017). The efficacy, safety, and feasibility of inhaled amikacin for the treatment of difficult-to-treat non-tuberculous mycobacterial lung diseases. *BMC Infect. Dis.* 17:558. doi: 10.1186/s12879-017-2665-5

Yuan, J., Liu, Y., Yang, Z., Cai, Y., Deng, Z., Qin, P., et al. (2009). *Mycobacterium abscessus* post-injection abscesses from extrinsic contamination of multiple-dose bottles of normal saline in a rural clinic. *Int. J. Infect. Dis.* 13, 537–542. doi: 10.1016/j.ijid.2008.11.024

Zhang, J., Leifer, F., Rose, S., Chun, D. Y., Thaisz, J., Herr, T., et al. (2018). Amikacin liposome inhalation suspension (ALIS) penetrates non-tuberculous mycobacterial biofilms and enhances amikacin uptake into macrophages. *Front. Microbiol.* 9:915. doi: 10.3389/fmicb.2018.00915

Conflict of Interest Statement: The authors declare that the research was conducted in the absence of any commercial or financial relationships that could be construed as a potential conflict of interest.

frontiers in Microbiology

REVIEW
published: 12 September 2018
doi: 10.3389/fmicb.2018.02179

The Role of Antibiotic-Target-Modifying and Antibiotic-Modifying Enzymes in *Mycobacterium abscessus* Drug Resistance

*Sakshi Luthra[1], Anna Rominski[1] and Peter Sander[1,2]**

[1] Institute of Medical Microbiology, University of Zurich, Zurich, Switzerland, [2] National Center for Mycobacteria, Zurich, Switzerland

OPEN ACCESS

Edited by:
Thomas Dick,
Rutgers, The State University of New Jersey, Newark, United States

Reviewed by:
Uday Suryan Ganapathy,
Rutgers, The State University of New Jersey, Newark, United States
Juan Manuel Belardinelli,
Colorado State University, United States

***Correspondence:**
Peter Sander
psander@imm.uzh.ch

Specialty section:
This article was submitted to Antimicrobials, Resistance and Chemotherapy, a section of the journal Frontiers in Microbiology

Received: 02 July 2018
Accepted: 24 August 2018
Published: 12 September 2018

Citation:
Luthra S, Rominski A and Sander P (2018) The Role of Antibiotic-Target-Modifying and Antibiotic-Modifying Enzymes in Mycobacterium abscessus Drug Resistance. Front. Microbiol. 9:2179. doi: 10.3389/fmicb.2018.02179

The incidence and prevalence of non-tuberculous mycobacterial (NTM) infections have been increasing worldwide and lately led to an emerging public health problem. Among rapidly growing NTM, *Mycobacterium abscessus* is the most pathogenic and drug resistant opportunistic germ, responsible for disease manifestations ranging from "curable" skin infections to only "manageable" pulmonary disease. Challenges in *M. abscessus* treatment stem from the bacteria's high-level innate resistance and comprise long, costly and non-standardized administration of antimicrobial agents, poor treatment outcomes often related to adverse effects and drug toxicities, and high relapse rates. Drug resistance in *M. abscessus* is conferred by an assortment of mechanisms. Clinically acquired drug resistance is normally conferred by mutations in the target genes. Intrinsic resistance is attributed to low permeability of *M. abscessus* cell envelope as well as to (multi)drug export systems. However, expression of numerous enzymes by *M. abscessus*, which can modify either the drug-target or the drug itself, is the key factor for the pathogen's phenomenal resistance to most classes of antibiotics used for treatment of other moderate to severe infectious diseases, like macrolides, aminoglycosides, rifamycins, β-lactams and tetracyclines. In 2009, when *M. abscessus* genome sequence became available, several research groups worldwide started studying *M. abscessus* antibiotic resistance mechanisms. At first, lack of tools for *M. abscessus* genetic manipulation severely delayed research endeavors. Nevertheless, the last 5 years, significant progress has been made towards the development of conditional expression and homologous recombination systems for *M. abscessus*. As a result of recent research efforts, an erythromycin ribosome methyltransferase, two aminoglycoside acetyltransferases, an aminoglycoside phosphotransferase, a rifamycin ADP-ribosyltransferase, a β-lactamase and a monooxygenase were identified to frame the complex and multifaceted intrinsic resistome of *M. abscessus*, which clearly contributes to complications in treatment of this highly resistant pathogen. Better knowledge of the underlying mechanisms of drug resistance in *M. abscessus* could improve selection of more effective chemotherapeutic regimen and promote

development of novel antimicrobials which can overwhelm the existing resistance mechanisms. This article reviews the currently elucidated molecular mechanisms of antibiotic resistance in *M. abscessus*, with a focus on its drug-target-modifying and drug-modifying enzymes.

Keywords: non-tuberculous mycobacteria, *Mycobacterium abscessus*, antibiotic, drug resistance, resistance genes, antibiotic-target-modifying enzymes, antibiotic-modifying enzymes

INTRODUCTION

Non-tuberculous mycobacteria (NTM) encompass all species of mycobacteria that do not cause tuberculosis (TB) or leprosy (Lee et al., 2015). NTM are ubiquitous in the environment and occasionally infect humans with various predisposing conditions like cystic fibrosis, bronchiectasis or immunosuppression, causing a variety of pathological conditions including pulmonary, skin and soft tissue infections and disseminated diseases (Chan and Iseman, 2013). The last few decades saw an alarming increase in the incidence and prevalence of NTM-pulmonary disease throughout the globe. Importantly, more than 90% of all reported NTM-pulmonary disease cases involved infections with the *Mycobacterium avium* complex (comprising of *M. avium*, *Mycobacterium chimaera* and *Mycobacterium intracellulare*) or *Mycobacterium abscessus*, accentuating the medical importance of these emerging pathogens (Hoefsloot et al., 2013; Ryu et al., 2016; Wu et al., 2018). For a long while, it was believed that infections with genetically diverse NTM strains were exclusively acquired upon exposure to the environment. However, a recent whole genome analysis of more than 1000 *M. abscessus* clinical isolates from different geographical locations, revealed the presence of genetically clustered strains in patients. This suggests a human-to-human transmission of *M. abscessus*, presumably through indirect mechanisms like cough aerosols or surface contamination (Bryant et al., 2016).

Mycobacterium abscessus is an opportunistic pathogen, ubiquitous in the environment, that often causes infections in humans with compromised natural defenses such as patients with cystic fibrosis or other chronic lung diseases (Sanguinetti et al., 2001; Brown-Elliott and Wallace, 2002; Howard, 2006; Griffith et al., 2007). A current taxonomic classification suggests separation of *M. abscessus* into three distinct subspecies: *M. abscessus* subsp. *abscessus*, *M. abscessus* subsp. *bolletii,* and *M. abscessus* subsp. *massiliense* (Tortoli et al., 2016). Although a saprophyte in water and soil, following lung infection *M. abscessus* can swiftly grow and survive intra-cellularly within macrophages as well as in extra-cellular caseous lesions and airway mucus (Wu et al., 2018). Several factors contribute to the success of this rapidly growing mycobacterium. A plethora of intrinsic resistance mechanisms renders almost all clinically used antibiotics ineffective against *M. abscessus* (Nessar et al., 2012). In addition, the presence of a highly dynamic open pan-genome in *M. abscessus* might explain the ease with which the bacterium evolves and adapts to a wide-spectrum of stressful environmental conditions encountered in diverse habitats (Choo et al., 2014; Wu et al., 2018). Importantly, the respiratory habitat of *M. abscessus* brings it in close proximity to highly virulent pathogens (for example, *Pseudomonas aeruginosa* in cystic fibrosis lung) which can serve as donors of novel drug resistance or virulence genes (Ripoll et al., 2009).

Treatment of an *M. abscessus* pulmonary infection is very difficult owing to the bacterium's high-level innate resistance towards most antibiotics commonly used for Gram-negative and Gram-positive bacterial infections including majority of β-lactams, tetracyclines, aminoglycosides and macrolides. In addition, anti-TB drugs including first-line drugs (such as rifampicin and isoniazid) as well as some second-line agents (such as capreomycin) are ineffective against this pathogen (**Table 1**). Thus, the term "incurable nightmare" is often used to describe *M. abscessus* (Brown-Elliott et al., 2012; Nessar et al., 2012). So far, no reliable antibiotic regimen has been established for *M. abscessus* pulmonary disease. Antibiotic administration is largely empirical and relies on *in vitro* antibiotic susceptibility testing and definitive subspecies identification (Griffith et al., 2007; Ryu et al., 2016). Treatment of *M. abscessus* pulmonary disease as recommended by the British Thoracic Society involves administration of a multi-drug regimen encompassing intravenous antibiotics - amikacin, tigecycline, and imipenem along with an oral macrolide (clarithromycin or azithromycin) for clinical isolates susceptible to macrolides, during the initial treatment phase. For the continuation phase of treatment, nebulised amikacin and an oral macrolide combined with one to three of the following oral antibiotics: linezolid, clofazimine, minocycline, co-trimoxazole, and moxifloxacin are generally recommended (Haworth et al., 2017). Standard of care calls for continuation of antibiotic therapy for a minimum of 12 months after culture conversion. However, microbiological eradication of *M. abscessus* bacilli from lung tissues, using recommended antibiotic regimens, is rare and recurrence is often after completion of a treatment course and successful symptom management (Jarand et al., 2011; Stout et al., 2016).

As a result of extensive, repeated or inappropriate use of macrolides and aminoglycosides, which inhibit protein biosynthesis by binding to the large and small ribosomal subunits, respectively, *M. abscessus* strains with clinically acquired pan-macrolide and pan-aminoglycoside resistance have emerged, due to mutation(s) in the corresponding 23S (*rrl*) and 16S (*rrs*) rRNA genes (Wallace et al., 1996; Prammananan et al., 1998; Maurer et al., 2012; Nessar et al., 2012). Acquired resistance to macrolides and aminoglycosides severely limits the remaining treatment options and highlights the urgent need for new antimicrobial agents.

Mechanisms underpinning intrinsic drug resistance of *M. abscessus* are multi-fold and fall into two main groups: first, the presence of a highly impermeable cell envelope

TABLE 1 | Drug susceptibility of *Mycobacterium abscessus* wild-type and isogenic mutants in comparison to screening concentrations for *M. tuberculosis* with decreased susceptibility.

Antimicrobial agent	*M. tuberculosis** (mg/L)	*M. abscessus* MIC (mg/L)	*M. abscessus* mutant MIC (mg/L)	Reference
Isoniazid	0.1	>512	*katG*$^{+}$ *(M. tb)*: 32	Pers. Communication
Rifampicin	1.0	128	Δ*arr*: 0.25	Rominski et al., 2017a
Ethambutol	5.0	64 (polymorphism in target gene)	N.A.	Alcaide et al., 1997
Capreomycin	2.5	>256	Δ*eis2*: 4	Rominski et al., 2017c
Clarithromycin	N.D.	64	Δ*erm*: 0.5	Choi et al., 2012
Kanamycin B	N.D.	8	Δ*aac(2′)*: 0.125	Rominski et al., 2017c
Amikacin	1.0	4	Δ*eis2*: 0.25	Rominski et al., 2017c
Streptomycin	1.0	32	Δ*str(3′′)*: 2	Dal Molin et al., 2017
Tetracycline	N.D.	60	Δ*tetX*: 4	Rudra et al., 2018
Amoxicillin	N.D.	>256	Δ*bla*: 8	Dubée et al., 2015
Ampicillin	N.D.	>256	Δ*bla*: 4	Dubée et al., 2015

Epidemiologic cutoff values (ECOFF; MGIT960) as defined by Cambau et al. (2015); MIC, minimal inhibitory concentration; N.A., Not available; N.D., Not determined.

and/or multi-drug efflux pumps might reduce the effective concentration of antibiotics within the bacterial cells; second, the genome of *M. abscessus* encodes several putative enzymes which can inactivate antibiotics by modification and/or degradation or lower the affinity of the drug for its target by modifying the target (Ripoll et al., 2009; Nessar et al., 2012). For long, molecular investigations aimed at elucidating antibiotic resistance mechanisms of *M. abscessus* were limited, however, significant progress has been made in recent years owing to the development of efficient tools for genetic manipulation of this bacterium (**Figure 1**). In this article, we provide an up-to-date overview of the main molecular mechanisms of antibiotic resistance in *M. abscessus* with a focus on the drug-target-modifying or drug-modifying enzymes and discuss the potential impact on clinical treatment. We also discuss how this knowledge could facilitate the discovery and development of new improved antimicrobial agents or help rescue the function of currently available antibiotics against *M. abscessus* and provide an update on the latest research underway to combat multi-drug resistant *M. abscessus* infections.

ANTIBIOTIC-TARGET-MODIFYING ENZYMES IN *M. abscessus*

Macrolide Resistance: MAB_2297 [*erm*(41)] Encoded Erythromycin Ribosome Methylase

Macrolides are among the most successful antibiotics in the world and are highly prescribed for infections caused by non-tuberculous mycobacteria. A multidrug regimen recommended for *M. abscessus* infections almost always includes macrolides, particularly clarithromycin or azithromycin. Macrolides target the nascent polypeptide exit tunnel within the 50S ribosomal subunit, which accommodates the newly synthesized polypeptide chain as it emerges from the ribosome. Following macrolide binding, the elongation of polypeptide chain continues up to a few amino acids before the peptidyl-tRNA dissociates from the ribosome thereby arresting protein synthesis (Wilson, 2014).

In bacteria, innate resistance towards macrolides is most often the result of increased efflux, ribosomal methyltransferases and GTP-dependent macrolide kinases (Pawlowski et al., 2018). A well-studied example of macrolide resistance by target modification in bacteria is the erythromycin ribosome methylase (Erm) enzyme, which specifically methylates A2058 nucleotide of 23S rRNA and lowers the macrolide affinity for ribosome exit tunnel (Blair et al., 2015). An Erm methyltransferase is also responsible for inducible macrolide resistance in *M. abscessus* (**Figure 1**). Interestingly, the *erm*(41) gene, first described by Nash et al. (2009), is only functional in two out of three subspecies of the *M. abscessus* complex. The subspecies *M. massiliense* harbors deletions in its *erm*(41) gene copy which render the Erm(41) enzyme inactive and the bacterium susceptible to macrolides. This may explain why patients with *M. massiliense* infections have better treatment outcomes than patients with *M. abscessus* or *M. bolletii* infections. To further complicate matters, a T/C polymorphism at position 28 of the *erm*(41) sequence determines the appearance of inducible macrolide resistance in *M. bolletii* and *M. abscessus* subspecies. Only those isolates that harbor a T28 *erm*(41) sequevar develop inducible macrolide resistance. Phenotypic detection of inducible macrolide resistance in the *M. abscessus* complex by drug susceptibility testing requires extended incubation (14 days rather than 3 days) in the presence of the drug (Nash et al., 2009; Kim et al., 2010).

A functional role of *erm*(41) in inducible resistance to macrolides has been confirmed by genetic studies. Deletion of *erm*(41) in *M. abscessus* lowered the minimal inhibitory concentration (MIC) of clarithromycin by 128-fold (**Table 1**), while introduction of a functional *M. abscessus erm*(41) gene into *M. massiliense* led to a 64-fold increase in the clarithromycin MIC on day 14 (Choi et al., 2012). Inducible Erm(41)-dependent rRNA methylation severely affects the efficacy of macrolides against *M. abscessus*. The long duration of partially effective macrolide therapy, eventually favors the emergence of isolates with high-level constitutive macrolide resistance. Mutations that alter the

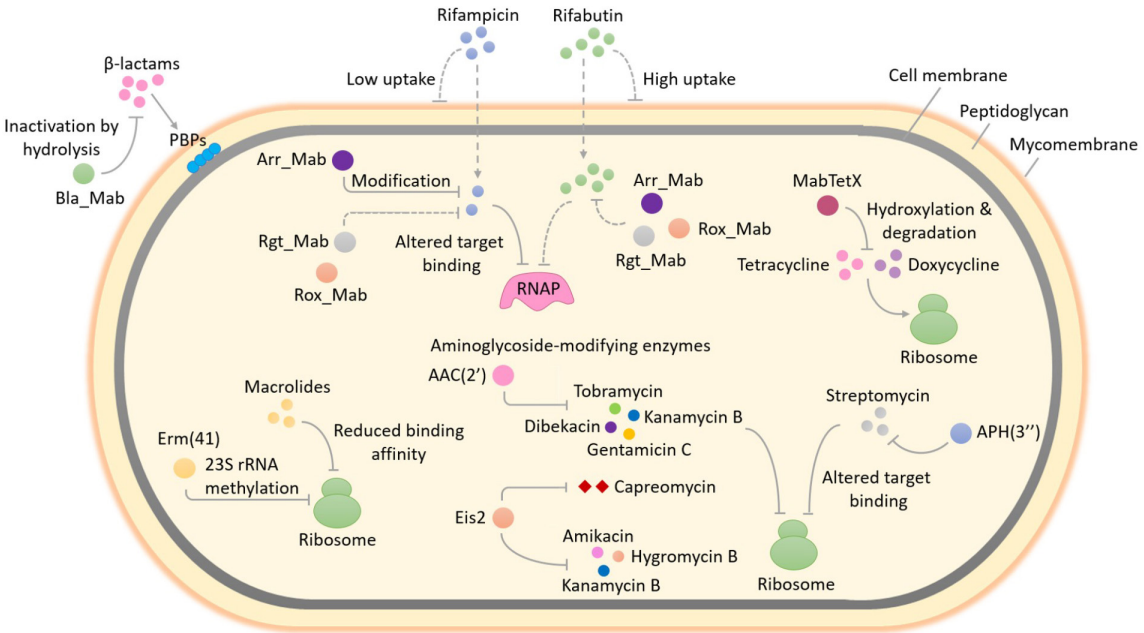

FIGURE 1 | Enzyme-mediated antibiotic resistance in *Mycobacterium abscessus*. *M. abscessus* is intrinsically resistant to a large and diverse array of antimicrobial agents. The occurrence of several enzymes that can modify and/or degrade antibiotics or alter their targets in *M. abscessus* enables it to resist the action of multiple classes of antibiotics. This figure provides an overview of the well-studied as well as some unexplored enzyme-mediated resistance mechanisms in *M. abscessus*. Methylation of 23S rRNA by Erm(41), an erythromycin ribosome methylase, lowers the binding affinity of macrolides for the ribosome exit tunnel and confers macrolide resistance. The expression of *erm*(41) gene in *M. abscessus* is induced upon exposure to macrolides, therefore this type of resistance by target modification is known as inducible macrolide resistance. The addition of different chemical groups including acyl and phosphate groups to vulnerable sites on the aminoglycoside molecule by *M. abscessus* enzymes can prevent the binding of aminoglycoside to its ribosomal target due to steric hindrance and result in resistance. A diverse group of enzymes that differ in the aminoglycosides that they can modify as well as in the region of the antibiotic that is modified, are found in *M. abscessus*. These include two putative acetyltransferases - AAC(2′) and Eis2 and one putative phosphotransferase - APH(3″). The substrate aminoglycosides for each enzyme are shown. In addition to aminoglycosides, Eis2 can also modify other ribosome-targeting antibiotics like capreomycin. Resistance to rifampicin and other rifamycin antibiotics in *M. abscessus* involves covalent modification and drug inactivation by an ADP-ribosyltransferase, Arr_Mab. Apart from ADP-ribosylation, two additional group transfer mechanisms of rifampicin inactivation including glycosylation, phosphorylation as well as decomposition of rifampicin by monooxygenation, are widespread in environmental bacteria but have not been explored in mycobacteria. Being a saprophyte in soil, exposure to antibiotic producing actinomycetes that utilize a variety of rifamycin inactivating mechanisms in its natural habitat might have favored the selection of an unknown reservoir of rifamycin resistance genes in *M. abscessus*, for example, those encoding a rifamycin glycosyltransferase (Rgt_Mab) and/or a rifamycin monooxygenase (Rox_Mab) (dashed lines). *M. abscessus* also produces a tetracycline-degrading flavin monooxygenase, MabTetX that activates molecular oxygen to hydroxylate and destabilize the antibiotic, which subsequently undergoes non-enzymatic decomposition, thereby conferring resistance. Resistance to β-lactams in *M. abscessus* is afforded by the production of a hydrolytic β-lactamase enzyme, Bla_Mab with the ability to degrade a broad range of β-lactams including extended-spectrum cephalosporins and carbapenems. RNAP, RNA polymerase; PBPs, penicillin-binding proteins; AAC(2′), 2′-*N*-acetyltransferase; Eis2, enhanced intracellular survival protein 2; APH(3″), aminoglycoside 3″-*O*-phosphotransferase.

23S rRNA nucleotides 2058 and 2059 within the peptidyl-transferase center (PTC), are a frequent cause of constitutive macrolide resistance in *M. abscessus* (Wallace et al., 1996; Bastian et al., 2011; Brown-Elliott et al., 2015).

ANTIBIOTIC-MODIFYING ENZYMES IN *M. abscessus*

Aminoglycoside Resistance: MAB_4395 [*aac(2′)*] & MAB_4532c (*eis2*) Encoded Acetyltransferases; MAB_2385 Encoded 3″-*O*-Phosphotransferase

Aminoglycosides are among the broadest classes of antibiotics that interfere with specific steps in bacterial protein synthesis (Kohanski et al., 2010). All aminoglycosides primarily target the 16S rRNA component of 30S ribosomal subunit, however, their exact binding site and mode of action may differ slightly depending on their chemical structure. For example, 2-deoxystreptamine (2-DOS) aminoglycosides (such as kanamycin, amikacin, apramycin, arbekacin), which are chemically distinct from the non-DOS aminoglycosides (for example, streptomycin), specifically bind to the A-site region of small ribosomal subunit at the decoding center, encompassing conserved nucleotides A1492 and A1493 of 16S rRNA. 2-DOS aminoglycosides function by inhibiting the translocation of tRNA-mRNA complex through the ribosome. Additionally, several members of this class also induce protein mistranslation by promoting and stabilizing the interaction of non-cognate aminoacylated tRNAs with mRNA. In contrast, the non-DOS aminoglycoside streptomycin targets a different region of 16S rRNA in proximity of the decoding center

and mainly interferes with the delivery of aminoacylated tRNA to the A-site (Wilson, 2014).

Bacterial resistance to aminoglycosides may occur due to low cell permeability/efflux, mutations or modification of 16S rRNA, mutations in ribosomal protein genes and enzymatic drug modification. Drug and target modification being the most extensively studied and clinically relevant aminoglycoside resistance mechanisms in pathogenic bacteria. Covalent modification of key amino or hydroxyl groups within the aminoglycoside molecule by bacterial enzymes markedly decreases the binding affinity for the ribosomal target and confers aminoglycoside resistance. Aminoglycoside-modifying enzymes in bacteria can be grouped into three main classes namely, acetyltransferases, nucleotidyltransferases, and phosphotransferases (D'Costa et al., 2011; Blair et al., 2015). A worrying discovery that the genome of emerging pathogen *M. abscessus* encodes several putative aminoglycoside-modifying enzymes which include members of all three classes, came in 2009 when Ripoll et al first sequenced the complete genome of *M. abscessus* (Ripoll et al., 2009). Some predictions were later substantiated by drug susceptibility testing and biochemical analysis (Maurer et al., 2015). More recently, direct genetic evidence for a functional role of some of these putative aminoglycoside-modifying enzymes in *M. abscessus* intrinsic resistance to this antibiotic class, was obtained.

Similar to all other mycobacteria that have been studied so far (Aínsa et al., 1997), *M. abscessus* also harbors a 2′-*N*-acetyltransferase [AAC(2′)], encoded by MAB_4395 gene. This enzyme is capable of acetylating several aminoglycosides bearing a 2′ amino group including gentamicin C, dibekacin, tobramycin and kanamycin B (**Figure 1**). This was evident upon deletion of MAB_4395 in *M. abscessus* ATCC 19977 strain which led to a 4-64-fold reduction in the MICs of these aminoglycosides (**Table 1**) (Rominski et al., 2017c). Interestingly, another *N*-acetyltransferase capable of conferring aminoglycoside resistance in *M. abscessus* is a homolog of *Anabaena variabilis* enhanced intracellular survival (Eis) protein (**Figure 1**). Eis proteins are widespread in mycobacteria as well as other Gram-positive bacteria. Eis protein in *Mycobacterium tuberculosis* has been shown to enhance intracellular survival within macrophages by acetylating and activating dual-specificity protein phosphatase 16/mitogen-activated protein kinase phosphatase-7 (DUSP16/MPK-7), a JNK-specific phosphatase that inhibits inflammation, autophagy and subsequent death of infected macrophages (Shin et al., 2010; Kim et al., 2012). Furthermore, upregulation of *eis* gene expression owing to mutations in its promoter was associated with kanamycin resistance in one-third of clinical isolates encompassing a large collection of *M. tuberculosis* strains from diverse geographical locations (Zaunbrecher et al., 2009). More recently, structural and biochemical characterization of *M. tuberculosis* Eis revealed its unprecedented ability to acetylate multiple amines of several aminoglycosides (Chen et al., 2011).

Analysis of *M. abscessus* genome revealed two genes namely, MAB_4124 (*eis1*) and MAB_4532c (*eis2*), which show homology to *eis* from *M. tuberculosis* (Rv2416c) and *A. variabilis* (Ava_4977), respectively. Drug susceptibility testing could confirm a functional role for Eis2 but not Eis1, in intrinsic aminoglycoside resistance. Of note, deletion of MAB_4532c enhanced *M. abscessus* susceptibility towards a heterogenous group of aminoglycosides including the cornerstone drug amikacin as well as a non-aminoglycoside antibiotic capreomycin (**Table 1**) (Rominski et al., 2017c). Furthermore, heterologous expression of *eis2* in *Mycobacterium smegmatis* decreased amikacin susceptibility (Hurst-Hess et al., 2017). Capreomycin is a cyclic peptide antibiotic that inhibits protein synthesis by blocking peptidyl-tRNA translocation. The drug is particularly active against *M. tuberculosis* and commonly used as a second-line agent for the treatment of TB (Stanley et al., 2010; Wilson, 2014). Although remarkable, the discovery that *M. abscessus* Eis2 exhibits a broad-spectrum acetyltransferase activity is not a real surprise. In fact, recent structural and functional studies on Eis enzymes from *M. tuberculosis* (Eis_*Mtb*), *M. smegmatis* (Eis_*Msm*), and *A. variabilis* (Eis_*Ava*) revealed the presence of an unusually large and complex active site unlike in other aminoglycoside acetyltransferases. The unique structure equips Eis with a regio-versatile multi-acetylating acetyltransferase activity towards a broad range of substrates (Chen et al., 2012; Pricer et al., 2012; Jennings et al., 2013). However, there seems to be a notable difference between the acetylation activities of *M. abscessus* Eis2 and *M. tuberculosis* Eis especially towards capreomycin as the MIC of capreomycin in *M. abscessus* is about 100-fold higher than that in *M. tuberculosis* and this difference is almost completely abolished by the deletion of *eis2* gene (**Table 1**) (Rominski et al., 2017c).

Aminoglycoside acetyltransferases Eis2 and AAC(2′) do not appear to modify streptomycin, an aminoglycoside which exhibits moderate *in vitro* activity against *M. abscessus* (MIC: 32 mg/L) (Rominski et al., 2017c). Instead, a MAB_2385 encoded putative aminoglycoside 3′′-*O*-phosphotransferase is the main determinant for intrinsic streptomycin resistance in *M. abscessus* (**Figure 1**). Twelve putative aminoglycoside phosphotransferases are encoded in the genome of *M. abscessus* (Ripoll et al., 2009). Among them, MAB_2385 was found to be a close homolog of *aph(3′′)-Ic*, an aminoglycoside 3′′-*O*-phosphotransferase gene which was previously shown to confer streptomycin resistance in *Mycobacterium fortuitum* (Ramón-García et al., 2006). Deletion of MAB_2385 enhanced the susceptibility of *M. abscessus* towards streptomycin by 16-fold (**Table 1**). Furthermore, MAB_2385 was able to confer streptomycin resistance when heterologously expressed in *M. smegmatis* (Dal Molin et al., 2017). To the best of our knowledge other annotated aminoglycoside phosphotransferases (such as MAB_0163c, MAB_0313c, MAB_0327, MAB_0951, and MAB_1020) and aminoglycoside acetyltransferases (for example, MAB_0247c, MAB_0404c, MAB_0745, MAB_4235c, and MAB_4324c) have not been addressed experimentally, however, interesting regulatory features of drug resistance genes have been elucidated.

A WhiB7 like protein encoded by MAB_3508c was recently uncovered as a multi-drug inducible transcriptional regulator that modulates the expression of genes conferring aminoglycoside and macrolide resistance in *M. abscessus*. WhiB7, an autoregulatory transcriptional activator, is a determinant of

innate antibiotic resistance in mycobacteria. In *M. tuberculosis*, genes conferring antibiotic resistance including *ermMT* (Rv1988), *eis* (Rv2416c) and *tap* (Rv1258c) are induced in a *whiB7*-dependent manner, upon exposure to antibiotics. Similarly, the *erm*(41) and *eis2* genes in *M. abscessus* are included in the *whiB7* regulon (Hurst-Hess et al., 2017). A recent study by Pryjma et al. (2017) demonstrated that exposure to sub-inhibitory levels of clarithromycin, enhanced amikacin as well as clarithromycin resistance in *M. abscessus* in a *whiB7*-dependent manner. Of note, deletion of MAB_3508c rendered *M. abscessus* more susceptible to amikacin (fourfold) and clarithromycin (eightfold), while complementation with an intact gene copy restored resistance to these antibiotics, suggesting a role of *whiB7* in *M. abscessus* amikacin and clarithromycin resistance. Interestingly, pre-exposure to clarithromycin, which is a potent inducer of *M. abscessus whiB7*, enhanced the resistance of *M. abscessus* wild-type strain towards amikacin by fourfold but had no effect on amikacin susceptibility of a Δ*whiB7* mutant. In addition, pre-treatment with clarithromycin markedly increased resistance to itself in the wild-type strain but did not alter clarithromycin sensitivity of a Δ*whiB7* mutant. Furthermore, a quantitative reverse transcription-PCR assay revealed a *whiB7*-dependent upregulation of *eis2* and *erm*(41) genes following pre-exposure to clarithromycin. These observations support the following conclusions: (i) in *M. abscessus*, *whiB7* (MAB_3508c) activates the expression of genes which confer amikacin and clarithromycin resistance, i.e., *eis2* and *erm*(41), (ii) strong induction of *whiB7* following exposure to clarithromycin confers cross-resistance to amikacin in addition to activating inducible macrolide resistance (Pryjma et al., 2017). Thus, *in vitro* findings by Pryjma et al. (2017) suggest that front-line antibiotics, amikacin and clarithromycin may exhibit antagonistic effects when used in combination for the treatment of *M. abscessus* infections. This may at least partially explain the limited clinical efficacy of currently recommended multi-drug regimen for *M. abscessus* which almost always includes these two antibiotics.

Tetracycline Resistance: MAB_1496c Encoded Flavin Monooxygenase

Tetracyclines are a class of broad-spectrum natural product antibiotics that interfere with bacterial protein synthesis. These drugs bind with high affinity to the small ribosomal subunit and specifically interfere with the delivery of aminoacylated tRNA to the A-site (Kohanski et al., 2010; Wilson, 2014). While tetracyclines are an important class of ribosome-targeting antibiotics, their anthropogenic and prolific use in the clinic and agriculture has led to emergence of resistance among benign as well as pathogenic bacteria, thereby limiting their efficacy. Despite growing resistance, tetracyclines continue to remain one of the most successful and widely used chemotherapeutics against bacterial infections (Allen et al., 2010). Furthermore, a renaissance for tetracyclines is being fuelled by the development of next-generation derivatives such as tigecycline, approved for clinical use in 2005 and omadacycline and eravacycline, undergoing late-phase clinical trials (Kinch and Patridge, 2014). In fact, tigecycline is the only new antibiotic and the sole member of its class, which has been introduced in the treatment of recalcitrant *M. abscessus* lung disease with clinical evidence (Wallace et al., 2014).

Previously, resistance towards tetracyclines was thought to be exclusively mediated by two mechanisms namely, drug efflux and ribosome protection. However, evidence for enzymatic inactivation of tetracyclines by a family of flavin adenine dinucleotide (FAD)-dependent monooxygenases in both benign and pathogenic bacteria has been recently documented. Few well characterized examples of such tetracycline-modifying enzymes include TetX from the obligate anaerobe *Bacteroides fragilis* and Tet(56) found in human pathogen *Legionella longbeachae*, the causative agent of Legionnaires' disease and Pontiac fever (Yang et al., 2004; Park et al., 2017). Whether such a mechanism of tetracycline resistance existed in mycobacteria was not known until recently, when Rudra and colleagues demonstrated through elegant experiments, that high levels of intrinsic resistance towards tetracycline and second generation derivative doxycycline in *M. abscessus* was mediated by a flavin monooxygenase, MabTetX (**Figure 1**). Deletion of MAB_1496c (encoding a putative FAD binding monooxygenase) enhanced the susceptibility of *M. abscessus* towards tetracycline and doxycycline by 15–20-fold (**Table 1**), while a complemented ΔMAB_1496c strain exhibited even higher levels of resistance towards both antibiotics compared to the wild-type strain, supporting the notion that MAB_1496c is a primary determinant for *M. abscessus* intrinsic tetracycline resistance. Furthermore, UV-Visible and mass spectrometry assays with purified MAB_1496c protein provided evidence for hydroxylation and subsequent degradation of tetracycline and doxycycline by MabTetX (Rudra et al., 2018). Interestingly, MAB_1496c is not a member of the *whiB7* regulon, even though tetracycline is a strong inducer of *whiB7* in *M. abscessus* (Hurst-Hess et al., 2017). In fact, MabTetX expression is regulated by a TetR family repressor, $MabTetR_x$ (encoded by the upstream gene MAB_1497c) which represses the MAB_1497c-MAB_1496c operon by binding to a 35bp operator sequence *tetO*. This repression is relieved in the presence of tetracycline and doxycycline which can bind the repressor protein thereby preventing its interaction with the *tetO* operator (Rudra et al., 2018).

The glycylcycline antibiotic tigecycline, specifically designed to evade resistance by ribosome protection and efflux, is not invulnerable to modification by *Bacteroides* TetX, which was recently also identified in numerous clinically relevant pathogens (Volkers et al., 2011; Leski et al., 2013). Although tigecycline was found to be a poor substrate of TetX, alarmingly enzymatic activity of TetX was substantially improved upon acquisition of single amino acid substitutions to confer resistance at clinically relevant tigecycline concentrations when overexpressed in *Escherichia coli* (Linkevicius et al., 2016). Surprisingly, tigecycline resisted MabTetX-dependent degradation and did not induce its expression, which might contribute to its excellent *in vitro* activity and moderate clinical efficacy against *M. abscessus* (Rudra et al., 2018). However, selective pressure exerted by tigecycline will eventually favor

the emergence of *M. abscessus* isolates carrying extended-spectrum FAD-monooxygenases with the ability to modify glycylcyclines.

Another interesting feature is the ability of anhydrotetracycline (ATc), a degradation product of tetracycline with poor antibiotic activity which was recently shown to be a competitive inhibitor of TetX and Tet(56) flavin monooxygenases, to rescue antibiotic activities of tetracycline and doxycycline against *M. abscessus* expressing MabTetX (Park et al., 2017; Rudra et al., 2018). However, ATc was also found to induce MabTetX expression by binding the $MabTetR_x$ repressor, a property at odds with its MabTetX inhibition activity. While this finding together with the severe side effects associated with ATc use, makes it an unattractive drug candidate, it nevertheless represents a flexible starting point for developing MabTetX inhibitors with improved activity, better tolerability and minimal binding affinity towards $MabTetR_x$. Co-administration with a potent MabTetX monooxygenase inhibitor can potentially rescue the clinical efficacies of tetracycline and doxycycline which are currently inactive against the *M. abscessus* complex (Burgos et al., 2011; Rudra et al., 2018).

β-Lactam Resistance: MAB_2875 Encoded β-Lactamase

β-lactams constitute an important class of antibiotics that function by inhibiting cell wall synthesis in bacteria. The β-lactam structure closely resembles the terminal D-alanyl-D-alanine dipeptide of peptidoglycan, a substrate of penicillin binding proteins (also known as D, D-transpeptidases) that catalyze the final cross-linking step of peptidoglycan synthesis. Penicilloylation of the D, D-transpeptidase active site following treatment with β-lactams, disables the enzyme and prevents the formation of peptidoglycan cross-links, thereby interfering with cell wall biosynthesis (Kohanski et al., 2010). Despite being the cornerstones of antimicrobial chemotherapy and constituting one of the largest groups of antibiotics available today, only two members of the β-lactam class namely, cefoxitin (a cephalosporin) and imipenem (a carbapenem) form a part of the antibiotic arsenal for *M. abscessus*. Furthermore, cefoxitin and imipenem have been shown to exhibit only moderate *in vitro* activity against *M. abscessus* with MICs of 32 and 4 mg/L, respectively (Lavollay et al., 2014). Majority of the other β-lactam antibiotics are not effective against this bacterium.

Several possible mechanisms may contribute to β-lactam resistance in *M. abscessus*. Low mycomembrane permeability and β-lactamase production may reduce the effective concentration of β-lactams at the site of action. Alternatively, modification of transpeptidase profile of the cell by replacement of penicillin binding proteins (D, D-transpeptidases) with L, D-transpeptidases for instance, may reduce the activity of penicillins and cephalosporins that have lower affinity for L, D-transpeptidase (Wivagg et al., 2014). However, most of the abovementioned resistance mechanisms are relatively unexplored in this organism except for one. Recently it was shown that the genome of *M. abscessus* encodes a strong, constitutive class A β-lactamase (Bla_Mab) which renders it highly resistant towards most β-lactams (**Figure 1**). The *M. abscessus* β-lactamase Bla_Mab, encoded by MAB_2875 is endowed with an exceptional broad-spectrum activity and can effectively hydrolyse several members of first- and second-generation cephalosporins, carbapenems, and penams (Soroka et al., 2014). The currently recommended β-lactams namely imipenem and cefoxitin are substrates of Bla_Mab, however, they are hydrolysed at a very slow rate, which may contribute to their clinical efficacy. The instability of imipenem complicates drug susceptibility testing when generation times of test bacteria require incubations for several days as in the case of *M. abscessus* (Rominski et al., 2017b).

One strategy to overcome the hurdle of chromosomally encoded β-lactamase in *M. abscessus* is to co-administer a β-lactamase inhibitor with the failing β-lactam. Soroka and colleagues evaluated the *in vitro* efficacy of nitrocefin and meropenem in combination with approved β-lactamase inhibitors clavulanate, tazobactam, and sulbactam against Bla_Mab. Surprisingly, Bla_Mab inhibition was not detected for all the three inhibitor drugs (Soroka et al., 2014). This remarkable ability of Bla_Mab to resist inhibition even surpasses that of BlaC, a class A β-lactamase encoded by its relative *M. tuberculosis*. Although BlaC is able to reverse inhibition caused by tazobactam and sulbactam, and return to its native functional form, clavulanate can slowly but irreversibly inhibit this enzyme (Sagar et al., 2017). In fact, a recent demonstration of *in vitro* synergy between meropenem and clavulanate in 13 extensively drug resistant (XDR) *M. tuberculosis* strains raised a renewed interest in β-lactams for use in TB therapy (Hugonnet et al., 2009). Fortunately, a surprising finding that *M. abscessus* Bla_Mab is effectively disabled by the newly approved β-lactamase inhibitor avibactam provides a new hope for old antibiotics. A study by Dubée et al. (2015) showed that co-administering a small amount of avibactam (4 mg/L) with each of several representative antibiotics from three important β-lactam sub-classes (carbapenems, penams, and cephalosporins) lowered their MICs in *M. abscessus* CIP104536 strain to levels comparable to those observed in a β-lactamase deficient mutant. The authors also reported synergy between avibactam and amoxicillin within macrophages as well as in a zebrafish model of *M. abscessus* infection (Dubée et al., 2015). More recently, an *in vitro* synergy screen of 110 β-lactam - β-lactamase inhibitor combinations against an *M. abscessus* clinical isolate identified six potential hits. Five selected β-lactamase inhibitors encompassing both β-lactam-based (clavulanate, tazobactam, and sulbactam) as well as non-β-lactam-based inhibitors (avibactam and vaborbactam) were evaluated for synergistic effects with a large panel of β-lactams. Importantly, all observed synergy combinations exclusively involved non-β-lactam-based inhibitors, either avibactam or vaborbactam. Combinations of avibactam with each of the following drugs including ampicillin, amoxicillin, tebipenem, and panipenem displayed synergistic effects against *M. abscessus*. Furthermore, the carbapenems, tebipenem, and panipenem also exhibited synergy with a novel boronic acid β-lactamase inhibitor, vaborbactam (Aziz et al., 2018). Thus, non-β-lactam-based β-lactamase inhibitors such as avibactam and vaborbactam can potentially extend the spectrum

of β-lactams employed for the treatment of largely incurable, chronic *M. abscessus* pulmonary infections.

Rifamycin Resistance: MAB_0591 Encoded ADP-Ribosyltransferase

Rifampicin, a rifamycin antibiotic commonly employed as a first-line agent in the treatment of *M. tuberculosis* infections, hardly exhibits any activity towards the *M. abscessus* complex (MIC: 128 mg/L) (**Table 1**). Since rifamycins inhibit transcription by binding with high affinity to *rpoB* encoded β-subunit of bacterial RNA polymerase, resistance towards this group of antibiotics is most commonly conferred by point mutations within the target gene *rpoB*, especially in *M. tuberculosis* (Campbell et al., 2001). However, additional rifamycin resistance mechanisms that involve enzymatic drug inactivation are also prevalent in other mycobacterial species. The presence of a rifamycin ADP-ribosyltransferase in *M. smegmatis* was known for quite a while (Quan et al., 1997), however, only recently genetic studies involving gene knockout and heterologous expression unveiled the existence of a MAB_0591 encoded ADP-ribosyltransferase as the major determinant for high levels of innate rifamycin resistance in *M. abscessus* (**Figure 1**). Deletion of MAB_0591 enhanced the susceptibility of *M. abscessus* towards three tested rifamycins including rifaximin, rifapentine and rifampicin by 64–512-fold, respectively (Rominski et al., 2017a).

Surprisingly, a rifampicin derivative, rifabutin showed up as an attractive hit (MIC: 2.5 mg/L), when a set of 2,700 FDA-approved drugs were screened against a clinical isolate of *M. abscessus.* Rifabutin exhibited approximately 10-fold higher potency *in vitro* relative to rifampicin and rifapentine, against reference strains representative of all three subspecies of the *M. abscessus* complex as well as a collection of clinical isolates and its bactericidal activity was comparable to or better than that of clarithromycin, one of the cornerstone drugs for *M. abscessus* infections (Aziz et al., 2017). The higher efficacy of rifabutin relative to rifampicin in *M. abscessus* as well as in *M. tuberculosis* (with no known rifamycin inactivating enzymes) suggests its increased accumulation within the bacterial cells. This may be due to differences in membrane penetration or specificity of efflux systems towards different rifamycins (**Figure 1**). Based on the findings reported by Aziz et al. (2017), rifampicin analog rifabutin, appears to be a potential candidate for repurposing and its clinical efficacy in patients with *M. abscessus* pulmonary disease should be further explored.

CLINICAL RELEVANCE

Although the inherent ability of *M. abscessus* to exhibit resistance to a wide array of antibiotics has long been recognized, our knowledge of the prodigious diversity of mechanisms involved has improved immensely in recent years, owing to the development of tools for genetic manipulation of *M. abscessus*. A better understanding of the genetic basis of innate antibiotic resistance is a prerequisite for the discovery and development of synergistic drug combinations, where one agent serves to salvage the antibacterial activity of a failing antibiotic by inhibiting an intrinsic resistance mechanism. This is exemplified by the recent discovery that avibactam is a potent inhibitor of *M. abscessus* β-lactamase Bla_Mab. When used in combination, avibactam lowered the MICs of several β-lactams in *M. abscessus* by 4–32-fold (Dubée et al., 2015; Kaushik et al., 2017). Despite the success of β-lactamase inhibitors, the concept of designing drugs which target intrinsic resistance mechanisms in bacteria, has not gained substantial clinical exploitation beyond this antibiotic class (Brown, 2015). Recently, a repertoire of drug-modifying and target-modifying enzymes conferring innate resistance to aminoglycosides, tetracyclines, rifamycins, and macrolides in *M. abscessus* were delineated (Nash et al., 2009; Dal Molin et al., 2017; Rominski et al., 2017a,c; Rudra et al., 2018). Likewise, attempts to identify chemical entities which could potentially rescue the function of one or more key members from each aforementioned antibiotic group, should be pursued in the near future.

Since the discovery that mutations within *eis* promoter are associated with kanamycin resistance in *M. tuberculosis*, vigorous attempts to identify Eis inhibitors that can potentially rescue kanamycin activity in this pathogen have been pursued with notable success. Recently, several structurally diverse competitive Eis inhibitors with 1,2,4-triazino[5,6*b*]indole-3-thioether-based, sulfonamide-based, pyrrolo[1,5-*a*]pyrazine-based and isothiazole *S,S*-dioxide heterocyclic scaffolds were identified by high-throughput screenings of large compound libraries. Importantly, few promising inhibitors could completely restore kanamycin susceptibility in a kanamycin resistant *M. tuberculosis* strain *in vitro* at concentrations that were non-cytotoxic to mammalian cells (Green et al., 2012; Garzan et al., 2016, 2017; Willby et al., 2016; Ngo et al., 2018). Remarkably, inhibitors designed for *M. tuberculosis* Eis, were also found to be active against Eis homologs in *M. smegmatis* and *A. variabilis* (Chen et al., 2012; Pricer et al., 2012). These findings give rise to an intriguing possibility that Eis_*Mtb* inhibitors may be able to overcome Eis2 mediated resistance towards aminoglycoside and/or non-aminoglycoside antibiotics like capreomycin and restore their effectiveness against *M. abscessus*. Hence efforts to explore the activity of Eis_*Mtb* inhibitors against *M. abscessus* Eis2 enzyme should be undertaken. Alternatively, extending drug discovery efforts towards targeting WhiB7, could be a possible strategy to tackle intrinsic macrolide and aminoglycoside resistance in *M. abscessus*. WhiB7 is a conserved transcriptional regulator in mycobacteria that co-ordinates intrinsic resistance to a wide range of ribosome-targeting drugs (Burian et al., 2012). Recent evidence suggests that genes which contribute to intrinsic aminoglycoside and macrolide resistance in *M. abscessus,* i.e., *eis2* and *erm*(41), are induced in a *whiB7*-dependent manner upon exposure to ribosomal antibiotics (Hurst-Hess et al., 2017). Thus, with the aim to kill two birds with one stone, compounds that prevent the induction of *eis2* and *erm*(41) resistance genes in *M. abscessus* by modulating the synthesis and/or activity of WhiB7, should be sought.

Since the discovery and development of compounds that can circumvent existing resistance mechanisms in *M. abscessus* is a daunting and time-consuming task, an immediate and relatively simple solution to improve treatment efficacy may

involve repurposing and repositioning of currently available antibiotics. A number of candidate drugs suited for this purpose have been reviewed in detail elsewhere (Wu et al., 2018) and are therefore only briefly mentioned here. For example, a systematic screening of a collection of FDA-approved drugs revealed rifabutin, an analog of rifampicin, exhibiting potent *in vitro* activity against *M. abscessus* (MIC: 2.5 mg/L) (Aziz et al., 2017). Similarly, clofazimine, a leprosy drug currently repurposed for treatment of TB, was also found to be active against *M. abscessus.* In addition to promising *in vitro* activity (MIC $\leq$ 1 mg/L), clofazimine displayed adequate clinical efficacy and safety when evaluated in patients with *M. abscessus* pulmonary infections (Yang et al., 2017). Likewise, a novel oxazolidinone LCB01-0371, presently in Phase II clinical development for TB, exhibited high potency against *M. abscessus* compared to linezolid, an FDA-approved drug of the same class (Kim et al., 2017). Moreover, some aminoglycosides such as kanamycin A, apramycin, isepamicin, and arbekacin were also found to exhibit potent *in vitro* activity against *M. abscessus* (MICs $\leq$ 1 mg/L) (Rominski et al., 2017c). Besides these, other compounds that have been extensively studied for their inhibitory effects against *M. abscessus* encompass anti-TB drug bedaquiline, some TB actives like indole-2-carboxamides and piperidinol-based compound 1 (PIPD1), as well as second generation thiacetazone derivatives like D6, D15, and D17 (Dupont et al., 2016, 2017; Franz et al., 2017; Halloum et al., 2017; Kozikowski et al., 2017).

In addition, several recent studies have reported *in vitro* synergies between novel combinations of existing antibiotic classes. For example, vancomycin, an inhibitor of cell wall synthesis, exhibited synergy with clarithromycin, an inhibitor of protein synthesis, in *M. abscessus* (Mukherjee et al., 2017). Likewise, a combination of tigecycline (which inhibits protein synthesis) with teicoplanin (which disrupts peptidoglycan synthesis) displayed a strong synergistic effect against *M. abscessus* (Aziz et al., 2018). Since the mycobacterial cell envelope forms a major permeability barrier, drugs that perturb cell wall integrity, are likely to synergize with drugs having intracellular targets (Le Run et al., 2018). Such combinations based on mechanistic drug action should be further explored for synergistic effects against *M. abscessus.* For example, PIPD1 and indole-2-carboxamides, which disrupt mycolic acid synthesis by targeting MmpL3 transporter in mycobacteria (Dupont et al., 2016; Franz et al., 2017), may be able to potentiate the effects of other drugs modulating intracellular targets.

Taken together, a huge reservoir of intrinsic resistance genes combined with an unusually high evolutionary potential of its genome to acquire resistance renders almost all available antibiotics ineffective against *M. abscessus.* Therefore, in the long run, a better understanding of natural resistance mechanisms in *M. abscessus* will help jump start drug discovery projects for (i) compounds that can rescue current antibiotics by neutralizing intrinsic resistance (termed antibiotic resistance breakers), (ii) new drugs with one or more improved properties like ability to resist enzymatic modification and/or degradation, high affinity for modified or mutated targets, better solubility/uptake and low propensity for efflux (Brown, 2015). In the short run, available knowledge from studies seeking synergy between antibiotics together with those investigating potential candidates for repurposing, will aid in the development of dosing regimens that display adequate clinical efficacy and resistance to which will only emerge slowly.

OUTLOOK AND PERSPECTIVES

Molecular genetic tools that allow investigators to systematically probe gene function in mycobacteria by generation of unmarked gene deletions and functional complementation, have proven extremely useful in dissecting the intrinsic resistome of *M. abscessus* while genetic investigations in other NTM species are still lagging behind. Using the available genetic 'toolkit,' 7 orthologs of known resistance gene families have been discovered so far in *M. abscessus* that provide resistance or 'immunity' against antibiotics targeting major cellular pathways including cell wall synthesis (β-lactams), RNA synthesis (rifamycins) and protein synthesis (macrolides, aminoglycosides, and tetracyclines). The impressive resistance diversity shown by *M. abscessus* is expected given its natural habitat is shared by many antibiotic producers, primarily the soil dwelling actinomycetes which are also reservoirs of extensively diverse resistance elements (Pawlowski et al., 2016; Crofts et al., 2017; Koteva et al., 2018). Exposure to a variety of noxious antimicrobial molecules in the soil might have favored selection of specialized and diverse resistance mechanisms in *M. abscessus* as well as in other NTM species.

Till now, the approach that researchers used to systematically probe the intrinsic resistome of *M. abscessus* involved analysis of few selected genes identified based on homology to known resistance determinants from other bacteria. As a result, this approach mainly revealed genes within *M. abscessus* that were involved in previously known resistance mechanisms and disguised the presence of potential determinants of entirely new resistance mechanisms that lack characterized homologs in other bacteria. To capture the remarkable resistance diversity of *M. abscessus* as well as other environmental NTM with unprecedented depth, future studies in this field should incorporate next-generation approaches that provide a comprehensive genome-wide definition of loci required for antibiotic resistance, using cutting-edge technologies. One such technique which can efficiently mine resistance determinants with novel sequences as well as assign resistance functions to known genes that were not previously shown to be involved in drug resistance, is the most recent incarnation of insertional mutagenesis, called transposon insertion sequencing (TIS) (Chao et al., 2016).

The utility of TIS in elucidating novel antibiotic resistance functions is highlighted by its recent application to the discovery of a repertoire of previously unknown intrinsic factors impacting resistance to antibiotics of different classes including oxazolidinones, fluoroquinolones, and aminoglycosides in pathogens of high clinical concern such as *Staphylococcus aureus*, *P. aeruginosa* and *E. coli* (Gallagher et al., 2011; Shan et al., 2015; Rajagopal et al., 2016). Screening large collections

of transposon insertion mutants for antibiotic susceptibility using TIS approach, has identified promising novel targets for drugs that can restore or enhance susceptibility to existing antibiotics. For example, analysis of insertion mutants spanning all non-essential *S. aureus* genes for fitness defects resulting from exposure to antibiotics, identified pathways/genes including *graRS* and *vraFG* (*graRS*/*vraFG*), *fmtA*, *mprF*, *SAOUHSC_01025,* and *SAOUHSC_01050* which if inhibited, can greatly improve the efficacy of existing antibiotics including daptomycin, vancomycin, gentamicin, ciprofloxacin, oxacillin, and linezolid and extend their utility for treating *S. aureus* infections (Rajagopal et al., 2016).

In the coming years, high-throughput next-generation strategies like TIS will undoubtedly rise to prominence in the NTM drug resistance field and radically advance our understanding of resistance mechanisms in *M. abscessus* and other emerging NTM pathogens. Such breakthrough technologies will greatly impact the kinds of questions which can be addressed in this field, for example, which resistance elements unique to *M. abscessus* render it unusually more drug resistant than other NTM species? or does *M. abscessus* already carry genes which confer resistance to novel NTM drugs in development?

AUTHOR CONTRIBUTIONS

All authors listed have made a substantial, direct and intellectual contribution to the work, and approved it for publication.

FUNDING

Research in the group of PS was supported by the Swiss National Science Foundation (#31003A_153349), Lungenliga Schweiz, the Institute of Medical Microbiology and the University of Zurich.

ACKNOWLEDGMENTS

We acknowledge the members of the research group for stimulating discussions and support.

REFERENCES

Aínsa, J. A., Pérez, E., Pelicic, V., Berthet, F. X., Gicquel, B., and Martín, C. (1997). Aminoglycoside 2′-N-acetyltransferase genes are universally present in mycobacteria: characterization of the aac(2′)-Ic gene from *Mycobacterium tuberculosis* and the aac(2')-Id gene from *Mycobacterium smegmatis*. *Mol. Microbiol.* 24, 431–441.

Alcaide, F., Pfyffer, G. E., and Telenti, A. (1997). Role of embB in natural and acquired resistance to ethambutol in Mycobacteria. *Antimicrob. Agents Chemother.* 41, 2270–2273.

Allen, H. K., Donato, J., Wang, H. H., Cloud-Hansen, K. A., Davies, J., and Handelsman, J. (2010). Call of the wild: antibiotic resistance genes in natural environments. *Nat. Rev. Microbiol.* 8, 251–259. doi: 10.1038/nrmicro2312

Aziz, D. B., Low, J. L., Wu, M.-L., Gengenbacher, M., Teo, J. W. P., Dartois, V., et al. (2017). Rifabutin is active against *Mycobacterium abscessus* complex. *Antimicrob. Agents Chemother.* 61:e00155-17. doi: 10.1128/AAC.00155-17

Aziz, D. B., Teo, J. W. P., Dartois, V., and Dick, T. (2018). Teicoplanin - tigecycline combination shows synergy against *Mycobacterium abscessus*. *Front. Microbiol.* 9:932. doi: 10.3389/fmicb.2018.00932

Bastian, S., Veziris, N., Roux, A.-L., Brossier, F., Gaillard, J.-L., Jarlier, V., et al. (2011). Assessment of clarithromycin susceptibility in strains belonging to the *Mycobacterium abscessus* group by erm(41) and rrl sequencing. *Antimicrob. Agents Chemother.* 55, 775–781. doi: 10.1128/AAC.00861-10

Blair, J. M. A., Webber, M. A., Baylay, A. J., Ogbolu, D. O., and Piddock, L. J. V. (2015). Molecular mechanisms of antibiotic resistance. *Nat. Rev. Microbiol.* 13, 42–51. doi: 10.1038/nrmicro3380

Brown, D. (2015). Antibiotic resistance breakers: can repurposed drugs fill the antibiotic discovery void? *Nat. Rev. Drug Discov.* 14, 821–832. doi: 10.1038/nrd4675

Brown-Elliott, B. A., Nash, K. A., and Wallace, R. J. (2012). Antimicrobial susceptibility testing, drug resistance mechanisms, and therapy of infections with nontuberculous mycobacteria. *Clin. Microbiol. Rev.* 25, 545–582. doi: 10.1128/CMR.05030-11

Brown-Elliott, B. A., Vasireddy, S., Vasireddy, R., Iakhiaeva, E., Howard, S. T., Nash, K., et al. (2015). Utility of sequencing the erm(41) gene in isolates of *Mycobacterium abscessus* subsp. abscessus with low and intermediate clarithromycin MICs. *J. Clin. Microbiol.* 53, 1211–1215. doi: 10.1128/JCM.02950-14

Brown-Elliott, B. A., and Wallace, R. J. (2002). Clinical and taxonomic status of pathogenic nonpigmented or late-pigmenting rapidly growing Mycobacteria. *Clin. Microbiol. Rev.* 15, 716–746. doi: 10.1128/CMR.15.4.716-746.2002

Bryant, J. M., Grogono, D. M., Rodriguez-Rincon, D., Everall, I., Brown, K. P., Moreno, P., et al. (2016). Population-level genomics identifies the emergence and global spread of a human transmissible multidrug-resistant nontuberculous mycobacterium. *Science* 354, 751–757. doi: 10.1126/science.aaf8156

Burgos, M. I., Fernández, R. A., Celej, M. S., Rossi, L. I., Fidelio, G. D., and Dassie, S. A. (2011). Binding of the highly toxic tetracycline derivative, anhydrotetracycline, to bovine serum albumin. *Biol. Pharm. Bull.* 34, 1301–1306. doi: 10.1248/bpb.34.1301

Burian, J., Ramón-García, S., Howes, C. G., and Thompson, C. J. (2012). WhiB7, a transcriptional activator that coordinates physiology with intrinsic drug resistance in *Mycobacterium tuberculosis*. *Expert Rev. Anti Infect. Ther.* 10, 1037–1047. doi: 10.1586/eri.12.90

Cambau, E., Viveiros, M., Machado, D., Raskine, L., Ritter, C., Tortoli, E., et al. (2015). Revisiting susceptibility testing in MDR-TB by a standardized quantitative phenotypic assessment in a European multicentre study. *J. Antimicrob. Chemother.* 70, 686–696. doi: 10.1093/jac/dku438

Campbell, E. A., Korzheva, N., Mustaev, A., Murakami, K., Nair, S., Goldfarb, A., et al. (2001). Structural mechanism for rifampicin inhibition of bacterial RNA polymerase. *Cell* 104, 901–912. doi: 10.1016/S0092-8674(01)00286-0

Chan, E., and Iseman, M. (2013). Underlying host risk factors for nontuberculous Mycobacterial lung disease. *Semin. Respir. Crit. Care Med.* 34, 110–123. doi: 10.1055/s-0033-1333573

Chao, M. C., Abel, S., Davis, B. M., and Waldor, M. K. (2016). The design and analysis of transposon insertion sequencing experiments. *Nat. Rev. Microbiol.* 14, 119–128. doi: 10.1038/nrmicro.2015.7

Chen, W., Biswas, T., Porter, V. R., Tsodikov, O. V., and Garneau-Tsodikova, S. (2011). Unusual regioversatility of acetyltransferase Eis, a cause of drug resistance in XDR-TB. *Proc. Natl. Acad. Sci.* 108, 9804–9808. doi: 10.1073/pnas.1105379108

Chen, W., Green, K. D., Tsodikov, O. V., and Garneau-Tsodikova, S. (2012). The aminoglycoside multi-acetylating activity of the enhanced intracellular survival (Eis) protein from *Mycobacterium smegmatis* and its inhibition. *Biochemistry* 51, 4959–4967. doi: 10.1021/bi3004473

Choi, G.-E., Shin, S. J., Won, C.-J., Min, K.-N., Oh, T., Hahn, M.-Y., et al. (2012). Macrolide treatment for *Mycobacterium abscessus* and *Mycobacterium massiliense* infection and inducible resistance. *Am. J. Respir. Crit. Care Med.* 186, 917–925. doi: 10.1164/rccm.201111-2005OC

Choo, S. W., Wee, W. Y., Ngeow, Y. F., Mitchell, W., Tan, J. L., Wong, G. J., et al. (2014). Genomic reconnaissance of clinical isolates of emerging human pathogen *Mycobacterium abscessus* reveals high evolutionary potential. *Sci. Rep.* 4:4061. doi: 10.1038/srep04061

Crofts, T. S., Gasparrini, A. J., and Dantas, G. (2017). Next-generation approaches to understand and combat the antibiotic resistome. *Nat. Rev. Microbiol.* 15, 422–434. doi: 10.1038/nrmicro.2017.28

Dal Molin, M., Gut, M., Rominski, A., Haldimann, K., Becker, K., and Sander, P. (2017). Molecular mechanisms of intrinsic streptomycin resistance in *Mycobacterium abscessus*. *Antimicrob. Agents Chemother.* 62:e01427-17. doi: 10.1128/AAC.01427-17

D'Costa, V. M., King, C. E., Kalan, L., Morar, M., Sung, W. W. L., Schwarz, C., et al. (2011). Antibiotic resistance is ancient. *Nature* 477, 457–461. doi: 10.1038/nature10388

Dubée, V., Bernut, A., Cortes, M., Lesne, T., Dorchene, D., Lefebvre, A.-L., et al. (2015). β-Lactamase inhibition by avibactam in *Mycobacterium abscessus*. *J. Antimicrob. Chemother.* 70, 1051–1058. doi: 10.1093/jac/dku510

Dupont, C., Viljoen, A., Dubar, F., Blaise, M., Bernut, A., Pawlik, A., et al. (2016). A new piperidinol derivative targeting mycolic acid transport in *Mycobacterium abscessus*. *Mol. Microbiol.* 101, 515–529. doi: 10.1111/mmi.13406

Dupont, C., Viljoen, A., Thomas, S., Roquet-Banères, F., Herrmann, J.-L., Pethe, K., et al. (2017). Bedaquiline inhibits the ATP synthase in *Mycobacterium abscessus* and is effective in infected zebrafish. *Antimicrob. Agents Chemother.* 61, 1–15. doi: 10.1128/AAC.01225-17

Franz, N. D., Belardinelli, J. M., Kaminski, M. A., Dunn, L. C., Calado Nogueira de Moura, V., Blaha, M. A., et al. (2017). Design, synthesis and evaluation of indole-2-carboxamides with pan anti-mycobacterial activity. *Bioorg. Med. Chem.* 25, 3746–3755. doi: 10.1016/j.bmc.2017.05.015

Gallagher, L. A., Shendure, J., and Manoil, C. (2011). Genome-scale identification of resistance functions in *Pseudomonas aeruginosa* using Tn-seq. *mBio* 2:e00315-10. doi: 10.1128/mBio.00315-10

Garzan, A., Willby, M. J., Green, K. D., Gajadeera, C. S., Hou, C., Tsodikov, O. V., et al. (2016). Sulfonamide-based inhibitors of aminoglycoside acetyltransferase Eis abolish resistance to kanamycin in *Mycobacterium tuberculosis*. *J. Med. Chem.* 59, 10619–10628. doi: 10.1021/acs.jmedchem.6b01161

Garzan, A., Willby, M. J., Ngo, H. X., Gajadeera, C. S., Green, K. D., Holbrook, S. Y. L., et al. (2017). Combating enhanced intracellular survival (Eis)-mediated kanamycin resistance of *Mycobacterium tuberculosis* by novel pyrrolo[1,5-a]pyrazine-based Eis inhibitors. *ACS Infect. Dis.* 3, 302–309. doi: 10.1021/acsinfecdis.6b00193

Green, K. D., Chen, W., and Garneau-Tsodikova, S. (2012). Identification and characterization of inhibitors of the aminoglycoside resistance acetyltransferase Eis from *Mycobacterium tuberculosis*. *ChemMedChem* 7, 73–77. doi: 10.1002/cmdc.201100332

Griffith, D. E., Aksamit, T., Brown-Elliott, B. A., Catanzaro, A., Daley, C., Gordin, F., et al. (2007). An official ATS/IDSA statement: diagnosis, treatment, and prevention of nontuberculous mycobacterial diseases. *Am. J. Respir. Crit. Care Med.* 175, 367–416. doi: 10.1164/rccm.200604-571ST

Halloum, I., Viljoen, A., Khanna, V., Craig, D., Bouchier, C., Brosch, R., et al. (2017). Resistance to thiacetazone derivatives active against *Mycobacterium abscessus* involves mutations in the MmpL5 transcriptional repressor MAB_4384. *Antimicrob. Agents Chemother.* 61, e02509-16. doi: 10.1128/AAC.02509-16

Haworth, C. S., Banks, J., Capstick, T., Fisher, A. J., Gorsuch, T., Laurenson, I. F., et al. (2017). British thoracic society guideline for the management of non-tuberculous mycobacterial pulmonary disease (NTM-PD). *BMJ Open Respir. Res.* 4:e000242. doi: 10.1136/bmjresp-2017-000242

Hoefsloot, W., van Ingen, J., Andrejak, C., Ängeby, K., Bauriaud, R., Bemer, P., et al. (2013). The geographic diversity of nontuberculous mycobacteria isolated from pulmonary samples: an NTM-NET collaborative study. *Eur. Respir. J.* 42, 1604–1613. doi: 10.1183/09031936.00149212

Howard, S. T. (2006). Spontaneous reversion of *Mycobacterium abscessus* from a smooth to a rough morphotype is associated with reduced expression of glycopeptidolipid and reacquisition of an invasive phenotype. *Microbiology* 152, 1581–1590. doi: 10.1099/mic.0.28625-0

Hugonnet, J., Tremblay, L. W., Boshoff, H. I., Barry, C. E., and Blanchard, J. S. (2009). Meropenem-clavulanate is effective against extensively drug-resistant *Mycobacterium tuberculosis*. *Science* 323, 1215–1218. doi: 10.1126/science.1167498

Hurst-Hess, K., Rudra, P., and Ghosh, P. (2017). *Mycobacterium abscessus* WhiB7 regulates a species-specific repertoire of genes to confer extreme antibiotic resistance. *Antimicrob. Agents Chemother.* 61, e01347-17. doi: 10.1128/AAC.01347-17

Jarand, J., Levin, A., Zhang, L., Huitt, G., Mitchell, J. D., and Daley, C. L. (2011). Clinical and microbiologic outcomes in patients receiving treatment for *Mycobacterium abscessus* pulmonary disease. *Clin. Infect. Dis.* 52, 565–571. doi: 10.1093/cid/ciq237

Jennings, B. C., Labby, K. J., Green, K. D., and Garneau-Tsodikova, S. (2013). Redesign of substrate specificity and identification of aminoglycoside binding residues of Eis from *Mycobacterium tuberculosis*. *Biochemistry* 52, 5125–5132. doi: 10.1021/bi4002985

Kaushik, A., Gupta, C., Fisher, S., Story-Roller, E., Galanis, C., Parrish, N., et al. (2017). Combinations of avibactam and carbapenems exhibit enhanced potencies against drug-resistant *Mycobacterium abscessus*. *Future Microbiol.* 12, 473–480. doi: 10.2217/fmb-2016-0234

Kim, H.-Y., Kim, B. J., Kook, Y., Yun, Y.-J., Shin, J. H., Kim, B.-J., et al. (2010). *Mycobacterium massiliense* is differentiated from *Mycobacterium abscessus* and *Mycobacterium bolletii* by erythromycin ribosome methyltransferase gene (erm) and clarithromycin susceptibility patterns. *Microbiol. Immunol.* 54, 347–353. doi: 10.1111/j.1348-0421.2010.00221.x

Kim, K. H., An, D. R., Song, J., Yoon, J. Y., Kim, H. S., Yoon, H. J., et al. (2012). *Mycobacterium tuberculosis* Eis protein initiates suppression of host immune responses by acetylation of DUSP16/MKP-7. *Proc. Natl. Acad. Sci. U.S.A.* 109, 7729–7734. doi: 10.1073/pnas.1120251109

Kim, T. S., Choe, J. H., Kim, Y. J., Yang, C., Kwon, H., Jeong, J., et al. (2017). Activity of LCB01-0371, a novel oxazolidinone, against *Mycobacterium abscessus*. *Antimicrob. Agents Chemother.* 61, e02752-16. doi: 10.1128/AAC.02752-16

Kinch, M. S., and Patridge, E. (2014). An analysis of FDA-approved drugs for infectious disease: antibacterial agents. *Drug Discov. Today* 19, 1510–1513. doi: 10.1016/j.drudis.2014.05.012

Kohanski, M. A., Dwyer, D. J., and Collins, J. J. (2010). How antibiotics kill bacteria: from targets to networks. *Nat. Rev. Microbiol.* 8, 423–435. doi: 10.1038/nrmicro2333

Koteva, K., Cox, G., Kelso, J. K., Surette, M. D., Zubyk, H. L., Ejim, L., et al. (2018). Rox, a rifamycin resistance enzyme with an unprecedented mechanism of action. *Cell Chem. Biol.* 25, 403–412.e5. doi: 10.1016/j.chembiol.2018.01.009

Kozikowski, A. P., Onajole, O. K., Stec, J., Dupont, C., Viljoen, A., Richard, M., et al. (2017). Targeting mycolic acid transport by indole-2-carboxamides for the treatment of *Mycobacterium abscessus* infections. *J. Med. Chem.* 60, 5876–5888. doi: 10.1021/acs.jmedchem.7b00582

Lavollay, M., Dubée, V., Heym, B., Herrmann, J.-L., Gaillard, J.-L., Gutmann, L., et al. (2014). In vitro activity of cefoxitin and imipenem against *Mycobacterium abscessus* complex. *Clin. Microbiol. Infect.* 20, O297–O300. doi: 10.1111/1469-0691.12405

Le Run, E., Arthur, M., and Mainardi, J.-L. (2018). In vitro and intracellular activity of imipenem combined to rifabutin and avibactam against *Mycobacterium abscessus*. *Antimicrob. Agents Chemother* 62:e00623-18. doi: 10.1128/AAC.00623-18

Lee, M.-R., Sheng, W.-H., Hung, C.-C., Yu, C.-J., Lee, L.-N., and Hsueh, P.-R. (2015). *Mycobacterium abscessus* complex infections in humans. *Emerg. Infect. Dis.* 21, 1638–1646. doi: 10.3201/2109.141634

Leski, T. A., Bangura, U., Jimmy, D. H., Ansumana, R., Lizewski, S. E., Stenger, D. A., et al. (2013). Multidrug-resistant tet(X)-containing hospital isolates in Sierra Leone. *Int. J. Antimicrob. Agents* 42, 83–86. doi: 10.1016/j.ijantimicag.2013.04.014

Linkevicius, M., Sandegren, L., and Andersson, D. I. (2016). Potential of tetracycline resistance proteins to evolve tigecycline resistance. *Antimicrob. Agents Chemother.* 60, 789–796. doi: 10.1128/AAC.02465-15

Maurer, F. P., Bruderer, V. L., Castelberg, C., Ritter, C., Scherbakov, D., Bloemberg, G. V., et al. (2015). Aminoglycoside-modifying enzymes determine the innate susceptibility to aminoglycoside antibiotics in rapidly growing mycobacteria. *J. Antimicrob. Chemother.* 70, 1412–1419. doi: 10.1093/jac/dku550

Maurer, F. P., Ruegger, V., Ritter, C., Bloemberg, G. V., and Bottger, E. C. (2012). Acquisition of clarithromycin resistance mutations in the 23S rRNA gene of *Mycobacterium abscessus* in the presence of inducible erm(41). *J. Antimicrob. Chemother.* 67, 2606–2611. doi: 10.1093/jac/dks279

Mukherjee, D., Wu, M.-L., Teo, J. W. P., and Dick, T. (2017). Vancomycin and clarithromycin show synergy against *Mycobacterium abscessus* in vitro. *Antimicrob. Agents Chemother.* 61, e01298-17. doi: 10.1128/AAC.01298-17

Nash, K. A., Brown-Elliott, A. B., and Wallace, R. J. (2009). A novel gene, erm(41), confers inducible macrolide resistance to clinical isolates of *Mycobacterium abscessus* but is absent from *Mycobacterium chelonae*. *Antimicrob. Agents Chemother.* 53, 1367–1376. doi: 10.1128/AAC.01275-08

Nessar, R., Cambau, E., Reyrat, J. M., Murray, A., and Gicquel, B. (2012). *Mycobacterium abscessus*: a new antibiotic nightmare. *J. Antimicrob. Chemother.* 67, 810–818. doi: 10.1093/jac/dkr578

Ngo, H. X., Green, K. D., Gajadeera, C. S., Willby, M. J., Holbrook, S. Y. L., Hou, C., et al. (2018). Potent 1,2,4-triazino[5,6b]indole-3-thioether inhibitors of the kanamycin resistance enzyme Eis from *Mycobacterium tuberculosis*. *ACS Infect. Dis.* 4, 1030–1040. doi: 10.1021/acsinfecdis.8b00074

Park, J., Gasparrini, A. J., Reck, M. R., Symister, C. T., Elliott, J. L., Vogel, J. P., et al. (2017). Plasticity, dynamics, and inhibition of emerging tetracycline-resistance enzymes. *Nat. Chem. Biol.* 13, 730–736. doi: 10.1038/nchembio.2376

Pawlowski, A. C., Stogios, P. J., Koteva, K., Skarina, T., Evdokimova, E., Savchenko, A., et al. (2018). The evolution of substrate discrimination in macrolide antibiotic resistance enzymes. *Nat. Commun.* 9:112. doi: 10.1038/s41467-017-02680-0

Pawlowski, A. C., Wang, W., Koteva, K., Barton, H. A., McArthur, A. G., and Wright, G. D. (2016). A diverse intrinsic antibiotic resistome from a cave bacterium. *Nat. Commun.* 7:13803. doi: 10.1038/ncomms13803

Prammananan, T., Sander, P., Brown, B. A., Frischkorn, K., Onyi, G. O., Zhang, Y., et al. (1998). A single 16S ribosomal RNA substitution is responsible for resistance to amikacin and other 2-deoxystreptamine aminoglycosides in Mycobacterium abscessus and Mycobacterium chelonae. *J. Infect. Dis.* 177, 1573–1581. doi: 10.1086/515328

Pricer, R. E., Houghton, J. L., Green, K. D., Mayhoub, A. S., and Garneau-Tsodikova, S. (2012). Biochemical and structural analysis of aminoglycoside acetyltransferase Eis from *Anabaena variabilis*. *Mol. Biosyst.* 8, 3305–3313. doi: 10.1039/c2mb25341k

Pryjma, M., Burian, J., Kuchinski, K., and Thompson, C. J. (2017). Antagonism between front-line antibiotics clarithromycin and amikacin in the treatment of *Mycobacterium abscessus* infections is mediated by the whiB7 gene. *Antimicrob. Agents Chemother.* 61, e01353-17. doi: 10.1128/AAC.01353-17

Quan, S., Venter, H., and Dabbs, E. R. (1997). Ribosylative inactivation of rifampin by *Mycobacterium smegmatis* is a principal contributor to its low susceptibility to this antibiotic. *Antimicrob. Agents Chemother.* 41, 2456–2460.

Rajagopal, M., Martin, M. J., Santiago, M., Lee, W., Kos, V. N., Meredith, T., et al. (2016). Multidrug intrinsic resistance factors in *Staphylococcus aureus* identified by profiling fitness within high-diversity transposon libraries. *mBio* 7: e00950-16. doi: 10.1128/mBio.00950-16

Ramón-García, S., Otal, I., Martin, C., Gomez-Lus, R., and Ainsa, J. A. (2006). Novel streptomycin resistance gene from *Mycobacterium fortuitum*. *Antimicrob. Agents Chemother.* 50, 3920–3922. doi: 10.1128/AAC.00223-06

Ripoll, F., Pasek, S., Schenowitz, C., Dossat, C., Barbe, V., Rottman, M., et al. (2009). Non mycobacterial virulence genes in the genome of the emerging pathogen *Mycobacterium abscessus*. *PLoS One* 4:e5660. doi: 10.1371/journal.pone.0005660

Rominski, A., Roditscheff, A., Selchow, P., Böttger, E. C., and Sander, P. (2017a). Intrinsic rifamycin resistance of *Mycobacterium abscessus* is mediated by ADP-ribosyltransferase MAB_0591. *J. Antimicrob. Chemother.* 72, 376–384. doi: 10.1093/jac/dkw466

Rominski, A., Schulthess, B., Müller, D. M., Keller, P. M., and Sander, P. (2017b). Effect of β-lactamase production and β-lactam instability on MIC testing results for *Mycobacterium abscessus*. *J. Antimicrob. Chemother.* 72, 3070–3078. doi: 10.1093/jac/dkx284

Rominski, A., Selchow, P., Becker, K., Brülle, J. K., Dal Molin, M., and Sander, P. (2017c). Elucidation of *Mycobacterium abscessus* aminoglycoside and capreomycin resistance by targeted deletion of three putative resistance genes. *J. Antimicrob. Chemother.* 72, 2191–2200. doi: 10.1093/jac/dkx125

Rudra, P., Hurst-Hess, K., Lappierre, P., and Ghosh, P. (2018). High levels of intrinsic tetracycline resistance in *Mycobacterium abscessus* are conferred by a tetracycline-modifying monooxygenase. *Antimicrob. Agents Chemother.* 62:e00119-18. doi: 10.1128/AAC.00119-18

Ryu, Y. J., Koh, W.-J., and Daley, C. L. (2016). Diagnosis and treatment of nontuberculous mycobacterial lung disease: clinicians' perspectives. *Tuberc. Respir. Dis.* 79, 74–84. doi: 10.4046/trd.2016.79.2.74

Sagar, A., Haleem, N., Bashir, Y. M., and Ashish, A. (2017). Search for non-lactam inhibitors of mtb β-lactamase led to its open shape in apo state: new concept for antibiotic design. *Sci. Rep.* 7:6204. doi: 10.1038/s41598-017-06023-3

Sanguinetti, M., Ardito, F., Fiscarelli, E., La Sorda, M., D'Argenio, P., Ricciotti, G., et al. (2001). Fatal pulmonary infection due to multidrug-resistant *Mycobacterium abscessus* in a patient with cystic fibrosis. *J. Clin. Microbiol.* 39, 816–819. doi: 10.1128/JCM.39.2.816-819.2001

Shan, Y., Lazinski, D., Rowe, S., Camilli, A., and Lewis, K. (2015). Genetic basis of persister tolerance to aminoglycosides in *Escherichia coli*. *mBio* 6:e00078-15. doi: 10.1128/mBio.00078-15

Shin, D.-M., Jeon, B.-Y., Lee, H.-M., Jin, H. S., Yuk, J.-M., Song, C.-H., et al. (2010). *Mycobacterium tuberculosis* Eis regulates autophagy, inflammation, and cell death through redox-dependent signaling. *PLoS Pathog.* 6:e1001230. doi: 10.1371/journal.ppat.1001230

Soroka, D., Dubée, V., Soulier-Escrihuela, O., Cuinet, G., Hugonnet, J.-E., Gutmann, L., et al. (2014). Characterization of broad-spectrum *Mycobacterium abscessus* class A β-lactamase. *J. Antimicrob. Chemother.* 69, 691–696. doi: 10.1093/jac/dkt410

Stanley, R. E., Blaha, G., Grodzicki, R. L., Strickler, M. D., and Steitz, T. A. (2010). The structures of the anti-tuberculosis antibiotics viomycin and capreomycin bound to the 70S ribosome. *Nat. Struct. Mol. Biol.* 17, 289–293. doi: 10.1038/nsmb.1755

Stout, J. E., Koh, W.-J., and Yew, W. W. (2016). Update on pulmonary disease due to non-tuberculous mycobacteria. *Int. J. Infect. Dis.* 45, 123–134. doi: 10.1016/j.ijid.2016.03.006

Tortoli, E., Kohl, T. A., Brown-Elliott, B. A., Trovato, A., Leão, S. C., Garcia, M. J., et al. (2016). Emended description of *Mycobacterium abscessus*, *Mycobacterium abscessus* subsp. *abscessus* and *Mycobacterium abscessus* subsp. *bolletii* and designation of *Mycobacterium abscessus* subsp. *massiliense* comb. nov. *Int. J. Syst. Evol. Microbiol.* 66, 4471–4479. doi: 10.1099/ijsem.0.001376

Volkers, G., Palm, G. J., Weiss, M. S., Wright, G. D., and Hinrichs, W. (2011). Structural basis for a new tetracycline resistance mechanism relying on the TetX monooxygenase. *FEBS Lett.* 585, 1061–1066. doi: 10.1016/j.febslet.2011.03.012

Wallace, R. J., Dukart, G., Brown-Elliott, B. A., Griffith, D. E., Scerpella, E. G., and Marshall, B. (2014). Clinical experience in 52 patients with tigecycline-containing regimens for salvage treatment of *Mycobacterium abscessus* and *Mycobacterium chelonae* infections. *J. Antimicrob. Chemother.* 69, 1945–1953. doi: 10.1093/jac/dku062

Wallace, R. J., Meier, A., Brown, B. A., Zhang, Y., Sander, P., Onyi, G. O., et al. (1996). Genetic basis for clarithromycin resistance among isolates of *Mycobacterium chelonae* and *Mycobacterium abscessus*. *Antimicrob. Agents Chemother.* 40, 1676–1681.

Willby, M. J., Green, K. D., Gajadeera, C. S., Hou, C., Tsodikov, O. V., Posey, J. E., et al. (2016). Potent inhibitors of acetyltransferase Eis Overcome kanamycin resistance in *Mycobacterium tuberculosis*. *ACS Chem. Biol.* 11, 1639–1646. doi: 10.1021/acschembio.6b00110

Wilson, D. N. (2014). Ribosome-targeting antibiotics and mechanisms of bacterial resistance. *Nat. Rev. Microbiol.* 12, 35–48. doi: 10.1038/nrmicro3155

Wivagg, C. N., Bhattacharyya, R. P., and Hung, D. T. (2014). Mechanisms of β-lactam killing and resistance in the context of *Mycobacterium tuberculosis*. *J. Antibiot.* 67, 645–654. doi: 10.1038/ja.2014.94

Wu, M.-L., Aziz, D. B., Dartois, V., and Dick, T. (2018). NTM drug discovery: status, gaps and the way forward. *Drug Discov. Today* 23, 1502–1519. doi: 10.1016/j.drudis.2018.04.001

Yang, B., Jhun, B. W., Moon, S. M., Lee, H., Park, H. Y., Jeon, K., et al. (2017). Clofazimine-containing regimen for the treatment of *Mycobacterium abscessus* lung disease. *Antimicrob. Agents Chemother.* 61:e02052-16. doi: 10.1128/AAC.02052-16

Yang, W., Moore, I. F., Koteva, K. P., Bareich, D. C., Hughes, D. W., and Wright, G. D. (2004). TetX Is a Flavin-dependent monooxygenase conferring resistance to tetracycline antibiotics. *J. Biol. Chem.* 279, 52346–52352. doi: 10.1074/jbc.M409573200

Zaunbrecher, M. A., Sikes, R. D., Metchock, B., Shinnick, T. M., and Posey, J. E. (2009). Overexpression of the chromosomally encoded aminoglycoside acetyltransferase Eis confers kanamycin resistance in *Mycobacterium tuberculosis*. *Proc. Natl. Acad. Sci. U.S.A.* 106, 20004–20009. doi: 10.1073/pnas.0907925106

Conflict of Interest Statement: The authors declare that the research was conducted in the absence of any commercial or financial relationships that could be construed as a potential conflict of interest.

The reviewer UG and handling Editor declared their shared affiliation at time of review.

frontiers in Microbiology

ORIGINAL RESEARCH
published: 05 April 2018
doi: 10.3389/fmicb.2018.00649

Mechanistic and Structural Insights Into the Unique TetR-Dependent Regulation of a Drug Efflux Pump in *Mycobacterium abscessus*

Matthias Richard[1], Ana Victoria Gutiérrez[1,2], Albertus J. Viljoen[1], Eric Ghigo[3], Mickael Blaise[1] and Laurent Kremer[1,4]**

[1] CNRS UMR 9004, Institut de Recherche en Infectiologie de Montpellier, Université de Montpellier, Montpellier, France, [2] Unité de Recherche, Microbes, Evolution, Phylogeny and Infection, Institut Hospitalier Universitaire Méditerranée Infection, Marseille, France, [3] Centre National de la Recherche Scientifique, Campus Joseph Aiguier, Marseille, France, [4] Institut National de la Santé et de la Recherche Médicale, Institut de Recherche en Infectiologie de Montpellier, Montpellier, France

OPEN ACCESS

Edited by:
Thomas Dick,
Rutgers University, United States

Reviewed by:
Peter Sander,
Universität Zürich, Switzerland
Kyle Rohde,
University of Central Florida,
United States

***Correspondence:**
Mickael Blaise
mickael.blaise@irim.cnrs.fr
Laurent Kremer
laurent.kremer@irim.cnrs.fr

Specialty section:
This article was submitted to Antimicrobials, Resistance and Chemotherapy, a section of the journal Frontiers in Microbiology

Received: 13 February 2018
Accepted: 20 March 2018
Published: 05 April 2018

Citation:
Richard M, Gutiérrez AV, Viljoen AJ, Ghigo E, Blaise M and Kremer L (2018) Mechanistic and Structural Insights Into the Unique TetR-Dependent Regulation of a Drug Efflux Pump in Mycobacterium abscessus. Front. Microbiol. 9:649. doi: 10.3389/fmicb.2018.00649

Mycobacterium abscessus is an emerging human pathogen causing severe pulmonary infections and is refractory to standard antibiotherapy, yet few drug resistance mechanisms have been reported in this organism. Recently, mutations in *MAB_4384* leading to up-regulation of the MmpS5/MmpL5 efflux pump were linked to increased resistance to thiacetazone derivatives. Herein, the DNA-binding activity of MAB_4384 was investigated by electrophoretic mobility shift assays using the palindromic sequence $IR_{S5/L5}$ located upstream of *mmpS5/mmpL5*. Introduction of point mutations within $IR_{S5/L5}$ identified the sequence requirements for optimal binding of the regulator. Moreover, formation of the protein/$IR_{S5/L5}$ complex was severely impaired for MAB_4384 harboring D14N or F57L substitutions. $IR_{S5/L5}$*/lacZ* reporter fusions in *M. abscessus* demonstrated increased β-galactosidase activity either in strains lacking a functional MAB_4384 or in cultures treated with the TAC analogs. In addition, X-ray crystallography confirmed a typical TetR homodimeric structure of MAB_4384 and unraveled a putative ligand binding site in which the analogs could be docked. Overall, these results support drug recognition of the MAB_4384 TetR regulator, alleviating its binding to $IR_{S5/L5}$ and steering up-regulation of MmpS5/MmpL5. This study provides new mechanistic and structural details of TetR-dependent regulatory mechanisms of efflux pumps and drug resistance in mycobacteria.

Keywords: ***Mycobacterium abscessus*, TetR regulator, MmpL, efflux pump, structure, thiacetazone analogs, EMSA**

INTRODUCTION

Mycobacterium abscessus is a rapid growing mycobacterium (RGM) that has recently become an important health problem (Mougari et al., 2016). This non-tuberculous mycobacterial (NTM) pathogen can cause serious cutaneous, disseminated or pulmonary infections, particularly in cystic fibrosis (CF) patients. In CF patients, infection with *M. abscessus* is correlated with a decline in lung function and poses important challenges during last-resort lung transplantation (Esther et al., 2010; Smibert et al., 2016). An epidemiological study has recently documented the prevalence

and transmission of *M. abscessus* between hospital settings throughout the world, presumably *via* fomites and aerosols and uncovered the emergence of dominant circulating clones that have spread globally (Bryant et al., 2016). In addition, *M. abscessus* exhibits innate resistance to many different classes of antimicrobial agents, rendering infections with this microorganism extremely difficult to treat (Nessar et al., 2012; van Dorn, 2017). Recent studies have started to unveil the basis of the multi-drug resistance characterizing *M. abscessus,* uncovering a wide diversity of mechanisms or regulatory networks. These involve, for example, the induction of the *erm(41)* encoded 23S rRNA methyltransferase and mutations in the 23S *rRNA* that lead to clarithromycin resistance (Nash et al., 2009), the presence of a broad spectrum β-lactamase that limits the use of imipenem (Dubée et al., 2015; Lefebvre et al., 2016, 2017) or the presence of *eis2,* encoding an acetyltransferase that modifies aminoglycosides, specifically induced by *whiB7*, which contributes to the intrinsic resistance to amikacin (Hurst-Hess et al., 2017; Rominski et al., 2017b). Other studies reported the role of the ADP-ribosyltransferase MAB_0591 as a major contributor to rifamycin resistance (Rominski et al., 2017a) whereas MAB_2385 was identified as an important determinant in innate resistance to streptomycin (Dal Molin et al., 2018).

Recently, we reported the activity of a library of thiacetazone (TAC) derivatives against *M. abscessus* and identified several compounds exhibiting potent activity against a vast panel of clinical strains isolated from CF and non-CF patients (Halloum et al., 2017). High resistance levels to these compounds were linked to mutations in a putative transcriptional repressor MAB_4384, together with a strong up-regulation of the divergently oriented adjacent locus encoding a putative MmpS5/MmpL5 transporter system. That ectopic overexpression of MmpS5/MmpL5 in *M. abscessus* also increased the minimal inhibitory concentration (MIC) to analogs of TAC further suggested that these two proteins may act as an active efflux pump which was sufficient to confer drug resistance (Halloum et al., 2017). In addition to uncovering new leads for future drug developments, this study also highlighted a novel mechanism of drug resistance in *M. abscessus*. Unexpectedly, an important difference relies on the fact that, in *M. tuberculosis*, MmpS5/MmpL5 acts as a multi-substrate efflux pump causing low resistance levels to antitubercular compounds such as clofazimine, bedaquiline, and azoles (Milano et al., 2009; Andries et al., 2014; Hartkoorn et al., 2014) whereas the *M. abscessus* strains overexpressing MmpS5/MmpL5 are very resistant to the TAC analogs but fail to show cross-resistance against clofazimine or bedaquiline (Halloum et al., 2017). This implies that, despite their high primary sequence identity, the MmpS5/MmpL5 orthologs from *M. tuberculosis* and *M. abscessus* do not share the same substrate specificity. Moreover, whereas Rv0678, the cognate regulator of MmpS5/MmpL5 in *M. tuberculosis* belongs to the MarR family (Radhakrishnan et al., 2014), MAB_4384 is part of the TetR family of regulators and the change in the transcriptional level of *mmpS5/mmpL5* was much more pronounced in the *M. abscessus* mutants than in the *M. tuberculosis* mutants (Milano et al., 2009; Hartkoorn et al., 2014).

The TetR transcriptional regulatory factors are common single component signal transduction systems found in bacteria. These proteins possess a conserved helix-turn-helix (HTH) signature at the N-terminal of the DNA-binding domain as well as a ligand binding domain (LBD) located at the C-terminal part (Cuthbertson and Nodwell, 2013). They often act as repressors and interact with a specific DNA target to prevent or abolish transcription in the absence of an effector. In contrast, the binding of a specific ligand to the LBD induces structural changes, conducting the dissociation of the repressor from the target DNA, and the subsequent transcription of the TetR-regulated genes. Being largely associated with resistance to antibiotics and regulation of genes coding for small molecule exporters, TetR regulators also govern expression of antibiotic biosynthesis genes, quorum sensing and in distinct aspects in bacterial physiology/virulence (Cuthbertson and Nodwell, 2013). A recent global analysis indicated that the TetR regulators represent the most abundant class of regulators in mycobacteria, the vast majority remaining uncharacterized (Balhana et al., 2015). In order to provide new insight into the mechanism of gene regulation by TetR regulators in mycobacteria and to describe a new and specific drug resistance mechanism in *M. abscessus*, we focused our efforts on the molecular and structural characterization of the MAB_4384-dependent regulation of MmpS5/MmpL5.

In this study, a combination of genetic and biochemical analyses was applied to determine the specificity of this regulatory system in *M. abscessus* and to describe the contribution of key residues that are important in driving the DNA-binding of MAB_4384 to its operator. We report also the crystal structure of the MAB_4384 TetR regulator. Overall, the results provide new insights into the regulation of members of the MmpL family and on a novel mechanism of drug resistance in *M. abscessus*.

MATERIALS AND METHODS

Plasmids, Strains, Growth Conditions, and Reagents

The *Mycobacterium abscessus* subsp. *abscessus* CIP104536^T reference strain and all derived mutant strains are listed in Supplementary Table S1. Strains were grown in Middlebrook 7H9 broth (BD Difco) supplemented with 0.05% Tween 80 (Sigma-Aldrich) and 10% oleic acid, albumin, dextrose, catalase (OADC enrichment; BD Difco) (7H9$^{T/OADC}$) at 30°C or in Sauton's medium in the presence of antibiotics, when required. On plates, colonies were selected either on Middlebrook 7H10 agar (BD Difco) supplemented with 10% OADC enrichment (7H10^{OADC}) or on LB agar. For drug susceptibility testing, cultures were grown in Cation-Adjusted Mueller-Hinton Broth (CaMHB; Sigma-Aldrich). The TAC analogs D6, D15, and D17 were synthesized as reported previously (Coxon et al., 2013) and dissolved in DMSO. Other antibiotics were purchased from Sigma-Aldrich.

Cloning of Wild-Type and Mutated MAB_4384 and Site-Directed Mutagenesis

MAB_4384 was PCR-amplified from *M. abscessus* CIP104536^T purified genomic DNA using the *MAB_4384_full* primers (Supplementary Table S2) and Phusion polymerase (Thermo Fisher Scientific). The amplicon was cloned into pET32a restricted with KpnI and HindIII (New England Biolabs), enabling the introduction of *MAB_4384* in frame with the thioredoxin and poly-histidine tags as well as a Tobacco Etch Virus protease (TEV) cleavage site between the N-terminus of MAB_4384 and the tags. The *MAB_4384* alleles harboring the g40a (D14N) and t169c (F57L) mutations were PCR-amplified using the primers described above and using the purified genomic DNA of the two spontaneous resistant *M. abscessus* strains to TAC analogs reported previously (Halloum et al., 2017). The double mutant carrying both g40a and t169c mutations was obtained from the *MAB_4384* (g40a) allele using the PCR-driven primer overlap extension method (Aiyar et al., 1996). Briefly, two separate PCR reactions were set up using Phusion polymerase. The first was generated using the forward primer *MAB_4384_full* Fw and a reverse internal primer *MAB_4384_DM* Rev harboring the nucleotide substitution responsible for the mutation. The second PCR was set up with an internal forward primer *MAB_4384_DM* Fw overlapping the internal reverse primer *MAB_4384_DM* Rev and with the original reverse primer *MAB_4384_full* Rev. PCR products were purified, annealed and amplified by a last PCR amplification with the *MAB_4384_full* primers. All mutated genes were cloned into pET32a, as described for wild-type *MAB_4384*.

Expression and Purification of MAB_4384 Variants

The various pET32a-derived constructs containing either the wild-type or the mutated *MAB_4384* gene alleles were used to transform *Escherichia coli* strain BL21 Rosetta 2 (DE3) (Novagen). Cultures were grown in Luria-Bertani (LB) medium containing 200 μg/mL ampicillin and 30 μg/mL chloramphenicol until an optical density at 600 nm (OD_{600}) of between 0.6 and 1.0 was reached. Liquid cultures were then placed on icy water for 30 min prior to the addition of 1 mM isopropyl β-D-1-thiogalactopyranoside (IPTG) and incubation for an additional 20 h at 16°C. Bacteria were then collected by centrifugation (6,000 × *g*, 4°C, 60 min) and the pellets were resuspended in lysis buffer (50 mM Tris-HCl pH 8, 200 mM NaCl, 20 mM imidazole, 5 mM β-mercaptoethanol, 1 mM benzamidine). Cells were opened by sonication and the lysate clarified by centrifugation (28,000 × *g*, 4°C, 45 min) and subjected to a first step of nickel affinity chromatography (IMAC) (Ni-NTA Sepharose, GE Healthcare Life Sciences). After elution, the protein was dialyzed overnight at 4°C in a buffer containing 50 mM Tris-HCl pH 8, 200 mM NaCl, 5 mM β-mercaptoethanol and TEV protease (1 mg of protease/50 mg of total protein) to cleave the thioredoxin and histidine tags from the recombinant proteins. The dialyzed preparations were purified again by IMAC, followed by an anion exchange chromatography step (HiTrap Q Fast Flow, GE Healthcare Life Sciences) as well as a final polishing step using size exclusion chromatography (SEC) (Sephadex^{TM} 75 10/300 GL, GE Healthcare Life Sciences) and a buffer containing 50 mM Tris-HCl pH 8, 200 mM NaCl and 5 mM β-mercaptoethanol.

The selenomethionine-substituted protein was expressed in the methionine auxotroph *E. coli* strain B834 (DE3) (Novagen). A 1L culture was grown very densely in LB medium containing 200 μg/mL ampicillin for 36 h at 37°C. Bacteria were harvested by centrifugation and the pellets resuspended in minimal medium A without antibiotic and methionine traces (M9 medium, trace elements, 0.4% glucose, 1 μM $MgSO_4$, 0.3 mM $CaCl_2$, biotin and thiamine at 1 μg/mL). After an additional wash in medium A, the bacterial pellet was resuspended in 6L of medium A containing 200 μg/mL ampicillin and incubated for 2 h at 37°C. Finally, S/L selenomethionine was added at a final concentration of 100 μg/mL. After 30 min of incubation, expression of the protein was induced with 1 mM IPTG for 5 h at 37°C. The protein was purified using a protocol similar to the one used for the proteins expressed in the *E. coli* strain BL21 Rosetta 2(DE3).

Determination of Oligomeric States of MAB_4384 by Size Exclusion Chromatography

The oligomeric state of MAB_4384 and MAB_4384:DNA complex in solution were assessed on an ENrich^{TM} SEC 650 size exclusion column (Bio-Rad) run on an ÄKTA pure 25M chromatography system (GE Healthcare Life Science). The protein, DNA or protein:DNA complex were eluted with 50 mM Tris-HCl pH 8, 200 mM NaCl and 5 mM β-mercaptoethanol at a flow rate of 0.4 mL/min at 4°C. MAB_4384 (dimer) was concentrated to 3.9 mg/mL, while DNA was at 2.8 mg/mL and complexes were formed at different protein(dimer)/DNA molar ratios of 1:1, 2:1, 3:1. The molecular weights were determined based on a calibration curve generated using the Gel Filtration Markers Kit (Sigma-Aldrich) for proteins ranging from 12,400 to 200,000 Da. The column void volume was assessed with the elution peak of dextran blue. The apparent mass was obtained by plotting the partition coefficient K_{av} against the log values of the molecular weights of the standard proteins.

Disruption of *MAB_4384* and *mmpL5* in *M. abscessus*

To generate *MAB_4384* and *mmpL5* knock-out mutants, internal fragments of the genes were PCR-amplified using Phusion polymerase and the specific oligonucleotide sets: *MAB_4384*::pUX1 Fw with *MAB_4384*::pUX1 Rev and *mmpL5*::pUX1 Fw with *mmpL5*::pUX1 Rev, respectively, digested with NheI and BamHI and ligated to NheI-BamHI-linearized pUX1 (Supplementary Table S1), a suicide vector specifically designed to perform gene inactivation in *M. abscessus* (Viljoen et al., 2018). Electrocompetent *M. abscessus* was transformed with the plasmids pUX1-*MAB_4384* and pUX1-*mmpL5* and plated on 250 μg/mL kanamycin LB plates. After 5 days of incubation at 37°C, red fluorescent colonies were selected and gene disruption resulting from homologous recombination

between the plasmid DNA and the target genes was confirmed by PCR and sequencing with appropriate primers (Supplementary Table S2).

Quantitative Real-Time PCR

Isolation of RNA, reverse transcription and qRT-PCR were done as reported earlier (Halloum et al., 2017) using the primers listed in Supplementary Table S2.

Drug Susceptibility Assessment

The MICs were determined according to the CLSI guidelines (Woods et al., 2011), as reported earlier (Halloum et al., 2017).

Electrophoretic Mobility Shift Assays

First, a typical DNA binding motif recognized by the TetR regulator, often composed of palindromic sequences or inverted repeats, was identified *in silico* within the intergenic region located between *MAB_4384* and the *MAB_4383c (mmpS5$_{Mabs}$)/MAB_4382c (mmpL5$_{Mabs}$)* gene cluster, hereafter referred to as IR$_{S5/L5}$, using the MEME Suite 4.20.0 online tool[1] (Bailey et al., 2009). A 45 bp double stranded DNA fragment (Probe 1) containing the 27 bp palindromic sequence was labeled with fluorescein at their 5′ ends (Sigma-Aldrich). Increasing amounts of purified MAB_4384 protein were co-incubated with 280 nM of the fluorescein-labeled probes in 1X Tris Base/acetic acid/EDTA (TAE) buffer for 1 h at room temperature. The samples were then subjected to 6% native polyacrylamide gel electrophoresis for 30 min at 100 V in 1X TAE buffer. Gel shifts were visualized by fluorescence using an Amersham Imager 600 (GE Healthcare Life Sciences). All additional modified probes listed Supplementary Table S2 and used in this study were synthetized and used in electrophoretic mobility shift assay (EMSA) assays, as described above.

Construction of β-Galactosidase Reporter Strains and β-Gal Assays

The *lacZ* reporter gene encoding the β-galactosidase was amplified from the *E. coli* HB101 using primers listed in Supplementary Table S2. The amplicon was cloned into pMV261 cut with BamHI and HindIII, thus yielding pMV261_P$_{hsp60}$_*lacZ*. The 208 bp intergenic region IR$_{S5/L5}$ was amplified by PCR using *M. abscessus* CIP104536^T genomic DNA and the *MAB_4384*_P$_{S5/L5}$ primers (Supplementary Table S2) and subsequently cut with XbaI and BamHI. The *hsp60* promoter was removed from pMV261_P$_{hsp60}$_*lacZ* construct by restriction using XbaI and BamHI and replaced with IR$_{S5/L5}$, thus creating pMV261_P$_{S5/L5}$_*lacZ*. A promoterless pMV261_*lacZ* construct was also generated by removing the *hsp60* promoter from the pMV261_P$_{hsp60}$_*lacZ* with BamHI and XbaI, blunting the overhang extremities using the T4 DNA Polymerase and self-religation.

The β-galactosidase activity of the *M. abscessus* strains carrying either wild-type or mutated *MAB_4384* alleles and the various β-gal reporter constructs was monitored streaking the strains directly on 7H10^{OADC} agar plates supplemented with 100 μg/mL kanamycin and 50 μg/mL X-gal (Sigma-Aldrich). The quantification of the β-gal activity was also assayed in liquid medium using a protocol adapted from Miller's method. Briefly, a 10 mL culture in Sauton's medium supplemented with 0.025% tyloxapol was grown until the OD_{600} reached 0.6–1. Cultures were collected by centrifugation (4,000 × *g* for 10 min at 4°C) and the bacterial pellets were resuspended in 700 μL 1X phosphate-buffered saline (PBS) prior to mechanical lysis by bead beating (3 min treatment, 30 Hz). Lysates were finally centrifuged at 16,000 × *g* for 10 min at 4°C. 10 μL of clarified lysate were co-incubated 30 min at 37°C with 100 μL of reaction buffer (60 mM Na_2HPO_4, 40 mM NaH_2PO_4, 10 mM KCl, 1 mM $MgSO_4$, 50 mM β-mercaptoethanol) in 96-well plates. Enzymatic reactions were initiated by adding 35 μL of 2-Nitrophenyl β-D-galactopyranoside (ONPG, Sigma-Aldrich) at 4 mg/mL and absorbance was recorded at 420 nm at 34°C using a Multimode Microplate Reader POLARstar Omega (BMG Labtech). The β-galactosidase specific activity ($SA_{\beta-Gal}$) was calculated using the following formula: $SA_{\beta-Gal}$ = ($Absorbance_{420nm}$ × min^{-1})/(OD_{280nm} × liter of culture). To test the β-gal-induction by the TAC analogs, the drugs were added directly to the cultures grown in Sauton's medium (OD_{600} = 0.6–1) and incubated with slow shaking for 96 h at 37°C. The β-gal activity was determined as described above.

Crystallization, Data Collection, and Refinement

The MAB_4384 crystals were grown in sitting drops in MR Crystallization Plates (Hampton Research) at 18°C by mixing 1.5 μl of protein solution concentrated to 4.7 mg/mL with 1.5 μl of reservoir solution made of 100 mM sodium cacodylate pH 6.5, 200 mM $MgCl_2$, 16% PEG 8000 and 5% DMSO. Crystals were briefly soaked in 100 mM Cacodylate buffer pH 6.5, 200 mM $MgCl_2$, 16% PEG 8000, 5% DMSO and 10% PEG 400 prior to being cryo-cooled in liquid nitrogen. The selenomethionine-substituted MAB_4384 crystals were obtained in sitting drops in 96-well SWISSCI MRC plates (Molecular Dimension) at 18°C by mixing 0.8 μl of protein solution concentrated to 2.5 mg/mL with 0.8 μl of reservoir solution consisting of 35% (v/v) 1,4 dioxane. Crystals were cryo-cooled without any additional cryo-protection. Data were processed with *XDS* and scaled and merged with *XSCALE* (Kabsch, 2010). Data collection statistics are presented in **Table 1**. The MAB_4384 structure was solved by the single wavelength anomalous dispersion method. *AutoSol* from the *Phenix* package was used to solve the structure (Adams et al., 2010). Twelve of the fourteen potential selenium sites in the asymmetric unit were found using a resolution cutoff of 3.4 Å for the search of the Se atoms. After density modification, a clear electron density map for the two TetR monomers allowed initial model building. The resulting partial model was used to perform molecular replacement with the 1.9 Å native dataset using *Phaser* (McCoy et al., 2007) from the *Phenix* package (Adams et al., 2010). *Coot* (Emsley et al., 2010) was used for manual rebuilding while structure refinement and validation were performed with

[1]http://meme-suite.org

TABLE 1 | Data collection and refinement statistics.

	MAB_4384 native	Selenium peak
Data collection statistics		
Beamline	ESRF-ID30B	ESRF-ID30B
Wavelength (Å)	0.979	0.979
Resolution range (Å)	36.5–1.9 (1.96–1.9)	47–2.3 (2.38–2.3)
Space group	P 1 21 1	P 1 21 1
Unit cell (Å,°)	40.8 100.8 56.0 90 105.8 90	41.4 99.3 55.7 90 106.9 90
Total reflections	73028 (7378)	126590 (12013)
Unique reflections	31705 (3193)	18983 (1849)
Multiplicity	2.3 (2.3)	6.7 (6.5)
Completeness (%)	92.1 (93.4)	98.6 (98.1)
Mean I/sigma (I)	11.09 (1.06)	11.66 (1.36)
Wilson B-factor (Å^2)	33.9	46.02
R-meas	0.06 (0.92)	0.13 (1.21)
CC1/2	0.99 (0.51)	0.97 (0.67)
CC*	1 (0.82)	0.99 (0.89)
Data refinement statistics		
Reflections used in refinement	31695 (3193)	
Reflections used for R-free	2000 (201)	
R-work	0.184 (0.312)	
R-free	0.213 (0.351)	
Number of non-H atoms	3460	
Macromolecules	3178	
Solvent	282	
Protein residues	402	
RMS bonds (Å)	0.002	
RMS angles (°)	0.45	
Ramachandran favored (%)	98.99	
Ramachandran allowed (%)	1.01	
Ramachandran outliers (%)	0.00	
Rotamer outliers (%)	0.95	
Average B-factor (Å^2)	43.6	
Macromolecules	43.2	
Solvent	47.6	
PDB accession number	5OVY	

The values in parenthesis are for the last resolution shell.

the *Phenix* package (Adams et al., 2010). The statistics for data collection and structure refinement are displayed in **Table 1**. Figures were prepared with PyMOL[2]. The atomic coordinates and the structure factors for the reported MAB_4384 crystal structure has been deposited at the Protein Data bank (accession number 5OVY).

Docking of TAC Analogs Into the Ligand Binding Site

Docking studies was performed with *PyRx* (Dallakyan and Olson, 2015) running *AutoDock Vina* (Trott and Olson, 2010). Search was done with grid dimensions of 39.45, 39.05, 29.25 Å and origin coordinates at $x = -17.8$, $y = 6.9$, $z = 0.63$. The search was performed on chain B of the crystal structure of MAB_4384 without any additional model modification.

[2]www.pymol.org

RESULTS

MAB_4384 Specifically Regulates Susceptibility to TAC Analogs in *M. abscessus*

We recently showed that mutations in the MAB_4384 regulator were associated with the transcriptional induction of the divergently oriented adjacent genes coding for an MmpS5/MmpL5 efflux pump and accounting for high resistance levels toward various TAC analogs (Halloum et al., 2017). To gain more insight into this drug resistance mechanism in *M. abscessus,* detailed genetic, functional and structural characterizations of the MAB_4384 regulator were undertaken. First, the expression profile of 19 *mmpL* genes was analyzed by qRT-PCR using the *M. abscessus* D15_S4 strain which possesses an early stop codon in *MAB_4384* resulting in high resistance levels to the TAC analogs D6, D15 and D17 (MIC > 200 μg/mL), presumably due to derepression of the MmpS5/MmpL5 efflux pump machinery (Halloum et al., 2017). The results clearly showed a pronounced increase in the expression level of *MAB_4382c* (*mmpL5*) mRNA in D15_S4 in comparison to the wild-type strain as reported previously, while no marked effect on the remaining *mmpL* genes was detected **(Figure 1A)**. The expression levels of *tgs1*, encoding the primary triacylglycerol synthase responsible for the accumulation of triglycerides in *M. abscessus* (Viljoen et al., 2016) was included as unrelated gene control. As expected, expression of *tgs1* stayed unchanged **(Figure 1A)**. To further confirm these results, the *MAB_4384* and *MAB_4382c* genes were inactivated by homologous recombination using the recently developed genetic tool dedicated to facilitate gene disruption in *M. abscessus* (Viljoen et al., 2018), as illustrated in Supplementary Figures S1A,B. The mutant strain, designated *MAB_4384*::pUX1, failed to show morphological changes (Supplementary Figure S1C) and grew similarly to its parental strain and the *MAB_4382c*::pUX1 mutant (Supplementary Figure S1D), suggesting that *MAB_4384* does not play a significant role under normal *in vitro* conditions. However, this mutant exhibited high resistance levels to D6, D15, and D17 (MIC > 200 μg/mL, corresponding to >8-, >32-, and >16-fold-increases in MIC levels, respectively) (**Table 2**) similarly to our previous results for D15_S4 (Halloum et al., 2017), thus validating the expected phenotype of the strain. Analysis of the transcriptional profile of all 19 *mmpL* genes in *MAB_4384*::pUX1 confirmed the results obtained in the D15_S4 strain **(Figure 1B)**. Interestingly, expression of *MAB_4384* itself was significantly induced in *MAB_4384*::pUX1, **(Figure 1C)**, albeit lower than the expression level of *mmpL5*, thus indicating that MAB_4384 is self-regulated.

Overall, these results suggest that MAB_4384 is a unique and highly specific regulator controlling expression of *mmpL5* in *M. abscessus*, which was strongly up-regulated in the absence of MAB_4384.

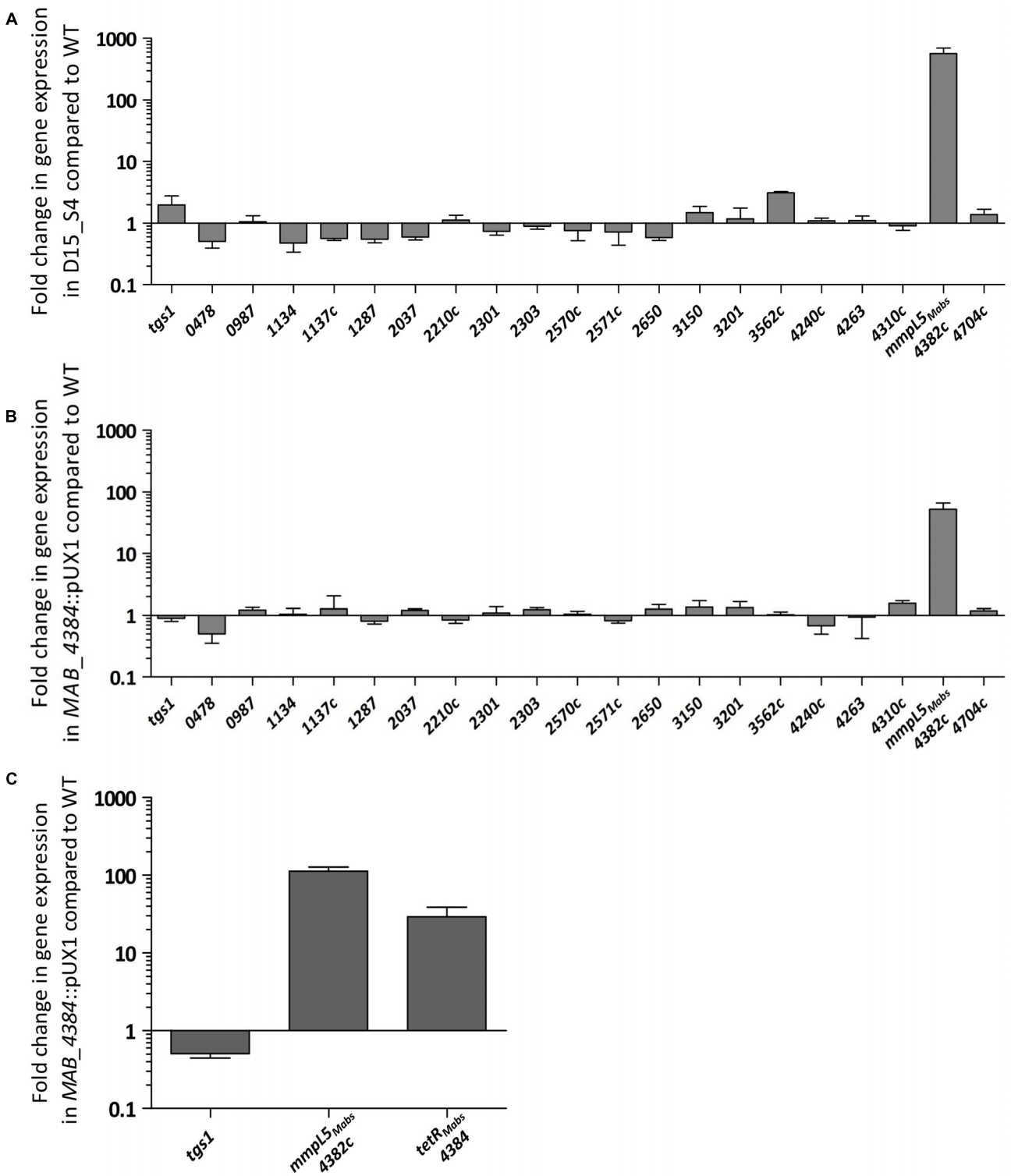

FIGURE 1 | MAB_4384 is a specific repressor of the *mmpS5/mmpL5* locus in *M. abscessus*. Transcriptional profile of 19 *mmpL* in *M. abscessus* expressed in fold induction relative to expression in the wild-type strain (CIP104536^T) in **(A)** the D15_S4 spontaneous mutant resistant to TAC analogs containing a stop codon in *MAB_4384* and in **(B)** *MAB_4384*::pUX1 in which *MAB_4384* has been disrupted by homologous recombination. *tgs1* was included as a non-relevant control gene. Error bars indicate standard deviation. **(C)** Expression of MAB_*4384* in *M. abscessus.* Fold induction levels of *MAB_4384* were calculated in *MAB_4384*::pUX1 relative to the parental strain. Error bars indicate standard deviation. Relative gene expression was calculated using the $\Delta\Delta$Ct method with correction for PCR efficiency. Data is representative of three independent experiments.

TABLE 2 | Drug susceptibility profile of *M. abscessus* S strains inactivated in either *MAB_4384* (*tetR* gene) or *MAB_4382c* (*mmpL5* gene).

	MIC (μg/mL)				
Strain	**D6**	**D15**	**D17**	**CFZ**	**BDQ**
CIP104536^T	25	6.2	12.5	1.6	0.05
MAB_4384::pUX1	>200	>200	>200	1.6	0.05
MAB_4382c::pUX1	12.5	6.2	6.2	1.6	0.05

The MIC (μg/mL) was determined in CaMH medium. Data are representative of three independent experiments. CFZ, clofazimine; BDQ, bedaquiline.

MAB_4384 Negatively Regulates Expression of *mmpS5/mmpL5*

The pMV261_$P_{S5/L5}$_*lacZ* plasmid was constructed, containing the β-galactosidase gene as a reporter in *M. abscessus* to further confirm the negative regulation of MAB_4384 on the target gene (*mmpS5/mmL5* locus) expression. To do this, the 208 bp intergenic region located between *MAB_4384* and *mmpS5/mmpL5* **(Figure 2A)**, designated $IR_{S5/L5}$, was cloned upstream of *lacZ*. pMV261_$P_{S5/L5}$_*lacZ* was subsequently introduced in parental smooth (S) and rough (R) variants of *M. abscessus* as well as in three different strains carrying single point mutations in MAB_4384 (M1A, F57L, and D14N), previously selected for their high resistance phenotype to TAC analogs (Halloum et al., 2017). In addition, pMV261_P_{hsp60}_*lacZ* allowing constitutive expression of *lacZ* under the control of the strong *hsp60* promoter was produced. As expected, pMV261_P_{hsp60}_*lacZ* led to high expression of *lacZ* in the wild-type strain and in the mutants compared to the promoter-less plasmid, as evidenced by the production of intense blue colonies and a strong β-Gal activity **(Figure 2B)**. In contrast, whereas $IR_{S5/L5}$ resulted in very low expression of LacZ in the wild-type strains, characterized by a pale blue color on plates and low β-Gal activity in liquid-grown cultures, a pronounced *lacZ* induction was detected in all three mutant strains **(Figure 2B)**. Strikingly, the *lacZ* expression levels in these strains was almost comparable to the one observed in the pMV261_P_{hsp60}_*lacZ*-containing strains.

Overall, these results indicate that expression of *lacZ* is strongly repressed in the presence of an intact MAB_4384 regulator and that under derepressed conditions, the promoter driving expression of *mmpS5/mmpL5* appears almost as strong as the *hsp60* promoter.

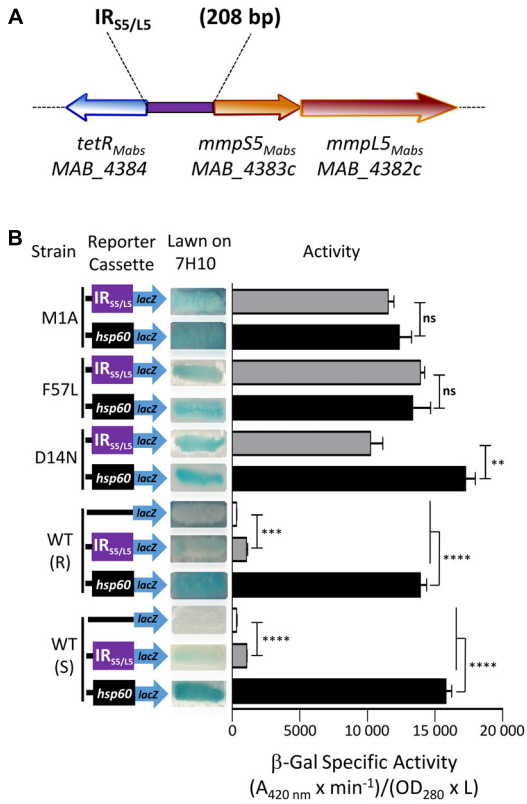

FIGURE 2 | Identification of a MAB_4384-dependent regulatory promoter region in *M. abscessus*. **(A)** Schematic representation of the genome organization of *MAB_4384* and the *mmpS5/mmpL5* gene cluster in *M. abscessus* with the purple rectangle indicating the $IR_{S5/L5}$ intergenic region cloned upstream of the *lacZ* reporter construct. **(B)** The effect of MAB_4384 on *mmpS5/mmpL5* expression was assayed by constructing a plasmid with the *lacZ* reporter under control of $IR_{S5/L5}$. A positive control plasmid consisting of the constitutive expression of *lacZ* under the control of the *hsp60* promoter and a negative control consisting of a promoter-less *lacZ* were also generated. All constructs were introduced into wild-type smooth (S) and rough (R) variants as well as into three different strains harboring single point mutations in MAB_4384 (M1A, D14N and F57L replacements). Exponentially growing *M. abscessus* cultures were streaked onto 7H10 plates containing 100 μg/mL kanamycin and 50 μg/mL X-gal. The plates were subsequently incubated for 3–4 days at 37°C and visualized for their appearance with respect to white-to-blue coloration. The β-galactosidase specific activity ($SA_{\beta-Gal}$) was quantified in liquid cultures using ONPG as a substrate. Results were obtained from three independent experiments and the error bars represent standard deviation. The capped lines indicate the groups compared. For statistical analysis, the Student's *t*-test was applied with ns, **, ***, **** indicating non-significant, $p < 0.01$, $p < 0.001$, and $p < 0.0001$, respectively.

MAB_4384 Binds to a Palindromic Sequence Within $IR_{S5/L5}$

Motif-based sequence analysis using MEME (Bailey et al., 2009) revealed the presence of a 27 bp segment within the divergently oriented $IR_{S5/L5}$ intergenic region and harboring a palindromic sequence **(Figure 3A)**. To test whether this motif represents a DNA binding site for MAB_4384, EMSA was first performed using increasing concentrations of purified MAB_4384 expressed in *E. coli* in the presence of a 45 bp fragment of $IR_{S5/L5}$ (Probe 1; **Figure 3B**) carrying extra nucleotides flanking the palindromic sequence. Under these conditions, a DNA–protein complex was seen **(Figure 3C)**. To confirm the specificity of the binding, a competition assay with increasing concentrations of the corresponding unlabeled probe (cold probe) was carried out, leading to a dose-dependent decrease of the DNA–protein complex **(Figure 3C)**. In addition, in the presence of an excess of a non-related labeled probe, the shift was maintained, thus indicating that a specific protein–DNA complex was seen only when MAB_4384 was incubated with DNA containing the specific inverted repeat sequence. To better define the

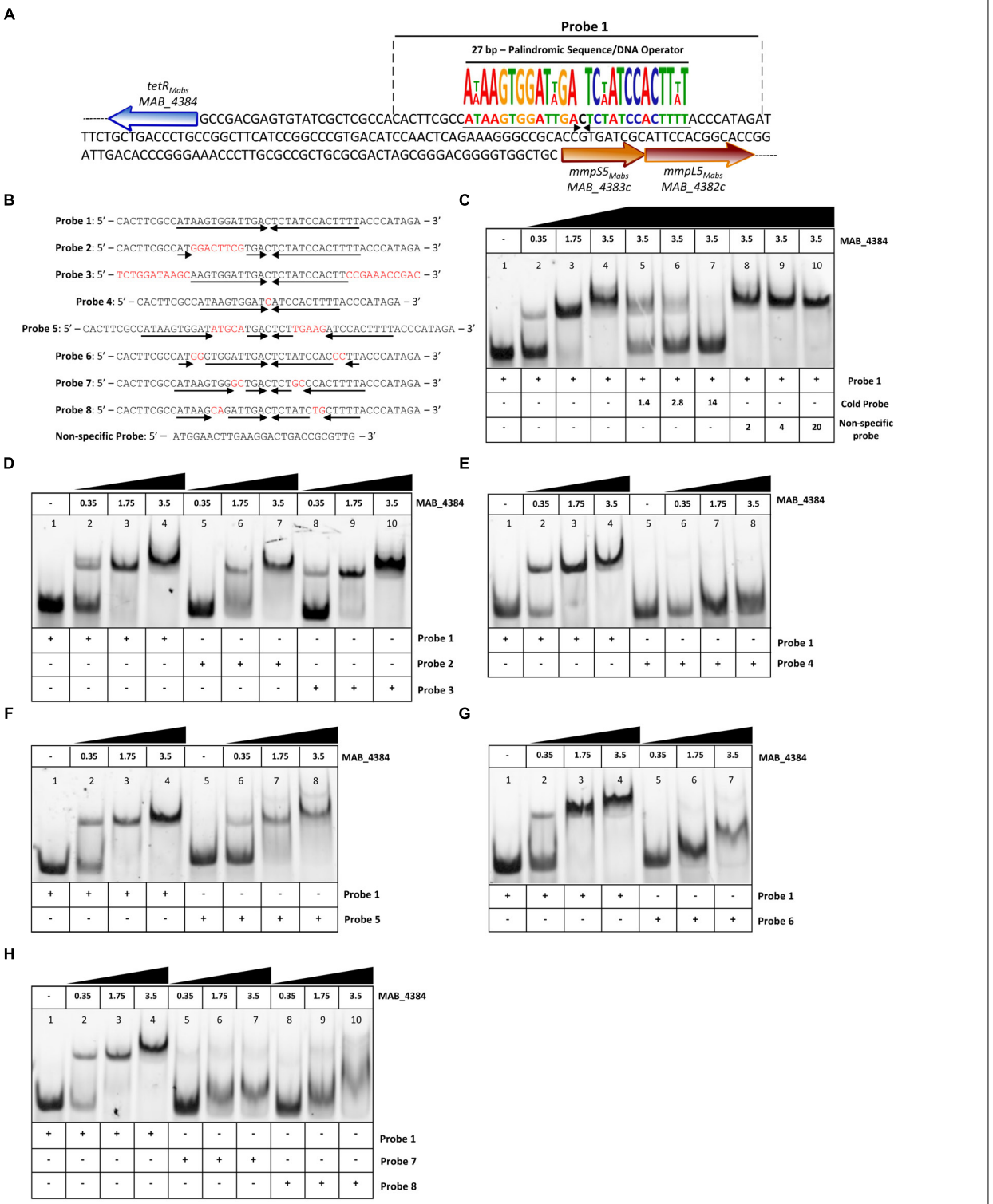

FIGURE 3 | Binding activity of MAB_4384 to a palindromic region within $IR_{S5/L5}$. **(A)** DNA sequence of $IR_{S5/L5}$ and representation of the operator composed of a 27 bp region containing two degenerated inverted sequences of 13 nucleotides each (black arrows) and separated by a one nucleotide spacer. The probe used to perform the EMSA is delimited by dotted lines (Probe 1). **(B)** DNA sequences of all the various 5′ fluorescein-labeled probes used in this study. **(C)** EMSA and competition assay using probe 1. Protein and DNA concentrations are expressed in μM. In competition assays, the concentration of Probe 1 was fixed at 280 nM. Gel shifts were revealed by fluorescence emission. **(D–H)** EMSA using Probes 2 to 8, each time compared to the shift profile obtained with Probe 1. Experiments were reproduced three times with similar results.

minimal motif and the importance of the nucleotides involved in recognition and binding of the protein, a large set of fluorescein-labeled probes differing in their size and/or sequence were next assayed **(Figure 3B).** In the presence of Probe 2, in which only the right inverted sequence was conserved, a delay in the DNA shift was observed (partial in the presence of 1.75 μM of protein as compared to the reaction in the presence of Probe 1). Shifts using Probe 3, where the extra nucleotides surrounding the palindromic sequence were changed randomly were comparable to those obtained with Probe 1 **(Figure 3D)**, indicating that the extra-palindromic sequence does not influence protein binding. With Probe 4, where the inverted repeats were shortened by six nucleotides, the formation of the DNA–protein complex was severely impeded even with the highest concentration of protein tested (3.5 μM) **(Figure 3E)**. Increasing the spacer between the two inverted repeats by 10 nucleotides (Probe 5) negatively impacted the shift **(Figure 3F)**. Substitutions of two nucleotides at the extremities in each repeat sequence (Probe 6) was accompanied by a pronounced shift alteration **(Figure 3G)** and similar results were obtained when di-nucleotide substitutions occurred at other positions within the conserved palindromic sequence (Probes 7 and 8) **(Figure 3H)**.

Overall, these results confirm that a strict preservation of this inverted sequence and space separating these two motifs are crucial for binding of MAB_4384 to its target.

Asp14 and Phe57 Are Critical for Optimal DNA-Binding Activity of MAB_4384

Multiple primary sequence alignments of the MAB_4384 N-terminus with other TetR regulators with known three-dimensional structures indicate that the N-terminus Asp14 residue is well conserved in several other Tet regulators **(Figure 4A)**. Similarly, Phe57 was also found to be part of a highly conserved stretch of amino acids in these proteins, although, in some instances, Phe was replaced by bulky/hydrophobic residues **(Figure 4A)**. The importance of the conservation of these two residues for the function of MAB_4384 and presumably also for that of the other TetR regulators, was next assessed by EMSA using the purified MAB_4384 mutated variants. As compared to the shift profile with wild-type MAB_4384, the production of the DNA–protein complex was severely impaired in the presence of either MAB_4384 (D14N) **(Figure 4C)** or MAB_4384 (F57L) **(Figure 4D)** and fully abrogated in the presence of the double mutant (D14N/F57L) **(Figure 4E)**.

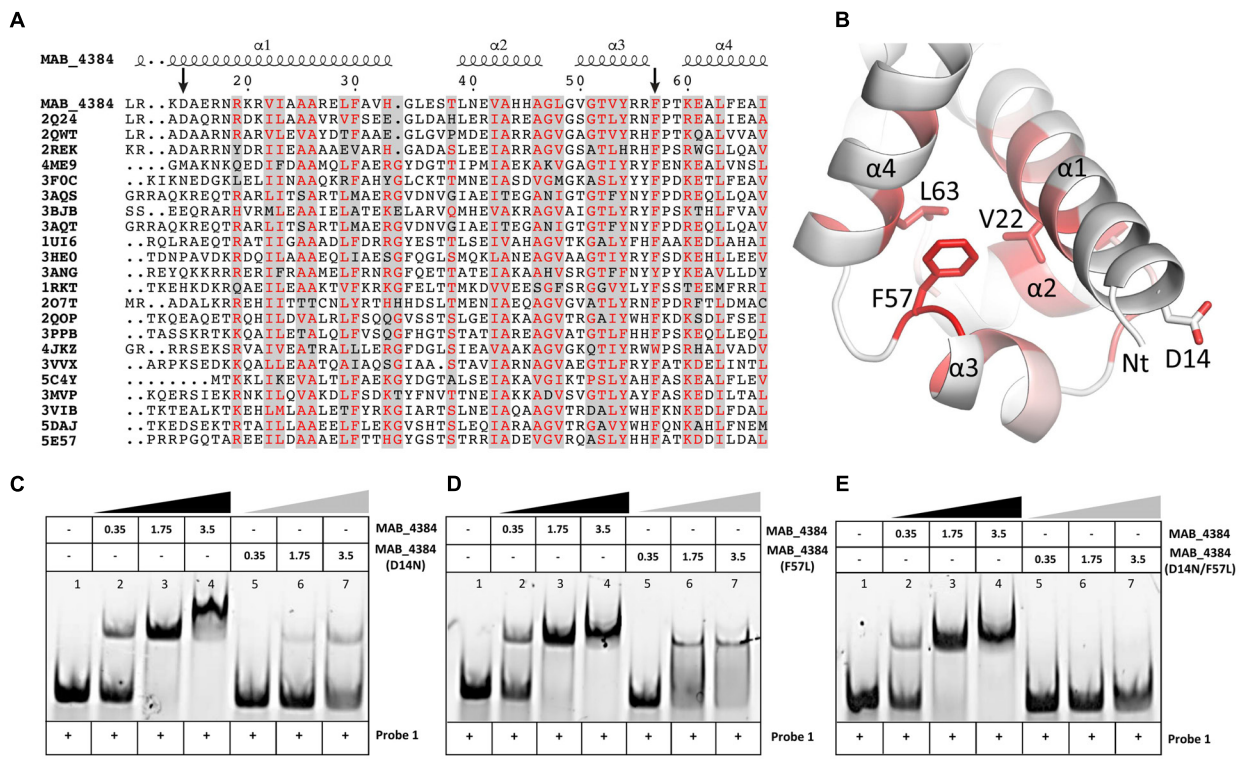

FIGURE 4 | D14N and F57L mutations abrogate binding of MAB_4384 to its palindromic DNA target. **(A)** Multiple primary sequence alignments of MAB_4384 N-terminus with other TetR family members whose crystal structures are known (PDB code indicated) from different microorganisms showing the conservation of the Asp14 and Phe57 residues (indicated with black arrows). **(B)** Mapping of the mutations on the crystal structure of MAB_4384, the degree of residue conservation (obtained from the sequence alignment in **A**) is represented by the coloration, from white (low conservation) to red (high conservation). **(A,B)** Were prepared using the ENDscript server (http://endscript.ibcp.fr/ESPript/ENDscript/). EMSA were performed using increasing concentrations (in μM) of the purified MAB_4384 (D14N) **(C)**, MAB_4384 (F57L) **(D)** or MAB_4384 (D14N/F57L) **(E)** in the presence of Probe 1. Wild-type MAB_4384 was included as a positive control in each assay. The concentration of Probe 1 was fixed at 280 nM. Gel shifts were revealed by fluorescence emission. Three independent experiments were performed with similar results.

Overall, these results support the importance of both residues in the DNA-binding capacity of MAB_4384 and the impaired ability of the mutants to bind to the operator is in agreement with the derepression of *lacZ* transcription in the *M. abscessus* strains carrying the D14N or F57L mutations **(Figure 2B)**.

Oligomeric States of MAB_4384 and MAB_4384:DNA in Solution

To further characterize the MAB_4384:DNA complex formation, we next assessed its stability in solution by SEC **(Figure 5)**. The oligomeric state of MAB_4384 in solution has an apparent 42.6 kDa molecular weight as compared to its 24.7 kDa theoretical molecular mass calculated from its primary sequence, thus highlighting the dimeric state of MAB_4384 in solution. MAB_4384 (dimer) was next incubated with the non-fluorescent DNA Probe 1 **(Figure 3A)** in a 1:1 molar ratio. A stable complex elution peak at 12.6 mL clearly shifted from the elution peak of MAB_4384 and DNA alone **(Figure 5)**, allowing deduction of the molecular mass of the protein:DNA complex at 102 kDa. As the DNA alone in solution appeared on SEC as a 24.5 kDa molecule, these results strongly suggest the existence of two MAB_4384 dimers bound to one DNA molecule as such a complex would possess a molecular mass of 109.7 kDa (2×42.6 kDa + 24.5 kDa). This 2-to-1 binding mode was further corroborated by the fact that an elution peak corresponding to free DNA can be seen at 14.4 mL when we mixed the MAB_4384 dimer and DNA in a 1:1 ratio. Moreover, increasing the molar ratio of the MAB_4384 dimer:DNA complex (2:1 and 3:1) did not yield larger protein:DNA complexes (data not shown), suggesting that, at a 1:1 molar ratio, the operator is already saturated by the protein. This observation is not unique as two TetR dimers have been shown to bind their DNA targets in other microorganisms, such as in *Staphylococcus aureus* (Grkovic et al., 2001) or in *Thermus thermophilus* (Agari et al., 2012).

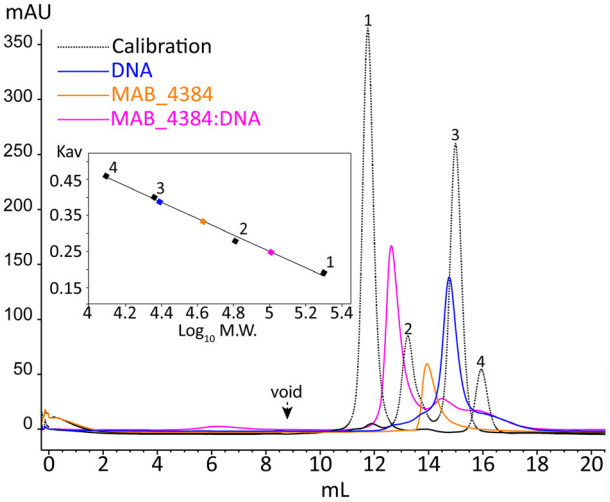

FIGURE 5 | Oligomerization of MAB_4384 and the MAB_4384:DNA complex in solution. The oligomeric states of MAB_4384 alone or complexed to its DNA target were determined by size exclusion chromatography. The elution profile of the proteins, used for the calibration is displayed as a dashed black line. Calibration was established using β-amylase (200 kDa) (1), bovine serum albumin (66 kDa) (2), carbonic anhydrase (29 kDa) (3), and cytochrome C (12.4 kDa) (4), eluting with estimated volumes of 11.7, 13.2, 14.9, 15.9 mL, respectively. The void volume was determined with the elution volume (8.8 mL) of dextran blue. MAB_4384 (dimer) was at a concentration of 3.9 mg/mL. The elution profiles of MAB_4384 dimer, DNA target and MAB_4384 bound to the DNA target are shown in orange, blue, and pink and their respective elution peaks were at 13.9, 14.7, and 12.6 mL. K_{av} indicates the partition coefficient.

Crystal Structure of MAB_4384

To understand, at a molecular basis, how the D14N or F57L mutations generate resistance to TAC analogs, we first crystallized and determined the X-ray structure of MAB_4384. Although the structure of the protein could not be solved by molecular replacement, the phase problem was overcome with the SAD method using crystals of selenomethionine-substituted MAB_4384 **(Table 1)**. The crystal structure of the native protein was subsequently solved with the partial model obtained from the SAD data and refined to a resolution of 1.9 Å. The asymmetric unit contains two subunits. Chain A was modeled from residues Asp14 to Thr213, indicating that the first thirteen residues, one residual Gly residue from the tag and the last eight residues in the C-terminus were not visible in the electron density. Chain B showed also disordered regions as the first ten residues, one Gly residue from the tag in N-terminus as well as the last nine residues in the C-terminus, could not be modeled. Analysis of the crystal packing using the *PISA* server (Krissinel and Henrick, 2007) predicted the existence of a stable homodimer formed within the crystal, consistent with other TetR regulators (Cuthbertson and Nodwell, 2013) and with the SEC profile of MAB_4384 in solution **(Figure 5)**.

The two subunits are very similar as their superposition leads to a root mean square deviation (r.m.s.d.) of 0.53 Å over 198 aligned residues. The N-terminus comprises the DNA binding domain (DBD), followed by the LBD. The DBD is composed of three α-helices α1: residues 12–33, α2: 39–46, and α3: 50–56, where helices 2 and 3 form a helix-turn-helix (HTH) motif. The LBD is made of seven α-helices, α4: 60–82, α5: 88–104, α6: 107–114, α7: 121–143, α8: 155–170, α9: 178–188, and α10: 205–211 **(Figure 6A)**. The surface of dimerization of about 1,700 $Å^2$ is mediated by 31 residues mainly from helices α8 and α9 of each subunit and involves numerous interactions notably five salt bridges, fourteen hydrogen bonds and van der Waals interactions.

Interestingly, we noticed the presence of extra electron density in the LBD of chain B in a rather hydrophobic pocket **(Figure 6B)**. Although we could not interpret this density, we hypothesize that it may correspond to a compound present in the crystallization solution, such as PEG. Search for structural homologs in the PDBeFold server indicated that the closest structure to MAB_4384 corresponds to the LfrR TetR transcriptional regulator from *Mycobacterium smegmatis* bound to proflavin (PDB id : 2V57) (Bellinzoni et al., 2009) with an r.m.s.d. of 2.6 Å and sharing 16% primary sequence identity with MAB_4384. However, only one subunit of each structure could

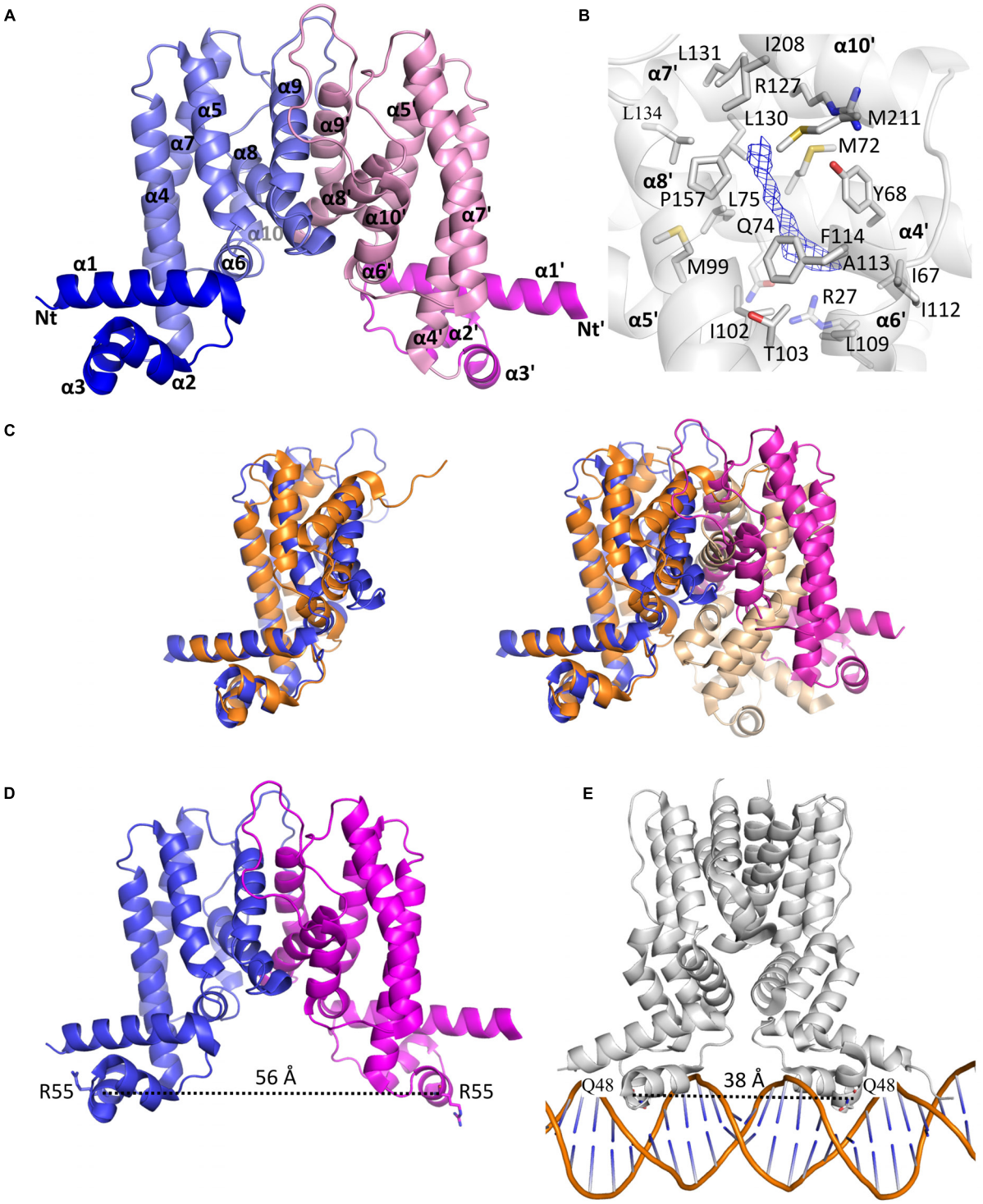

FIGURE 6 | The homodimeric crystal structure of MAB_4384. **(A)** Overall structure of the MAB_4384 dimer displayed as cartoon representation. The LBDs of each subunit are colored in slate and pink while the DNA binding domains are colored in blue and magenta. Helices are indicated by the α signs followed by numbers, Nt and Ct stands for N-terminus and C-terminus and ' is for chain B. **(B)** Putative ligand binding pocket in the LBD of MAB_4384. The Fo-Fc simulated annealed omit map contoured at 3 σ level is shown in blue. Residues that are 4 Å around the electron density blob and that are potential amino acids of the ligand binding site are shown as sticks. **(C)** Structural comparison of MAB_4384 with the crystal structure of the *M. smegmatis* LfrR repressor (PDB id: 2V57). The left panel represents the superposition of one monomer of MAB_4384 (in blue) on one monomer of LfrR (in orange). The superposition of the two homodimers is shown on the right panel, the two subunits of MAB_4384 are in blue and magenta and the two monomers of LfrR are in orange and wheat. **(D,E)** The figures compare the distance between the two DNA binding domains in MAB_4384 **(D)** and in the crystal structure of the *M. smegmatis* TetR Ms6564 protein bound to its DNA target (PDB id: 4JL3).

be superposed as the overall dimers differed largely **(Figure 6C)**. LrfR represses the expression of the LfrA efflux pump (Buroni et al., 2006) and mediates resistance to ethidium bromide, acriflavine, and fluoroquinolones (Takiff et al., 1996).

Due to the occurrence of an extra electron density within the LBD of MAB_4384 and that the closest structure of MAB_4384 is LfrR in its ligand bound form, it is very likely that MAB_4384 was crystallized in its open conformation, i.e., its derepressed form that is not able to interact with DNA. This was assessed by determining the distance between two residues from the DBD susceptible to interact with DNA. Residues Arg55 from chains A and B are about 56 Å apart **(Figure 6D)**. In comparison, the distances between the equivalent residues in various TetR:DNA complexes are largely reduced. In the TetR:DNA complex (PDB id: 4PXI) from *Streptomyces coelicolor* this distance is 45 Å (Bhukya et al., 2014), in the TetR:DNA complex from *M. smegmatis* (PDB id: 4JL3) (Yang et al., 2013) **(Figure 6E)**, *E. coli* (PDB id: 1QPI) (Orth et al., 2000), *Corynebacterium glutamicum* (PDB id: 2YVH) (Itou et al., 2010) or *Staphylococcus aureus* (PDB id: 1JT0) (Schumacher et al., 2002) the distances are 38 Å, 30 Å, 42 Å, and 37 Å, respectively. From these results it can be inferred that the DBDs of MAB_4384 are too far from each other to bind to the DNA groove. These observations combined with the presence of an unidentified ligand in the LBD strongly suggest that the MAB_4384 structure is in an open conformation.

Structural Basis of the Resistant Phenotype of the Mutants

To determine the impact of the mutations in the spontaneous resistant *M. abscessus* mutants, the D14N and F57L residues were mapped on the crystal structure of MAB_4384. Asp14 is located at the beginning of helix α1 and is conserved in several TetR protein members **(Figures 4A,B)**. Residues from helix α1 are often found in contact with DNA as seen in several TetR:DNA crystal structures. Nonetheless, due to the acidic nature of Asp, it is more likely that this residue repulses DNA. We, therefore, hypothesize that it may instead contribute to the correct positioning of other residues located in its close vicinity. Alternatively, repulsion may promote important interactions of DNA with other residues. Indeed, in other collected datasets at lower resolution (data not shown), Asp14 was found to establish a salt bridge interaction, thereby stabilizing the side chain of Arg17 that could interact with DNA. In the absence of a crystal structure of MAB_4384 bound to DNA it is, however, difficult to convincingly affirm the impact of the D14N substitution. However, neither the repulsion of DNA nor the establishment of a salt bridge would be possible if Asn is present instead of Asp, presumably explaining the loss of DNA binding activity of the TetR D14N mutant.

The role of Phe57 situated on helix α3 is more obvious as this position appears always occupied by bulky residues (Phe, Tyr, or Trp) in numerous TetR proteins **(Figure 4A)**. The side chain of Phe57 contacts the side chains of Val22 from helix α1 and Leu63 from helix α4 **(Figure 4B)**. Phe57 is very likely to perform an important structural role in stabilizing the DBD. Replacement with a less bulky side chain such as Leu would abolish these contacts with helices α1 and α4 residues, thus perturbing the overall structural fold of this domain and suppressing the DNA-binding capacity of MAB_4384.

Drug Recognition of MAB_4384 Induces Expression of MmpS5/MmpL5

TetR regulators can respond to small molecules and the best characterized member of this family of regulators is *E. coli* TetR itself. It confers resistance to tetracycline by regulating the expression of the tetracycline TetA efflux pump (Hillen and Berens, 1994). When tetracycline binds to TetR, the regulator loses affinity for the operators, conducting derepression of *tetA* and extrusion of tetracycline out of the bacteria (Lederer et al., 1995). To investigate whether TAC derivatives could bind to the LBD of MAB_4384, *in silico* docking was performed. Despite using a large grid box covering the entire LBD, all three compounds seem to be accommodated by the same binding pocket **(Figure 7A)**. Interestingly, this pocket positioned exactly where the extra electron density was seen in the LBD **(Figure 6B)**. All the compounds bind with similar energies in the aforementioned hydrophobic binding pocket. A slightly stronger interaction for the most hydrophobic derivative D17 was nonetheless observed. D17 and D6 that seem to bind stronger are more hydrophobic and in their best docking poses their thiosemicarbazide group is differently oriented as compared to D15.

Next, we determined whether expression of *mmpS5/mmpL5* can be conditionally induced by the substrates that are extruded by the efflux pump system. This was achieved by determining the effect of the D6, D15, and D17 analogs on LacZ production using the pMV261_$P_{S5/L5}$_*lacZ* reporter strain in *M. abscessus* incubated in Sauton's medium with various drug concentrations consisting of 1X, 2.5X, and 5X the MIC for D15 and of 0.5X, 1X, and 2.5X for D6 and D17. Kinetic studies indicated that optimal expression was obtained after 96 h of treatment (data not shown). The LacZ assay showed that transcription was induced by the TAC analogs in a dose-dependent manner whereas non-related drugs such as amikacin or the DMSO control had no effects **(Figure 7B)**. In comparison with the basal transcriptional level in Sauton's medium (no drug control), the addition of TAC derivatives in the cultures resulted in a reproducible 2.5- to 5-fold increase in the detection of β-Gal activity with D17 being the most potent inducer at 2.5X MIC. However, ethionamide, an antitubercular drug that, like the TAC and TAC analogs, requires to be activated by the EthA monooxygenase (Baulard et al., 2000; DeBarber et al., 2000; Dover et al., 2007; Halloum et al., 2017) failed to induce *lacZ* at 5X MIC (previously determined at 16 μg/ml). Induction of *lacZ* by D17 treatment was further confirmed at a transcriptional level from the pMV261_$P_{S5/L5}$_*lacZ* cultures treated with 2.5× MIC of D17 for 8 h **(Figure 7C**, left). This effect was specific to D17 as no gene induction was observed in the DMSO-treated cultures. Consistently, transcription profiling of *mmpS5* and *mmpL5* in the D17-exposed cultures clearly showed a marked induction level as compared to the DMSO-treated cultures and no effect on *tgs1* expression **(Figure 7C**, right).

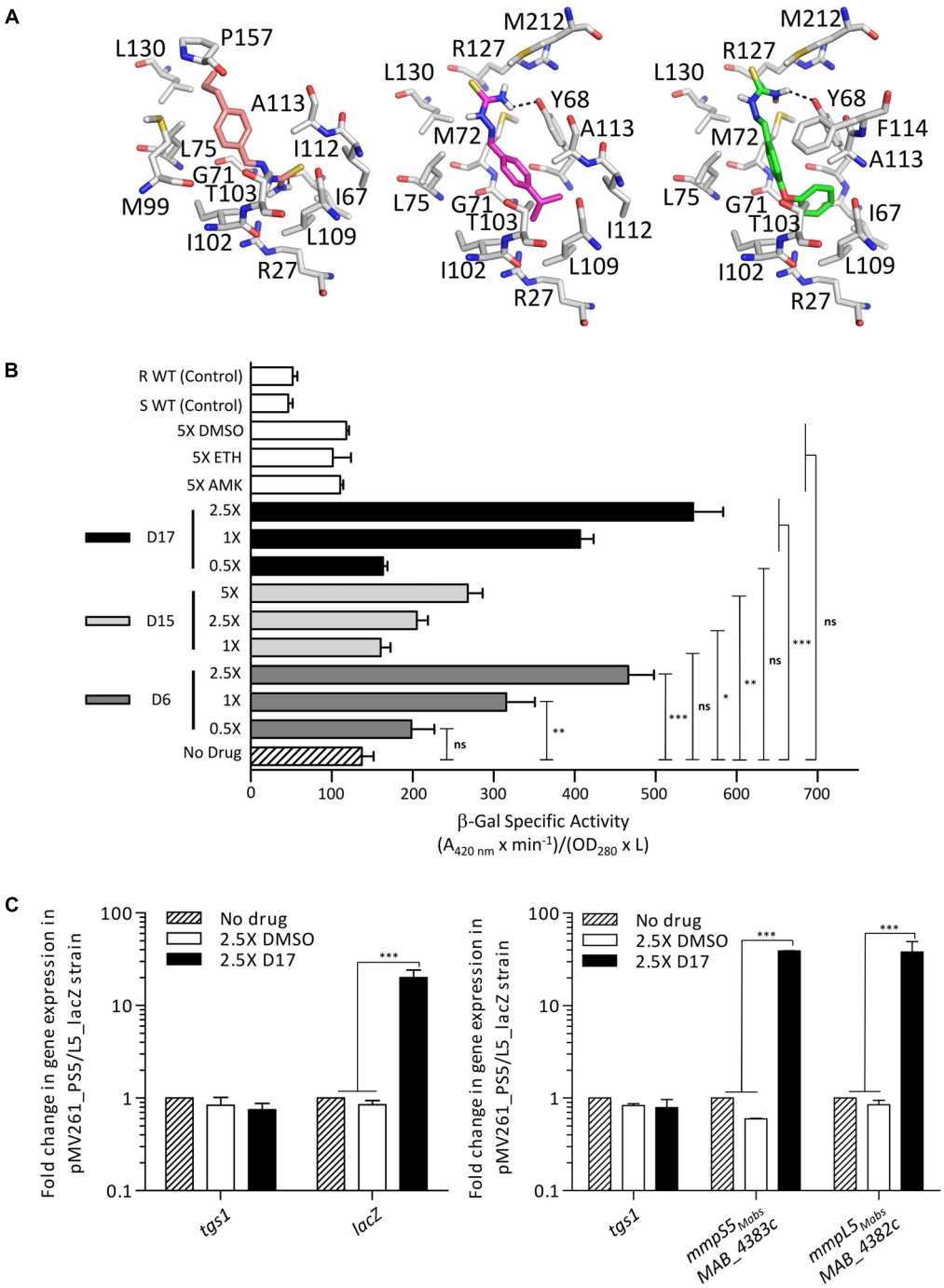

FIGURE 7 | $IR_{S5/L5}$ can be induced by structural analogs of thiacetazone. **(A)** Docking of TAC derivatives in the ligand binding site of MAB_4384. All the residues involved in van der Waals, hydrophobic bonds or hydrogen bonds (in black dashes) are displayed as sticks. D15 in salmon has a binding energy of ΔG = –6.6 kcal/mol, D6 in magenta has a ΔG = –7.3 kcal/mol, and D17 seems to bind slightly stronger with a ΔG = –8.3kcal/mol. **(B)** Conditional induction of *lacZ* by structural analogs of TAC in *M. abscessus*. Induction of β-Gal activity in wild-type *M. abscessus* S carrying pMV261_$P_{S5/L5}$_*lacZ* was assayed using mid-log phase cultures incubated with increasing drug concentrations varying from 1X to 5X the MIC for D15 and varying from 0.5X to 2.5X the MIC for D6 and D17. Inductions were performed for 96 h at 37°C. The β-galactosidase specific activity ($SA_{\beta-Gal}$) was quantified in liquid cultures using ONPG as a substrate. Amikacin (AMK) and ethionamide (ETH) were included as unrelated drug controls. **(C)** Transcriptional profile of *lacZ* in the *M. abscessus* pMV261_$P_{S5/L5}$_*lacZ* reporter strain exposed to 2.5X the MIC of D17 for 8 h (left). *tgs1* was included as a non-relevant control. Replacing D17 by an equal volume of DMSO had no effect on *lacZ* transcription. Transcriptional induction of $mmpS5_{Mabs}$ and $mmpL5_{Mabs}$ following exposure to 2.5X the MIC of D17 for 8 h (right). Results were obtained from three independent experiments and the error bars represent standard deviation. For statistical analysis the Student's *t*-test was applied with ns, *, **, ***, **** indicating non-significant, $p < 0.05$, $p < 0.01$, $p < 0.001$, and $p < 0.0001$, respectively.

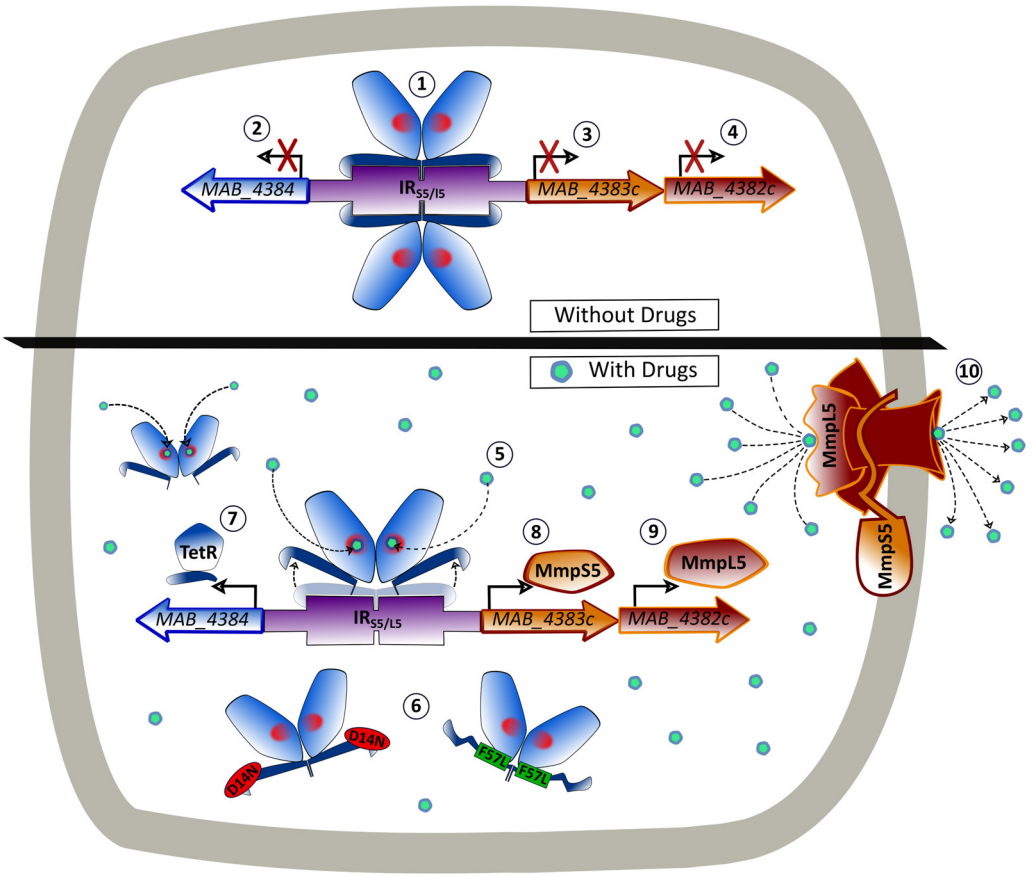

FIGURE 8 | Model of the binding of MAB_4384 to its operator and regulation of the MmpS5/MmpL5 efflux pump machinery. In the absence of drug, two MAB_4384 dimers bind to their DNA operator located in the intergenic region ($IR_{S5/L5}$) between the divergently transcribed *MAB_4384* (encoding the TetR regulator) and *MAB_4383c/MAB_4382c* (encoding the MmpS5/MmpL5 efflux pump) (1). This action represses the transcription of *MAB_4384* (2), *MAB_4383c* (3) and *MAB_4382c* (4), predisposing the bacteria to drug susceptibility. When the TAC derivatives bind to MAB_4384 (5) or if MAB_4384 harbors the D14N or F57L mutations (6), the regulator loses affinity for the operator, leading to derepression of *MAB_4384* itself (7), *MAB_4383c* (8) and *MAB_4382c* (9). This triggers high levels of expression of the MmpS5/MmpL5 complex in the plasma membrane and the subsequent export of the TAC analogs outside the bacteria (10), reducing susceptibility to the compounds.

Together, these results support the view that TAC analogs, which are substrates of MmpS5/mmpL5, are also effectors of MAB_4384-induced transcription of *mmpS5/mmpL5*.

DISCUSSION

Herein, a combination of genetic, biochemical and structural studies was used to demonstrate that MAB_4384 is part of the TetR family of regulators, which represses the transcriptional expression of the MmpS5/MmpL5 efflux pump. MAB_4384 belongs to the type I class TetR family of regulators, characterized by a divergent orientation to one of the adjacent target genes (Cuthbertson and Nodwell, 2013). In *M. tuberculosis,* MmpS5/MmpL5 is under the control of the MarR repressor Rv0678 (Radhakrishnan et al., 2014) and mutations in this regulator leads to drug resistance (Andries et al., 2014; Hartkoorn et al., 2014; Zhang et al., 2015). EMSA indicated a direct binding of Rv0678 to the intergenic region located between *mmpS5* and *Rv0678*. However, shifts were also found using the promoter regions of *mmpS2-mmpL2*, *mmpS4-mmpL4,* and *Rv0991-Rv0992* (Radhakrishnan et al., 2014), suggesting that a single regulator can control expression of several *mmpS/mmpL* loci. Our analysis indicates that, despite the fact that *M. abscessus* possesses the highest number of *mmpL* genes among all mycobacterial species studied (Viljoen et al., 2017), the MAB_4384 regulator is highly specific to the *mmpS5/mmpL5* pair as demonstrated by the lack of transcriptional regulation of a large set of *mmpL* genes and the presence of a unique inverted DNA sequence target that was not found elsewhere in the chromosome. This unique trait might also be reflected by the modest structural homology of MAB_4384 with other TetR crystal structures. The tight regulation and the high specificity of interaction with its target DNA, however, cannot be solely explained on the basis of the MAB_4384 crystal structure and the structure of the MAB_4384:DNA complex is, therefore, greatly warranted to dissect these underlying mechanisms. Nevertheless, our structural analysis underscores the strategy employed by *M. abscessus* to acquire mutations

impacting the DNA-binding capacity or the folding/stability of the DBD of MAB_4384 to become resistant.

EMSA and *lacZ* reporter fusions confirmed that D14N and F57L mutations, alleviating the DNA-binding activity of MAB_4384, cause a strong up-regulation of *mmpS5/mmpL5* gene expression, in agreement with our previous qRT-PCR analyses (Halloum et al., 2017). This leads to extrusion of the TAC derivatives out of the cells, contributing to the high MIC values for TAC derivatives against these mutants, as illustrated in **Figure 8**. Expression of multi-drug resistant efflux pumps can also be conditionally induced using structurally diverse substrates (Kaatz and Seo, 1995; Rosenberg et al., 2003; Buroni et al., 2006). This induction is caused by the direct interaction of these substrates with the repressors, interfering with binding of the repressors to their target operators and resulting in increased expression of the pumps. Here, we show inducible β-galactosidase activity following treatment with D6, D15, or D17, a mechanism that is very likely to be meditated by MAB_4384. This view is reinforced by the fact that docking studies highlighted the possibility that all three analogs could be accommodated in the LBD of the protein, which perfectly coincided with the extra electron density observed. Since, the LBD are remote from the DBD, the derepression of TetR family regulators involves allosteric mechanisms that include conformational changes transmitted largely within the same subunit (Ramos et al., 2005). The interaction of ligands with the LBD captures a conformational state where the DBD is repositioned relative to the LBD in a way that the dimer is prevented from binding to its target DNA. However, definitive proof of this mechanism awaits the elucidation of the crystal structure of the D17-bound form of MAB_4384, as reported for instance with the hexadecyl octanoate-bound EthR repressor (Frénois et al., 2004) or the LfrR regulator complexed with proflavine (Bellinzoni et al., 2009). Lack of inducible *lacZ* expression in *M. abscessus* cultures exposed to amikacin, for which mutations in 16S rRNA represent a major mechanism of resistance (Prammananan et al., 1998), indicates that MmpL5-mediated efflux cannot mediate resistance toward this antibiotic in line with the lack of cross-resistance toward amikacin observed for TAC derivative-spontaneous resistant mutants (Halloum et al., 2017). The specificity of the MAB_4384-driven resistance mechanism described herein is further supported by the lack of *lacZ* induction during exposure to ETH, that similarly to TAC and TAC analogs, requires bio-transformation by EthA, whose expression is also dependent on the EthR regulator belonging to the TetR family (Baulard et al., 2000; Engohang-Ndong et al., 2004; Halloum et al., 2017). Together, these findings strongly suggest that when TAC analogs bind to MAB_4384, the regulator loses affinity for its DNA target, resulting in up-regulation of *mmpS5/mmpL5* and export of the drugs from the cells **(Figure 8)**. These results also point out the selectivity of this efflux-based mechanism. Indeed, no change in the MIC of clofazimine or bedaquiline were noticed in a *MAB_4384*-disrupted strain, which appears intriguing as MmpL5 has been reported as a multi-substrate efflux pump responsible for low-level resistance to both of these drugs in *M. tuberculosis* (Hartkoorn et al., 2014). The LBD of MAB_4384 potentially can accommodate bulky molecules and might thus indicate that MAB_4384 is involved in efflux of other types of compounds in addition to TAC analogs. However, we could neither dock clofazimine nor bedaquiline in the LBD of MAB_4384 (not shown). Several reasons can be put forth to explain these species-specific variations. In *M. tuberculosis*, expression of MmpL5 is under the control of a MarR regulator rather than a TetR regulator. Alternatively, we have previously reported the occurrence in *M. abscessus* of three *mmpS5/mmpL5* paralogs (Halloum et al., 2017), thus, it remains possible that either of the two remaining genes may participate in co-resistance to these drugs in *M. abscessus*.

The highly pronounced expression of *lacZ* under derepressed conditions found in the M1A, F57L, or D14N mutant strains, almost at levels similar to those driven by the strong and constitutive *hsp60* promoter, confirmed the very high expression levels of *mmpS5* and *mmpL5* detected by qRT-PCR and probably explains the very high level of resistance of the mutants (MIC $>$ 200 μg/mL). This contrasts also with findings where MmpL5 mediates only low-levels of resistance in *M. tuberculosis* (Andries et al., 2014; Hartkoorn et al., 2014), presumably because expression of *mmpL5* is driven by a weaker promoter than in *M. abscessus*. That *mmpS5/mmpL5* expression is tightly controlled suggests that the MmpS5/MmpL5 machinery may exert an important function in the assembly and/or maintenance of the cell wall by exporting a yet unidentified lipid, as already reported for several MmpL transporters in *M. tuberculosis* (Chalut, 2016; Viljoen et al., 2017). Alternatively, they may participate in adaptation during the infection process. However, the growth curves of the wild-type or the strain constitutively expressing high levels of MmpL5 (due to the M1A mutation in MAB_4384) were comparable *in vitro*. In addition, microinjections of the different strains were done in the zebrafish embryo, an animal model previously developed to study the early events of the *M. abscessus* infection (Bernut et al., 2014, 2015). No differences in virulence were noticed between the wild-type and MAB_4384 (M1A) strains (Supplementary Figure S2). Interestingly, the *mmpS5/mmpL5* locus was found to be induced when *M. abscessus* was exposed to a defined, synthetic medium that mimics the composition of CF sputum (Miranda-CasoLuengo et al., 2016). This may be part of a complex adaptive transcriptional response to the mucus layer of the CF airways that leads to the chronic infections of *M. abscessus*.

In summary, this study provides new functional and structural insights into TetR-dependent regulation of MmpL efflux pumps in mycobacteria. Considering the exceptionally high abundance of TetR transcriptional regulators (more than 130) as well as the important MmpL repertoire (around 30) in *M. abscessus*, one can anticipate that mechanisms similar to the one described here are exploited by this pathogen to express its intrinsic resistance level to other antibiotics.

ETHICS STATEMENT

Zebrafish experiments were done at IRIM, according to European Union guidelines for handling of laboratory animals

(http://ec.europa.eu/environment/chemicals/lab_animals/home_en.htm) and approved by the Direction Sanitaire et Vétérinaire de l'Hérault and Comité d'Ethique pour l'Expérimentation Animale de la Région Languedoc Roussillon (CEEA-LR) under the reference CEEA-LR-1145.

AUTHOR CONTRIBUTIONS

MR, AVG, AV, MB, and LK acquired and analyzed the data. EG, MB, and LK wrote the manuscript. LK conceived and designed the study.

FUNDING

This work was supported by the Fondation pour la Recherche Médicale (FRM) (grant number DEQ20150331719 to LK; grant number ECO20160736031 to MR) and by the InfectioPôle Sud for funding the Ph.D. Fellowship of AVG.

ACKNOWLEDGMENTS

The authors wish to thank G. S. Coxon for the generous gift of the TAC analogs. The crystallographic data were collected on beamline ID30B at the European Synchrotron Radiation Facility (ESRF), Grenoble, France. The authors are grateful to Local Contact at the ESRF for providing assistance in using beamline ID30B.

SUPPLEMENTARY MATERIAL

The Supplementary Material for this article can be found online at: https://www.frontiersin.org/articles/10.3389/fmicb.2018.00649/full#supplementary-material

REFERENCES

Adams, P. D., Afonine, P. V., Bunkóczi, G., Chen, V. B., Davis, I. W., Echols, N., et al. (2010). *PHENIX*: a comprehensive Python-based system for macromolecular structure solution. *Acta Crystallogr. D Biol. Crystallogr.* 66, 213–221. doi: 10.1107/S0907444909052925

Agari, Y., Sakamoto, K., Kuramitsu, S., and Shinkai, A. (2012). Transcriptional repression mediated by a TetR family protein, PfmR, from *Thermus thermophilus* HB8. *J. Bacteriol.* 194, 4630–4641. doi: 10.1128/JB.00668-12.

Aiyar, A., Xiang, Y., and Leis, J. (1996). Site-directed mutagenesis using overlap extension PCR. *Methods Mol. Biol.* 57, 177–191. doi: 10.1385/0-89603-332-5:177

Andries, K., Villellas, C., Coeck, N., Thys, K., Gevers, T., Vranckx, L., et al. (2014). Acquired resistance of *Mycobacterium tuberculosis* to bedaquiline. *PLoS One* 9:e102135. doi: 10.1371/journal.pone.0102135

Bailey, T. L., Boden, M., Buske, F. A., Frith, M., Grant, C. E., Clementi, L., et al. (2009). MEME SUITE: tools for motif discovery and searching. *Nucleic Acids Res.* 37, W202–W208. doi: 10.1093/nar/gkp335

Balhana, R. J. C., Singla, A., Sikder, M. H., Withers, M., and Kendall, S. L. (2015). Global analyses of TetR family transcriptional regulators in mycobacteria indicates conservation across species and diversity in regulated functions. *BMC Genomics* 16:479. doi: 10.1186/s12864-015-1696-9

Baulard, A. R., Betts, J. C., Engohang-Ndong, J., Quan, S., McAdam, R. A., Brennan, P. J., et al. (2000). Activation of the pro-drug ethionamide is regulated in mycobacteria. *J. Biol. Chem.* 275, 28326–28331. doi: 10.1074/jbc.M003744200

Bellinzoni, M., Buroni, S., Schaeffer, F., Riccardi, G., De Rossi, E., and Alzari, P. M. (2009). Structural plasticity and distinct drug-binding modes of LfrR, a mycobacterial efflux pump regulator. *J. Bacteriol.* 191, 7531–7537. doi: 10.1128/JB.00631-09

Bernut, A., Dupont, C., Sahuquet, A., Herrmann, J.-L., Lutfalla, G., and Kremer, L. (2015). Deciphering and imaging pathogenesis and cording of *Mycobacterium abscessus* in zebrafish embryos. *J. Vis. Exp.* 103:53130. doi: 10.3791/53130

Bernut, A., Herrmann, J.-L., Kissa, K., Dubremetz, J.-F., Gaillard, J.-L., Lutfalla, G., et al. (2014). *Mycobacterium abscessus* cording prevents phagocytosis and promotes abscess formation. *Proc. Natl. Acad. Sci. U.S.A.* 111, E943–E952. doi: 10.1073/pnas.1321390111

Bhukya, H., Bhujbalrao, R., Bitra, A., and Anand, R. (2014). Structural and functional basis of transcriptional regulation by TetR family protein CprB from *S. coelicolor* A3(2). *Nucleic Acids Res.* 42, 10122–10133. doi: 10.1093/nar/gku587

Bryant, J. M., Grogono, D. M., Rodriguez-Rincon, D., Everall, I., Brown, K. P., Moreno, P., et al. (2016). Emergence and spread of a human-transmissible multidrug-resistant nontuberculous mycobacterium. *Science* 354, 751–757. doi: 10.1126/science.aaf8156

Buroni, S., Manina, G., Guglierame, P., Pasca, M. R., Riccardi, G., and De Rossi, E. (2006). LfrR is a repressor that regulates expression of the efflux pump LfrA in *Mycobacterium smegmatis*. *Antimicrob. Agents Chemother.* 50, 4044–4052. doi: 10.1128/AAC.00656-06

Chalut, C. (2016). MmpL transporter-mediated export of cell-wall associated lipids and siderophores in mycobacteria. *Tuberclosis* 100, 32–45. doi: 10.1016/j.tube.2016.06.004

Coxon, G. D., Craig, D., Corrales, R. M., Vialla, E., Gannoun-Zaki, L., and Kremer, L. (2013). Synthesis, antitubercular activity and mechanism of resistance of highly effective thiacetazone analogues. *PLoS One* 8:e53162. doi: 10.1371/journal.pone.0053162

Cuthbertson, L., and Nodwell, J. R. (2013). The TetR family of regulators. *Microbiol. Mol. Biol. Rev.* 77, 440–475. doi: 10.1128/MMBR.00018-13

Dal Molin, M., Gut, M., Rominski, A., Haldimann, K., Becker, K., and Sander, P. (2018). Molecular mechanisms of intrinsic streptomycin resistance in *Mycobacterium abscessus*. *Antimicrob. Agents Chemother.* 62:e01427-17. doi: 10.1128/AAC.01427-17

Dallakyan, S., and Olson, A. J. (2015). Small-molecule library screening by docking with PyRx. *Methods Mol. Biol.* 1263, 243–250. doi: 10.1007/978-1-4939-2269-7_19

DeBarber, A. E., Mdluli, K., Bosman, M., Bekker, L. G., and Barry, C. E. (2000). Ethionamide activation and sensitivity in multidrug-resistant *Mycobacterium tuberculosis*. *Proc. Natl. Acad. Sci. U.S.A.* 97, 9677–9682. doi: 10.1073/pnas.97.17.9677

Dover, L. G., Alahari, A., Gratraud, P., Gomes, J. M., Bhowruth, V., Reynolds, R. C., et al. (2007). EthA, a common activator of thiocarbamide-containing drugs acting on different mycobacterial targets. *Antimicrob. Agents Chemother.* 51, 1055–1063. doi: 10.1128/AAC.01063-06

Dubée, V., Bernut, A., Cortes, M., Lesne, T., Dorchene, D., Lefebvre, A.-L., et al. (2015). β-Lactamase inhibition by avibactam in *Mycobacterium abscessus*. *J. Antimicrob. Chemother.* 70, 1051–1058. doi: 10.1093/jac/dku510

Emsley, P., Lohkamp, B., Scott, W. G., and Cowtan, K. (2010). Features and development of coot. *Acta Crystallogr. D Biol. Crystallogr.* 66, 486–501. doi: 10.1107/S0907444910007493

Engohang-Ndong, J., Baillat, D., Aumercier, M., Bellefontaine, F., Besra, G. S., Locht, C., et al. (2004). EthR, a repressor of the TetR/CamR family implicated in ethionamide resistance in mycobacteria, octamerizes cooperatively on its operator. *Mol. Microbiol.* 51, 175–188. doi: 10.1046/j.1365-2958.2003.03809.x

Esther, C. R., Esserman, D. A., Gilligan, P., Kerr, A., and Noone, P. G. (2010). Chronic *Mycobacterium abscessus* infection and lung function decline

in cystic fibrosis. *J. Cyst. Fibros.* 9, 117–123. doi: 10.1016/j.jcf.2009.12.0001

Frénois, F., Engohang-Ndong, J., Locht, C., Baulard, A. R., and Villeret, V. (2004). Structure of EthR in a ligand bound conformation reveals therapeutic perspectives against tuberculosis. *Mol. Cell* 16, 301–307. doi: 10.1016/j.molcel.2004.09.020

Grkovic, S., Brown, M. H., Schumacher, M. A., Brennan, R. G., and Skurray, R. A. (2001). The staphylococcal QacR multidrug regulator binds a correctly spaced operator as a pair of dimers. *J. Bacteriol.* 183, 7102–7109. doi: 10.1128/JB.183.24.7102-7109.2001

Halloum, I., Viljoen, A., Khanna, V., Craig, D., Bouchier, C., Brosch, R., et al. (2017). Resistance to thiacetazone derivatives active against *Mycobacterium abscessus* involves mutations in the MmpL5 transcriptional repressor MAB_4384. *Antimicrob. Agents Chemother.* 61:11e01225-17. doi: 10.1128/AAC.02509-16

Hartkoorn, R. C., Uplekar, S., and Cole, S. T. (2014). Cross-resistance between clofazimine and bedaquiline through upregulation of MmpL5 in *Mycobacterium tuberculosis*. *Antimicrob. Agents Chemother.* 58, 2979–2981. doi: 10.1128/AAC.00037-14

Hillen, W., and Berens, C. (1994). Mechanisms underlying expression of Tn10 encoded tetracycline resistance. *Annu. Rev. Microbiol.* 48, 345–369. doi: 10.1146/annurev.mi.48.100194.002021

Hurst-Hess, K., Rudra, P., and Ghosh, P. (2017). *Mycobacterium abscessus* WhiB7 regulates a species-specific repertoire of genes to confer extreme antibiotic resistance. *Antimicrob. Agents Chemother.* 61:e01347-17. doi: 10.1128/AAC.01347-17

Itou, H., Watanabe, N., Yao, M., Shirakihara, Y., and Tanaka, I. (2010). Crystal structures of the multidrug binding repressor *Corynebacterium glutamicum* CgmR in complex with inducers and with an operator. *J. Mol. Biol.* 403, 174–184. doi: 10.1016/j.jmb.2010.07.042

Kaatz, G. W., and Seo, S. M. (1995). Inducible NorA-mediated multidrug resistance in *Staphylococcus aureus*. *Antimicrob. Agents Chemother.* 39, 2650–2655. doi: 10.1128/AAC.39.12.2650

Kabsch, W. (2010). Integration, scaling, space-group assignment and post-refinement. *Acta Crystallogr. D Biol. Crystallogr.* 66, 133–144. doi: 10.1107/S0907444909047374

Krissinel, E., and Henrick, K. (2007). Inference of macromolecular assemblies from crystalline state. *J. Mol. Biol.* 372, 774–797. doi: 10.1016/j.jmb.2007.05.022

Lederer, T., Takahashi, M., and Hillen, W. (1995). Thermodynamic analysis of tetracycline-mediated induction of Tet repressor by a quantitative methylation protection assay. *Anal. Biochem.* 232, 190–196. doi: 10.1006/abio.1995.0006

Lefebvre, A.-L., Dubée, V., Cortes, M., Dorchêne, D., Arthur, M., and Mainardi, J.-L. (2016). Bactericidal and intracellular activity of β-lactams against *Mycobacterium abscessus*. *J. Antimicrob. Chemother.* 71, 1556–1563. doi: 10.1093/jac/dkw022

Lefebvre, A.-L., Le Moigne, V., Bernut, A., Veckerlé, C., Compain, F., Herrmann, J.-L., et al. (2017). Inhibition of the β-lactamase BlaMab by avibactam improves the *in vitro* and *in vivo* efficacy of imipenem against *Mycobacterium abscessus*. *Antimicrob. Agents Chemother.* 61:e02440-16. doi: 10.1128/AAC.02440-16

McCoy, A. J., Grosse-Kunstleve, R. W., Adams, P. D., Winn, M. D., Storoni, L. C., and Read, R. J. (2007). *Phaser* crystallographic software. *J. Appl. Crystallogr.* 40, 658–674. doi: 10.1107/S0021889807021206

Milano, A., Pasca, M. R., Provvedi, R., Lucarelli, A. P., Manina, G., Ribeiro, A. L., et al. (2009). Azole resistance in *Mycobacterium tuberculosis* is mediated by the MmpS5-MmpL5 efflux system. *Tuberclosis* 89, 84–90. doi: 10.1016/j.tube.2008.08.003

Miranda-CasoLuengo, A. A., Staunton, P. M., Dinan, A. M., Lohan, A. J., and Loftus, B. J. (2016). Functional characterization of the *Mycobacterium abscessus* genome coupled with condition specific transcriptomics reveals conserved molecular strategies for host adaptation and persistence. *BMC Genomics* 17:553. doi: 10.1186/s12864-016-2868-y

Mougari, F., Guglielmetti, L., Raskine, L., Sermet-Gaudelus, I., Veziris, N., and Cambau, E. (2016). Infections caused by *Mycobacterium abscessus*: epidemiology, diagnostic tools and treatment. *Expert Rev. Anti Infect. Ther.* 14, 1139–1154. doi: 10.1080/14787210.2016.1238304

Nash, K. A., Brown-Elliott, B. A., and Wallace, R. J. (2009). A novel gene, *erm(41)*, confers inducible macrolide resistance to clinical isolates of *Mycobacterium abscessus* but is absent from *Mycobacterium chelonae*. *Antimicrob. Agents Chemother.* 53, 1367–1376. doi: 10.1128/AAC.01275-08

Nessar, R., Cambau, E., Reyrat, J. M., Murray, A., and Gicquel, B. (2012). *Mycobacterium abscessus*: a new antibiotic nightmare. *J. Antimicrob. Chemother.* 67, 810–818. doi: 10.1093/jac/dkr578

Orth, P., Schnappinger, D., Hillen, W., Saenger, W., and Hinrichs, W. (2000). Structural basis of gene regulation by the tetracycline inducible Tet repressor-operator system. *Nat. Struct. Biol.* 7, 215–219. doi: 10.1038/73324

Prammananan, T., Sander, P., Brown, B. A., Frischkorn, K., Onyi, G. O., Zhang, Y., et al. (1998). A single 16S ribosomal RNA substitution is responsible for resistance to amikacin and other 2-deoxystreptamine aminoglycosides in *Mycobacterium abscessus* and *Mycobacterium chelonae*. *J. Infect. Dis.* 177, 1573–1581. doi: 10.1086/515328

Radhakrishnan, A., Kumar, N., Wright, C. C., Chou, T.-H., Tringides, M. L., Bolla, J. R., et al. (2014). Crystal structure of the transcriptional regulator Rv0678 of *Mycobacterium tuberculosis*. *J. Biol. Chem.* 289, 16526–16540. doi: 10.1074/jbc.M113.538959

Ramos, J. L., Martínez-Bueno, M., Molina-Henares, A. J., Terán, W., Watanabe, K., Zhang, X., et al. (2005). The TetR family of transcriptional repressors. *Microbiol. Mol. Biol. Rev.* 69, 326–356. doi: 10.1128/MMBR.69.2.326-356.2005

Rominski, A., Roditscheff, A., Selchow, P., Böttger, E. C., and Sander, P. (2017a). Intrinsic rifamycin resistance of *Mycobacterium abscessus* is mediated by ADP-ribosyltransferase MAB_0591. *J. Antimicrob. Chemother.* 72, 376–384. doi: 10.1093/jac/dkw466

Rominski, A., Selchow, P., Becker, K., Brülle, J. K., Dal Molin, M., and Sander, P. (2017b). Elucidation of *Mycobacterium abscessus* aminoglycoside and capreomycin resistance by targeted deletion of three putative resistance genes. *J. Antimicrob. Chemother.* 72, 2191–2200. doi: 10.1093/jac/dkx125

Rosenberg, E. Y., Bertenthal, D., Nilles, M. L., Bertrand, K. P., and Nikaido, H. (2003). Bile salts and fatty acids induce the expression of *Escherichia coli* AcrAB multidrug efflux pump through their interaction with Rob regulatory protein. *Mol. Microbiol.* 48, 1609–1619. doi: 10.1046/j.1365-2958.2003.03531.x

Schumacher, M. A., Miller, M. C., Grkovic, S., Brown, M. H., Skurray, R. A., and Brennan, R. G. (2002). Structural basis for cooperative DNA binding by two dimers of the multidrug-binding protein QacR. *EMBO J.* 21, 1210–1218. doi: 10.1093/emboj/21.5.1210

Smibert, O., Snell, G. I., Bills, H., Westall, G. P., and Morrissey, C. O. (2016). *Mycobacterium abscessus* complex - a particular challenge in the setting of lung transplantation. *Expert Rev. Anti Infect. Ther.* 14, 325–333. doi: 10.1586/14787210.2016.1138856

Takiff, H. E., Cimino, M., Musso, M. C., Weisbrod, T., Martinez, R., Delgado, M. B., et al. (1996). Efflux pump of the proton antiporter family confers low-level fluoroquinolone resistance in *Mycobacterium smegmatis*. *Proc. Natl. Acad. Sci. U.S.A.* 93, 362–366. doi: 10.1073/pnas.93.1.362

Trott, O., and Olson, A. J. (2010). AutoDock Vina: improving the speed and accuracy of docking with a new scoring function, efficient optimization, and multithreading. *J. Comput. Chem.* 31, 455–461. doi: 10.1002/jcc.21334

van Dorn, A. (2017). Multidrug-resistant *Mycobacterium abscessus* threatens patients with cystic fibrosis. *Lancet Respir. Med.* 5:15. doi: 10.1016/S2213-2600(16)30444-1

Viljoen, A., Blaise, M., de Chastellier, C., and Kremer, L. (2016). MAB_3551c encodes the primary triacylglycerol synthase involved in lipid accumulation in *Mycobacterium abscessus*. *Mol. Microbiol.* 102, 611–627. doi: 10.1111/mmi.13482

Viljoen, A., Dubois, V., Girard-Misguich, F., Blaise, M., Herrmann, J.-L., and Kremer, L. (2017). The diverse family of MmpL transporters in mycobacteria: from regulation to antimicrobial developments. *Mol. Microbiol.* 104, 889–904. doi: 10.1111/mmi.13675

Viljoen, A., Gutiérrez, A. V., Dupont, C., Ghigo, E., and Kremer, L. (2018). A simple and rapid gene disruption strategy in *Mycobacterium abscessus*: on the design and application of glycopeptidolipid mutants. *Front. Cell. Infect. Microbiol.* 8:69. doi: 10.3389/fcimb.2018.00069

Woods, G. L., Brown-Elliott, B. A., Conville, P. S., Desmond, E. P., Hall, G. S., Lin, G., et al. (2011). *Susceptibility Testing of Mycobacteria, Nocardiae and Other Aerobic Actinomycetes: Approved Standard*, 2nd Edn. Wayne, PA: Clinical and Laboratory Standards Institute.

Yang, S., Gao, Z., Li, T., Yang, M., Zhang, T., Dong, Y., et al. (2013). Structural basis for interaction between *Mycobacterium smegmatis* Ms6564, a TetR family master regulator, and its target DNA. *J. Biol. Chem.* 288, 23687–23695. doi: 10.1074/jbc.M113.468694

Zhang, S., Chen, J., Cui, P., Shi, W., Zhang, W., and Zhang, Y. (2015). Identification of novel mutations associated with clofazimine resistance in *Mycobacterium tuberculosis*. *J. Antimicrob. Chemother.* 70, 2507–2510. doi: 10.1093/jac/dkv150

Conflict of Interest Statement: The authors declare that the research was conducted in the absence of any commercial or financial relationships that could be construed as a potential conflict of interest.

frontiers in Microbiology

ORIGINAL RESEARCH
published: 04 July 2018
doi: 10.3389/fmicb.2018.01428

GlnR Activation Induces Peroxide Resistance in Mycobacterial Biofilms

*Yong Yang[1], Jacob P. Richards[1,2], Jennifer Gundrum[1] and Anil K. Ojha[1,3]**

[1] Division of Genetics, Wadsworth Center, New York State Department of Health, Albany, NY, United States, [2] Department of Infectious Diseases and Microbiology, University of Pittsburgh, Pittsburgh, PA, United States, [3] Department of Biomedical Sciences, University at Albany, Albany, NY, United States

Mycobacteria spontaneously form surface-associated multicellular communities, called biofilms, which display resistance to a wide range of exogenous stresses. A causal relationship between biofilm formation and emergence of stress resistance is not known. Here, we report that activation of a nitrogen starvation response regulator, GlnR, during the development of *Mycobacterium smegmatis* biofilms leads to peroxide resistance. The resistance arises from induction of a GlnR-dependent peroxide resistance (*gpr*) gene cluster comprising of 8 ORFs (MSMEG_0565-0572). Expression of *gpr* increases the NADPH to NADP ratio, suggesting that a reduced cytosolic environment of nitrogen-starved cells in biofilms contributes to peroxide resistance. Increased NADPH levels from *gpr* activity likely support the activity of enzymes involved in nitrogen assimilation, as suggested by a higher threshold of nitrogen supplement required by a *gpr* mutant to form biofilms. Together, our study uniquely interlinks a nutrient sensing mechanism with emergence of stress resistance during mycobacterial biofilm development. The *gpr* gene cluster is conserved in several mycobacteria that can cause nosocomial infections, offering a possible explanation for their resistance to peroxide-based sterilization of medical equipment.

Keywords: mycobacteria, biofilms, peroxide, starvation, GlnR

OPEN ACCESS

Edited by:
Thomas Dick,
Rutgers, The State University of New Jersey, Newark, United States

Reviewed by:
John T. Belisle,
Colorado State University, United States
Tanya Parish,
Infectious Disease Research Institute, United States

***Correspondence:**
Anil K. Ojha
anil.ojha@health.ny.gov

Specialty section:
This article was submitted to Antimicrobials, Resistance and Chemotherapy, a section of the journal Frontiers in Microbiology

Received: *27 April 2018*
Accepted: *11 June 2018*
Published: *04 July 2018*

Citation:
Yang Y, Richards JP, Gundrum J and Ojha AK (2018) GlnR Activation Induces Peroxide Resistance in Mycobacterial Biofilms. Front. Microbiol. 9:1428. doi: 10.3389/fmicb.2018.01428

INTRODUCTION

Under most detergent-free *in vitro* conditions, mycobacterial species grow as surface-associated, three-dimensionally organized multicellular communities, called biofilms, which develop through dedicated genetic programs (Ojha et al., 2005, 2008; Weiss and Stallings, 2013; Gupta et al., 2015; Chuang et al., 2016; Yang et al., 2017; Clary et al., 2018). Biofilm-like multicellular aggregates of non-tuberculous mycobacteria (NTMs) have also been reported from clinical and environmental specimens (Feazel et al., 2009; Bosio et al., 2012; Mullis and Falkinham, 2013; Fennelly et al., 2016). Biofilms of *Mycobacterium avium*, a prominent member of NTMs, have been implicated in pathogenesis (Rose and Bermudez, 2014), although biofilms of other pathogenic mycobacterial species including *M. tuberculosis* in the context of their host environments remain to be evaluated. Further clinical significance of mycobacterial biofilms is highlighted by at least two unique phenotypes, which are not associated with their single-cell planktonic counterparts. First, mycobacterial biofilms harbor a sizable subpopulation of bacilli that can survive extreme conditions including exposure to antibiotics and antiseptics (Falkinham, 2007; Ojha et al., 2008; Rose et al., 2015; Yang et al., 2017; Clary et al., 2018). Second, biofilm growth of some mycobacterial species, including the pathogenic species *M. canettii*, fosters horizontal gene transfer

(Nguyen et al., 2010; Boritsch et al., 2016), which possibly accelerates the propagation of drug resistance mutations in these species. Although mycobacterial biofilms are increasingly being recognized as potential targets for effective anti-mycobacterial strategies, mechanisms underlying the emergence of stress tolerance in biofilms remain unknown.

Biofilm development in the model mycobacterial species, *M. smegmatis*, is a genetically programmed process that appears to occur in distinct stages, each demarcated by its specific genetic requirements (Ojha et al., 2005; Ojha and Hatfull, 2007; Yang et al., 2017). While the cell surface glycopeptidolipid (GPL) is necessary for optimum substratum attachment, a nucleoid-associated protein, Lsr2, is required for cell–cell aggregation (Yang et al., 2017). Moreover, gene expression analysis of an extragenic suppressor of an *lsr2* mutant revealed that cell–cell aggregation is a critical checkpoint in the developmental process (Yang et al., 2017). Expression levels of 83 genes are dependent on intercellular aggregation and aggregated growth (Yang et al., 2017), suggesting that the physicochemical interactions among cells induce transcriptional reprogramming for further maturation of architecture and physiological adaptation of resident cells.

A large number of 83 aggregation-dependent genes are under the control of GlnR, a conserved OmpR-like transcription factor that regulates nitrogen assimilation in response to its limited availability (Amon et al., 2008; Jenkins et al., 2013; Yang et al., 2017). GlnR-dependent upregulation of three ammonium transporters (Amt), glutamine/glutamate synthases (GlnA) and nitrite/nitrate reductases facilitate efficient assimilation of environmental nitrogen in a cell (Amon et al., 2008; Yang et al., 2017). In addition, GlnR also induces urecase, amidase, xanthin permeases, which likely maximize the total intracellular nitrogen pool (Jenkins et al., 2013). However, the fact that GlnR induces over 100 genes in mycobacteria opens up questions about its wider influence in mycobacterial growth and adaptation. Studies in other species support a global role of GlnR, extending beyond nitrogen assimilation. In *Saccharopolyspora erythraea,* GlnR controls the expression of carbohydrate ATP-binding cassette (ABC) transporters, thereby facilitating carbon uptake in response to nitrogen starvation (Liao et al., 2015). Similarly, GlnR also appears to control the expression of a key phosphate-sensing regulator, PhoP, in *S. erythraea,* implying a possible role of GlnR in phosphorous homeostasis (Yao and Ye, 2016). In addition to controlling nutrient balance in bacteria, GlnR also influences secondary metabolism in actinomycetes. In *Streptomyces coelicolor* and *Streptomyces avermitilis*, GlnR modulates the synthesis of antibiotics by directly regulating the transcription of pathway-specific genes (He et al., 2016; Urem et al., 2016). Lastly, GlnR also controls osmolyte levels in *S. coelicolor* (Shao et al., 2015), and pH homeostasis in *Streptococcus salivarius* (Huang and Chen, 2016).

Given a global role of GlnR in other species, we asked whether its activation during biofilm development in *M. smegmatis* has any significance beyond nitrogen assimilation. We report here that GlnR activation for nitrogen assimilation during biofilm growth also increases resistance to peroxide. The phenotype is caused by induction of a GlnR-dependent peroxide resistance (*gpr*) cluster of genes. The *gpr* cluster is comprised of 8 open reading frames (ORFs) – MSMEG_0565-0572– encoding genes of diverse functions. The upstream region of this uncharacterized operon has binding sites for both GlnR and SoxR, which is a MarR-family transcription factor that responds to oxidative stress to maintain redox homeostasis (Dietrich et al., 2008; Jenkins et al., 2013). However, *gpr* induction responds differently to GlnR and SoxR activities. While GlnR is a strong positive regulator of *gpr*, inducing it by ∼100-fold under limiting nitrogen, SoxR is a modest negative regulator causing twofold de-repression under peroxide stress. Emergence of peroxide resistance through a nutrient sensing mechanism provides a direct link between form and function of mycobacterial biofilms.

MATERIALS AND METHODS

Bacterial Strains and Growth Conditions

All plasmids and strains used in this study are listed in Supplementary Tables S1 and S2, respectively. Unless indicated, *M. smegmatis*, mc^2155 (wild-type), was maintained at 37°C in 7H9ADC (Becton Dickinson) with 0.05% (v/v) Tween-80 for planktonic cultures. 7H10ADC agar (Becton Dickinson) was used for plate cultures. When necessary, hygromycin, kanamycin, and zeocin were added at 150, 20, or 25 μg/mL, respectively, to culture recombinant strains. *Escherichia coli* (DH5α) was grown at 37°C in LB broth or LB agar. Pellicle biofilms of *M. smegmatis* strains were grown as described earlier (Yang et al., 2017). Briefly, 10 μL of saturated planktonic cultures were inoculated into 10 mL of detergent-free Sauton's medium or modified M63 medium in either 60 mm polystyrene dishes or 12-well polystyrene plates, and incubated stationary at 30°C untill indicated time. The N_0 version of Sauton's medium was prepared by omitting asparagine, and by replacing the ferric ammonium citrate with ferric citrate. The $N_{1/2}$ version was prepared by reducing the initial concentrations of the above mentioned nitrogen sources by half.

Construction of Mutants and Plasmids

Mutations in *M. smegmatis* mc^2155 were constructed using recombineering as described previously (Yang et al., 2017). Briefly, allelic exchange substrates for a given target gene were generated by SOEing-PCR on either side of a *loxP* flanked zeocin-resistant cassette using the respective primers listed in Supplementary Table S3. The purified PCR-products were electroporated into an electrocompetent recombineering strain, mc^2155-pJV53-SacB, and plated on 7H10ADC with 25 μg/mL zeocin. Mutant genotypes of zeo^r colonies were confirmed by PCR. The recombineering plasmid, pJV53-SacB, was rescued from mutants by plating them on 7H10ADC with 15% sucrose, and screening sucrose resistant colonies for kanamycin sensitivity. The zeo^r marker was removed by excision using a Cre recombinase expressed from pCre-SacB, which was electroporated into the rescued mutant cells and transformants were screened for loss of zeo^r. The zeo^s colonies were screened on 7H10ADC with 15% sucrose to obtain clones

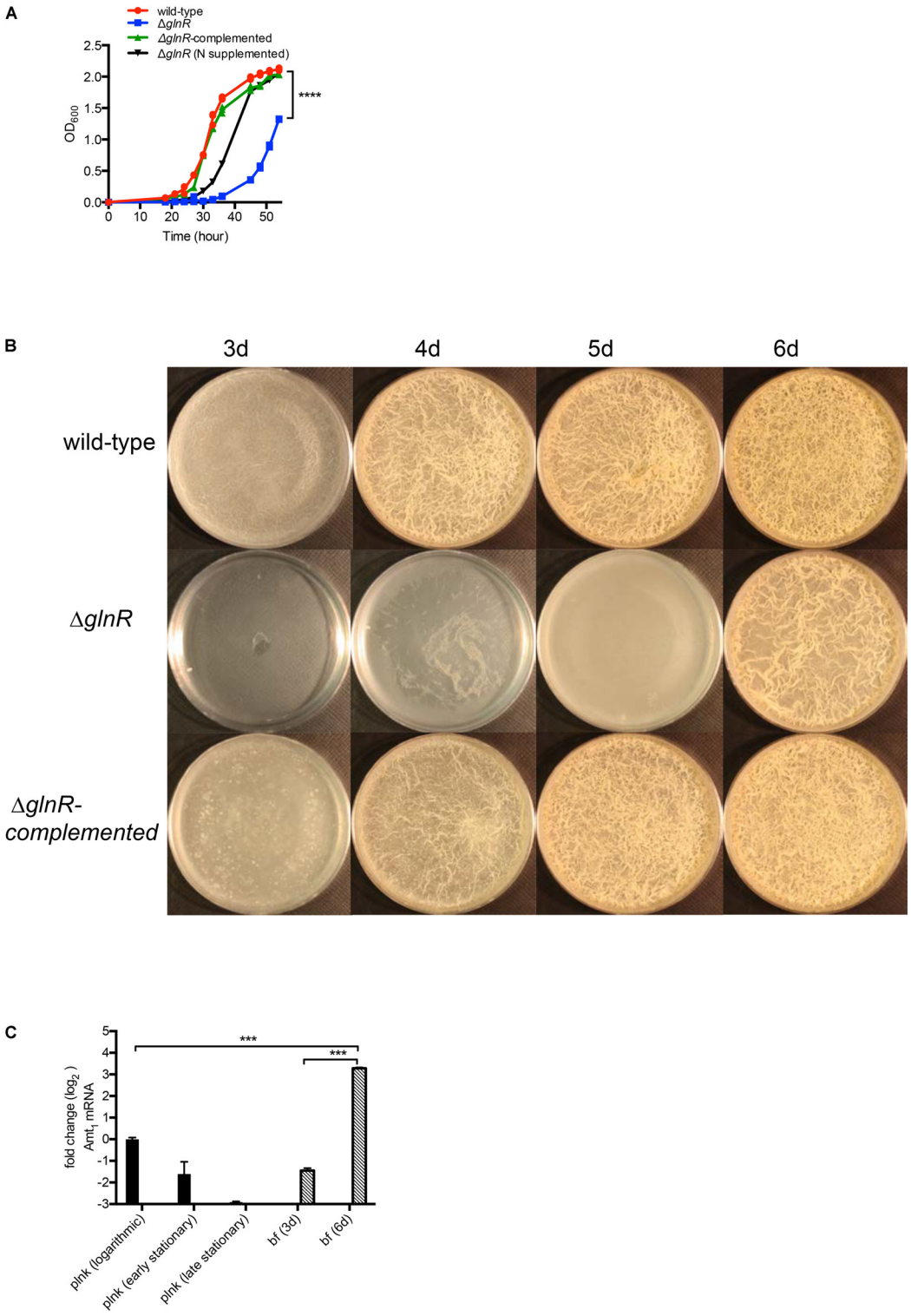

FIGURE 1 | GlnR-dependent growth of *M. smegmatis* in planktonic and biofilm cultures in Sauton's medium. **(A)** Planktonic growth of wild-type, Δ*glnR* and Δ*glnR*-complemented strains in Sauton's medium with 0.05% (v/v) Tween80. Growth of Δ*glnR* is also rescued by supplementation of Sauton's medium with 0.5% (w/v) casamino acid and 0.2% (w/v) ammonium sulfate. **(B)** A top-down view of pellicle biofilms of wild-type, Δ*glnR* and Δ*glnR* complemented strains in detergent-free Sauton's medium at the indicated time point. **(C)** Expression of a GlnR-dependent ammonium transporter (Amt_1) in planktonic (plnk) and biofilm (bf) cultures of wild-type *M. smegmatis* at indicated stages of growth. Logarithmic, early- and late-stationary phases of planktonic cultures correspond to OD 0.3, 1.5 and 2.5, respectively. Stages of biofilms at which cells were harvested are indicated as days after incubation. Expression was determined by real-time PCR and normalized with the SigA transcripts. Data represent mean of two independent experiments. *** and **** denote $p < 0.001$ and 0.0001, respectively (*t*-test).

without the pCre-SacB plasmid. The rescued unmarked mutants were complemented as indicated.

RNA-seq

Mycobacterium smegmatis mc^{2}155 and Δ*glnR* were grown in detergent-free Sauton's medium to form matured pellicle biofilms. Total RNA was extracted using a Qiagen RNeasy kit and contaminating DNA was removed with the turbo DNA-free kit (Thermo Fisher Scientific). For each sample, 5 μg of total RNA was processed for rRNA removal using the Ribo Zero kit (Illumina). Strand-specific DNA libraries were then prepared with 100 ng of mRNA using the Scriptseq Complete Kit- Bacteria (Illumina). Libraries were sequenced on the NextSeq500 platform (Illumina) and analyzed by Rockhopper (McClure et al., 2013) at default settings using the reference genome of *M. smegmatis* mc^2 155 (NC_008596).

RT-qPCR

All oligonucleotides used for RT-qPCR are listed in Supplementary Table S3. DNA-free RNA for RT-qPCR was extracted as described for RNA-seq. For each sample, 200 ng of RNA was used for reverse transcription using the Maxima First Strand cDNA Synthesis Kit (Thermo Fisher Scientific). RT-qPCR was performed on an Applied Biosystems 7000 fast RT-qPCR System (Applied Biosystems) with SYBR Green Master Mix following the manufacturer's instructions. Relative expression of target gene is calculated either as $2^{-\Delta Ct(gene-SigA)}$ or $2^{-\Delta Ct(target\ gene1-SigA)-\Delta Ct(target\ gene2-SigA)}$, in which SigA transcript was the endogenous control.

Antibiotics and Peroxide Sensitivity Assays

Exponential phase culture (OD_{600} = 0.3) of each strain grown in Sauton's medium with 0.05% (v/v) Tween80 was harvested and washed once with phosphate buffered saline with 0.05% Tween-80 (PBST). Approximately 2 × 10^7 CFU/mL of each strain was resuspended in nitrogen-free (N_0) Sauton's medium with 0.05% (v/v) Tween80 at 37°C for 3 h. 400 μg/mL rifampicin, 1 μg/mL streptomycin or 20 mM H_2O_2 were added and incubated at

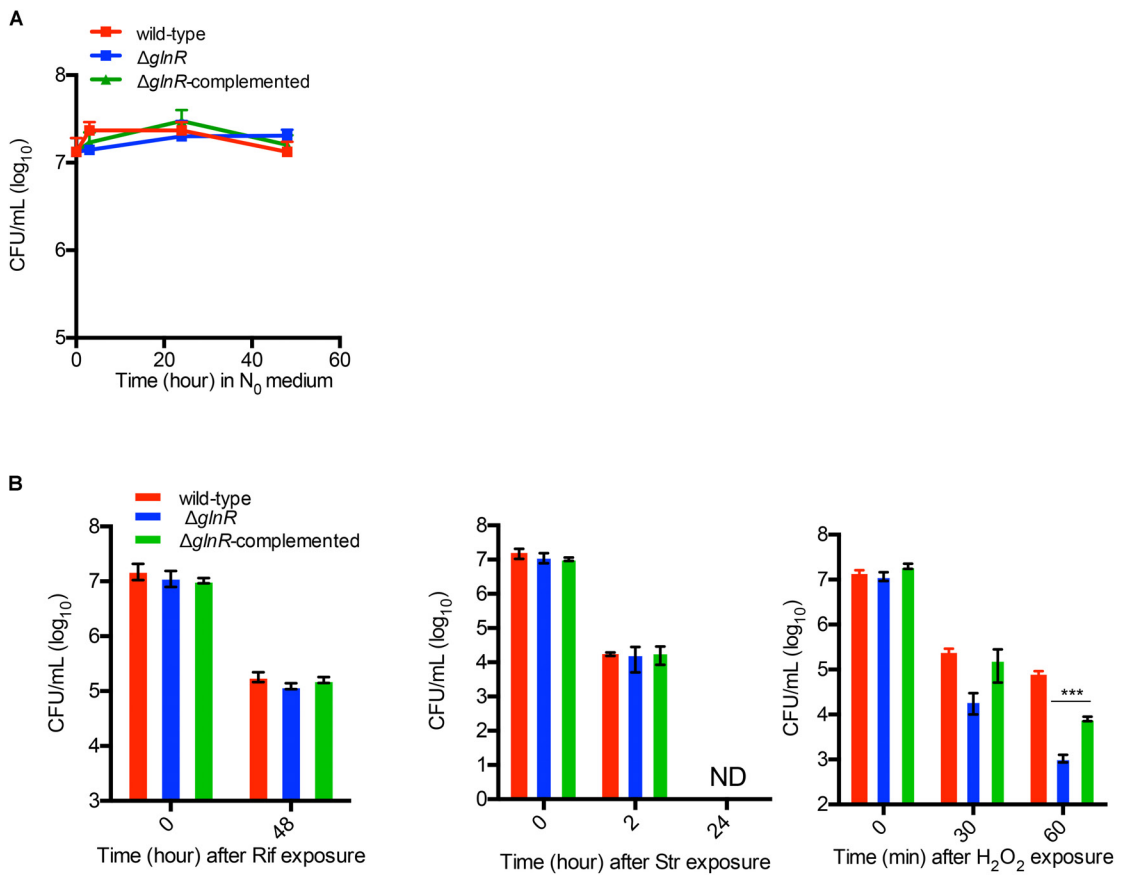

FIGURE 2 | GlnR-dependent resistance of *M. smegmatis* to hydrogen peroxide under nitrogen-limiting condition. **(A)** Survival of wild-type, Δ*glnR* and Δ*glnR*-complemented strains in nitrogen-free Sauton's (N_0) medium for up to 48 h. Exponentially growing cells (OD 0.3) cultured in Sauton's medium with 0.05% (v/v) Tween80 were washed and resuspended in N_0 medium for indicated time points prior to plating the dilutions on 7H10ADC plate. **(B)** Effect of streptomycin (Str; 1 μg/mL), rifampicin (Rif; 400 μg/mL), and hydrogen peroxide (H_2O_2; 20 mM) on survival of wild-type, Δ*glnR* and Δ*glnR* -complemented strains in N_0 medium. Cells were incubated in N_0 medium for 6 h prior to exposure to each condition for the indicated period of time. Data are representative of mean of three biologically independent experiments. *** indicates p (t-test) < 0.001.

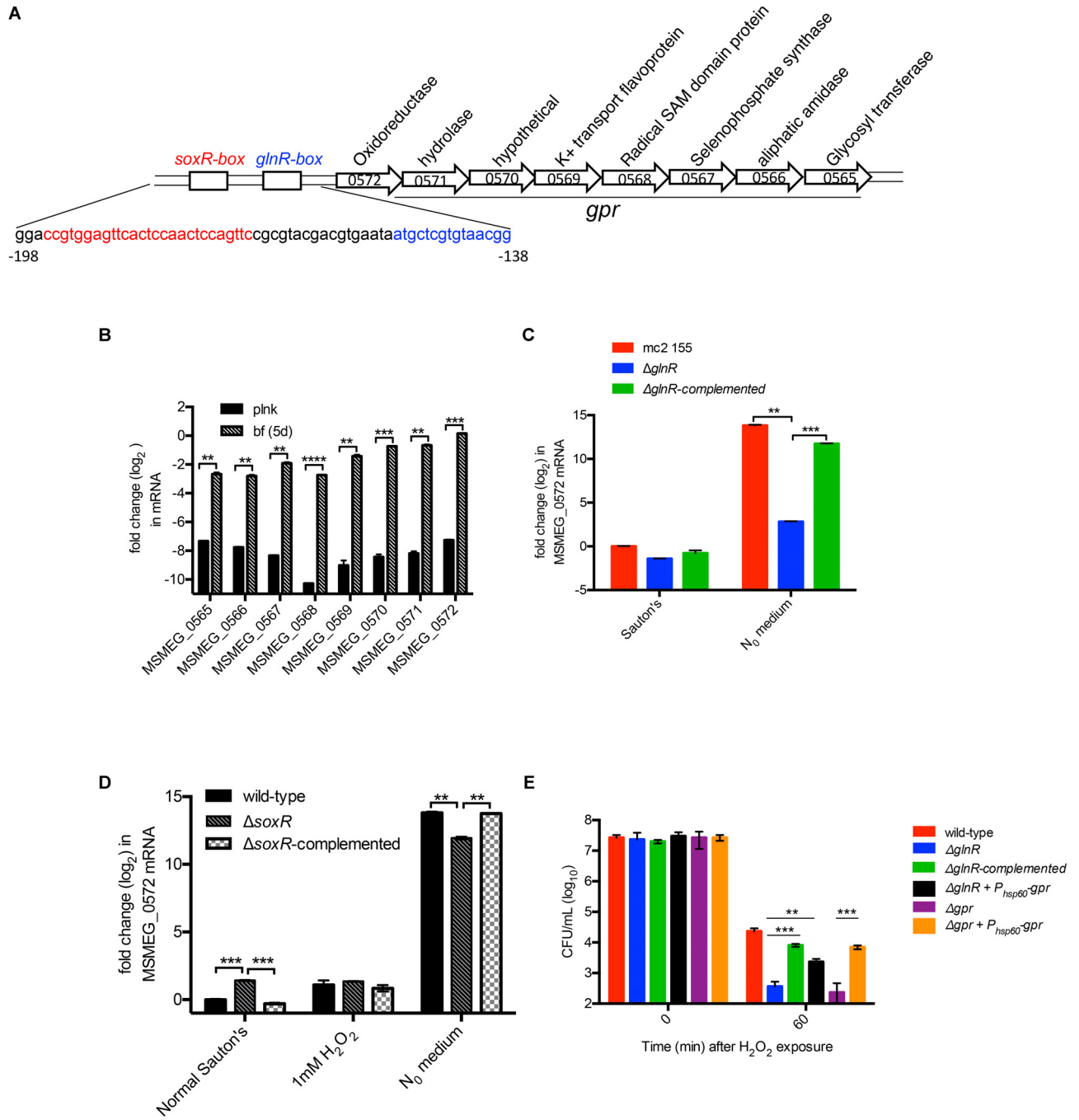

FIGURE 3 | GlnR-dependent peroxide resistance in *M. smegmatis* results from activation of a cluster comprising of eight genes (MSMEG_0565 to 0572), called *gpr*. **(A)** Schematic representation of *gpr* and the upstream GlnR and SoxR-binding regions, called *GlnR*-box and *SoxR*-box, respectively. Nucleotide sequence of the two regions are indicated below in their corresponding color codes. **(B)** Expression of each of the eight genes in *gpr* cluster in logarithmic phase (OD 0.3) planktonic culture and in 6-day biofilms, both cultured in Sauton's medium. Transcripts were normalized with SigA transcripts. **(C)** GlnR-dependent induced expression of *gpr* cluster (represented by MSMEG_0572) in N_0 medium. Indicated strains were cultured in normal Sauton's medium untill OD 0.3 and transferred to N_0 medium for 3 h prior to mRNA analysis by real-time PCR. Cells collected from Sauton's medium before exposure to N_0 medium were used as reference. Fold-change relative to transcript level in wild-type cells in Sauton's medium was calculated. **(D)** Expression of *gpr* (represented by MSMEG_0572) is unresponsive to SoxR and peroxide in Sauton's medium. Indicated strains were cultured and processed as described for **(C)**, except that an additional set exposed to a sub-lethal concentration (1 mM) of H_2O_2 for 60 min was also included. **(E)** Expression of *gpr* is sufficient to restore peroxide resistance in Δ*glnR* mutant. Viability of the indicated strains before (0 min) and after 30 min of exposure to 20 mM H_2O_2. Data in **(B–E)** represent mean of three biologically independent experiments. ** and *** indicates p (t-test) < 0.01 and <0.001, respectively.

37°C for the indicated period; unexposed cultures were used as control. At the indicated time point, the exposed and unexposed cultures were diluted and plated on 7H10ADC for bacterial viability.

Measurement of Intracellular NADPH/NADP Ratio

Average intracellular NADPH/NADP ratios of planktonic culture and biofilms were measured according to previous publication with minor modifications (Vilcheze et al., 2005). Briefly, exponential phase planktonic and biofilm cultures from normal and N_0 Sauton's medium were harvested and washed once with PBS and then resuspended in PBS. Large aggregates from biofilms were broken up by 8–10 repeated passaging through 18-G needles. 1.5 mL single cell suspensions at density of 10^8–10^9 CFU/mL of each strain were pelleted and resuspended in 0.75 mL 0.2 M HCl (for NADP extraction) or 0.75 mL of 0.2 M NaOH (for NADPH extraction). After 10 min at 55°C, the suspensions were cooled to 0°C and neutralized by adding either 0.75 mL of 0.1 M NaOH for NADP extraction or 0.75 mL of 0.1 M HCl for NADPH extraction, while vortexing at high speed. After incubation for 10 min on ice, the suspensions were centrifuged at 3000 rpm for 10 min at 4°C. The supernatants were filtered and transferred to a new tube and used immediately. The concentrations of NADP and NADPH in the suspensions were determined by spectrophotometric measurement of the rate of 3-[4,5-dimethylthiazol-2-yl]-2,5-diphenyltetrazolium bromide (Sigma # M2128) reduction by the glucose-6-phosphate dehydrogenase (Sigma # G6378) in the presence of phenazine ethosulfate (Sigma # P4544) at 570 nm. The rate of 3-[4,5-dimethylthiazol-2-yl]-2,5-diphenyltetrazolium bromide reduction is proportional to the concentration of the nucleotides. Purified NADP (Sigma # 10128031001) and NADPH (Sigma # 10107824001) were used for standard curves, which were used for determination of the nucleotides in each sample. Serial dilutions of samples were tested to ensure the values were in the linear range of the NADP/NADPH standard curve.

Peroxide Sensitivity Assay for Microfluidic Biofilms

Biofilms as microcolonies were grown in a CellASIC ONIX (Cat # EV262) microfluidic platform, using CellASIC microfluidic plates (M04S-03) with headspace of 150 μm. Approximately 10^6 CFU/mL of bacteria in 10 μL media were perfused at a pressure of 1.7 kPa (0.25 psi) into each culture chamber of the plate for 6 s, followed by no perfusion for 30 min. This allowed optimum attachment of single cells to the culture chamber surface at a density that then grew into separate colony biofilms. For microfluidic culturing, detergent-free Sauton's media was perfused across each culture chamber at the manufacturer's recommendation of a dual pressure of 3.4 kPa (0.5 psi) at 37°C for 4 days to provide adequate nourishment and minimal stress to biofilm-like colonies. Incubation of Δ*glnR* was extended by an additional day to allow colony biofilms to grow to the same size as wild type. Colony biofilms were exposed to 20 mM H_2O_2 in Sauton's media via microfluidic perfusion for 3 h followed by overnight perfusion of Sauton's media with 1 μg/mL Calcein AM to stain survivors. Images of colony biofilms were collected by confocal laser scanning microscopy (CLSM) at 20× magnification under green channel (excitation 488 nm). Corresponding DIC image of each colony was also captured for overlaying the fluorescence signal. The images were analyzed by ImageJ. To compare the numbers of surviving cells among strains after H_2O_2 exposure, the number of green CalceinAM-stained cells was calculated from the maximum intensity projection of the z-stacks of each biofilm-like colony, normalized to colony surface area. For each strain, at least three biofilm-like colonies over two fields of view were analyzed.

RESULTS

GlnR and Biofilm Formation in *M. smegmatis*

In our earlier study we identified 61 genes induced during maturation of *M. smegmatis* biofilms to be GlnR-dependent (Jenkins et al., 2013; Yang et al., 2017). We therefore tested the effect of *glnR* mutation on development of *M. smegmatis* biofilms. Deletion of *glnR* produced no apparent phenotype in modified M63 medium, which was used in our earlier study (Yang et al., 2017) (Supplementary Figure S1). However, the mutation caused delayed planktonic growth and retarded biofilm development in Sauton's medium (**Figures 1A,B**), which has poorer nitrogen source relative to the modified M63 medium. Lack of adequate nitrogen source in Sauton's medium appeared to be the primary cause for Δ*glnR* phenotype, because the mutant growth could be substantially rescued by addition of casamino acid as supplemental nitrogen source (**Figure 1A**). Moreover, similar to the observation in modified M63 medium (Yang et al., 2017), late-stage (6-day) biofilms of wild-type (mc^2155) *M. smegmatis* in Sauton's medium also exhibited > 50-fold induction of a GlnR-dependent ammonium transporter (MSMEG_2425; Amt_1) (**Figure 1C**). The induction was not observed in planktonic culture of the strain (**Figure 1C**), indicating that nitrogen availability in the medium is sufficiently high to prevent peak level of GlnR activation in planktonic cells, but not high enough to do so in biofilms. Based on these findings, and to maintain consistent growth conditions used in previous studies of GlnR mutant of *M. smegmatis* (Jenkins et al., 2013), we chose to use Sauton's medium for this study.

Growth retardation of Δ*glnR* in planktonic cultures (**Figure 1A**) suggests that a basal activity of the regulator is necessary for optimum uptake of nitrogen sources. Delayed but matured biofilm development by Δ*glnR* raised the possibility of either an alternative mechanism of induction of GlnR-dependent genes, or existence of alternative pathways for nitrogen assimilation. To investigate these possibilities we compared the transcriptomes of 6-day biofilms of wild-type and Δ*glnR* strains. Expression of GlnR-dependent genes was significantly retarded in biofilms of Δ*glnR* mutant, compared to the wild-type (Supplementary Table S4), suggesting that

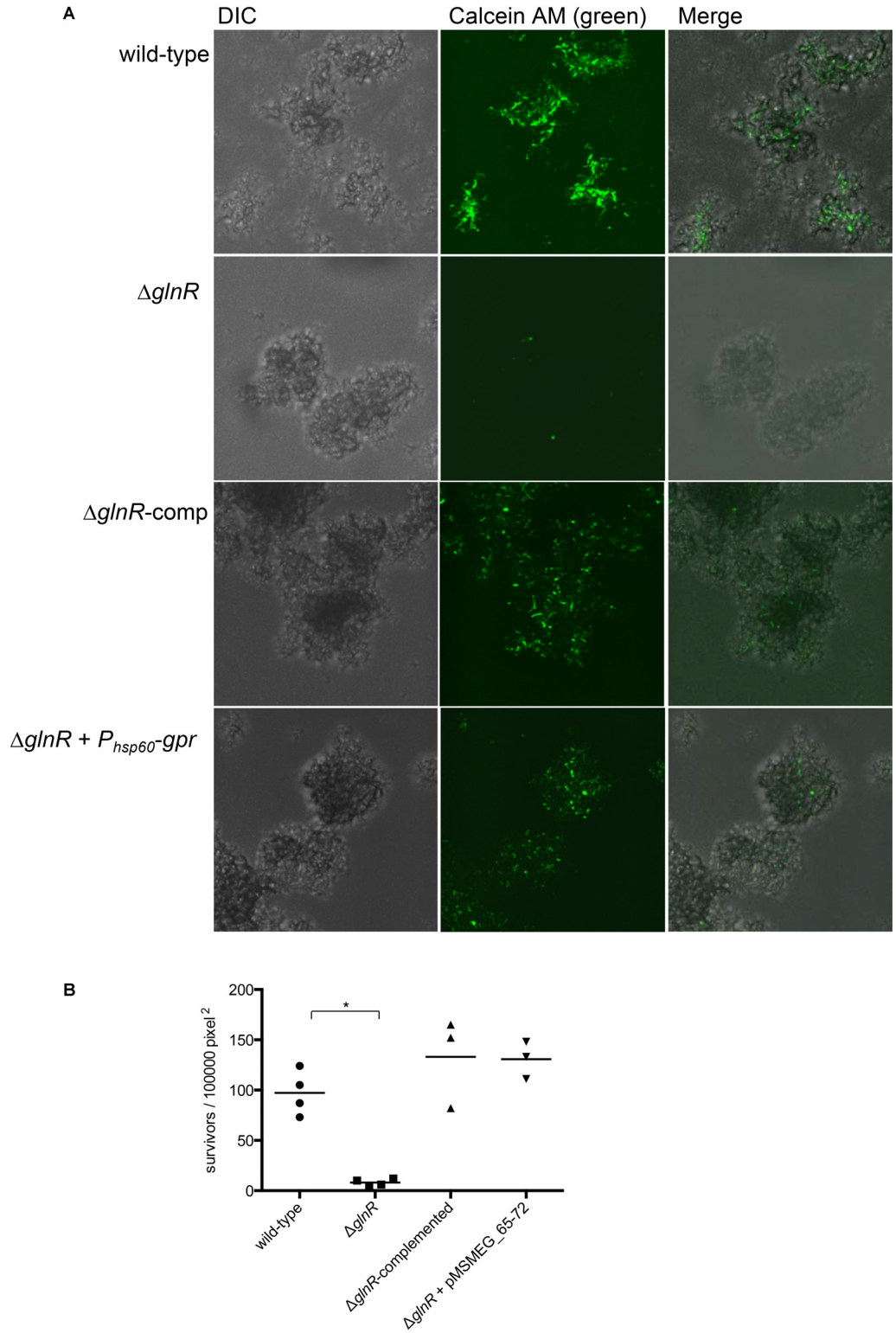

FIGURE 4 | GlnR-dependent expression of *gpr* induces peroxide resistance in *M. smegmatis* biofilms. **(A)** Visualization of peroxide resistant survivors (green) in 4-day biofilms of the indicated strains. Biofilms, cultured in CellASIC Onix microfluidic system perfused with Sauton's medium, were exposed with the medium containing 20 mM H_2O_2 for 3 h prior to staining with Calcein AM (1 μg/mL). Distributions of live cells (green) in colony biofilms were determined from images acquired by confocal microscopy. The micrographs represent maximum intensity projection of green signal across *z*-stacks analyzed by ImageJ. **(B)** A summary plot of frequency of green cells in four independent biofilms of wild-type and mutants, and three for the complemented strains. Data represent mean from 3 to 4 independent biofilms of each strain formed in a microfluidic chamber. *denotes p (Mann–Whitney) < 0.05.

secondary mechanisms of nitrogen assimilation are triggered in the mutant. This was further substantiated by upregulation in Δ*glnR* mutant biofilms of acetamidase (*amiE* or MSMEG_5335) and D-amino acid dehydrogenase (Supplementary Table S4).

GlnR Activation and Peroxide Resistance

A global effect of GlnR on gene expression patterns (Jenkins et al., 2013; Jessberger et al., 2013; Yang et al., 2017) raised a possibility that its activation during adaptation of *M. smegmatis* to low nitrogen may also impact other functions of cells. We investigated the effect of GlnR on persistence under stress exposure by comparing the sensitivity of nitrogen-starved cells of wild-type, Δ*glnR* and Δ*glnR* complemented strains to two commonly used anti-TB antibiotics: rifampicin (Rif) and streptomycin (Str) at 10X MIC. We also included hydrogen peroxide – a routinely used sterilizing agent for control of biofilm-related contaminants of surgical equipment in nosocomial settings (Falagas et al., 2011). We excluded isoniazid (INH) due to its selective activity on growing cells. We chose to test GlnR-activated planktonic cells by exposing them to N_0-Sauton's medium. GlnR was activated within 3 h of exposure to N_0-Sauton's medium (Supplementary Figure S2). Because viability of Δ*glnR* remains unaltered during the first 48 h of exposure to the N_0-Sauton's medium (**Figure 2A**), the exposure periods to the stressors were kept within this time limit. All three strains appeared equally sensitive to high concentrations of Rif and Str (**Figure 2B**). Interestingly, Δ*glnR* mutant showed significantly greater sensitivity to peroxide exposure in a 60-min period (**Figure 2B**), and the phenotype was substantially reversed in the complemented strain (**Figure 2B**).

Peroxide Resistance Arises From GlnR-Dependent Induction of *gpr*

To determine the basis of GlnR-dependent peroxide resistance we analyzed the nucleotide sequence of GlnR-dependent genes. Upstream region of one of the GlnR-dependent operons comprising of 8 ORFs (MSMEG_0565 to MSMEG_0572) contained binding sites for both GlnR and SoxR (Dietrich et al., 2008; Jenkins et al., 2013) (**Figure 3A**). Since SoxR plays important role in redox homeostasis in many bacterial species (Storz and Imlay, 1999), we speculated that this locus could be under dual regulation of SoxR and GlnR, and that its activation by either of the two regulators possibly confers peroxide resistance. Biofilm-specific expression of all 8 ORFs in Sauton's medium was verified by RT-qPCR (**Figure 3B**). We next tested the role of SoxR and GlnR in activation of the operon using MSMEG_0572 as a representative member. As expected from earlier studies (Jenkins et al., 2013; Jessberger et al., 2013; Yang et al., 2017), expression of the operon in wild-type cells was highly (>500 fold) induced upon 3-h exposure to N_0 Sauton's medium in a GlnR-dependent manner (**Figure 3C**). However, SoxR activity appears to have very modest (∼2-fold) negative effect on the induction of the operon (**Figure 3D**). Interestingly, exposure to peroxide did not induce the operon (**Figure 3D**). Together, these expression profiles indicate that regulation of the operon exclusively depends on GlnR under the tested conditions.

We next asked if expression of MSMEG_0565-72 operon is necessary and sufficient to exhibit GlnR-dependent peroxide resistance. A deletion mutant of the operon exhibited similar level of peroxide sensitivity as Δ*glnR* under N_0-Sauton's medium (**Figure 3E**), and the phenotype was rescued by plasmid-borne expression of the operon by a constitutive (P_{hsp60}) promoter. Importantly, constitutive expression of the operon by P_{hsp60} promoter was also able to substantially rescue peroxide sensitivity of Δ*glnR*, indicating that peroxide resistance in *M. smegmatis* is primarily contributed by GlnR-dependent activation of MSMEG_0565-72 operon. We therefore call this operon as GlnR-dependent peroxide resistance or *gpr*.

To obtain a direct evidence for roles of *glnR* and *gpr* in peroxide resistance of *M. smegmatis* biofilms, we employed a microfluidic-based growth model to visualize surviving cells in peroxide exposed biofilms by confocal microscopy. To calibrate the growth model we first determined the timing of activation of GlnR by using a reporter strain of *M. smegmatis*, which

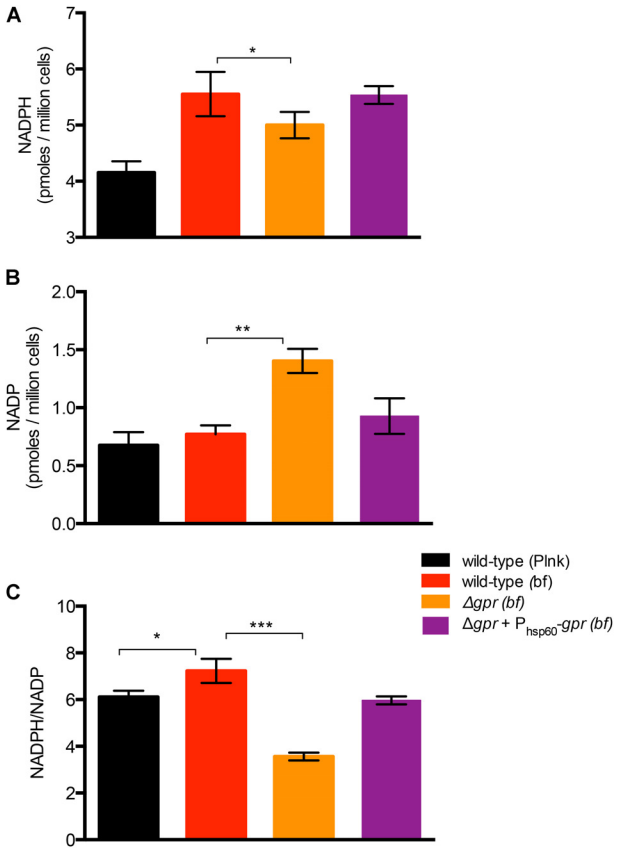

FIGURE 5 | Role of *gpr* in maintenance of redox homeostasis of *M. smegmatis*. **(A,B)** Levels of oxidized (NADP) form of nicotinamide adenine dinucleotide phosphate in biofilms of wild-type, Δ*gpr* and the complemented strains cultured in normal Sauton's medium. **(C)** Ratio of NADPH to NADP calculated from **(A,B)**. Data represent mean of three biologically independent experiments *, **, and *** indicate *p* (*t*-test) < 0.05, 0.01, and 0.001, respectively.

harbored constitutively expressing mCherry and Dendra-2 fused to the promoter of Amt_1 (MSMEG_2425). Expression of Dendra-2 in biofilms could be visualized after 4 days of growth in Sauton's medium (Supplementary Figure S3). Subsequent incubation led to bacterial growth in the flow channels, leading to increased backflow pressure. We therefore used 4-day stage of wild type biofilms for our analysis, although biofilms of Δ*glnR* were cultured for an additional day to allow them to achieve similar size as wild-type. Following peroxide exposure, live cells in biofilms were probed by calcein AM, which remains non-fluorescent until its passive diffusion to the cytosol and hydrolysis by intracellular hydrolases produces fluorescent calcein (Rego et al., 2017). Compared to wild-type biofilms, the number of viable cells in peroxide exposed Δ*glnR* biofilms was significantly reduced (**Figures 4A,B**). The mutant phenotype could be complemented by plasmid-borne expression of either *glnR* from its native promoter or a constitutive expression of *gpr* from the hsp60 promoter. We thus conclude that induced expression of *gpr* upon activation of GlnR during maturation of *M. smegmatis* biofilms directly contributes to their peroxide resistance.

Physiological Role of *gpr* in Biofilm Development

Nitrogen assimilation in majority of bacterial species occurs at the expense of the redox currency, NADPH (van Heeswijk et al., 2013), which serves as a co-factor for several enzymes, including glutamate synthase, involved in synthesis of ammonia and amino acids. Two subunits of NADPH-dependent glutamate

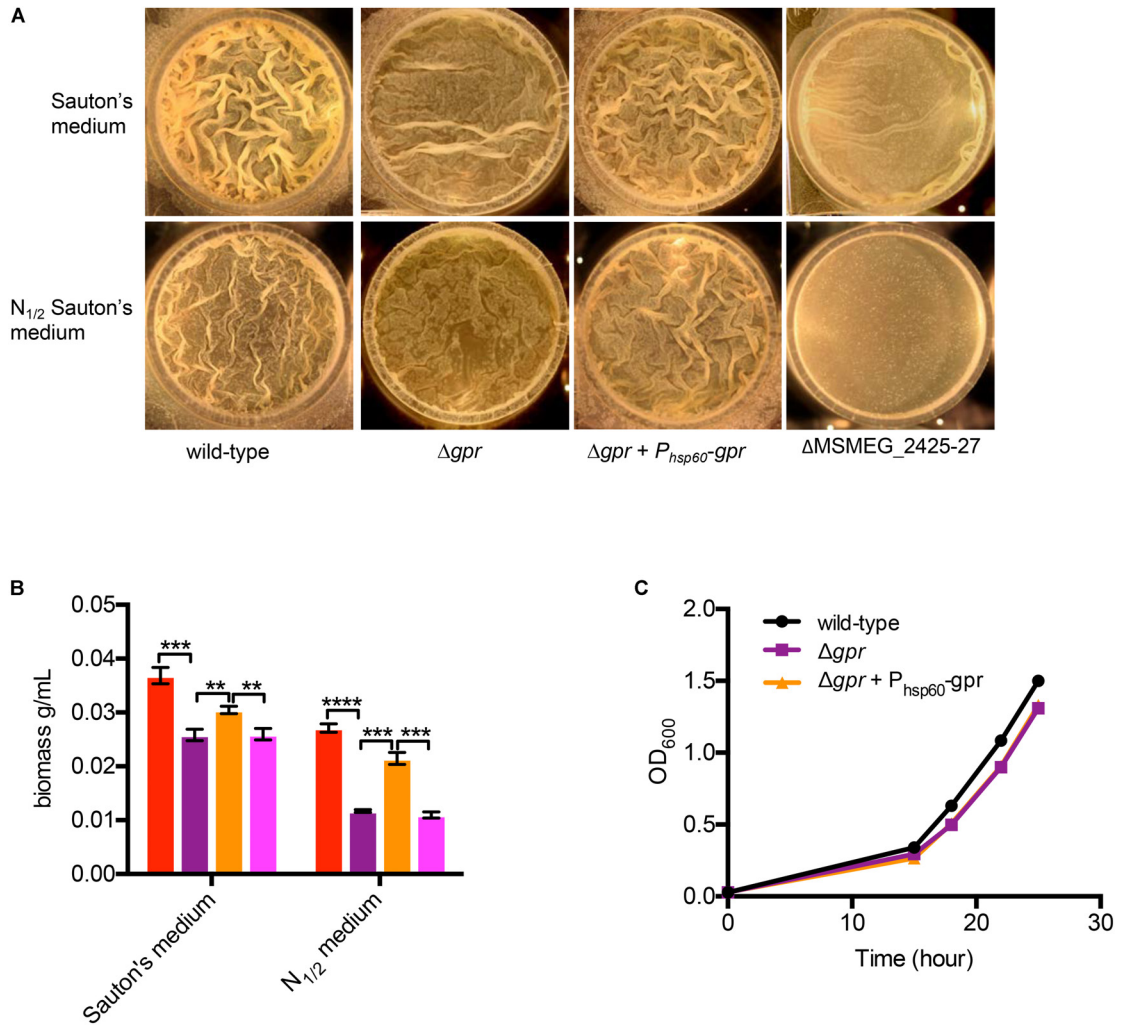

FIGURE 6 | Role of *gpr* in biofilm formation of *M. smegmatis*. **(A)** A top-down view of pellicle biofilms of the indicated strains after days of growth in detergent-free Sauton's medium and modified Sauton's medium with half the normal nitrogen source ($N_{1/2}$). In contrast to the wild type, which formed thick-textured biofilms in both medium, Δamt_1 and Δ*gpr* mutants formed untextured biofilms in $N_{1/2}$ Sauton's medium, and the phenotype was partially rescued by nitrogen restoration in normal Sauton's medium. **(B)** Biomass of the pellicles described in **(A)** from three independent experiments. The order of columns in the plot corresponds to the order in which the strains are indicated in **(A)**. Data represent mean of three biologically independent experiments. **, ***, and **** denote $p < 0.01$, 0.001, and 0.0001, respectively (*t*-test). **(C)** Planktonic growth of the indicated strains in $N_{1/2}$ Sauton's medium.

synthase, encoded by MSMEG_3225 and MSMEG_3226, are induced in biofilms by ∼30-fold (Yang et al., 2017), and their induction is GlnR-dependent (Supplementary Table S4). This suggests a greater demand of NADPH for nitrogen-starved cells in biofilms. This is consistent with ∼5-fold increase NADPH/NADP ratio after 3 h of incubation of wild-type cells in N_0-Sauton's medium, relative to normal Sauton's medium (Supplementary Figure S4). The increase in the ratio appears to be contributed by a modest decrease (<2-fold) in NADPH, relative to NADP (∼7-fold), suggesting that NADPH is likely regenerated from existing NADP by reductases induced in nitrogen-starved cells. Regeneration of NADPH, as opposed to new synthesis, is preferred perhaps due to lack of nutrients in N_0-Sauton's medium. We therefore hypothesized that induction of the putative reductases encoded by genes in *gpr* cluster likely regenerate NADPH pool to meet the metabolic demand of nitrogen-starved cells. Nitrogen-starved Δ*gpr* mutant indeed produced a lower NADPH/NADP ratio than wild-type and complemented cells (Supplementary Figure S4). The decreased ratio in the mutant was due to reciprocal change in NADP and NADPH levels, consistent with the idea that existing NADP are reduced to regenerate NADPH (Supplementary Figure S4).

To test *gpr*-dependent redox homeostasis during biofilm development, we first compared the NADPH and NADP levels between planktonic and wild-type cells. Interestingly,

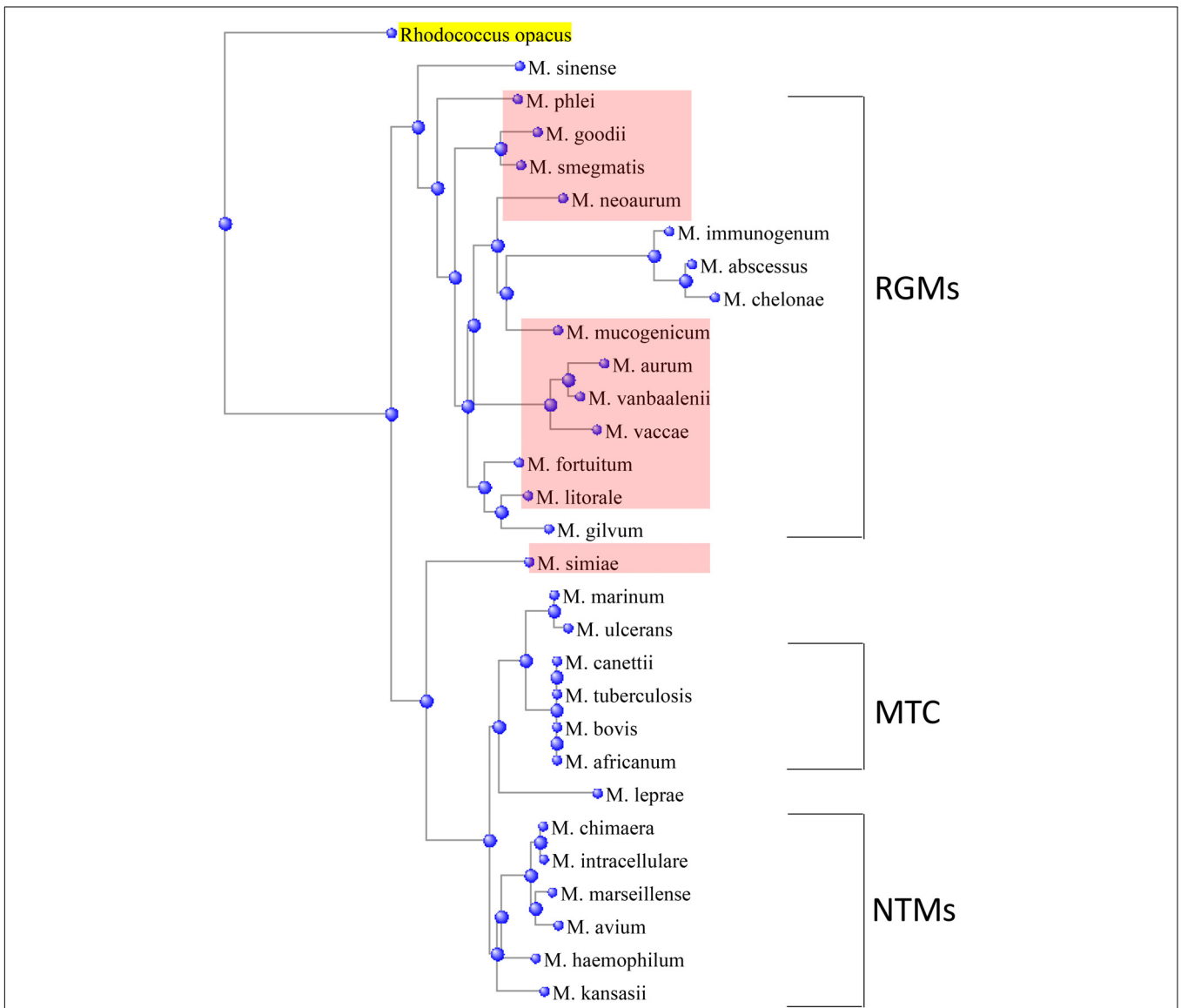

FIGURE 7 | Presence of *gpr* locus in a subset (shaded pink) of rapidly growing mycobacteria (RGMs), which are depicted in relationship to the other RGMs, slow-growing non-tuberculous mycobacteria (NTMs), and *Mycobacterium tuberculosis* complex (MTC), based on their similarities in 16S rRNA sequences. A member of NTM, *Mycobacterium simiae,* is an outlier. The phylogenetic tree was constructed by distance method using *Rhodococcus opacus* as an outgroup.

the average NADPH/NADP ratio in biofilm cells of wild-type increased by ∼18%, relative to its planktonic counterpart, indicating that biofilm cells have a more reduced cytosolic environment (**Figure 5C**). The increase in the ratio resulted from a disproportionate increase in NADPH (∼34%), compared to NADP, which was maintained at a steady level (**Figures 5A,B**). This suggests increase in both new synthesis of NADP and its reduction. This was in contrast to the scenario observed in planktonic cells in N_0-Sauton's medium (Supplementary Figure S4). Expectedly, the average NADPH/NADP ratio in biofilms of Δ*gpr* mutant declined by nearly 50%, relative to wild-type, and the phenotype was substantially restored in the complemented strain (**Figures 5A–C**). Decline in the ratio in the mutant was due to accumulation of NADP, with concomitant decrease in NADPH (**Figures 5A–C**). Together, we infer that GlnR-dependent induction of *gpr* in a subpopulation of biofilm cells that experience nitrogen starvation is critical for maintenance of higher NADPH pool to meet their metabolic demand.

A corollary to *gpr*-dependent redox homeostasis is that Δ*gpr* mutant has impaired ability to assimilate nitrogen that impacts its growth in biofilms. Relative to wild-type, biofilm growth of Δ*gpr* cells in normal Sauton's medium was moderately retarded, but the effect was more pronounced in nitrogen-depleted ($N_{1/2}$) Sauton's medium, which has been shown to increase GlnR-dependency of *M. smegmatis* in biofilms (Yang et al., 2017) (**Figures 6A,B**). A mutant lacking a GlnR-dependent operon (MSMEG_2425-27), which was previously shown to display nitrogen-responsive biofilm defect (Yang et al., 2017), served as a reference in our analysis of Δ*gpr* phenotype (**Figures 6A,B**). Phenotype of Δ*gpr* could be complemented by plasmid-borne expression of *gpr* (**Figures 6A,B**). The defect was specific to biofilm culture, as no difference in planktonic growth of Δ*gpr* mutant was observed (**Figure 6C**).

Our preliminary attempts to identify specific gene(s) of *gpr* that could complement Δ*gpr* phenotype were unsuccessful (data not shown), suggesting that interaction between multiple genes of the cluster give rise to its function.

DISCUSSION

Mycobacteria express and utilize dedicated genes to build stress resistant biofilms (Richards and Ojha, 2014), raising a possibility that genetic programs involved in adaptation of resident cells within the architecture, and those in stress resistance overlap with each other. In this study, we provide evidence supporting this hypothesis by demonstrating a causal relationship between nitrogen-starvation response exhibited by biofilm cells and emergence of peroxide resistance in these cells. Peroxide resistance is likely a result of recalibration of NADPH/NADP ratio, skewed toward a more reduced cytosolic environment, to meet the increasing demand of NADPH for nitrogen assimilation in starved cells. These cells likely reside in interiors of biofilms, as suggested by localization of GlnR-activated cells in these regions of biofilms (Supplementary Figure S3). It is noteworthy that *E. coli* also acquire greater resistance to peroxide upon exposure to nitrogen starvation (Jenkins et al., 1988), although underlying mechanism remains unknown in this species.

The contribution of *gpr* cluster in maintenance of NADPH pool suggests specific function of encoded reductases in the process, although identity of these enzymes and their mechanisms remain open to further investigation. MSMEG_0572 appears to represent DsrE-family reductases, which are conserved in a wide range of environmental species of bacteria. Moreover, similar to MSMEG_0572, its orthologs in these species exhibit a syntenic arrangement with respect to the remaining seven genes of *gpr* cluster, suggesting that the entire cluster has migrated across genomes during evolution. This also raises the possibility that the cluster could function as a unit, rendering a possible explanation to our inability in identifying individual genes responsible for the phenotype associated with Δ*gpr* strain. Interestingly, one of the genes in the cluster, MSMEG_0567, is homologous to selenophosphate synthetase, which is directly involved in the synthesis of selenocysteine (Sec) (Turanov et al., 2011). Sec in prokaryotes is incorporated in polypeptide by a set of specialized accessory factors, which facilitate Sec-tRNA to decode the UGA codon (Krol, 2002). The UGA codon in mRNA decoded as Sec must have a downstream Sec insertion sequence (SECIS), which forms a unique stem-loop structure recognized by the accessory factors that recruit Sec-tRNA during translation (Krol, 2002). Bioinformatics search using bSECIS program (Zhang and Gladyshev, 2005) of all *gpr* ORFs identified a SECIS element comprising of 39 bp downstream of UGA codon of MSMEG_0571, suggesting that the codon in this ORF is decoded as Sec, thereby giving rise to a selenoprotein. The resulting selenoprotein is extended by 518 amino acids (aa) to terminate at the originally annotated stop codon (UAG) of MSMEG_0569 (Supplementary Figure S5). BLAST search of thus encoded 818aa long selenoprotein encompassing MSMEG_0567 to MSMEG_0569 reveals a conserved nitrilase-like domain in the N-terminal region and a flavin-dependent oxidoreductase domain in the C-terminal region (Supplementary Figure S5). This domain architecture is consistent with the fact that majority of the selenopoteins known so far are oxidoreductase (Hatfield et al., 2014), supporting the function of *gpr* cluster in redox homeostasis. The *gpr* cluster also includes a putative aliphatic amidase (MSMEG_0566), which could directly contribute to nitrogen assimilation.

A homology search for *gpr* cluster in 29 mycobacterial species reveals its presence in only a few members, which are evolutionarily linked based on 16S rRNA phylogeny (**Figure 7**). Most of these species are classified as rapidly growing mycobacteria (RGM) (Runyon, 1959). Interestingly, *gpr* is absent in a clinically important RGM, *M. abscessus*, suggesting that its transfer to RGM from a common ancestor is a relatively recent evolutionary event. Moreover, evidence of horizontal gene transfer is supported by the presence of *gpr* in the only slow-growing non-tuberculosis mycobacteria, *M. simiae* (**Figure 7**). Presence of *gpr* in *M. mucogenicum*, *M. goodii,* and *M. simiae,* which are emerging pathogens in nosocomial infections (van Ingen et al., 2008; Adekambi, 2009; Parikh and Grant, 2017; Salas and Klein, 2017), raises clinical significance of our findings and

possibly offers insight into resistance of these species to peroxide-mediated sterilization of surgical and medical equipment.

Lack of *gpr* in a majority of mycobacteria suggests a different mechanism of GlnR-dependent nitrogen assimilation in these species, consistent with the differences between GlnR activities in *M. smegmatis* and *M. tuberculosis* as described previously (Williams et al., 2015). Further understanding of molecular underpinnings of these differences is likely to identify a role of GlnR in biofilm development and associated stress tolerance in these species.

AUTHOR CONTRIBUTIONS

AO and YY conceived this study. YY, JR, JG, and AO designed, performed, and analyzed the experiments. YY and AO wrote the manuscript.

FUNDING

AO received funding from the NIH (AI107595).

ACKNOWLEDGMENTS

The authors acknowledged technical help from Advanced Light Microscopy and Image Analysis, Applied Genomic Technologies, and Media core laboratories of the Wadsworth Center.

SUPPLEMENTARY MATERIAL

The Supplementary Material for this article can be found online at: https://www.frontiersin.org/articles/10.3389/fmicb.2018.01428/full#supplementary-material

REFERENCES

Adekambi, T. (2009). *Mycobacterium mucogenicum* group infections: a review. *Clin. Microbiol. Infect.* 15, 911–918. doi: 10.1111/j.1469-0691.2009.03028.x

Amon, J., Brau, T., Grimrath, A., Hanssler, E., Hasselt, K., Holler, M., et al. (2008). Nitrogen control in *Mycobacterium smegmatis*: nitrogen-dependent expression of ammonium transport and assimilation proteins depends on the OmpR-type regulator GlnR. *J. Bacteriol.* 190, 7108–7116. doi: 10.1128/JB.00855-08

Boritsch, E. C., Khanna, V., Pawlik, A., Honore, N., Navas, V. H., Ma, L., et al. (2016). Key experimental evidence of chromosomal DNA transfer among selected tuberculosis-causing mycobacteria. *Proc. Natl. Acad. Sci. U.S.A.* 113, 9876–9881. doi: 10.1073/pnas.1604921113

Bosio, S., Leekha, S., Gamb, S. I., Wright, A. J., Terrell, C. L., and Miller, D. V. (2012). *Mycobacterium fortuitum* prosthetic valve endocarditis: a case for the pathogenetic role of biofilms. *Cardiovasc. Pathol.* 21, 361–364. doi: 10.1016/j.carpath.2011.11.001

Chuang, Y. M., Dutta, N. K., Hung, C. F., Wu, T. C., Rubin, H., and Karakousis, P. C. (2016). Stringent response factors PPX1 and PPK2 play an important role in *Mycobacterium tuberculosis* metabolism, biofilm formation, and sensitivity to isoniazid *in vivo*. *Antimicrob. Agents Chemother.* 60, 6460–6470. doi: 10.1128/AAC.01139-16

Clary, G., Sasindran, S. J., Nesbitt, N., Mason, L., Cole, S., Azad, A., et al. (2018). *Mycobacterium abscessus* smooth and rough morphotypes form antimicrobial-tolerant biofilm phenotypes but are killed by acetic acid. *Antimicrob. Agents Chemother.* 62:e1782-17. doi: 10.1128/AAC.01782-17

Dietrich, L. E., Teal, T. K., Price-Whelan, A., and Newman, D. K. (2008). Redox-active antibiotics control gene expression and community behavior in divergent bacteria. *Science* 321, 1203–1206. doi: 10.1126/science.1160619

Falagas, M. E., Thomaidis, P. C., Kotsantis, I. K., Sgouros, K., Samonis, G., and Karageorgopoulos, D. E. (2011). Airborne hydrogen peroxide for disinfection of the hospital environment and infection control: a systematic review. *J. Hosp. Infect.* 78, 171–177. doi: 10.1016/j.jhin.2010.12.006

Falkinham, J. O. III. (2007). Growth in catheter biofilms and antibiotic resistance of *Mycobacterium avium*. *J. Med. Microbiol.* 56(Pt 2), 250–254. doi: 10.1099/jmm.0.46935-0

Feazel, L. M., Baumgartner, L. K., Peterson, K. L., Frank, D. N., Harris, J. K., and Pace, N. R. (2009). Opportunistic pathogens enriched in showerhead biofilms. *Proc. Natl. Acad. Sci. U.S.A.* 106, 16393–16399. doi: 10.1073/pnas.0908446106

Fennelly, K. P., Ojano-Dirain, C., Yang, Q., Liu, L., Lu, L., Progulske-Fox, A., et al. (2016). Biofilm formation by *Mycobacterium abscessus* in a lung cavity. *Am. J. Respir. Crit. Care Med.* 193, 692–693. doi: 10.1164/rccm.201508-1586IM

Gupta, K. R., Kasetty, S., and Chatterji, D. (2015). Novel functions of (p)ppGpp and Cyclic di-GMP in mycobacterial physiology revealed by phenotype microarray analysis of wild-type and isogenic strains of *Mycobacterium smegmatis*. *Appl. Environ. Microbiol.* 81, 2571–2578. doi: 10.1128/AEM.03999-14

Hatfield, D. L., Tsuji, P. A., Carlson, B. A., and Gladyshev, V. N. (2014). Selenium and selenocysteine: roles in cancer, health, and development. *Trends Biochem. Sci.* 39, 112–120. doi: 10.1016/j.tibs.2013.12.007

He, J. M., Zhu, H., Zheng, G. S., Liu, P. P., Wang, J., Zhao, G. P., et al. (2016). Direct involvement of the master nitrogen metabolism regulator GlnR in antibiotic biosynthesis in *Streptomyces*. *J. Biol. Chem.* 291, 26443–26454. doi: 10.1074/jbc.M116.762476

Huang, S. C., and Chen, Y. Y. (2016). Role of VicRKX and GlnR in pH-dependent regulation of the *Streptococcus salivarius* 57.I Urease Operon. *mSphere* 1:e33-16. doi: 10.1128/mSphere.00033-16

Jenkins, D. E., Schultz, J. E., and Matin, A. (1988). Starvation-induced cross protection against heat or H2O2 challenge in *Escherichia coli*. *J. Bacteriol.* 170, 3910–3914. doi: 10.1128/jb.170.9.3910-3914.1988

Jenkins, V. A., Barton, G. R., Robertson, B. D., and Williams, K. J. (2013). Genome wide analysis of the complete GlnR nitrogen-response regulon in *Mycobacterium smegmatis*. *BMC Genomics* 14:301. doi: 10.1186/1471-2164-14-301

Jessberger, N., Lu, Y., Amon, J., Titgemeyer, F., Sonnewald, S., Reid, S., et al. (2013). Nitrogen starvation-induced transcriptome alterations and influence of transcription regulator mutants in *Mycobacterium smegmatis*. *BMC Res. Notes* 6:482. doi: 10.1186/1756-0500-6-482

Krol, A. (2002). Evolutionarily different RNA motifs and RNA-protein complexes to achieve selenoprotein synthesis. *Biochimie* 84, 765–774. doi: 10.1016/S0300-9084(02)01405-0

Liao, C. H., Yao, L., Xu, Y., Liu, W. B., Zhou, Y., and Ye, B. C. (2015). Nitrogen regulator GlnR controls uptake and utilization of non-phosphotransferase-system carbon sources in actinomycetes. *Proc. Natl. Acad. Sci. U.S.A.* 112, 15630–15635. doi: 10.1073/pnas.1508465112

McClure, R., Balasubramanian, D., Sun, Y., Bobrovskyy, M., Sumby, P., Genco, C. A., et al. (2013). Computational analysis of bacterial RNA-Seq data. *Nucleic Acids Res.* 41:e140. doi: 10.1093/nar/gkt444

Mullis, S. N., and Falkinham, J. O. III. (2013). Adherence and biofilm formation of *Mycobacterium avium*, *Mycobacterium intracellulare* and *Mycobacterium abscessus* to household plumbing materials. *J. Appl. Microbiol.* 115, 908–914. doi: 10.1111/jam.12272

Nguyen, K. T., Piastro, K., Gray, T. A., and Derbyshire, K. M. (2010). Mycobacterial biofilms facilitate horizontal DNA transfer between strains of *Mycobacterium smegmatis*. *J. Bacteriol.* 192, 5134–5142. doi: 10.1128/JB.00650-10

Ojha, A., Anand, M., Bhatt, A., Kremer, L., Jacobs, W. R. Jr., and Hatfull, G. F. (2005). GroEL1: a dedicated chaperone involved in mycolic acid biosynthesis during biofilm formation in mycobacteria. *Cell* 123, 861–873. doi: 10.1016/j.cell.2005.09.012

Ojha, A., and Hatfull, G. F. (2007). The role of iron in *Mycobacterium smegmatis* biofilm formation: the exochelin siderophore is essential in limiting iron

conditions for biofilm formation but not for planktonic growth. *Mol. Microbiol.* 66, 468–483. doi: 10.1111/j.1365-2958.2007.05935.x

Ojha, A. K., Baughn, A. D., Sambandan, D., Hsu, T., Trivelli, X., Guerardel, Y., et al. (2008). Growth of *Mycobacterium tuberculosis* biofilms containing free mycolic acids and harbouring drug-tolerant bacteria. *Mol. Microbiol.* 69, 164–174. doi: 10.1111/j.1365-2958.2008.06274.x

Parikh, R. B., and Grant, M. (2017). *Mycobacterium goodii* endocarditis following mitral valve ring annuloplasty. *Ann. Clin. Microbiol. Antimicrob.* 16:14. doi: 10.1186/s12941-017-0190-4

Rego, E. H., Audette, R. E., and Rubin, E. J. (2017). Deletion of a mycobacterial divisome factor collapses single-cell phenotypic heterogeneity. *Nature* 546, 153–157. doi: 10.1038/nature22361

Richards, J. P., and Ojha, A. K. (2014). Mycobacterial Biofilms. *Microbiol. Spectr.* 2:MGM2-0004-2013. doi: 10.1128/microbiolspec.MGM2-0004-2013

Rose, S. J., Babrak, L. M., and Bermudez, L. E. (2015). *Mycobacterium avium* possesses extracellular DNA that contributes to biofilm formation, structural integrity, and tolerance to antibiotics. *PLoS One* 10:e0128772. doi: 10.1371/journal.pone.0128772

Rose, S. J., and Bermudez, L. E. (2014). *Mycobacterium avium* biofilm attenuates mononuclear phagocyte function by triggering hyperstimulation and apoptosis during early infection. *Infect. Immun.* 82, 405–412. doi: 10.1128/IAI.00820-13

Runyon, E. H. (1959). Anonymous mycobacteria in pulmonary disease. *Med. Clin. North Am.* 43, 273–290. doi: 10.1016/S0025-7125(16)34193-1

Salas, N. M., and Klein, N. (2017). *Mycobacterium goodii*: an emerging nosocomial pathogen: a case report and review of the literature. *Infect. Dis. Clin. Pract.* 25, 62–65. doi: 10.1097/IPC.0000000000000428

Shao, Z., Deng, W., Li, S., He, J., Ren, S., Huang, W., et al. (2015). GlnR-mediated regulation of ectABCD transcription expands the role of the GlnR regulon to osmotic stress management. *J. Bacteriol.* 197, 3041–3047. doi: 10.1128/JB.00185-15

Storz, G., and Imlay, J. A. (1999). Oxidative stress. *Curr. Opin. Microbiol.* 2, 188–194. doi: 10.1016/S1369-5274(99)80033-2

Turanov, A. A., Xu, X. M., Carlson, B. A., Yoo, M. H., Gladyshev, V. N., and Hatfield, D. L. (2011). Biosynthesis of selenocysteine, the 21st amino acid in the genetic code, and a novel pathway for cysteine biosynthesis. *Adv. Nutr.* 2, 122–128. doi: 10.3945/an.110.000265

Urem, M., Swiatek-Polatynska, M. A., Rigali, S., and van Wezel, G. P. (2016). Intertwining nutrient-sensory networks and the control of antibiotic production in *Streptomyces*. *Mol. Microbiol.* 102, 183–195. doi: 10.1111/mmi.13464

van Heeswijk, W. C., Westerhoff, H. V., and Boogerd, F. C. (2013). Nitrogen assimilation in *Escherichia coli*: putting molecular data into a systems perspective. *Microbiol. Mol. Biol. Rev.* 77, 628–695. doi: 10.1128/MMBR.00025-13

van Ingen, J., Boeree, M. J., Dekhuijzen, P. N., and van Soolingen, D. (2008). Clinical relevance of *Mycobacterium simiae* in pulmonary samples. *Eur. Respir. J.* 31, 106–109. doi: 10.1183/09031936.00076107

Vilcheze, C., Weisbrod, T. R., Chen, B., Kremer, L., Hazbon, M. H., Wang, F., et al. (2005). Altered NADH/NAD+ ratio mediates coresistance to isoniazid and ethionamide in mycobacteria. *Antimicrob. Agents Chemother.* 49, 708–720. doi: 10.1128/AAC.49.2.708-720.2005

Weiss, L. A., and Stallings, C. L. (2013). Essential roles for *Mycobacterium tuberculosis* Rel beyond the production of (p)ppGpp. *J. Bacteriol.* 195, 5629–5638. doi: 10.1128/JB.00759-13

Williams, K. J., Jenkins, V. A., Barton, G. R., Bryant, W. A., Krishnan, N., and Robertson, B. D. (2015). Deciphering the metabolic response of *Mycobacterium tuberculosis* to nitrogen stress. *Mol. Microbiol.* 97, 1142–1157. doi: 10.1111/mmi.13091

Yang, Y., Thomas, J., Li, Y., Vilcheze, C., Derbyshire, K. M., Jacobs, W. R., et al. (2017). Defining a temporal order of genetic requirements for development of mycobacterial biofilms. *Mol. Microbiol.* 105, 794–809. doi: 10.1111/mmi.13734

Yao, L. L., and Ye, B. C. (2016). Reciprocal regulation of GlnR and PhoP in response to nitrogen and phosphate limitations in *Saccharopolyspora erythraea*. *Appl. Environ. Microbiol.* 82, 409–420. doi: 10.1128/AEM.02960-15

Zhang, Y., and Gladyshev, V. N. (2005). An algorithm for identification of bacterial selenocysteine insertion sequence elements and selenoprotein genes. *Bioinformatics* 21, 2580–2589. doi: 10.1093/bioinformatics/bti400

Conflict of Interest Statement: The authors declare that the research was conducted in the absence of any commercial or financial relationships that could be construed as a potential conflict of interest.

frontiers in Microbiology

REVIEW
published: 18 July 2018
doi: 10.3389/fmicb.2018.01613

Challenges of NTM Drug Development

*Joseph O. Falkinham III**

Department of Biological Sciences, Virginia Tech, Blacksburg, VA, United States

Discovery and development of antibiotics active against the environmental opportunistic non-tuberculous mycobacteria (NTM) have been retarded by innate antibiotic-resistance of NTM cells and methodological challenges in the laboratory. The basis for the innate resistance of NTM cells is its lipid rich outer membrane that results in hydrophobic cells and the outer membrane's impermeability, and the residence of NTM cells in phagocytic cells, and the slow growth and dormancy of NTM. Laboratory challenges include: the choice of species and strains for screening and measurement of anti-NTM activity, the high frequency colony switching between antibiotic-susceptible and resistant variants, the preference of NTM to adhere to surfaces and form biofilms, and the aggregation of NTM cells. Understanding these challenges can guide and inform our approaches to discovery and development of antibiotics with activity against NTM.

Keywords: slow growth, rapid metabolism, adaptation, impermeable, hydrophobic, dormancy, biofilms, intracellular

OPEN ACCESS

Edited by:
Thomas Dick,
Rutgers, The State University of New Jersey, United States

Reviewed by:
David E. Griffith,
The University of Texas Health Science Center at Tyler, United States
César de la Fuente,
Massachusetts Institute of Technology, United States

***Correspondence:**
Joseph O. Falkinham III
jofiii@vt.edu

Specialty section:
This article was submitted to Antimicrobials, Resistance and Chemotherapy, a section of the journal Frontiers in Microbiology

Received: *11 April 2018*
Accepted: *28 June 2018*
Published: *18 July 2018*

Citation:
Falkinham JO III (2018) Challenges of NTM Drug Development. Front. Microbiol. 9:1613. doi: 10.3389/fmicb.2018.01613

INTRODUCTION TO THE NON-TUBERCULOUS MYCOBACTERIA (NTM)

The term non-tuberculous mycobacteria (NTM) encompass a large number (>150) *Mycobacterium* species that are environmental opportunistic pathogens causing pulmonary disease and skin infections in adults and cervical lymphadenitis in children (Marras and Daley, 2002). There is growing awareness of the emergence of NTM as causative agents of nosocomial infections (Marras and Daley, 2002). In the United States the species most commonly reported as causing disease are *Mycobacterium avium* subsp. *hominissuis, Mycobacterium intracellulare, Mycobacterium chimaera, Mycobacterium kansasii,* and *Mycobacterium abscessus* complex. Proven sources of infection include NTM from drinking water, potting soils, and medical equipment. Routes of infection include aerosols from water, dusts from soil, and water and soil contact with abraded or injured skin (Falkinham, 2015).

Humans are surrounded by NTM. NTM have been shown to be normal residents of drinking water distribution systems and premise plumbing; in fact, they grow in distribution systems between the treatment plant and buildings (Falkinham et al., 2001). Premise plumbing is an ideal habitat for the NTM. The water is heated and the low concentration of organic carbon is sufficient to support NTM growth. Although NTM can be grown on rich laboratory medium, they are oligotrophs able to grow on the small amount of organic matter in drinking water (George et al., 1980; Norton et al., 2004). Periods of water stagnation brought about by increased water age and oxygen consumption do not limit NTM growth, as they can grow at 12% oxygen as well as in air (21% oxygen) and can even grow, albeit at half the rate, at 6% oxygen (Lewis and Falkinham, 2015). Finally, NTM cells are surrounded by a lipid-rich outer membrane (Brennan and Nikaido, 1995) that makes NTM cells hydrophobic (van Oss et al., 1975) and impermeable

(Jarlier and Nikaido, 1994). Hydrophobicity leads to the preferential attachment of NTM cells to the walls of any container or pipe, so the slowly growing NTM cells cannot be washed out. Surveys of household plumbing of *M. avium* patients showed that in 50% of the households the NTM isolates from the houses were of the same species and shared the same *rep*-PCR DNA fingerprint patterns (Falkinham, 2011). It is important to note that later work has shown that VNTR-RFLP is more discriminatory than *rep*-PCR (Iakhiaeva et al., 2016). Further, *M. avium* was common in plumbing of homes with a water heater temperatures of 125° F (50° C) or less, but rare if the water heater temperature was 130° F (55° C) or higher. That has led to a current study of the role of water heaters in increasing numbers of *M. avium* in premise plumbing. All the factors listed above undoubtedly contributed to the colonization and growth of *M. chimaera* in heater-coolers that have been shown to generate *M. chimaera*-laden aerosols and infected patients undergoing cardiac surgery (Sax et al., 2015).

CHALLENGES TO DEVELOPMENT OF ANTI-NTM ANTIBIOTICS

Introduction

The foregoing brief introduction to the NTM is necessary before discussion of how NTM physiologic and genetic features of NTM are challenges to antibiotic development. The challenges fall into two categories: those involving difficulties in overcoming innate genetic and physiologic traits of NTM (**Table 1**) and difficulties in measuring anti-NTM antibiotic activity in the laboratory (**Table 2**). The approach that follows focuses first on laboratory challenges of susceptibility measurements and then turns to challenges due to innate NTM resistance to antibiotics. In a number of instances, it will be clear that a single NTM feature drives antibiotic resistance and laboratory measurement problems. Finally, a table is included to suggest possible solutions to the challenges (**Table 3**).

Laboratory Challenges

NTM Strain Selection

When searching among libraries of synthetic or nature compounds for anti-mycobacterial activity the choice of *Mycobacterium* spp. strains is of paramount importance. First, do not use strains of *Mycobacterium smegmatis* as indicators of potential anti-NTM activity by novel compounds in spite of their rapid rate of growth and ease of handling. Current isolates of *M. smegmatis* have been linearly cultivated for so long, that they do not resemble the original ATCC deposit. Most of the *M. smegmatis* isolates being used are derivatives of ATCC strain 607, and those lab-adapted strains have lost many unique characteristics – slow growth, hydrophobicity, and impermeability – that directly increase antibiotic susceptibility. Thus, measurements of minimal inhibitory concentrations (MIC) are not useful to guide compound selection as the *M. smegmatis* strains in use are unusually susceptible to a wide range of antibiotics. Prolonged, linear cultivation of NTM isolates selects for variants that can grow faster, have lost hydrophobicity and impermeability. Even employing *M. smegmatis* as a primary screen can be misleading, as some compounds that do not display anti-*M. smegmatis* inhibition has activity against *M. avium, M. intracellulare*, or *M. abscessus*. It is best to identify the ultimate target NTM species (e.g., *M. avium*) and measure MICs against representatives of that species (**Table 3**).

Another problem concerns selection of isolates from patients for measurement of MIC to guide and select antibiotics for therapy. More than a single isolate needs to be selected and its susceptibility measured (CSLI, 2011), as it has been shown that colonies of *M. avium* from AIDS patients having identical morphology, yielded different patterns of susceptibility to antibiotics (von Reyn et al., 1995). Further, as NTM-infected patients may be infected by more than a single NTM species as detected directly (Wallace et al., 1998) or evidenced by relapse (Boyle et al., 2016), selection of single colonies may lead to an incorrect assessment of the antibiotic of choice.

TABLE 1 | Non-tuberculous mycobacteria (NTM) antibiotic development challenges for NTM due to laboratory measurement of antibiotic susceptibility.

Mycobacterium species strain selection
Colonial variation
Preference for surface adherence and biofilm formation
Cell aggregation
Dormancy
Residence in phagocytic cells

TABLE 2 | Non-tuberculous mycobacteria antibiotic development challenges due to innate traits of NTM.

Hydrophobic cells
Lipid-rich impermeable outer membrane
Slow growth
Dormancy
Adaptation

TABLE 3 | Possible solutions to challenges impeding antibiotic development for NTM.

Challenge	Possible solution
Laboratory problem	
Strain selection	Measure MIC in target *Mycobacterium* spp.
Colonial variation	Confirm colony type
	Initiate cultures from single colony type
Preference for adherence	Measure MIC of biofilm-grown
Aggregation	Measure MIC in early growth phase
Adaptation	Measure MIC throughout growth
Intracellular	Measure MIC in phagocytic cells
Innate NTM trait	
Hydrophobic cells	Amphipathic antibiotics
	Combine with OM-targeted antibiotic
Lipid-rich, impermeable OM	Amphipathic antibiotics
	Combine with OM-targeted antibiotic
Slow growth	Patience
Dormancy	Combine with resuscitation factors
Adaptation	Combine with RNA or protein synthesis inhibitor

NTM Colonial Variation

Another problem associated with strain choice is that NTM strains can display alternative colonial variants. For *M. avium* and *M. intracellulare*, isolates exhibit either a transparent or opaque colony form (McCarthy, 1970; Stormer and Falkinham, 1989). Likewise, *M. abscessus* complex isolates can exhibit either a rough and smooth colonial morphology (Howard et al., 2006). In *M. avium* and *M. intracellulare* the transparent (T) "Mexican Hat" colony morphology is found upon primary culture from patients. The transparent (T) variant is slow-growing, hydrophobic, virulent, and antibiotic-resistant compared to the opaque (O) variant that emerges during laboratory medium cultivation (Schaefer et al., 1970). The opaque (O) variants are faster growing, less hydrophobic, and antibiotic-sensitive compared to the isogenic transparent (T) variants. In *M. avium,* single colony isolates switch between the T and O forms; colony variation is fully reversible (McCarthy, 1970). The frequency of colony variants of the opposite type amongst isolates of *M. avium* is approximately 1 in 1,000 (Stormer and Falkinham, 1989). Thus, in a barely turbid culture of one-hundred million (10^8) *M. avium* (T) variant cells, there are approximately one-hundred thousand (10^5 O) cells. Thus, special care must be taken to sample every culture to ensure that the frequency of colonies of the opaque (O) type are always less than or equal to 1 in 1,000 (**Table 3**).

As the alternative colonial variants have different susceptibilities to antibiotics (McCarthy, 1970; Stormer and Falkinham, 1989), measurement of MIC values may not provide the guidance to direct either chemotherapy or selection of promising novel anti-mycobacterial compounds. For example, as transparent (T) colony variants predominate in patients, selection of an isogenic opaque (O) variant for MIC measurement will lead to choice of an antibiotic that may lack activity against the patient's transparent (T) variant. This may be the basis, in part, for the lack of any correlation between MIC measurements and prediction of therapeutic success (Sison et al., 1996; Van Engen et al., 2010; Schön and Chryssanthou, 2017). It might also result in the advancement of a compound for further testing based on MIC values from an opaque (O) variant, that will be ineffective in patients as the transparent variant (T) is resistant to the compound.

NTM Hydrophobicity and Measurement of Antibiotic Susceptibility

Non-tuberculous mycobacteria hydrophobicity also creates problems in measuring MICs to guide compound selection or patient therapy. As NTM are hydrophobic, they prefer surface attachment and growth rather than replicating in aqueous suspension. That means that the NTM cells are not in suspension, but rather adhere to the walls of the individual wells in 96-well plates used to measure MICs as recommended by Clinical and Laboratory Standards Institute (CSLI, 2011). Measurements of NTM cells adhering to the walls of water heaters and pipes in households and hospitals, in medical equipment (e.g., heater-coolers), and in test tubes in the laboratory shows that the majority of NTM cells (>99%) are surface-attached (Falkinham et al., 2001; Falkinham, 2011). This observation alone provides a reason why measurement of antibiotic susceptibility in tubes or 96-well plates has not provided guidance for therapeutic efficacy in patients (Sison et al., 1996; Van Engen et al., 2010; Schön and Chryssanthou, 2017). Simply, measurement of turbidity of cell suspensions does not accurately reflect the number of total cells; most are not in suspension but adhering to the wells or tubes. The solution is to use methods to measure MIC of biofilm-grown cells in biofilms (**Table 3**).

Non-tuberculous mycobacteria preference for adherence and biofilm-formation (Falkinham et al., 2001; Falkinham, 2011) also explain why disinfection of hospital pipes and medical equipment generally fails. The NTM cells in the biofilms survive disinfection and can re-inoculate the water.

A second hydrophobicity-driven problem reducing the utility of standard methods of MIC measurement (CSLI, 2011) is the spontaneous aggregation of NTM cells. Typically, early growth of NTM cells in laboratory medium (e.g., M7H9 broth) can be followed by increases in turbidity, but upon reaching the mid to late exponential phase of growth turbidity disappears and visible aggregates of various dimensions appear. Thus, for many NTM isolates, antibiotic susceptibility cannot be measured with accuracy. Aggregation between NTM cells is driven by hydrophobicity, just as hydrophobicity drives the adherence of NTM to the walls of tubes and wells (van Oss et al., 1975). The best solution to this problem is to measure MIC of isolates during the early phases of cell growth, before aggregation occurs (**Table 3**). This may require amplification, such as PCR or dyes, to increase the signal from the low cell numbers.

There are no other current useful approaches to reduce the aggregation of NTM cells, as the use of detergent reduces cell-surface hydrophobicity and abolishes aggregation, but increases NTM permeability and growth rate, and thereby the susceptibility to antibiotics. Selection of non-aggregating variants of NTM isolates is not a solution, as the non-aggregating variants have reduced cell hydrophobicity and altered outer membrane composition. Thus, the cells are not representative of those recovered from the patient. This is represented by the laboratory-culture-induced selection of opaque (O) variants of the transparent (T) variants that are isolated from patients.

NTM Adherence and Biofilm Formation

Non-tuberculous mycobacteria cells prefer surface adherence to residence in suspension, whether in humans, in water, or in laboratory growth medium. Surface attachment allows NTM cells to reduce the interaction of their hydrophobic surfaces with the positive and negative charges in aqueous suspension. Once the NTM cells adhere, they can grow to form a biofilm that consists of NTM and other microbial cells within a polymeric matrix consisting of polysaccharide, lipid, DNA, and protein (Mullis and Falkinham, 2013). The layers of cells within the matrix are relatively impermeable to antibiotics and disinfectants. There are significant differences in the susceptibility to chlorine (Falkinham, 2003; Steed and Falkinham, 2006) or antibiotics (Falkinham, 2007) of *M. avium* cells grown and exposed in biofilms compared to suspension-grown and exposed cells. The increased resistance of *M. avium* cells in biofilms to antimicrobial agents, compared to those grown and exposed in suspension, prevents obtaining an accurate measurement of disinfectant-

or antibiotic-susceptibility for guidance in water treatment or patient care. Again, the solution to biofilm formation is to measure MICs of NTM cells grown in biofilms (**Table 3**).

That is not the only problem of NTM biofilm formation. Surprisingly, cells of *M. avium* grown in biofilms, yet harvested and exposed as single cell suspensions were significantly more tolerant of chlorine or antibiotics than cells grown and exposed in suspension (Steed and Falkinham, 2006; Falkinham, 2007). That tolerance was transient, as cells lost the increased resistance to chlorine or antibiotics exhibited by suspension-grown cells following overnight growth in fresh medium (Steed and Falkinham, 2006; Falkinham, 2007). I speculate that such a physiologic adaptation (adaptation, because cells are not permanently altered in susceptibility) is a consequence of growth of NTM-cells in a biofilm.

NTM Dormancy

NTM-dormancy has been demonstrated in a variety of NTM species, particularly in *M. avium* (Archuleta et al., 2005). *M. avium* cells subjected to nutrient starvation entered a dormant stage in which cells are effectively non-growing and thereby resistant to any antibiotic challenge (Archuleta et al., 2005). Whether such NTM-dormant cells are in patient tissue or in the wells of an antibiotic-containing medium, such non-growing cells would be expected to be resistant to most antibiotics, as the antibiotics do not actively destroy cell components.

As demonstrated by the studies of Larry Wayne, the slow decrease in oxygen levels as *M. tuberculosis* triggers the formation of lung tubercles, points out that dormancy of *M. tuberculosis* is triggered by the absence of oxygen. Those dormant cells can, under certain conditions, be triggered to grow again. The discovery of proteins that can induce growth in such dormant cells, suggests an approach to measurement of MIC of cells suspected to be dormant; namely resuscitate the dormant cells (Wivagg and Hung, 2012) and measure the MIC following the subsequent growth (**Table 3**).

NTM Residence in Phagocytic Cells

Non-tuberculous mycobacteria cells are not only found within phagocytic cells in infected individuals, but also in granulomas in infected organs like the lungs and liver. NTM-cells in granulomas have not only the NTM outer membrane to protect them, but they also have the layers of host, human cells that make up the granuloma. When considering that it is likely that the majority of NTM-cells are located within mammalian phagocytic cells in infected individuals, a problem of permeability re-appears. Here, it is not the NTM cell's impermeability that is the only factor, but rather the impermeability of the phagocytic cell's membrane now plays a role. Recognition of that fact led David Yajko and his colleagues to measure antibiotic susceptibility of NTM cells in human macrophages (Yajko et al., 1991). However, as discussed above, impermeability can be possibly overcome using combinations of agents; namely, one agent to increase the permeability of the phagocytic cell's membrane to achieve bacteriostatic or bactericidal concentrations within those cells and a second for killing or inhibiting the growth of the NTM cells (**Table 3**). Documentation that the MICs of the intracellular NTM cells were higher than those of the NTM cells alone, forces us to consider this approach.

Innate Resistance of NTM to Antibiotics

NTM Hydrophobicity and Impermeability and NTM Susceptibility to Antibiotics

Both the hydrophobic and impermeable NTM outer membrane are major and independent contributors to the lack of susceptibility of NTM to commonly used antibiotics (Rastogi et al., 1981; Jarlier and Nikaido, 1994; Brennan and Nikaido, 1995). NTM are the most hydrophobic of bacteria (van Oss et al., 1975), due to the fact that cells are surrounded by the lipid-rich outer membrane that comprises 30% of the cell mass (Brennan and Nikaido, 1995). Hydrophobicity, measured as water droplet contacts angles on filters covered with NTM cells are high ($\geq$75°) almost resembling water droplets on a freshly waxed automobile. The non-polar cell surface prevents the adherence or binding of antibiotics that carry positive or negative charges.

The lipid-rich outer membrane is also impermeable. Measurement of rates of uptake of compounds showed the uptake of charged antibiotics, nutrients, metals, oxyanions, and disinfectants was only 1% of the rate measured in rapidly growing bacteria such as *Escherichia coli* (Jarlier and Nikaido, 1994). Thus, not only is adherence of charged compounds reduced, but the rate of transport though the outer membrane is greatly reduced. Therefore, it is not surprising that NTM exhibit resistance to most commonly used antibiotics. That having been stated, it is important to point out that the targets for antibiotic action, for example the 23S rRNA for the erythromycin-family antibiotic clarithromycin, are intact and resemble those in other bacteria. That can be shown by exposing NTM cells to antibiotics or other anti-microbial compounds in the presence of detergent. Detergent disrupts the outer membrane, reducing hydrophobicity and increasing permeation, artificially creating phenocopy cells that are antibiotic-susceptible.

One successful route to development of anti-NTM antibiotics is to synthesize hydrophobic derivatives of existing antibiotics. That approach was taught in a paper describing the synthesis of effective anti-NTM drugs through the addition of hydrophobic groups, starting with an ineffective and hydrophilic drug (Rastogi et al., 1988). Although those drugs are not in use, there is the example of synthesizing hydrophobic derivatives of erythromycin, a common antibiotic with little activity against NTM. Hydrophobic derivatives of erythromycin, namely clarithromycin and azithromycin have been shown effective in treating NTM-infected patients whether suffering from NTN pulmonary disease or NTM bacteremia. Following that rational for anti-NTM antibiotic development, a family of Amphipathic dendritic amphiphiles were synthesized and their anti-NTM activity measured (**Table 3**). These compounds consist of a fatty acid tail linked to (Williams et al., 2007; Falkinham et al., 2012). A number of these compounds displayed strong antibiotic activity against *M. avium, M. intracellulare*, and *M. abscessus* with MICs all below 10 μg/mL (Williams et al., 2007; Falkinham et al., 2012).

Another successful approach to overcoming the hydrophobic barrier of the NTM outer membrane is through combinations

of antibiotics (**Table 3**). For example, the antibiotic ethambutol is an inhibitor of formation of the arabinogalactan polymer that links the NTM outer membrane to the peptidoglycan cell wall. Although ethambutol is not a first line drug, it acts synergistically with other antibiotics with targets within cells. Ethambutol reduces the hydrophobic and impermeable outer membrane barrier resulting in increased transport of the second drug (Yajko et al., 1988). That demonstrated example of rational synergism, suggests that the search for anti-NTM antibiotics includes screening methods to identify those that target and disrupt the outer membrane and then measure MICs of those compounds in combination with drugs whose targets are intracellular. Adoption of this view strongly suggests that screening natural and synthetic compounds for anti-NTM activity include all possible combinations and screening in combination with known, albeit low, anti-NTM active antibiotics such as ethambutol.

NTM Slow Growth and Adaptation

The unique structural feature of the mycobacteria; namely the presence of a long chain lipid and wax-rich outer membrane, is the major determinant of their physiology, growth, ecology, and epidemiology (Brennan and Nikaido, 1995). As the outer membrane makes up 30% of the total mycobacterial cell weight, its synthesis reduces energy available for production of new cells. Consequently, NTM grow slowly with a generation time of 1 doubling per day under nutrient-rich conditions at 37°C. However, it is important to point out that the NTM do not replicate slowly because of a slow rate of metabolism. NTM metabolism, as reflected by oxygen uptake and ATP production, is as active as that of rapidly growing bacteria; the NTM simply expend a great deal of energy making the outer membrane. That rapid rate of metabolism means that NTM cells can induce gene products that protect against environmental stress before cells divide.

In *M. avium*, growth rate modulates antibiotic susceptibility. The susceptibility of *M. avium* cells to antibiotics or chlorine is greater in medium that supports more rapid growth compared to a minimal, nutrient-poor medium (Falkinham, 2003). In measuring antibiotic MICs of NTM isolates, it is valuable to examine and identify MICs on a daily basis (**Table 3**). For example, inspection of MICs for the antibiotic clarithromycin against strains of *Mycobacterium abscessus* identified some whose MIC values increased over time. Significantly, the MIC measured after 3 days incubation was significantly lower than that measured at 7 days (Nash et al., 2009). Further examination of that behavior led to the discovery of an erythromycin methylase that protected cells from inhibition of protein synthesis due to its induction and synthesis leading to methylation of the 23S rRNA target of clarithromycin (Nash et al., 2009).

The studies of Maaløe and Kjeldgaard (1966) taught microbiologists the concept of "balanced" and "unbalanced" growth and the relationship of growth rate to the efficacy of antibiotics. Growth of microorganisms in the absence of antibiotics leads to "balanced" conditions where the increases in the amount of DNA, RNA, protein, and cell walls are proportionate with the growth rate. Exposure of cells growing under "balanced" conditions to an antibiotic unbalances growth. For example, as antibiotics have a single target (e.g., DNA polymerase), it follows that exposure to an antibiotic that inhibits the activity of DNA polymerase would lead to an "unbalanced" condition where increases in of DNA, are not proportionate with increases in cell mass. "Unbalanced" growth of microbial cells leads to death, particularly in rapidly dividing cells (e.g., *E. coli*). However, unlike *E. coli*, NTM cells can react to antibiotic stress by synthesizing proteins and other cell constituents able to protect the cells before they are forced to divide (24 h/generation).

To explain NTM-adaptation further, what follows are the results of a study of *M. avium* heat-adaptation. My students and I have found heat-tolerance in *M. avium* isolates recovered from plumbing biofilm samples collected from homes of *M. avium*-infected patients. The isolates are able to survive exposure to 60°C for 3 h without any loss in colony-forming units; they are only killed at 65°C. This data is in contrast to published data on heat-susceptibility of NTM species (Schulze-Röbbecke and Buchholtz, 1992). As the patient, plumbing, and water-provider *M. avium* isolates shared an identical VNTR-RFLP DNA fingerprint patterns (Iakhiaeva et al., 2016) and heat-tolerance was an adaptation, we hypothesized that passage through the home's water heater may have triggered an adaptive response leading to increased heat-tolerance. Accordingly, we grew the household *M. avium* strains at 25°, 30°, 35°, and 42° (the latter the highest temperature of growth for *M. avium*) and measured their susceptibilities to 55°, 60°, and 65°C. Further, we measured the cell concentration of trehalose that has been shown to be a modulator of temperature-susceptibility. Compared to cells grown at 25°C, cells grown at 42°C had 10-times more trehalose/cell protein. Further, cells grown at 42°C were significantly more tolerant to survival at 60°C compared to those grown at 25°C.

CONCLUDING COMMENTS

The foregoing information provides strong support for the notion that the search for novel anti-NTM antibiotics will continue to be difficult. It is already well-established that laboratory measures of antibiotic MICs of suspension-grown NTM cells do not provide guidance for therapy (Sison et al., 1996; Van Engen et al., 2010; Schön and Chryssanthou, 2017). The challenges involve both methods of measuring antibiotic susceptibility of NTM strains in the laboratory (**Table 1**) as well as developing novel anti-NTM antibiotics that can overcome innate characters of these waterborne opportunistic pathogens (**Table 2**). I have suggested several solutions to these problems (**Table 3**), but further approaches are needed.

First, identification of suitable novel anti-NTM antibiotics requires development of accurate laboratory measures of NTM antibiotic susceptibility. That requires choice of species and strains coupled with the development of accurate measures of suspension-, biofilm-, and intracellular- (e.g., macrophage) NTM susceptibility (**Table 1**). Those *in vitro* measures must be supplemented with ways to prevent NTM cell aggregation, without altering NTM susceptibility.

The second challenge facing development of anti-NTM antibiotics involves efforts to overcome NTM cell surface hydrophobicity and outer membrane impermeability (**Table 2**). A starting point might be the realization that successful anti-NTM drug therapy involves synergistic combinations; one antibiotic to disrupt or inhibit the outer membrane, and a second antibiotic to inhibit a critical cellular process (i.e., DNA, RNA, or protein and outer membrane synthesis) and hence unbalance growth. For such an approach, high throughput screening involving pairs or compounds seems the likely tool.

AUTHOR CONTRIBUTIONS

JF researched, practiced, and wrote the article.

REFERENCES

Archuleta, R. J., Hoppes, P. Y., and Primm, T. P. (2005). *Mycobacterium avium* enters a state of metabolic dormancy in response to starvation. *Tuberculosis* 85, 147–158. doi: 10.1016/j.tube.2004.09.002

Boyle, D. P., Zembower, T. R., and Qi, C. (2016). Relapse versus reinfection of *Mycobacterium avium* complex pulmonary disease. *Ann. Am. Thor. Soc.* 13, 1956–1961. doi: 10.1513/AnnalsATS.201605-344BC

Brennan, P. J., and Nikaido, H. (1995). The envelope of *Mycobacteria*. *Annu. Rev. Biochem.* 64, 29–63. doi: 10.1146/annurev.bi.64.070195.000333

CSLI (2011). *Susceptibility Testing of Mycobacteria, nocardiae, and other Aerobic Actinomycetes; Approved Standard*, 2nd Edn. Wayne, PA: Clinical and Laboratory Standards Institute.

Falkinham, J. O. (2003). Factors influencing the chlorine susceptibility of *Mycobacterium avium*, *Mycobacterium intracellulare*, and *Mycobacterium scrofulaceum*. *Appl. Environ. Microbiol.* 69, 5685–5689. doi: 10.1128/AEM.69.9.5685-5689.2003

Falkinham, J. O. (2007). Growth in catheter biofilms and antibiotic resistance of *Mycobacterium avium*. *J. Med. Microbiol.* 56, 250–254. doi: 10.1099/jmm.0.46935-0

Falkinham, J. O. (2011). Nontuberculous *Mycobacteria* from household plumbing of patients with nontuberculous *Mycobacteria* disease. *Emerg. Infect. Dis.* 17, 419–424. doi: 10.3201/eid1703.101510

Falkinham, J. O., Maisuria, B. B., Actis, M. L., Hardrict, S. N., Macri, R. V., Sugandhi, E. W., Williams, A. A., et al. (2012). Antibacterial activities of dendritic amphiphiles against nontuberculous *Mycobacteria*. *Tuberculosis* 92, 173–181. doi: 10.1016/j.tube.2011.12.002

Falkinham, J. O., Norton, C. D., and LeChevallier, M. W. (2001). Factors influencing numbers of *Mycobacterium avium*, *Mycobacterium intracellulare*, and other *Mycobacteria* in drinking water distribution systems. *Appl. Environ. Microbiol.* 67, 1225–1231. doi: 10.1128/AEM.67.3.1225-1231.2001

Falkinham, J. O. (2015). Environmental sources of nontuberculous *Mycobacteria*. *Clin. Chest Med.* 36, 35–41. doi: 10.1016/j.ccm.2014.10.003

George, K. L., Parker, B. C., Gruft, H., and Falkinham, J. O. (1980). Epidemiology of infection by nontuberculous *Mycobacteria*. II. Growth and survival in natural waters. *Am. Rev. Respir. Dis.* 122, 89–94.

Howard, S. T., Rhoades, E., Recht, J., Pang, X., Alsup, A., Kolter, R., et al. (2006). Spontaneous reversion of *Mycobacterium abscessus* from a smooth to a rough morphotype is associated with reduced expression of glycopeptidolipid and reacquisition of an invasive phenotype. *Microbiology* 152, 1581–1590. doi: 10.1099/mic.0.28625-0

Iakhiaeva, E., Howard, S. T., Brown-Elliott, B. A., McNulty, S., Newman, K. L., Falkinham, J. O. III, et al. (2016). Variable number tandem repeat (VNTR) of respiratory and household water biofilm isolates of *Mycobacterium avium* subspecies "*hominissuis*" with establishment of a PCR database. *J. Clin. Microbiol.* 54, 891–901. doi: 10.1128/JCM.02409-15

Jarlier, V., and Nikaido, H. (1994). *Mycobacteria* l cell wall: structure and role in natural resistance to antibiotics. *FEMS Microbiol. Lett.* 123, 11–18. doi: 10.1111/j.1574-6968.1994.tb07194.x

Lewis, A. H., and Falkinham, J. O. (2015). Microaerobic growth and anaerobic survival of *Mycobacterium avium*, *Mycobacterium intracellulare* and *Mycobacterium scrofulaceum*. *Int. J. Mycobacteriol.* 4, 25–30. doi: 10.1016/j.ijmyco.2014.11.066

Maaløe, O., and Kjeldgaard, N. O. (1966). *Control of Macromolecular Synthesis: A Study of DNA, RNA, and Protein Synthesis in Bacteria*. New York, NY: W. A. Benjamin.

Marras, T. K., and Daley, C. L. (2002). Epidemiology of human and pulmonary infection with nontuberculous *Mycobacteria*. *Clin. Chest Med.* 23, 553–567. doi: 10.1016/S0272-5231(02)00019-9

McCarthy, C. M. (1970). Spontaneous and induced mutation in *Mycobacterium avium*. *Infect. Immun.* 2, 223–228.

Mullis, S. N., and Falkinham, J. O. (2013). Adherence and biofilm formation of *Mycobacterium avium*, *Mycobacterium intracellulare* and *Mycobacterium abscessus* to household plumbing materials. *J. Appl. Microbiol.* 115, 908–914. doi: 10.1111/jam.12272

Nash, K. A., Brown-Elliott, B. A., and Wallace, R. J. Jr (2009). A novel gene, erm(41), confers inducible macrolide resistance to clinical isolates of *Mycobacterium abscessus* but is absent from *Mycobacterium chelonae*. *Antimicrob. Agents Chemother.* 53, 1367–1376. doi: 10.1128/AAC.01275-08

Norton, C. D., LeChevallier, M. W., and Falkinham, J. O. (2004). Survival of *Mycobacterium avium* in a model distribution system. *Water Res.* 38, 1457–1466. doi: 10.1016/j.watres.2003.07.008

Rastogi, N., Moreau, B., Capmau, M. L., Goh, K. S., and David, H. L. (1988). Antibacterial activity of amphipathic derivatives of isoniazid against *Mycobacterium avium* complex. *Zentralbl. Bakteriol. Mikrobiol. Hyg. A* 268, 456–462.

Rastogi, N., Frehel, C., Ryter, A., Ohayon, H., Lesourd, M., and David, H. L. (1981). Multiple drug resistance of *Mycobacterium avium*: is the wall architecture responsible for the exclusion of antimicrobial agents. *Antimicrob. Agents Chemother.* 20, 666–677. doi: 10.1128/AAC.20.5.666

Sax, H., Bloemberg, G., Hasse, B., Sommerstein, R., Kohler, P., Achermann, Y., et al. (2015). Prolonged outbreak of *Mycobacterium chimaera* infection after open-chest heart surgery. *Clin. Infect. Dis.* 61, 67–75. doi: 10.1093/cid/civ198

Schaefer, W. B., Davis, C. L., and Cohn, M. L. (1970). Pathogenicity of transparent, opaque, and rough variants of *Mycobacterium avium* in chickens and mice. *Am. Rev. Respir. Dis.* 102, 499–506.

Schön, T., and Chryssanthou, E. (2017). Minimum inhibitory concentration distributions for *Mycobacterium avium* complex – towards evidence-based susceptibility breakpoints. *Int. J. Infect. Dis.* 55, 122–124. doi: 10.1016/j.ijid.2016.12.027

Schulze-Röbbecke, R., and Buchholtz, K. (1992). Heat susceptibility of aquatic *Mycobacteria*. *Appl. Environ. Microbiol.* 58, 1869–1873.

Sison, J. P., Yao, Y., Kemper, C. A., Hamilton, J. R., Brummer, E., Stevens, D. A., and Deresinski, S. C. (1996). Treatment of *Mycobacterium avium* complex infection: do the results of in vitro susceptibility tests predict therapeutic outcome in humans? *J. Infect. Dis.* 173, 677–683. doi: 10.1093/infdis/173.3.677

Steed, K. A., and Falkinham, J. O. (2006). Effect of growth in biofilms on chlorine susceptibility of *Mycobacterium avium* and *Mycobacterium intracellulare*. *Appl. Environ. Microbiol.* 72, 4007–4100. doi: 10.1128/AEM.02573-05

Stormer, R. S., and Falkinham, J. O. (1989). Differences in antimicrobial susceptibility of pigmented and unpigmented colonial variants of *Mycobacterium avium*. *J. Clin. Microbiol.* 27, 2459–2465.

Van Engen, J., van der Laan, T., Dekhuijzen, R., Boeree, M., and van Soolingen, D. (2010). In vitro drug susceptibility of 2275 clinical non-tuberculous *Mycobacterium* isolates of 49 species in the Netherlands. *Int. J. Antimicrob. Agents* 35, 169–173. doi: 10.1016/j.ijantimicag.2009.09.023

van Oss, C. J., Gillman, C. F., and Neumann, A. W. (1975). *Phagocytic Engulfment and Cell Adhesiveness as Cellular Phenomena*. New York, NY: Marcel Dekker.

von Reyn, C. F., Jacobs, N. J., Arbeit, R. D., Maslow, J. N., and Niemczyk, S. (1995). Polyclonal *Mycobacterium avium* infections in patients with AIDS: variations

in antimicrobial susceptibilities of different strains of *M. avium* isolated from the same patient. *J. Clin. Microbiol.* 33, 1008–1010.

Wallace, R. J. Jr., Zhang, Y., Brown, B. A., Dawson, D., Murphy D. T., Wilson, R., et al. (1998). Polyclonal *Mycobacterium avium* complex infections in patients with nodular bronchiectasis. *Am. J. Respir. Crit. Care Med*. 158, 1235–1244. doi: 10.1164/ajrccm.158.4.9712098

Williams, A. A., Sugandhi, E. W., Macri, R. V., Falkinham, J. O., and Gandour, R. D. (2007). Antimicrobial activity of long-chain, water-soluble, dendritic tricarboxylato amphiphiles. *J. Antimicrob. Chemother.* 59, 451–458. doi: 10.1093/jac/dkl503

Wivagg, C. N., and Hung, D. T. (2012). Resuscitation-promoting factors are required for β-lactam tolerance and the permeability barrier of *Mycobacterium tuberculosis*. *Antimicrob. Agents Chemother.* 56, 1591–1594. doi: 10.1128/AAC.06027-11

Yajko, D. M., Nassos, P. S., Sanders, C. A., and Hadley, W. K. (1991). Effects of antimicrobial agents on survival of *Mycobacterium avium* complex inside alveolar macrophages obtained from patients with human immunodeficiency virus infection. *Antimicrob. Agents Chemother.* 35, 1621–1625. doi: 10.1128/AAC.35.8.1621

Yajko, D. M., Kirihara, J., Sanders, C., Nassos, P., and Hadley, W. K. (1988). Antimicrobial synergism against *Mycobacterium avium* complex strains Isolated from patients with acquired immune deficiency syndrome. *Antimicrob. Agents Chemother*. 32, 1392–1395. doi: 10.1128/AAC.32.9.1392

Conflict of Interest Statement: The author declares that the research was conducted in the absence of any commercial or financial relationships that could be construed as a potential conflict of interest.

frontiers in Microbiology

ORIGINAL RESEARCH
published: 16 May 2018
doi: 10.3389/fmicb.2018.00915

Amikacin Liposome Inhalation Suspension (ALIS) Penetrates Non-tuberculous Mycobacterial Biofilms and Enhances Amikacin Uptake Into Macrophages

Jimin Zhang[1]†, Franziska Leifer[1]†, Sasha Rose[1,2], Dung Yu Chun[1], Jill Thaisz[1], Tracey Herr[1], Mary Nashed[1], Jayanthi Joseph[2], Walter R. Perkins[1] and Keith DiPetrillo[1]*

[1] Insmed Incorporated, Bridgewater, NJ, United States, [2] Department of Biomedical Sciences, College of Veterinary Medicine, Oregon State University, Corvallis, OR, United States

OPEN ACCESS

Edited by:
Thomas Dick,
Rutgers, The State University of New Jersey, Newark, United States

Reviewed by:
Murugesan V. S. Rajaram,
The Ohio State University, United States
Nagendran Tharmalingam,
Alpert Medical School, Brown University, United States

***Correspondence:**
Jimin Zhang
jimin.zhang@insmed.com

†These authors have contributed equally to this work.

Specialty section:
This article was submitted to Antimicrobials, Resistance and Chemotherapy, a section of the journal Frontiers in Microbiology

Received: 28 February 2018
Accepted: 20 April 2018
Published: 16 May 2018

Citation:
Zhang J, Leifer F, Rose S, Chun DY, Thaisz J, Herr T, Nashed M, Joseph J, Perkins WR and DiPetrillo K (2018) Amikacin Liposome Inhalation Suspension (ALIS) Penetrates Non-tuberculous Mycobacterial Biofilms and Enhances Amikacin Uptake Into Macrophages. Front. Microbiol. 9:915. doi: 10.3389/fmicb.2018.00915

Non-tuberculous mycobacteria (NTM) cause pulmonary infections in patients with structural lung damage, impaired immunity, or other risk factors. Delivering antibiotics to the sites of these infections is a major hurdle of therapy because pulmonary NTM infections can persist in biofilms or as intracellular infections within macrophages. Inhaled treatments can improve antibiotic delivery into the lungs, but efficient nebulization delivery, distribution throughout the lungs, and penetration into biofilms and macrophages are considerable challenges for this approach. Therefore, we developed amikacin liposome inhalation suspension (ALIS) to overcome these challenges. Nebulization of ALIS has been shown to provide particles within the respirable size range that distribute to both central and peripheral lung compartments in humans. The *in vitro* and *in vivo* efficacy of ALIS against NTM has been demonstrated previously. The key mechanistic questions are whether ALIS penetrates NTM biofilms and enhances amikacin uptake into macrophages. We found that ALIS effectively penetrated throughout NTM biofilms and concentration-dependently reduced the number of viable mycobacteria. Additionally, we found that ALIS improved amikacin uptake by ∼4-fold into cultured macrophages compared with free amikacin. In rats, inhaled ALIS increased amikacin concentrations in pulmonary macrophages by 5- to 8-fold at 2, 6, and 24 h post-dose and retained more amikacin at 24 h in airways and lung tissue relative to inhaled free amikacin. Compared to intravenous free amikacin, a standard-of-care therapy for refractory and severe NTM lung disease, ALIS increased the mean area under the concentration-time curve in lung tissue, airways, and macrophages by 42-, 69-, and 274-fold. These data demonstrate that ALIS effectively penetrates NTM biofilms, enhances amikacin uptake into macrophages, both *in vitro* and *in vivo*, and retains amikacin within airways and lung tissue. An ongoing Phase III trial, adding ALIS to guideline based therapy, met its primary endpoint of culture conversion by month 6. ALIS represents a promising new treatment approach for patients with refractory NTM lung disease.

Keywords: non-tuberculous mycobacteria, amikacin, biofilm, macrophage uptake, ALIS, LAI, Arikayce, Arikace

INTRODUCTION

Non-tuberculous mycobacteria (NTM) are commonly found throughout the environment and cause pulmonary infections in patients with structural lung damage, impaired immunity, or other risk factors (Johnson and Odell, 2014; van Ingen and Kuijper, 2014). Lung disease is the most common manifestation of NTM infections (NTM lung disease; NTM-LD) and patients typically present with either nodular bronchiectatic disease or fibrocavitary disease (Johnson and Odell, 2014). Various mycobacterial species can cause NTM-LD, but species from the *Mycobacterium avium* complex (MAC; including *avium*, *intracellulare*, *chimaera*, and others) are the most common (Johnson and Odell, 2014).

Non-tuberculous mycobacteria can persist extracellularly in biofilms or intracellularly within macrophages and other cells in infected hosts. NTM biofilms are evident in both expectorated sputum samples and in alveolar walls of explanted lungs from infected patients (Qvist et al., 2015). Several lines of evidence demonstrate that MAC species can also live as intracellular infections within monocytes and macrophages (Appelberg, 2006; Awuh and Flo, 2017). *In vitro*, several MAC strains grew well (9- to 43-fold increases) inside isolated human peripheral blood monocytes cultured with human serum, but failed to grow extracellularly in the presence of human serum (Nozawa et al., 1984). In mice systemically infected with *M. avium*, the mycobacteria proliferated in spleen, liver, and lung tissues over the course of several months (Frehel et al., 1991). Electron microscopy localized the mycobacteria exclusively within cells, with no extracellular mycobacteria detected in thin tissue sections of livers and spleens (Frehel et al., 1991). Clinical case reports have also described intracellular MAC infections in humans, with *M. avium* detected inside peripheral blood leukocytes and bone marrow aspirate (Graham et al., 1984; Moffie et al., 1989). These findings indicate that MAC species can live and replicate within macrophages. Therefore, delivering effective antibiotic concentrations into NTM biofilms and cells infected with NTM are important components of treatment.

Mycobacterium avium complex species are generally sensitive *in vitro* to aminoglycoside antibiotics, such as amikacin (Brown-Elliott et al., 2013; Cowman et al., 2016), that exhibit concentration-dependent bactericidal effects. However, amikacin and other aminoglycoside antibiotics accumulate poorly in cells, which can limit their effectiveness against intracellular infections (Kesavalu et al., 1990). One way to increase intracellular amikacin delivery is to package the antibiotic into liposomes, which are nanometer sized vesicles composed of a phospholipid bilayer membrane surrounding an aqueous interior compartment (Gregoriadis, 1976a). The physical characteristics of liposomes (small size, low toxicity, tissue/cell targeting) and their capability for delayed or triggered release of cargo molecules make them highly useful drug carriers (Gregoriadis, 1976b). In fact, liposome encapsulation has been shown to improve the ability of amikacin to kill intracellular *M. avium* infections in macrophages (Kesavalu et al., 1990). Moreover, intravenous injection of liposome-encapsulated amikacin improved treatment of systemic *M. avium* infections compared to free amikacin (Cynamon et al., 1989; Ehlers et al., 1996; Petersen et al., 1996), reducing mycobacterial counts in liver and spleen at doses 100-fold lower than free amikacin (Ehlers et al., 1996).

Despite the effectiveness of liposome-encapsulated amikacin against disseminated *M. avium* infections, intravenous administration of liposomal amikacin failed to provide long-term benefit against pulmonary infections in mice (Ehlers et al., 1996). NTM-LD is particularly difficult to treat because it requires delivery of high amounts of antibiotics to the lung while keeping systemic concentrations low to avoid toxicities (Olivier et al., 2014). Inhalation delivery of liposomal amikacin directly into the lungs may address this problem, but this approach faces three major delivery hurdles: (1) efficient nebulization delivery of liposomes to the lungs; (2) distribution of the liposomes throughout the lungs; and, (3) penetration into biofilms and macrophages to reach the sites of infection. Therefore, we developed amikacin liposome inhalation suspension (ALIS), also referred to in previous publications as Arikayce, Arikace or liposomal amikacin for inhalation (LAI), to overcome these challenges and improve the treatment of NTM-LD.

To provide efficient nebulization delivery to the lungs, ALIS was designed to have a high drug to lipid ratio and to retain a consistent fraction of amikacin within the liposome during the nebulization process. ALIS liposomes are composed of dipalmitoylphosphatidylcholine (DPPC) and cholesterol at a 2:1 weight ratio, with 70 mg/mL of amikacin and 47 mg/mL of lipid (DPPC and cholesterol combined). The high drug loading is achieved through a proprietary infusion process that mixes a stream of lipids dissolved in ethanol with a stream of amikacin sulfate dissolved in water at a specific flow rate ratio (Li et al., 2008), causing amikacin to be in a semi-soluble, coacervated state during liposome formation. The high drug load within each liposome is critical to deliver an effective dose of amikacin to NTM-LD patients in about 14 min using a product-specific eFlow® nebulizer (Lamira™ Nebulizer System; PARI Respiratory Equipment, Inc.). The liposomes are relatively small (<300 nm in diameter) and release about 30% of the initial amikacin load during nebulization. Approximately 67% of the aerosol droplets produced are within the respirable range (<5.0 μm), which enables 43% of the nominal liposome dose to be deposited in the lungs of NTM-LD patients after nebulization (Olivier et al., 2016).

Once inhaled into the lungs, ALIS must disperse throughout the lungs and penetrate through mucus to reach infected areas. In healthy animals dosed with ALIS by inhalation, amikacin was distributed evenly throughout the lungs after single and multiple doses, with equal amikacin concentrations in all lobes of both lungs (Malinin et al., 2016). Similarly, inhaled ALIS distributed throughout the lungs in both healthy volunteers (Weers et al., 2009) and patients with NTM-LD (Olivier et al., 2016); the ratio of distribution to central and peripheral lung regions was approximately 1.6–2.0 (Weers et al., 2009; Olivier et al., 2016) and more than 50% of the deposited dose was detectable in the lung 24 h post-dose (Olivier et al., 2016). Mucus represents a further barrier to distribution of inhaled particles, but ALIS

liposomes effectively diffuse through 500–1000 μm thick human mucus in 30 min (Meers et al., 2008). These studies show that inhaled ALIS can distribute across lung regions and through mucus.

The final delivery challenge for ALIS is reaching sites of infection where NTM reside. Previous work demonstrated *in vitro* efficacy with ALIS against multiple *M. avium* and *M. abscessus* strains in a THP-1 macrophage model of infection (Rose et al., 2014). Furthermore, inhaled, nebulized ALIS reduced the NTM burden in mice with respiratory *M. avium* infections (Rose et al., 2014). However, the mechanistic data demonstrating ALIS penetration into NTM biofilms and macrophages are limited. Therefore, we evaluated a range of ALIS concentrations against *M. avium* biofilms and we also quantified ALIS uptake into macrophages, both *in vitro* and in rats given inhaled ALIS.

MATERIALS AND METHODS

Preparation and Characterization of ALIS Containing TAMRA-Amikacin

Amikacin liposome inhalation suspension was prepared using a microscale flow focusing method. DPPC (NOF America; cat # COATSOME® MC-6060) and cholesterol (Avanti Polar Lipids; cat # 700000) were dissolved at a 2:1 weight ratio in 100% ethanol at 20 mg/mL. Amikacin sulfate was dissolved in sterile, deionized water at 80 mg/mL (53.4 mg/mL amikacin base; pH adjusted to 6.7 using 5 M NaOH). For studies requiring fluorescent liposomes, 0.01% AF647-labeled dipalmitoylphosphatidylethanolamine (DPPE; Avanti Polar Lipids; cat # 850705) was included in the lipid solution and 3% tetramethylrhodamine (TAMRA)-amikacin (AAT Bioquest) was included in the amikacin stock. The lipid and amikacin solutions were infused (17 and 34 mL/min flow rates, respectively) through a Y connector, mixed with 2/3 volumes of 275 mM sodium citrate buffer at pH 8, and the resulting liposome suspension was diluted 1:1 in the collection vial with 1.5% NaCl. Samples were subsequently washed via tangential flow filtration using 2 EMD Millipore Pellicon XL cassettes (500 kDa polyethersulfone membrane; cat # PXB500C50).

Total amikacin concentrations in the liposome suspensions were measured by high-performance liquid chromatography (HPLC) using a Hypersil GOLD C18 column (175 Å, 3 μm, 150 mm × 4.6 mm; Thermo Fisher; cat. # 25003-154630) with a mobile phase of 65% methanol, 35% water, and 0.3% pentafluoropropionic acid (PFPA). An aliquot of each liposome suspension was centrifuged in an Amicon Ultra-0.5 centrifugal filter unit with Ultracel-30 KDa membrane to separate free amikacin, and the amount of free amikacin was then determined by HPLC. The lipid concentrations were measured by HPLC using an XBridge C8 column (130 Å, 3.5 μm, 150 mm × 4.6 mm; Waters; cat. # 186003055) with a mobile phase A consisting of 49.9% acetonitrile, 49.9% water, 0.1% acetic acid, and 0.1% triethylamine and mobile phase B consisting of 44.9% acetonitrile, 45% isopropyl alcohol, 10% water, 0.1% acetic acid, and 0.1% triethylamine. Liposome sizes were determined using a Mobius dynamic light scattering instrument (MOB-131, Wyatt Technology).

To confirm the TAMRA-amikacin concentration in the final sample of fluorescent ALIS, liposomes were dissolved with octylthioglucoside detergent to eliminate any minor-self quenching effect and TAMRA fluorescence was measured on a plate reader (Biotek Synergy NEO; BioTek Instruments, Inc., Winooski, VT, United States). Standards with decreasing percentages of TAMRA-amikacin mixed with amikacin (total amikacin concentration fixed at 80 mg/mL) were measured simultaneously and the final TAMRA-amikacin concentration of 0.44% in the ALIS sample was calculated from the standard curve. The same amount (0.44%) of TAMRA-amikacin was used for the free amikacin sample.

Mycobacterium avium Biofilm Assays

The biofilm studies were performed with the A5 strain of *M. avium* subspecies *hominissuis* that was originally isolated from an AIDS patient with a pulmonary infection. For imaging studies, mycobacteria were cultured for 7 days in 2-well chamber slides to establish biofilms. The biofilms were treated with 512 μg/mL of fluorescently labeled ALIS (AF647) for 4 h, fixed with 4% paraformaldehyde for 15 min, stained with Syto9 for 15 min, and sealed with a coverslip. Biofilms were imaged with a Zeiss LSM 780 confocal scanning microscope (630× magnification) and Zen 2.3 software. For efficacy studies, mycobacteria were cultured on plates containing Middlebrook 7H10 agar supplemented with 10% oleic acid-albumin-dextrose-catalase (OADC; Hardy Diagnostics, Santa Maria, CA, United States) at 37°C for 7–10 days and then resuspended into Hank's Balanced Salt Solution (HBSS; Corning, Corning, NY, United States) at 3×10^8 CFU/mL using optical density. Input suspensions were serially diluted 10-fold and plated to determine the inoculum for each experiment. The input suspension was added to flat-bottom, 96-well polystyrene plates (150 μL/well) and biofilms were formed statically at room temperature for 7 days. After 7 days, supernatants were removed and replaced with HBSS containing 60 mM lactose ± increasing concentrations of either 100% ALIS or 70% ALIS/30% free amikacin (total amikacin concentrations tested were 16, 32, 64, 128, 256, 512, or 1024 μg/mL). Biofilms were treated for 4 days and then disrupted by pipetting the supernatant 50 times. The mixture was serially diluted 10-fold to a final dilution of 10^4 and the 10^2–10^4 dilutions were spot plated in duplicate to quantify CFU. Three independent experiments were performed on different days, with three technical replicates for each condition tested.

Macrophage Uptake Assay

THP-1 human peripheral blood monocytes (ATCC; cat. # TIB-202) were seeded in 12-well plates at 1.2×10^6 cells/well in RPMI-1640 media (ATCC; cat. # 30-2001) containing 10% fetal bovine serum (FBS; HyClone; cat. # SH30070.03) and 50 ng/mL phorbol myristate acetate to induce attachment and differentiation into macrophages. After 24 h, the media was replaced with fresh RPMI media containing 5% FBS. After another 24 h, the media was replaced with 1 mL of fresh RPMI media with 5% FBS,

and 250 μL of ALIS (0.44% TAMRA-amikacin), free amikacin (0.44% TAMRA-amikacin), or control solution were added to respective wells to achieve the final desired concentrations (8, 16, 32, 64, or 128 μg/mL total amikacin). ALIS and free amikacin stocks were dissolved in 300 mM lactose solution. Following 4- or 24-h incubation periods, the media was removed, and then the cells were washed once with phosphate-buffered saline (PBS) and harvested into a 96-well plate. The cells were centrifuged at 300 × *g*, washed twice with PBS, and suspended in 200 μL of PBS. A small aliquot of the cell suspension was removed for imaging and the remaining cell suspension was used to quantify TAMRA-amikacin fluorescence using a Guava easyCyte 6HT flow cytometer (Millipore) with Easy Check beads as an internal control. The mean fluorescence intensity (MFI) was measured for 5,000 cells and normalized to the TAMRA fluorescence added to each well to account for any slight differences. The assay was repeated in three independent experiments, and then averages and standard errors of the mean were calculated for each treatment condition.

Macrophage Imaging

The aliquot removed prior to flow cytometry analysis was transferred to another 96-well plate and fixed in 4% formaldehyde. Fixed cells were mounted to glass slides with ProLong™ Diamond Antifade Mountant with 4′,6-diamidino-2-phenylindole (DAPI; Thermo Fisher; cat. # P36962) and coverslips were sealed with clear nail polish. Samples were imaged with a Zeiss Axio fluorescence microscope (400× magnification) and Zen 2.3 software. Settings were kept constant while imaging all samples from the same timepoint.

Animals and Housing Conditions

Male, Han-Wistar rats were purchased from Charles River Laboratories, group-housed in plastic cages, and maintained with an average room temperature of 69°F (range 68–78°F), an average room humidity of 49% (range 30–70%), and a 12-h light cycle (light on 6:00–18:00). Animals received standard chow (Purina diet; cat. #5053) and water *ad libitum* throughout the study, except during the nebulization period. This study was carried out in accordance with the recommendations of the Guide for the Care and Use of Laboratory Animals. The protocol was approved by the animal care and use committee at Rutgers University.

Evaluation of Macrophage Content in Cells Collected by Bronchoalveolar Lavage

Four naïve rats were anesthetized under isoflurane anesthesia and bronchoalveolar lavage (BAL) was performed with 2 mL of PBS. The BAL fluid was centrifuged at 2,000 × *g*, the resulting cell pellet was resuspended in FACS staining buffer, and Fc receptors were blocked for 30 min at 4°C. Cells were stained for 30 min with an Alexa Fluor 700 anti-rat CD45 antibody (BioLegend, San Diego, CA, United States), an Alexa Fluor 488 mouse anti-rat CD11b antibody (Bio-Rad, Hercules, CA, United States), a mouse anti-rat CD11c antibody (Bio-Rad) pre-conjugated with Cy5, and a biotin-conjugated mouse anti-rat CD68 antibody (Bio-Rad), followed by a phycoerythrin-conjugated streptavidin (BioLegend). Finally, all cell samples were stained with DAPI. Cell populations were analyzed using a BD Influx Cell Sorter (BD Biosciences, San Jose, CA, United States), and flow cytometry compensation setting was performed with UltraComp eBeads™ (Thermo Fisher Scientific, Waltham, MA, United States) and with cell samples. The NR8383 rat alveolar macrophage cell line was used as a positive control for staining and flow cytometry.

Administration of ALIS and Free Amikacin

For inhalation dosing, rats were placed into plastic tube restrainers and loaded into an ONARES nose-only inhalation delivery system (CH Technologies, Westwood, NJ, United States). Drug suspension/solution (40 mL of ALIS or free amikacin) was split between two Aeroneb Pro nebulizers (Aerogen, Chicago, IL, United States) placed in series along the air flow (3 L/min) into the ONARES chamber. The aerosol concentration in the ONARES chamber was sampled 5 min after the start of nebulization by drawing aerosol through a Pall #61631 glass-fiber filter (MilliporeSigma, St. Louis, MO, United States) at 0.25 L/min for 5 min. The filters were stored at 4°C in a glass vial for subsequent amikacin measurements. Nebulization continued until 40 mL of drug solution/suspension was nebulized and the nebulizers ran clear for one additional minute (total nebulization time was 60–90 min).

The study consisted of three experimental groups: ALIS (40 mL at 53.4 mg/mL amikacin base); low-dose free amikacin (40 mL at 20.0 mg/mL amikacin base); and, high-dose free amikacin (40 mL at 53.4 mg/mL amikacin base). Each timepoint for each experimental group required a separate nebulization group consisting of 10 rats; lungs were collected from 2 rats immediately post-dose at the end of the nebulization period to determine the deposited dose of amikacin, and the remaining 8 rats were euthanized together at one timepoint, either 2, 6, or 24 h post-dose. Therefore, each experimental group consisted of 30 rats total, with $n = 6$ euthanized immediately post-dose to measure deposited doses (2 from each of 3 nebulization groups) and $n = 8$ euthanized at each timepoint of 2, 6, and 24 h.

The distribution of intravenous amikacin into pulmonary macrophages, airways, and lung tissue was also assessed using a similar study design. Ten rats in each group were injected with a 20 mg/mL amikacin solution in 0.9% NaCl at 5 mL/kg to achieve a dose of 100 mg/kg. From each group, 2 animals were euthanized 0.25 h post-dose (similar to the immediately post-dose group for the nebulization studies) and the remaining 8 were euthanized together at either 2, 6, or 24 h post-dose. BAL fluid and cell pellets, lungs, and plasma were collected from each rat as described below.

Blood, Bronchoalveolar Lavage Fluid, and Lung Tissue Collection

At the appropriate timepoint after dosing, rats were weighed and deeply anesthetized with isoflurane, blood was collected

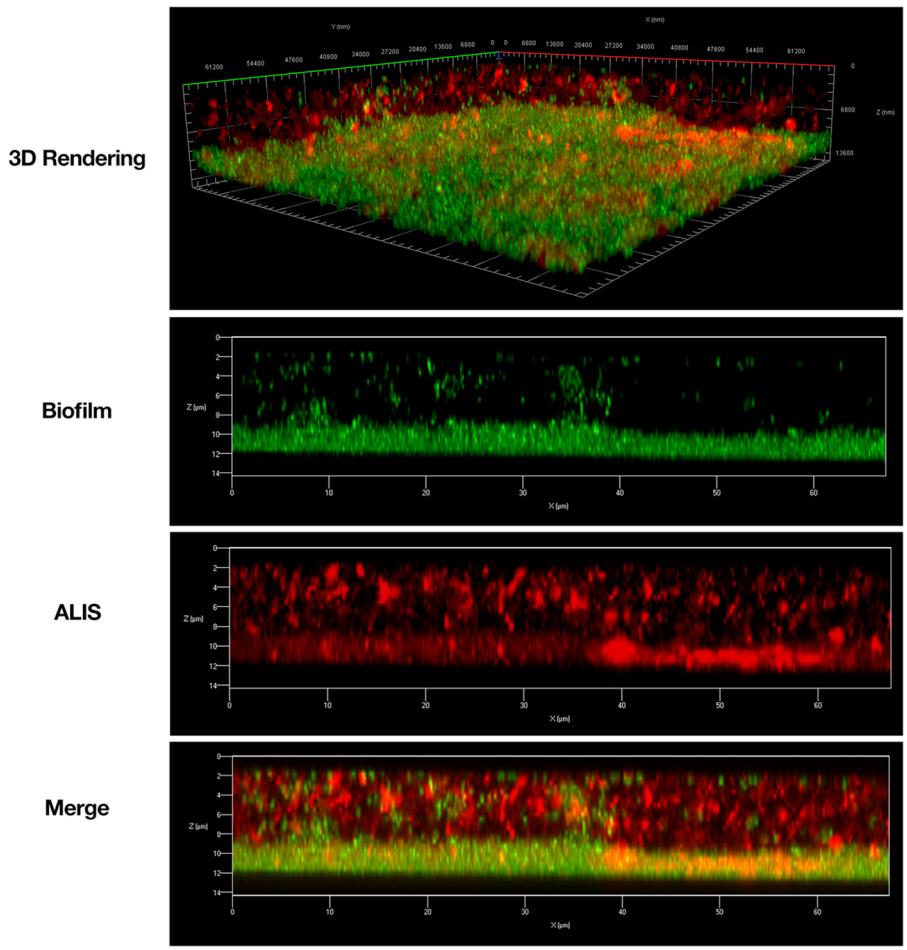

FIGURE 1 | Amikacin liposome inhalation suspension (ALIS) penetrated *Mycobacterium avium* biofilms. Biofilms (strain A5) were established for 7 days in 2-well chamber slides, treated with 512 μg/mL of AF657-labeled ALIS (red) for 4 h, fixed, stained with Syto9 (green), and imaged with a Zeiss LSM 780 confocal scanning microscope (630× magnification).

by retroorbital bleeding into ethylenediaminetetraacetic acid (EDTA) coated BD Microtainer® tubes (cat. # 02 669-33; Becton Dickinson, Franklin Lakes, NJ, United States), and then rats were euthanized by exsanguination. The lungs were lavaged with 2 mL of PBS and the BAL fluid was collected. Lungs were excised, weighed, rinsed in PBS, placed in 5 mL Eppendorf tubes, and flash frozen in liquid nitrogen. Blood samples were kept on ice prior to centrifugation at 20,817 × *g* for 10 min, and then the plasma was collected and stored at −80°C until analysis. BAL fluid was centrifuged at 2,000 × *g* for 3 min and the supernatant was removed and stored at −80°C. The cell pellet was resuspended in 1 mL of fresh PBS and centrifuged at 2,000 × *g* for 3 min. The supernatant was discarded and the cell pellet was stored at −80°C until analysis.

Quantification of Sample Amikacin Concentrations

Amikacin standards were generated in each sample matrix: cultured NR8383 rat alveolar macrophage cells were used for BAL cell pellet standards; PBS was utilized for BAL fluid standards; lung homogenate from naïve rats was employed for lung homogenate standards; and, plasma from naïve rats was used for plasma standards. For each standard curve, a 1.0 mg/mL intermediate in the appropriate matrix was first prepared from a primary amikacin stock of 20.0 mg/mL in 20% methanol and 80% water, then further diluted to 100 μg/mL in the appropriate matrix and serially diluted to make calibration standards. Quality control samples were also prepared from the highest standard. Experimental samples were mixed with an equal volume of internal standard working solution (gentamicin C1 in water) and 10% trichloroacetic acid, vortexed for 5 s, and centrifuged at 21,130 × *g* at 4°C for 15 min. Depending on the analytical range, the supernatant was mixed with either equal volume or 10× volume of mobile phase A (0.2% formic acid and 0.1% heptafluorobutyric acid in water) and 10 μL was injected into a Phenomenex Kinetex Phenyl-Hexyl column (4.6 mm × 50 mm; 2.6 μm; 50°C; 1 mL/min) with an elution gradient consisting of mobile phase A and mobile phase B (100% acetonitrile). Liquid chromatography, tandem mass spectrometry (LC-MS/MS) was

performed using a Sciex API4500 mass spectrometer (AB SCIEX, Framingham, MA, United States).

Quantification of Protein Concentrations

A portion of rat BAL cell pellet lysate and lung homogenate samples were retained for protein quantification using a Pierce™ BCA Protein Assay Kit (Thermo Fisher) according to the manufacturer's instructions.

Statistical Analyses

Statistical analyses were performed with GraphPad Prism (La Jolla, CA, United States). Because the inoculation levels were different between the three independent biofilm experiments (P = 0.0007 by one-way ANOVA with Tukey post-test), the CFU count for each concentration was normalized as percent of the untreated CFU count within each experiment and then group means and standard errors were calculated. Significant changes from the untreated control group were identified by one-way ANOVA with Dunnett's multiple comparisons test. For the *in vitro* macrophage uptake experiments, the data were analyzed by two-way ANOVA with Tukey post-test. For the *in vivo* studies, differences between the dose groups at each timepoint were determined by one-way analysis of variance (ANOVA) with Tukey post-test. $P < 0.05$ was considered significant.

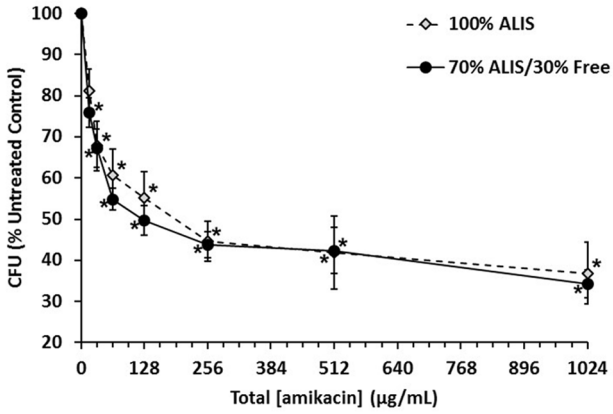

FIGURE 2 | Amikacin liposome inhalation suspension (ALIS) reduced viable cell counts in *Mycobacterium avium* biofilms. Biofilms (strain A5) were established for 7 days in plastic 96-well plates and then treated for 4 days with either 100% ALIS or a 70% ALIS/30% free amikacin mixture that replicates the ratio of liposomal to free amikacin after nebulization. Three independent experiments were performed on different days, with three technical replicates for each condition tested. The colony forming unit (CFU) count for each concentration was normalized as percent of the untreated CFU count within each experiment and then group means and standard errors were calculated. *$P < 0.05$ compared to no amikacin by one-way ANOVA with Dunnett's multiple comparisons post-test.

RESULTS

ALIS Penetrates and Kills *Mycobacterium avium* Biofilms

During respiratory NTM infection, one of the niches the bacteria can reside within are biofilms. ALIS is effective at treating NTM infections, but it is unknown if it can penetrate and kill NTM biofilms. We treated *M. avium* biofilms for 4 h with AF647-labeled ALIS to evaluate whether the liposomes can penetrate into the biofilm. Mycobacteria formed a dense biofilm on the slide surface, with more diffuse bacteria and extracellular biofilm components above (**Figure 1**). Liposomes were visible throughout the biofilm, indicating that the liposomes penetrated through the extracellular components and reached the cell dense region (**Figure 1**). We also tested whether increasing concentrations of ALIS can effectively kill the mycobacteria within the biofilms, using both 100% ALIS and a mix of 70% ALIS/30% free amikacin that represents the ratio of liposomal/free amikacin after nebulization. ALIS concentration-dependently reduced viable cell counts in biofilms at concentrations greater than 16 μg/mL, and the 100% ALIS and 70% ALIS/30% free amikacin treatment groups were equally effective (**Figure 2**).

ALIS Enhanced *in Vitro* Amikacin Uptake Into Macrophages Compared to Free Amikacin

Non-tuberculous mycobacteria are intracellular pathogens that mainly reside within macrophages during infection, creating an additional challenge to deliver effective antibiotic concentrations inside the cell. Taking this important point into consideration, we used fluorescently labeled amikacin to investigate macrophage uptake of ALIS. The fluorescent ALIS formulation produced for uptake studies contained 0.44% TAMRA-amikacin; therefore, we used the same 0.44% TAMRA-amikacin concentration in the free amikacin sample for all experiments to ensure that the total fluorescence added was equal for each comparison between ALIS and free amikacin. The batch of fluorescent ALIS had characteristics similar to a previous engineering batch (ENG1505) of ALIS that represents a typical batch produced by the manufacturing process (**Table 1**).

To confirm that TAMRA conjugation did not alter macrophage uptake of amikacin, we performed a pilot study using mass spectrometry to measure the ratio of TAMRA-labeled to unlabeled amikacin in the cell pellet after 24-h incubation with

TABLE 1 | Characteristics of fluorescent ALIS batch used in macrophage uptake studies.

Parameter	Fluorescent ALIS	Batch ENG1505[1]
Particle diameter (nm), Nicomp	221 ± 98	321 ± 134
DPPC:Chol (w:w)	1.91	2.06
Drug (amikacin base)/Lipid	0.86	1.38
Amikacin encapsulation	88.3%	100%

[1]*Batch ENG1505 represents a typical batch produced by the ALIS manufacturing process.*

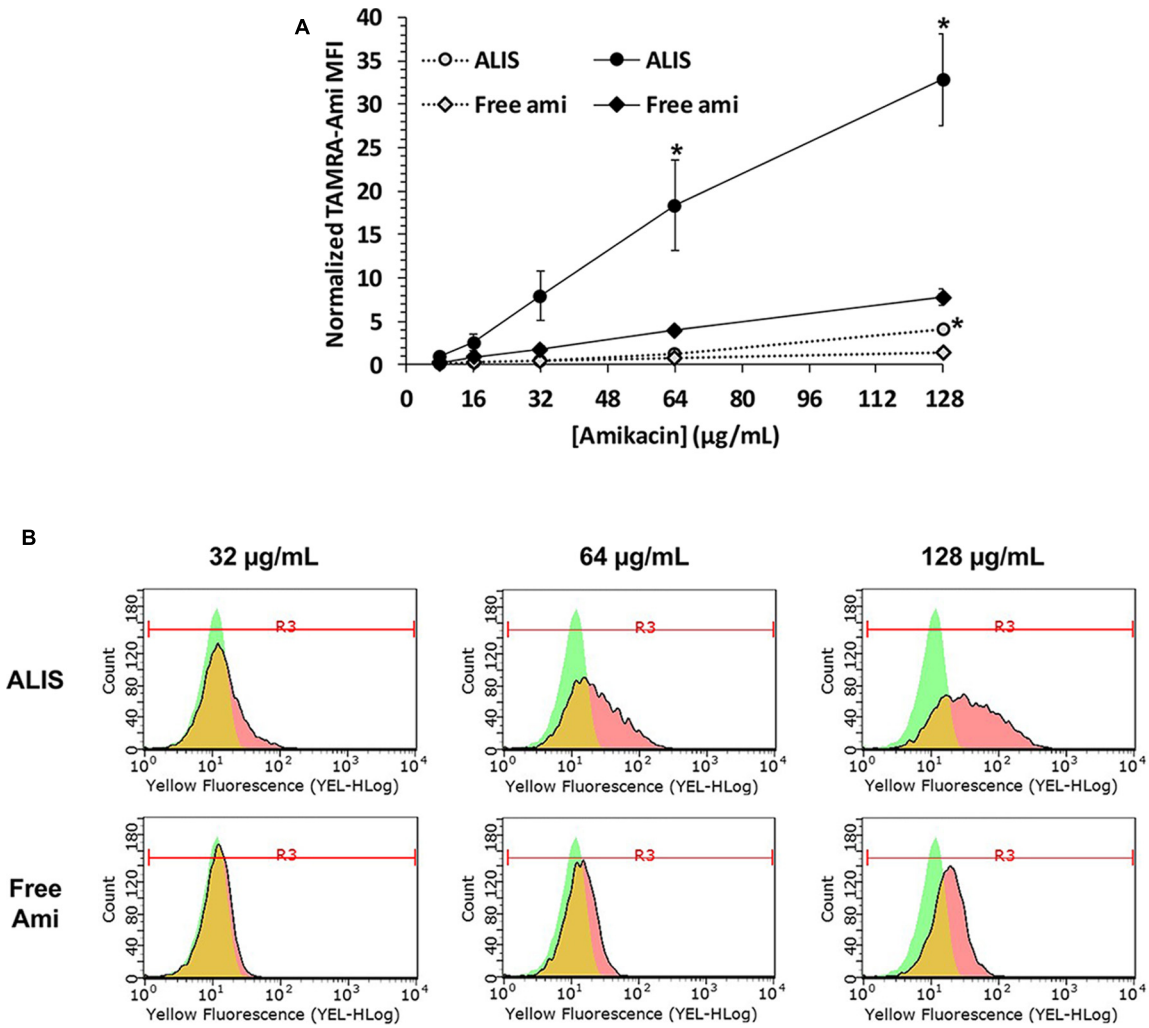

FIGURE 3 | Quantification of liposomal and free amikacin uptake into human macrophages by flow cytometry. ALIS demonstrated higher uptake into differentiated THP-1 macrophages than free amikacin at each concentration. Macrophages were exposed to increasing concentrations of either ALIS or free amikacin (0.44% labeled with TAMRA) for 4 h (gray symbols) or 24 h (black symbols) and, cell monolayers were resuspended, then cellular TAMRA fluorescence was quantified by flow cytometry. Panel **(A)** shows normalized mean fluorescence intensity (MFI) at each concentration averaged from three independent experiments. Panel **(B)** shows representative flow cytometry histograms with gating for the MFI after 24 h treatment from one experiment. Green represents control cells, red represents cells treated with ALIS or free amikacin, and yellow indicates overlap between the two histograms. $^*P < 0.05$ vs. free amikacin at the same concentration and timepoint.

free amikacin or ALIS. Cells treated with either free amikacin or ALIS had the same ratio of unlabeled/TAMRA-labeled amikacin (data not shown).

We quantified the uptake of various concentrations of free or liposomal TAMRA-amikacin into human macrophages after incubation for 4 or 24 h. Amikacin uptake was low after 4-h incubation, but cells treated with 128 μg/mL ALIS contained significantly more amikacin than cells treated with the same concentration of free amikacin (**Figure 3A**). After 24-h incubation, macrophages treated with ALIS generally contained ∼4-fold more amikacin than cells exposed to the same concentrations of free amikacin, with significant differences between ALIS and free amikacin groups exposed to 64 and 128 μg/mL concentrations (**Figure 3A**). The flow cytometry histograms demonstrated unimodal distributions for both free and liposomal amikacin at all concentrations tested (**Figure 3B**).

Fluorescence microscopy images taken after 24-h incubation were consistent with the flow cytometry measurements. Macrophages exposed to 32, 64, or 128 μg/mL of ALIS clearly exhibited TAMRA fluorescence, whereas TAMRA fluorescence was sparse and dim in cells incubated with the same concentrations of free amikacin (**Figure 4**).

ALIS Enhanced *in Vivo* Amikacin Uptake Into Macrophages Compared to Free Amikacin

To establish a method to collect pulmonary macrophages, we used flow cytometry to determine the percentage of

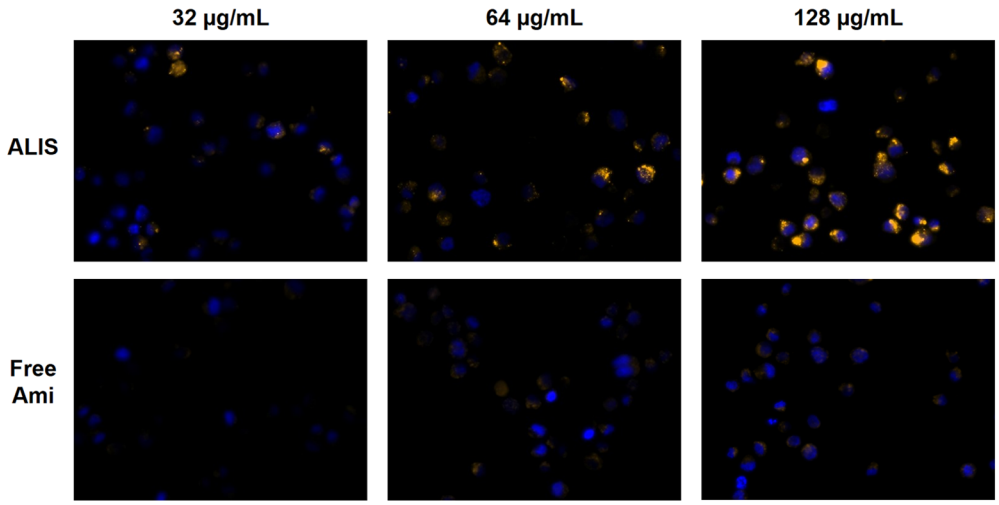

FIGURE 4 | Visualization of liposomal and free amikacin uptake in human macrophages by fluorescence microscopy. ALIS demonstrated higher uptake into differentiated THP-1 macrophages than free amikacin at each concentration. Macrophages were exposed to increasing concentrations of either liposomal or free amikacin (0.44% labeled with TAMRA) for 24 h and then TAMRA fluorescence was visualized by a Zeiss Axio fluorescence microscope (400× magnification) using constant settings for all experimental conditions. Yellow: TAMRA amikacin; Blue: DAPI-stained DNA.

macrophages among cells collected by BAL from naïve rats. Side and forward scatter differentiated single cells from other debris and cell aggregates in the sample, and high DAPI fluorescence identified dead cells for removal from the analysis (**Figure 5**). $CD45^+$ staining identified leukocytes and $CD11c^{high}/CD11b^{low}$ staining differentiated alveolar macrophages within the leukocyte population (**Figure 5**). High $CD68^+$ staining confirmed the identity of macrophages. Overall, 82.0 ± 3.3% of live cells isolated by BAL were alveolar macrophages.

Because the percentage of macrophages collected by BAL was high, we used total BAL cells for subsequent studies evaluating *in vivo* amikacin uptake into macrophages from rats given either ALIS or free amikacin by nebulization. From each nebulization group, we euthanized two rats immediately post-dose and measured the amikacin dose deposited in the lungs. The amikacin doses delivered to the nose or deposited in the lungs were not significantly different between the ALIS and low-dose amikacin groups (**Table 2**), but high-dose amikacin achieved significantly higher delivered and deposited doses than the other groups (**Table 2**).

We collected cells in the BAL fluid after inhalation administration of ALIS or free amikacin and measured amikacin concentrations in the cell pellets. The amount of protein in the cell pellets was not different between dosing groups at any timepoint (**Table 3**), indicating consistent collection of cells across the different dose groups. Cells harvested from the BAL fluid from rats dosed with ALIS exhibited 5- to 8-fold higher amikacin concentrations than BAL cells collected from rats dosed with low-dose free amikacin (**Figure 6A**). Additionally, the ALIS group contained 4- to 6-fold higher amikacin concentrations in the BAL cell pellet compared to the high-dose free amikacin group (**Figure 6A**), despite a twofold lower deposited dose in the ALIS group.

We also quantified amikacin levels in BAL fluid (representing amikacin collected from airways) and found that samples from rats in the ALIS group had significantly higher amikacin concentrations at 2 h post-dose than BAL fluid samples from rats in the low-dose amikacin group (**Figure 6B**). Despite a higher dose deposited in the lungs, high-dose amikacin did not achieve significantly higher BAL fluid concentrations than ALIS (**Figure 6B**). At 24 h post-dose, the ALIS group exhibited significantly higher BAL fluid amikacin concentrations than both groups administered free amikacin (**Figure 6B**).

Following each BAL procedure, we excised and froze the lungs for measurement of tissue amikacin concentrations. Lung concentrations at 2 and 6 h post-dose in the ALIS group were significantly higher than those in the low-dose amikacin group (although the two groups achieved similar deposited doses) and equivalent to amikacin concentrations in the high-dose amikacin group (despite a ∼2-fold lower deposited dose with ALIS; **Figure 6C**). At 24 h post-dose, lung concentrations in the ALIS group were significantly higher than both low- and high-dose amikacin (**Figure 6C**).

Plasma amikacin concentrations were not significantly different between the ALIS and low dose amikacin groups at 2 and 6 h post-dose (**Figure 6D**). Plasma concentrations were significantly higher in the ALIS group relative to the low-dose amikacin group, but not the high-dose group, at 24 h post-dose (**Figure 6D**).

Because intravenous amikacin is a common treatment for refractory NTM infections, we also evaluated the distribution of amikacin into pulmonary macrophages, airways, and lung tissue after an intravenous bolus dose. The 100 mg/kg dose

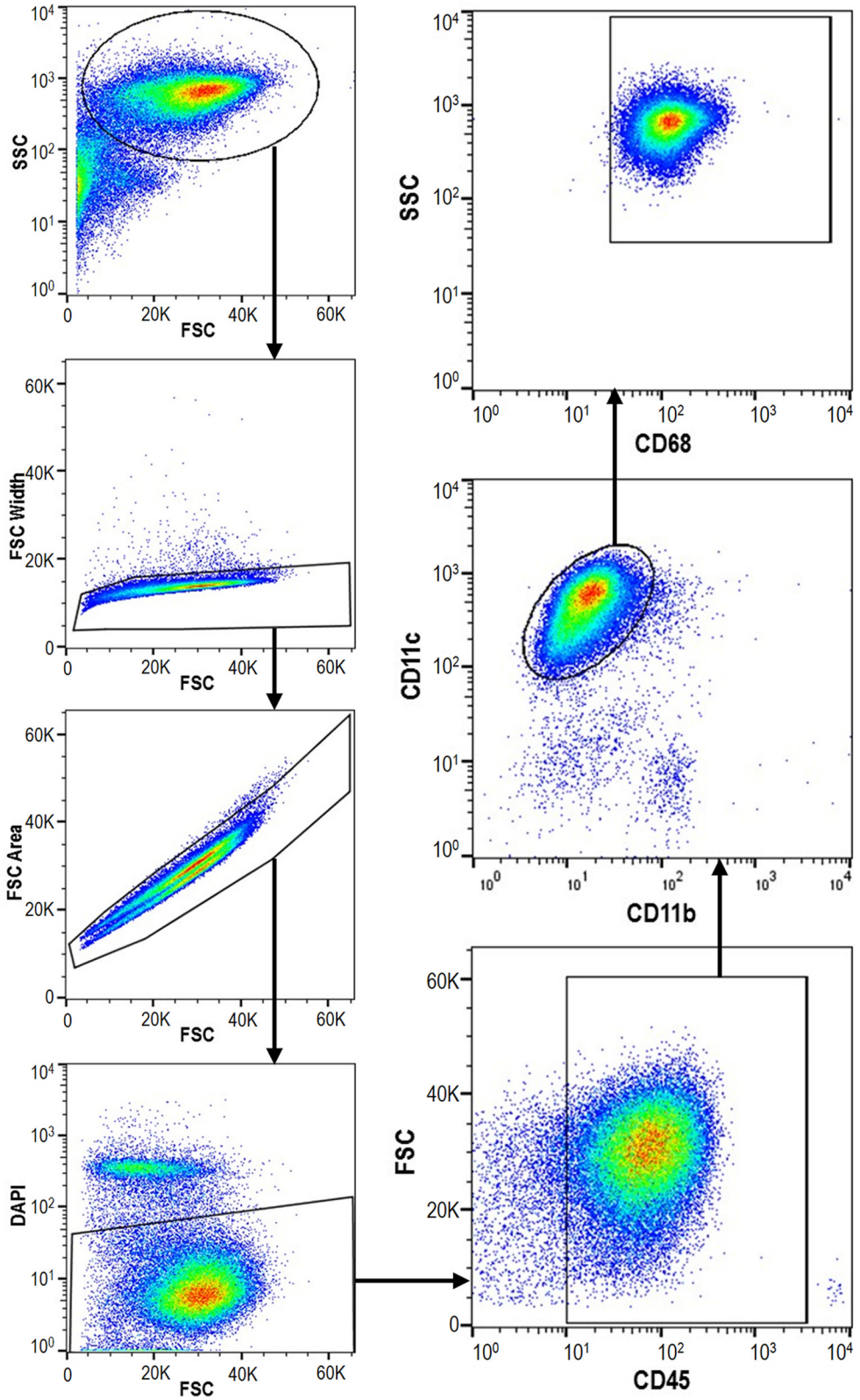

FIGURE 5 | Macrophages represent >80% of cells isolated by bronchoalveolar lavage (BAL). Cells were collected from lungs of naïve rats (n = 4) by BAL, labeled with antibodies differentiating macrophages from other leukocytes, and counted by flow cytometry. SSC, side scatter; FSC, forward scatter.

TABLE 2 | Delivered and deposited amikacin doses in rats administered either ALIS or free amikacin by nebulization.

	ALIS	Amikacin (low dose)	Amikacin (high dose)
Delivered dose (mg/kg BW)	96 ± 4	67 ± 3	161 ± 37*
Deposited dose (μg/g lung)	977 ± 106	507 ± 64	2283 ± 308**

*Delivered dose was calculated as the aerosol concentration (calculated from filter samples captured during nebulization) × respiratory minute volume × duration of nebulization/body weight. The deposited dose was measured as the lung amikacin concentration immediately post-dose in two rats from each nebulization group. Values represent mean ± SEM. *P < 0.05 vs. low-dose amikacin; n = 3 filters per group. **P < 0.05 vs. both low-dose amikacin and ALIS; n = 6 rats per group.*

TABLE 3 | Protein concentrations of cell pellets collected by bronchoalveolar lavage (BAL).

Timepoint	ALIS	Amikacin (low dose)	Amikacin (high dose)	*P*-value
2	79 ± 8	98 ± 10	72 ± 12	0.1957
6	90 ± 10	78 ± 7	91 ± 7	0.4570
24	108 ± 13	101 ± 19	115 ± 16	0.8320

BAL cell pellet protein concentrations (μg/mL) were measured by BCA protein assay. n = 8 per timepoint in each group.

given intravenously was comparable to the 96 mg/kg amikacin dose delivered by ALIS nebulization. The mean peak plasma concentration at 0.25 h post-dose was 337 μg/mL and the mean lung concentration at that timepoint was 94 μg/g, approximately 10-fold lower than the 977 μg/g deposited dosed achieved with nebulized ALIS (**Table 2**). In pulmonary macrophages, amikacin concentrations were less than 0.004 μg/μg protein throughout the 24-h time course and the area under the curve (AUC) was 274-fold lower than the macrophage AUC following ALIS inhalation (**Table 4**). Similarly, AUCs in BAL fluid and lung tissue were 69- and 42-fold lower, respectively, after intravenous dosing compared with inhalation dosing of ALIS (**Table 4**).

DISCUSSION

Amikacin liposome inhalation suspension was designed to provide efficient nebulization delivery of liposomes to the lungs, distribute to both central and peripheral regions of the lungs, and penetrate into biofilms and macrophages to reach the sites of infection. Li et al. (2008) showed that ALIS nebulization provides a consistent combination of encapsulated and free amikacin and forms aerosol droplets within the respirable range, and Meers et al. (2008) and Malinin et al. (2016) demonstrated that ALIS distributes well throughout different lobes of the lungs and into peripheral airways. The data presented herein clearly establish that ALIS can penetrate *M. avium* biofilms and into macrophages.

Amikacin liposome inhalation suspension effectively penetrated *M. avium* biofilms to reduce the number of viable bacteria; this was true for 100% ALIS as well as 70% ALIS/30% free amikacin (representing nebulized ALIS). *In vivo*, ALIS retained more amikacin at 24 h in airways and lung tissue compared to free amikacin, which would increase the duration of amikacin exposure at the sites of biofilm infections within mucus and alveolar walls.

Additionally, ALIS significantly enhanced amikacin uptake into macrophages compared with free amikacin. Using flow cytometry to quantify TAMRA fluorescence in macrophages, we found that the liposomal formulation enhanced amikacin uptake following 4- and 24-h incubations. Enhanced uptake with ALIS relative to free amikacin was also evident by fluorescence microscopy. These *in vitro* studies relied on the use of fluorescent amikacin, but we confirmed in a pilot study that TAMRA-conjugation did not alter uptake of free amikacin into macrophages. These data demonstrate that ALIS significantly increased amikacin uptake into human macrophages by ∼4-fold relative to free amikacin over a range of concentrations. The finding of improved uptake into macrophages *in vitro* is consistent with published data showing that ALIS kills intracellular *M. avium* infections in macrophages better than free amikacin (Rose et al., 2014).

Pulmonary macrophages from rats dosed with ALIS exhibited 5- to 8-fold higher amikacin levels compared with cells from animals given low-dose free amikacin, although the deposited dose immediately after nebulization was not significantly different between the groups. Additionally, the ALIS group exhibited significantly higher amikacin concentrations in BAL fluid and lung tissue relative to the low-dose amikacin group. These results show that the ALIS formulation retains amikacin within macrophages, airways, and lung tissue significantly better than free amikacin. Furthermore, high-dose amikacin deposited twofold more amikacin in the lungs immediately post-dose compared to ALIS, but failed to produce macrophage amikacin concentrations equaling those in the ALIS treatment group (4- to 6-fold lower with high-dose amikacin vs. ALIS). Amikacin levels in the bronchoalveolar space and lung tissue declined more over 24 h after administration of high-dose free amikacin relative to ALIS, indicating that free amikacin passes out of the lungs faster than ALIS. Taken together, these data provide strong evidence that inhaled ALIS can deliver more amikacin into macrophages *in vivo* than free drug. Importantly, simply depositing more free amikacin into the lungs failed to match the macrophage amikacin concentrations achieved with ALIS.

Intravenous amikacin is commonly used in patients with severe or refractory NTM-LD, but we found that free amikacin penetrated very poorly into lung tissue, airways, and pulmonary macrophages after intravenous administration. Compared to intravenous amikacin, ALIS achieved ∼42-, ∼69-, and ∼274-fold higher amikacin exposures in lung tissue, airways, and pulmonary macrophages, respectively, with ∼5-fold lower plasma exposure. Although intravenous amikacin is the current standard of care, ALIS delivered more antibiotic to sites relevant for NTM lung infections with substantially lower systemic exposure.

Amikacin liposome inhalation suspension has been shown to effectively treat NTM-LD in both preclinical studies and

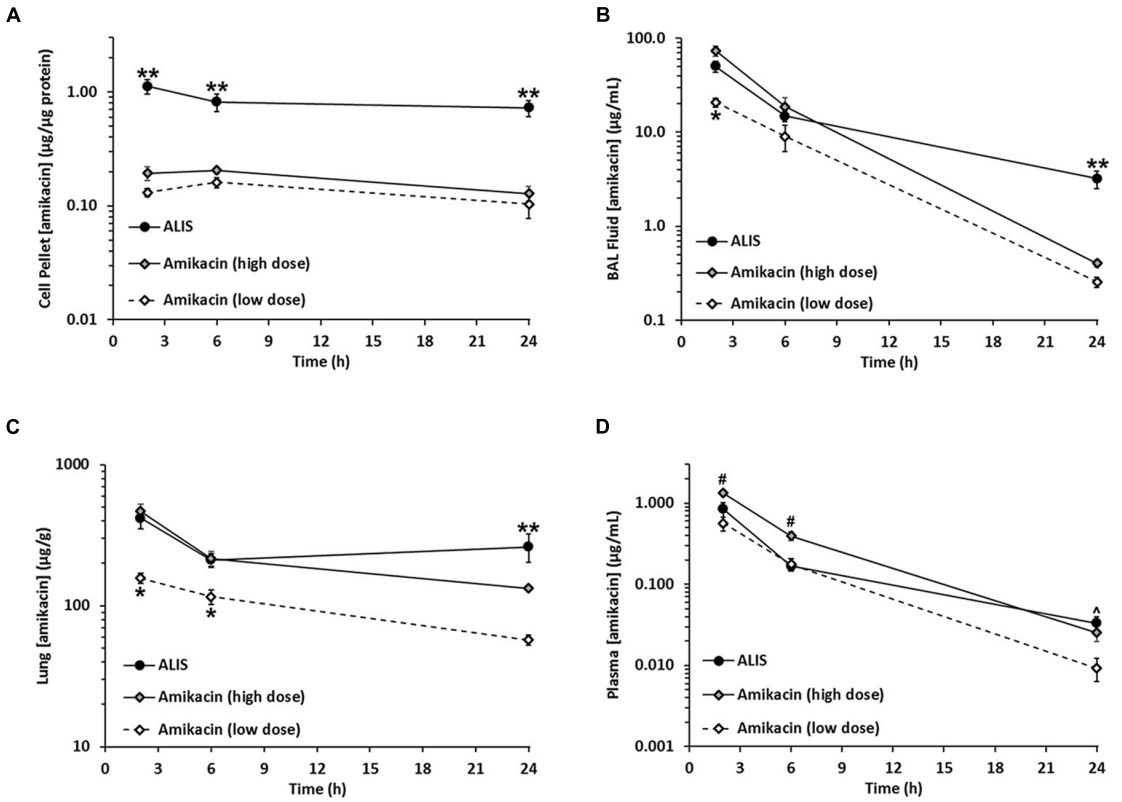

FIGURE 6 | Amikacin liposome inhalation suspension (ALIS) enhanced amikacin uptake into macrophages and retained more amikacin in airways and lung tissue. Rats were administered either ALIS or free amikacin by nebulization and BAL cells (representing >80% macrophages) **(A)**, BAL fluid **(B)**, lungs **(C)**, and plasma **(D)** were collected at 2, 6, or 24 h after the end of nebulization. Amikacin concentrations were quantified by LC-MS/MS. The delivered and deposited doses for each group are presented in **Table 2**. $^{*}P < 0.05$ vs. both high-dose amikacin and ALIS groups. $^{**}P < 0.05$ vs. both low and high-dose amikacin groups. $^{\#}P < 0.05$ vs. both ALIS and low-dose amikacin groups. $\hat{}P < 0.05$ vs. the low-dose amikacin group. $n = 8$ rats per group.

TABLE 4 | Summary of macrophage, airway, lung tissue, and plasma exposures.

				Fold difference	
	IV Amikacin	**Inh Amikacin**	**ALIS**	**ALIS vs. IV Amikacin**	**ALIS vs. Inh Amikacin**
Macrophages	0.1	2.9	17.8	274.2	6.1
Airways	4.2	142.5	292.6	69.5	2.1
Lung tissue	162.1	2771.0	6917.0	42.7	2.5
Plasma	22.6	3.1	3.8	0.2	1.2

Values represent area under the curve (AUC) calculated for each group using the mean concentrations at each timepoint. AUC_{2-24} was calculated for macrophage, airway, and plasma exposures, whereas AUC_{0-24} was calculated for lung exposure.

clinical trials. In mice with pulmonary *M. avium* infections, inhalation administration of ALIS lowered viable mycobacteria in the lungs by more than 2 log units (Rose et al., 2014). A Phase II trial of patients with refractory NTM-LD demonstrated that ALIS increased the proportion of patients who achieved negative sputum cultures compared with placebo, and the time to first negative sputum culture was shorter with ALIS treatment versus placebo (Olivier et al., 2017). Based on top-line results, an ongoing Phase III study met the primary endpoint by demonstrating that the addition of ALIS to guideline based therapy eliminated evidence of NTM-LD caused by MAC in sputum by month 6 in a greater proportion of patients than guideline based therapy alone (Insmed, 2018).

Overall, the data presented herein demonstrate that ALIS delivers amikacin to pulmonary macrophages, airways, and lung tissue better than free amikacin given by either inhalation or intravenous administration. Simply delivering more free amikacin to the lungs by nebulization failed to match the macrophage uptake or duration of exposure achieved by ALIS, indicating the benefit of the liposomal formulation. This mechanism of improved delivery into pulmonary macrophages and retention within airways and lung tissue has been shown

to effectively treat refractory NTM-LD in clinical trials and represents a promising new therapy for patients.

AUTHOR CONTRIBUTIONS

FL, JZ, SR, WP, and KD contributed conception and design of the studies. KD performed the statistical analyses. FL and KD wrote the manuscript. JZ, DC, SR, MN, JJ, JT, and TH performed the experiments. All authors contributed to manuscript revision, and then read and approved the submitted version.

FUNDING

This work was funded by Insmed Incorporated.

ACKNOWLEDGMENTS

Special thanks to Daniel Martin in the High Resolution Microscopy Facility, Department of Biomedical Engineering at Rutgers University for assistance with biofilm imaging.

REFERENCES

Appelberg, R. (2006). Pathogenesis of *Mycobacterium avium* infection: typical responses to an atypical mycobacterium? *Immunol. Res.* 35, 179–190. doi: 10.1385/IR:35:3:179

Awuh, J. A., and Flo, T. H. (2017). Molecular basis of mycobacterial survival in macrophages. *Cell Mol. Life Sci.* 74, 1625–1648. doi: 10.1007/s00018-016-2422-8

Brown-Elliott, B. A., Iakhiaeva, E., Griffith, D. E., Woods, G. L., Stout, J. E., Wolfe, C. R., et al. (2013). In vitro activity of amikacin against isolates of *Mycobacterium avium* complex with proposed MIC breakpoints and finding of a 16S rRNA gene mutation in treated isolates. *J. Clin. Microbiol.* 51, 3389–3394. doi: 10.1128/JCM.01612-13

Cowman, S., Burns, K., Benson, S., Wilson, R., and Loebinger, M. R. (2016). The antimicrobial susceptibility of non-tuberculous mycobacteria. *J. Infect.* 72, 324–331. doi: 10.1016/j.jinf.2015.12.007

Cynamon, M. H., Swenson, C. E., Palmer, G. S., and Ginsberg, R. S. (1989). Liposome-encapsulated-amikacin therapy of *Mycobacterium avium* complex infection in beige mice. *Antimicrob. Agents Chemother.* 33, 1179–1183. doi: 10.1128/AAC.33.8.1179

Ehlers, S., Bucke, W., Leitzke, S., Fortmann, L., Smith, D., Hansch, H., et al. (1996). Liposomal amikacin for treatment of *M. avium* infections in clinically relevant experimental settings. *Zentralbl. Bakteriol.* 284, 218–231. doi: 10.1016/S0934-8840(96)80097-1

Frehel, C., de Chastellier, C., Offredo, C., and Berche, P. (1991). Intramacrophage growth of *Mycobacterium avium* during infection of mice. *Infect. Immun.* 59, 2207–2214.

Graham, B. S., Hinson, M. V., Bennett, S. R., Gregory, D. W., and Schaffner, W. (1984). Acid-fast bacilli on buffy coat smears in the acquired immunodeficiency syndrome: a lesson from Hansen's bacillus. *South Med. J.* 77, 246–248. doi: 10.1097/00007611-198402000-00029

Gregoriadis, G. (1976a). The carrier potential of liposomes in biology and medicine (first of two parts). *N. Engl. J. Med.* 295, 704–710. doi: 10.1056/NEJM197609232951305

Gregoriadis, G. (1976b). The carrier potential of liposomes in biology and medicine (second of two parts). *N. Engl. J. Med.* 295, 765–770. doi: 10.1056/NEJM197609302951406

Insmed (2018). *Insmed Press Release*. Available at: http://investor.insmed.com/releasedetail.cfm?releaseid=1053237 [accessed February 27, 2018].

Johnson, M. M., and Odell, J. A. (2014). Nontuberculous mycobacterial pulmonary infections. *J. Thorac. Dis.* 6, 210–220. doi: 10.3978/j.issn.2072-1439.2013.12.24

Kesavalu, L., Goldstein, J. A., Debs, R. J., Duzgunes, N., and Gangadharam, P. R. (1990). Differential effects of free and liposome encapsulated amikacin on the survival of *Mycobacterium avium* complex in mouse peritoneal macrophages. *Tubercle* 71, 215–217. doi: 10.1016/0041-3879(90)90079-N

Li, Z., Zhang, Y., Wurtz, W., Lee, J. K., Malinin, V. S., Durwas-Krishnan, S., et al. (2008). Characterization of nebulized liposomal amikacin (Arikace) as a function of droplet size. *J. Aerosol. Med. Pulm. Drug Deliv.* 21, 245–254. doi: 10.1089/jamp.2008.0686

Malinin, V., Neville, M., Eagle, G., Gupta, R., and Perkins, W. R. (2016). Pulmonary deposition and elimination of liposomal amikacin for inhalation and effect on macrophage function after administration in rats. *Antimicrob. Agents Chemother.* 60, 6540–6549. doi: 10.1128/AAC.00700-16

Meers, P., Neville, M., Malinin, V., Scotto, A. W., Sardaryan, G., Kurumunda, R., et al. (2008). Biofilm penetration, triggered release and in vivo activity of inhaled liposomal amikacin in chronic *Pseudomonas aeruginosa* lung infections. *J. Antimicrob. Chemother.* 61, 859–868. doi: 10.1093/jac/dkn059

Moffie, B. G., Krulder, J. W., and de Knijff, J. C. (1989). Direct visualization of mycobacteria in blood culture. *N. Engl. J. Med.* 320, 61–62. doi: 10.1056/NEJM198901053200115

Nozawa, R. T., Kato, H., and Yokota, T. (1984). Intra- and extracellular susceptibility of *Mycobacterium avium*-intracellulare complex to aminoglycoside antibiotics. *Antimicrob. Agents Chemother.* 26, 841–844. doi: 10.1128/AAC.26.6.841

Olivier, K. N., Griffith, D. E., Eagle, G., McGinnis, J. P. I. I., Micioni, L., Liu, K., et al. (2017). Randomized trial of liposomal amikacin for inhalation in nontuberculous mycobacterial lung disease. *Am. J. Respir. Crit. Care Med.* 195, 814–823. doi: 10.1164/rccm.201604-0700OC

Olivier, K. N., Maas-Moreno, R., Whatley, M., Cheng, K. T., Lee, J., Folio, L., et al. (2016). Airway deposition and retention of liposomal amikacin for inhalation in patients with pulmonary nontuberculous mycobacterial disease. *Am. J. Respir. Crit. Care Med.* 193:A3732.

Olivier, K. N., Shaw, P. A., Glaser, T. S., Bhattacharyya, D., Fleshner, M., Brewer, C. C., et al. (2014). Inhaled amikacin for treatment of refractory pulmonary nontuberculous mycobacterial disease. *Ann. Am. Thorac. Soc.* 11, 30–35. doi: 10.1513/AnnalsATS.201307-231OC

Petersen, E. A., Grayson, J. B., Hersh, E. M., Dorr, R. T., Chiang, S. M., Oka, M., et al. (1996). Liposomal amikacin: improved treatment of *Mycobacterium avium* complex infection in the beige mouse model. *J. Antimicrob. Chemother.* 38, 819–828. doi: 10.1093/jac/38.5.819

Qvist, T., Eickhardt, S., Kragh, K. N., Andersen, C. B., Iversen, M., Hoiby, N., et al. (2015). Chronic pulmonary disease with *Mycobacterium abscessus* complex is a biofilm infection. *Eur. Respir. J.* 46, 1823–1826. doi: 10.1183/13993003.01102-2015

Rose, S. J., Neville, M. E., Gupta, R., and Bermudez, L. E. (2014). Delivery of aerosolized liposomal amikacin as a novel approach for the treatment of nontuberculous mycobacteria in an experimental model of pulmonary infection. *PLoS One* 9:e108703. doi: 10.1371/journal.pone.0108703

van Ingen, J., and Kuijper, E. J. (2014). Drug susceptibility testing of nontuberculous mycobacteria. *Future Microbiol.* 9, 1095–1110. doi: 10.2217/fmb.14.60

Weers, J., Metzheiser, B., Taylor, G., Warren, S., Meers, P., and Perkins, W. R. (2009). A gamma scintigraphy study to investigate lung deposition and clearance of inhaled amikacin-loaded liposomes in healthy male volunteers. *J. Aerosol. Med. Pulm. Drug Deliv.* 22, 131–138. doi: 10.1089/jamp.2008.0693

Conflict of Interest Statement: Authors JZ, FL, SR, DC, JT, TH, MN, WP, and KD were employed by Insmed Incorporated. The other author JJ declares no competing interests. The funder, Insmed Incorporated, had no role in study design, data collection and analysis, but was involved in the decision to publish the manuscript.

frontiers in Microbiology

ORIGINAL RESEARCH
published: 20 September 2018
doi: 10.3389/fmicb.2018.02231

Optimization and Lead Selection of Benzothiazole Amide Analogs Toward a Novel Antimycobacterial Agent

Mary A. De Groote[1†], Thale C. Jarvis[2†], Christina Wong[2], James Graham[2], Teresa Hoang[2], Casey L. Young[2], Wendy Ribble[2], Joshua Day[2], Wei Li[1], Mary Jackson[1], Mercedes Gonzalez-Juarrero[1], Xicheng Sun[2] and Urs A. Ochsner[2]*

[1] *Mycobacteria Research Laboratories, Department of Microbiology, Immunology and Pathology, Colorado State University, Fort Collins, CO, United States,* [2] *Crestone, Inc., Boulder, CO, United States*

OPEN ACCESS

Edited by:
Veronique Anne Dartois, Rutgers, The State University of New Jersey, Newark, United States

Reviewed by:
Philip Hipskind, Lgenia Inc, United States
Courtney Cortez Aldrich, University of Minnesota Twin Cities, United States

***Correspondence:**
Urs A. Ochsner
uochsner@crestonepharma.com

† These authors have contributed equally to this work

Specialty section:
This article was submitted to Antimicrobials, Resistance and Chemotherapy, a section of the journal Frontiers in Microbiology

Received: *30 May 2018*
Accepted: *31 August 2018*
Published: *20 September 2018*

Citation:
De Groote MA, Jarvis TC, Wong C, Graham J, Hoang T, Young CL, Ribble W, Day J, Li W, Jackson M, Gonzalez-Juarrero M, Sun X and Ochsner UA (2018) Optimization and Lead Selection of Benzothiazole Amide Analogs Toward a Novel Antimycobacterial Agent. Front. Microbiol. 9:2231. doi: 10.3389/fmicb.2018.02231

Mycobacteria remain an important problem worldwide, especially drug resistant human pathogens. Novel therapeutics are urgently needed to tackle both drug-resistant tuberculosis (TB) and difficult-to-treat infections with nontuberculous mycobacteria (NTM). Benzothiazole adamantyl amide had previously emerged as a high throughput screening hit against *M. tuberculosis* (*Mtb*) and was subsequently found to be active against NTM as well. For lead optimization, we applied an iterative process of design, synthesis and screening of several 100 analogs to improve antibacterial potency as well as physicochemical and pharmacological properties to ultimately achieve efficacy. Replacement of the adamantyl group with cyclohexyl derivatives, including bicyclic moieties, resulted in advanced lead compounds that showed excellent potency and a mycobacteria-specific spectrum of activity. MIC values ranged from 0.03 to 0.12 μg/mL against *M. abscessus* (*Mabs*) and other rapid- growing NTM, 1–2 μg/mL against *M. avium* complex (MAC), and 0.12–0.5 μg/mL against *Mtb.* No pre-existing resistance was found in a collection of $n = 54$ clinical isolates of rapid-growing NTM. Unlike many antibacterial agents commonly used to treat mycobacterial infections, benzothiazole amides demonstrated bactericidal effects against both *Mtb* and *Mabs*. Metabolic labeling provided evidence that the compounds affect the transfer of mycolic acids to their cell envelope acceptors in mycobacteria. Mapping of resistance mutations pointed to the trehalose monomycolate transporter (MmpL3) as the most likely target. *In vivo* efficacy and tolerability of a benzothiazole amide was demonstrated in a mouse model of chronic NTM lung infection with *Mabs*. Once daily dosing over 4 weeks by intrapulmonary microspray administration as 5% corn oil/saline emulsion achieved statistically significant CFU reductions compared to vehicle control and non-inferiority compared to azithromycin. The benzothiazole amides hold promise for development of a novel therapeutic agent with broad antimycobacterial activity, though further work is needed to develop drug formulations for direct intrapulmonary delivery via aerosol.

Keywords: NTM, tuberculosis, antibacterial therapeutics, benzothiazole amide, MmpL3, efficacy, tolerability, aerosol

INTRODUCTION

Infections with non-tuberculous mycobacteria (NTM) are increasing in incidence (Falkinham, 2013; Prevots and Marras, 2015; Strollo et al., 2015; Vinnard et al., 2016; Prevots et al., 2017; Spaulding et al., 2017) and are notoriously difficult to treat (Henkle et al., 2017; Lande et al., 2018). Resistance of NTM to disinfectants may contribute to hospital acquired infections (Caskey et al., 2018) especially in cystic fibrosis disease where infection is common as patients age (Nick et al., 2016; Martiniano et al., 2017). Increasing evidence suggests that there is a protective effectiveness of the Bacillus Calmette-Guerin (BCG) vaccination against NTM disease (Zimmermann et al., 2018). Tuberculosis may give some cross-protection to NTM infection. With the declining incidence of TB in the US, NTM may fill this immunity void and we will see rising numbers of cases and will be challenged with treating NTM infection as the tuberculosis prevalence is at an all-time low in the US. Given that the US has never undertaken a BCG vaccination strategy like most other nations there may be a niche for NTM infections. NTM are ubiquitous in the environment and disease due to these organisms are heterogeneous disorders with pulmonary manifestations being the most common presentation. Lung disease manifests as nodular bronchiectasis and/or fibrocavitary disease. Some individuals will remain culture positive but clinically stable, but those with significant respiratory symptoms and radiographic abnormalities including destructive cavitary manifestations and microbiological evidence of an NTM will require treatment as disease progression frequently occurs and mortality can be high (Fleshner et al., 2016). Increasing prevalence of NTM will continue to occur as the population ages (Falkinham, 2003). Immune dysfunction has been seen in patients with pulmonary NTM (Cowman et al., 2018). Since many patients have underlying host predispositions they are susceptible to re-infection and may need intermittent treatment when symptomatic infection recurs (Lake et al., 2016). Treatment of non-tuberculous mycobacterial lung disease (NTM-LD) is challenging for several reasons including the relative resistance of NTM to currently available drugs and the difficulty in tolerating prolonged treatment with multiple drugs (Philley et al., 2016).

There are virtually no antimicrobial drug discovery programs specifically targeting NTM. Although therapeutic agents developed to treat *Mtb* infections often lack activity against NTM, it remains an attractive approach to initiate new NTM drug discovery projects via screening a library of TB active compounds against NTM, which has indeed resulted in high hit rates (Low et al., 2017). In fact, our development candidate, benzothiazole adamantyl amide, was discovered via that approach in a screening for *Mabs* whole cell activity of a library composed of hits from a previous *Mtb* screening (Franzblau et al., 2012). Another strategy for NTM drug discovery is to revisit or repurpose older drugs. A potential role for clofazimine in NTM treatment regimens has been suggested, since this agent showed bactericidal activity and synergy with amikacin or clarithromycin, both of which are commonly used antibiotics to treat NTM infections (Ferro et al., 2016). Semisynthetic spectinamides derived from the old spectinomycin discovered over half a century ago have shown potent activity against MDR and XDR tuberculosis (Liu et al., 2017).

NTM treatment regimens differ by species (Daley and Glassroth, 2014; Kasperbauer and De Groote, 2015), particularly between rapid growers (RGM) comprised of *M. abscessus* (*Mabs*) complex (*M. abscessus*, ssp. *abscessus*, *bolletti*, and *massiliensis*), *M. chelonae, M. fortuitum*, and others; and slow growers represented by *M. avium, M. intracellulare,* and *M. chimaera* (*M. avium* complex, or MAC). *M. abscessus* (*Mabs*) is particularly difficult to treat (Haworth et al., 2017). This organism is capable of forming more virulent rough phenotypes and smooth forms that tend to form biofilms (Claeys and Robinson, 2018) associated with antibiotic drug resistance (Clary et al., 2018). Resistance to macrolides, a cornerstone class of therapeutic agents, is innate in certain *Mabs* subspecies that carry an inducible methylase genetic element and the presence of this gene affects the outcomes (Koh, 2017; Choi et al., 2018). This resistance is detected clinically as well as in the laboratory (Carvalho et al., 2018) and is an important development limiting effective therapy (Kasperbauer and De Groote, 2015). Therapy involves multiple agents and recalcitrant or severe infections are optimally managed with the addition of an injectable agent (De Groote and Huitt, 2006; Philley et al., 2016). Therapeutic intolerances and side effects limit adherence to treatment regimens and affect outcomes. In addition, the potency of available agents is relatively low. Thus, there is a compelling need for novel antibiotics that are more potent and better tolerated.

The most common form of NTM disease is lung disease. NTM can result in chronic progressive lung disease especially for those with known risk factors, the most common of which is aging. Patients with cystic fibrosis, chest structural abnormalities and pre-existing lung disease such as bronchiectasis and autoimmune diseases and their treatments are all risk factors for infection and disease. For pulmonary disease, direct delivery to the airway would allow greater penetration and less systemic exposure. An inhaled route of delivery would be advantageous for intermittent therapy, in particular to suppress systemic side effects. Advances have been made in the area of aerosol delivery carriers and devices. The success of inhalational therapies with liposomal amikacin (Olivier et al., 2014; Caimmi et al., 2018) and Arikayce™ (Olivier et al., 2017) has paved the way for new therapies in this category. The development of a multicenter clinical trial network will allow more rapid enrollment in new drug treatment trials (Kevin Winthrop, personal communication).

Much remains to be done in the field of NTM as this has been a neglected area of drug development. As more treatment response surrogate markers are discovered, the future holds great promise for utilization of biomarkers to match therapeutic regimens to appropriate patient subpopulations and to monitor treatment response (Asakura et al., 2015) similar to biomarker work in TB to enhance drug development (Sigal et al., 2017). This will require clinical studies involving multi-center cooperative studies to ensure an adequate number of enrollees. In addition, diseases like Buruli ulcer caused by *M. ulcerans* are emerging infections in need of novel treatment approaches (Tai et al., 2018; Zingue et al., 2018). Wound healing is prolonged and problematic (O'Brien

et al., 2018) and topical therapy for Buruli ulcer or *M. marinum* cutaneous infections may have some utility depending on drug penetration into deeper tissues (Simoes et al., 2016). Mycobacteria live in lipid-rich host environments (Aguilar-Ayala et al., 2018; Ayyappan et al., 2018) so a lipophilic drug might be attractive for a variety of disease manifestations if lipophilicity can be managed. There is always the need to balance good drug properties such as hydrophilicity with the impenetrable lipid rich cell walls of mycobacteria. In addition to delivery improvements, future work to optimize potency against members of the slowly growing mycobacteria, particularly (MAC), will be a priority.

MATERIALS AND METHODS

Synthesis of Benzothiazole Amide Analogs

Unsubstituted benzothiazole adamantyl amide had emerged as a hit during screening of a focused library of TB-actives (Franzblau et al., 2012) for compounds that also possessed activity against *M. abscessus*. This scaffold represented the starting point for a campaign to elucidate the structure-activity relationship in greater detail. The initial strategy involved trimming of the adamantyl group to a minimum of lipophilic structure required for activity. The general synthetic route started from substituted 2-amino-benzothiazole intermediates and variably substituted cycloalkyl carboxylic acids under standard amide coupling conditions using 1-[Bis(dimethylamino)methylene]-1H-1,2,3-triazolo[4,5-b]pyridinium 3-oxide hexafluoro-phosphate (HATU) in the presence of N,N-diisopropylethylamine (DIEA) in dichloroethane (DCE). A detailed description of chemical synthesis, purification and SAR of substituted benzothiazole cyclohexyl amides is presented elsewhere (Graham et al., 2018). The products were purified by column chromatography using ethyl acetate and hexanes as eluents and fully characterized by NMR and LC-MS. Purity of the lead analogs described here was >95%.

Microbiological Evaluation of Benzothiazole Amide Compounds

NTM clinical isolates were from University of Colorado Hospital (De Groote et al., 2014a). *M. chimaera* strains were provided by the CDC (van Ingen et al., 2017), Reference strain *Mabs* 19977 and other bacterial strains, including anaerobes, were from ATCC, BEI Resources, or from the biorepository at Crestone, Inc. The avirulent *Mtb* strain H37Rv mc^2 6206 is a *leuC leuD* mutant derivative of strain mc^2 6020 (Δ*lysA* Δ*panCD*) and was provided by Dr. Bill Jacobs (Sambandamurthy et al., 2005). Compounds were tested for antimicrobial activity against mycobacteria and other pathogens following guidelines published by the Clinical Laboratory Standards Institute (CLSI). Muller-Hinton broth (MHB, 3 days) was used for rapid-growing NTM and Middlebrook medium (7H9 + OADC, 7 days) for slow-growing NTM and for *Mtb* (CLSI, 2003). Accurate endpoint minimum inhibitory concentration (MIC) values were obtained after addition of resazurin for 24 h to monitor viable cells colorimetrically (Khalifa et al., 2013). Protein and serum binding of compounds was tested by MIC determination in the presence of human albumin (45 mg/mL) or 50% complement-inactivated human serum. Potential non-specific effects on membranes were monitored in a hemolysis assay, where equine erythrocytes were exposed to compounds over a concentration range of up to 128 μg/mL in 10 mM Tris-HCl buffered 0.9% saline (pH 7.5) for 10 min at room temperature, centrifuged and evaluated for absence of erythrocyte pellets and buffer discoloration due to hemolysis. Spontaneous resistant mutants were isolated by plating 10^9-10^{10} *Mabs* ATCC 19977 cells onto 7H11-ADC agar plates containing benzothiazole amide compounds at multiples of their MIC, followed by colony purification on selective agar, preparation of genomic DNA, PCR amplification and sequencing of the *mmpL3* gene. For time-kill assays, cultures of *Mabs* and *Mtb* were diluted with broth to cell densities of 10^5-10^6 CFU/mL, compounds and control agents were added at 10 times their MICs and samples were removed for colony enumeration over a period of 5 days (*Mabs*) and 21 days (*Mtb*). Synergy studies applied the MIC checkerboard method of CRS400393 with 10 commercially available antibiotics, and the fractional inhibitory concentration index (FIC-I) was determined (Li et al., 2017). Metabolic labeling assays using [^{14}C]acetate of *Mabs* ATCC19977 cultures either untreated or treated with benzothiazole amides at 2 and 10 times their MICs and lipid extraction and analysis were performed as described (Li et al., 2014).

Preliminary Determination of Pharmacological Properties

ADMET assays were performed through NIAID Preclinical Services and Eurofins. Potential for cytotoxicity was monitored in HepG2 cells after 72 h growth in the presence of test compounds, either prepared as 10-point 3-fold serial dilutions or at a fixed 10 μM concentration. Cell viability was measured using the CellTiter-Glo® Luminescent Cell Viability Assay (Promega) or via fluorescent image analysis. Cytotoxicity was expressed as IC_{50} or as percent reduction of viable cells relative to a reference compound. Metabolic stability of compounds was evaluated via incubation with human liver microsomes at 37°C and quantitative analysis of parent compound by LC-MS/MS in samples removed at 0, 5, 15, 30, and 45 min (Obach, 1999). For cytochrome P450 (CYP) inhibition assays, compounds were prepared as a 7-point dilution series and incubated with human liver microsomes in buffer containing 2 mM NADPH and probe substrate. After incubation at 37°C for the optimal time (10–60 min) the reactions were processed for quantitative LC-MS/MS analysis of probe substrate metabolites in order to calculate IC_{50} values (Walsky and Obach, 2004). Thermodynamic solubility of compounds in aqueous media was determined by incubation in 50 mM potassium phosphate buffer (pH 7.4) for 24 h, followed by HPLC-UV detection of compound in the filtrate (Analiza, Cleveland, OH, United States).

Efficacy and Tolerability Assessment

In vivo assessment of efficacy and tolerability of benzothiazole amide CRS400226 was assessed in a granulocyte macrophage colony stimulated factor-knockout (GM-CSF KO) mouse model of *Mabs* infection (Gonzalez-Juarrero et al., 2012; De Groote et al., 2014b). This study was carried out at Colorado State University which maintains a centralized IACUC registered by

the USDA and accredited by the Association for Assessment and Accreditation of Laboratory Animal Care (AAALAC) International. The protocols were reviewed and approved by the CSU Animal Care and Usage Committee (ACUC) prior to development of the experimental infections. Male GM/CSF-KO mice were bred from the Gonzalez-Juarrero Lab colony at Colorado State University in the Painter Center for Laboratory Animal Resources. Mice at least 2 months old and at least 20 grams of weight were selected and acclimated for 1 week in the BSL3 laboratory prior to infection. Inoculum was prepared from a stock vial of *Mabs* strain #21, a clinical isolate, in 4 mL ddH2O to a targeted dose of 10^6 CFU/50 μL. The actual CFU in the inoculum used for infection was determined by plating of serial dilutions onto 7H11 agar plates, followed by colony enumeration after 4 days. The mice were infected via intratracheal aerosol delivery using a Penn-Century microsprayer. Actual bacterial deposition in the lungs was determined in three mice that were sacrificed to remove the lungs for bead homogenization in 500 uL of PBS, and CFU determination in serial dilutions of the homogenate. Established infections were confirmed after 10 days, again by determination of CFU in the lungs of three mice. Post infection, animals were monitored daily and weights recorded weekly, to ensure <20% weight loss and to adjust drug dosing to the actual weight. Four groups of $n = 5$ mice were included in the study, and treatment started 10 days post infection. The benzothiazole amide CRS400226 was formulated in saline containing 5% corn oil and 0.05% Tween-80. CRS400226 and vehicle were administered via intrapulmonary liquid aerosol delivery (50 μL/dose) via liquid Penn-Century MicroSprayer (liquid) 5 days per week over a 4-week treatment course. Azithromycin (TOCRIS #1A/203325) was prepared as a solution in 0.6% acetic acid and was administered via oral gavage of 0.1 mL to achieve a dose of 100 mg/kg. One group of mice served as untreated controls. After 4 weeks of treatment, the mice were sacrificed and the lung lobes separated. The left lobes of the lungs were homogenized in PBS and plated to determine bacterial load. The middle right lobes were placed in 4% paraformaldehyde and processed for histology.

RESULTS

Improved Potency of Advanced Lead Compounds and *in vitro* Profiling

Following previous screening of compound collections against *Mtb* (Falzari et al., 2005; Franzblau et al., 2012), initial hits with modest activity against *Mabs* ATCC 19977 emerged from a whole cell activity screen of small molecule compound libraries. This led to the identification of scaffolds with broad antimycobacterial spectrum, such as the adamantyl amides. We applied an iterative process of design-synthesis-screen and increased potency by 1–2 orders of magnitude compared to the initial library hits (Graham et al., 2018). Optimization of the adamantyl amide series resulted in compound CRS400226, an adamantyl benzothiazole amide. Due to its high lipophilicity and consequent potential for nonspecific binding, the adamantyl group was eventually replaced with cyclohexyl derivatives, such as in CRS400153. Some loss of activity, particularly against slow-growing NTM, was noted when comparing the cyclohexyl derivatives to adamantyl compounds. A breakthrough in structure-activity relationship was achieved with bicyclic moieties, such as in CRS400359 and CRS400393, which resulted in improved potency against both rapid- and slow-growing NTM as well against *Mtb*. The properties of these advanced leads with regard to *in vitro* activity and ADMET profiles are shown in **Table 1**. The lead compounds demonstrated a very narrow, mycobacteria-specific spectrum of activity, without appreciable activity against other aerobic or anaerobic bacteria. *In vitro* activity and MIC distributions were further investigated for the top compounds against rapid-growing NTM clinical isolates. MIC ranges and MIC_{90} values, defined as the minimum concentration required to inhibit growth of at least 90% of all strains tested, are shown in **Table 2**. Advanced lead compounds had MIC_{90} of ≤1 μg/mL against all mycobacteria tested, which included $n = 20$ *Mabs*, $n = 11$ *M. chelonae*, $n = 11$ *M. fortuitum,* and $n = 12$ other rapid-growing NTM. Outlier strains with elevated MIC values for benzothiazole amides were not found and the MIC ranges were tight, while commonly used antibiotics such as amikacin, linezolid, and azithromycin showed bimodal MIC distributions (**Supplementary Figure S1**). Reduced susceptibility (MIC ≥ 8 μg/mL) to at least one of these three antibiotics was observed for 45 of 54 (83%) of the clinical isolates. The benzothiazole amides were equally active against drug-resistant strains, which is consistent with the absence of preexisting resistance to an agent directed against a novel target. Lead compound CRS400393 demonstrated MIC values ranging from ≤0.03 to 0.5 μg/mL against rapid-growing NTM, MIC = 1–2 μg/mL against MAC, and MIC ≤ 0.12 μg/mL against *Mtb*. Notably, all mycobacterial species were susceptible, including isoniazid, rifampin, or fluoroquinolone resistant strains of *Mtb*, and activity was maintained under low oxygen conditions and against intracellular *Mtb*, as shown for CRS400226 (**Supplementary Table S2**). In addition, lead compounds have so far shown favorable *in vitro* ADMET properties with regard to cytotoxicity, hemolysis, CYP inhibition, and metabolic stability, although *in vivo* safety and toxicity data have not yet been generated for the more potent analogs. Aqueous solubility was low (<3 μM) and protein binding was high (>95%) for all compounds of this series, likely attributable to the highly hydrophobic moieties of the compounds.

Mode of Action and Target Identification

Benzothiazole amides showed bactericidal activity in time-kill assays. CRS400226 at concentrations of 25 μM (10 μg/mL) caused a reduction in *Mtb* of 3 Log_{10} CFU within 7 days. CRS400393 was bacteriostatic against *Mabs*, for 3 days, followed by a drop of 2 Log_{10} CFU after 5 days. Importantly, no regrowth was observed following a single addition of compound due to emergence of resistance (**Figure 1**). *In vitro* checkerboard synergy assays of the benzothiazole amides showed additive effects with many commonly used antimycobacterial agents (amikacin, ciprofloxacin, azithromycin, tobramycin, clofazimine, linezolid, and cefoxitin), and indifference when combined with doxycycline or bedaquiline (**Supplementary Table S3**).

TABLE 1 | *In vitro* activity of advanced benzothiazole amides.

Compound	CRS400226	CRS400153	CRS400359	CRS400393
Structure	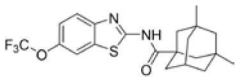	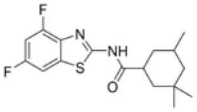	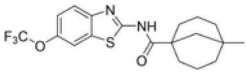	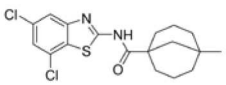
RAPID-GROWING NTM, MIC (μg/mL)				
M. abscessus ATCC 19977	0.25	0.5	≤0.06	0.03
M. abscessus massiliense 119	0.25	0.5	≤0.06	0.03
M. chelonae 93	0.5	0.25	0.12	0.03
M. fortuitum 41	0.12	0.25	0.12	0.06
M. peregrinum ATCC 700686	≤0.06	0.12	0.12	0.03
SLOW-GROWING NTM, MIC (μg/mL)				
M. avium 101	2	16	2	2
M. intracellulare 1956	1	8	2	2
M. chimaera 1502055	1	NT	2	1
M. tuberculosis H37Rv mc^2 6206	0.5	1	0.5	≤0.12
SPECTRUM Of ACTIVITY, MIC (μg/mL)				
S. aureus ATCC 29213	>64	>64	>64	>64
E. faecalis ATCC 29212	>64	>64	>64	>64
S. pyogenes ATCC 19615	>64	>64	>64	>64
S. pneumoniae ATCC 49619	64	8	32	32
E. coli tolC CGSC 5633[a]	>64	>64	>64	64
E. coli ATCC 25922 + PMBN[b]	>64	>64	>64	>64
P. aeruginosa ATCC 35151	>64	>64	64	64
C. albicans ATCC 10231	NT	NT	64	>64
Anaerobes (n > 20 strains)[c]	>16	NT	NT	>32
ADMET PROPERTIES				
HepG2 cytotox., IC_{50} (μM [μg/mL])	69 (29)	NT	10 (4)	>10 (>4)
Hemolysis (μg/mL)	128	128	>128	128
Solubility (μM), phosphate buffer	<3	3	<3	<3
Protein (albumin) binding (%)	>95	>95	>95	>95
Protein (serum) binding (%)	>95	>95	>95	>95
Metabolic stability (μL/min/mg)[d]	124	NT	NT	NT
CYP2B6 inhibition, 10 μM (%)	<50	NT	30	39
CYP3A inhibition, 10 μM (%)	<50	NT	0	26
OTHER PROPERTIES				
Molecular weight (M.W.)	424.5	338.42	398.4	383.3
cLogP	6.67	5.31	6.70	6.48

[a] *Efflux mutant strain of E. coli.*
[b] *Permeabilized strain of E. coli; PMBN, polymyxin B nonapeptide.*
[c] *Including genus Clostridium, Bifidobacterium, Fusobacterium, Peptostreptococcus, Bacteroides, Lactobacillus, Veillonella, Blautia, Parvimonas, Finegoldia, Coprococcus, Actinomyces, Eubacterium, and Prevotella.*
[d] *Clearance measured in human liver microsome assay.*
NT, not tested.

Mode-of-action studies were performed with CRS400153 and CRS400226, which represent the cyclohexyl and the adamantyl subseries of benzothiazole amides, respectively. Evidence was obtained that compounds from both subseries at 2x MIC and 10x MIC affect the transfer of mycolic acids to their cell envelope acceptors in both *Mabs* and *Mtb*, most likely through the inhibition of the trehalose monomycolate transporter, MmpL3. Indeed, metabolic labeling with [^{14}C]acetate of *Mabs* ATCC19977 cultures either untreated or treated with benzothiazole amides at 2x and 10x MIC resulted in a concentration-dependent inhibition of mycolic acid transfer to both arabinogalactan and trehalose dimycolates, a hallmark of MmpL3 inhibitors (**Supplementary Figure S4**). Moreover, spontaneous *Mabs* ATCC19977 mutants resistant to CRS400153 were isolated with a frequency of 6×10^{-9} at 4x MIC and were found to harbor non-synonymous mutations in

TABLE 2 | *In vitro* Activity (MIC, μg/mL) of benzothiazole amides and control agents against rapid-growing NTM clinical Isolates.

Compound	*M. abscessus* ($n = 20$)		*M. chelonae* ($n = 11$)		*M. fortuitum* ($n = 11$)		Other NTM ($n = 12$)[a]	
	MIC range	MIC_{90}[b]	MIC range	MIC_{90}	MIC range	MIC_{90}	MIC range	MIC_{90}
CRS400226	0.25–2	0.5	0.5–0.5	0.5	0.12–0.5	0.5	0.12–1	0.5
CRS400153	0.5–2	1	0.5–1	1	0.5–0.5	0.5	0.25–1	1
CRS400359	0.06–2	0.25	0.25–0.5	0.25	0.06–1	1	0.12–2	0.5
CRS400393	≤0.03– 0.25	0.25	0.12–0.12	0.12	≤0.03–0.5	0.25	0.12–0.5	0.5
Amikacin	1–>16	16	16–>16	>16	0.5–4	2	0.5–16	16
Linezolid	0.5–>8	>8	1–8	8	0.5–>8	>8	0.5–>8	>8
Azithromycin	0.12–>8	>8	0.12–0.5	0.5	0.12–>8	>8	0.12–>8	>8

[a]*Other rapid-growing NTM included two strains each of M. peregrinum, M. mucogenicum, M. massiliense, M. bolletii, M. phocaicum, and M. porcinum.*
[b]*MIC_{90} defined as the minimum drug concentration that inhibited growth of ≥90% of the strains tested.*

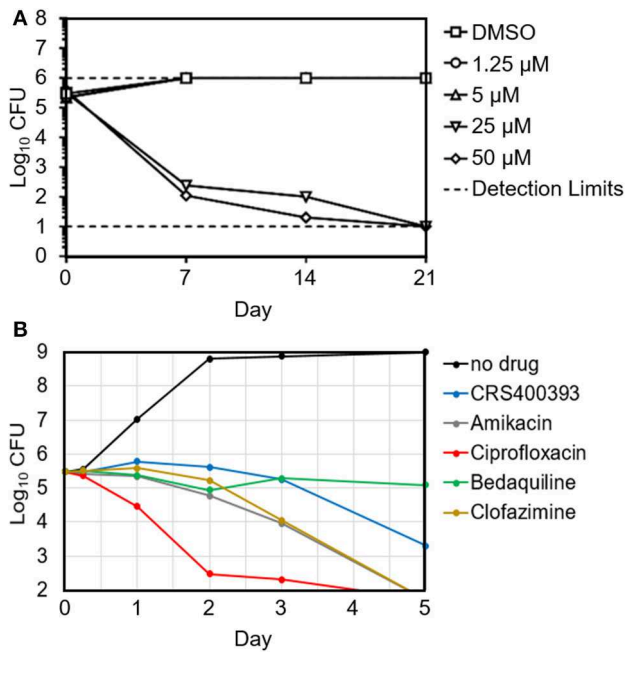

FIGURE 1 | Time-kill kinetics of *Mtb* H37Rv in the presence of increasing concentrations of CRS400226 **(A)** and of *Mabs* 21 in the presence of CRS400393 or other antimycobacterial agents at 10x MIC **(B)**, indicating bactericidal activity.

MmpL3 (L551S, I306S, or A309P). These mutations were sufficient to confer reduced susceptibility (4 to >32-fold MIC increase) to CRS400153 and CRS400359 when introduced via recombineering into the isogenic background of Mabs ATCC19977. Moreover, testing of 15 additional analogs from the same compound subclass indicated that all of them displayed 8–64-fold reduced activity against CRS400153-resistant mutants harboring mutations in MmpL3. Interestingly, the same A309P and L551S mutations were previously reported to decrease 16- to 64-fold the susceptibility of *M. abscessus* to MmpL3 inhibitors of the indole-2-carboxamide and piperidinol series (Dupont et al., 2016; Franz et al., 2017) (unpublished data). The I306 residue has not previously been associated with resistance to MmpL3 inhibitors but maps in the fifth transmembrane region of the transporter, very close to A309 and to a conserved serine residue (S302 in *M. abscessus*, S288 in Mtb) shown to confer resistance to a variety of MmpL3 inhibitors in Mtb (Belardinelli et al., 2016). These data strongly suggest that compounds from the structural class of benzothiazole cyclohexyl amides such as CRS400153 kill *M. abscessus* through the direct or indirect inhibition of MmpL3. The fact that CRS400153 showed no effect on the membrane potential and electrochemical pH gradient of Mtb intact cells and inverted membrane vesicles (data not shown) supports a direct mechanism of inhibition of the transporter (Li et al., 2018).

In vivo Efficacy and Tolerability

Several compounds were screened in mouse PK and tolerability studies to evaluate various doses and routes of administration. Although essentially insoluble in water, we found CRS400226 was soluble in corn oil at concentrations up to 250 mg/mL. Oral dosing of this compound at 100 mg/kg in female CD-1 mice resulted in very low plasma levels of 2.3 μg/mL at 1 h and 2.0 μg/mL at 8 h. Although highly tolerated, it became clear that the lipophilic nature and high protein binding of the compounds precluded oral routes of administration for efficacy. Instead, intrapulmonary delivery methods for treatment of lung infections such as NTM and *Mtb* were explored. CRS400226 was synthesized in multi-gram quantities to support *in vivo* studies and was further developed for this delivery pathway. These initial attempts to formulate CRS400226 as a corn oil/saline emulsion afforded the opportunity to obtain proof-of-concept *in vivo* efficacy. We assessed CRS400226 against *Mabs* 21 in a 28-day mouse model of chronic NTM lung infection in granulocyte macrophage colony stimulated factor-knockout (GM-CSF KO) mice, which represent a clinically relevant model of human infection (De Groote et al., 2014b). Actual dose deposited in the lungs was 4.53 Log_{10} CFU, which increased to 4.98 Log_{10} CFU after 10 days of infection, as determined in groups of three mice. Intratracheal administration of CRS400226 at 25 mg/kg once daily, 5 days per week for 4 weeks resulted in a statistically significant ($p = 0.0005$) reduction of 0.64 Log_{10} CFU compared to the vehicle control (**Figure 2A**). Azithromycin at 100 mg/kg achieved 0.38 Log_{10} CFU reduction

when compared to the untreated group ($p = 0.05$), though the data points in the azithromycin group were more scattered than in the other groups. There was no statistical difference ($p = 0.17$) in the bacterial burden between the CRS400226 and azithromycin treated groups. No animals died during the 4-week course of the efficacy model, though all treatment groups demonstrated a slight decrease in weight ranging from 1.6 to 7.8%. CRS400226 was well tolerated up to 4 weeks of treatment, without any observed adverse side effects (**Figure 2B**). Histology showed that the azithromycin treated animals had only minimal pathologic evidence of inflammatory infiltrates with one animal displaying normal appearing lung tissue. CRS400226 treated animals had only very mild areas of airway-centric inflammation compared to the peribronchial inflammatory infiltrate seen in the vehicle treated group. The untreated and vehicle treated lung tissue demonstrated scattered nodules and more significant inflammatory infiltrates. In many of the animal lungs, evidence of bronchiectasis was observed and inflamed peri-bronchial lymphoid tissue (**Supplementary Figure S5**).

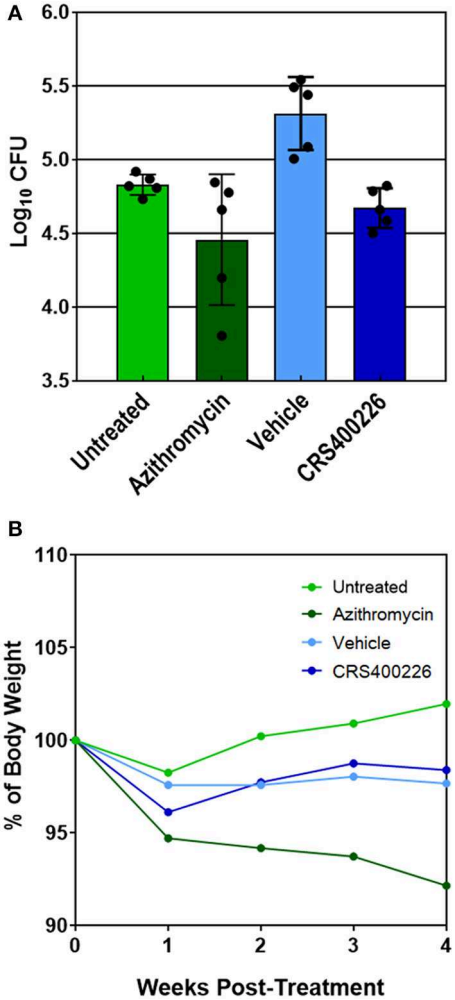

FIGURE 2 | GM-CSF KO mouse model of *Mabs* lung infection demonstrating efficacy **(A)** and tolerability **(B)** of CRS400226. The Penn Century microsprayer was used for delivery of 5×10^5 to 1×10^6 bacteria to the lungs. Starting 10 days later, the test compound was dosed once daily over 4 weeks by intratracheal microspray administration as 5% corn oil/saline emulsion. CRS400226 at 25 mg/kg daily for 28 days resulted in a statistically significant ($p = 0.0005$) reduction of 0.64 Log_{10} CFU compared to the vehicle control.

DISCUSSION

We have developed a lead series that exhibits broad antimycobacterial activity, which could revolutionize the treatment of NTM, while simultaneously adding much-needed novel agents to the *Mtb* treatment armamentaria. The strength of the benzothiazole amide series is that advanced lead compounds are very potent *in vitro* and mid-stage compounds showed *in vivo* efficacy. Good potency of the benzothiazole amides was demonstrated against a collection of rapid growing NTM clinical isolates which included many strains that were resistant to amikacin, linezolid, or azithromycin illustrating the high prevalence of non-susceptibility of NTM to many antibiotics commonly used to treat NTM infections and the need for novel agents whose activity is not affected by existing resistance mechanisms. Apparent MIC values against slow-growing NTM and *Mtb* were 3higher compared to the MIC values seen against rapid-growing NTM. This has been attributed to differences in the media used to test the different mycobacterial species, specifically to the presence of albumin (5 mg/mL) in the OADC supplement used for slow- growing NTMs and for *Mtb*, causing an MIC shift of the relatively highly (>95%) protein-bound compounds (**Supplementary Table S6**). CRS400393 showed additivity and no antagonism when combined with other antimycobacterial agents, an essential property for treating chronic NTM infections that often require combination drug regimens. Another favorable property of the benzothiazole amides is their narrow spectrum, since such a mycobacterial-specific agent may prove more tolerable for prolonged duration of therapy, i.e., by not affecting the beneficial gut microbiome that protects the host from gastroenteric side effects such as *Clostridium difficile* infections that often arise from exposure to broad-spectrum antibiotics.

The apparent target of benzothiazole amides, MmpL3, is a mycolate transporter essential for assembly of the outer membrane and has high potential to improve and shorten current drug-susceptible and drug-resistant tuberculosis chemotherapies (Li et al., 2016, 2018). Several MmpL3 inhibitors with different chemical scaffolds have been reported (Poce et al., 2013, 2016; Li et al., 2014; Rayasam, 2014; Stec et al., 2016). One compound, SQ109, which is unrelated to our compound series, has been in clinical development through Phase II (Sacksteder et al., 2012; Tahlan et al., 2012). The nature of the membrane-bound MmpL3 target favors lipophilic and therefore poorly water-soluble inhibitors. Efforts to optimize oral drug-like properties such as improving compound solubility have largely resulted in loss of activity. This potential limitation had been discovered through detailed SAR of the early lead compound CRS400153, by exploring hydrophilic substitutions at the 4-, 5-, 6-, and 7-position of the benzothiazole moiety, such as a hydroxyl, tertiary amine, and ether or ester groups. In all cases, these

hydrophilic substitutions resulted in MIC > 64 μg/mL against *M. abscessus* compared to MIC = 0.5 μg/mL for the 4,6-diF-benzothiazole analog CRS400153, except for the 7-OH benzothiazole analog which retained some activity with an MIC range of 2–16 μg/mL against *M. abscessus* (compound #37) (Graham et al., 2018). Our lead compounds are very potent, but have very low solubility (≤3 μM), high protein binding (MIC ≥ 16 μg/mL in 50% serum) and low oral bioavailability due to their lipophilic nature, precluding their utility as oral agents. Therefore, further development will focus on inhalational therapy for NTM first and possibly development of a topical formulation later. Similar approaches have been reported for aerosolized liposomal amikacin (Rose et al., 2014) and for inhaled dry powder capreomycin with the potential of rendering patients non-infectious (Dharmadhikari et al., 2013). Our proof-of-concept efficacy study used corn oil for formulation, and we noted an increased bacterial burden in the vehicle treated group compared to the untreated group, which is likely attributable to corn oil being a carbon source for mycobacteria, increasing their replication; hence, developing a more sophisticated formulation will be paramount.

The desired target product profile for this drug includes (1) broad-spectrum coverage of the clinically-relevant mycobacteria *Mabs,* MAC and *Mtb*, (2) bactericidal activity, (3) antibacterial potency equal or better compared to antibiotics currently used in the standard of care for NTM infections, (4) suitability for inhaled therapy via aerosol, (5) dosing frequency preferably once or twice a day, (6) excellent safety profile suitable for treating chronic infections and for pediatric use, (7) low propensity for resistance development, (8) compatibility with other antibacterial drug cocktails, and (9) shelf-life of at least 2 years. Our data indicate that the benzothiazole amides already meet the criteria regarding the *in vitro* antimyobacterial activity and low resistance frequencies. The next steps will be the evaluation of the compounds regarding efficacy, safety, tolerability, and chemical stability. Cytotoxicity studies, however, have been limited by the low solubility of the compounds, which made testing at high concentrations impossible, and potential effect may be masked due to the high protein binding of the compounds.

In conclusion, the limitations of the scaffold are high lipophilicity, high protein binding, and poor PK with oral dosing. Such challenges in drug development can often be overcome by exquisite potency of the agents and improved formulation and delivery methods. A recent example of an antimycobacterial drug with some undesirable physicochemical properties is bedaquiline, which nonetheless was developed successfully and became the first FDA-approved TB drug in 40 years (Palomino and Martin, 2013).

In vivo efficacy and tolerability of mid-stage lead compound CRS400226 provides exciting evidence of the potential for this series; new analogs have already shown further potency increases, providing a solid foundation for further optimization. Next steps will include testing of pharmacokinetic properties, metabolic stability, toxicity and efficacy of the most recent potent compounds such as CRS400393 against NTM and *Mtb* as inhaled therapy, hopefully leading to IND-enabling studies.

AUTHOR CONTRIBUTIONS

MD, UO, XS, JD, and TJ conceived the project and designed the strategy. Experiments were carried out by CW, JG, JD, and XS (chemical synthesis and SAR), TH, CY, and UO (*in vitro* susceptibility and other microbiological assays), WL and MJ (mode-of-action studies) and MG-J (*in vivo* efficacy). WR was Project Manager and assisted with data analysis. MD and UO wrote the manuscript.

FUNDING

Initial funding was obtained from the American Lung Association and NTM Info & Research (NTMir) and the Cystic Fibrosis Foundation through grants awarded to MD (CSU), followed by funding from NIH via SBIR Phase I and II grants GM110848 to Crestone, Inc. (PIs TJ, MD, and XS) and AI116525 to MJ and MG-J. The content is solely the responsibility of the authors and does not necessarily represent the official views of the NIH.

ACKNOWLEDGMENTS

We thank Scott Franzblau (Univ. Illinois at Chicago) for providing screening hits. We are grateful to Jim Boyce at NIAID preclinical services (Task Order A19) for performing *in vitro* activity and ADMET assays. NTM strains were provided by Denver Health, and *Mtb* H37Rv mc^{2}6206 was provided by Dr. Bill Jacobs (Albert Einstein College of Medicine, NY).

SUPPLEMENTARY MATERIAL

The Supplementary Material for this article can be found online at: https://www.frontiersin.org/articles/10.3389/fmicb.2018.02231/full#supplementary-material

REFERENCES

Aguilar-Ayala, D. A., Cnockaert, M., Vandamme, P., Palomino, J. C., Martin, A., and Gonzalez, Y. M. J. (2018). Antimicrobial activity against *Mycobacterium tuberculosis* under *in vitro* lipid-rich dormancy conditions. *J. Med. Microbiol.* 67, 282–285. doi: 10.1099/jmm.0.000681

Asakura, T., Funatsu, Y., Ishii, M., Namkoong, H., Yagi, K., Suzuki, S., et al. (2015). Health-related quality of life is inversely correlated with C-reactive protein and age in *Mycobacterium avium* complex lung disease: a cross-sectional analysis of 235 patients. *Respir. Res.* 16:145. doi: 10.1186/s12931-015-0304-5

Ayyappan, J. P., Vinnard, C., Subbian, S., and Nagajyothi, J. F. (2018). Effect of *Mycobacterium tuberculosis* infection on adipocyte physiology. *Microbes Infect.* 20, 81–88. doi: 10.1016/j.micinf.2017.10.008

Belardinelli, J. M., Yazidi, A., Yang, L., Fabre, L., Li, W., Jacques, B., et al. (2016). Structure-function profile of MmpL3, the essential mycolic acid

transporter from *Mycobacterium tuberculosis*. *ACS Infect. Dis.* 2, 702–713. doi: 10.1021/acsinfecdis.6b00095

Caimmi, D., Martocq, N., Trioleyre, D., Guinet, C., Godreuil, S., Daniel, T., et al. (2018). Positive effect of Liposomal Amikacin for inhalation on *Mycobacterium abcessus* in Cystic Fibrosis patients. *Open Forum Infect. Dis.* 5:ofy034. doi: 10.1093/ofid/ofy034

Carvalho, N. F. G., Pavan, F., Sato, D. N., Leite, C. Q. F., Arbeit, R. D., and Chimara, E. (2018). Genetic correlates of clarithromycin susceptibility among isolates of the *Mycobacterium abscessus* group and the potential clinical applicability of a PCR-based analysis of erm(41). *J. Antimicrob. Chemother.* 73, 862–866. doi: 10.1093/jac/dkx476

Caskey, S., Moore, J. E., and Rendall, J. C. (2018). *In vitro* activity of seven hospital biocides against *Mycobacterium abscessus:* implications for patients with cystic fibrosis. *Int. J. Mycobacteriol.* 7, 45–47. doi: 10.4103/ijmy.ijmy_197_17

Choi, H., Jhun, B. W., Kim, S. Y., Kim, D. H., Lee, H., Jeon, K., et al. (2018). Treatment outcomes of macrolide-susceptible *Mycobacterium abscessus* lung disease. *Diagn. Microbiol. Infect. Dis.* 90, 293–295. doi: 10.1016/j.diagmicrobio.2017.12.008

Claeys, T. A., and Robinson, R. T. (2018). The many lives of nontuberculous mycobacteria. *J. Bacteriol*. doi: 10.1128/JB.00739-17. [Epub ahead of print].

Clary, G., Sasindran, S. J., Nesbitt, N., Mason, L., Cole, S., Azad, A., et al. (2018). *Mycobacterium abscessus* smooth and rough morphotypes form antimicrobial-tolerant biofilm phenotypes but are killed by acetic acid. *Antimicrob. Agents Chemother.* 62:e01782-17. doi: 10.1128/AAC.01782-17

CLSI (2003). *Susceptibility Testing of Mycobacteria, Nocardiae, and Other Aerobic Actinomycetes*. Wayne, PA: Clinical Laboratory Standards Institute Approved Standard M24-A.

Cowman, S. A., Jacob, J., Hansell, D. M., Kelleher, P., Wilson, R., Cookson, W. O. C., et al. (2018). Whole-blood gene expression in pulmonary nontuberculous Mycobacterial infection. *Am. J. Respir. Cell Mol. Biol.* 58, 510–518. doi: 10.1165/rcmb.2017-0230OC

Daley, C. L., and Glassroth, J. (2014). Treatment of pulmonary nontuberculous Mycobacterial infections: many questions remain. *Ann. Am. Thorac. Soc.* 11, 96–97. doi: 10.1513/AnnalsATS.201311-399ED

De Groote, M. A., Gibbs, S., de Moura, V. C., Burgess, W., Richardson, K., Kasperbauer, S., et al. (2014a). Analysis of a panel of rapidly growing Mycobacteria for resistance to aldehyde-based disinfectants. *Am. J. Infect. Control* 42, 932–934. doi: 10.1016/j.ajic.2014.05.014

De Groote, M. A., and Huitt, G. (2006). Infections due to rapidly growing Mycobacteria. *Clin. Infect. Dis.* 42, 1756–1763. doi: 10.1086/504381

De Groote, M. A., Johnson, L., Podell, B., Brooks, E., Basaraba, R., and Gonzalez-Juarrero, M. (2014b). GM-CSF knockout mice for preclinical testing of agents with antimicrobial activity against *Mycobacterium abscessus*. *J. Antimicrob. Chemother.* 69, 1057–1064. doi: 10.1093/jac/dkt451

Dharmadhikari, A. S., Kabadi, M., Gerety, B., Hickey, A. J., Fourie, P. B., and Nardell, E. (2013). Phase, I., single-dose, dose-escalating study of inhaled dry powder capreomycin: a new approach to therapy of drug-resistant tuberculosis. *Antimicrob. Agents Chemother.* 57, 2613–2619. doi: 10.1128/AAC.02346-12

Dupont, C., Viljoen, A., Dubar, F., Blaise, M., Bernut, A., Pawlik, A., et al. (2016). A new piperidinol derivative targeting mycolic acid transport in *Mycobacterium abscessus*. *Mol. Microbiol.* 101, 515–529. doi: 10.1111/mmi.13406

Falkinham, J. O. (2003). The changing pattern of nontuberculous Mycobacterial disease. *Can. J. Infect. Dis.* 14, 281–286. doi: 10.1155/2003/323058

Falkinham, J. O. III. (2013). Ecology of nontuberculous Mycobacteria–where do human infections come from? *Semin. Respir. Crit. Care Med.* 34, 95–102. doi: 10.1055/s-0033-1333568

Falzari, K., Zhu, Z., Pan, D., Liu, H., Hongmanee, P., and Franzblau, S. (2005). *In vitro* and *in vivo* activities of macrolide derivatives against *Mycobacterium tuberculosis*. *Antimicrob. Agents Chemother.* 49, 1447–1454. doi: 10.1128/AAC.49.4.1447-1454.2005

Ferro, B. E., Meletiadis, J., Wattenberg, M., de Jong, A., van Soolingen, D., Mouton, J. W., et al. (2016). Clofazimine prevents the regrowth of *Mycobacterium abscessus* and *Mycobacterium avium* type strains exposed to amikacin and clarithromycin. *Antimicrob. Agents Chemother.* 60, 1097–1105. doi: 10.1128/AAC.02615-15

Fleshner, M., Olivier, K. N., Shaw, P. A., Adjemian, J., Strollo, S., Claypool, R. J., et al. (2016). Mortality among patients with pulmonary non-tuberculous Mycobacteria disease. *Int. J. Tuberc. Lung Dis.* 20, 582–587. doi: 10.5588/ijtld.15.0807

Franz, N. D., Belardinelli, J. M., Kaminski, M. A., Dunn, L. C., Calado Nogueira de Moura, V., Blaha, M. A., et al. (2017). Design, synthesis and evaluation of indole-2-carboxamides with pan anti-mycobacterial activity. *Bioorg. Med. Chem.* 25, 3746–3755. doi: 10.1016/j.bmc.2017.05.015

Franzblau, S. G., DeGroote, M. A., Cho, S. H., Andries, K., Nuermberger, E., Orme, I. M., et al. (2012). Comprehensive analysis of methods used for the evaluation of compounds against *Mycobacterium tuberculosis*. *Tuberculosis* 92, 453–488. doi: 10.1016/j.tube.2012.07.003

Gonzalez-Juarrero, M., Woolhiser, L. K., Brooks, E., DeGroote, M. A., and Lenaerts, A. J. (2012). Mouse model for efficacy testing of antituberculosis agents via intrapulmonary delivery. *Antimicrob. Agents Chemother.* 56, 3957–3959. doi: 10.1128/AAC.00464-12

Graham, J., Wong, C. E., Day, J., McFaddin, E., Ochsner, U., Hoang, T., et al. (2018). Discovery of benzothiazole amides as potent antimycobacterial agents. *Bioorg. Med. chem. Lett.* doi: 10.1016/j.bmcl.2018.08.026. [Epub ahead of print].

Haworth, C. S., Banks, J., Capstick, T., Fisher, A. J., Gorsuch, T., Laurenson, I. F., et al. (2017). British Thoracic Society Guideline for the management of non-tuberculous Mycobacterial pulmonary disease (NTM-PD). *BMJ Open Respir. Res.* 4:e000242. doi: 10.1136/bmjresp-2017-000242

Henkle, E., Novosad, S. A., Shafer, S., Hedberg, K., Siegel, S. A. R., Ku, J., et al. (2017). Long-term outcomes in a population-based cohort with respiratory nontuberculous Mycobacteria isolation. *Ann. Am. Thorac. Soc.* 14, 1120–1128. doi: 10.1513/AnnalsATS.201610-801OC

Kasperbauer, S. H., and De Groote, M. A. (2015). The treatment of rapidly growing Mycobacterial infections. *Clin. Chest Med.* 36, 67–78. doi: 10.1016/j.ccm.2014.10.004

Khalifa, R., Nasser, M., Gomaa, A., Osman, N., and Salem, H. (2013). Resazurin Microtiter Assay Plate method for detection of susceptibility of multidrug resistant *Mycobacterium tuberculosis* to second-line anti-tuberculous drugs. *Egypt. J. Chest Dis. Tuberc.* 62, 241–247. doi: 10.1016/j.ejcdt.2013.05.008

Koh, W. J. (2017). Nontuberculous Mycobacteria-overview. *Microbiol. Spectr.* 5:TNMI7-0024-2016. doi: 10.1128/microbiolspec.TNMI7-0024-2016

Lake, M. A., Ambrose, L. R., Lipman, M. C., and Lowe, D. M. (2016). "Why me, why now?" Using clinical immunology and epidemiology to explain who gets nontuberculous mycobacterial infection. *BMC Med.* 14:54. doi: 10.1186/s12916-016-0606-6

Lande, L., George, J., and Plush, T. (2018). *Mycobacterium avium* complex pulmonary disease: new epidemiology and management concepts. *Curr. Opin. Infect. Dis.* 31, 199–207. doi: 10.1097/QCO.0000000000000437

Li, W., Obregon-Henao, A., Wallach, J. B., North, E. J., Lee, R. E., Gonzalez-Juarrero, M., et al. (2016). Therapeutic potential of the *Mycobacterium tuberculosis* Mycolic Acid Transporter, MmpL3. *Antimicrob. Agents Chemother.* 60, 5198–5207. doi: 10.1128/AAC.00826-16

Li, W., Sanchez-Hidalgo, A., Jones, V., de Moura, V. C., North, E. J., and Jackson, M. (2017). Synergistic interactions of MmpL3 inhibitors with antitubercular compounds *in vitro*. *Antimicrob. Agents Chemother.* 61:e02399-16. doi: 10.1128/AAC.02399-16

Li, W., Upadhyay, A., Fontes, F. L., North, E. J., Wang, Y., Crans, D. C., et al. (2014). Novel insights into the mechanism of inhibition of MmpL3, a target of multiple pharmacophores in *Mycobacterium tuberculosis*. *Antimicrob. Agents Chemother.* 58, 6413–6423. doi: 10.1128/AAC.03229-14

Li, W., Yazidi, A., Pandya, A. N., Hegde, P., Tong, W., Calado Nogueira de Moura, V., et al. (2018). MmpL3 as a target for the treatment of drug-resistant nontuberculous Mycobacterial infections. *Front. Microbiol.* 9:1547. doi: 10.3389/fmicb.2018.01547

Liu, J., Bruhn, D. F., Lee, R. B., Zheng, Z., Janusic, T., Scherbakov, D., et al. (2017). Structure-activity relationships of spectinamide antituberculosis agents: a dissection of ribosomal inhibition and native efflux avoidance contributions. *ACS Infect. Dis.* 3, 72–88. doi: 10.1021/acsinfecdis.6b00158

Low, J. L., Wu, M. L., Aziz, D. B., Laleu, B., and Dick, T. (2017). Screening of TB actives for activity against nontuberculous Mycobacteria delivers high hit rates. *Front Microbiol.* 8:1539. doi: 10.3389/fmicb.2017.01539

Martiniano, S. L., Davidson, R. M., and Nick, J. A. (2017). Nontuberculous Mycobacteria in cystic fibrosis: updates and the path forward. *Pediatr. Pulmonol.* 52, S29–S36. doi: 10.1002/ppul.23825

Nick, J. A., Pohl, K., and Martiniano, S. L. (2016). Nontuberculous Mycobacterial infections in cystic fibrosis: to treat or not to treat? *Curr. Opin. Pulm. Med.* 22, 629–636. doi: 10.1097/MCP.0000000000000317

Obach, R. S. (1999). Prediction of human clearance of twenty-nine drugs from hepatic microsomal intrinsic clearance data: an examination of *in vitro* half-life approach and nonspecific binding to microsomes. *Drug Metab. Dispos.* 27, 1350–1359.

O'Brien, D. P., Friedman, N. D., McDonald, A., Callan, P., Hughes, A., Walton, A., et al. (2018). Wound healing: natural history and risk factors for delay in Australian patients treated with antibiotics for *Mycobacterium ulcerans* disease. *PLoS Negl. Trop. Dis.* 12:e00 06357. doi: 10.1371/journal.pntd.0006357

Olivier, K. N., Griffith, D. E., Eagle, G., McGinnis, J. P. II., Micioni, L., Liu, K., et al. (2017). Randomized trial of liposomal amikacin for inhalation in nontuberculous Mycobacterial lung disease. *Am. J. Respir. Crit. Care Med.* 195, 814–823. doi: 10.1164/rccm.201604-0700OC

Olivier, K. N., Shaw, P. A., Glaser, T. S., Bhattacharyya, D., Fleshner, M., Brewer, C. C., et al. (2014). Inhaled amikacin for treatment of refractory pulmonary nontuberculous Mycobacterial disease. *Ann. Am. Thorac. Soc.* 11, 30–35. doi: 10.1513/AnnalsATS.201307-231OC

Palomino, J. C., and Martin, A. (2013). TMC207 becomes bedaquiline, a new anti-TB drug. *Future Microbiol.* 8, 1071–1080. doi: 10.2217/fmb.13.85

Philley, J. V., DeGroote, M. A., Honda, J. R., Chan, M. M., Kasperbauer, S., Walter, N. D., et al. (2016). Treatment of non-tuberculous Mycobacterial lung disease. *Curr. Treat. Options Infect. Dis.* 8, 275–296. doi: 10.1007/s40506-016-0086-4

Poce, G., Bates, R. H., Alfonso, S., Cocozza, M., Porretta, G. C., Ballell, L., et al. (2013). Improved BM212 MmpL3 inhibitor analogue shows efficacy in acute murine model of tuberculosis infection. *PLoS ONE* 8:e56980. doi: 10.1371/journal.pone.0056980

Poce, G., Consalvi, S., and Biava, M. (2016). MmpL3 inhibitors: diverse chemical scaffolds inhibit the same target. *Mini Rev. Med. Chem.* 16, 1274–1283. doi: 10.2174/1389557516666160118105319

Prevots, D. R., Loddenkemper, R., Sotgiu, G., and Migliori, G. B. (2017). Nontuberculous Mycobacterial pulmonary disease: an increasing burden with substantial costs. *Eur. Respir. J.* 49:1700374. doi: 10.1183/13993003.00374-2017

Prevots, D. R., and Marras, T. K. (2015). Epidemiology of human pulmonary infection with nontuberculous Mycobacteria: a review. *Clin. Chest Med.* 36, 13–34. doi: 10.1016/j.ccm.2014.10.002

Rayasam, G. V. (2014). MmpL3 a potential new target for development of novel anti-tuberculosis drugs. *Expert Opin. Ther. Targets* 18, 247–256. doi: 10.1517/14728222.2014.859677

Rose, S. J., Neville, M. E., Gupta, R., and Bermudez, L. E. (2014). Delivery of aerosolized liposomal amikacin as a novel approach for the treatment of nontuberculous Mycobacteria in an experimental model of pulmonary infection. *PLoS ONE* 9:e108703. doi: 10.1371/journal.pone.0108703

Sacksteder, K. A., Protopopova, M., Barry, C. E. III, Andries, K., and Nacy, C. A. (2012). Discovery and development of SQ109: a new antitubercular drug with a novel mechanism of action. *Future Microbiol.* 7, 823–837. doi: 10.2217/fmb.12.56

Sambandamurthy, V. K., Derrick, S. C., Jalapathy, K. V., Chen, B., Russell, R. G., Morris, S. L., et al. (2005). Long-term protection against tuberculosis following vaccination with a severely attenuated double lysine and pantothenate auxotroph of *Mycobacterium tuberculosis*. *Infect. Immun.* 73, 1196–1203. doi: 10.1128/IAI.73.2.1196-1203.2005

Sigal, G. B., Segal, M. R., Mathew, A., Jarlsberg, L., Wang, M., Barbero, S., et al. (2017). Biomarkers of tuberculosis severity and treatment effect: a directed screen of 70 host markers in a randomized clinical trial. *EBioMed.* 25, 112–121. doi: 10.1016/j.ebiom.2017.10.018

Simoes, S., Carvalheiro, M., and Gaspar, M. M. (2016). Lipid-based nanocarriers for Cutaneous Leishmaniais and Buruli Ulcer management. *Curr. Pharm. Des.* 22, 6577–6586. doi: 10.2174/1381612822666160701083812

Spaulding, A. B., Lai, Y. L., Zelazny, A. M., Olivier, K. N., Kadri, S. S., Prevots, D. R., et al. (2017). Geographic distribution of nontuberculous Mycobacterial species identified among clinical isolates in the United States, 2009-2013. *Ann. Am. Thorac. Soc.* 14, 1655–1661. doi: 10.1513/AnnalsATS.201611-860OC

Stec, J., Onajole, O. K., Lun, S., Guo, H., Merenbloom, B., Vistoli, G., et al. (2016). Indole-2-carboxamide-based MmpL3 inhibitors show exceptional antitubercular activity in an animal model of tuberculosis infection. *J. Med. Chem.* 59, 6232–6247. doi: 10.1021/acs.jmedchem.6b00415

Strollo, S. E., Adjemian, J., Adjemian, M. K., and Prevots, D. R. (2015). The burden of pulmonary nontuberculous Mycobacterial disease in the United States. *Ann. Am. Thorac. Soc.* 12, 1458–1464. doi: 10.1513/AnnalsATS.201503-173OC

Tahlan, K., Wilson, R., Kastrinsky, D. B., Arora, K., Nair, V., Fischer, E., et al. (2012). SQ109 targets MmpL3, a membrane transporter of trehalose monomycolate involved in mycolic acid donation to the cell wall core of *Mycobacterium tuberculosis*. *Antimicrob. Agents Chemother.* 56, 1797–1809. doi: 10.1128/AAC.05708-11

Tai, A. Y. C., Athan, E., Friedman, N. D., Hughes, A., Walton, A., and O'Brien, D. P. (2018). Increased severity and spread of *Mycobacterium ulcerans*, Southeastern Australia. *Emerg. Infect. Dis.* 24. doi: 10.3201/eid2401.171070

van Ingen, J., Kohl, T. A., Kranzer, K., Hasse, B., Keller, P. M., Katarzyna Szafranska, A., et al. (2017). Global outbreak of severe *Mycobacterium chimaera* disease after cardiac surgery: a molecular epidemiological study. *Lancet Infect. Dis.* 17, 1033–1041. doi: 10.1016/S1473-3099(17)30324-9

Vinnard, C., Longworth, S., Mezochow, A., Patrawalla, A., Kreiswirth, B. N., and Hamilton, K. (2016). Deaths related to nontuberculous Mycobacterial infections in the United States, 1999-2014. *Ann. Am. Thorac. Soc.* 13, 1951–1955. doi: 10.1513/AnnalsATS.201606-474BC

Walsky, R. L., and Obach, R. S. (2004). Validated assays for human cytochrome P450 activities. *Drug Metab. Dispos.* 32, 647–660. doi: 10.1124/dmd.32.6.647

Zimmermann, P., Finn, A., and Curtis, N. (2018). Does BCG vaccination protect against Non-tuberculous Mycobacterial infection? A systematic review and meta-analysis. *J. Infect. Dis.* 218, 679–687. doi: 10.1093/infdis/jiy207

Zingue, D., Bouam, A., Tian, R. B. D., and Drancourt, M. (2018). Buruli Ulcer, a prototype for ecosystem-related infection, caused by *Mycobacterium ulcerans*. *Clin. Microbiol. Rev.* 31:e00 045-17. doi: 10.1128/CMR.00045-17

Conflict of Interest Statement: UO, XS, JD, TJ, CW, JG, JD, XS, TH, and CY are employees of Crestone, Inc.

The remaining authors declare that the research was conducted in the absence of any commercial or financial relationships that could be construed as a potential conflict of interest.

frontiers in Microbiology

MINI REVIEW
published: 25 September 2018
doi: 10.3389/fmicb.2018.02273

Mycobacterium abscessus and β-Lactams: Emerging Insights and Potential Opportunities

*Elizabeth Story-Roller[1], Emily C. Maggioncalda[1], Keira A. Cohen[2] and Gyanu Lamichhane[1]**

[1] Division of Infectious Diseases, School of Medicine, Johns Hopkins University, Baltimore, MD, United States, [2] Division of Pulmonary and Critical Care Medicine, School of Medicine, Johns Hopkins University, Baltimore, MD, United States

β-lactams, the most widely used class of antibiotics, are well-tolerated, and their molecular mechanisms of action against many bacteria are well-documented. *Mycobacterium abscessus* (*Mab*) is a highly drug-resistant rapidly-growing nontuberculous mycobacteria (NTM). Only in recent years have we started to gain insight into the unique relationship between β-lactams and their targets in *Mab*. In this mini-review, we summarize recent findings that have begun to unravel the molecular basis for overall efficacy of β-lactams against *Mab* and discuss emerging evidence that indicates that we have yet to harness the full potential of this antibiotic class to treat *Mab* infections.

Keywords: *Mycobacterium abscessus*, β-lactams, peptidoglycan, LD-transpeptidase, β-lactamase inhibitor

OPEN ACCESS

Edited by:
Thomas Dick, Rutgers, The State University of New Jersey, Newark, United States

Reviewed by:
Marcel Behr, McGill University, Canada
Bavesh Davandra Kana, University of the Witwatersrand, South Africa

***Correspondence:**
Gyanu Lamichhane
lamichhane@jhu.edu

Specialty section:
This article was submitted to Antimicrobials, Resistance and Chemotherapy, a section of the journal Frontiers in Microbiology

Received: *30 May 2018*
Accepted: *05 September 2018*
Published: *25 September 2018*

Citation:
Story-Roller E, Maggioncalda EC, Cohen KA and Lamichhane G (2018) Mycobacterium abscessus and β-Lactams: Emerging Insights and Potential Opportunities. Front. Microbiol. 9:2273. doi: 10.3389/fmicb.2018.02273

INTRODUCTION

Although *Mycobacterium abscessus* (*Mab*) was first discovered in 1953 (Moore and Frerichs, 1953), it was only recently that genomic sequencing differentiated the *Mab* complex into three subspecies: *M. abscessus sensu stricto*, *M. abscessus* subsp. *bolletii*, and *M. abscessus* subsp. *massiliense* (Adekambi et al., 2004, 2006; Viana-Niero et al., 2008). These subspecies exhibit differential susceptibilities to certain antibiotics and differential clinical outcomes.

Mab can cause pulmonary disease in addition to skin and soft tissue infections, lymphadenitis, and disseminated disease. *Mab* is sometimes considered a respiratory colonizer; however, in the setting of immunosuppression or structural lung disease, such as cystic fibrosis (CF) and bronchiectasis, *Mab* can cause chronic pulmonary disease. In CF patients, *Mab* infections are often incurable and associated with rapid lung function decline (Griffith et al., 2007; Esther et al., 2010; Benwill and Wallace, 2014). The cure rate for *Mab* lung disease is only 30–50% (Jarand et al., 2011), with a recent review reporting sputum culture conversion rates as low as 25% with antibiotic treatment alone (Diel et al., 2017).

Poor treatment outcomes of *Mab* infection have been ascribed to both innate and acquired drug resistance. *Mab* is intrinsically resistant to multiple antibiotic classes which has been attributed to various factors (Brown-Elliott and Wallace, 2002; Nessar et al., 2012; van Ingen et al., 2012). Acquired resistance has further limited therapeutic options (Flume, 2016). Current treatment regimens are suboptimal, as they require several months of intravenous multidrug therapy with potentially cytotoxic antibiotics and produce poor outcomes (Wallace et al., 1985; Floto et al., 2016).

In this review, we will briefly summarize *Mab* treatment recommendations, discuss unique molecular targets of β-lactams in *Mab,* and highlight emerging insights into how β-lactams may be leveraged to treat individuals infected with *Mab*.

CURRENT *Mab* TREATMENT RECOMMENDATIONS

The US Cystic Fibrosis Foundation and European Cystic Fibrosis Society recently developed consensus guidelines for management of *Mab* lung disease in CF patients (Floto et al., 2016). Similar to tuberculosis, *Mab* infection is treated with multidrug regimens divided into an intensive phase, followed by a continuation phase. Per recent guidelines, the intensive phase of *Mab* therapy should consist of an oral macrolide, combined with 3–12 weeks of intravenous amikacin, plus at least one of the following: intravenous cefoxitin, imipenem, or tigecycline (Floto et al., 2016). Guidelines for the continuation phase include a daily oral macrolide, inhaled amikacin, and two to three additional oral antibiotics, including minocycline, clofazimine, moxifloxacin, and linezolid.

Macrolides have historically been considered the backbone of treatment against *Mab*. They have relatively low toxicity, are orally bioavailable (Griffith et al., 2007; Floto et al., 2016), and exhibit consistent activity against *Mab in vitro* (Griffith et al., 2007). However, subspecies *abscessus* and *bolletii* harbor a functional *erm*(41) gene, which confers inducible macrolide resistance and can limit the effectiveness of this drug class. In contrast, subspecies *massiliense* carries a non-functional *erm*(41) gene (Nash et al., 2009), thus cannot exhibit inducible macrolide resistance and is associated with improved outcomes on macrolide-based regimens (Koh et al., 2011). Consequently, the CF guidelines recommend subspeciation of *Mab* complex, which many clinical laboratories are not equipped to perform routinely. Therefore, some CF centers prescribe initial treatment regimens comprised of intravenous amikacin plus either cefoxitin or imipenem, rather than a macrolide (Philley et al., 2016).

Cefoxitin and imipenem are currently the only two β-lactams included in the guidelines for treatment of *Mab* infections. This antibiotic class has been largely understudied against *Mab* and may be a potential untapped resource in combating this highly-resistant microbe.

MECHANISM OF ACTION OF β-LACTAMS AGAINST *Mab*

β-lactams are the most widely-used antibiotic class to treat bacterial infections (Hamad, 2010) and their safety and efficacy profiles have been well-established. There are five subclasses of β-lactams currently available in the clinical setting: penicillins, cephalosporins, monobactams, carbapenems, and penems. β-lactams have been studied extensively for treatment of drug-resistant *Mycobacterium tuberculosis* (*Mtb*) infections, which is summarized elsewhere (Story-Roller and Lamichhane, 2018). Certain β-lactam subclasses also exhibit activity against *Mab* (Lavollay et al., 2014; Kaushik et al., 2015; Lefebvre et al., 2016). While initial insights into the molecular mechanism of action of β-lactams against mycobacteria were gleaned largely from *Mtb*, recent studies have begun to elucidate the relationship between *Mab* and β-lactams (Lavollay et al., 2014; Lefebvre et al., 2016; Kumar et al., 2017a).

β-lactams exert their activity by inhibiting synthesis of an essential component of the bacterial cell wall, the peptidoglycan (PG) (Hartmann et al., 1972). The building block of PG is a disaccharide with a stem peptide comprised of four or five amino acids; specifically *N*-acetyl-glucosamine-*N*-acetyl-muramic acid-L-alanyl-D-glutaminyl-*meso*-diaminopimelyl-D-alanyl-D-alanine in *Mab* (Lavollay et al., 2011). Polymerization of disaccharides by transglycosylases and stem peptides by transpeptidases produces a three-dimensional macromolecule, the PG (**Figure 1**).

The dominant model of PG architecture was largely established by studies using model organisms, such as *E. coli*. According to this historical model, the final step of PG synthesis is catalyzed by D,D-transpeptidases (DDT), also known as penicillin binding proteins, which link the 4th amino acid of one stem peptide to the 3rd amino acid of the adjacent stem peptide, thereby generating a 4 →3-linked peptide network. However, as early as 1974, it became clear that the chemical architecture of mycobacterial PG, and therefore the enzymes necessary for its synthesis, were distinct from those described in the historical model. This study reported that stem peptides in the PG of *M. smegmatis, Mtb,* and *M. bovis* BCG were predominantly cross-linked with non-canonical linkages between the 3rd amino acid of one peptide and the 3rd amino acid of another (Wietzerbin et al., 1974). That same year, this group also demonstrated that the enzyme, L,D-transpeptidase (LDT), generated these 3 →3 linkages in *Streptococcus faecalis* (Coyette et al., 1974).

The first direct evidence demonstrating that stem peptides in *Mab* PG are predominantly cross-linked by 3 →3 linkages was reported in 2011 (Lavollay et al., 2011). Subsequently, five putative LDTs, Ldt_{Mab1-5}, were identified in *Mab* (Mattoo et al., 2017) and the first crystal structure of one of these enzymes, Ldt_{Mab2}, was described (Kumar et al., 2017a). These studies confirmed that *Mab* utilizes both LDTs and DDTs to generate 3 →3 and 4 →3 linkages between stem peptides, respectively (**Figure 1**). The majority of linkages in *Mab* are 3 →3, which suggests that LDTs are at least as important as DDTs for synthesis of its PG. Several studies report that genes involved in PG synthesis and remodeling are largely conserved across mycobacteria, implying a similar PG chemical composition, architecture, and metabolism (Sanders et al., 2014; Mattoo et al., 2017). A review of PG biosynthesis in *Mtb* by Pavelka et al. is recommended for further insight into mycobacterial PG biology (Pavelka et al., 2014).

LDTs ARE PREFERENTIALLY INHIBITED BY CARBAPENEMS AND CEPHALOSPORINS

β-lactams mimic the *C*-terminal end of the native stem peptide of PG, bind to the active site of transpeptidases, and irreversibly inhibit their enzymatic activity (Park and Strominger, 1957). As the historical model considered DDTs to be the only enzymes that synthesized PG, they were assumed to be the sole targets of β-lactams. The discovery of LDTs (Mainardi et al., 2005) prompted inquiry into whether β-lactams also interacted with this enzyme

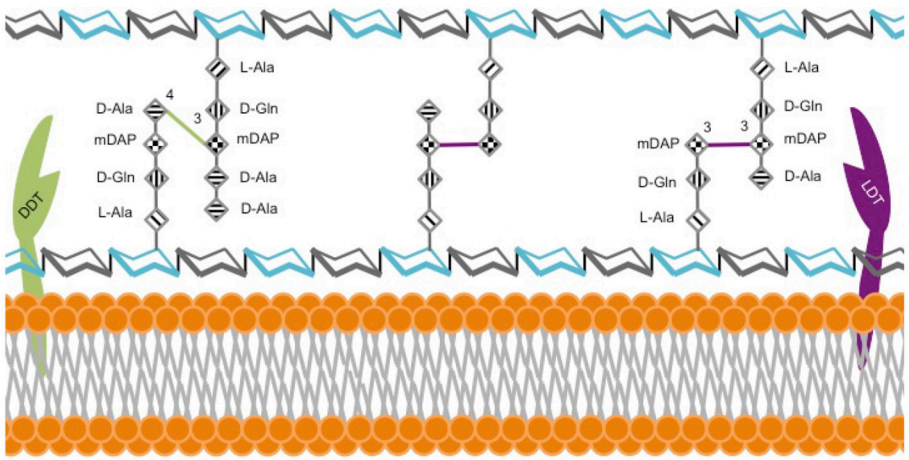

FIGURE 1 | Model of *M. abscessus* peptidoglycan. The hexagonal structures depict sugars *N*-acetylglucosamine (gray) and *N*-acetylmuramic acid (cyan). L-alanine (L-Ala), D-glutamine (D-Gln), *meso*-diaminopimelic acid (m-DAP) and D-alanine (D-Ala).

class. Subsequent studies have demonstrated that LDTs and DDTs of mycobacteria differ in their binding affinities to β-lactam subclasses and are consequently inhibited by different subclasses to varying degrees (Dubee et al., 2012; Kumar et al., 2017b). DDTs are effectively bound and inhibited by all β-lactam subclasses, whereas *Mab* LDTs are preferentially bound and inhibited by carbapenems and to a lesser extent by cephalosporins (Kumar et al., 2017a,b).

Although the crystal structures of LDTs of *Mab* bound to β-lactams are not yet available, several groups have reported crystal structures of LDTs of *Mtb* bound to carbapenems and penems (Kim et al., 2013; Li et al., 2013; Bianchet et al., 2017; Kumar et al., 2017b; Steiner et al., 2017). As LDTs and DDTs of *Mab* are differentially inhibited by β-lactam subclasses, comprehensive inhibition of PG synthesis will likely require simultaneous administration of multiple β-lactams belonging to different subclasses to optimally inhibit the two enzyme classes.

FACTORS THAT DETERMINE POTENCY OF β-LACTAMS AGAINST *Mab*

The major molecular factors limiting effectiveness of β-lactams against *Mab* are β-lactamase activity and the bacterial cell wall. Factors that commonly affect other antibiotic classes, including poor permeability of the cellular envelope, low affinity of antibiotic targets, drug efflux pumps, and chromosomally-encoded neutralizing enzymes, have been elegantly summarized elsewhere (Nessar et al., 2012; van Ingen et al., 2012).

β-Lactamases

The potent activity of the chromosomally-encoded β-lactamase, Bla_{Mab}, is primarily responsible for poor efficacy of β-lactams against *Mab* (Soroka et al., 2014). β-lactamases hydrolyze the β-lactam ring, thereby inactivating these antibiotics (Kasik et al., 1971). Not only does Bla_{Mab} degrade several β-lactams with significantly higher efficiency than BlaC of *Mtb*, Bla_{Mab} is not effectively inhibited by common β-lactamase inhibitors (BLI) clavulanate, tazobactam, and sulbactam (Soroka et al., 2017); agents that inhibit BlaC of *Mtb* (Wang et al., 2006). The observation that these BLIs do not reduce the minimum inhibitory concentration (MIC) of β-lactams against *Mab* in a whole-cell assay (Kaushik et al., 2017) is additional confirmation that β-lactamase activity in *Mab* is more robust than in *Mtb*. Subspecies *massiliense* harbors an additional β-lactamase, Bla_{Mmas} (Ramirez et al., 2017).

Bla_{Mab} is inactivated by avibactam (Dubee et al., 2015a), a recently-developed BLI whose core chemical composition differs from older BLIs and lacks a β-lactam ring (Coleman, 2011). Observations that avibactam reduces the MIC of several β-lactams against *Mab* provides further validation of its efficacy against both the Bla_{Mab} protein and whole-cell *Mab* (Dubee et al., 2015a; Kaushik et al., 2017; Lefebvre et al., 2017). A recent study showed avibactam not only inhibits β-lactamases but also inhibits LDTs (Edoo et al., 2018). A recombinant *Mab* strain lacking bla_{Mab} exhibited increased sensitivity to β-lactams and was rendered susceptible to amoxicillin and ceftaroline (Lefebvre et al., 2016). This study also observed that β-lactams plus avibactam exhibited similar efficacy against the parental *Mab* strain as compared to each drug alone against Δbla_{Mab}, suggesting that avibactam fully inhibits Bla_{Mab}. While Bla_{Mab} and Bla_{Mmas} hydrolyze penicillins and cephalosporins with similar efficacy, Bla_{Mmas} also exhibits mild carbapenemase activity, a potential concern as it suggests an evolutionary movement toward β-lactamases with extended spectra (Ramirez et al., 2017). This study also noted that Bla_{Mmas} is structurally similar to other acquired carbapenemases normally found in gram negative bacteria, such as KPC-2 and SFC-1. Avibactam activity against Bla_{Mmas} has not yet been assessed and further study is warranted.

Cell Wall

Mycobacteria possess an unusually thick cell wall composed of layers of complex hydrophobic molecules including fatty acids,

mycolic acids, lipoproteins, glycopeptidolipids (GPL), and largely insoluble PG and arabinogalactan layers. Although poorly-understood in *Mab*, epigenetic factors generating differential levels of these molecules, especially GPLs, are associated with two distinct colony morphotypes—rough and smooth—within a clonal population. The rough morphotype tends to be associated with higher rates of antimicrobial resistance, including against β-lactams (Cangelosi et al., 1999; Greendyke and Byrd, 2008; Lavollay et al., 2014). Additionally, glycosylation of lipoproteins limits permeability of the cell wall to antibiotics that inhibit PG synthesis (Becker et al., 2017). Cell wall porins are also partially responsible for β-lactam resistance, as they allow transport of small hydrophilic molecules across the membrane, which interact with targets within the cytoplasm to potentially activate expression of drug resistance genes (Nguyen and Thompson, 2006; Nessar et al., 2012).

ACTIVITY OF β-LACTAMS AGAINST *Mab*

We identified thirty-five studies with documented MIC ranges of β-lactams against clinical isolates of *Mab* globally (**Table 1**). These data serve to highlight the high degree of variability in observed MIC ranges among clinical isolates, even within each study, and this variability is partially why standardized treatment regimens against *Mab* are often not practical in the clinical setting. Imipenem and cefoxitin were the most commonly-tested β-lactams and nearly all studies included *Mab* strains that were resistant to these agents based on established MIC breakpoints (Woods et al., 2011). Only in four studies were all strains susceptible or intermediate to cefoxitin (Lee et al., 2012; Lavollay et al., 2014; Singh et al., 2014; Jeong et al., 2017). Two studies performed subspeciation and observed that all strains of subspecies *massiliense* and/or *bolletii* were either susceptible or intermediate to imipenem, whereas subspecies *abscessus* exhibited higher MICs to this drug (Lavollay et al., 2014; Singh et al., 2014). The reason for this is not currently known. Although seventeen studies also evaluated additional β-lactams, it is evident that this antibiotic class is largely understudied against *Mab*.

FURTHER POTENTIATION OF β-LACTAMS AGAINST *Mab* BY BLIs

Several studies have investigated the ability of BLIs to potentiate β-lactams against *Mab*, both *in vitro* and *in vivo*. The combination of amoxicillin and avibactam effectively reduced abscess formation and prolonged survival of zebrafish infected with *Mab* reference strain ATCC 19977 compared to amoxicillin alone (Dubee et al., 2015a). A subsequent study found that a combination of imipenem and avibactam also prolonged zebrafish survival compared to imipenem alone (Lefebvre et al., 2017). Avibactam also decreases the MIC of ceftaroline against *Mab* (Dubee et al., 2015b). Combinations of carbapenems and avibactam against clinical isolates of *Mab* showed that avibactam reduced MICs to therapeutically-achievable levels (Kaushik et al., 2017). The greatest MIC reductions were noted with tebipenem, ertapenem, and panipenem; demonstrating that avibactam can successfully overcome β-lactamase activity and further suggests that carbapenems, especially those developed after imipenem, such as doripenem, biapenem and tebipenem, have untapped potential for use against *Mab* (Kaushik et al., 2017).

SYNERGY STUDIES WITH β-LACTAMS AND OTHER DRUGS

As combination regimens are essential for clinical management of *Mab* infections, several studies have evaluated antibiotic synergy against *Mab* with mixed results (Cremades et al., 2009; Shen et al., 2010; Bastian et al., 2011; Choi et al., 2012; van Ingen et al., 2012; Oh et al., 2014; Singh et al., 2014; Ferro et al., 2016; Mukherjee et al., 2017; Aziz et al., 2018; Pryjma et al., 2018; Schwartz et al., 2018; Zhang et al., 2018). *In vitro* studies have shown variable synergy of β-lactams in combination with other drugs. One study found no evidence of synergy among combinations of either imipenem or ertapenem with various other antibiotics (Cremades et al., 2009). However, another study reported high levels of synergy against *Mab* clinical isolates when clofazimine and amikacin were combined with several β-lactam subclasses (Schwartz et al., 2018). In a final study, rifampin combined with either doripenem or biapenem significantly reduced the MICs of both drugs to within therapeutic levels, compared with each carbapenem alone (Kaushik et al., 2015).

DUAL β-LACTAMS FOR *Mab*

Given that different subclasses of β-lactams target distinct aspects of mycobacterial cell wall biosynthesis, *Mab* regimens that contain two β-lactams from different subclasses may have high efficacy in *Mab*. As mentioned above, mycobacterial DDTs are inhibited by all β-lactams, whereas LDTs are preferentially inhibited by carbapenems and cephalosporins (Kumar et al., 2017a,b). A combination of cefdinir and doripenem was observed to be synergistic against *Mab* 19977 (Kumar et al., 2017a), demonstrating that dual β-lactams have therapeutic potential against *Mab*. This promising finding warrants further investigation into the effects of dual β-lactams against clinical isolates of *Mab,* further potentiation with BLIs, and additional *in vivo* studies.

PRECLINICAL MODELS AND CLINICAL TRIALS

At least two groups have taken initiatives to develop animal models of *Mab* infection (Lerat et al., 2014; Obregon-Henao et al., 2015). Two studies have assessed efficacy of antibiotic treatment of mice infected with *Mab*, one of which included a β-lactam, cefoxitin. Lerat et al. assessed regimens containing clarithromycin, amikacin, or cefoxitin monotherapy vs. a three-drug combination in nude mice infected with *Mab* ATCC 19977. Cefoxitin monotherapy was equally effective as triple therapy, resulting in prolonged survival and reduced splenic bacillary

TABLE 1 | MIC range (ug/mL) for β-lactam antibiotics against clinical isolates of *M. abscessus*.

Description of *M. abscessus* clinical isolates	BIA	DOR	ERT	FAR	IPM	MEM	PAN	TEB	FEP	CMZ	FOX	CRO	AMC	References
3 isolates from US (TX)					8–64						16–512			Woods et al., 2000
8 isolates from Japan					8–16	8–16	4–16				16–>32		>32	Ito et al., 2003
92 isolates from Taiwan					1–>64	8–>64					8–256			Yang et al., 2003
48 isolates from South Korea					1–64						16–128			Lee et al., 2007
167 isolates from Taiwan					<0.5–>64					<1–>32	<2–>256			Huang et al., 2008
74 isolates from Korea					4–>16						<16–64			Park et al., 2008
45 isolates from South Korea					2–64						4–128			Jeon et al., 2009
108 isolates from US (UT)		16–>32	32–>32		2–>32	32–>32								Chihara et al., 2010
40 isolates from Taiwan					1–256						16–256			Huang et al., 2010
3 isolates from India (Mumbai)					64						256	64	32	Set et al., 2010
37 isolates from US (TX)					4–>16									Brown-Elliott et al., 2012
86 clinical isolates from Japan (63 subsp. abscessus, 23 massiliense)					2–64 4–64									Harada et al., 2012
6 isolates from Taiwan					32–64				>32		32–64	>64	>64	Lee et al., 2012
177 isolates from UK					<4–>16				>32		<16–>128	<8–>64	16–>32	Broda et al., 2013
43 isolates from France/Germany (15 subsp. abscessus, 14 massiliense, 14 bolletii)					<4–16 <4 <4–8						8–16 8–32 8–32			Lavollay et al., 2014
143 isolates from Japan (90 subsp. abscessus, 53 bolletii)					2–64 1–64				16–>256 1–>256			>32 1–>32	8–>256 2–>256	Yoshida et al., 2013
70 isolates from China					1–64						16–128			Zhuo et al., 2013
30 isolates from Brazil (6 subsp. abscessus, 24 bolletii)											32–256 32–256	>64 >64	>64 >64	Candido et al., 2014
70 isolates from China (Beijing) (45 subsp. abscessus, 25 bolletii)					<0.5–16 2–16						4–64 16–>256			Nie et al., 2014
14 isolates from Taiwan (4 subsp. abscessus, 10 bolletii)					16–32 16–64				32–>32 >32		32–128 32–64	>64 >64	>64 >64	Lee et al., 2014
67 isolates from France (42 subsp. abscessus, 21 massiliense, 24 bolletii)					4–32 4–8 4–16						2–64 2–8 2–64			Singh et al., 2014

(Continued)

TABLE 1 | Continued

Description of *M. abscessus* clinical isolates	BIA	DOR	ERT	FAR	IPM	MEM	PAN	TEB	FEP	CMZ	FOX	CRO	AMC	References
38 isolates from Australia (20 subsp. abscessus, 18 massiliense)					8–>64 4–>64				>32 >32		32–>128 32–>128	64–>64 64–>64	64–>64 >64	Chua et al., 2015
3 isolates from US (MD)	6.25–12.5	3.12–6.25	>25	40–80	>25	>25	>80	40–80						Kaushik et al., 2015
55 isolates from China						<4–>32				<16–>64	<16–>128		<8–>32	Pang et al., 2015
313 isolates from Singapore					4–>64						4–>128	‘		Tang et al., 2015
22 isolates from China					0.5–256						8–256			Li et al., 2016
78 isolates from US (TX) (67 subsp. abscessus, 11 massiliense)			4 4		8–16 8–16	8–16 8–16								Brown-Elliott et al., 2016
30 isolates from Iran					1–256	1–64					2–256			Heidarieh et al., 2016
165 isolates from France					4–>64				16–>32		8–128	8–>64	2–>64	Mougari et al., 2016
13 isolates from Japan				>2	2–16	8–64		4–>4	32–>64	8–64				Hatakeyama et al., 2017
20 isolates from South Korea (10 subsp. abscessus, 10 massiliense)					2–32 8–64						16–32 16–64			Jeong et al., 2017
28 isolates from US (MD)	16–128	8–128	64–>256	64–256	4–32	8–128	32–256	128–>256						Kaushik et al., 2017
67 isolates from Taiwan (28 subsp. abscessus, 38 massiliense, 1 bolletii)					8–>64 4–>64 32						16–128 16–>128 64			Lee et al., 2017
28 isolates from US (MD)					4–>64				16–>32		16–>128	32–>64	32–>64	Schwartz et al., 2018
64 isolates from US (FL)					<4–>16						<16–>128		16–>32	Sfeir et al., 2018

BIA, biapenem; DOR, doripenem; ERT, ertapenem; FAR, faropenem; IPM, imipenem; MEM, meropenem; PAN, panipenem; TEB, tebipenem; FEP, cefepime; CMZ, cefmetazole; FOX, cefoxitin; CRO, ceftriaxone; AMC, amoxicillin.

loads compared to untreated controls (Lerat et al., 2014). Several clinical trials assessing efficacy of non-β-lactam antibiotics against NTMs have been undertaken (clinicaltrials.gov). To date, there are no published clinical trials that have specifically investigated β-lactams for the treatment of *Mab*; however, we are hopeful that an increasing awareness of β-lactams as viable treatment options may lead to clinical trials with this class in the future.

FUTURE DIRECTIONS AND CONCLUSIONS

There is a dearth of research exploring β-lactams as potential treatments for *Mab*. Given the increasing prevalence of highly drug-resistant *Mab* isolates leading to poor clinical outcomes, new therapeutic approaches are needed to adequately treat these infections. Given our understanding of the differential mechanisms of β-lactam subclasses, and the ability of certain BLIs to overcome β-lactamase activity, currently-available β-lactams are a largely untapped resource for *Mab* treatment. Of the β-lactam subclasses, carbapenems/penems have the greatest activity against *Mab*, followed by cephalosporins, then penicillins. As noted above (Kumar et al., 2017a), it is likely that combinations of different β-lactam subclasses are required to fully inhibit PG synthesis in *Mab*. This insight may partially explain why prior studies evaluating β-lactams individually have not shown significant efficacy against this microbe. Further investigation may identify novel treatments utilizing combinations of β-lactams that optimally inhibit the distinct enzymatic targets present in *Mab*.

Appropriate selection of companion BLIs is another area in which β-lactams can be potentiated for use against *Mab*. Several studies have demonstrated efficacy of the BLI avibactam in inhibiting Bla_{Mab} activity, which is a major factor contributing to the high MIC of most β-lactams against *Mab*. However, avibactam is currently only available as a coformulated combination with ceftazidime, which itself does not appear to have activity against *Mab* (Dubee et al., 2015a; Kaushik et al., 2017). If avibactam were to be made available as an individual formulation, this would significantly increase its clinical usefulness, as regimens could be tailored to combine it with any β-lactam shown to be effective against a particular microbe or strain. Recently, two novel carbapenem-BLI combinations have been developed. These are meropenem-vaborbactam, which was recently FDA-approved for use against gram-negative organisms, and imipenem-relebactam, which is currently in phase II clinical trials (Zhanel et al., 2018). There are no published studies assessing efficacy of these BLIs against *Mab*, but their coformulation with carbapenems may confer greater potential for clinical use and further studies with these drugs are certainly warranted. It is possible that β-lactam-BLI combinations will become integral to effective treatment of drug-resistant *Mab* in the future. Additional animal studies as well as clinical trials with this drug class will be essential for the development of novel treatment regimens with improved clinical outcomes. Furthermore, repurposing already FDA-approved β-lactams for use against *Mab* may allow for expedited clinical implementation of regimens that show promise in preclinical models.

AUTHOR CONTRIBUTIONS

ES-R, EM, KC, and GL discussed relevant literature. ES-R and KC focused on clinical aspects of the literature and EM focused on the basic biology. ES-R, EM, KC, and GL wrote the manuscript.

ACKNOWLEDGMENTS

This work was supported by the Cystic Fibrosis Foundation grant LAMICH17GO and NIH grant R21 AI121805. ES-R was supported by the NIH T32 AI007291. The content is solely the responsibility of the authors and does not necessarily represent the official views of the Cystic Fibrosis Foundation or the National Institutes of Health.

REFERENCES

Adekambi, T., Berger, P., Raoult, D., and Drancourt, M. (2006). rpoB gene sequence-based characterization of emerging non-tuberculous mycobacteria with descriptions of *Mycobacterium bolletii* sp. nov., *Mycobacterium phocaicum* sp. nov. and *Mycobacterium aubagnense* sp. nov. *Int. J. Syst. Evol. Microbiol.* 56, 133–143. doi: 10.1099/ijs.0.63969-0

Adekambi, T., Reynaud-Gaubert, M., Greub, G., Gevaudan, M. J., La Scola, B., Raoult, D., et al. (2004). Amoebal coculture of "*Mycobacterium massiliense*" sp. nov. from the sputum of a patient with hemoptoic pneumonia. *J. Clin. Microbiol.* 42, 5493–5501. doi: 10.1128/JCM.42.12.5493-5501.2004

Aziz, D. B., Teo, J. W. P., Dartois, V., and Dick, T. (2018). Teicoplanin – tigecycline combination shows synergy against *Mycobacterium abscessus*. *Front. Microbiol.* 9:932. doi: 10.3389/fmicb.2018.00932

Bastian, S., Veziris, N., Roux, A. L., Brossier, F., Gaillard, J. L., Jarlier, V., et al. (2011). Assessment of clarithromycin susceptibility in strains belonging to the Mycobacterium abscessus group by erm(41) and rrl sequencing. *Antimicrob. Agents Chemother.* 55, 775–781. doi: 10.1128/AAC.00861-10

Becker, K., Haldimann, K., Selchow, P., Reinau, L. M., Dal Molin, M., and Sander, P. (2017). Lipoprotein glycosylation by protein-O-mannosyltransferase (MAB_1122c) contributes to low cell envelope permeability and antibiotic resistance of *Mycobacterium abscessus*. *Front. Microbiol.* 8:2123. doi: 10.3389/fmicb.2017.02123

Benwill, J. L., and Wallace, R. J. Jr. (2014). *Mycobacterium abscessus*: challenges in diagnosis and treatment. *Curr. Opin. Infect. Dis.* 27, 506–510. doi: 10.1097/QCO.0000000000000104

Bianchet, M. A., Pan, Y. H., Basta, L. A. B., Saavedra, H., Lloyd, E. P., and Lamichhane, G. (2017). Structural insight into the inactivation of *Mycobacterium tuberculosis* non-classical transpeptidase LdtMt2 by biapenem and tebipenem. *BMC Biochem.* 18:8. doi: 10.1186/s12858-017-0082-4

Broda, A., Jebbari, H., Beaton, K., Mitchell, S., and Drobniewski, F. (2013). Comparative drug resistance of *Mycobacterium abscessus* and *M. chelonae* isolates from patients with and without cystic fibrosis in the United Kingdom. *J. Clin. Microbiol.* 51, 217–223. doi: 10.1128/JCM.02260-12

Brown-Elliott, B. A., Killingley, J., Vasireddy, S., Bridge, L., and Wallace, R. J. Jr. (2016). *In vitro* comparison of ertapenem, meropenem, and imipenem against isolates of rapidly growing mycobacteria and nocardia by use of broth microdilution and Etest. *J. Clin. Microbiol.* 54, 1586–1592. doi: 10.1128/JCM.00298-16

Brown-Elliott, B. A., Mann, L. B., Hail, D., Whitney, C., and Wallace, R. J. Jr. (2012). Antimicrobial susceptibility of nontuberculous mycobacteria from eye infections. *Cornea* 31, 900–906. doi: 10.1097/ICO.0b013e31823f8bb9

Brown-Elliott, B. A., and Wallace, R. J. Jr. (2002). Clinical and taxonomic status of pathogenic nonpigmented or late-pigmenting rapidly growing mycobacteria. *Clin. Microbiol. Rev.* 15, 716–746. doi: 10.1128/CMR.15.4.716-746.2002

Candido, P. H., Nunes Lde, S., Marques, E. A., Folescu, T. W., Coelho, F. S., De Moura, V. C., et al. (2014). Multidrug-resistant nontuberculous mycobacteria isolated from cystic fibrosis patients. *J. Clin. Microbiol.* 52, 2990–2997. doi: 10.1128/JCM.00549-14

Cangelosi, G. A., Palermo, C. O., Laurent, J. P., Hamlin, A. M., and Brabant, W. H. (1999). Colony morphotypes on Congo red agar segregate along species and drug susceptibility lines in the *Mycobacterium avium*-intracellulare complex. *Microbiology* 145, 1317–1324. doi: 10.1099/13500872-145-6-1317

Chihara, S., Smith, G., and Petti, C. A. (2010). Carbapenem susceptibility patterns for clinical isolates of *Mycobacterium abscessus* determined by the Etest method. *J. Clin. Microbiol.* 48, 579–580. doi: 10.1128/JCM.01930-09

Choi, G. E., Min, K. N., Won, C. J., Jeon, K., Shin, S. J., and Koh, W. J. (2012). Activities of moxifloxacin in combination with macrolides against clinical isolates of *Mycobacterium abscessus* and *Mycobacterium massiliense*. *Antimicrob. Agents Chemother.* 56, 3549–3555. doi: 10.1128/AAC.00685-12

Chua, K. Y., Bustamante, A., Jelfs, P., Chen, S. C., and Sintchenko, V. (2015). Antibiotic susceptibility of diverse *Mycobacterium abscessus* complex strains in New South Wales, Australia. *Pathology* 47, 678–682. doi: 10.1097/PAT.0000000000000327

Coleman, K. (2011). Diazabicycloоctanes (DBOs): a potent new class of non-β-lactam β-lactamase inhibitors. *Curr. Opin. Microbiol.* 14, 550–555. doi: 10.1016/j.mib.2011.07.026

Coyette, J., Perkins, H. R., Polacheck, I., Shockman, G. D., and Ghuysen, J. M. (1974). Membrane-bound DD-carboxypeptidase and LD-transpeptidase of *Streptococcus faecalis* ATCC 9790. *Eur. J. Biochem.* 44, 459–468. doi: 10.1111/j.1432-1033.1974.tb03504.x

Cremades, R., Santos, A., Rodriguez, J. C., Garcia-Pachon, E., Ruiz, M., and Royo, G. (2009). *Mycobacterium abscessus* from respiratory isolates: activities of drug combinations. *J. Infect. Chemother.* 15, 46–48. doi: 10.1007/s10156-008-0651-Y

Diel, R., Ringshausen, F., Richter, E., Welker, L., Schmitz, J., and Nienhaus, A. (2017). Microbiological and clinical outcomes of treating non-*Mycobacterium avium* complex nontuberculous mycobacterial pulmonary disease: a systematic review and meta-analysis. *Chest* 152, 120–142. doi: 10.1016/j.chest.2017.04.166

Dubee, V., Bernut, A., Cortes, M., Lesne, T., Dorchene, D., Lefebvre, A. L., et al. (2015a). β-Lactamase inhibition by avibactam in *Mycobacterium abscessus*. *J. Antimicrob. Chemother.* 70, 1051–1058. doi: 10.1093/jac/dku510

Dubee, V., Soroka, D., Cortes, M., Lefebvre, A. L., Gutmann, L., Hugonnet, J. E., et al. (2015b). Impact of β-lactamase inhibition on the activity of ceftaroline against *Mycobacterium tuberculosis* and *Mycobacterium abscessus*. *Antimicrob. Agents Chemother.* 59, 2938–2941. doi: 10.1128/AAC.05080-14

Dubee, V., Triboulet, S., Mainardi, J. L., Etheve-Quelquejeu, M., Gutmann, L., Marie, A., et al. (2012). Inactivation of *Mycobacterium tuberculosis* L,D-transpeptidase Ldt_{Mt1} by carbapenems and cephalosporins. *Antimicrob. Agents Chemother.* 56, 4189–4195. doi: 10.1128/AAC.00665-12

Edoo, Z., Iannazzo, L., Compain, F., Li De La Sierra Gallay, I., Van Tilbeurgh, H., Fonvielle, M., et al. (2018). Synthesis of avibactam derivatives and activity on β-lactamases and peptidoglycan biosynthesis enzymes of mycobacteria. *Chemistry* 24, 8081–8086. doi: 10.1002/chem.201800923

Esther, C. R. Jr., Esserman, D. A., Gilligan, P., Kerr, A., and Noone, P. G. (2010). Chronic *Mycobacterium abscessus* infection and lung function decline in cystic fibrosis. *J. Cyst. Fibros.* 9, 117–123. doi: 10.1016/j.jcf.2009.12.001

Ferro, B. E., Srivastava, S., Deshpande, D., Pasipanodya, J. G., Van Soolingen, D., Mouton, J. W., et al. (2016). Failure of the amikacin, cefoxitin, and clarithromycin combination regimen for treating pulmonary *Mycobacterium abscessus* infection. *Antimicrob. Agents Chemother.* 60, 6374–6376. doi: 10.1128/AAC.00990-16

Floto, R. A., Olivier, K. N., Saiman, L., Daley, C. L., Herrmann, J. L., Nick, J. A., et al. (2016). US cystic fibrosis foundation and European Cystic Fibrosis Society consensus recommendations for the management of non-tuberculous mycobacteria in individuals with cystic fibrosis. *Thorax* 71, i1–22. doi: 10.1136/thoraxjnl-2015-207360

Flume, P. A. (2016). US cystic fibrosis foundation and European Cystic Fibrosis Society consensus recommendations for the management of non-tuberculous mycobacteria in individuals with cystic fibrosis. *J. Cyst. Fibros.* 15, 139–140. doi: 10.1016/S1569-1993(16)00018-7

Greendyke, R., and Byrd, T. F. (2008). Differential antibiotic susceptibility of *Mycobacterium abscessus* variants in biofilms and macrophages compared to that of planktonic bacteria. *Antimicrob. Agents Chemother.* 52, 2019–2026. doi: 10.1128/AAC.00986-07

Griffith, D. E., Aksamit, T., Brown-Elliott, B. A., Catanzaro, A., Daley, C., Gordin, F., et al. (2007). An official ATS/IDSA statement: diagnosis, treatment, and prevention of nontuberculous mycobacterial diseases. *Am. J. Respir. Crit. Care Med.* 175, 367–416. doi: 10.1164/rccm.200604-571ST

Hamad, B. (2010). The antibiotics market. *Nat. Rev. Drug Discov.* 9, 675–676. doi: 10.1038/nrd3267

Harada, T., Akiyama, Y., Kurashima, A., Nagai, H., Tsuyuguchi, K., Fujii, T., et al. (2012). Clinical and microbiological differences between *Mycobacterium abscessus* and *Mycobacterium massiliense* lung diseases. *J. Clin. Microbiol.* 50, 3556–3561. doi: 10.1128/JCM.01175-12

Hartmann, R., Holtje, J. V., and Schwarz, U. (1972). Targets of penicillin action in *Escherichia coli*. *Nature* 235, 426–429. doi: 10.1038/235426a0

Hatakeyama, S., Ohama, Y., Okazaki, M., Nukui, Y., and Moriya, K. (2017). Antimicrobial susceptibility testing of rapidly growing mycobacteria isolated in Japan. *BMC Infect. Dis.* 17:197. doi: 10.1186/s12879-017-2298-8

Heidarieh, P., Mirsaeidi, M., Hashemzadeh, M., Feizabadi, M. M., Bostanabad, S. Z., Nobar, M. G., et al. (2016). *In vitro* antimicrobial susceptibility of nontuberculous mycobacteria in Iran. *Microb. Drug Resist.* 22, 172–178. doi: 10.1089/mdr.2015.0134

Huang, T. S., Lee, S. S., Hsueh, P. R., Tsai, H. C., Chen, Y. S., Wann, S. R., et al. (2008). Antimicrobial resistance of rapidly growing mycobacteria in western Taiwan: SMART program 2002. *J. Formos. Med. Assoc.* 107, 281–287. doi: 10.1016/S0929-6646(08)60088-1

Huang, Y. C., Liu, M. F., Shen, G. H., Lin, C. F., Kao, C. C., Liu, P. Y., et al. (2010). Clinical outcome of *Mycobacterium abscessus* infection and antimicrobial susceptibility testing. *J. Microbiol. Immunol. Infect.* 43, 401–406. doi: 10.1016/S1684-1182(10)60063-1

Ito, K., Hashimoto, K., and Ogata, H. (2003). Activity of cephems and carbapenems against clinically isolated *Mycobacterium abscessus*. *Kekkaku* 78, 587–590. doi: 10.11400/kekkaku1923.78.587

Jarand, J., Levin, A., Zhang, L., Huitt, G., Mitchell, J. D., and Daley, C. L. (2011). Clinical and microbiologic outcomes in patients receiving treatment for *Mycobacterium abscessus* pulmonary disease. *Clin. Infect. Dis.* 52, 565–571. doi: 10.1093/cid/ciq237

Jeon, K., Kwon, O. J., Lee, N. Y., Kim, B. J., Kook, Y. H., Lee, S. H., et al. (2009). Antibiotic treatment of *Mycobacterium abscessus* lung disease: a retrospective analysis of 65 patients. *Am. J. Respir. Crit. Care Med.* 180, 896–902. doi: 10.1164/rccm.200905-0704OC

Jeong, S. H., Kim, S. Y., Huh, H. J., Ki, C. S., Lee, N. Y., Kang, C. I., et al. (2017). Mycobacteriological characteristics and treatment outcomes in extrapulmonary *Mycobacterium abscessus* complex infections. *Int. J. Infect. Dis.* 60, 49–56. doi: 10.1016/j.ijid.2017.05.007

Kasik, J. E., Severson, C. D., Stearns, N. A., and Thompson, J. S. (1971). Immunologic distinction of mycobacterial β-lactamase. *J. Lab. Clin. Med.* 78, 982.

Kaushik, A., Gupta, C., Fisher, S., Story-Roller, E., Galanis, C., Parrish, N., et al. (2017). Combinations of avibactam and carbapenems exhibit enhanced potencies against drug-resistant *Mycobacterium abscessus*. *Fut. Microbiol.* 12, 473–480. doi: 10.2217/fmb-2016-0234

Kaushik, A., Makkar, N., Pandey, P., Parrish, N., Singh, U., and Lamichhane, G. (2015). Carbapenems and rifampin exhibit synergy against *Mycobacterium tuberculosis* and *Mycobacterium abscessus*. *Antimicrob. Agents Chemother.* 59, 6561–6567. doi: 10.1128/AAC.01158-15

Kim, H. S., Kim, J., Im, H. N., Yoon, J. Y., An, D. R., Yoon, H. J., et al. (2013). Structural basis for the inhibition of *Mycobacterium tuberculosis* L,D-transpeptidase by meropenem, a drug effective against extensively drug-resistant strains. *Acta Crystallogr. D Biol. Crystallogr.* 69, 420–431. doi: 10.1107/S0907444912048998

Koh, W. J., Jeon, K., Lee, N. Y., Kim, B. J., Kook, Y. H., Lee, S. H., et al. (2011). Clinical significance of differentiation of *Mycobacterium massiliense* from *Mycobacterium abscessus*. *Am. J. Respir. Crit. Care Med.* 183, 405–410. doi: 10.1164/rccm.201003-0395OC

Kumar, P., Chauhan, V., Silva, J. R. A., Lameira, J., D'andrea, F. B., Li, S. G., et al. (2017a). *Mycobacterium abscessus* L,D-transpeptidases are susceptible to inactivation by carbapenems and cephalosporins but not penicillins. *Antimicrob. Agents Chemother.* 61:e00866-17. doi: 10.1128/AAC.00866-17

Kumar, P., Kaushik, A., Lloyd, E. P., Li, S. G., Mattoo, R., Ammerman, N. C., et al. (2017b). Non-classical transpeptidases yield insight into new antibacterials. *Nat. Chem. Biol.* 13, 54–61. doi: 10.1038/nchembio.2237

Lavollay, M., Dubee, V., Heym, B., Herrmann, J. L., Gaillard, J. L., Gutmann, L., et al. (2014). *In vitro* activity of cefoxitin and imipenem against *Mycobacterium abscessus* complex. *Clin. Microbiol. Infect.* 20, O297–O300. doi: 10.1111/1469-0691.12405

Lavollay, M., Fourgeaud, M., Herrmann, J. L., Dubost, L., Marie, A., Gutmann, L., et al. (2011). The peptidoglycan of *Mycobacterium abscessus* is predominantly cross-linked by L,D-transpeptidases. *J. Bacteriol.* 193, 778–782. doi: 10.1128/JB.00606-10

Lee, M. C., Sun, P. L., Wu, T. L., Wang, L. H., Yang, C. H., Chung, W. H., et al. (2017). Antimicrobial resistance in *Mycobacterium abscessus* complex isolated from patients with skin and soft tissue infections at a tertiary teaching hospital in Taiwan. *J. Antimicrob. Chemother.* 72, 2782–2786. doi: 10.1093/jac/dkx212

Lee, M. R., Cheng, A., Lee, Y. C., Yang, C. Y., Lai, C. C., Huang, Y. T., et al. (2012). CNS infections caused by *Mycobacterium abscessus* complex: clinical features and antimicrobial susceptibilities of isolates. *J. Antimicrob. Chemother.* 67, 222–225. doi: 10.1093/jac/dkr420

Lee, M. R., Ko, J. C., Liang, S. K., Lee, S. W., Yen, D. H., and Hsueh, P. R. (2014). Bacteraemia caused by *Mycobacterium abscessus* subsp. *abscessus* and *M. abscessus* subsp. *bolletii*: clinical features and susceptibilities of the isolates. *Int. J. Antimicrob. Agents* 43, 438–441. doi: 10.1016/j.ijantimicag.2014.02.007

Lee, S. M., Kim, J., Jeong, J., Park, Y. K., Bai, G. H., Lee, E. Y., et al. (2007). Evaluation of the broth microdilution method using 2,3-diphenyl-5-thienyl-(2)-tetrazolium chloride for rapidly growing mycobacteria susceptibility testing. *J. Korean Med. Sci.* 22, 784–790. doi: 10.3346/jkms.2007.22.5.784

Lefebvre, A. L., Dubee, V., Cortes, M., Dorchene, D., Arthur, M., and Mainardi, J. L. (2016). Bactericidal and intracellular activity of β-lactams against *Mycobacterium abscessus*. *J. Antimicrob. Chemother.* 71, 1556–1563. doi: 10.1093/jac/dkw022

Lefebvre, A. L., Le Moigne, V., Bernut, A., Veckerle, C., Compain, F., Herrmann, J. L., et al. (2017). Inhibition of the β-lactamase Bla_{Mab} by avibactam improves the *in vitro* and *in vivo* efficacy of imipenem against *Mycobacterium abscessus*. *Antimicrob. Agents Chemother.* 61:e02440-16. doi: 10.1128/AAC.02440-16

Lerat, I., Cambau, E., Roth Dit Bettoni, R., Gaillard, J. L., Jarlier, V., Truffot, C., et al. (2014). *In vivo* evaluation of antibiotic activity against *Mycobacterium abscessus*. *J. Infect. Dis.* 209, 905–912. doi: 10.1093/infdis/jit614

Li, W. J., Li, D. F., Hu, Y. L., Zhang, X. E., Bi, L. J., and Wang, D. C. (2013). Crystal structure of L,D-transpeptidase Ldt_{Mt2} in complex with meropenem reveals the mechanism of carbapenem against *Mycobacterium tuberculosis*. *Cell Res.* 23, 728–731. doi: 10.1038/cr.2013.53

Li, Y. M., Tong, X. L., Xu, H. T., Ju, Y., Cai, M., and Wang, C. (2016). Prevalence and antimicrobial susceptibility of *Mycobacterium abscessus* in a General Hospital, China. *Biomed. Environ. Sci.* 29, 85–90. doi: 10.3967/bes2016.009

Mainardi, J. L., Fourgeaud, M., Hugonnet, J. E., Dubost, L., Brouard, J. P., Ouazzani, J., et al. (2005). A novel peptidoglycan cross-linking enzyme for a β-lactam-resistant transpeptidation pathway. *J. Biol. Chem.* 280, 38146–38152. doi: 10.1074/jbc.M507384200

Mattoo, R., Lloyd, E. P., Kaushik, A., Kumar, P., Brunelle, J. L., Townsend, C. A., et al. (2017). Ldt_{Mav2}, a nonclassical transpeptidase and susceptibility of *Mycobacterium avium* to carbapenems. *Fut. Microbiol.* 12, 595–607. doi: 10.2217/fmb-2016-0208

Moore, M., and Frerichs, J. B. (1953). An unusual acid-fast infection of the knee with subcutaneous, abscess-like lesions of the gluteal region; report of a case with a study of the organism, *Mycobacterium abscessus*. *J. Invest. Dermatol.* 20, 133–169. doi: 10.1038/jid.1953.18

Mougari, F., Amarsy, R., Veziris, N., Bastian, S., Brossier, F., Bercot, B., et al. (2016). Standardized interpretation of antibiotic susceptibility testing and resistance genotyping for *Mycobacterium abscessus* with regard to subspecies and erm41 sequevar. *J. Antimicrob. Chemother.* 71, 2208–2212. doi: 10.1093/jac/dkw130

Mukherjee, D., Wu, M. L., Teo, J. W. P., and Dick, T. (2017). Vancomycin and clarithromycin show synergy against *Mycobacterium abscessus in vitro*. *Antimicrob. Agents Chemother.* 61: e01298-17. doi: 10.1128/AAC.01298-17

Nash, K. A., Brown-Elliott, B. A., and Wallace, R. J. Jr. (2009). A novel gene, erm(41), confers inducible macrolide resistance to clinical isolates of *Mycobacterium abscessus* but is absent from *Mycobacterium chelonae*. *Antimicrob. Agents Chemother.* 53, 1367–1376. doi: 10.1128/AAC.01275-08

Nessar, R., Cambau, E., Reyrat, J. M., Murray, A., and Gicquel, B. (2012). *Mycobacterium abscessus*: a new antibiotic nightmare. *J. Antimicrob Chemother.* 67, 810–818. doi: 10.1093/jac/dkr578

Nguyen, L., and Thompson, C. J. (2006). Foundations of antibiotic resistance in bacterial physiology: the mycobacterial paradigm. *Trends Microbiol* 14, 304–312. doi: 10.1016/j.tim.2006.05.005

Nie, W., Duan, H., Huang, H., Lu, Y., Bi, D., and Chu, N. (2014). Species identification of *Mycobacterium abscessus* subsp. *abscessus* and *Mycobacterium abscessus* subsp. *bolletii* using rpoB and hsp65, and susceptibility testing to eight antibiotics. *Int. J. Infect. Dis.* 25, 170–174. doi: 10.1016/j.ijid.2014.02.014

Obregon-Henao, A., Arnett, K. A., Henao-Tamayo, M., Massoudi, L., Creissen, E., Andries, K., et al. (2015). Susceptibility of *Mycobacterium abscessus* to antimycobacterial drugs in preclinical models. *Antimicrob. Agents Chemother.* 59, 6904–6912. doi: 10.1128/AAC.00459-15

Oh, C. T., Moon, C., Park, O. K., Kwon, S. H., and Jang, J. (2014). Novel drug combination for *Mycobacterium abscessus* disease therapy identified in a Drosophila infection model. *J. Antimicrob. Chemother.* 69, 1599–1607. doi: 10.1093/jac/dku024

Pang, H., Li, G., Zhao, X., Liu, H., Wan, K., and Yu, P. (2015). Drug susceptibility testing of 31 antimicrobial agents on rapidly growing mycobacteria isolates from China. *Biomed. Res. Int.* 2015:419392. doi: 10.1155/2015/419392

Park, J. T., and Strominger, J. L. (1957). Mode of action of penicillin. *Science* 125, 99–101. doi: 10.1126/science.125.3238.99

Park, S., Kim, S., Park, E. M., Kim, H., Kwon, O. J., Chang, C. L., et al. (2008). *In vitro* antimicrobial susceptibility of *Mycobacterium abscessus* in Korea. *J. Korean Med. Sci.* 23, 49–52. doi: 10.3346/jkms.2008.23.1.49

Pavelka, M. S. Jr., Mahapatra, S., and Crick, D. C. (2014). Genetics of peptidoglycan biosynthesis. *Microbiol. Spectr.* 2:MGM2-0034-2013. doi: 10.1128/microbiolspec.MGM2-0034-2013

Philley, J. V., Degroote, M. A., Honda, J. R., Chan, M. M., Kasperbauer, S., Walter, N. D., et al. (2016). Treatment of non-tuberculous mycobacterial lung disease. *Curr. Treat Options Infect. Dis.* 8, 275–296. doi: 10.1007/s40506-016-0086-4

Pryjma, M., Burian, J., and Thompson, C. J. (2018). Rifabutin acts in synergy and is bactericidal with frontline *Mycobacterium abscessus* antibiotics clarithromycin and tigecycline, suggesting a potent treatment combination. *Antimicrob. Agents Chemother.* 62:e00283-18. doi: 10.1128/AAC.00283-18

Ramirez, A., Ruggiero, M., Aranaga, C., Cataldi, A., Gutkind, G., De Waard, J. H., et al. (2017). Biochemical characterization of β-lactamases from *Mycobacterium abscessus* complex and genetic environment of the β-lactamase-encoding gene. *Microb. Drug Resist.* 23, 294–300. doi: 10.1089/mdr.2016.0047

Sanders, A. N., Wright, L. F., and Pavelka, M. S. Jr. (2014). Genetic characterization of mycobacterial L,D-transpeptidases. *Microbiology* 160, 1795–1806. doi: 10.1099/mic.0.078980-0

Schwartz, M., Fisher, S., Story-Roller, E., Lamichhane, G., and Parrish, N. (2018). Activities of dual combinations of antibiotics against multidrug-resistant nontuberculous mycobacteria recovered from patients with cystic fibrosis. *Microb. Drug Resist.* doi: 10.1089/mdr.2017.0286. [Epub ahead of print].

Set, R., Rokade, S., Agrawal, S., and Shastri, J. (2010). Antimicrobial susceptibility testing of rapidly growing mycobacteria by microdilution–experience of a tertiary care centre. *Indian J. Med. Microbiol.* 28, 48–50. doi: 10.4103/0255-0857.58729

Sfeir, M., Walsh, M., Rosa, R., Aragon, L., Liu, S. Y., Cleary, T., et al. (2018). *Mycobacterium abscessus* complex infections: a retrospective cohort study. *Open Forum Infect. Dis.* 5:ofy022. doi: 10.1093/ofid/ofy022

Shen, G. H., Wu, B. D., Hu, S. T., Lin, C. F., Wu, K. M., and Chen, J. H. (2010). High efficacy of clofazimine and its synergistic effect with amikacin against rapidly growing mycobacteria. *Int. J. Antimicrob. Agents* 35, 400–404. doi: 10.1016/j.ijantimicag.2009.12.008

Singh, S., Bouzinbi, N., Chaturvedi, V., Godreuil, S., and Kremer, L. (2014). *In vitro* evaluation of a new drug combination against clinical isolates belonging to the *Mycobacterium abscessus* complex. *Clin. Microbiol. Infect.* 20, O1124–O1127. doi: 10.1111/1469-0691.12780

Soroka, D., Dubee, V., Soulier-Escrihuela, O., Cuinet, G., Hugonnet, J. E., Gutmann, L., et al. (2014). Characterization of broad-spectrum *Mycobacterium abscessus* class A β-lactamase. *J. Antimicrob. Chemother.* 69, 691–696. doi: 10.1093/jac/dkt410

Soroka, D., Ourghanlian, C., Compain, F., Fichini, M., Dubee, V., Mainardi, J. L., et al. (2017). Inhibition of β-lactamases of mycobacteria by avibactam and clavulanate. *J. Antimicrob. Chemother.* 72, 1081–1088. doi: 10.1093/jac/dkw546

Steiner, E. M., Schneider, G., and Schnell, R. (2017). Binding and processing of β-lactam antibiotics by the transpeptidase Ldt_{Mt2} from *Mycobacterium tuberculosis*. *FEBS J.* 284, 725–741. doi: 10.1111/febs.14010

Story-Roller, E., and Lamichhane, G. (2018). Have we realized the full potential of β-lactams for treating drug-resistant TB? *IUBMB Life* 70, 881–888. doi: 10.1002/iub.1875.

Tang, S. S., Lye, D. C., Jureen, R., Sng, L. H., and Hsu, L. Y. (2015). Rapidly growing mycobacteria in Singapore, 2006–2011. *Clin. Microbiol. Infect.* 21, 236–241. doi: 10.1016/j.cmi.2014.10.018

van Ingen, J., Boeree, M. J., Van Soolingen, D., and Mouton, J. W. (2012). Resistance mechanisms and drug susceptibility testing of nontuberculous mycobacteria. *Drug Resist. Updat* 15, 149–161. doi: 10.1016/j.drup.2012.04.001

Viana-Niero, C., Lima, K. V., Lopes, M. L., Rabello, M. C., Marsola, L. R., Brilhante, V. C., et al. (2008). Molecular characterization of *Mycobacterium massiliense* and *Mycobacterium bolletii* in isolates collected from outbreaks of infections after laparoscopic surgeries and cosmetic procedures. *J. Clin. Microbiol.* 46, 850–855. doi: 10.1128/JCM.02052-07

Wallace, R. J. Jr., Swenson, J. M., Silcox, V. A., and Bullen, M. G. (1985). Treatment of nonpulmonary infections due to *Mycobacterium fortuitum* and *Mycobacterium chelonei* on the basis of *in vitro* susceptibilities. *J. Infect. Dis.* 152, 500–514. doi: 10.1093/infdis/152.3.500

Wang, F., Cassidy, C., and Sacchettini, J. C. (2006). Crystal structure and activity studies of the *Mycobacterium tuberculosis* β-lactamase reveal its critical role in resistance to β-lactam antibiotics. *Antimicrob. Agents Chemother.* 50, 2762–2771. doi: 10.1128/AAC.00320-06

Wietzerbin, J., Das, B. C., Petit, J. F., Lederer, E., Leyh-Bouille, M., and Ghuysen, J. M. (1974). Occurrence of D-alanyl-(D)-meso-diaminopimelic acid and meso-diaminopimelyl-meso-diaminopimelic acid interpeptide linkages in the peptidoglycan of Mycobacteria. *Biochemistry* 13, 3471–3476. doi: 10.1021/bi00714a008

Woods, G. L., B. A., Brown-Elliot, P. S., Conville, E. P., Desmond, G. S., Hall, G., et al. (2011). *Susceptibility Testing of Mycobacteria, Nocardiae, and Other Aerobic Actinomycetes, 2nd Edn.* Wayne, PA: Clinical and Laboratory Standards Institute.

Woods, G. L., Bergmann, J. S., Witebsky, F. G., Fahle, G. A., Boulet, B., Plaunt, M., et al. (2000). Multisite reproducibility of Etest for susceptibility testing of *Mycobacterium abscessus*, *Mycobacterium chelonae*, and *Mycobacterium fortuitum*. *J. Clin. Microbiol.* 38, 656–661.

Yang, S. C., Hsueh, P. R., Lai, H. C., Teng, L. J., Huang, L. M., Chen, J. M., et al. (2003). High prevalence of antimicrobial resistance in rapidly growing mycobacteria in Taiwan. *Antimicrob. Agents Chemother.* 47, 1958–1962. doi: 10.1128/AAC.47.6.1958-1962.2003

Yoshida, S., Tsuyuguchi, K., Suzuki, K., Tomita, M., Okada, M., Hayashi, S., et al. (2013). Further isolation of *Mycobacterium abscessus* subsp. *abscessus* and subsp. *bolletii* in different regions of Japan and susceptibility of these isolates to antimicrobial agents. *Int. J. Antimicrob. Agents* 42, 226–231. doi: 10.1016/j.ijantimicag.2013.04.029

Zhanel, G. G., Lawrence, C. K., Adam, H., Schweizer, F., Zelenitsky, S., Zhanel, M., et al. (2018). Imipenem-relebactam and meropenem-vaborbactam: two novel carbapenem-β-lactamase inhibitor combinations. *Drugs* 78, 65–98. doi: 10.1007/s40265-017-0851-9

Zhang, Z., Lu, J., Song, Y., and Pang, Y. (2018). *In vitro* activity between linezolid and other antimicrobial agents against *Mycobacterium abscessus* complex. *Diagn. Microbiol. Infect. Dis.* 90, 31–34. doi: 10.1016/j.diagmicrobio.2017.09.013

Zhuo, F. L., Sun, Z. G., Li, C. Y., Liu, Z. H., Cai, L., Zhou, C., et al. (2013). Clinical isolates of *Mycobacterium abscessus* in Guangzhou area most possibly from the environmental infection showed variable susceptibility. *Chin. Med. J. (Engl).* 126, 1878–1883.

Conflict of Interest Statement: The authors declare that the research was conducted in the absence of any commercial or financial relationships that could be construed as a potential conflict of interest.

frontiers in Microbiology

ORIGINAL RESEARCH
published: 10 October 2018
doi: 10.3389/fmicb.2018.02417

Novel Screen to Assess Bactericidal Activity of Compounds Against Non-replicating *Mycobacterium abscessus*

*Bryan J. Berube, Lina Castro, Dara Russell, Yulia Ovechkina and Tanya Parish**

TB Discovery Research, Infectious Disease Research Institute, Seattle, WA, United States

Mycobacterium abscessus infections are increasing worldwide. Current drug regimens are largely ineffective, yet the current development pipeline for *M. abscessus* is alarmingly sparse. Traditional discovery efforts for *M. abscessus* assess the capability of a new drug to inhibit bacterial growth under nutrient-rich growth conditions, but this does not predict the impact when used in the clinic. The disconnect between *in vitro* and *in vivo* activity is likely due to the genetic and physiological adaptation of the bacteria to the environmental conditions encountered during infection; these include low oxygen tension and nutrient starvation. We sought to fill a gap in the drug discovery pipeline by establishing an assay to identify novel compounds with bactericidal activity against *M. abscessus* under non-replicating conditions. We developed and validated a novel screen using nutrient starvation to generate a non-replicating state. We used alamarBlue® to measure metabolic activity and demonstrated this correlates with bacterial viability under these conditions. We optimized key parameters and demonstrated reproducibility. Using this assay, we determined that niclosamide was bactericidal against non-replicating bacilli, highlighting its potential to be included in *M. abscessus* regimens. In contrast, most other drugs currently used in the clinic for *M. abscessus* infections, were completely inactive, potentially explaining their poor efficacy. Thus, our assay allows for rapid identification of bactericidal compounds in a model using conditions that are more relevant *in vivo*. This screen can be used in a high-throughput way to identify novel agents with properties that promise an increase in efficacy, while also shortening treatment times.

Keywords: *Mycobacterium abscessus*, nutrient starvation, high-throughput screen, drug discovery, non-replicating, niclosamide

OPEN ACCESS

Edited by:
Thomas Dick,
Rutgers, The State University of New Jersey, United States

Reviewed by:
Giovanna Poce,
Università degli Studi di Roma "La Sapienza", Italy
Umayal Lakshmanan,
*Agency for Science, Technology and Research (A*STAR), Singapore*

***Correspondence:**
Tanya Parish
Tanya.Parish@idri.org

Specialty section:
This article was submitted to Antimicrobials, Resistance and Chemotherapy, a section of the journal Frontiers in Microbiology

Received: *18 May 2018*
Accepted: *20 September 2018*
Published: *10 October 2018*

Citation:
Berube BJ, Castro L, Russell D, Ovechkina Y and Parish T (2018) Novel Screen to Assess Bactericidal Activity of Compounds Against Non-replicating Mycobacterium abscessus. Front. Microbiol. 9:2417. doi: 10.3389/fmicb.2018.02417

INTRODUCTION

Infections by nontubercular mycobacteria (NTMs), including *Mycobacterium avium* complex and *Mycobacterium abscessus* complex, are a growing public health concern (Nessar et al., 2012). Traditionally considered an opportunistic pathogen, *M. abscessus* predominantly causes pulmonary disease in patients with cystic fibrosis (CF), chronic obstructive pulmonary disease (COPD), or bronchiectasis. However, recent trends suggest *M. abscessus* infection among otherwise healthy

individuals is also on the rise with recent studies showing a 3% increase in prevalence per year (Prevots et al., 2010). Additionally, many cases likely go misdiagnosed as *Mycobacterium tuberculosis* infections due to their similarity in disease presentation and colony morphology upon microscopic examination of sputum smears. This not only underestimates the number of *M. abscessus* infections worldwide but also leads to improper antibacterial treatment (Brown-Elliott et al., 2012).

The increase in NTM infections is troubling in part due to NTMs being particularly refractory to antibiotic treatment with *M. abscessus* resistant to all front-line anti-tuberculosis drugs (Brown-Elliott and Philley, 2017). The American Thoracic Society/Infectious Disease Society of America guidelines state that no current drug regimens are proven efficacious against pulmonary *M. abscessus* infection (Griffith et al., 2007). Drug regimens can be tailored to individuals based on laboratory drug susceptibility testing and individual tolerance to drugs, but generally include a macrolide-based antimicrobial in combination with intravenously administered agents (CF Foundation Clinical Care Guidelines; Griffith et al., 2007). Current guidelines from the Center for Disease Control and Prevention list amikacin, cefoxitin, and clarithromycin as the leading drugs for treatment of *M. abscessus* infection (Lee et al., 2015). These regimens are not only ineffective (29–58% cure rate) but also lead to considerable toxic side-effects due to a typical course of treatment lasting 18–24 months (Jeon et al., 2009; Jarand et al., 2011; Koh et al., 2017; Wu et al., 2018). Antibiotic treatment alone also leads to higher relapse rates than highly invasive surgical procedures involving resection of infected tissue (Griffith et al., 1993; Jarand et al., 2011). These highly invasive procedures should be seen as a last resort, but due to the failure of current drug regimens, these procedures are often the only realistic path to a relapse-free cure (Griffith et al., 2007).

Failure of current drug regimens against *M. abscessus* is likely multi-factorial. One factor is intrinsic antibiotic resistance (Nessar et al., 2012). *M. abscessus* has a waxy cell wall composed of peptidoglycan, arabinogalactan, and long-chain mycolic acids, which is relatively impermeable to antibacterial compounds (Jarlier and Nikaido, 1990; Brennan and Nikaido, 1995). *M. abscessus* also possesses efflux pumps capable of exporting drug, as well as enzymes capable of modifying antibiotics or their targets (Nasiri et al., 2017). These factors make it difficult for drugs not only to enter the cell but also to remain effective if they get past the cell wall. In the few small-scale screens for compounds active against *M. abscessus*, screens suffered from low hit rates compared to other mycobacterial species (Chopra et al., 2011; Gupta et al., 2017; Low et al., 2017).

A major factor in the failure of current drug regimens is the diversity of niches and physiological states encountered by the bacterium during infection, which are not adequately captured with current *in vitro* model systems. The disease pathology of *M. abscessus* infection is similar to that of *M. tuberculosis* (Griffith et al., 2007; Koh, 2017). *M. abscessus* is phagocytosed by macrophages in the lung, but prevents phagosomal acidification and can survive for an extended time (Laencina et al., 2018). During this time physiological and transcriptional changes can lead to phenotypic resistance (tolerance) to drugs (Adams et al., 2011; Larsson et al., 2012). As the infection progresses, NTMs are contained in necrotic granulomas and eventually survive extracellularly in caseum, where they likely experience both low oxygen tensions and/or nutrient starvation (Wu et al., 2018). In *M. tuberculosis*, these conditions lead to a non-replicating state controlled by the DosR regulon, which is characterized by low metabolic activity and enhanced resistance to antibiotics (Wayne and Hayes, 1996; Xie et al., 2005; Leistikow et al., 2010; Sarathy et al., 2018). In this state, *M. tuberculosis* maintains a basal level of metabolic activity to ensure bacterial viability, and the electron transport chain (ETC) is required to maintain the proton-motive force and generate ATP (Rao et al., 2008; Cook et al., 2014).

The ability of *M. abscessus* to survive nutrient starvation or low oxygen tensions has not been established. However, *M. abscessus* does contain a DosR regulon (Gerasimova et al., 2011) and is known to survive in biofilms in the lung of CF patients (Qvist et al., 2015). Additionally, other NTMs have been shown to establish latent infections in patients with subsequent reactivation to active disease (Rosenmeier et al., 1991; Tsilimparis et al., 2014). Together with the similarity in disease progression to TB disease, we believe it is highly likely *M. abscessus* can survive in patients in a dormant state. Previous screens against *M. abscessus* specifically addressed drug activity against actively growing, metabolically active bacteria (Chopra et al., 2011; Gupta et al., 2017; Low et al., 2017). Such efforts will miss compounds which are active against non-replicating or metabolically inactive cells.

The current state of the drug pipeline for NTMs was recently reviewed (Wu et al., 2018), highlighting the need for novel screens to address different physiological conditions encountered by NTMs during infection, including nutrient starvation. Our study aimed to fill part of that gap by developing and validating a novel assay to identify compounds with bactericidal activity against non-replicating *M. abscessus* generated by nutrient starvation. This will allow screening of compound libraries for compounds with sterilizing capabilities under a physiological state likely to be relevant to *in vivo* infection. We demonstrate that a number of drugs currently employed to treat *M. abscessus* infection are inactive in this assay, highlighting the need for drug discovery and development campaigns specifically targeted against *M. abscessus*.

MATERIALS AND METHODS

Mycobacterium abscessus Culture

Mycobacterium abscessus strain # 103 was purchased directly from BEI Resources (NIAID, NIH) and was cultured in Middlebrook 7H9 medium containing 10% v/v OADC (Oleic Acid, Albumin, Dextrose, Catalase; Becton Dickinson) supplement and 0.05% v/v Tween 80 (7H9-OADC-Tw). Cultures were maintained standing at 37°C. Viable bacteria were determined by colony forming units by plating 10-fold serial dilutions onto Middlebrook 7H10 agar plus 10% v/v OADC supplement. For starvation, mid-log cultures were harvested and resuspended in phosphate-buffered saline (PBS) + 0.05% v/v

Tyloxapol (PBS-Tyl) at an OD_{590} of 0.4. Cultures were incubated shaking at 100 rpm for 96 h at 37°C before use. Cultures were harvested and resuspended in PBS-Tyl to an OD_{590} of 0.5 and 50 μL was dispensed into 96-well plates using a Multidrop Combi.

Preparation of Assay Plates

Compound plates were prepared as described (Ollinger et al., 2013). In brief, 10 mM stock solutions in DMSO were prepared as a 10-point twofold serial dilution in 96-well plates using a Biomek 3000. For the final assay plate, 50 μL of PBS-Tyl was dispensed into each well of a 96-well plate (μCLEAR plates Greiner). Compounds or controls (2 μL of each) were added to each well using a Biomek 4000. The final assay plate contained DMSO as a negative inhibition control and 25 μM niclosamide as a positive control for bacterial killing (**Figure 1**). The final concentration of DMSO in all wells was 2%. Plates were inoculated with 50 μL of bacterial culture; 50 μL of PBS-Tyl was dispensed into column 12 (contamination control). Assay plates were incubated in a humidified incubator for 48 h at 37°C after which 50 μL of 20% v/v alamarBlue® in PBS-Tyl (Bio-Rad) was added using a Multidrop Combi. Plates were incubated at 37°C for 24 h and relative fluorescent units (RFUs) measured at Ex560/Em590 using a BioTek Synergy 4.

Data Analysis and Statistics

The mean value from the buffer-only wells (background) was subtracted. The coefficient of variance (CV) was calculated as:

$$CV = \frac{\frac{SD}{\sqrt{n}}}{AVG}$$

Z′ was calculated by the following formula:

$$Z' = \frac{\left(\mathrm{AVG_{max}} - \frac{3\mathrm{SD_{max}}}{\sqrt{n}}\right) - \left(\mathrm{AVG_{min}} + \frac{3\mathrm{SD_{min}}}{\sqrt{n}}\right)}{\mathrm{AVG_{max}} - \mathrm{AVG_{min}}}$$

where AVG is the average RFU, SD is standard deviation, and *n* is the number of controls per plate. The signal-to-background (S/B) ratio is calculated as the mean of the maximum signal wells divided by the mean of the background (no bacteria) wells.

RESULTS

Rationale and Establishment of Assay Parameters

We sought to develop a screen to identify compounds with bactericidal activity against non-replicating *M. abscessus*. We used nutrient starvation to generate a non-replicating state, since this is relevant *in vivo* and is technically feasible. We first established the ability of *M. abscessus* to survive under nutrient starvation. We grew *M. abscessus* to mid-log phase and resuspended in buffer to induce complete nutrient starvation. After 96 h, we adjusted the cultures to an OD_{590} of 0.25 (~2.5×10^7 CFU) and monitored survival. After a further 72 h, bacterial counts were $2.6 \pm 0.4 \times 10^7$ CFU/mL (n = 6, three biological replicates), indicating *M. abscessus* is capable of surviving under non-replicating, nutrient starvation conditions. Our data confirmed that there was no increase in viable bacteria during this time and thus the bacilli are in a non-replicating state.

We needed a rapid measure of bacterial viability which was amenable to high throughput and required minimal manipulation. Since the ETC is essential under nutrient-starvation, we predicted that respiration would be a good measure of bacterial viability. We tested alamarBlue®, which uses the reducing power of the cell to convert resazurin to resorufin, since we could use fluorescence as the readout. We tested the correlation between bacterial viability, measured by optical density, and respiratory output measured by alamarBlue® turnover. We generated nutrient-starved bacteria after incubation in PBS-Tyl and then measured OD_{590} and RFU for twofold serial dilutions, starting at an OD_{590} of 1.0. Optical density correlated in a linear fashion to respiratory output up to an OD_{590} of 0.25 (**Figure 2A** and **Supplementary Figure 1**). Above this level, the RFU signal flattened, likely due to a complete turnover of any alamarBlue® present in the wells or having reached the upper limit of detection of the microplate reader. We confirmed a linear correlation between fluorescence and colony forming units, which determined that a reduction of alamarBlue® signal by 90% is equivalent to ≥1-log reduction in CFU (**Figure 2B** and **Supplementary Figure 2**). We varied a number of parameters (data not shown) and selected the key parameters for the inoculum as 50 μL of a starting culture with a final OD_{590} in the assay plate of 0.25 for assay validation. We established the remaining parameters of the assay as starvation for 96 h, exposure to compounds for 48 h, and incubation with alamarBlue® for 24 h. These parameters gave us sufficient signal to background and signal to noise ratios.

Reference Compound Activity Under Nutrient–Starvation Conditions

We next sought a control compound which would have rapid bactericidal activity against *M. abscessus* under starvation conditions. We selected a number of compounds based on current treatment guidelines for *M. abscessus* infection, as well as compounds known to be active against non-replicating bacteria. Surprisingly, almost all the compounds we tested were inactive, including most of those currently used as part of *M. abscessus* drug regimens (**Table 1**). Only three of the tested compounds inhibited alamarBlue® turnover by at least 90%, i.e., MBC_{90} (**Table 1**). Kanamycin and amikacin had MBC_{90} values of 39 and 16 μM, respectively, while niclosamide was the most effective compound with a MBC_{90} of 8.4 μM (**Table 1**) and maximal activity at 25 μM (**Figure 3**).

Confirmation of Assay Serving as a Measure of Bactericidal Activity

To confirm our screen's ability to serve as a measure of bacterial killing, we assayed *M. abscessus* survival over time in the presence of niclosamide. Concentrations of niclosamide below the MBC_{90} (3.1and 6.3 μM) had minimal activity (**Figure 4A**), while concentrations above the MBC_{90} had >1-log reduction in CFU

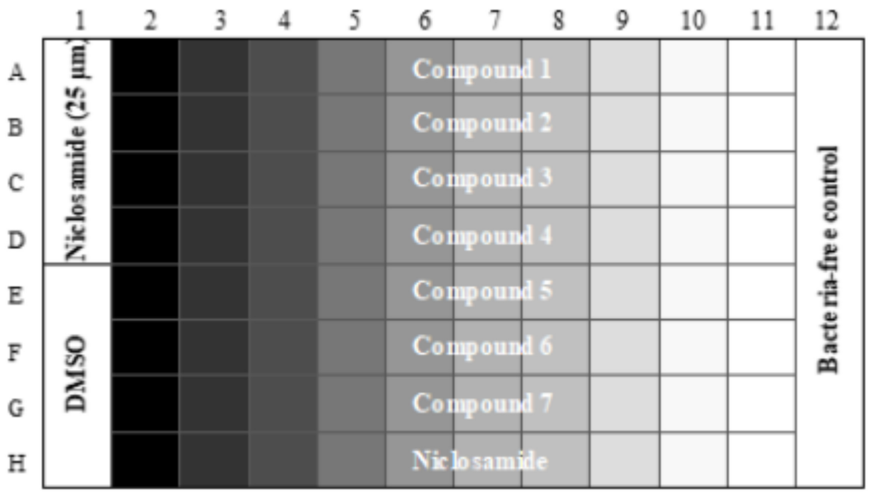

FIGURE 1 | Final assay plate layout. Column 1 contains positive control (Niclosamide) in Rows A–D and negative control (DMSO) in Rows E–H. Column 12 contains bacteria-free control wells. Compounds are tested in Rows A–G as 10-pt serial twofold dilutions. Row H contains a control twofold dilution of niclosamide starting at 25 μM in Column 2.

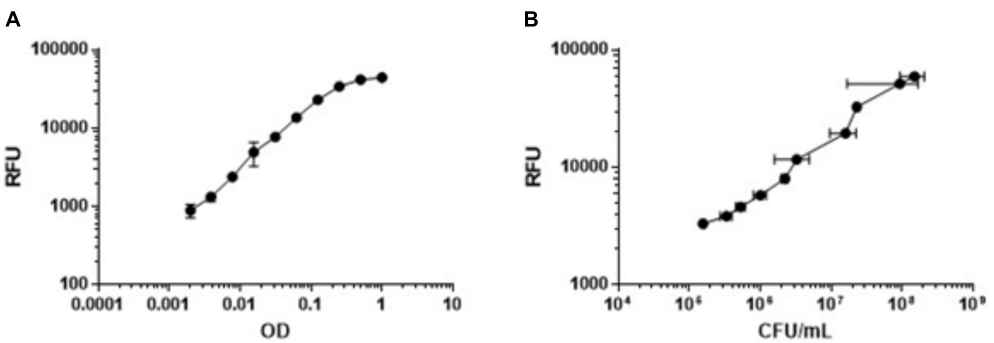

FIGURE 2 | Metabolic activity measured by alamarBlue® correlates with OD_{590} and bacterial viability. Nutrient-starved bacteria were generated in PBS-Tyl. Bacteria were serially diluted twofold and metabolic activity was measured by alamarBlue turnover after 24 h (RFU). **(A)** OD was measured at 590 nm. **(B)** Bacterial viability was measured by determining CFU. Data are average ± SD of three replicates.

within three days; 25 μM reduced bacterial viability by 1.5-log CFU (**Figure 4A**). This data corresponds to the concentration–response curve seen in **Figure 3**, where 25 μM niclosamide caused the greatest reduction in alamarBlue® turnover. At higher concentrations (50 and 100 μM), niclosamide had reduced activity due to solubility issues. We measured alamarBlue® turnover each day. **Figure 4B** shows bacterial viability correlates in a linear fashion with RFU in our assay (R^2 = 0.59). Over time, niclosamide killed *M. abscessus*, and there was a concomitant decrease in alamarBlue® turnover (**Figure 4B**). These data confirm that alamarBlue® can be used as a readout for bacterial viability.

Validation of High-Throughput Screen

We tested the reproducibility of our screen by testing for intra-experiment and inter-experiment variability (Iversen et al., 2004). We ran three separate experiments each containing duplicate plates with full 96-well plates of the maximum signal (2% DMSO), minimum signal (25 μM niclosamide) and dose–response curves (niclosamide 10-point, twofold dilutions). Inter- and intra-assay variability were low (**Figure 5A**). The average CV across all DMSO control plates was 11%, while average CV for niclosamide plates was only 5% (**Table 2**), both well below the minimum standard for CV of 20% specified in the assay guidance manual (Iversen et al., 2004). The curves for niclosamide were consistent within and across runs (**Figure 5B**) with an average MBC_{90} of 9.1 ± 3.2 μM and MBC_{50} of 5.0 ± 0.9 μM across 48 replicates and an average Z′ score for these plates of 0.84 ± 0.16 (n = 6; **Table 2**). Thus, the assay is reproducible and suitable for high throughput screening.

DISCUSSION

The drug development pipeline for *M. abscessus* is extremely sparse at a time when infections worldwide are on the rise

TABLE 1 | Activity of drugs against non-replicating *M. abscessus*.

Compound	MBC_{90} (μM)
Niclosamide	8.4 ± 0.5
Amikacin	16 ± 0.5
Kanamycin	39 ± 2.3
Ebselen	>100
Cefoxitin	>200
Tiacumicin	>200
Rifampicin	>200
Clarithromycin	>200
Imipenem	>200
Linezolid	>200
Azithromycin	>200
Ethambutol	>200
Ciprofloxacin	>200
Levofloxacin	>200
Moxifloxacin	>200

Nutrient-starved bacteria were exposed to compounds for 48 h, alamarBlue was added, and RFU measured after 24 h. MBC_{90} is the concentration required to reduce alamarBlue turnover by 90% as determined by the Gompertz equation. Data are mean ± SD of at least two independent biological replicates.

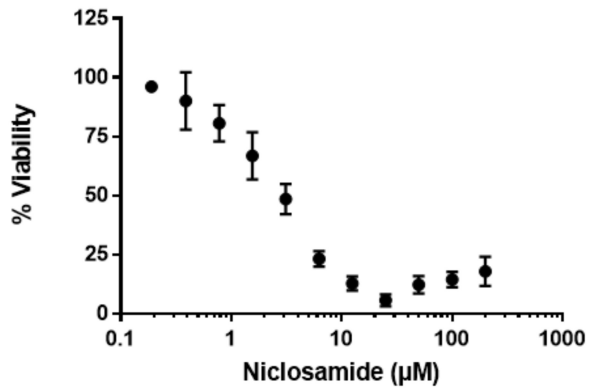

FIGURE 3 | Niclosamide has potent activity against non-replicating bacteria. Nutrient-starved bacteria were exposed to nicolsamide for 72 h. alamarBlue® was added, and RFU measured after 24 h. RFUs were normalized to the DMSO control to express % viability. Data are mean ± SD of four independent biological replicates.

and current drug regimens are highly ineffective (Griffith et al., 2007). Recently, a call was issued for the development of novel assays to assess the efficacy of compounds against *M. abscessus* under various physiological states with the hope these assays might lead to hits that are more physiologically relevant, and thus more likely to be successful in the clinic. In this work, we describe one such assay that specifically identifies compounds that are bactericidal to nutrient-starved *M. abscessus*.

Nearly all tested compounds were completely inactive against non-replicating *M. abscessus* (**Table 1**). This could be due to an inability of the compounds to penetrate the *M. abscessus* cell wall or to their inactivity under nutrient-starvation conditions. Surprisingly, we found only one of the drugs recommended by the Center for Disease Control and Prevention to treat *M. abscessus* was active in this assay. Amikacin, an aminoglycoside inhibitor of the 30S ribosomal subunit, had a MBC_{90} of 16 μM, indicating this drug actively targets non-replicating *M. abscessus*. On the other hand, cefoxitin and clarithromycin were completely inactive (**Table 1**). Inactivity of cefoxitin is potentially explained by its mechanism of action. As a beta-lactam antibiotic, cefoxitin targets the cell wall of actively dividing cells, a potential liability against non-replicating *M. abscessus*. Clarithromycin was also inactive in this assay, despite being a protein synthesis inhibitor like amikacin. One possible explanation is the known induction of clarithromycin resistance in some *M. abscessus* isolates (Benwill and Wallace, 2014; Koh, 2017). Whatever the mechanism, it is troubling two of the three recommended treatments for *M. abscessus* are inactive. It is tempting to speculate the general inactivity of the tested compounds against non-replicating *M. abscessus* may play a role in the failure of these drugs to adequately treat patients. More work needs to be done to assess their efficacy under other physiological states likely encountered by *M. abscessus* during infection.

We did identify two other compounds capable of killing non-replicating *M. abscessus*, namely kanamycin and niclosamide. Kanamycin, like amikacin, is an aminoglycoside inhibitor of ribosomal translocation (Misumi and Tanaka, 1980) and is commonly used as a second-line drug in regimens to treat multidrug-resistant tuberculosis (MDR-TB). However, kanamycin has considerable negative side effects shared with amikacin (Lane et al., 1977; Jiang et al., 2017). First, kanamycin is not orally bioavailable; it is given as an injectable drug, making its delivery more difficult than drugs available as pills. Second, patients undergoing prolonged aminoglycoside treatment can experience nephrotoxicity, as well as significant hearing loss, and thus must undergo repeated testing to determine whether treatment can continue (Ariano et al., 2008; Al-Malky et al., 2015; Garinis et al., 2017). With current drug regimens for *M. abscessus* lasting 18–24 months, kanamycin is not an ideal drug to be included in a new regimen.

Niclosamide was the most effective compound in this assay, causing 1–2 log-CFU kill in just three days (**Figure 4**). Niclosamide, an anti-tapeworm drug, is an inhibitor of oxidative phosphorylation, potentially working by inhibiting production of adenosine triphosphate (ATP) (Frayha et al., 1997; Chen et al., 2018). Niclosamide is an essential medicine according to the World Health Organization and is available as a chewable tablet (World Health Organization [WHO], 2017), although there are issues with solubility, absorption, and distribution to tissues (Chen et al., 2018). Recent work has been done to improve pharmacokinetic (PK) and pharmacodynamic (PD) properties of niclosamide, which could lead to its use to treat various bacterial infections (Mook et al., 2015). Our work suggests niclosamide could be used as part of a drug regimen to treat *M. abscessus*. If PK/PD properties were suitable to provide adequate exposure in the

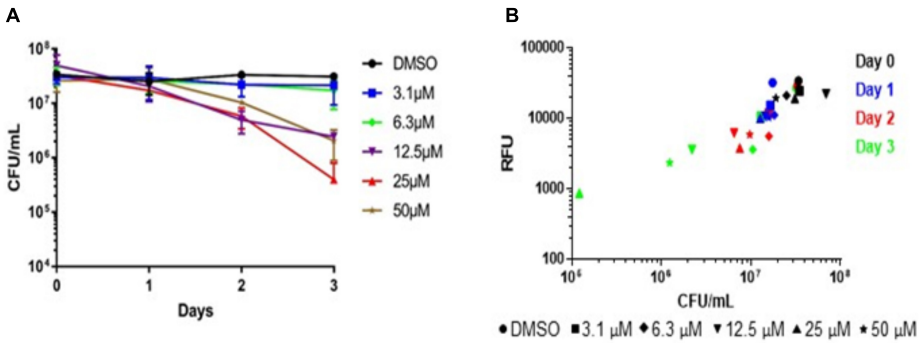

FIGURE 4 | Metabolic activity correlates with bactericidal activity. Nutrient-starved bacteria were exposed to compounds for 24–72 h, alamarBlue® was added and RFU measured after 24 h. Aliquots from the same samples were used to determine: **(A)** Bacterial viability (CFU; data are the average ± SD of 2 biological replicates); **(B)** metabolic activity.

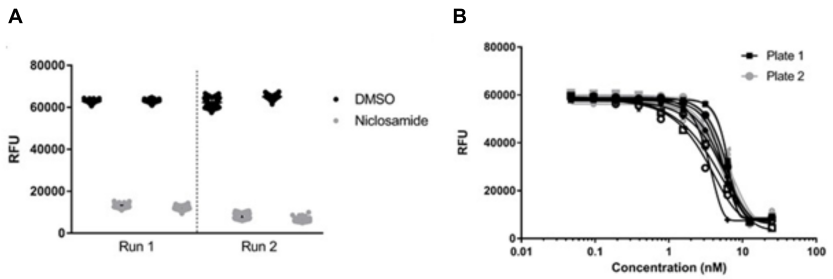

FIGURE 5 | Validation of high-throughput screen. **(A)** Metabolic activity measured by alamarBlue® turnover was plotted for individual plates from each of two separate biological runs. **(B)** Activity of niclosamide was determined in 16 technical replicates across two different plates. Line of best fit was plotted by the Gompertz equation. Data are representative of three independent biological replicates.

TABLE 2 | Assay reproducibility and robustness testing.

Run	Plate	Z′	% CV DMSO	% CV Niclosamide	S/B
1	1	0.82	1	6	23
	2	0.94	1	7	23
2	1	0.90	3	16	22
	2	0.90	2	7	23
3	1	0.50	13	15	18
	2	0.96	11	15	18
Mean		0.84	5	11	21
SD		0.16	5	4	2

The final assay was run in three independent runs containing two plates each of minimum signal (2% DMSO), maximum signal (25 μM niclosamide), and niclosamide CRCs with positive and negative controls. Nutrient-starved bacteria were exposed to compounds for 48 h, alamarBlue® was added, and RFU measured after 24 h. Z′, % CV, and signal/background (S/B) ratio were calculated for each experimental run.

lungs, niclosamide might be able to target non-replicating bacilli residing in granulomas or caseum and help clear the infection.

CONCLUSION

In conclusion, we have developed a new assay to find anti-mycobacterial agents with activity against non-replicating bacilli, where positive hits can be followed up for bactericidal activity by plating for CFU. This assay allows us to screen for compounds that are bactericidal within a short period (3 days), increasing the possibility that we can identify rapidly bactericidal agents that could have an impact on the treatment of *M. abscessus* infections. We used this assay to determine that niclosamide is a rapidly bactericidal agent against non-replicating *M. abscessus*.

AUTHOR CONTRIBUTIONS

BB and TP conceived the experiments. BB, LC, YO, and TP designed all the experiments. BB, LC, DR performed the

experiments. BB, LC, and TP wrote the manuscript. All authors edited and approved the final manuscript.

FUNDING

This work was funded in part by NIAID of the National Institutes of Health under award number R01AI099188 and by the Bill and Melinda Gates Foundation, under grant OPP1024038. The content is solely the responsibility of the authors and does not necessarily represent the official views of the National Institutes of Health.

SUPPLEMENTARY MATERIAL

The Supplementary Material for this article can be found online at: https://www.frontiersin.org/articles/10.3389/fmicb.2018.02417/full#supplementary-material

REFERENCES

Adams, K. N., Takaki, K., Connolly, L. E., Wiedenhoft, H., Winglee, K., Humbert, O., et al. (2011). Drug tolerance in replicating mycobacteria mediated by a macrophage-induced efflux mechanism. *Cell* 145, 39–53. doi: 10.1016/j.cell.2011.02.022

Al-Malky, G., Dawson, S. J., Sirimanna, T., Bagkeris, E., and Suri, R. (2015). High-frequency audiometry reveals high prevalence of aminoglycoside ototoxicity in children with cystic fibrosis. *J. Cyst. Fibros.* 14, 248–254. doi: 10.1016/j.jcf.2014.07.009

Ariano, R. E., Zelenitsky, S. A., and Kassum, D. A. (2008). Aminoglycoside-induced vestibular injury: maintaining a sense of balance. *Ann. Pharmacother.* 42, 1282–1289. doi: 10.1345/aph.1L001

Benwill, J. L., and Wallace, R. J. Jr. (2014). *Mycobacterium abscessus*: challenges in diagnosis and treatment. *Curr. Opin. Infect. Dis.* 27, 506–510. doi: 10.1097/QCO.0000000000000104

Brennan, P. J., and Nikaido, H. (1995). The envelope of mycobacteria. *Annu. Rev. Biochem.* 64, 29–63. doi: 10.1146/annurev.bi.64.070195.000333

Brown-Elliott, B. A., Nash, K. A., and Wallace, R. J. Jr. (2012). Antimicrobial susceptibility testing, drug resistance mechanisms, and therapy of infections with nontuberculous mycobacteria. *Clin. Microbiol. Rev.* 25, 545–582. doi: 10.1128/CMR.05030-11

Brown-Elliott, B. A., and Philley, J. V. (2017). Rapidly growing mycobacteria. *Microbiol. Spectr.* 5, 1–19. doi: 10.1128/microbiolspec.TNMI7-0027-2016

Chen, W., Mook, R. A., Premont, R. T., and Wang, J. (2018). Niclosamide_ beyond an antihelminthic drug. *Cell. Signal.* 41, 89–96. doi: 10.1016/j.cellsig.2017.04.001

Chopra, S., Matsuyama, K., Hutson, C., and Madrid, P. (2011). Identification of antimicrobial activity among FDA-approved drugs for combating *Mycobacterium abscessus* and *Mycobacterium chelonae*. *J. Antimicrob. Chemother.* 66, 1533–1536. doi: 10.1093/jac/dkr154

Cook, G. M., Hards, K., Vilchèze, C., Hartman, T., and Berney, M. (2014). Energetics of respiration and oxidative phosphorylation in mycobacteria. *Microbiol. Spectr.* 2, 1–20. doi: 10.1128/microbiolspec.MGM2-0015-2013.f1

Frayha, G. J., Smyth, J. D., Gobert, J. G., and Savel, J. (1997). The mechanisms of action of antiprotozoal and anthelmintic drugs in man. *Gen. Pharmacol.* 28, 273–299. doi: 10.1016/S0306-3623(96)00149-8

Garinis, A. C., Cross, C. P., Srikanth, P., Carroll, K., Feeney, M. P., Keefe, D. H., et al. (2017). The cumulative effects of intravenous antibiotic treatments on hearing in patients with cystic fibrosis. *J. Cyst. Fibros.* 16, 401–409. doi: 10.1016/j.jcf.2017.01.006

Gerasimova, A., Kazakov, A. E., Arkin, A. P., Dubchak, I., and Gelfand, M. S. (2011). Comparative genomics of the dormancy regulons in mycobacteria. *J. Bacteriol.* 193, 3446–3452. doi: 10.1128/JB.00179-11

Griffith, D. E., Aksamit, T., Brown-Elliott, B. A., Catanzaro, A., Daley, C., Gordin, F., et al. (2007). American thoracic society documents an official ATS/IDSA statement: diagnosis, treatment, and prevention of nontuberculous mycobacterial diseases. *Am. J. Respir. Crit. Care Med.* 175, 367–416. doi: 10.1164/rccm.200604-571ST

Griffith, D. E., Girard, W. M., and Wallace, R. J. (1993). Clinical features of pulmonary disease caused by rapidly growing mycobacteria an analysis of 154 patients. *Am. Rev. Respir. Dis.* 147, 1271–1278. doi: 10.1164/ajrccm/147.5.1271

Gupta, R., Netherton, M., Byrd, T. F., and Rohde, K. H. (2017). Reporter-based assays for high-throughput drug screening against *Mycobacterium abscessus*. *Front. Microbiol.* 8:2204. doi: 10.3389/fmicb.2017.02204

Iversen, P. W., Beck, B., Chen, Y.-F., Dere, W., Devanarayan, V., Eastwood, B. J., et al. (2004). "HTS assay validation," in *Assay Guidance Manual*, eds G. S. Sittampalam, N. P. Coussens, K. Brimacombe, A. Grossman, M. Arkin, D. Auld, et al. (Rockville, MD: Bethesda).

Jarand, J., Levin, A., Zhang, L., Huitt, G., Mitchell, J. D., and Daley, C. L. (2011). Clinical and microbiologic outcomes in patients receiving treatment for *Mycobacterium abscessus* pulmonary disease. *Clin. Infect. Dis.* 52, 565–571. doi: 10.1093/cid/ciq237

Jarlier, V., and Nikaido, H. (1990). Permeability barrier to hydrophilic solutes in *Mycobacterium chelonei*. *J. Bacteriol.* 172, 1418–1423. doi: 10.1128/jb.172.3.1418-1423.1990

Jeon, K., Kwon, O. J., Lee, N. Y., Kim, B.-J., Kook, Y.-H., Lee, S.-H., et al. (2009). Antibiotic treatment of *Mycobacterium abscessus* lung disease a retrospective analysis of 65 patients. *Am. J. Respir. Crit. Care Med.* 180, 896–902. doi: 10.1164/rccm.200905-0704OC

Jiang, M., Karasawa, T., and Steyger, P. S. (2017). Aminoglycoside-induced cochleotoxicity: a review. *Front. Cell. Neurosci.* 11:308. doi: 10.3389/fncel.2017.00308

Koh, W.-J. (2017). Nontuberculous mycobacteria—overview. *Microbiol. Spectr.* 5, 1–7. doi: 10.1128/microbiolspec.TNMI7-0024-2016

Koh, W.-J., Jeong, B.-H., Kim, S.-Y., Jeon, K., Un Park, K., Woo Jhun, B., et al. (2017). Clinical infectious diseases mycobacterial characteristics and treatment outcomes in *Mycobacterium abscessus* lung disease. *Clin. Infect. Dis.* 64, 309–316. doi: 10.1093/cid/ciw724

Laencina, L., Dubois, V., Le Moigne, V., Viljoen, A., Majlessi, L., Pritchard, J., et al. (2018). Identification of genes required for *Mycobacterium abscessus* growth in vivo with a prominent role of the ESX-4 locus. *Proc. Natl. Acad. Sci. U.S.A.* 115, E1002–E1011. doi: 10.1073/pnas.1713195115

Lane, A. Z., Wright, G. E., and Blair, D. C. (1977). Ototoxicity and nephrotoxicity of amikacin: an overview of phase II and phase III experience in the United States. *Am. J. Med.* 62, 911–918. doi: 10.1016/0002-9343(77)90660-X

Larsson, C., Luna, B., Ammerman, N. C., Maiga, M., Agarwal, N., Bishai, W. R., et al. (2012). Gene expression of *Mycobacterium tuberculosis* putative transcription factors whiB1-7 in redox environments. *PLoS One* 7:e37516. doi: 10.1371/journal.pone.0037516

Lee, M. R., Sheng, W. H., Hung, C. C., Yu, C. J., Lee, L. N., and Hsueh, P. R. (2015). *Mycobacterium abscessus* complex infections in humans. *Emerg. Infect. Dis.* 21, 1638–1646. doi: 10.3201/2109.141634

Leistikow, R. L., Morton, R. A., Bartek, I. L., Frimpong, I., Wagner, K., and Voskuil, M. I. (2010). The *Mycobacterium tuberculosis* DosR regulon assists in metabolic homeostasis and enables rapid recovery from nonrespiring dormancy. *J. Bacteriol.* 192, 1662–1670. doi: 10.1128/JB.00926-09

Low, J. L., Wu, M.-L., Aziz, D. B., Laleu, B., and Dick, T. (2017). Screening of TB actives for activity against nontuberculous mycobacteria delivers high hit rates. *Front. Microbiol.* 8:1539. doi: 10.3389/fmicb.2017.01539

Misumi, M., and Tanaka, N. (1980). Mechanism of inhibition of translocation by kanamycin and viomycin: a comparative study with fusidic acid. *Biochem. Biophys. Res. Commun.* 92, 647–654. doi: 10.1016/0006-291X(80)90382-4

Mook, R. A., Wang, J., Ren, X.-R., Chen, M., Spasojevic, I., Barak, L. S., et al. (2015). Structure-activity studies of Wnt/Î^2-catenin inhibition in the Niclosamide

chemotype: identification of derivatives with improved drug exposure. *Bioorg. Med. Chem.* 23, 5829–5838. doi: 10.1016/j.bmc.2015.07.001

Nasiri, M. J., Haeili, M., Ghazi, M., Goudarzi, H., Pormohammad, A., Imani Fooladi, A. A., et al. (2017). New insights in to the intrinsic and acquired drug resistance mechanisms in mycobacteria. *Front. Microbiol.* 8:681. doi: 10.3389/fmicb.2017.00681

Nessar, R., Cambau, E., Reyrat, J. M., Murray, A., and Gicquel, B. (2012). *Mycobacterium abscessus*: a new antibiotic nightmare. *J. Antimicrob. Chemother.* 67, 810–818. doi: 10.1093/jac/dkr578

Ollinger, J., Bailey, M. A., Moraski, G. C., Casey, A., Florio, S., Alling, T., et al. (2013). A dual read-out assay to evaluate the potency of compounds active against *Mycobacterium tuberculosis*. *PLoS One* 8:e60531. doi: 10.1371/journal.pone.0060531

Prevots, D. R., Shaw, P. A., Strickland, D., Jackson, L. A., Raebel, M. A., Blosky, M. A., et al. (2010). Nontuberculous mycobacterial lung disease prevalence at four integrated health care delivery systems. *Am. J. Respir. Crit. Care Med.* 182, 970–976. doi: 10.1164/rccm.201002-0310OC

Qvist, T., Eickhardt, S., Kragh, K. N., Andersen, C. B., Iversen, M., Hoiby, N., et al. (2015). Chronic pulmonary disease with *Mycobacterium abscessus* complex is a biofilm infection. *Eur. Respir. J.* 46, 1823–1826. doi: 10.1183/13993003.01102-2015

Rao, S. P. S., Alonso, S., Rand, L., Dick, T., and Pethe, K. (2008). The protonmotive force is required for maintaining ATP homeostasis and viability of hypoxic, nonreplicating *Mycobacterium tuberculosis*. *Proc. Natl. Acad. Sci. U.S.A.* 105, 11945–11950. doi: 10.1073/pnas.0711697105

Rosenmeier, G. J., Keeling, J. H., Grabski, W. J., McCollough, M. L., and Solivan, G. A. (1991). Latent cutaneous *Mycobacterium fortuitum* infection in a healthy man. *J. Am. Acad. Dermatol.* 25(5 Pt 2), 898–902. doi: 10.1016/S0190-9622(08)80362-3

Sarathy, J. P., Via, L. E., Weiner, D., Blanc, L., Boshoff, H., Eugenin, E. A., et al. (2018). Extreme drug tolerance of *Mycobacterium tuberculosis* in caseum. *Antimicrob. Agents Chemother.* 62, e02266-17. doi: 10.1128/AAC.02266-17

Tsilimparis, N., Defreitas, D., Debus, E. S., and Reeves, J. G. (2014). Latent mycobacterium avium infection causing a mycotic suprarenal aortic aneurysm in a human immunodeficiency virus-positive patient. *Ann. Vasc. Surg.* 28, 1035.e1-4. doi: 10.1016/j.avsg.2013.06.036

Wayne, L. G., and Hayes, L. G. (1996). An in vitro model for sequential study of shiftdown of *Mycobacterium tuberculosis* through two stages of nonreplicating persistence. *Infect. Immun.* 64, 2062–2069.

World Health Organization [WHO] (2017). *Essential Medicines*, 17th Edn. Available at: http://www.who.int/medicines/services/essmedicines_def/en/index.html

Wu, M.-L., Aziz, D. B., Dartois, V., and Dick, T. (2018). NTM drug discovery: status, gaps and the way forward. *Drug Discov. Today* 23, 1502–1519. doi: 10.1016/j.drudis.2018.04.001

Xie, Z., Siddiqi, N., and Rubin, E. J. (2005). Differential antibiotic susceptibilities of starved *Mycobacterium tuberculosis* isolates. *Antimicrob. Agents Chemother.* 49, 4778–4780. doi: 10.1128/AAC.49.11.4778-4780.2005

Conflict of Interest Statement: The authors declare that the research was conducted in the absence of any commercial or financial relationships that could be construed as a potential conflict of interest.

frontiers in Microbiology

ORIGINAL RESEARCH
published: 07 September 2018
doi: 10.3389/fmicb.2018.02095

Tedizolid Activity Against Clinical *Mycobacterium abscessus* Complex Isolates—An *in vitro* Characterization Study

Ying Wei Tang[1], *Bernadette Cheng*[2], *Siang Fei Yeoh*[3], *Raymond T. P. Lin*[2,4] *and Jeanette W. P. Teo*[2]*

[1] Department of Biological Sciences, National University Singapore, Singapore, Singapore, [2] Department of Laboratory Medicine, National University Hospital, Singapore, Singapore, [3] Pharmacy, National University Hospital, Singapore, Singapore, [4] National Public Health Laboratory, Ministry of Health, Singapore, Singapore

Mycobacterium abscessus complex consist of three rapidly growing subspecies: *M. abscessus*, *M. massiliense,* and *M. bolletii*. They are clinically important human pathogens responsible for opportunistic pulmonary and skin and soft tissue infections. Treatment of *M. abscessus* infections is difficult due to *in vitro* resistance to most antimicrobial agents. Tedizolid (TZD) is a next-generation oxazolidinone antimicrobial with a wide spectrum of activity even against multidrug resistant Gram-positive bacteria. In this study, the *in vitro* activity of TZD against the *M. abscessus* complex ($n = 130$) was investigated. Susceptibility testing by broth microdilution showed lower TZD minimum inhibitory concentrations (MICs) when compared to linezolid. The MIC_{50} and MIC_{90} was 1 mg/L and 4 mg/L, respectively across all *M. abscessus* complex members, reflecting no difference in subspecies response to TZD. Pre-exposure of *M. abscessus* complex to subinhibitory concentrations of TZD did not trigger any inducible drug resistance. Single-drug time kill assays and bactericidal activity assays demonstrated bacteriostatic activity of TZD in all three *M. abscessus* subspecies, even at high drug concentrations of 4 to 8x MIC. Combination testing of TZD with clarithromycin, doxycycline and amikacin using the checkerboard approach showed no antagonistic interactions. TZD may be an effective therapeutic antimicrobial agent for the treatment of *M. abscessus* infections.

Keywords: multidrug resistant (MDR), inducible resistance, oxazolidinone, time-kill, repurposable drugs

OPEN ACCESS

Edited by:
Thomas Dick,
Rutgers, The State University of New Jersey, Newark, United States

Reviewed by:
Timothy Barkham,
Tan Tock Seng Hospital, Singapore
Avi Peretz,
The Baruch Padeh Medical Center, Poriya, Israel

***Correspondence:**
Jeanette W. P. Teo
jeanette_teo@nuhs.edu.sg

Specialty section:
This article was submitted to Antimicrobials, Resistance and Chemotherapy, a section of the journal Frontiers in Microbiology

Received: *18 July 2018*
Accepted: *16 August 2018*
Published: *07 September 2018*

Citation:
Tang YW, Cheng B, Yeoh SF, Lin RTP and Teo JWP (2018) Tedizolid Activity Against Clinical Mycobacterium abscessus Complex Isolates—An in vitro Characterization Study. Front. Microbiol. 9:2095. doi: 10.3389/fmicb.2018.02095

INTRODUCTION

Mycobacterium abscessus complex consists of three rapidly-growing mycobacteria (RGM) subspecies: *M. abscessus* subspecies *abscessus*, *M. abscessus* subspecies *massiliense* and *M. abscessus* subspecies *bolletii* (Lee et al., 2015). They have emerged as clinically important multi-drug resistant (MDR) human pathogens responsible for a wide spectrum of skin and soft tissue infections (SSTIs), opportunistic infections in immunocompromised patients and pulmonary infections in patients with chronic pulmonary disease or cystic fibrosis (Nessar et al., 2012). Nosocomial outbreaks of *M. abscessus* have been reported worldwide, highlighting its clinical significance (Nessar et al., 2012). *M. abscessus* complex accounts for approximately 65–80% of pulmonary infections caused by RGM (Koh et al., 2011). In Singapore, *M. abscessus* complex is the most prevalent RGM isolated

in hospitals and accounts for approximately 35% of all non-tuberculous mycobacteria (NTM) infections (Tang et al., 2015).

M. abscessus pulmonary infections are infamously difficult to treat, with low cure rates ranging from 30 to 50%. This is attributed to natural resistance to most antimicrobial agents (Van Ingen et al., 2012). Existing treatment regimens are combination-based therapies usually consisting of a macrolide antibiotic such as clarithromycin (CLR), amikacin (AMK) and either cefoxitin (FOX), imipenem (IPM), or tigecycline (TGC) (Van Ingen et al., 2012). The administration of combination therapy (usually CLR and AMK) is lengthy, lasting for periods of between 2 and 4 months before clinical and microbiological improvements are noticeable (Huang et al., 2010). And the lack of alternative antimicrobial options further complicates the treatment of NTM infections (Benwill and Wallace, 2014).

Tedizolid (TZD) is a next-generation oxazolidinone antibiotic approved by the Food and Drug Administration (FDA) in 2014 for the treatment of acute bacterial skin and skin structure infections (ABSSSI) caused by certain *Streptococcus* spp. and methicillin-resistant *Staphylococcus aureus* (MRSA). Phase three clinical trials demonstrated non-inferiority of TZD to the first-in-class oxazolidinone LZD for the treatment of ABSSI, with improved clinical efficacy against MRSA and slightly improved safety profile (Moran et al., 2014). Oxazolidinones are protein synthesis inhibitors (Rybak et al., 2014) whose action is primarily bacteriostatic (Rybak et al., 2014). *In vitro*, TZD has demonstrated activity against acid-fast bacilli such as slow-growing *Mycobacterium tuberculosis* and the rapidly-growing *Mycobacterium fortuitum* (Kisgen et al., 2014). TZD MIC values against NTM were equivalent or 1- to 8-fold lower than those of LZD, indicating improved *in vitro* potency (Brown-Elliott and Wallace, 2017). Another study showed that TZD exhibited good bacteriostatic activity against *M. abscessus*, with MICs two- to 16-fold lower as compared to LZD (Compain et al., 2018). The combination of *in vitro* activity against MDR Gram-positive bacteria, an oral dosage formulation and once-daily dosing makes TZD a promising investigational antimicrobial therapeutic agent (Kisgen et al., 2014).

In this study, we explored the potential use of TZD for anti-mycobacterial therapy by characterizing the *in vitro* activity of TZD against 130 clinical isolates of *M. abscessus* complex members.

MATERIALS AND METHODS

Mycobacterial Isolates and Genetic Characterization

A total of 130 retrospective non-duplicate clinical *M. abscessus* complex isolates were evaluated. This collection consisted of 43 *M. abscessus* isolates, 82 *M. massiliense* isolates and five *M. bolletii* isolates. The subspecies of the *M. abscessus* complex isolates was determined by multi-locus sequencing employing the *rpoB* and *hsp65* genes (Macheras et al., 2011). CLR resistance was analyzed by full-length sequencing of the *erm*(41) and *rrl* genes (Aziz et al., 2017). For *erm*(41), the full-length 673 bp gene sequence was examined for T/C polymorphism at the 28th nucleotide position as well as for gene deletions. *erm*(41) T28 sequevars have wild-type inducible CLR resistance whilst C28 sequevars are phenotypically CLR susceptible (Choi et al., 2012). For the *rrl* gene, the nucleotides 2058–2059, associated with CLR resistance were examined.

MIC Determination

Antibiotic powders of TZD, CLR, and LZD were purchased from MedChem Express (NJ, USA). Antimicrobial susceptibility testing of TZD, CLR and LZD were performed using the microdilution method according to the Clinical & Laboratory Standards Institute (CLSI) guidelines (CLSI, 2015). The working range for all tested antimicrobials was 0.125–64 mg/L. For TZD and LZD, the inoculated microdilution plates were incubated at 30°C for 3–5 days before growth was assessed by visual inspection. The MIC was determined as the concentration of antibiotic at which there was no visible growth. *Staphylococcus aureus* ATCC (American type culture collection) 6538 and *Enterococcus faecalis* ATCC 29212 were used as susceptibility testing quality control strains. The MIC for the control strains fell within the acceptable MIC range of 0.25–1 mg/L for both TZD and LZD (Woods et al., 2011; Brown-Elliott and Wallace, 2017). For TZD, there are currently no interpretative criteria for RGM. For LZD, RGM with MICs of $\leq$8 were classified as sensitive and $\geq$32 as resistant (Woods et al., 2011).

Bactericidal/Static Activity Determination

For the bactericidal/static activity determination assay, *M. abscessus* isolates ($n = 7$), *M. massiliense* isolates ($n = 15$) and *M. bolletii* ($n = 5$) were tested. After three days of TZD incubation at 30°C, the entire 96-well microtiter plate well contents corresponding to the two-fold diluted TZD concentrations (64–0.0625 mg/L) were plated and the CFU determined. The Minimum Bactericidal Concentration (MBC) of TZD against the tested isolates was defined as the lowest drug concentration required to induce $\geq$99.9% cell death as compared to the untreated control at the 0 h time point. For bactericidal antibiotics, the MBC is classified as $\leq$4 times the MIC while the MBC is usually >4 times the MIC for bacteriostatic antibiotics.

TZD Time Kill Assay for the *M. abscessus* Complex

Time-kill assays were performed according to CLSI guidelines (CLSI, 1999) and were setup for a single isolate each of *M. abscessus*, *M. massiliense* and *M. bolletii* using a 10^6 CFU/mL inoculum exponential growth phase bacterial suspension. Two-fold increasing concentrations of TZD (from 0.25 to 8x MIC) and a drug-free growth control was used. At time intervals of 0, 4, 8, 12, 24, 36, 48, 72, 96, and 120 h CFU enumerations were made. Bactericidal activity was defined as a $\geq$3-$\log_{10}$ decrease in CFU/mL at 120 h when compared to the 0 h time point. All time-kill experiments were performed in duplicate and the mean CFU counts plotted.

TZD Pre-exposure Assay

erm(41) confers inducible macrolide resistance in the *M. abscessus* complex, observable phenotypically at day 14 of

TABLE 1 | MICs of tedizolid, clarithromycin and linezolid for 130 clinical isolates of *Mycobacterium abscessus* complex.

Antimicrobial agent	*M. abscessus* complex (*n* = 130)	MIC_{50}	MIC_{90}	MIC range (mg/L)	Susceptibility (%)*
Tedizolid	*M. abscessus* (43)	1	4	0.0625–8	N/A
	M. bolletii (5)	4	4	1–8	N/A
	M. massiliense (82)	1	4	0.0625–8	N/A
	Total (130)	1	4	0.0625–8	N/A
Linezolid	*M. abscessus* (43)	8	>32	0.0625–>32	53.5
	M. bolletii (5)	32	>32	8– >32	20
	M. massiliense (82)	8	>32	0.5–>32	53.7
	Total (130)	8	>32	0.0625–>32	52.3
Clarithromycin*	*M. abscessus* (43)	>16	>16	0.0625–>16	20.9
	M. bolletii (5)	>16	>16	1–>16	40
	M. massiliense (82)	0.5	12	0.0625–>16	76.8
	Total (130)	1	>16	0.0625–>16	55.4

*For LZD, isolates with MICs of ≤8 were classified as sensitive and ≥32 were resistant (Woods et al., 2011).
For CLR, isolates with MICs of ≤2 were classified as sensitive and ≥8 were resistant.

incubation (Rubio et al., 2015). To examine if a similar inducible phenomenon existed for TZD, *M. abscessus* complex isolates were pre-exposed to sub-inhibitory concentrations of TZD prior to MIC determination as previously described (Aziz et al., 2017). TZD pre-exposure assays were performed for three isolates each of *M. abscessus*, *M. massiliense* and *M. bolletii*. Briefly, 10^6 CFU/mL bacterial suspension was treated with TZD at a sub-inhibitory concentration of 0.25 mg/L for *M. abscessus* and *M. massiliense* isolates, and at 1 mg/L for *M. bolletii* isolates, four-fold lower than their MIC_{50} values. An untreated, drug-free culture was setup as a growth control. The MICs were determined at day 3 and at day 14.

Synergy Studies Using Checkerboard Titration Assay

The *in vitro* interactions of TZD and CLR, TZD and DOX, as well as TZD and AMK were investigated by the checkerboard approach using the broth microdilution method as previously described (Kaushik et al., 2015). Five isolates of *M. abscessus*, four *M. massiliense* and five *M. bolletii* isolates were used for evaluation. The fractional inhibitory concentration index ($\sum$FIC) for each isolate was calculated as follows: $\sum \text{FIC} = \frac{MIC\ of\ antibiotic\ 1\ in\ combination}{MIC\ of\ antibiotic\ 1\ only} + \frac{MIC\ of\ antibiotic\ 2\ in\ combination}{MIC\ of\ antibiotic\ 2\ only}$. Synergy was defined as a FIC index of ≤0.5, indifference by a FIC index of >0.5 to ≤4 and antagonism when the FIC index was >4.

RESULTS

Susceptibility of *M. abscessus* Complex Isolates to Tedizolid, Clarithromycin, and Linezolid

For TZD, the MIC range was 0.0625–8 mg/L, compared to 0.0625–>32 mg/L for LZD. The MIC_{50} and MIC_{90} for TZD was 1 and 4 mg/L, consistent across all three subspecies suggesting that the 3 subspecies were similarly responsive to TZD. In general, the TZD MICs were 2- to 16-fold lower than those of LZD. Due to the lack of interpretive criteria for TZD for RGM, susceptibility rates were not assigned (**Table 1**). For LZD, 52.3% of all isolates were susceptible (MIC ≤ 8 mg/L); 53.5% of *M. abscessus*, 20% of *M. bolletii* and 53.7% of *M. massiliense* (**Table 1**).

For CLR, the MIC_{50} and MIC_{90} were both >16 mg/L for *M. abscessus* and *M. bolletii*, as compared to 1 and 12 mg/L for *M. massiliense*. According to CLSI interpretive criteria for susceptibility (CLSI, 2017), 55.4% (72/130) of all isolates were susceptible to CLR (MIC < 2 mg/L). *M. massiliense* isolates showed susceptibility rates of 76.8%. This is consistent with the observation that *M. massiliense* usually possesses a truncated non-functional *erm*(41) (Chew et al., 2017). In contrast, *M. abscessus* (20.9% susceptible) and *M. bolletii* isolates (0% susceptible) showed higher rates of resistance to CLR. The susceptible *M. abscessus* isolates were *erm*(41) C28 sequevar.

TZD Does Not Exhibit Bactericidal Activity Against the *M. abscessus* Complex

Time kill assays were performed using TZD for one isolate each of *M. abscessus* (MIC = 2 mg/L), *M. bolletii* (MIC = 8 mg/L) and *M. massiliense* (MIC = 0.25 mg/L). TZD did not exhibit bactericidal activity in all three subspecies, even at concentrations of 4- and 8-fold higher than the MIC determined by the microdilution method (**Figure 1**). There was a general decline in CFU count over time for *M. bolletii* and *M. massiliense*. Bacterial regrowth (0.2 $\log_{10}$CFU/ml greater than the starting inoculum) was observed at time point 72 h for *M. abscessus* for all drug concentrations (0.5–8x MIC), following which a reduction in CFU was only observed at concentrations of 4x and 8x MIC. For *M. bolletii*, regrowth was noted at time point 120 h for concentrations of 0.25x and 1x MIC. Regrowth was observed at time point 12 h for 0.25x MIC and 72 h for 0.5x MIC for *M. massiliense* (**Figure 1**).

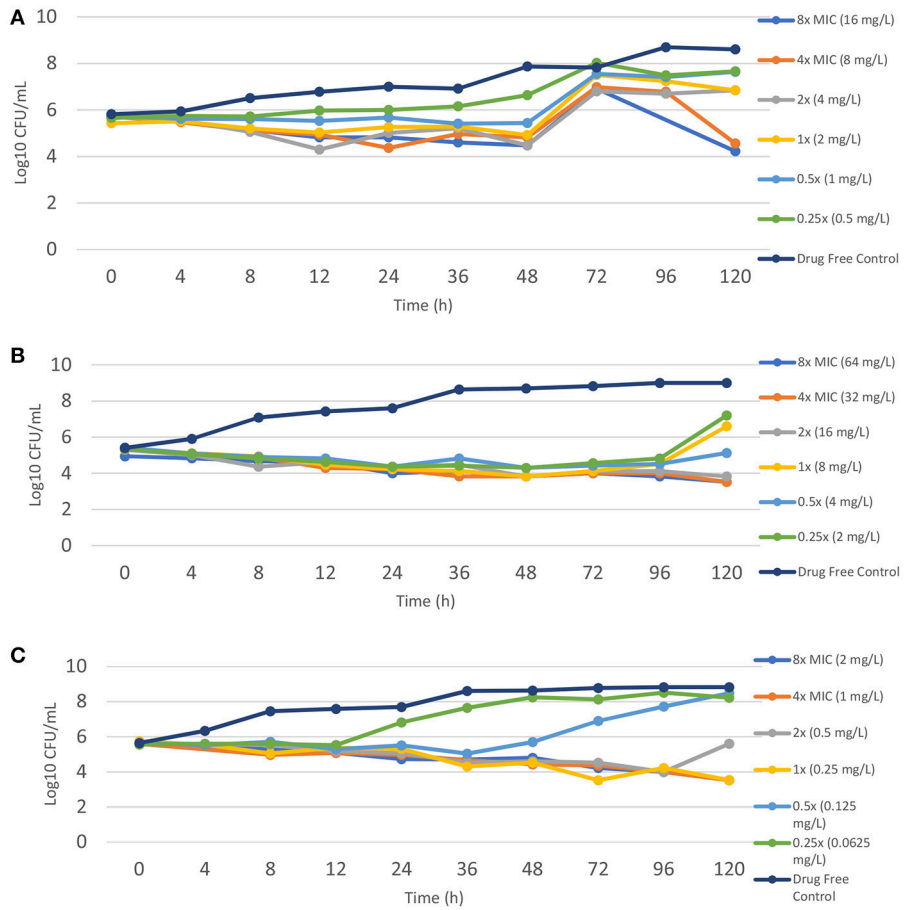

FIGURE 1 | Time kill kinetics of tedizolid against different *M. abscessus* subspecies **(A)** *M. abscessus* (TZD MIC = 2 mg/L); **(B)** *M. bolletii* (TZD MIC = 8 mg/L); *M. massiliense* (TZD MIC = 0.5 mg/L). Each point represents the mean of duplicate determinations.

TZD Exhibits Bacteriostatic Activity Against *M. abscessus* Complex

TZD exhibited bacteriostatic activity against all tested isolates of the *M. abscessus* complex (**Table 2**). The MBC of all three subspecies was greater than four times of MIC, which is characteristic of a bacteriostatic antimicrobial agent.

TZD Pre-exposure Does Not Induce Resistance

Pre-treatment of *three M. abscessus*, *M. bolletii* and *M. massiliense* isolates to sub-inhibitory concentrations of TZD did not affect MICs (**Table 3**). MICs after pre-exposure to TZD were similar to those without pre-exposure, suggesting that *M. abscessus* did not harbor inducible TZD resistance mechanisms.

Checkerboard Testing of TZD in Combination With Clarithromycin, Doxycycline and Amikacin Suggests Interactions That Are Largely Indifferent

Amikacin (AMK) and clarithromycin (CLR) are currently the only two antimicrobial agents with reliable *in vitro* activity against *M. abscessus* (Tang et al., 2015). TZD in combination with CLR, DOX and AMK were evaluated for antimicrobial activity against five isolates of *M. abscessus*, four isolates of *M. bolletii* and five isolates of *M. massiliense* by checkerboard synergy approach (**Table 4**). No instances of antagonism were observed in any antimicrobial combination tested. Indifference was the primary interaction accounting for 90.5% of all interactions. For the combination of TZD and CLR, all interactions were indifferent. One instance of synergistic interaction was observed in the *erm*(41) C28 sequevar *M. bolletii* isolate for the combination of TZD and DOX. In two *erm*(41) T28 sequevar *M. abscessus* isolates and one *M. massiliense* isolate, synergistic interactions were observed for the combination of TZD and AMK (**Table 4**). Overall, the findings suggest that TZD has no interaction when used in combination with CLR, DOX and AMK against *M. abscessus*.

DISCUSSION

M. abscessus pulmonary infections are notoriously difficult to treat with low cure rates of 30–50% (5). This has

TABLE 2 | Determination of the MBC and antibacterial mode of tedizolid against the *Mycobacterium abscessus* complex.

M. abscessus complex	MBC range (mg/L)	Median MBC (mg/L)	MIC range (mg/L)	Median MIC (mg/L)	Mode of action
M. abscessus ($n = 7$)	>64	>64	0.125–8	4	Bacteriostatic
M. bolletii ($n = 5$)	8–>64	32	1–8	4	Bacteriostatic
M. massiliense ($n = 15$)	16–>64	>64	0.125–8	0.5	Bacteriostatic

TABLE 3 | MICs of *Mycobacterium abscessus* complex after exposure to sub-inhibitory concentrations of tedizolid.

M. abscessus complex*	TZD MIC (mg/L)	
	No pre-exposure	After pre-exposure
M. abscessus #1	4	2
M. abscessus #2	4	2
M. abscessus #3	8	4
M. bolletii #1	0.5	1
M. bolletii #2	0.5	0.5
M. bolletii #3	4	2
M. massiliense #1	4	2
M. massiliense #2	4	4
M. massiliense #3	4	4

*Three unique isolates of each subspecies were used for testing.

spurred drug repurposing, defined as the "off-label" usage of existing antimicrobials (Palomino and Martin, 2014). LZD was initially developed for the treatment of infections caused by β-lactam-resistant Gram-positive bacteria, but it is now a recommended second-line drug for the treatment of MDR and extensively drug-resistant tuberculosis (Dheda et al., 2017). Furthermore, TZD has demonstrated *in vitro* activity against mycobacterial pathogens such as *Mycobacterium tuberculosis* and *Mycobacterium fortuitum* (Kisgen et al., 2014).

In our study, the potential of TZD for the treatment of *M. abscessus* complex infections was investigated *in vitro*. In comparison to two recent studies, our TZD MIC range of 0.0625–8 mg/L ($MIC_{50} = 1$ mg/L, $MIC_{90} = 4$ mg/L) for 43 *M. abscessus* isolates was lower than the MIC range of 0.12–>32 μg/mL ($MIC_{50} = 4\,\mu g/mL$, $MIC_{90} = 8\,\mu g/mL$) reported by Brown-Elliott and Wallace (2017) and the MIC range of 1–16 μg/mL ($MIC_{50} = 2\,\mu g/mL$, $MIC_{90} = 8\,\mu g/mL$) reported by Compain et al. (2018). For the 82 *M. massiliense* isolates a TZD MIC range of 0.0625–8 mg/L ($MIC_{50} = 1$ mg/mL, $MIC_{90} = 4$ mg/mL) was obtained. Brown-Elliott & Wallace Jr. reported a TZD MIC range of 0.12–>32 μg/mL ($MIC_{50} = 2\,\mu g/mL$, $MIC_{90} = 4\,\mu g/mL$) for a smaller set of 12 isolates whilst Compain et al. reported a MIC range of 1–8 μg/mL ($MIC_{50} = 4\,\mu g/mL$, $MIC_{90} = 8\,\mu g/mL$) for 14 *M. massiliense* isolates (n=14). The TZD MIC range of 1–8 mg/L (MIC_{50} and $MIC_{90} = 4$ mg/L) for 5 *M. bolletii* isolates were comparable to the MIC range of 1–4 mg/L ($MIC_{50} = 2\,\mu g/mL$, $MIC_{90} = 4\,\mu g/mL$) as determined by Compain et al. (2018).

There are currently no CLSI recommended TZD breakpoints for Mycobacteria but LZD is considered a reliable surrogate antimicrobial agent for TZD susceptibility, with the European Committee on Antimicrobial Susceptibility Testing (EUCAST) recommending the reporting of isolates susceptible to LZD as also susceptible to TZD (EUCAST, 2016). LZD susceptibility was found to be highly predictive of TZD susceptibility, with high categorical agreement between MIC values of LZD and TZD, and low rates of very major errors for Gram-positive bacteria (e.g., *Staphylococcus* spp. and *Enterococcus* spp.) (Zurenko et al., 2014). All 130 *M. abscessus* isolates were susceptible to TZD when a breakpoint ≤8 mg/L was applied. Although the suitability of LZD as a surrogate for TZD susceptibility has only been recommended for Gram-positive bacteria, these findings suggest that *M. abscessus* may be more susceptible to TZD than LZD.

In *M. tuberculosis* oxazolidinone resistance is associated with point mutations in the 23S rRNA gene (*rrl*) and in the 50S ribosomal protein L3 (Klitgaard et al., 2015; McNeil et al., 2017). *rrl* and L3 mutant strains were resistant to LZD and cross-resistant to sutezolid, a next-generation oxazolidinone currently in clinical development with improved potency against *M. tuberculosis* (McNeil et al., 2017). Furthermore, Gram-positive bacteria with 23S rRNA gene mutations were found to have high LZD (16 mg/L) and TZD MICs (>1 mg/L) as reported in a 2011–2012 surveillance report of TZD activity (Bensaci and Sahm, 2017). In our study, 5 isolates with high TZD MIC (8 mg/L) had their full–length *rrl* gene sequenced. All the sequenced isolates possessed a wild type *rrl* gene. This suggests alternative resistance mechanisms, such as efflux pumps (Gupta et al., 2006). We acknowledge our study limitation where mutations in bacterial 50S ribosomal protein L3, which are associated with oxazolidinone resistance, were not investigated.

This is currently the first study (to the best of our knowledge) to perform a time-kill assay for all three subspecies of the *M. abscessus* complex. TZD exhibits little concentration-dependent killing and no significant bactericidal activity against the three subspecies at all tested drug concentrations (0.5x−8x MIC). Compain et al. reported similar time-kill kinetics for *M. abscessus* ATCC 19977/CIP 104536, with no bactericidal activity at TZD concentrations of 4 and 8 mg/L. Bacterial regrowth was observed in *M. abscessus* in the logarithmic phase of growth for TZD concentrations tested. In comparison, regrowth was only observed at lower TZD concentrations of 0.25x and 1x MIC for *M. bolletii* and 0.25x and 0.5x MIC for *M. massiliense*. These findings were consistent with the findings by Ferro et al. (2015)

TABLE 4 | FIC index for tedizolid tested in combination with clarithromycin, doxycycline and amikacin against the *Mycobacterium abscessus* complex.

			MIC (mg/L)				FIC index[#]		FIC index[#]		FIC index[#]	
***M. abscessus* complex**	**Susceptibility to CLR**	***erm*(41)[$]**	**TZD**	**CLR**	**DOX**	**AMK**	**TZD + CLR**	**Interaction**	**TZD + DOX**	**Interaction**	**TZD + AMK**	**Interaction**
M. abscessus ($n = 1$)	S	C28 sequevar	1	2	1	1	1.000	Indifference	1.000	Indifference	0.625	Indifference
M. abscessus ($n = 4$)	R	T28 sequevar	3	>16	1	1	1.000	Indifference	1.000	Indifference	0.625	Indifference
M. abscessus	R	T28 sequevar	4	>16	1	16	1.016	Indifference	0.625	Indifference	0.375	Synergistic
M. abscessus	R	T28 sequevar	1	>16	1	2	1.016	Indifference	1.000	Indifference	1.063	Indifference
M. abscessus	R	T28 sequevar	8	>16	1	2	1.016	Indifference	1.125	Indifference	0.750	Indifference
M. bolletii ($n = 1$)	S	C28 sequevar	1	1	8	16	1.016	Indifference	0.313	Synergistic	0.53	Indifference
M. bolletii ($n = 3$)	R	T28 sequevar	8	>16	2	16	1.016	Indifference	0.563	Indifference	1.008	Indifference
M. bolletii	R	T28 sequevar	4	>16	1	8	1.500	Indifference	0.625	Indifference	0.563	Indifference
M. bolletii	R	T28 sequevar	4	>16	4	0.5	1.016	Indifference	0.625	Indifference	0.750	Indifference
M. massiliense ($n = 5$)	S	Deleted	0.25	0.25	2	2	1.016	Indifference	0.563	Indifference	0.625	Indifference
M. massiliense	S	Deleted	2	2	1	1	2.016	Indifference	1.000	Indifference	0.750	Indifference
M. massiliense	S	Deleted	1	1	2	2	0.516	Indifference	0.625	Indifference	0.375	Synergistic
M. massiliense	S	Deleted	0.125	0.125	1	2	1.016	Indifference	0.750	Indifference	0.750	Indifference
M. massiliense	S	Deleted	1	1	1	1	1.016	Indifference	0.750	Indifference	1.000	Indifference

[$] *T28 sequevar are CLR resistant, C28 sequevars are CLR susceptible. Deleted, refers to 274 bp erm(41) gene deletion characteristic in the M. massiliense subspecies.*
[#] *FIC index was calculated as [(MIC of tedizolid in combination/MIC of tedizolid alone) + (MIC of second antibiotic in combination/MIC of second antibiotic alone)]. Only FIC index <0.5 was considered as a synergistic interaction.*

where regrowth was also observed for AMK and CLR after 72 hours even at concentrations of 2x to 8x MIC. The findings suggest that a TZD concentration of ≥4x MIC may be required to induce significant killing activity against *M. abscessus*, whereas a TZD concentration of 1x/2x MIC sufficiently reduces bacterial counts in *M. bolletii* and *M. massiliense* over time. Similar to other active antimicrobials against *M. abscessus* complex, TZD exhibits a bacteriostatic effect that is more pronounced in *M. bolletii* and *M. massiliense* than *M. abscessus*.

Synergy studies of TZD with CLR, DOX, AMK demonstrated that all combinations primarily showed indifferent interactions with no instances of antagonism. A similar study performed by Compain et al. reported indifferent interactions of TZD with TGC, AMK and ciprofloxacin, with the combination of CLR and TZD showing one synergistic interaction out of 6 tested isolates. The findings suggest that TZD could be used in the existing combination regime of CLR and AMK with no antagnostic interactions.

AUTHOR CONTRIBUTIONS

YT drafted the manuscript and performed the experiments. BC performed the experiments. SY provided clinical feedback and scientific review. RL provided clinical feedback and scientific review. JT drafted the manuscript and oversaw the project execution.

REFERENCES

Aziz, D. B., Low, J. L., Wu, M. L., Gengenbacher, M., Teo, J. W. P., Dartois, V., et al. (2017). Rifabutin Is active against *Mycobacterium abscessus* complex. *Antimicrob. Agents Chemother.* 61:e00155–e00117.

Bensaci, M., and Sahm, D. (2017). Surveillance of tedizolid activity and resistance: *in vitro* susceptibility of Gram-positive pathogens collected over 5 years from the United States and Europe. *Diagn. Microbiol. Infect. Dis.* 87, 133–138. doi: 10.1016/j.diagmicrobio.2016.10.009

Benwill, J. L., and Wallace, R. J. (2014). Mycobacterium abscessus: challenges in diagnosis and treatment. *Curr. Opin. Infect. Dis.* 27, 506–510. doi: 10.1097/QCO.0000000000000104

Brown-Elliott, B. A., and Wallace, R. J. (2017). *In Vitro* Susceptibility testing of tedizolid against nontuberculous Mycobacteria. *J. Clin. Microbiol.* 55, 1747–1754. doi: 10.1128/JCM.00274-17

Chew, K. L., Cheng, J. W. S., Hudaa Osman, N., Lin, R. T. P., and Teo, J. W. P. (2017). Predominance of clarithromycin-susceptible *Mycobacterium massiliense* subspecies: characterization of the *Mycobacterium abscessus* complex at a tertiary acute care hospital. *J. Med. Microbiol.* 66, 1443–1447. doi: 10.1099/jmm.0.000576

Choi, G. E., Shin, S. J., Won, C. J., Min, K. N., Oh, T., Hahn, M. Y., et al. (2012). Macrolide treatment for mycobacterium abscessus and *Mycobacterium massiliense* infection and inducible resistance. *Am. J. Respir. Crit. Care Med.* 18, 917–925. doi: 10.1164/rccm.201111-2005OC

CLSI (1999). Methods for determining bactericidal activity of antimicrobial agents; approved guideline M26-A. *Clin. Lab. Stand. Inst.* 19:7.

CLSI (2015). *Methods for Dilution Antimicrobial Susceptibility Tests for Bacteria That Grow Aerobically. Approved Standard, 10*th Edn. CLSI document M07-A10, 1–87.

CLSI (2017). *Performance Standards for Antimicrobial Susceptibility Testing.* Perform Stand Antimicrob susceptibility Test 282.

Compain, F., Soroka, D., Heym, B., Gaillard, J. L., Herrmann, J. L., Dorchène, D., et al. (2018). *In vitro* activity of tedizolid against the *Mycobacterium abscessus* complex. *Diagn. Microbiol. Infect. Dis.* 90, 186–189. doi: 10.1016/j.diagmicrobio.2017.11.001

Dheda, K., Gumbo, T., Maartens, G., Dooley, K. E., McNerney, R., Murray, M., et al. (2017). The epidemiology, pathogenesis, transmission, diagnosis, and management of multidrug-resistant, extensively drug-resistant, and incurable tuberculosis. *Lancet Respir. Med*. doi: 10.1016/S2213-2600(17)30079-6. [Epub ahead of print].

EUCAST (2016). *Breakpoint Tables for Interpretation of MICs and Zone Diameters European Committee on Antimicrobial Susceptibility Testing Breakpoint Tables for Interpretation of MICs and Zone Diameters*. Växjö: EUCAST Development Laboratory for Antimicrobial Susceptibility Testing of bacteria c/o Clinical Microbiology.

Ferro, B. E., Van Ingen, J., Wattenberg, M., Van Soolingen, D., and Mouton, J. W. (2015). Time-kill kinetics of antibiotics active against rapidly growing mycobacteria. *J. Antimicrob. Chemother.* 70, 811–817. doi: 10.1093/jac/dku431

Gupta, A. K., Chauhan, D. S., Srivastava, K., Das, R., Batra, S., Mittal, M., et al. (2006). Estimation of efflux mediated multi-drug resistance and its correlation with expression levels of two major efflux pumps in Mycobacteria. *J. Commun. Dis.* 38, 246–254.

Huang, Y.C., Liu, M.F., Shen, G.H., Lin, C.F., Kao, C.C., Liu, P.Y., et al. (2010). Clinical outcome of *Mycobacterium abscessus* infection and antimicrobial susceptibility testing. *J. Microbiol. Immunol. Infect.* 43, 401–406. doi: 10.1016/S1684-1182(10)60063-1

Kaushik, A., Makkar, N., Pandey, P., Parrish, N., Singh, U., and Lamichhane, G. (2015). Carbapenems and rifampin exhibit synergy against *Mycobacterium tuberculosis* and *Mycobacterium abscessus*. *Antimicrob. Agents Chemother.* 59, 6561–6567. doi: 10.1128/AAC.01158-15

Kisgen, J. J., Mansour, H., Unger, N. R., and Childs, L. M. (2014). Tedizolid: A new oxazolidinone antimicrobial. *Am. J. Health Syst. Pharm*. 71, 621–633. doi: 10.2146/ajhp130482

Klitgaard, R. N., Ntokou, E., Nørgaard, K., Biltoft, D., Hansen, L. H., Trædholm, N. M., et al. (2015). Mutations in the bacterial ribosomal protein l3 and their association with antibiotic resistance. *Antimicrob. Agents Chemother.* 59, 3518–3528. doi: 10.1128/AAC.00179-15

Koh, W. J., Jeon, K., Lee, N. Y., Kim, B. J., Kook, Y. H., Lee, S. H., et al. (2011). Clinical significance of differentiation of *Mycobacterium massiliense* from *Mycobacterium abscessus*. *Am. J. Respir. Crit. Care Med.* 183, 405–410. doi: 10.1164/rccm.201003-0395OC

Lee, M. R., Sheng, W. H., Hung, C. C., Yu, C. J., Lee, L. N., and Hsueh, P. R. (2015). *Mycobacterium abscessus* complex infections in humans. *Emerging Infect. Dis.* 21, 1638–1646. doi: 10.3201/2109.141634

Macheras, E., Roux, A. L., Bastian, S., Leão, S. C., Palaci, M., Sivadon-Tardy, V., et al. (2011). Multilocus sequence analysis and rpoB sequencing of *Mycobacterium abscessus* (sensu lato) strains. *J. Clin. Microbiol.* 49, 491–499. doi: 10.1128/JCM.01274-10

McNeil, M. B., Dennison, D. D., Shelton, C., and Parish, T. (2017). *In vitro* isolation and characterization of oxazolidinone resistant *Mycobacterium tuberculosis*. *Antimicrob. Agents Chemother.* 61:e01296–e01217. doi: 10.1128/AAC.01296-17

Moran, G. J., Fang, E., Corey, G. R., Das, A. F., De Anda, C., and Prokocimer, P. (2014). Tedizolid for 6 days versus linezolid for 10 days for acute bacterial skin and skin-structure infections (ESTABLISH-2): A randomised, double-blind, phase 3, non-inferiority trial. *Lancet Infect. Dis.* 14, 696–705. doi: 10.1016/S1473-3099(14)70737-6

Nessar, R., Cambau, E., Reyrat, J. M., Murray, A., and Gicquel, B. (2012). *Mycobacterium abscessus*: A new antibiotic nightmare. *J. Antimicrob. Chemother.* 67, 810–818. doi: 10.1093/jac/dkr578

Palomino, J. C., and Martin, A. (2014). Drug resistance mechanisms in Mycobacterium tuberculosis. *Antibiotics (Basel).* 2, 317–340. doi: 10.3390/antibiotics3030317

Rubio, M., March, F., Garrigó, M., Moreno, C., Español, M., and Coll, P. (2015). Inducible and acquired clarithromycin resistance in the *Mycobacterium abscessus* complex. *PLoS ONE* 10:e0140166. doi: 10.1371/journal.pone.0140166

Rybak, J. M., Marx, K., and Martin, C. A. (2014). Early experience with tedizolid: clinical efficacy, pharmacodynamics, and resistance. *Pharmacotherapy*. 34, 1198–1208. doi: 10.1002/phar.1491

Tang, S. S., Lye, D. C., Jureen, R., Sng, L. H., and Hsu, L. Y. (2015). Rapidly growing mycobacteria in Singapore, 2006-2011. *Clin. Microbiol. Infect.* 21, 236–241. doi: 10.1016/j.cmi.2014.10.018

Van Ingen, J., Boeree, M. J., Van Soolingen, D., and Mouton, J. W. (2012). Resistance mechanisms and drug susceptibility testing of nontuberculous mycobacteria. *Drug Resistance Updates* 15, 149–161. doi: 10.1016/j.drup.2012.04.001

Woods, G. L., Brown-Elliott, B. A., Conville, P. S., Desmond, E. P., Hall, G. S., and Lin, G. (2011). Susceptibility testing of mycobacteria, nocardiae, and other aerobic actinomycetes; approved standard-second edition. *Clin. Lab. Stand. Inst*. 26, 1–61.

Zurenko, G., Bien, P., Bensaci, M., Patel, H. N., and Thorne, G. (2014). Use of linezolid susceptibility test results as a surrogate for the susceptibility of gram-positive pathogens to tedizolid, a novel oxazolidinone. *Ann. Clin. Microbiol. Antimicrob.* 13:46. doi: 10.1186/s12941-014-0046-0

Conflict of Interest Statement: The authors declare that the research was conducted in the absence of any commercial or financial relationships that could be construed as a potential conflict of interest.

The handling editor declared a past co-authorship with one of the authors JT.

frontiers in Microbiology

MINI REVIEW
published: 24 September 2018
doi: 10.3389/fmicb.2018.02271

Therapy for *Mycobacterium kansasii* Infection: Beyond 2018

*Michelle S. DeStefano[1], Carolyn M. Shoen[1] and Michael H. Cynamon[1,2]**

[1] Central New York Research Corporation, Syracuse, NY, United States, [2] Veterans Affairs Medical Center, Syracuse, NY, United States

The current standard of care therapy for pulmonary *Mycobacterium kansasii* infection is isoniazid (300 mg/day), rifampin (600 mg/day), and ethambutol (15 mg/kg/day) for 12 months after achieving sputum culture negativity. Rifampin is the key drug in this regimen. The contribution of isoniazid is unclear since its *in vitro* MICs against *M. kansasii* are near the peak achievable serum levels and more than 100-fold greater than the MICs for *Mycobacterium tuberculosis*. Ethambutol likely decreases the emergence of rifampin resistant organisms. There are several new drug classes (e.g., quinolones, macrolides, nitroimidazoles, diarylquinolines, and clofazimine) that exhibit antimycobacterial activities against *M. tuberculosis* but have not yet been adequately studied against *M. kansasii* infections. The evaluation of *in vitro* activities of these agents as well as their study in new regimens in comparison to the standard of care regimen in mouse infection models should be undertaken. This knowledge will inform development of human clinical trials of new regimens in comparison to the current standard of care regimen. It is likely that shorter and more effective therapy is achievable with currently available drugs.

Keywords: *M. kansasii*, antimycobacterials, mouse models, non-tuberculous mycobacteria, pulmonary infection

OPEN ACCESS

Edited by:
Thomas Dick,
Rutgers, The State University of New Jersey, Newark, United States

Reviewed by:
Amanda S. MacLeod,
Duke University, United States
Tianyu Zhang,
Guangzhou Institutes of Biomedicine and Health (CAS), China
Eric Nuermberger,
Johns Hopkins University, United States

***Correspondence:**
Michael H. Cynamon
Michael.Cynamon@va.gov

Specialty section:
This article was submitted to Antimicrobials, Resistance and Chemotherapy, a section of the journal Frontiers in Microbiology

Received: *28 June 2018*
Accepted: *05 September 2018*
Published: *24 September 2018*

Citation:
DeStefano MS, Shoen CM and Cynamon MH (2018) Therapy for Mycobacterium kansasii Infection: Beyond 2018. Front. Microbiol. 9:2271. doi: 10.3389/fmicb.2018.02271

INTRODUCTION

Mycobacterium kansasii (*M. kansasii*) is a group I non-tuberculous mycobacterium (NTM) (Buhler and Pollack, 1953). These organisms are ubiquitous in the environment and are often found in aquatic settings (Amha et al., 2017). Seven genotypes, or subtypes have been identified, along with an intermediate (I/II) and atypical (IIb) subtype (Bakuła et al., 2018). Types I and II are the most common clinical subtypes found while types III-VII have generally only been recovered from environmental samples (Taillard et al., 2003).

Mycobacterium kansasii causes infection in both immunocompetent and immunosuppressed individuals. Additionally, it is the non-tuberculous mycobacterium most frequently found in immunocompetent patients. It is also the second most frequent mycobacterium found in HIV-infected patients and is only surpassed by *Mycobacterium avium* complex (Canueto-Quintero et al., 2003). The number of NTM infections is increasing and are geographically wide-spread. *M. kansasii* is the second most prevalent cause of NTM disease in the United States, China, South American countries, and some European countries such as Poland, Slovakia, and the United Kingdom (Hoefsloot et al., 2013).

Mycobacterium kansasii causes lung disease that clinically and radiologically resembles tuberculosis. The American Thoracic Society (ATS) and the Infectious Diseases Society of America (IDSA) recommend a combination of three anti-tuberculosis drugs, isoniazid (INH) at 300 mg/day, rifampin (RIF) at 600 mg/day, and ethambutol (EMB) at 15 mg/kg/day for treatment of *M. kansasii*

pulmonary disease in HIV negative individuals. Treatment should be continued for 1 year after culture negativity (Griffith et al., 2007).

Mycobacterium kansasii infection is challenging to treat since the course of therapy requires multiple drugs and treatment periods of up to 2 years. Long periods of treatment often give rise to additional problems including patient non-adherence to the treatment plan, expense, and potential drug interactions and/or adverse events (Larsson et al., 2017). There are several antimycobacterial drugs that are effective against tuberculosis and other NTMs that might be better alternatives to the current three drug combination. The British Thoracic Society recommends the inclusion of a macrolide, such as azithromycin (AZI) at 250 mg/day or 500 mg of clarithromycin (CLA) twice a day as an alternative to INH (Haworth et al., 2017).

The focus of this review is to discuss *in vitro* susceptibility testing, *in vivo* evaluation in animal models, and clinical reports or studies utilizing these antimycobacterial agents. We will also discuss future efforts that should be undertaken to improve the clinical outcome of *M. kansasii* pulmonary infection.

IN VITRO SUSCEPTIBILITY TESTING

In vitro susceptibility testing of *M. kansasii* to antimycobacterial agents has been accomplished using several different methodologies, including agar dilution, broth macrodilution or microdilution method, or BACTEC. Investigations to determine the minimal inhibitory concentration (MIC) of antimicrobials against *M. kansasii* have been performed on multiple clinical isolates. **Table 1** contains the MIC_{50} and MIC_{90} (defined as the lowest concentration at which 50 and 90% of the clinical isolates tested were inhibited, respectively) of drugs currently used to treat *M. kansasii* infection, as well as other drugs used to treat tuberculosis and some NTM infections. The list includes oxazolidinones, quinolones, macrolides, riminophenazines, diarylquinolines, nitroimidazoles, glycylcyclines, and rifamycins.

Throughout the literature there is a divergence in the MIC values for CLA and AZI. The reported MIC values of susceptible strains of *M. kansasii* for CLA are generally consistent with those listed in **Table 1** with the MIC_{50} 0.12 and MIC_{90} 0.5 μg/mL. Other MIC values reported are: 0.125–0.25 μg/mL (Griffith et al., 2003), $MIC_{50} \leq 0.06$ MIC_{90} 0.125 μg/mL (Guna et al., 2005), MIC_{50} 0.25 and MIC_{90} 0.5 μg/mL (Witzig and Fransblau, 1993), and MIC_{50} 0.125, MIC_{90} 0.25 μg/mL (Brown et al., 1992). Although a more recent study (Li et al., 2016) suggests that CLA resistance is related to the Subtype I phenotype of *M. kansasii* and reports much higher MIC_{90} values (MIC_{50} 0.25, MIC_{90} 128 μg/mL). Subtype 1 is the most prevalent type of *M. kansasii* worldwide. In the same study the MIC values of AZI (MIC_{50} 16 MIC_{90} 32 μg/mL) are similar to those reported in **Table 1** (MIC_{50} 8 MIC_{90} 8 μg/mL). It is possible that these higher values are due to cross resistance with CLA as there are CLA resistant isolates identified in the same study. Other studies report MIC values of >8 μg/mL (Yew et al., 1994). Conversely, there are also reports of MIC values of AZI being similar to those seen with clarithromycin (Brown et al., 1992; Klemens and Cynamon, 1994).

The clinical MIC cutoff for EMB to define susceptibility/resistance against *M. kansasii* is 4 μg/ml, however, there is growing evidence that many *M. kansasii* isolates are resistant to EMB by this definition (**Table 1**). Patients diagnosed with this infection are not routinely evaluated for EMB susceptibility, therefore, resistance may be more prevalent than previously thought. It has been suggested that resistance to EMB (and INH) in *M. kansasii* occurs when a patient develops RIF resistance while on the standard regimen (Hjelm et al., 1992; Griffith et al., 2003). In a 2016 study, isolates belonging to *M. kansasii* Subtype I were found to exhibit greater resistance to EMB than the other subtypes (Li et al., 2016) although the differences were not statistically significant perhaps due to their small sample size. In a study looking at isolates from Poland, Germany, and Netherlands, 97.9% of the isolates were EMB resistant (all subtypes with the exception of Subtype V), however, published results from other countries indicates a resistance range for EMB of 0–94% as well as variable methods used to determine susceptibility (Bakuła et al., 2018). This raises the question whether EMB and INH should be used as companion drugs to rifampin when newer, potentially more efficacious drugs are currently available.

A model of intracellular *M. kansasii* infection has been designed to mimic the pharmacodynamics and pharmacokinetics between infected macrophages and therapeutic agents (Srivastava et al., 2015; Srivastava and Gumbo, 2018). The hollow fiber model of *M. kansasii* has been adapted from similar models for *Mycobacterium tuberculosis* and *M. avium* complex (Deshpande et al., 2010; Srivastava and Gumbo, 2011). It has been reported that this system evaluates compound efficacy, rank orders kill rates compared to standard regimens, and assesses antibiotic tolerance by the use of efflux pump inhibitors. In the case where samples were available from moxifloxacin (MOX) treated patients, analysis of bronchial secretions, alveolar macrophages and lung epithelium lining fluid were used to simulate optimal doses and breakpoints for resistance with the aid of computer software (Srivastava et al., 2015). This preclinical disease model will provide valuable additional information to help select the appropriate agents for *in vivo* testing and perhaps subsequent evaluation in clinical studies.

The immune status of a patient determines the course of infection and the selection of an appropriate regimen. RIF is currently the cornerstone for the therapy of *M. kansasii* infection, but in patients co-infected with HIV, RIF presents a problem since it increases the hepatic metabolism of protease inhibitors, often used for the treatment of HIV infection (Brown-Elliott et al., 2012). Rifabutin (RBT) has less effect on the hepatic metabolism, therefore, it is often used as an alternative to RIF in HIV-infected patients. Rifapentine (RPT) is an alternative to RIF or RBT. All three rifamycins have demonstrated good *in vitro* activity against *M. kansasii* (Cynamon and Sklaney, 2013).

Linezolid (LZD), an oxazalidinone, is currently an option for multi-drug resistant tuberculosis infections and has been shown to have good *in vitro* activity against *M. kansasii* (**Table 1**), but there are significant toxicity issues with this drug. These

TABLE 1 | MIC (μg/ml) of various compounds against *M. kansasii*.

Drug	MIC_{50}	MIC_{90}	Method	*N*	Reference
Linezolid	1	2	Broth microdilution	20	Shoen et al., 2018
Sutezolid	0.125	0.25	Broth microdilution	20	Shoen et al., 2018
Tedizolid	0.5	1.0	Broth microdilution	20	Shoen et al., 2018
Contezolid	1.0	1.0	Broth microdilution	20	Shoen et al., 2018
Isoniazid	0.5	16.0	Broth microdilution	169	Da Silva Telles et al., 2005
Ethambutol	16	16.0	Broth microdilution	169	Da Silva Telles et al., 2005
Clofazimine	0.5	2.0	Broth microdilution	169	Da Silva Telles et al., 2005
Bedaquiline	0.06	>16.0	Broth microdilution	84	Pang et al., 2017
Delamanid	0.025	0.1	Agar dilution	20	Doi and Disratthakit, 2006
Pretomanid	12.5	12.5	Agar dilution	20	Doi and Disratthakit, 2006
Clarithromycin	0.12	0.5	BACTEC	148	Alcaide et al., 2004
Azithromycin	8.0	8.0	BACTEC	19	Witzig and Fransblau, 1993
Moxifloxacin	0.06	0.06	BACTEC	148	Alcaide et al., 2004
Levofloxacin	0.12	0.12	BACTEC	148	Alcaide et al., 2004
Tigecycline	≤0.06	<0.12	Broth microdilution	11	Wallace et al., 2002
Rifampin	0.06	0.125	Broth microdilution	22	Cynamon and Sklaney, 2013
Rifabutin	0.004	0.015	Broth microdilution	22	Cynamon and Sklaney, 2013
Rifapentine	0.015	0.125	Broth microdilution	22	Cynamon and Sklaney, 2013

toxicity issues make the use of this drug for *M. kansasii* therapy problematic. The newer oxazolidinones, tedizolid, and contezolid, have fewer side effects than LZD, and have good *in vitro* activity against *M. kansasii* (Shoen et al., 2018).

Four other drugs that are used to treat drug resistant tuberculosis have also shown good *in vitro* activity against *M. kansasii* (**Table 1**). They are clofazimine (CFZ) (riminophenazine), bedaquiline (diarylquinoline), delamanid (nitroimidazole), and pretomanid (nitroimidazopyran) although the MIC_{50} of pretomanid is significantly high and therefore may not be a viable candidate compound. Attempting to correlate *in vitro* efficacy with achievable serum levels is not always useful when selecting compounds for *in vivo* testing and treatment.

Several factors affecting serum levels and compound availability have to be considered. These include tissue/cell accumulation, interaction with other drugs, and length of treatment (single dosing versus multiple doses). CFZ illustrates the complexity of this issue. A single 200 mg dose in humans results in peak plasma levels of 0.41 μg/ml, which is lower than reported MIC values (**Table 1**), however, CFZ concentrates in macrophages and tissues long-term due to its highly lipophilic character (Cholo et al., 2012). INH treatment with CFZ increases the plasma concentration and reduces tissue concentration of CFZ (Haworth et al., 2017). Several studies with other antimycobacterial agents allude to a synergistic relationship with CFZ when evaluated in combination therapy against a variety of NTM species (McGuffin et al., 2017).

Since treatment for *M. kansasii* and other NTM infections consist of a multi-drug regimen, a comprehensive review of each compound's known characteristics need to be considered to better predict potential efficacy. The established method for evaluation of *in vitro* combination therapy, "the checkerboard" has been used to define synergy or antagonism between two compounds. It is not clear whether results from this method correlate with those from *in vivo* modeling. New methods are being developed for prioritizing drug combinations, however, they have not yet been utilized for modeling regimens of *M. kansasii* therapy. Due to the lack of resources available for *M. kansasii* research it continues to be important to utilize available information on candidate compounds from *in vitro* combination studies focused on *M. tuberculosis* to advise our prioritization of regimens for *M. kansasii*.

ANIMAL STUDIES

Relatively little research has been done utilizing animal models to develop new therapies for NTM generally (Soni et al., 2016) and *M. kansasii* infection specifically. Research into the efficacy of compounds has largely been limited to drugs currently in use to treat tuberculosis or licensed drugs such as quinolones and macrolides. Due to the emerging importance of this infection, and the challenges of treatment for patients with resistant infections, more research into the development of an appropriate animal model to test new therapeutics is needed.

A review of the available literature indicates that several different strains of mice, levels of inocula, and routes of infection have been used, all with the ability to sustain a measurable bioburden. Presently there is no standard model and the strains of mice and routes of infection used are varied. Described below is a summary of the available literature on animal studies evaluating antimycobacterial compounds against *M. kansasii*.

BALB/c athymic (nude) mice infected with 10^7 CFU *M. kansasii* intravenously resulted in disseminated infection (Graybill and Bocanegra, 2001). Untreated control mice succumbed to the infection after about 2 months. Therapy given daily for 21 days was started 1-week post-infection. Increasing doses of RPT (0.15, 0.3, and 0.6 mg/kg), AZI (10, 15, 30, 50, and

TABLE 2 | *In vivo* results of *M. kansasii* intranasal infection in mice.

Mouse strain	Inoculum	Drug regimen (n)	Log_{10} CFU ± S.D.
Beige	1.4×10^6 CFU	Early controls (6)	7.47 ± 0.35
		Late controls (6)	8.70 ± 0.044
		Gatifloxacin 100 mg/kg (5)	6.50 ± 0.41
		Clarithromycin 200 mg/kg (5)	5.38 ± 0.64
		Gatifloxacin/Clarithromycin (6)	5.78 ± 0.35
		Rifampin 20 mg/kg (6)	6.30 ± 0.64
		Rifampin/Clarithromycin (5)	5.00 ± 0.13
		Linezolid 100 mg/kg (6)	7.03 ± 0.13
		Clarithromycin/Linezolid (6)	5.23 ± 1.02
		Gatifloxacin/Linezolid (6)	5.71 ± 1.27
			Cynamon et al., 2003
Mouse strain	**Inoculum**	**Drug regimen (n)**	**Median log counts***
C57BL/6J	8×10^4 CFU	Early controls (8)	5.39 (5.00–5.72)
		Late controls (8)	6.45 (6.40–6.69)
		Azithromycin 100 mg/kg (7)	4.95 (4.76–5.04)
		Rifalazil 10 mg/kg (8)	2.86 (2.21–3.12)
		Rifalazil/Azithromycin (5)	2.11 (1.48–2.70)
		Rifampin 10 mg/kg (8)	5.79 (5.53–6.23)
		Rifampin/Azithromycin (7)	4.40 (4.15–4.89)
			Cynamon and Buswell, 2002
Mouse strain	**Inoculum**	**Drug regimen (n)**	**Median log counts***
C57BL/6J	4.4×10^5 CFU	Early controls (5)	6.94 (6.23–7.08)
		Late controls (7)	7.73 (7.56–8.01)
		Rifalazil 1 mg/kg (6)	6.29 (5.85–6.45)
		Rifalazil 5 mg/kg (8)	4.76 (4.64–4.92)
		Rifalazil 10 mg/kg (8)	2.18 (1.95–2.45)
		Rifampin 20 mg/kg (7)	5.45 (5.13–5.72)
		Gatifloxacin 100 mg/kg (7)	4.48 (4.22–4.68)
			Cynamon and Monica, 2003

**95% confidence interval.*

150 mg/kg) and EMB (10, 25, and 100 mg/kg) were evaluated in a survival study. RPT dosed at 0.6 mg/kg, AZI at 15 mg/kg, and EMB at 10 mg/kg or higher doses of each prolonged survival. There was no difference in survival between RPT and AZI. The investigators also evaluated bioburden reduction in the spleens and livers of mice treated with RPT and AZI alone and in combination. The results indicated that the combination was no more effective than RPT alone.

In another study, beige mice (C57BL/6J background) were infected intravenously with 10^7 CFU of *M. kansasii* and treated 1-week post-infection, 5 days/week for 4 weeks. AZI 200 mg/kg, CLA 200 mg/kg, EMB 125 mg/kg, RIF 20 mg/kg, and CFZ 20 mg/kg were evaluated for activity compared to untreated controls. Viable cell counts were enumerated from the spleens and lungs. RIF reduced lung CFUs by about 1 log compared to the early controls and yielded the greatest reduction in organisms in the lungs. AZI and CLA had similar, but modest activity (Klemens and Cynamon, 1994).

In a study using beige mice infected intranasally with approximately 10^6 CFU of *M. kansasii*, treatment with gatifloxacin (GAT) 100 mg/kg, CLA 200 mg/kg, LZD 100 mg/kg, RIF 20 mg/kg, GAT + CLA, CLA + LZD, GAT + LZD, and RIF + CLA was given for 4 weeks, 5 days/week. All of the treatment groups were significantly better than the early controls (evaluated at the initiation of therapy, 1-week post-infection). CLA was more effective than any other monotherapy. CLA combined with LZD, GAT, or RIF was better than any single drug therapy (Cynamon et al., 2003; **Table 2**).

More recent studies with immunocompetent C57BL/6J mice demonstrate that *M. kansasii* can also survive and replicate in these mice. Two studies were carried out where mice were infected with approximately 5×10^5 CFU/mouse via the intranasal route. In the first experiment, RIF 10 mg/kg, rifalazil (RZL) 10 mg/kg, AZI 100 mg/kg and combinations of RIF + AZI and RZL + AZI were evaluated. All treatment groups were significantly better than the early controls. The combination of RZL + AZI was the most effective treatment group (Cynamon and Buswell, 2002; **Table 2**). In the second experiment, 4 weeks (5 days/week) of GAT 100 mg/kg and RIF 20 mg/kg were compared to increasing doses of RZL (1, 5,

and 10 mg/kg). The individual drugs were also compared to a combination of GAT + RZL10 mg/kg. All single agents and the combination regimen had significant activity compared to the early controls (evaluated 1-week post-infection). There was a dose response with RZL and the combination of RZL + GAT reduced lung CFUs to an undetectable level after 4 weeks of therapy (Cynamon and Monica, 2003; **Table 2**).

Although the published literature is limited regarding the use of *M. kansasii* infection models as a screening tool to evaluate recently licensed or new experimental compounds, the above studies suggest that these models should be used to determine if more effective therapy is achievable and whether their use may lead to a shorter duration of therapy compared to the current standard regimen.

CLINICAL RESEARCH

Rifampin, INH, and EMB (ATS/IDSA) or RIF, CLA (or AZI), EMB (British Thoracic Society) are suggested regimens for treatment of *M. kansasii* infection in humans taking between 12–18 months depending on the sputum culture time of conversion. The standard treatment regimen is effective in most instances; however, therapy is lengthy and it does not provide a cure for all patients (Santin et al., 2009). Treatment failure is almost always associated with resistance to RIF and/or CLA (Brown-Elliott et al., 2012). The Clinical and Laboratory Standards Institute (CLSI) currently recommends testing all initial patient isolates of *M. kansasii* for RIF and CLA *in vitro* susceptibility. Broth dilution is the suggested methodology utilizing cation-adjusted Mueller Hinton broth and 5% OADC (oleic acid, albumin, dextrose, catalase) enrichment as the media (Griffith et al., 2007). When isolates are RIF resistant (MIC > 1 μg/ml), the suggestion is to test secondary agents such as AMK, EMB, LZD, MOX, RBT, and trimethoprim-sulfamethoxazole for *in vitro* activity (Brown-Elliott et al., 2012).

The current method for testing and interpretation of the MIC for INH in the clinical laboratory utilizes the critical concentrations (0.2 μg/ml, 1 μg/ml) for *M. tuberculosis* susceptibility testing. This results in a false interpretation of INH resistance because the MIC values for *M. kansasii* usually range from 0.5 μg/ml to 5 μg/ml (Brown-Elliott et al., 2012). Heifets' work illustrated this issue stating that of more than 100 *M. kansasii* isolates evaluated by agar dilution methodology almost all were completely resistant to 0.2 μg/ml and susceptible, or partially resistant to 1 μg/ml of INH (Heifets, 1991). MIC testing of INH is not recommended.

Although infection can occur in other organs or become disseminated, the focus of our literature review of clinical outcomes is pulmonary infection caused by *M. kansasii.* A systematic review of microbiological and clinical treatment outcomes for *M. kansasii* pulmonary infections highlighted the lack of randomized controlled clinical trials for this infection (Diel et al., 2017; Haworth et al., 2017). A small cohort of prospective and retrospective observational studies exist and a few representative studies are discussed below.

A prospective study by the British Thoracic Society evaluated 173 patients with pulmonary *M. kansasii* infection. Prior to species identification, 149 of these patients were treated with regimens of INH + RIF + EMB, INH + RIF + EMB + PZA, or INH + RIF + PZA + streptomycin. Once *M. kansasii* was identified patients were given RIF + EMB for an additional 9 months (Jenkins et al., 1994). The remaining 24 patients received 9 months of RIF + EMB. Their results suggested that the RIF + EMB was acceptable treatment for non-immune compromised patients. Only 11% of their patients had positive sputum cultures after 3 months of therapy. Fifteen patients (9.7%) of the 154 patients who entered the post-chemotherapy follow up period relapsed between 6 and 50 (median 23) months.

In a retrospective study of 111 patients diagnosed with *M. kansasii* lung disease and treated with RIF + EMB + INH supplemented with streptomycin during the initial 2–3 months, 75 patients completed 12 months of therapy (Santin et al., 2009). After a 41.5-month median follow-up, five (6.6%) patients relapsed. The authors concluded that a 12-month course is adequate for most, but not all patients.

A prospective trial by Griffith et al. (2003) evaluated a thrice-weekly regimen of CLA 1000 mg (two female patients who weighed <50 kg received 500 mg), EMB 25 mg/kg, and RIF 600 mg in 18 patients with *M. kansasii* lung disease. This regimen yielded a durable cure with no relapse after a follow-up of 46 ± 8 months (mean time ± standard deviation) for the 14 patients that completed therapy. Four patients were lost to follow-up. The mean time to sputum conversion was 1 ± 0.9 months and the mean duration of therapy was 13.4 ± 0.9 months (Griffith et al., 2003).

FUTURE EFFORTS

The efficacy of INH when added to RIF + EMB should be measured in an appropriate mouse model to evaluate the contribution of INH to the standard regimen. New drug regimens should be tested in a mouse model of *M. kansasii* infection and compared to RIF + EMB ± INH to determine comparative efficacy. Similar to *in vitro* evaluation, multiple clinical isolates of *M. kansasii* should be studied in a mouse model to ensure that isolate differences do not affect efficacy in the mouse model. It is preferable to deliver the inoculum by the aerosol or intranasal route since this method most closely parallels the human pulmonary route of infection.

Initially, 4 weeks of treatment should be used to determine which regimens to evaluate in more detail (i.e., longer duration of therapy followed by a non-treatment observation period). It is yet to be determined whether one particular mouse strain is preferable to another. It would be of interest to evaluate C3HeB/FeJ mice as a potential model system for *M. kansasii* infection since they develop lesions similar to humans when infected with *M. tuberculosis* (Driver et al., 2012; Harper et al., 2012).

Several agents included in **Table 1** (bedaquiline, delamanid, MOX, tedizolid, contezolid, CFZ, and CLA) should be studied

in a mouse model of *M. kansasii* infection to determine whether they can improve outcomes with regard to efficacy and duration of therapy. CFZ added to INH + RIF + PZA in mice infected with tuberculosis was shown to decrease the time needed to achieve a durable cure (Tyagi et al., 2015; Ammerman et al., 2018). It should be determined whether CFZ has a similar effect with RIF + EMB or in the case of possible RIF resistance, a combination of CFZ with 2 other drugs in *M. kansasii* infections.

Several tuberculosis clinical trials with RIF suggest that doses of 20 and 35 mg/kg are both well tolerated and more efficacious than the standard 10 mg/kg dose (600 mg daily) (Tiberi et al., 2018). Higher doses of RIF should be evaluated to assess whether this treatment is also beneficial in reducing the lung bioburden of *M. kansasii* infected mice.

In order to accomplish randomized controlled clinical trials evaluating new regimens for therapy of pulmonary *M. kansasii* infection it is necessary to develop a clinical trials consortium, similar to the Mycoses Study Group[1]. This would enable multiple clinical trial sites to recruit and enter patients into clinical trials. In 2009 the European based MTB clinical trial consortium TBnet, formed the Non-tuberculous Mycobacteria Network European Trials Group (NTM-NET). NTM-NET is an international consortium of clinical NTM researchers that is primarily focused in Europe[2] and is able to provide limited funding for NTM research. Perhaps now is an appropriate time for a Non-tuberculous Mycobacteria Study Group funded by NIAID to advance clinical trials for NTM infections by providing opportunities and resources for this important work.

AUTHOR CONTRIBUTIONS

MD, CS, and MC have equally contributed to the research of the content, writing, and editing of this article. All authors have approved the final version of the article.

ACKNOWLEDGMENTS

This manuscript is dedicated to Dr. Leonid B. Heifets for his many contributions to expanding our understanding of susceptibility testing of mycobacteria.

[1] http://www.msgerc.org

[2] http://www.ntm-net.org

REFERENCES

Alcaide, F., Calatayud, L., Santín, M., and Martín, R. (2004). Comparative in vitro activities of linezolid, telithromycin, clarithromycin, levofloxacin, moxifloxacin, and four conventional antimycobacterial drugs against *Mycobacterium kansasii*. *Antimicrob. Agents Chemother.* 48, 4562–4565. doi: 10.1128/AAC.48.12.4562-4565

Amha, Y. M., Anwar, M. Z., Kumaraswamy, R., Henschel, A., and Ahmad, F. (2017). Mycobacteria in municipal wastewater treatment and reuse: microbial diversity for screening the occurrence of clinically and environmentally relevant species in arid regions. *Environ. Sci. Technol.* 51, 3048–3056. doi: 10.1021/acs.est.6b05580

Ammerman, N. C., Swanson, R. V., Bautista, E. M., Almeida, D. V., Saini, V., Omansen, T. F., et al. (2018). Impact of clofazimine dosing on treatment-shortening of the first-line regimen in a mouse model of tuberculosis. *Antimicrob. Agents Chemother.* 62:e636-18. doi: 10.1128/AAC.00636-18

Bakuła, Z., Modrzejewska, M., Pennings, L., Proboszcz, M., Safianowska, A., Bielecki, J., et al. (2018). Drug susceptibility profiling and genetic determinants of drug resistance in *Mycobacterium kansasii*. *Antimicrob. Agents Chemother.* 62:e1788-17. doi: 10.1128/AAC.01788-17

Brown, B. A., Wallace, R. J. Jr., and Onyi, G. O. (1992). Activities of clarithromycin against eight slowly growing species of nontuberculous mycobacteria, determined by using a broth microdilution MIC system. *Antimicrob. Agents Chemother.* 36, 1987–1990.

Brown-Elliott, B. A., Nash, K. A., and Wallace, R. J. Jr. (2012). Antimicrobial susceptibility testing, drug resistance mechanisms, and therapy of infections with nontuberculous mycobacteria. *Clin. Microbiol. Rev.* 25, 545–582. doi: 10.1128/CMR.05030-11

Buhler, V. B., and Pollack, A. (1953). Human infection with atypical acid-fast organisms. *Am. J. Clin. Pathol.* 23, 363–374.

Canueto-Quintero, J., Caballero-Granado, F. J., Herrero-Romero, M., Domínguez-Castellano, A., Martín-Rico, P., Verdú, V. E., et al. (2003). Epidemiological, clinical, and prognostic differences between the diseases caused by *Mycobacterium kansasii* and *Mycobacterium tuberculosis* in patients infected with human immunodeficiency virus: a multicenter study. *Clin. Infect. Dis.* 37, 584–590. doi: 10.1155/2017/4545721

Cholo, M. C., Steel, H. C., Fourie, P. B., Germishuizen, W. A., and Anderson, R. (2012). Clofazimine: current status and future prospects. *J. Antimicrob. Chemother.* 67, 290–298. doi: 10.1093/jac/dkr444

Cynamon, M., and Buswell, S. (2002). "Activities of rifampin, rifalazil and azithromycin in a mous model of *Mycobacterium kansasii* infection," in *Proceedings of the European Society of Mycobacteriology 23rd Annual Congress*, Dubrovnik.

Cynamon, M., and Sklaney, M. (2013). "Comparative in vitro activities of rifampin, rifapentine and rifabutin against *Mycobacterium kansasii*," in *Proceedings of the European Society of Mycobacteriology 34th Annual Congress*, Florence.

Cynamon, M. H., Elliott, S. A., DeStefano, M. S., and Yeo, A. E. T. (2003). Activity of clarithromycin alone and in combination in a murine model of *M. kansasii* infection. *J. Antimicrob. Chemother.* 52, 306–307.

Cynamon, M. H., and Monica, B. (2003). "Activities of rifalazil alone and in combination with gatifloxacin in a mouse model of *Mycobacterium kansasii* infection," in *Proceedings of the 43rd Interscience Conference on Antimicrobial Agents and Chemotherapy*, Chicago, IL.

Da Silva Telles, M. A., Chimara, E., Ferrazoli, L., and Riley, L. W. (2005). *Mycobacterium kansasii*: antibiotic susceptibility and PCR-restriction analysis of clinical isolates. *J. Med. Microbiol.* 54, 975–979.

Deshpande, D., Srivastava, S., Meek, C., Leff, R., Hall, G. S., and Gumbo, T. (2010). Moxifloxacin pharmacokinetics/pharmacodynamics and optimal dose and susceptibility breakpoint identification for treatment of disseminated *Mycobacterium avium* infection. *Antimicrob. Agents Chemother.* 54, 2534–2539. doi: 10.1128/AAC.01761-09

Diel, R., Ringshausen, F., Richter, E., Welker, L., Schmitz, J., and Nienhaus, A. (2017). Microbiological and clinical outcomes of treating non-*Mycobacterium avium* complex nontuberculous mycobacterial pulmonary disease a systematic review and meta-analysis. *Chest* 152, 120–142. doi: 10.1016/j.chest.2017.04.166

Doi, N., and Disratthakit, A. (2006). "Characteristic antimycobacterial spectra of the novel anti-TB drug candidates OPC-67683 and PA-824," in *Proceedings of the Interscience Conference on Antimicrobial Agents and Chemotherapy (ICAAC)*, San Francisco, CA, F1–F1377.

Driver, E. R., Ryan, G. J., Hoff, D. R., Irwin, S. M., Basaraba, R. J., Kramnik, I., et al. (2012). Evaluation of a mouse model of necrotic granuloma formation using C3HeB/FeJ mice for testing of drugs against *Mycobacterium tuberculosis*. *Antimicrob. Agents Chemother.* 56, 3181–3195. doi: 10.1128/AAC.00217-12

Graybill, J. R., and Bocanegra, R. (2001). Treatment alternatives for *Mycobacterium kansasii*. *J. Antimicrob. Chemother.* 47, 417–420.

Griffith, D. E., Aksamit, T., Brown-Elliott, B. A., Catanzaro, A., Daley, C., and Gordin, F. (2007). An official ATS/IDSA statement: diagnosis,treatment, and prevention of nontuberculous mycobacterial diseases. *Am. J. Respir. Crit. Care Med.* 175, 367–416.

Griffith, D. E., Brown-Elliott, B. A., and Wallace, R. J. Jr. (2003). Thrice-weekly clarithromycin-containing regimen for treatment of *Mycobacterium kansasii* infection. *J. Antimicrob. Chemother.* 37, 1178–1182. doi: 10.1086/378742

Guna, R., Munñoz, C., Domínguez, V., García-García, A., Gaálvez, G., de Juliaán-Ortiz, J. V., et al. (2005). *Mycobacterium kansasii* subtype I is associated with clarithromycin resistance in china. *J. Antimicrob. Chemother.* 55, 950–953. doi: 10.1093/jac/dki111

Harper, J., Sherry, C., Davis, S. L., Tasneen, R., Weir, M., Kramnik, I., et al. (2012). Mouse model of necrotic tuberculosis granulomas develops hypoxic lesions. *J. Infect. Dis.* 205, 595–602. doi: 10.1093/infdis/jir786

Haworth, C. S., Banks, J., Capstick, T., Fisher, A. J., Gorsuch, T., Laurenson, I. F., et al. (2017). British thoracic society guidelines for the management of non-tuberculous mycobacterial pulmonary disease (NTM-PD). *Thorax* 72, ii1–ii64. doi: 10.1136/thoraxjnl-2017-210927

Heifets, L. (1991). "Dilemmas and realities in drug susceptibility testing of *M. avium*-M. intracellulare and other slowly growing nontuberculous mycobacteria," in *Drug susceptibility in the chemotherapy of mycobacterial infections*, ed. L. Heifets (Boca Raton, FL: CRC Press), 136.

Hjelm, U., Kaustová, J., Kubín, M., and Hoffner, S. E. (1992). Susceptibility of *Mycobacterium kansasii* to ethambutol and its combination with rifamycins, ciprofloxacin and isoniazid. *Eur. J. Clin. Microbiol. Infect. Dis.* 11, 51–54. doi: 10.1007/BF01971272

Hoefsloot, W., van Ingen, J., Andrejak, C., Angeby, K., Bauriaud, R., Bemer, P., et al. (2013). The geographic diversity of nontuberculous mycobacteria isolated from pulmonary samples: an NTM-NETcollab. *Eur. Respir. J.* 42, 1604–1613. doi: 10.1183/09031936.00149212

Jenkins, P. A., Banks, J., Campbell, I. A., and Smith, A. P. (1994). *Mycobacterium kansasii* pulmonary infection: a prospective study of the results of nine months of treatment with rifampicin and ethambutol. research committee, British thoracic society. *Thorax* 49, 442–445. doi: 10.1136/thx.49.5.435

Klemens, S. P., and Cynamon, M. H. (1994). Activities of azithromycin and clarithromycin against nontuberculous mycobacteria in beige mice. *Antimicrob. Agents Chemother.* 38, 1455–1459.

Larsson, L. O., Polverino, E., Hoefsloot, W., Codecasa, L. R., Diel, R., Jenkins, S. G., et al. (2017). Pulmonary disease by non-tuberculous mycobacteria – clinical management, unmet needs and future perspectives. *Expert Rev. Respir. Med.* 11, 977–989. doi: 10.1080/17476348.2017.1386563

Li, Y., Pang, Y., Tong, X., Zheng, H., Zhao, Y., and Wang, C. (2016). *Mycobacterium kansasii* subtype I is associated with clarithromycin resistance in China. *Front. Microbiol.* 7:2097. doi: 10.3389/fmicb.2016.02097

McGuffin, S. A., Pottinger, P. S., and Harnisch, J. P. (2017). Clofazimine in nontuberculous mycobacterial infections: a growing niche. *Open Forum Infect. Dis.* 4:ofx147. doi: 10.1093/ofid/ofx147

Pang, Y., Zheng, H., Tan, Y., Song, Y., and Zhao, Y. (2017). In vitro activity of bedaquiline against nontuberculous mycobacteria in China. *Antimicrob. Agents Chemother.* 61:e2627-16. doi: 10.1128/AAC.02627-16

Santin, M., Dorca, J., Alcaide, F., Gonzalaz, F., Casas, S., Lopez, M., et al. (2009). Long-term relapses after 12-month treatment for *Mycobacterium kansasii* lung disease. *Eur. Respir. J.* 33, 148–152. doi: 10.1183/09031936.00024008

Shoen, C., Sklaney, M., and Cynamon, M. (2018). "Comparative in vitro activities of several oxazolidinones against *Mycobacterium kansasii*," in *Proceedings of the 18th International Congress on Infectious Diseases*, Buenos Aires.

Soni, I., De Groote, M. A., Dasgupta, A., and Chopra, S. (2016). Challenges facing the drug discovery pipeline for non-tuberculous mycobacteria. *J. Med. Microbiol.* 65, 1–8. doi: 10.1099/jmm.0.000198

Srivastava, S., and Gumbo, T. (2011). In vitro and in vivo modeling of anti-tuberculosis drugs and its impact on optimization of doses and regimens. *Curr. Pharm. Des.* 17, 2881–2888. doi: 10.2174/138161211797470192

Srivastava, S., and Gumbo, T. (2018). Clofazimine for the treatment of *Mycobacterium kansasii*. *Antimicrob. Agents Chemother.* 62:e248-18. doi: 10.1128/AAC.00248-18

Srivastava, S., Pasipanodya, J., Sherman, C. M., Meek, C., Leff, R., and Gumbo, T. (2015). Rapid drug tolerance and dramatic sterilizing effect of moxifloxacin monotherapy in a novel hollow-fiber model of intracellular *Mycobacterium kansasii* disease. *Antimicrob. Agents Chemother.* 59, 2273–2279. doi: 10.1128/AAC.04441-14

Taillard, C., Greub, G., Weber, R., Pfyffer, G. E., Bodmer, T., Zimmerli, S., et al. (2003). Clinical implications of *Mycobacterium kansasii* species heterogeneity: swiss national survey. *J. Clin. Microbiol.* 41, 1240–1244. doi: 10.1128/JCM.41.3.1240-1244.2003

Tiberi, S., du Plessis, N., Walzl, G., Vjecha, M. J., Rao, M., and Ntoumi, F. (2018). Tuberculosis: progress and advances in development of new drugs, treatment regimens, and host-directed therapies. *Lancet Infect. Dis.* 18, e183–e198. doi: 10.1016/S1473-3099(18)30110-5

Tyagi, S., Ammerman, N. C., Li, S. Y., Adamson, J., Converse, P. J., and Swanson, R. V. (2015). Clofazimine shortens the duration of the first-line treatment regimen for experimental chemotherapy of tuberculosis. *Proc. Natl. Acad. Sci. U.S.A.* 112, 869–874. doi: 10.1073/pnas.1416951112

Wallace, R. J., Brown-Elliott, B. A., Crist, C. J., Mann, L., and Wilson, R. W. (2002). Comparison of the in vitro activity of the glycylcycline tigecycline (formerly GAR-936) with those of tetracycline, minocycline, and doxycycline against isolates of nontuberculous mycobacteria. *Antimicrob. Agents Chemother.* 46, 3164–3167.

Witzig, R. S., and Fransblau, S. G. (1993). Susceptibility of *Mycobacterium kansasii* to ofloxacin, sparfloxacin, clarithromycin, azithromycin, and fusidic acid. *Antimicrob. Agents Chemother.* 37, 1997–1999.

Yew, W. W., Piddock, L. J., Li, M. S., Lyon, D., Chan, C. Y., and Cheng, A. F. (1994). In-vitro activity of quinolones and macrolides against mycobacteria. *J. Antimicrob. Chemother.* 34, 343–351.

Conflict of Interest Statement: The authors declare that the research was conducted in the absence of any commercial or financial relationships that could be construed as a potential conflict of interest.

frontiers in Microbiology

ORIGINAL RESEARCH
published: 11 May 2018
doi: 10.3389/fmicb.2018.00932

Teicoplanin – Tigecycline Combination Shows Synergy Against *Mycobacterium abscessus*

*Dinah B. Aziz[1,2], Jeanette W. P. Teo[3], Véronique Dartois[4] and Thomas Dick[4,5]**

[1] Department of Medicine, Yong Loo Lin School of Medicine, National University of Singapore, Singapore, Singapore, [2] Department of Pharmacy, Faculty of Science, National University of Singapore, Singapore, Singapore, [3] Department of Laboratory Medicine, National University Hospital, Singapore, Singapore, [4] The Public Health Research Institute, Rutgers, New Jersey Medical School, The State University of New Jersey, Newark, NJ, United States, [5] Department of Microbiology and Immunology, Yong Loo Lin School of Medicine, National University of Singapore, Singapore, Singapore

Lung disease caused by non-tuberculous mycobacteria (NTM), relatives of *Mycobacterium tuberculosis*, is increasing. *M. abscessus* is the most prevalent rapid growing NTM. This environmental pathogen is intrinsically resistant to most commonly used antibiotics, including anti-tuberculosis drugs. Current therapies take years to achieve cure, if cure if achieved. Thus, there is an urgent medical need to identify new, more efficacious treatments. Here, we explore the possibility of repurposing antibiotics developed for other indications. We asked whether novel two-drug combinations of clinically used antibiotics can be identified that show synergistic activity against this mycobacterium. An *in vitro* checkerboard titration assay was employed to test 180 dual combinations of 41 drugs against the clinical isolate *M. abscessus* Bamboo. The most attractive novel combination was further profiled against reference strains representing three sub-species (*M. abscessus* subsp. *abscessus*, *massiliense* and *bolletii*) and a collection of clinical isolates. This resulted in the identification of a novel synergistic antibiotic pair active against the *M. abscessus* complex: the glycopeptide teicoplanin with the glycylcycline tigecycline showed inhibitory activity at 2–3 μM (teicoplanin) and 1–2 μM (tigecycline). This novel combination can now be tested in *M. abscessus* animal models of infection and/or patients.

Keywords: *Mycobacterium abscessus*, teicoplanin, tigecycline, synergy, repurposing

OPEN ACCESS

Edited by:
Farhat Afrin,
Taibah University, Saudi Arabia

Reviewed by:
Yusuf Akhter,
Babasaheb Bhimrao Ambedkar University, India
Anna D. Tischler,
University of Minnesota, United States
Gyanu Lamichhane,
Johns Hopkins Medicine, United States

****Correspondence:***
Thomas Dick
td367@njms.rutgers.edu

Specialty section:
This article was submitted to Antimicrobials, Resistance and Chemotherapy, a section of the journal Frontiers in Microbiology

Received: *27 February 2018*
Accepted: *23 April 2018*
Published: *11 May 2018*

Citation:
Aziz DB, Teo JWP, Dartois V and Dick T (2018) Teicoplanin – Tigecycline Combination Shows Synergy Against Mycobacterium abscessus. Front. Microbiol. 9:932. doi: 10.3389/fmicb.2018.00932

INTRODUCTION

Among the rapid growing non-tuberculous mycobacteria (NTM), *M. abscessus* is the most common cause of lung disease (Griffith et al., 2007; Medjahed et al., 2010; Hoefsloot et al., 2013). A poor rate of successful chemotherapeutic treatment makes *M. abscessus* disease a chronic incurable infection (Griffith et al., 2007). The bacterium is intrinsically drug resistant to most antibiotics (Brown-Elliott et al., 2012; Nessar et al., 2012). Currently, *M. abscessus* infections are treated by a multi-drug regimen consisting of a macrolide (clarithromycin), amikacin and either cefoxitin or imipenem (Benwill and Wallace, 2014; Ryu et al., 2016). Different clinics may choose to add on additional antibiotics and recently, tigecycline has been used (Wallace et al., 2014; Floto et al., 2016). The treatment issues are further complicated by the ability of two out of three sub-species of *M. abscessus* to develop macrolide resistance upon exposure to sub-inhibitory concentrations of the drug (Nash et al., 2009; Bastian et al., 2011; Maurer et al., 2014).

Indeed, a recent study conducted in a hollow fiber model showed that the standard regimen of clarithromycin, amikacin, and cefoxitin exerted low sterilizing activity within the first 14 days of treatment, and re-growth of the bacteria was seen after this period due to inducible macrolide resistance (Ferro et al., 2016). Demonstrated transmission of *M. abscessus* between cystic fibrosis patients (Bryant et al., 2016) has increased the urgency to identify novel treatments for this NTM pathogen.

Screening for synergy interactions of approved drugs is an approach to new medicines that allows rapid bench-to-bedside translation (Hill and Cowen, 2015). A series of synergy studies have been conducted for *M. abscessus* and among the combinations that have been identified so far are imipenem + clarithromycin, imipenem + levofloxacin, clarithromycin + linezolid, clarithromycin + vancomycin, clofazimine + amikacin, tigecycline + clarithromycin, tigecycline + clofazimine, tigecycline + linezolid, clavulanate + meropenem, doripenem + rifampicin, biapenem + rifampicin, avibactam + ertapenem, avibactam + tebipenem, and avibactam + panipenem (Miyasaka et al., 2007; Cremades et al., 2009; Shen et al., 2010; van Ingen et al., 2012; Huang et al., 2013; Oh et al., 2014; Singh et al., 2014; Kaushik et al., 2015, 2017; Mukherjee et al., 2017).

To identify novel synergistic combinations, we carried out a large scale study using the checkerboard assay employing two different strategies. The first strategy was to screen combinations of β-lactams with β-lactamase inhibitors (Livermore, 1995; Bebrone et al., 2010). *M. abscessus* harbors the bla_{mab} gene encoding an Ambler class A β-lactamase (Soroka et al., 2014) and an inhibitor might restore activity of β-lactams against *M. abscessus*. The second strategy was to screen combinations of cell wall-targeting antibiotics with antibiotics that engage intracellular targets. This approach is based on our previous findings that vancomycin displayed (moderate) activity against *M. abscessus* (Aziz et al., 2017) and showed synergy with clarithromycin (Mukherjee et al., 2017). We screened a total of 180 dual drug combinations against a clinical isolate of *M. abscessus* and found that the combination of teicoplanin and tigecycline displayed synergistic activity. We characterized the *in vitro* activity of this novel combination against *M. abscessus* reference strains and diverse clinical isolates.

MATERIALS AND METHODS

Compounds

The 36 antibiotics and 5 β-lactamase inhibitors used in this study were obtained from commercial sources and dissolved according to the manufacturer's recommendations. Teicoplanin was obtained from Sigma-Aldrich, while tigecycline was obtained from Adooq BioScience. Both antibiotics were dissolved in 90% dimethyl sulfoxide (DMSO).

Bacterial Strains and Culture Media

Mycobacterium abscessus Bamboo (Yee et al., 2017) was used for screening of combinations and the subsequent confirmation of synergy hit combinations. For the checkerboard titration assay determination of the activity of the teicoplanin + tigecycline hit against the various *M. abscessus* subspecies within the *M. abscessus* complex, *M. abscessus* subsp. *abscessus* (ATCC 19977), *M. abscessus* subsp. *bolletii* (CCUG 50184-T) and *M. abscessus* subsp. *massiliense* (CCUG 48898-T) were used. Reference strains were obtained from the American Type Culture Collection (ATCC) and the Culture Collection University of Goteborg (CCUG), respectively. For further characterization of the teicoplanin + tigecycline combination in the macrolide resistance induction assay, *M. abscessus* subsp. *abscessus* (ATCC 19977) harboring the T28 sequevar of *erm41* gene, conferring inducible resistance upon exposure to sub-inhibitory concentrations of macrolides (Nash et al., 2009; Bastian et al., 2011) was used. For determination of synergy of teicoplanin + tigecycline against a variety of clinical isolates, strains were obtained from the strain collection of the clinical microbiology laboratory at the National University Hospital, Singapore. The strains were characterized by the lab as previously described (Aziz et al., 2017). For the evaluation of the bactericidal activity of the synergy combination *M. abscessus* subsp. *abscessus* (ATCC 19977) was used.

Liquid cultures were grown in standard mycobacterium medium, Middlebrook 7H9 broth (BD Difco) supplemented with 0.5% albumin, 0.2% glucose, 0.085% sodium chloride, 0.0003% catalase, 0.2% glycerol and 0.05% Tween 80. Solid cultures were grown on Middlebrook 7H10 agar (BD Difco) supplemented with 0.5% albumin, 0.2% glucose, 0.085% sodium chloride, 0.5% glycerol, 0.0003% catalase and 0.006% oleic acid.

Mycobacterium abscessus bacterial work was carried out under BSL-2 conditions according to approved biosafety protocols.

Checkerboard Titration Assay

This assay was carried out in 96-well microtiter plates as previously described (Hsieh et al., 1993; Kaushik et al., 2015), with some modifications. Drugs were tested within the range of concentrations of either 0–25 μM or 0–50 μM, at twofold serial dilutions. For each combination, 8 concentrations of a drug were tested for synergy against 11 concentrations of another drug. Hence, for each two-drug combination screened for synergy, 88 different combination concentrations are tested. A total of 180 different two-drug combinations were tested in this study. For the screening of combinations, this assay was carried out using the Tecan D300e Digital Dispenser for dispensing of drugs. For confirmation of the teicoplanin + tigecycline hit, as well as its subsequent characterization against sub-species, clinical isolates and induced cultures, drugs were dispensed manually. Results were reproducible between the two methods of dispensing drugs for this assay. Briefly, this assay was carried out in 96-well flat bottom plates, with two different compounds, with a starting inoculum of an optical density at 600 nm (OD_{600}) of 0.05 (10^7 colony forming units or cfu/mL) in a final volume of 200 μL. The culture for the starting inoculum was diluted from a pre-culture at mid-log phase (OD_{600} = 0.4 to 0.6). The plates were sealed using parafilm, put in an airtight container with moist tissue and incubated for 3 days at 37°C on an orbital shaker at 110 rpm. Each plate had a media-only control, a drug free control as well as a positive control of clarithromycin at 20 μM. After 3 days of

incubation, the cultures in the wells were manually re-suspended before OD_{600} was read in the plate reader (Tecan Infinite 200 Pro) and used to calculate growth inhibition percentage of each well. The Fractional Inhibitory Concentration Index (FICI) was used to analyze the results from the checkerboard assay. FICI was calculated by using the concentrations at which at least 90% inhibition of the culture in the well as compared to the drug free culture was observed. It was computed as FICI = [(concentration of drug A in combination/concentration of drug A when used alone) + (concentration of drug B in combination/concentration of drug B when used alone)] (Hsieh et al., 1993). Synergy is defined as FICI $\leq$ 0.5, indifference is defined as 0.5 < FICI $\leq$ 4, and antagonism is defined as FICI > 4 (Hsieh et al., 1993).

Macrolide Resistance Induction Assay

M. abscessus subsp. *abscessus* (ATCC 19977) mid-log phase culture was diluted to OD_{600} = 0.05 and treated with clarithromycin at a sub-inhibitory concentration of 0.075 μM (fourfold lower than clarithromycin MIC_{50} (concentration that causes 50% growth inhibition). An untreated culture was set up as a control. Cultures were grown to mid-log phase overnight and then subjected to the checkerboard titration assay as described above.

Bactericidal Assay

Bactericidal activity determinations were carried out in 14 mL round bottom tubes with the compounds added at set concentrations, with a starting inoculum of OD_{600} 0.05 (10^7 cfu/mL) in a final volume of 1 mL. The culture for the starting inoculum was diluted from a pre-culture at mid-log phase (OD_{600} = 0.4 to 0.6). Tubes were incubated for 3 days at 37°C with shaking at 160 rpm. After 3 days of drug exposure, 10 μL of the cultures were plated at different dilutions in 12 well plates containing 2 mL of 7H10 agar in each well. The plates were sealed with parafilm and incubated at 37°C for 4 days and then colonies were counted. We report fold-kill, which is the

TABLE 1 | Outcome of screening 110 combinations of β-lactams and β-lactamase inhibitors against *Mycobacterium abscessus* Bamboo: 6 two-drug hits.

			β-lactamase inhibitors				
			Non-β-lactam- based		β-lactam-based		
			AVI	VAB	CLA	SUL	TZB
β-lactams	Carbapenems	Biapenem	I	I	N.D	N.D	N.D
		Doripenem	I	I	I	I	I
		Ertapenem	I	I	N.D	N.D	N.D
		Faropenem	I	N.D	I	I	I
		Imipenem	I	I	I	I	I
		Meropenem	I	I	I	I	I
		Panipenem	S	S	I	I	I
		Tebipenem	S	S	N.D	N.D	N.D
	Cephalosporins	Cefaclor	I	I	I	I	I
		Cefprozil	I	N.D	I	I	I
		Cefoxitin	I	I	I	I	I
		Cefdinir	I	N.D	I	I	I
		Cefditoren	I	I	I	I	I
		Cefixime	I	I	I	I	I
		Ceftiofur	I	I	I	I	I
		Cefoperazone	I	I	I	I	I
		Ceftazidime	I	I	I	I	I
		Cefozopran	I	N.D	I	I	I
		Ceftobiprole	I	N.D	I	I	I
	Penicillins	Ampicillin	S	I	I	I	I
		Amoxicillin	S	I	I	I	I
		Cloxacillin	I	I	I	I	I
		Methicillin	I	N.D	I	I	I
		Piperacillin	I	I	I	I	I
		Ticarcillin	I	I	I	I	I

S, synergistic; I, indifferent; N.D, not determined. Synergy is defined as FICI ≤ 0.5. However, FICI values cannot be calculated for combinations involving β-lactamase inhibitors or other drugs that do not have MIC values when used individually. Hence, in the tables, synergistic interactions are defined as either combinations with FICI ≤ 0.5 or combinations that exhibit potentiation where a fourfold or more reduction in concentration of both drugs when used together is observed to inhibit 90% of growth as compared to when they are each used alone. Indifferent is defined as 0.5 < FICI ≤ 4. Where FICI cannot be calculated, 'indifferent' is defined as a less than fourfold in concentration of each antibiotic needed to achieve inhibition of 90% of growth when used together as compared to when the antibiotic is used alone. AVI, avibactam; VAB, vaborbactam; CLA, clavulanate; SUL, sulbactam; TZB, tazobactam.

reduction in cfu/mL of the treated culture compared to the time zero untreated control.

RESULTS

Screening of 180 Two-Drug Combinations for Synergy Against *M. abscessus* Identifies 11 Hits

We screened a total of 180 two-drug combinations of approved antibiotics for their growth inhibition potency against the clinical isolate *M. abscessus* Bamboo using the checkerboard assay. Hits were defined as combinations that showed at least a fourfold decrease in concentration of each drug that was needed to achieve 90% inhibition as compared to the concentration needed to achieve that same level of inhibition when either drug was used alone. Screening of β-lactam – β-lactamase inhibitor combinations, identified 6 hits out of 110 combinations (**Table 1**). Screening of combinations of cell envelope targeting drugs with antibiotics that inhibit intracellular targets, identified 5 hits out of 70 combinations (**Table 2**). Taken together, the screen identified 11 primary hits (6.1% hit rate) which were re-confirmed with fresh solids (**Table 3**).

Three of our combination hits, panipenem + avibactam, tebipenem + avibactam, and amoxicillin + avibactam were reported previously (Dubee et al., 2015a; Kaushik et al., 2017).

Out of our eight novel hits, the potencies of ampicillin + avibactam, panipenem + vaborbactam, tebipenem + vaborbactam, and ceftobiprole + linezolid were only modest, with MIC_{90} (concentrations that inhibit 90% of growth) of 25 + 19 μM, 50 + 2 μM, 10 + 10 μM, and 38 + 19 μM (**Table 3**).

One of our novel hits involved the glycopeptide ramoplanin in combination with clarithromycin, however, this is not unexpected since we had previously reported synergy between the glycopeptide vancomycin with clarithromycin (Mukherjee et al., 2017).

Three novel hits showed encouraging synergy effects: Ramoplanin + tigecycline, vancomycin + tigecycline and teicoplanin + tigecycline inhibited growth at 5 + 0.8 μM, 2 + 1 μM and 3 + 1 μM, respectively (**Table 3**). Ramoplanin, vancomycin, and teicoplanin are all glycopeptides. Ramoplanin is not well absorbed and unstable in the bloodstream due to hydrolysis of the lactone bond (Farver et al., 2005). This makes ramoplanin unsuitable to repurpose for use in treatment of *M. abscessus* lung infections. As teicoplanin shows systemic exposure upon intravenous or intramuscular administration and has been reported to have a better safety and efficacy profile compared to vancomycin (Svetitsky et al., 2009), we characterized the activity of teicoplanin in combination with the glycylcycline tigecycline in more detail.

Teicoplanin + Tigecycline Displays Activity Against Reference Strains Representing the Three Subspecies of the *M. abscessus* Complex

To determine whether the teicoplanin + tigecycline combination shows similar attractive potency across the three subspecies of the *M. abscessus* complex, we carried out the checkerboard titration assay to determine the FICI value of the combination against the reference strains *M. abscessus* subsp. *abscessus* ATCC 19977, *M. abscessus* subsp. *bolletii* CCUG 50184-T and *M. abscessus* subsp. *massiliense* CCUG 48898-T. The teicoplanin + tigecycline combination was synergistic against all three subspecies (**Table 4**). These results suggest that this novel combination is active across the phylogenetically divergent *M. abscessus* complex.

TABLE 2 | Outcome of screening 70 combinations of cell envelope-targeting antibiotics with antibiotics targeting intracellular targets against *M. abscessus* Bamboo: 5 synergistic two-drug hits.

			Antibiotics with intracellular targets						
			LZD	**LVX**	**MXF**	**AZM**	**CLR**	**TGC**	**RFB**
Cell envelope-targeting antibiotics	β-lactams	Doripenem	I	I	I	I	I	N.D	I
		Faropenem	I	I	I	I	I	N.D	I
		Imipenem	I	N.D	I	I	I	N.D	I
		Panipenem	I	I	I	I	I	N.D	I
		Cefoxitin	I	I	I	I	I	N.D	I
		Cefdinir	I	I	I	I	I	N.D	I
		Cefozopran	I	I	I	I	I	N.D	I
		Ceftiofur	I	I	I	I	I	N.D	I
		Ceftobiprole	S	I	I	I	I	N.D	I
	Glycopeptides	Ramoplanin	I	I	I	N.D	S	S	I
		Vancomycin	N.D	N.D	N.D	N.D	S[a]	S	I
		Teicoplanin	I	I	I	I	I	S	I
	Polymyxins	Colistin	N.D	I	I	N.D	N.D	N.D	N.D

S, synergistic; I, indifferent; N.D, not determined. For definition of terms see legend of ***Table 1****. LZD, linezolid; LVX, levofloxacin; MXF, moxifloxacin; AZM, azithromycin; CLR, clarithromycin; TGC, tigecycline; RFB, rifabutin.* [a]*Reported previously in Mukherjee et al. (2017).*

Teicoplanin + Tigecycline Retains Its Activity Against *M. abscessus* subsp. *abscessus* ATCC 19977 Cultures Displaying Induced Macrolide Resistance

The checkerboard titration assay was performed using *M. abscessus* subsp. *abscessus* ATCC 19977 cultures that had been exposed to a sub-inhibitory concentration of clarithromycin to induce macrolide resistance to determine whether the teicoplanin + tigecycline combination retains its activity under these conditions. The combination still exhibited synergy against the culture with induced macrolide resistance as seen by its FICI value of 0.22 (**Table 4**).

Teicoplanin + Tigecycline Shows Potent Activity Against *M. abscessus* Clinical Isolates

The teicoplanin + tigecycline combination showed potent growth inhibition activity against the screening strain as well as the reference strains representing the three subspecies of *M. abscessus*. This suggests that most clinical *M. abscessus* strains may be susceptible to this combination.

TABLE 3 | Reconfirmation of 11 two-drug hits identified from screening of 180 combinations against *M. abscessus* Bamboo.

Strategy	Combination	MIC_{90} (μM)	
		Alone	Combined
β-lactams + β-lactamase inhibitors	Panipenem + Avibactam	>50	50
		>50	6
	Tebipenem + Avibactam	46	13
		>50	0.8
	Ampicillin + Avibactam	>50	25
		>50	19
	Amoxicillin + Avibactam	>50	25
		>50	25
	Panipenem + Vaborbactam	>50	50
		>50	2
	Tebipenem + Vaborbactam	40	10
		>50	10
Cell envelope-targeting + antibiotics with intracellular targets	Ceftobiprole + Linezolid	>50	38
		>50	19
	Ramoplanin + Clarithromycin	30	5
		0.7	0.2
	Ramoplanin + Tigecycline	30	5
		7	0.8
	Vancomycin + Tigecycline	17	2
		6	1
	Teicoplanin + Tigecycline	25	3
		8	1

*The synergy or potentiation concentration of the 11 drug pair hits identified in the screens shown in **Tables 1**, **2** are reported. Results shown are the mean of two replicates. Standard deviations were ±50% of shown values.*

To provide evidence for a widespread susceptibility of *M. abscessus* to the teicoplanin + tigecycline combination, we tested its activity against a collection of clinical isolates covering various subspecies of *M. abscessus*, including clarithromycin resistant as well as clarithromycin sensitive strains. The combination displayed synergy against 70.4% of the isolates with FICI values ranging from 0.32 to 0.48 (**Table 5**). This result indicates that this combination is active against a large number of *M. abscessus* isolates.

Teicoplanin + Tigecycline Is Not Bactericidal Against *M. abscessus* subsp. *abscessus* ATCC 19977

To determine whether the teicoplanin + tigecycline combination shows bactericidal activity against *M. abscessus*, cultures were treated with the drug combination and the effect on viability was determined by cfu enumeration as described in Section "Materials and Methods." The teicoplanin + tigecycline combination showed no bactericidal activity.

DISCUSSION

A synergy screen of 180 dual antibiotic combinations against *M. abscessus* yielded a total of 11 hits. Six hits were obtained from combinations of β-lactams with β-lactamase inhibitors, and five hits from combinations of cell wall-targeting antibiotics with antibiotics that have intracellular targets.

From the analyses of combinations of β-lactams with β-lactamase inhibitors, the most striking observation is that all six hits involved a non-β-lactam-based β-lactamase inhibitor. 4 out of the 6 hits involved avibactam. This is consistent with previous reports showing that this inhibitor is effective against *M. abscessus*β-lactamases (Ehmann et al., 2012; Soroka et al., 2014; Dubee et al., 2015a; Kaushik et al., 2017). The remaining 2 hits involved the novel non-β-lactam-based β-lactamase inhibitor vaborbactam, which has not been previously studied for activity against *M. abscessus* β-lactamases. Activity of avibactam and now vaborbactam suggests that it may be worthwhile to characterize other types of non-β-lactam β-lactamase inhibitors like phosphonates, hydroxamates, or vanadate-catechol complexes, in combination with β-lactams for any potentiation effect of the combinations against *M. abscessus* (Bebrone et al., 2010).

It is to note that out of the three sub-classes of β-lactams we tested, avibactam appears not to improve the activity of cephalosporins, in contrast to a previous report describing potentiation between ceftaroline and avibactam against *M. abscessus* (Dubee et al., 2015b). A recent study by Kaushik et al. (2017) which focused on combinations of avibactam, sulbactam and tazobactam with carbapenems against *M. abscessus* reported 3 hits, with potentiation observed for combinations of avibactam with ertapenem, tebipenem, or panipenem (Kaushik et al., 2017). In this study, we could confirm potentiation for combinations of

avibactam with tebipenem or panipenem, however, we did not observe any potentiation between avibactam and ertapenem. Another study found potentiation between clavulanate and meropenem, which we also did not observe (Kaushik et al., 2015). The reasons for these discrepancies remain to be determined (Fisher et al., 2005). One possible explanation may be the use of different *M. abscessus* strains. This study used the clinical isolate *M. abscessus* Bamboo in the initial screening, while other studies used other strains including *M. abscessus* subsp. *abscessus* ATCC19977. In comparison to avibactam, vaborbactam improved the activity of selected compounds only from the carbapenems but not from the penicillins.

Vaborbactam is a new β-lactamase inhibitor and is the first one to contain a cyclic boronic acid structure (Lomovskaya et al., 2017). Despite its difference in structure from avibactam, both β-lactamase inhibitors were able to potentiate the activity of the same two carbapenems, panipenem and tebipenem. Panipenem is an earlier carbapenem and the drug needs to be administered together with betamipron to block its deactivation by dehydropeptidase I (Papp-Wallace et al., 2011). Tebipenem is a more recently discovered carbapenem and is the first oral drug of this class (Papp-Wallace et al., 2011).

From the analyses of combinations of cell wall-targeting antibiotics with drugs that have intracellular targets, we obtained five novel hits, with the teicoplanin + tigecycline combination being most attractive. Teicoplanin + tigecycline combination displayed synergy at a similar range across reference strains representing the three subspecies of *M. abscessus* with growth inhibitory combination concentrations of 2–3 μM teicoplanin + 1–2 μM tigecycline. The combination also retained

TABLE 4 | Synergy concentrations and FICI values of teicoplanin + tigecycline combination against *M. abscessus* screening strain and three reference strains of the *M. abscessus* sub-species.

Conditions	Strains	MIC_{90} (μM)				FICI
		Teicoplanin		Tigecycline		
		Alone	Combined	Alone	Combined	
(No pre-treatment)	*M. abscessus* Bamboo	25	3	8	1	0.27
	M. abscessus subsp. *abscessus*	10	2	6	2	0.42
	M. abscessus subsp. *bolletii*	10	2	8	2	0.39
	M. abscessus subsp. *massiliense*	14	2	7	2	0.36
Pre-treated with clarithromycin	*M. abscessus* subsp. *abscessus*	7	1.2	8.5	1.6	0.22

'Pre-treated with clarithromycin' shows the respective data for a strain displaying induced macrolide resistance due to pre-treatment with a sub-inhibitory concentration of clarithromycin (see section "Materials and Methods"). Results shown are the mean of two replicates. Standard deviation was ±50% of shown values. Synergy is defined as FICI ≤ 0.5. Checkerboard assay was conducted with 7H9 broth.

TABLE 5 | Synergy concentrations and FICI values of the teicoplanin + tigecycline combination against 14 clinical *M. abscessus* isolates.

Isolate code	*M. abscessus* sub-species	*erm41* sequevar	Clarithromycin susceptibility	MIC_{90} (μM)				FICI
				Teicoplanin		Tigecycline		
				Alone	Combined	Alone	Combined	
M199	*abscessus*	T28	Resistant	5	2	6	2	0.56
M337	*abscessus*	T28	Resistant	5	2	7	2	0.51
M404	*abscessus*	C28	Sensitive	6	2	4	1	0.53
M421	*abscessus*	T28	Resistant	17	3	4	0.6	0.37
M422	*abscessus*	T28	Resistant	6	1	6	1	0.44
M232	*bolletii*	T28	Resistant	21	5	18	2	0.39
M416	*bolletii*	N.D	Sensitive	4	2	5	1	0.63
M506	*bolletii*	C28	Sensitive	10	3	9	1	0.45
M111	*massiliense*	Deletion	Sensitive	10	2	10	2	0.48
M353	*massiliense*	Deletion	Sensitive	13	3	8	2	0.43
M357	*massiliense*	Deletion	Sensitive	12	2	8	1	0.33
M414	*massiliense*	Deletion	Sensitive	8	1	10	2	0.32
M444	*massiliense*	Deletion	Sensitive	7	3	6	1	0.48
M505	*massiliense*	Deletion	Sensitive	13	3	8	1	0.39

Results shown are the mean of two replicates. Standard deviations were ±50% of shown values. Synergy is defined as FICI ≤ 0.5. Indifference is defined as 0.5 < FICI ≤ 4, and antagonism is defined as FICI > 4. N.D, not determined.

activity against most clinical isolates. A limitation of the combinations tested in this category is, that we only tested combinations of tigecycline with glycopeptides and not with other classes of cell wall-targeting antibiotics such as β-lactams, and this should be explored in future studies.

Teicoplanin is a glycopeptide and acts by interacting with the D-ala-D-ala terminal of the muramyl-pentapeptide which results in inhibition of the cell wall peptidoglycan synthesis (Parenti, 1986). The drug is reported to have good tissue and cellular penetration (Parenti, 1986). Teicoplanin was found to have lower adverse event rates compared to the glycopeptide vancomycin (Svetitsky et al., 2009). Tigecycline is a glycylcycline acting via inhibiting protein synthesis (Olson et al., 2006). Both teicoplanin and tigecycline are administered intravenously, which may limit their application. However, it is noteworthy that despite this limitation tigecycline is used to treat *M. abscessus* infections (Wallace et al., 2014). The exact molecular mechanism by which the synergistic combination of teicoplanin + tigecycline exerts its activity remains to be determined. Tigecycline may have limited ability to penetrate the bacterium to gain access to its intracellular target. One may speculate that with the administration of teicoplanin together with tigecycline, teicoplanin is able to 'weaken' the bacterial cell wall and allow greater penetration of tigecycline into the bacterium.

CONCLUSION

This study has identified teicoplanin + tigecycline as a novel synergistic combination against *M. abscessus in vitro*. The drug pair can now be tested in *M. abscessus* animal models of infection and/or in patients.

AUTHOR CONTRIBUTIONS

DA, VD, and TD conceived the idea, developed the strategy, and wrote the manuscript. DA carried out the experiments. JT provided and characterized the clinical isolates.

FUNDING

Research reported in this publication was supported by the National Institute of Allergy and Infectious Diseases of the National Institutes of Health under Award Number R01AI132374 and by the Cystic Fibrosis Foundation under Award Number DICK17XX00 to TD. The content is solely the responsibility of the authors and does not necessarily represent the official views of the National Institutes of Health or the Cystic Fibrosis Foundation. This research was also supported by the Singapore Ministry of Health National Medical Research Council under its TCR Flagship grant NMRC/TCR/011-NUHS/2014 as part of the Singapore Programme of Research Investigating New Approaches to Treatment of Tuberculosis (SPRINT-TB; www.sprinttb.org). TD holds a Toh Chin Chye Visiting Professorship at the Department of Microbiology and Immunology, Yong Loo Lin School of Medicine, National University of Singapore.

ACKNOWLEDGMENTS

We thank Wei Chang Huang, Taichung Veterans General Hospital, Taichung, Taiwan for the *M. abscessus* Bamboo strain.

REFERENCES

Aziz, D. B., Low, J. L., Wu, M. L., Gengenbacher, M., Teo, J. W. P., Dartois, V., et al. (2017). Rifabutin is active against *Mycobacterium abscessus* complex. *Antimicrob. Agents Chemother.* 61:e00155-17. doi: 10.1128/AAC.00155-17

Bastian, S., Veziris, N., Roux, A. L., Brossier, F., Gaillard, J. L., Jarlier, V., et al. (2011). Assessment of clarithromycin susceptibility in strains belonging to the *Mycobacterium abscessus* group by erm(41) and rrl sequencing. *Antimicrob. Agents Chemother.* 55, 775–781. doi: 10.1128/AAC.00861-10

Bebrone, C., Lassaux, P., Vercheval, L., Sohier, J. S., Jehaes, A., Sauvage, E., et al. (2010). Current challenges in antimicrobial chemotherapy: focus on ss-lactamase inhibition. *Drugs* 70, 651–679. doi: 10.2165/11318430-000000000-00000

Benwill, J. L., and Wallace, R. J. Jr. (2014). *Mycobacterium abscessus*: challenges in diagnosis and treatment. *Curr. Opin. Infect. Dis.* 27, 506–510. doi: 10.1097/QCO.0000000000000104

Brown-Elliott, B. A., Nash, K. A., and Wallace, R. J. Jr. (2012). Antimicrobial susceptibility testing, drug resistance mechanisms, and therapy of infections with nontuberculous mycobacteria. *Clin. Microbiol. Rev.* 25, 545–582. doi: 10.1128/CMR.05030-11

Bryant, J. M., Grogono, D. M., Rodriguez-Rincon, D., Everall, I., Brown, K. P., Moreno, P., et al. (2016). Emergence and spread of a human-transmissible multidrug-resistant nontuberculous mycobacterium. *Science* 354, 751–757. doi: 10.1126/science.aaf8156

Cremades, R., Santos, A., Rodriguez, J. C., Garcia-Pachon, E., Ruiz, M., and Royo, G. (2009). *Mycobacterium abscessus* from respiratory isolates: activities of drug combinations. *J. Infect. Chemother.* 15, 46–48. doi: 10.1007/s10156-008-0651-y

Dubee, V., Bernut, A., Cortes, M., Lesne, T., Dorchene, D., Lefebvre, A. L., et al. (2015a). beta-Lactamase inhibition by avibactam in *Mycobacterium abscessus*. *J. Antimicrob. Chemother.* 70, 1051–1058. doi: 10.1093/jac/dku510

Dubee, V., Soroka, D., Cortes, M., Lefebvre, A. L., Gutmann, L., Hugonnet, J. E., et al. (2015b). Impact of beta-lactamase inhibition on the activity of ceftaroline against *Mycobacterium tuberculosis* and *Mycobacterium abscessus*. *Antimicrob. Agents Chemother.* 59, 2938–2941. doi: 10.1128/AAC.05080-14

Ehmann, D. E., Jahic, H., Ross, P. L., Gu, R. F., Hu, J., Kern, G., et al. (2012). Avibactam is a covalent, reversible, non-beta-lactam beta-lactamase inhibitor. *Proc. Natl. Acad. Sci. U.S.A.* 109, 11663–11668. doi: 10.1073/pnas.1205073109

Farver, D. K., Hedge, D. D., and Lee, S. C. (2005). Ramoplanin: a lipoglycodepsipeptide antibiotic. *Ann. Pharmacother.* 39, 863–868. doi: 10.1345/aph.1E397

Ferro, B. E., Srivastava, S., Deshpande, D., Pasipanodya, J. G., van Soolingen, D., Mouton, J. W., et al. (2016). Failure of the amikacin, cefoxitin, and clarithromycin combination regimen for treating pulmonary *Mycobacterium abscessus* infection. *Antimicrob. Agents Chemother.* 60, 6374–6376. doi: 10.1128/AAC.00990-16

Fisher, J. F., Meroueh, S. O., and Mobashery, S. (2005). Bacterial resistance to beta-lactam antibiotics: compelling opportunism, compelling opportunity. *Chem. Rev.* 105, 395–424. doi: 10.1021/cr030102i

Floto, R. A., Olivier, K. N., Saiman, L., Daley, C. L., Herrmann, J. L., Nick, J. A., et al. (2016). US cystic fibrosis foundation and European cystic fibrosis society consensus recommendations for the management of non-tuberculous mycobacteria in individuals with cystic fibrosis. *Thorax* 71(Suppl. 1), i1–i22. doi: 10.1136/thoraxjnl-2015-207360

Griffith, D. E., Aksamit, T., Brown-Elliott, B. A., Catanzaro, A., Daley, C., Gordin, F., et al. (2007). An official ATS/IDSA statement: diagnosis, treatment,

and prevention of nontuberculous mycobacterial diseases. *Am. J. Respir. Crit. Care Med.* 175, 367–416. doi: 10.1164/rccm.200604-571ST

Hill, J. A., and Cowen, L. E. (2015). Using combination therapy to thwart drug resistance. *Future Microbiol.* 10, 1719–1726. doi: 10.2217/fmb.15.68

Hoefsloot, W., van Ingen, J., Andrejak, C., Angeby, K., Bauriaud, R., Bemer, P., et al. (2013). The geographic diversity of nontuberculous mycobacteria isolated from pulmonary samples: an NTM-NET collaborative study. *Eur. Respir. J.* 42, 1604–1613. doi: 10.1183/09031936.00149212

Hsieh, M. H., Yu, C. M., Yu, V. L., and Chow, J. W. (1993). Synergy assessed by checkerboard. A critical analysis. *Diagn. Microbiol. Infect. Dis.* 16, 343–349.

Huang, C. W., Chen, J. H., Hu, S. T., Huang, W. C., Lee, Y. C., Huang, C. C., et al. (2013). Synergistic activities of tigecycline with clarithromycin or amikacin against rapidly growing mycobacteria in Taiwan. *Int. J. Antimicrob. Agents* 41, 218–223. doi: 10.1016/j.ijantimicag.2012.10.021

Kaushik, A., Gupta, C., Fisher, S., Story-Roller, E., Galanis, C., Parrish, N., et al. (2017). Combinations of avibactam and carbapenems exhibit enhanced potencies against drug-resistant *Mycobacterium abscessus*. *Future Microbiol.* 12, 473–480. doi: 10.2217/fmb-2016-0234

Kaushik, A., Makkar, N., Pandey, P., Parrish, N., Singh, U., and Lamichhane, G. (2015). Carbapenems and rifampin exhibit synergy against *Mycobacterium tuberculosis* and *Mycobacterium abscessus*. *Antimicrob. Agents Chemother.* 59, 6561–6567. doi: 10.1128/AAC.01158-15

Livermore, D. M. (1995). beta-Lactamases in laboratory and clinical resistance. *Clin. Microbiol. Rev.* 8, 557–584.

Lomovskaya, O., Sun, D., Rubio-Aparicio, D., Nelson, K., Tsivkovski, R., Griffith, D. C., et al. (2017). Vaborbactam: spectrum of beta-lactamase inhibition and impact of resistance mechanisms on activity in *Enterobacteriaceae*. *Antimicrob. Agents Chemother.* 61:e01443-17. doi: 10.1128/AAC.01443-17

Maurer, F. P., Castelberg, C., Quiblier, C., Bottger, E. C., and Somoskovi, A. (2014). Erm(41)-dependent inducible resistance to azithromycin and clarithromycin in clinical isolates of *Mycobacterium abscessus*. *J. Antimicrob. Chemother.* 69, 1559–1563. doi: 10.1093/jac/dku007

Medjahed, H., Gaillard, J. L., and Reyrat, J. M. (2010). *Mycobacterium abscessus*: a new player in the mycobacterial field. *Trends Microbiol.* 18, 117–123. doi: 10.1016/j.tim.2009.12.007

Miyasaka, T., Kunishima, H., Komatsu, M., Tamai, K., Mitsutake, K., Kanemitsu, K., et al. (2007). In vitro efficacy of imipenem in combination with six antimicrobial agents against *Mycobacterium abscessus*. *Int. J. Antimicrob. Agents* 30, 255–258. doi: 10.1016/j.ijantimicag.2007.05.003

Mukherjee, D., Wu, M. L., Teo, J. W. P., and Dick, T. (2017). Vancomycin and clarithromycin show synergy against *Mycobacterium abscessus* in vitro. *Antimicrob. Agents Chemother.* 61:e01298-17. doi: 10.1128/AAC.01298-17

Nash, K. A., Brown-Elliott, B. A., and Wallace, R. J. Jr. (2009). A novel gene, erm(41), confers inducible macrolide resistance to clinical isolates of *Mycobacterium abscessus* but is absent from *Mycobacterium chelonae*. *Antimicrob. Agents Chemother.* 53, 1367–1376. doi: 10.1128/AAC.01275-08

Nessar, R., Cambau, E., Reyrat, J. M., Murray, A., and Gicquel, B. (2012). *Mycobacterium abscessus*: a new antibiotic nightmare. *J. Antimicrob. Chemother.* 67, 810–818. doi: 10.1093/jac/dkr578

Oh, C. T., Moon, C., Park, O. K., Kwon, S. H., and Jang, J. (2014). Novel drug combination for *Mycobacterium abscessus* disease therapy identified in a *Drosophila* infection model. *J. Antimicrob. Chemother.* 69, 1599–1607. doi: 10.1093/jac/dku024

Olson, M. W., Ruzin, A., Feyfant, E., Rush, T. S., O'Connell, J., and Bradford, P. A. (2006). Functional, biophysical, and structural bases for antibacterial activity of tigecycline. *Antimicrob. Agents Chemother.* 50, 2156–2166. doi: 10.1128/AAC.01499-05

Papp-Wallace, K. M., Endimiani, A., Taracila, M. A., and Bonomo, R. A. (2011). Carbapenems: past, present, and future. *Antimicrob. Agents Chemother.* 55, 4943–4960. doi: 10.1128/AAC.00296-11

Parenti, F. (1986). Structure and mechanism of action of teicoplanin. *J. Hosp. Infect.* 7(Suppl. A), 79–83.

Ryu, Y. J., Koh, W. J., and Daley, C. L. (2016). Diagnosis and treatment of nontuberculous mycobacterial lung disease: clinicians' perspectives. *Tuberc. Respir. Dis.* 79, 74–84. doi: 10.4046/trd.2016.79.2.74

Shen, G. H., Wu, B. D., Hu, S. T., Lin, C. F., Wu, K. M., and Chen, J. H. (2010). High efficacy of clofazimine and its synergistic effect with amikacin against rapidly growing mycobacteria. *Int. J. Antimicrob. Agents* 35, 400–404. doi: 10.1016/j.ijantimicag.2009.12.008

Singh, S., Bouzinbi, N., Chaturvedi, V., Godreuil, S., and Kremer, L. (2014). In vitro evaluation of a new drug combination against clinical isolates belonging to the *Mycobacterium abscessus* complex. *Clin. Microbiol. Infect.* 20, O1124–O1127. doi: 10.1111/1469-0691.12780

Soroka, D., Dubee, V., Soulier-Escrihuela, O., Cuinet, G., Hugonnet, J. E., Gutmann, L., et al. (2014). Characterization of broad-spectrum *Mycobacterium abscessus* class A beta-lactamase. *J. Antimicrob. Chemother.* 69, 691–696. doi: 10.1093/jac/dkt410

Svetitsky, S., Leibovici, L., and Paul, M. (2009). Comparative efficacy and safety of vancomycin versus teicoplanin: systematic review and meta-analysis. *Antimicrob. Agents Chemother.* 53, 4069–4079. doi: 10.1128/AAC.00341-09

van Ingen, J., Totten, S. E., Helstrom, N. K., Heifets, L. B., Boeree, M. J., and Daley, C. L. (2012). In vitro synergy between clofazimine and amikacin in treatment of nontuberculous mycobacterial disease. *Antimicrob. Agents Chemother.* 56, 6324–6327. doi: 10.1128/AAC.01505-12

Wallace, R. J. Jr., Dukart, G., Brown-Elliott, B. A., Griffith, D. E., Scerpella, E. G., and Marshall, B. (2014). Clinical experience in 52 patients with tigecycline-containing regimens for salvage treatment of *Mycobacterium abscessus* and *Mycobacterium chelonae* infections. *J. Antimicrob. Chemother.* 69, 1945–1953. doi: 10.1093/jac/dku062

Yee, M., Klinzing, D., Wei, J. R., Gengenbacher, M., Rubin, E. J., and Dick, T. (2017). Draft genome sequence of *Mycobacterium abscessus* bamboo. *Genome Announc.* 5:e00388-17. doi: 10.1128/genomeA.00388-17

Conflict of Interest Statement: The authors declare that the research was conducted in the absence of any commercial or financial relationships that could be construed as a potential conflict of interest.

frontiers in Microbiology

ORIGINAL RESEARCH
published: 03 April 2019
doi: 10.3389/fmicb.2019.00693

Mycobacterium avium Infection in a C3HeB/FeJ Mouse Model

*Deepshikha Verma[1], Megan Stapleton[1], Jake Gadwa[1], Kridakorn Vongtongsalee[1], Alan R. Schenkel[1], Edward D. Chan[2,3,4] and Diane Ordway[1]**

[1] *Mycobacteria Research Laboratories, Department of Microbiology, Immunology and Pathology, Colorado State University, Fort Collins, CO, United States,* [2] *Department of Medicine, Denver Veterans Affairs Medical Center, Denver, CO, United States,* [3] *Departments of Medicine and Academic Affairs, National Jewish Health, Denver, CO, United States,* [4] *Division of Pulmonary Sciences and Critical Care Medicine, University of Colorado Anschutz Medical Campus, Aurora, CO, United States*

Infections caused by *Mycobacterium avium* complex (MAC) species are increasing worldwide, resulting in a serious public health problem. Patients with MAC lung disease face an arduous journey of a prolonged multidrug regimen that is often poorly tolerated and associated with relatively poor outcome. Identification of new animal models that demonstrate a similar pulmonary pathology as humans infected with MAC has the potential to significantly advance our understanding of nontuberculosis mycobacteria (NTM) pathogenesis as well as provide a tractable model for screening candidate compounds for therapy. One new mouse model is the C3HeB/FeJ which is similar to MAC patients in that these mice can form foci of necrosis in granulomas. In this study, we evaluated the ability of C3HeB/FeJ mice exposure to an aerosol infection of a rough strain of MAC 2285 to produce a progressive infection resulting in small necrotic foci during granuloma formation. C3HeB/FeJ mice were infected with MAC and demonstrated a progressive lung infection resulting in an increase in bacterial burden peaking around day 40, developed micronecrosis in granulomas and was associated with increased influx of $CD4^+$ Th1, Th17, and Treg lymphocytes into the lungs. However, during chronic infection around day 50, the bacterial burden plateaued and was associated with the reduced influx of $CD4^+$ Th1, Th17 cells, and increased numbers of Treg lymphocytes and necrotic foci during granuloma formation. These results suggest the C3HeB/FeJ MAC infection mouse model will be an important model to evaluate immune pathogenesis and compound efficacy.

Keywords: ***Mycobacterium avium*, C3HeB/FeJ mouse model, immunity, pathology, nontuberculosis mycobacteria**

OPEN ACCESS

Edited by:
Veronique Anne Dartois, Rutgers, The State University of New Jersey, United States

Reviewed by:
Eric Nuermberger, Johns Hopkins University, United States
Michael Henry Cynamon, Syracuse VA Medical Center, United States

****Correspondence:***
Diane Ordway
d.ordway@colostate.edu

Specialty section:
This article was submitted to Antimicrobials, Resistance and Chemotherapy, a section of the journal Frontiers in Microbiology

Received: *28 June 2018*
Accepted: *19 March 2019*
Published: *03 April 2019*

Citation:
Verma D, Stapleton M, Gadwa J, Vongtongsalee K, Schenkel AR, Chan ED and Ordway D (2019) Mycobacterium avium Infection in a C3HeB/FeJ Mouse Model. Front. Microbiol. 10:693. doi: 10.3389/fmicb.2019.00693

INTRODUCTION

Infections due to nontuberculosis mycobacteria (NTM) are increasing worldwide, resulting in a **serious** public health problem (Prevots and Marras, 2015). NTM are mycobacterial species other than *Mycobacterium tuberculosis* complex and *Mycobacterium leprae*, that can cause pulmonary and extrapulmonary disease in vulnerable individuals, and are reported throughout the world (Prevots and Marras, 2015; Bryant et al., 2016). Given the ubiquitous nature of NTM in the environment, it is likely that repeated exposures from multiple sources- such as shower heads, swimming pools, and Jacuzzi baths and soil- increases the likelihood of established disease in susceptible individuals (Chan et al., 2010; Bryant et al., 2016). Other reports demonstrate the

possibility that cystic fibrosis patients acquire NTM infection by contact to fomites or from patient to patient transmission (Bryant et al., 2016). Recent population-based studies have demonstrated this worldwide increase in NTM began in 2000 and currently in the United States, the prevalence of NTM lung disease exceeds that of tuberculosis by ∼10-fold (Epson et al., 2012; Prevots and Marras, 2015).

The most common NTM causing disease and outbreaks in the United States are species within the MAC—comprised of at least 9 species including *M. avium, M. intracellulare*, and *M. chimaera*, followed by *Mycobacterium abscessus* complex (including *M. abscessus* sensu stricto, *M. massiliense* and *M. bolletii*), *Mycobacterium chelonae* and *Mycobacterium kansasii* (De Groote and Huitt, 2006). The two most common preexisting conditions for NTM lung disease are emphysema and bronchiectasis, both of which may be acquired or heritable in origin (Chan et al., 2010; Prevots and Marras, 2015). Other host factors and phenotypes that are associated with NTM lung disease include advanced age, thin body habitus often with thoracic cage abnormalities such as scoliosis and pectus excavatum, gastroesophageal reflux, and use of inhaled corticosteroids and anti-tumor necrosis factor-alpha (anti-TNF-α) therapies (Shang et al., 2011; Bryant et al., 2016; Honda et al., 2018).

The two major clinical forms of MAC lung disease are manifested by two major radiographic patterns—the nodular bronchiectatic and fibrocavitary forms—which have differing lung pathology and bacterial burdens (Kartalija et al., 2013). MAC lung disease associated with upper lobe fibrocavitary pattern occurs dominantly in men with chronic obstructive pulmonary disease (COPD) (Glassroth, 2008). The fibrocavitary pattern is characterized by the formation of granulomas and increased bacterial burden (Gadkowski and Stout, 2008). The nodular-bronchiectasis form is often associated with immunocompetent women with granuloma formation in the airway walls and lower bacterial burdens (Glassroth, 2008). However, each type is not exclusively seen in one gender, and both types can be evident in a single patient (Okumura et al., 2008). The number of patients with MAC lung disease has increased worldwide, emphasizing the need for improved MAC modeling systems (Kartalija et al., 2013).

Treatment recommendations for MAC lung disease rely on a paucity of small clinical drug trials and mostly on expert opinion based on combined years of clinical experience (Griffith et al., 2007). Clarithromycin or azithromycin – used as part of a multidrug regimen – is currently the most important antibiotic in the treatment of MAC and many of the other NTM infections (Griffith et al., 2007; van Ingen et al., 2013). The present treatment guidelines for MAC lung disease recommend the combination of a macrolide (clarithromycin or azithromycin) with ethambutol and a rifamycin (rifampin), given for a minimum of 12 months after sputum culture conversion, with or without an aminoglycoside (streptomycin or amikacin given for the first several months) (Griffith et al., 2007; van Ingen et al., 2013). However, this recommended treatment regimen is only considered successful in roughly 50 to 60% of patients, with some recrudescence due to relapse and others due to a new infection from the environment (Griffith et al., 2007; van Ingen et al., 2013). The lack of success of the recommended treatment regimen (macrolide, ethambutol, rifamycin, aminoglycoside combination) is largely due to drug toxicities resulting in poor tolerability.

Four main animal models are routinely used for preclinical MAC experiments: C57BL/6, Balb/c, nude and beige mice infected by aerosol, intranasal, and intravenous exposure with MAC (Gangadharam et al., 1989; Pedrosa et al., 1994; Roger and Bermudez, 2001; Haug et al., 2013; Andrejak et al., 2015; Moraski et al., 2016; Blanchard et al., 2018). The majority of compound screening studies have been carried out with these mouse models due to their low cost and abundance of immunological reagents albeit a major drawback with them is a lack of necrotic granuloma formation (Abendano et al., 2014; Andrejak et al., 2015; Shin et al., 2015). In contrast, C3HeB/FeJ mice, develop highly organized encapsulated necrotic, hypoxic lesions following a *M. tuberculosis* infection (Kramnik et al., 2000; Obregon-Henao et al., 2013; Henao-Tamayo et al., 2015). Using a forward genetics approach, a region was identified as responsible for the 54.0-cM location of chromosome 1, termed the "super-susceptibility to tuberculosis-1" (*sst1*) locus (Kramnik et al., 2000). This locus was responsible for a reduced ability to control *M. tuberculosis* replication in the lungs. The susceptible *sst1* allele was also shown to be responsible for the formation of caseous necrosis in the lungs (Kramnik et al., 2000). The C3HeB/FeJ mouse model has been principally used to study compound screening, host immune response and vaccine efficacy with *M. tuberculosis* infection (Obregon-Henao et al., 2013; Henao-Tamayo et al., 2015) because they are capable of forming necrotic, hypoxic tubercle granulomas (Pichugin et al., 2009; Obregon-Henao et al., 2013; Henao-Tamayo et al., 2015). A MAC infection mouse model with the ability to develop necrotic granulomas is required to understand if a compound or vaccine-induced immune response can enter the site of necrosis to eradicate the bacilli.

Hence, we undertook a study to infect C3HeB/FeJ mice with an aerosol of a rough strain of *Mycobacterium avium* 2285 to determine if they develop a progressive infection and develop necrotic foci as well as characterize the cellular immune response. To better characterize the immune and pathologic responses induced by MAC infection in the C3HeB/FeJ mice would greatly improve the usefulness of this animal model for the testing of urgently needed new antimicrobial compounds and vaccines.

MATERIALS AND METHODS

Mice

Specific pathogen-free female C3Heb/FeJ, 6 to 8 weeks old, were purchased from the Jackson Laboratories (Bar Harbor, ME). Mice were maintained in the biosafety level 3 facilities at Colorado State University and were given sterile water, chow, bedding, and enrichment for the duration of the experiments. The specific-pathogen-free nature of the mouse colonies was demonstrated by testing sentinel animals. All experimental protocols were approved by the Animal Care and Use Committee of Colorado State University.

MAC Model

The *M. avium* 2285 strain with a rough colony morphology and positive for biofilm formation was obtained from a pulmonary MAC patient with a fibrocavitary form of disease (gift from Drs. Stephen Holland and Kenneth Olivier, National Institute of Allergy and Infectious Diseases). The *M. avium* 2285 strain was found to be of high virulence in Beige mouse model infected with a high dose aerosol (1.0×10^9 CFU) (unpublished data). The inoculum was prepared by thawing the bacterial vial, sonicating for 10 to 15 s, and vortexing to remove any clumps that formed during freezing. Thereafter, the mycobacterial suspension was obtained from the vial with a 1-ml tuberculin syringe fitted with a 26.5-gauge needle and expelled back into the vial. This procedure was repeated into the vial 20 times without removing the needle to mix the suspension and break up any small clumps of bacilli (Ordway et al., 2008b; Obregon-Henao et al., 2015).

C3HeB/FeJ mice were infected with MAC using a Glas-Col aerosol generator (Glas-Col, Terre Haute, IN, United States), using the clinical isolate *M. avium* 2285 rough strain (henceforth referred to as MAC 2285) calibrated to deliver 2,000 bacteria into the lungs per mouse (Obregon-Henao et al., 2013; Henao-Tamayo et al., 2015). The following day, five mice were euthanized and their whole lungs, spleens, and livers were harvested to determine the baseline bacterial burden. The organs were homogenized in phosphate-buffered saline (PBS), and serial dilutions were plated on nutrient 7H11 agar and tryptic soy agar (TSA) for 3 weeks at 37°C, then CFU were enumerated (Bryant et al., 2016).

The dose of MAC 2285 resulted in progressive infection without showing signs of mortality at the 2,000 CFU. The increased susceptibility of the C3HeB/FeJ mice to mycobacteria justified the use of lower infective doses of MAC 2285 compared to the other more resistant mice (C57BL/6, Balb/c, nude or beige) which require an infective dose of 1×10^8–1×10^{11} CFUs (Ji et al., 1994; Andrejak et al., 2015).

Animal Infection

Using a Glas-Col aerosol generator, C3HeB/FeJ mice were infected by an aerosol of the clinical isolate MAC 2285 rough strain calibrated to deliver 2,000 bacteria into the lung, spleen and liver per mouse (Obregon-Henao et al., 2013; Henao-Tamayo et al., 2015). The whole lung, spleen, and liver from the mice for each condition at each time point (n = 5) were harvested to quantify bacterial burden (lung, spleen and liver, n = 5), histological analysis (lungs, n = 5), and flow cytometric analyses (lung and spleen, n = 5) at 20, 30, 40, 50, and 60 days post-challenge. In brief, bacterial loads were determined by plating whole organ serial dilutions of organ homogenates onto nutrient 7H11 and TSA agar plates. The rationale for using both 7H11 and TSA plates are any additional environmental NTM contamination of our CFUs can be identified on the TSA plates. Colony forming units (CFU) were quantified after incubation for 3 weeks at 37°C. The tissues of additional groups of mice were analyzed for pathological and immune response analysis. The results shown in this study are representative of two independent experiments using five animals per time point.

Histological Analysis

The whole lung lobe from each mouse was fixed with 10% formalin in PBS. Sections from these tissues were stained with haematoxylin-eosin and with Ziehl-Neelsen acid-fast stains (Obregon-Henao et al., 2013; Henao-Tamayo et al., 2015).

Lung and Spleen Cell Digestion

Briefly, single cell suspensions were prepared as described previously (Ordway et al., 2008a; Shang et al., 2011; Obregon-Henao et al., 2013). The lungs and spleens were aseptically removed, teased apart and treated with a solution of deoxyribonuclease IV (DNAse) (Sigma Chemical, 30 μg/ml) and collagenase XI (Sigma Chemical, 0.7 mg/ml) for 45 min at 37°C. To obtain a single-cell suspension, the organs were gently passed through cell strainers (Becton Dickinson, Lincoln Park, NJ, United States). Any remaining erythrocytes were lysed with Gey's solution (0.15 M NH_4Cl, 10 mM $KHCO_3$) and the cells were washed with Dulbecco's modified Eagle's minimal essential medium. Cell suspensions from each individual mouse were incubated with monoclonal antibodies to various cytokines and cell surface markers labeled with fluorescein isothiocyanate (FITC), phycoerythrin (PE), peridinin chlorophyll-a protein (PerCP), or allophycocyanin (APC) at 4°C for 30 min in the dark as described previously (Ordway et al., 2008a; Shang et al., 2011; Obregon-Henao et al., 2013). Total cell numbers were determined by flow cytometry using BD™ Liquid Counting Beads, as described by the manufacturer (BD PharMingen, San Jose, CA, United States). All analyses were performed with an acquisition of at least 100,000 total events for T cells and 200,000 total events for antigen-presenting cells.

Cell Surface and Intracytoplasmic Cytokine Staining

Cells were first stained for cell surface markers as indicated above and thereafter the same cell suspensions were prepared for intracellular staining as described previously (Ordway et al., 2007, 2008a; Obregon-Henao et al., 2013). For flow cytometry analysis, single-cell suspensions prepared from the lungs of naïve and MAC 2285 infected mice were re-suspended in PBS containing 0.1% of sodium azide. Cells were incubated in the dark for 25 min at 37°C with pre-determined optimal titrations of specific antibody (directly conjugated to FITC, PE, PerCP, APC, Pacific Blue, or Alexa 700); or after biotin antibody incubations washed and incubated for 25 min more with streptavidin Qdot800 (Invitrogen), followed by two washes in PBS containing 4% sodium azide. Measurement of intracellular cytokines was conducted by pre-incubating lung cells with monensin (3 μM) (Golgi Stop, BD PharMingen), anti-CD3 and anti-CD28 (both at 0.2 $\mu g/10^6$ cells) for 4 h at 37°C, 5% CO_2. The cells were then surface stained, incubated for 30 min at 37°C, washed, fixed and permeabilized with Perm Fix/Perm Wash (BD Pharmingen). Finally, the cells were stained with fluorescently-labeled antibodies directed against intracellular Foxp3 (FJK-16s), IL-17 (clone N49-653) and IFN- γ many of the IFN-γ (clone B27) and separately with their respective isotype controls (BD Pharmingen) for a further 30 min. All the samples were run

on a Becton Dickinson LSR-II and data were analyzed using FACSDiva v5.0.1 software. Cells were gated on lymphocytes based on characteristic forward and side scatter profiles. Individual cell populations were identified according to their presence of specific fluorescent-labeled antibodies. All the analyses were performed with a minimum acquisition of 100,000 events for T cells and 200,000 events for macrophages and dendritic cells.

Statistical Analysis

Data are presented using the mean values from 5 mice per group performed in duplicate experiments. The Student *t*-test was used to assess statistical significance between groups of mice. In addition, bacterial burdens for each experimental condition were analyzed with GraphPad Prism version 4 (GraphPad Software, San Diego, CA), using analysis of variance (ANOVA) comparison test. Data are presented using the mean values ($n = 5$) plus or minus the standard error of the mean (SEM). Significance was considered with a P value of < 0.05 (Obregon-Henao et al., 2015).

RESULTS

Course of MAC Infection in C3HeB/FeJ Mice

Our goal was to assess the course of an aerosol infection during acute and chronic infection with MAC 2285 in mice. We evaluated aerosol exposure of a clinical, drug- resistant strain of MAC 2285 (∼2,000 bacilli per mouse) to determine if there is a progressive infection in the C3HeB/FeJ during the acute and relative chronic phases after infection.

Mice infected with MAC were evaluated for bacterial loads in the lungs (**Figure 1A**), spleens (**Figure 1B**), and livers (**Figure 1C**) after 1, 20, 30, 40, 50, and 60 days of infection.

C3HeB/FeJ mice showed an increase in bacterial burden 40 days after infection, peaking at ∼5.2 $\log_{10}$ CFU in the lungs (**Figure 1A**), followed by bacilli persisting in the lungs and plateauing at ∼5.1 $\log_{10}$ CFU during the chronic phase of disease. C3HeB/FeJ mice showed a delayed dissemination to the spleens (**Figure 1B**), and livers (**Figure 1C**) over the first 30 days of infection, followed by an increase of ∼4.0 $\log_{10}$ CFU in the spleens peaking at 50 days and ∼3.0. $\log_{10}$ CFU in the livers during the chronic phase of disease.

These results demonstrate that aerosol exposure of MAC can progress slowly over the acute and subacute phases of disease, reaching a peak in bacterial burden in the lungs ay day 40. Furthermore, by the chronic phase of the infection, the bacterial burden remained persistently elevated in all the organs examined (Kitahara et al., 1997; Boyle et al., 2015).

Development of Pathology in MAC Infection in C3HeB/FeJ Mice

The lung histopathology and acid-fast staining over the course of infection are shown in **Figure 2** (left / middle and right columns, respectively). As early as day 40 after infection, C3HeB/FeJ mice developed small pulmonary necrotic lesions (**Figure 2**, left / middle columns), and multiple extracellular clusters of bacilli were observed within these lesions (**Figure 2**, arrows). During the chronic stage, the lungs of MAC -infected C3HeB/FeJ mice developed increased numbers of granulomas, greater numbers of intracellular and extracellular acid fast bacilli and progressive development of lesions, with notable lung tissue inflammation and small areas of necrosis (**Figure 2** day 40–60). During the later stages of chronic disease much of the lung tissue was grossly consolidated, with inflammation and necrosis was evident. Overall, MAC infection of C3HeB/FeJ mice demonstrate disease progression resulting in pulmonary inflammation, lung consolidation and small foci of necrosis in pulmonary lesions.

Kinetic Influx of the T Cell Response in *M. avium* Infected C3HeB/FeJ Mice

T cells were gated with a primary gate on viable FSC^{low} vs. SSC^{low} lymphocytes and then on $CD3^+$ T cells and compared to the isotype controls (**Figures 3A–C**), and analyzed for changes in the total mean cell number of $CD3^+CD4^+$ and $CD3^+CD8^+$ cells over the course of infection.

T cells that migrated to the lungs of naive control and MAC-infected C3HeB/FeJ mice were harvested and analyzed by flow cytometry. Specifically, naive $CD3^+CD4^+$ and $CD3^+CD8^+$ T cells, as well as the kinetic influx of activated T effector cells ($CD3^+CD4^+CD44^{hi}$ and $CD3^+CD8^+CD44^{hi}$) and effector memory T cells ($CD3^+CD4^+CD44^{hi}CD127^+$ and $CD3^+CD8^+CD44^{hi}CD127^+$) were determined in naive mice and MAC-infected C3HeB/FeJ mice (Henao-Tamayo et al., 2014). As expected, at days 30 and 40, when bacterial burden increased (**Figure 1A**) and pathology began to develop (**Figure 2**), increased numbers of ($CD3^+CD4^+$ and $CD3^+CD8^+$ T cells) were already found in MAC-infected C3HeB/FeJ mice compared to naive mice (**Figures 3D,G**). In addition, in MAC infected C3HeB/FeJ mice the ($CD3^+CD4^+CD44^{hi}$ and $CD3^+CD8^+CD44^{hi}$) activated T effector cells showed a delay in trafficking into the lungs peaking on day 50 compared to the overall $CD4^+$ and $CD8^+$ populations (**Figures 3E,H**). Similarly, in the MAC infected C3HeB/FeJ mice, the effector memory T cells ($CD3^+CD4^+CD44^{hi}CD127^+$ and $CD3^+CD8^+CD44^{hi}CD127^+$) cells demonstrated a lag in reaching the lungs, peaking on day 50 compared to the overall $CD4^+$ and $CD8^+$ populations, thereafter, these memory T cells declined (**Figures 3F,I**).

Kinetic Influx of CD4 and CD8 T Cells Expressing IFN-γ, IL-17, and Foxp3 in MAC-Infected C3HeB/FeJ Mice

The kinetic influx of IFN- γ -producing $CD3^+CD4^+$ and $CD3^+CD8^+$ T cells, IL-17 producing $CD3^+CD4^+$ and $CD3^+CD8^+$ T cells, and suppressive T regulatory cells ($CD3^+CD4^+$ and $CD3^+CD8^+$ $CD25^+Foxp3^+$), were determined in the lungs of the MAC infected C3HeB/FeJ mice compared to naive mice. Interestingly, after day 40–50, when bacterial burden (**Figure 1A**) and pathology (**Figure 2**) were increasing, higher numbers of $CD4^+$ IFN-γ-producing T cells were found in the lungs which declined at 60 days (**Figures 4A,D**). However, with respect to $CD8^+$ IFN-γ-producing T cells in C3HeB/FeJ mice, what was observed

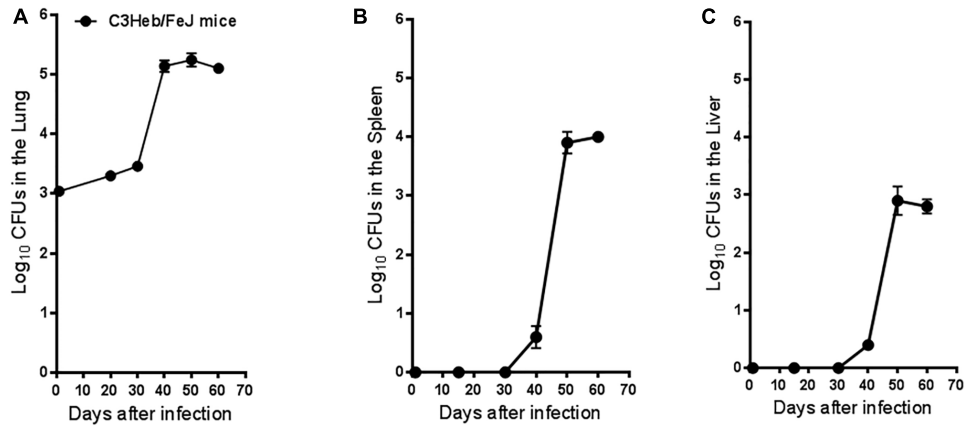

FIGURE 1 | *Mycobacterium avium* infection in C3HeB/FeJ mice. Bacterial counts in the lungs **(A)**, spleens **(B)**, and livers **(C)** of C3HeB/FeJ mice infected with 2,000 MAC 2285 rough strain per mouse are shown. CFU were determined at 1, 20, 30, 40, 50, and 60 days after infection by plating serial dilutions of organ homogenates on nutrient 7H11 and TSA agar and quantifying CFU after 3 weeks incubation at 37°C. The C3HeB/FeJ mice after 40 days of infection showed increased bacterial burden ∼4.5 to 5.0 $\log_{10}$ in the lungs followed by bacterial burden plateauing during chronic phase of infection ∼50–60 days **(A)**. The C3HeB/FeJ mice showed a delay in bacterial dissemination in both the spleens **(B)** and liver **(C)** peaking after ∼50–60 days to ∼4.0 $\log_{10}$ CFU in the spleen and ∼3.0 $\log_{10}$ CFU in the liver. Results represent the average of two experiments (n = 5 mice per time point) and are expressed as $\log_{10}$ CFU (±SEM).

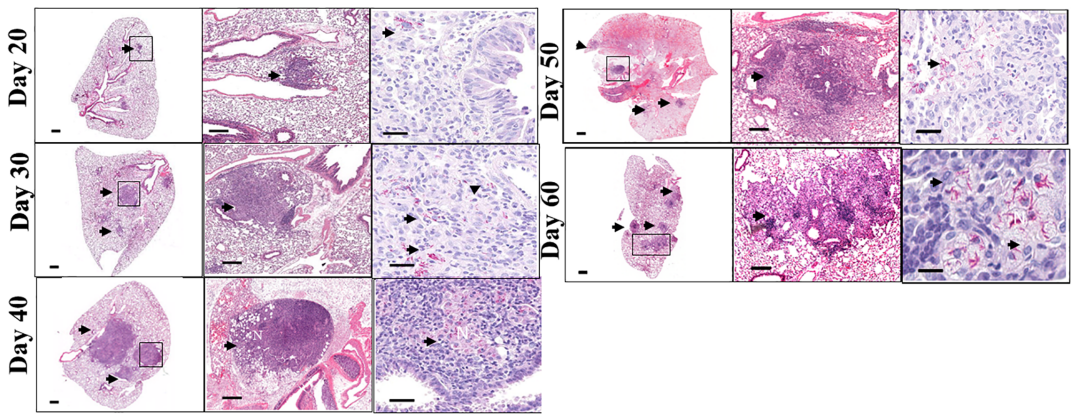

FIGURE 2 | Pulmonary pathology in *Mycobacterium avium* infection C3HeB/FeJ mice. Lung pathology of MAC-infected C3HeB/FeJ mice. Shown are representative photomicrographs of haematoxylin-eosin-stained (left and middle columns) and of acid-fast stain (right column) of the lungs of MAC -infected C3HeB/FeJ mice. As early as 20–30 days after infection, small granulomas are evident in C3HeB/FeJ mice. As disease progressed (day 40), significant increase in granuloma size and bacterial burden (denoted by acid-fast staining) are found. During chronic phase of infection between 50 and 60 days the number of granulomas increased with increased clusters of acid-fast-staining bacilli, accumulating in areas of necrosis (N) (arrows). Magnifications, 1X (left), 20X (middle) and 100X (right).

to be overall lower were observed and increased slightly between 40 and 50 days over the course of the infection compared to naive mice (**Figure 4B**). MAC-infected C3HeB/FeJ mice demonstrated increased numbers of $CD4^+$ and $CD8^+$ T cells producing IL-17 (**Figures 4B,E**), and regulatory T cell markers ($CD25^{hi}$ and Foxp3) (**Figures 4C,F**), that were associated with increased bacterial burden and organ pathology.

Kinetics of Macrophages and Dendritic Cells in *M. avium*-Infected C3HeB/FeJ Mice

Flow cytometric analysis was performed on MAC- infected C3HeB/FeJ mice and naïve mice in order to analyze the influx of $CD11b^+$ macrophages and $CD11c^+$ dendritic cells into the lungs. Between 40 and 50 days, a time at which the infection progressed, we observed a relative increase in cells staining positive for $CD11b^+$ and $CD11c^+$ MHC class II expression compared to the naïve mice (**Figures 5A,D**). This was consistent with the presence of increasing numbers of $CD11b^+$ and $CD11c^+$ cells expressing IL-27 (**Figures 5B,E**) and programmed death-ligand 1 (PD-L1) markers although both plateaued at 50 days of infection (**Figures 5C,F**) related with T cell immune suppression (Shu et al., 2017).

The slow increase of MHC II^+ macrophages and dendritic cells between 40 and 50 days of infection, was associated with an increase number of $CD4^+$ T cells producing IFN-γ and IL-17 increased arriving in the lungs at this later time range, whereas

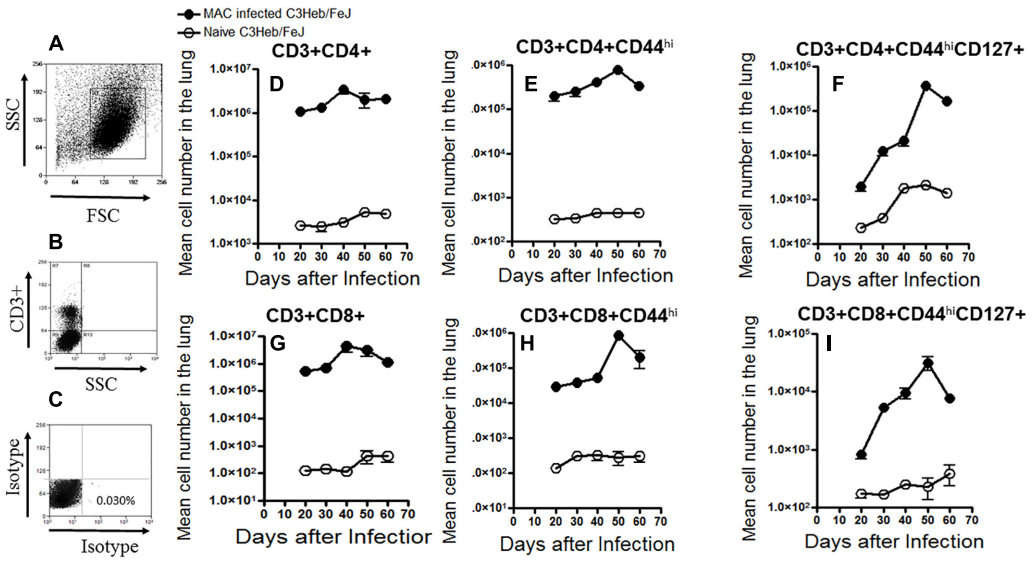

FIGURE 3 | Kinetic influx of CD4 and CD8 T cell effector and memory cells in *M. avium*-infected C3HeB/FeJ mice. Increased percentages of activated effector and memory T cells were present after a moderate-dose infection of MAC 2285 rough in C3HeB/FeJ mice analyzed by flow cytometry compared to naïve controls. T cells were gated with a primary gate on viable FSC^{low} vs. SSC^{low} lymphocytes compared to the isotype controls **(A–C)** and then on $CD3^+$ T cells, and analyzed for changes in the total mean cell number of $CD3^+CD4^+$ and $CD3^+CD8^+$ **(D,G)** cells over the course of infection. Shown are the numbers of activated effector T cells ($CD4^+CD44^{hi}$ and $CD8^+CD44^{hi}$) **(E,F)** and memory T cells ($CD4^+CD44^{hi}CD127^+$ and $CD8^+CD44^{hi}CD127^+$) **(F,I)** migrating to the lungs of C3HeB/FeJ mice peaking after 40–50 days of infection. During the later stages on day 60 of infection, C3HeB/FeJ mice expressed diminished numbers of activated effector and memory T cells. Results represent the mean number of cells of five mice for each condition from two independent experiments (±SEM).

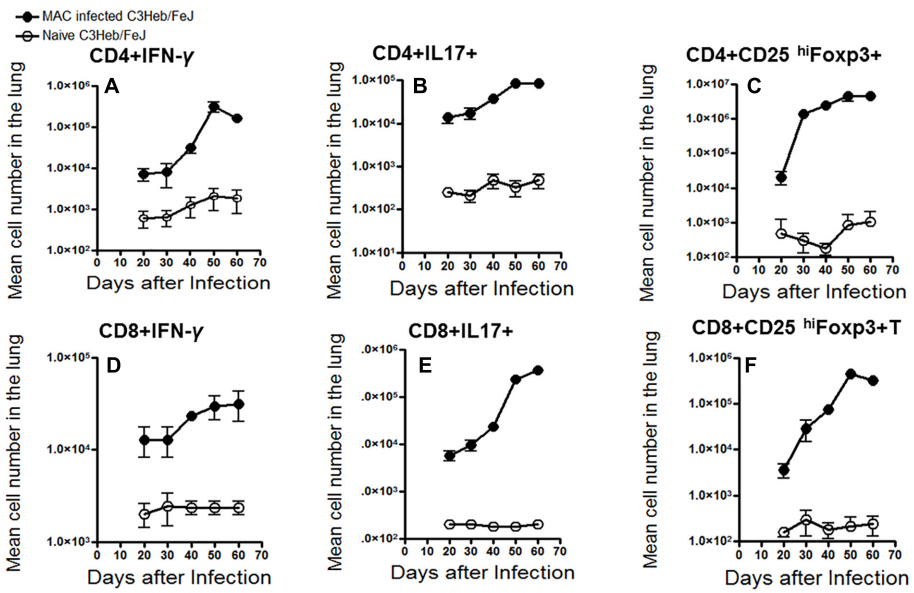

FIGURE 4 | Kinetic influx of CD4 and CD8 T cells expressing IFN-γ, IL-17, and Foxp3 in *M. avium*-infected C3HeB/FeJ mice. Lung cells obtained from MAC-infected C3HeB/FeJ and naive control mice were analyzed by flow cytometry. **(A–C)** show $CD4^+$ effector cells expressing IFN-γ, IL-17 and $CD25^{hi}$Foxp3. MAC-infected C3HeB/FeJ mice showed increased numbers of $CD4^+$IFN-γ^+ and $CD4^+$IL-17^+ producing cells peaking between 40 and 50 days after infection with concomitant increased numbers of $CD4^+CD25^{hi}Foxp3^+$ cell compared to the naïve mice. **(D–F)** show $CD8^+$ effector cells expressing IFN-γ, IL-17, and $CD25^{hi}$Foxp3. Interestingly, $CD8^+$IFN-γ^+ effector cells demonstrated decreased migration to the lungs with a concomitant increased number of $CD8^+$IL-17^+ and $CD8^+CD25^{hi}Foxp3^+$ cells compared to the naïve mice. The data are expressed as the mean number of pulmonary cells in each organ ± SEM (n = 5 mice for each condition from two independent experiments (±SEM).

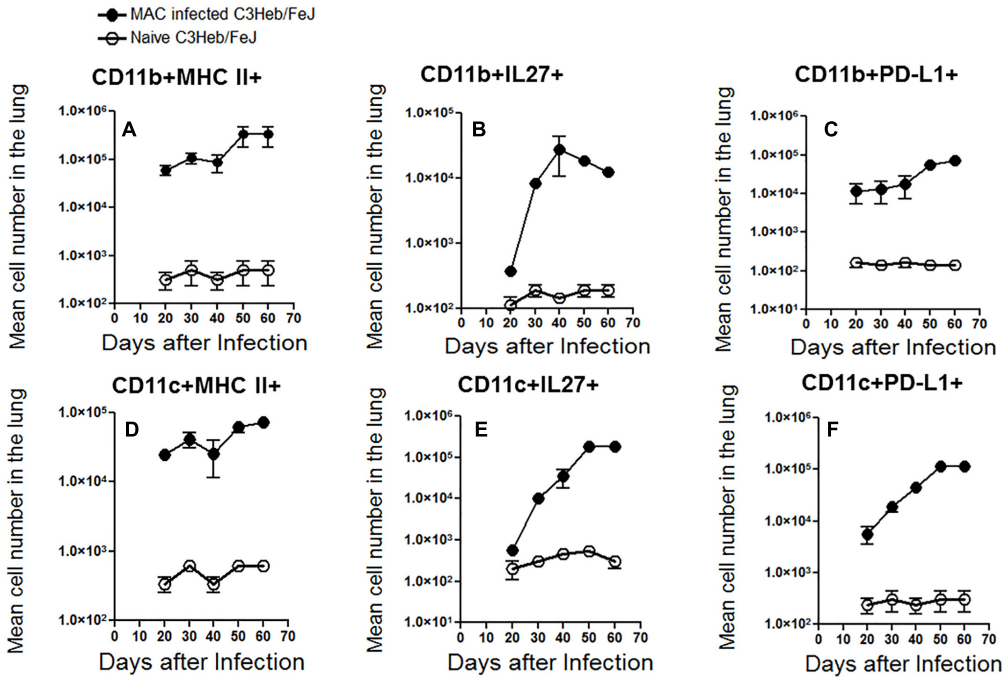

FIGURE 5 | Kinetic influx of CD11b$^+$ macrophages and CD11c$^+$ dendritic cells in *M. avium*-infected C3HeB/FeJ mice. After the indicated times of MAC infection of C3HeB/FeJ mice and naïve mice, the lung cells obtained were analyzed by flow cytometry. Kinetic influx of CD11b$^+$ macrophages and CD11c$^+$ dendritic cells expressing MHC-II$^+$ **(A,D)**, IL-27$^+$ **(B,E)** and PD-L1$^+$ **(C,F)** of MAC infected C3HeB/FeJ mice at the indicated times. The data are expressed as the mean number of pulmonary cells in each organ ± SEM (n = 5 mice per group). Results represent the mean number of cells of five mice for each condition from two independent experiments (±SEM).

there was only a modest increase in the number of CD8$^+$ T cells that produced IFN-γ (**Figure 4D**).

DISCUSSION

While MAC is less virulent than *M. tuberculosis*, these NTM are capable of causing chronic lung disease. Thus, development of a sustained progressive MAC infection in a mouse strain is an important endeavor to not only better characterize the immunopathogenesis in an *in vivo* model, but to also test candidate antimicrobials. Previous work using immunocompetent mouse strains demonstrated rapid clearance with lower amounts of MAC (Gangadharam, 1995), making such models suboptimal for more chronic human lung infection. In a MAC aerosol model using high doses of bacteria (1×10^9–1×10^{11} CFU per mouse) in comparing BALB/c, C57BL/6, Nude and Beige mice, the Nude mice were identified as the most sensitive mouse strain to MAC while treatment efficacy was most noticeable in BALB/c mice (Torrelles et al., 2002; van Ingen et al., 2013; Andrejak et al., 2015; Cha et al., 2015). Beige mice are not uncommonly utilized as an *in vivo* mouse model for MAC infection and display many immune deficiencies similar to those occuring in AIDS patients such as a dominant Th2 response resulting in enhanced susceptibility to infection with NTM following either intravenous or aerosol infection (Caverly et al., 2015). Indeed, dissemination of MAC from gut of the Beige mice was shown to be more rapid than that seen in wildtype C57BL/6 mice (Torrelles et al., 2002). The Beige mice also had a defect in the influx of neutrophils to the site of infection and transfusing exogenous neutrophils mitigated their susceptibility; neutrophil depletion studies with wildtype C56BL/6 mice demonstrated increased susceptibility (Torrelles et al., 2002). Subsequent studies in another mouse strain revealed that a defect in CXCR2 chemokine signaling impaired the early and rapid recruitment of neutrophils in response to MAC infection (Torrelles et al., 2002; van Ingen et al., 2013). Nevertheless, the initial discovery and further confirmation of sustained MAC disease in the Beige mouse have encouraged many investigators to use this model to screen potential chemotherapeutic compounds for the treatment of MAC disease (Obregon-Henao et al., 2015; van Ingen et al., 2013).

Finding demonstrate that C3HeB/FeJ mice infected with MAC (∼2,000 organisms per mouse) – as compared to an inoculum dose of 1×10^8–1×10^9 organisms per mouse typically utilized with infection of mouse models (Torrelles et al., 2002; van Ingen et al., 2013; Andrejak et al., 2015; Cha et al., 2015)-resulted in a progressive infection, distinct temporal immune responses, and histopathologic changes resulting in small foci of necrosis in the lungs.

More specifically, after 20 days of infection, the C3HeB/FeJ mice showed a burden of 3.5 $\log_{10}$ CFU in the lungs followed by an increase of 1.8 $\log_{10}$ CFU during the chronic phase of disease. C3HeB/FeJ mice showed a delayed dissemination to the

spleen, and liver, over the first 30 days of infection, followed by an increase of ∼4.0 $\log_{10}$ CFU in the spleen and ∼3.0 $\log_{10}$ CFU in the liver during the chronic phase of disease. An advantage of the C3HeB/FeJ model over the currently utilized MAC mouse models that use 1×10^8–1×10^9 CFU (Torrelles et al., 2002; van Ingen et al., 2013; Andrejak et al., 2015; Cha et al., 2015) to infect mice is that much fewer bacteria were used to infect the mice, mimicking the relative paucibacillary load seen in non-HIV infected subjects infected with NTM (Farhi et al., 1986; Hibiya et al., 2013; Kobashi et al., 2013).

Our prior studies with *M. tuberculosis* infection of C3HeB/FeJ mice demonstrated necrotic granulomas in the lungs during the chronic phase of the disease, allowing for bacterial replication, while fewer tubercular granulomas were present in the spleen and liver, leading to better bacterial clearance (Henao-Tamayo et al., 2015). However, presumably due to the reduced virulence of MAC compared to *M. tuberculosis*, MAC demonstrated a slower disease progression prior to 20 days where thereafter the development of small foci of necrosis appeared in MAC-infected granulomas. An additional advantage of the C3HeB/FeJ model over currently utilized MAC mouse models is the presence of small foci of necrosis in the granulomas - absent in the latter mouse strains (Torrelles et al., 2002; van Ingen et al., 2013; Andrejak et al., 2015; Cha et al., 2015) - since formation of these characteristic lesions is important in the pathogenesis of human NTM lung infections (Farhi et al., 1986; Hibiya et al., 2013; Kobashi et al., 2013).

Development of small foci of necrosis is an important aspect of NTM pathogenesis. Bacteria residing in necrotic granulomas have access to an abundant source of carbon in the form of cholesterol and triglycerides (Obregon-Henao et al., 2013), and this may be the reason for the relatively high NTM bacilli growth in these lesions. Furthermore, antibiotic penetration is significantly reduced in necrotic granulomas (Farhi et al., 1986), which could help explain the protracted antibiotic therapy required to eradicate NTMs. Thus, it is important to have these aspects in our mouse models that are utilized for compound and vaccine screening.

C3HeB/FeJ mice infected with MAC showed increased numbers of $CD11b^+$ macrophages and $CD11c^+$ dendritic cells expressing MHC class II during acute phase of the infection, however, this waned during the chronic phase of the disease when expression of IL-27 and PD-1L increased. Studies investigating macrophage deactivation by examining the expression of a panel of IFN-γ-inducible genes and activation of Janus kinase (JAK)-STAT pathway in MAC-infected macrophages showed reduced expression of IFN-γ-inducible genes—MHC class II gene Eβ; MHC class II transactivator; IFN regulatory factor-1; and Mg21, a gene coding for a GTP-binding protein in MAC-infected macrophages (Hussain et al., 1999). These studies support our results showing a reduction of MHC class II-expressing $CD11b^+$ macrophages and $CD11c^+$ dendritic cells during chronic disease (Taylor-Robinson et al., 1994).

C3HeB/FeJ mice infected with MAC was associated with increased numbers of $CD3^+CD4^+CD44^{hi}$ and $CD3^+CD8^+CD44^{hi}$ activated T effector cells and $CD3^+CD4^+CD44^{hi}CD127^+$ and $CD3^+CD8^+CD44^{hi}CD127^+$ memory T cells between 40 and 50 days after infection, followed by diminished numbers. In addition, C3HeB/FeJ mice were infected with MAC also demonstrated increased numbers of IFN- γ and IL-17 $CD4^+$ cells as well as increased $Foxp3^+CD4^+$ T regulatory cells during late chronic infection (60 days). Interestingly, MAC-infected C3HeB/FeJ mice displayed increasing numbers of $CD8^+$ T cells expressing IL-17 and Foxp3 over the course of the infection period but a modest increase of $CD8^+$IFN-γ^+ T cells. $CD4^+$ T cell depleted C57BL/6 mice clearly indicate a role for $CD4^+$ T cell needed for control of an intranasal infection of MAC (Florido et al., 1999). In this previous study, IFN-γ^+ depletion before and during MAC infection led to increased bacterial burden in then lung, spleen and liver, suggesting a protective role for IFN-γ against this pathogen.

In previous studies using C57BL/6 mice and C3HeB/FeJ mice, we reported that protection waned with specific alterations of the adaptive immune response, such as increased numbers of regulatory T cells (Henao-Tamayo et al., 2015), concomitant with reduced numbers of protective $CD8^+$ T cells. However, our previous studies infecting C3HeB/FeJ mice with *M. tuberculosis* (Henao-Tamayo et al., 2015) showed a reduction of both IFN-γ producing $CD4^+$ and $CD8^+$ T cell responses with a concomitant increase in the influx of $CD4^+$ and $CD8^+$ $Foxp3^+$ T regulatory cells. Due to the lower dose of MAC used to infect C3HeB/FeJ mice, it is plausible that MAC disease requires additional immune deficits to display progression or a higher infection dose.

A MAC-infected C3HeB/FeJ mouse model is supported by other murine studies showing early *in vivo* expression of IFN-γ during MAC-infection correlated with resistance to the infection (Gangadharam, 1995; Young and Bermudez, 2001; Appelberg, 2006). The use of specific neutralizing antibodies *in vivo* led to the identification of IFN-γ and TNF-α as protective cytokines acting at the effector level of resistance to MAC (Gangadharam, 1995; Young and Bermudez, 2001; Appelberg, 2006).

CONCLUSION

In conclusion, MAC infections are becoming an emerging problem worldwide. To deal with the increasing number of infected NTM patients and the resultant morbidity and mortality caused by these pathogens, multiple laboratories are focused on developing new preclinical models to screen new or repurposed compounds to fight the emergence of these pathogens. Our studies support the use of a MAC infected C3HeB/FeJ mouse model for testing candidate compounds against MAC.

ETHICS STATEMENT

This study was carried out in accordance with the recommendations of NRC Guide for the Care and Use of Laboratory Animals (National Research Council, 2010), the

requirements of the Public Health Service (PHS) Grants Administration Manual, and The Animal Welfare Act as amended. CSU files assurances with the DHHS Office of Extramural Research, Office of Laboratory Animal Welfare (OLAW), the Public Health Service, and adheres to NIH standards and practices for grantees. The protocol was approved by the Colorado State Universities Animal Care and Usage Committee.

AUTHOR CONTRIBUTIONS

DO, EC, AS, DV, and MS conceived and designed the study, acquired, analyzed, and interpreted the data, and drafted the manuscript. JG, KV, and AT analyzed and interpreted the data, and drafted and revised the manuscript. DO, EC, AS, and DV conceived and designed the study, analyzed and interpreted the data, and drafted, revised, and approved the manuscript.

DEDICATION

In memory of Dr. Ian Orme.

FUNDING

This work was supported by funding from the National Institutes of Health [Grant Nos. R21AIO99534-02 and AIO99534-02, and NIH/NIAID task order HHSN272201000009I/HHSN27200001, principal investigator (PI), Anne J. Lenaerts, co-PI, DO] (program officers, Christine Sizemore, Jim Boyce, and Andre McBride).

REFERENCES

Abendano, N., Tyukalova, L., Barandika, J. F., Balseiro, A., Sevilla, I. A., Garrido, J. M., et al. (2014). *Mycobacterium Avium* subsp. paratuberculosis isolates induce in vitro granuloma formation and show successful survival phenotype, common anti-inflammatory and antiapoptotic responses within ovine macrophages regardless of genotype or host of origin. *PLoS One* 9:e104238. doi: 10.1371/journal.pone.0104238

Andrejak, C., Almeida, D. V., Tyagi, S., Converse, P. J., Ammerman, N. C., and Grosset, J. H. (2015). Characterization of mouse models of *Mycobacterium avium* complex infection and evaluation of drug combinations. *Antimicrob. Agents Chemother.* 59, 2129–2135. doi: 10.1128/AAC.04841-14

Appelberg, R. (2006). Pathogenesis of *Mycobacterium avium* infection: typical responses to an atypical mycobacterium? *Immunol. Res.* 35, 179–190. doi: 10.1385/IR:35:3:179

Blanchard, J. D., Elias, V., Cipolla, D., Gonda, I., and Bermudez, L. E. (2018). Effective Treatment of *Mycobacterium avium* subsp. hominissuis and *Mycobacterium abscessus* species infections in macrophages, biofilm, and mice by using liposomal ciprofloxacin. *Antimicrob. Agents Chemother.* 62:e00440-18. doi: 10.1128/AAC.00440-18

Boyle, D. P., Zembower, T. R., Reddy, S., and Qi, C. (2015). Comparison of clinical features, virulence, and relapse among *Mycobacterium avium* complex species. *Am. J. Respir. Crit. Care Med.* 191, 1310–1317. doi: 10.1164/rccm.201501-0067OC

Bryant, J. M., Grogono, D. M., Rodriguez-Rincon, D., Everall, I., Brown, K. P., and Moreno, P. (2016). Emergence and spread of a human-transmissible multidrug-resistant nontuberculous mycobacterium. *Science* 354, 751–757. doi: 10.1126/science.aaf8156

Caverly, L. J., Caceres, S. M., Fratelli, C., Happoldt, C., Kidwell, K. M., Malcolm, K. C., et al. (2015). *Mycobacterium abscessus* morphotype comparison in a murine model. *PLoS One* 10:e0117657. doi: 10.1371/journal.pone.0117657

Cha, S. B., Jeon, B. Y., Kim, W. S., Kim, J.-S., Kim, H. M., Kwon, K. W., et al. (2015). Experimental reactivation of pulmonary *Mycobacterium avium* complex infection in a modified cornell-like murine model. *PLoS One* 10:e0139251. doi: 10.1371/journal.pone.0139251

Chan, E. D., Bai, X., Kartalija, M., Orme, I. M., and Ordway, D. J. (2010). Host immune response to rapidly growing mycobacteria, an emerging cause of chronic lung disease. *Am. J. Respir. Cell Mol. Biol.* 43, 387–393. doi: 10.1165/rcmb.2009-0276TR

De Groote, M. A., and Huitt, G. (2006). Infections due to rapidly growing mycobacteria. *Clin. Infect. Dis.* 42, 1756–1763. doi: 10.1086/504381

Epson, E., Cassidy, M., Marshall-Olson, A., Hedberg, K., and Winthrop, K. L. (2012). Patients with nontuberculous mycobacteria: comparison of updated and previous diagnostic criteria for lung disease. *Diagn. Microbiol. Infect. Dis.* 74, 98–100. doi: 10.1016/j.diagmicrobio.2012.05.035

Farhi, D. C., Mason, U. G. III, and Horsburgh, C. R. Jr. (1986). Pathologic findings in disseminated *Mycobacterium avium*-intracellulare infection. A report of 11 cases. *Am. J. Clin. Pathol.* 85, 67–72. doi: 10.1093/ajcp/85.1.67

Florido, M., Goncalves, A. S., Silva, R. A., Ehlers, S., Cooper, A. M., and Appelberg, R. (1999). Resistance of virulent *Mycobacterium avium* to gamma interferon-mediated antimicrobial activity suggests additional signals for induction of mycobacteriostasis. *Infect. Immun.* 67, 3610–3618.

Gadkowski, L. B., and Stout, J. E. (2008). Cavitary pulmonary disease. *Clin. Microbiol. Rev.* 21, 305–333. doi: 10.1128/CMR.00060-07

Gangadharam, P. R. (1995). Beige mouse model for *Mycobacterium avium* complex disease. *Antimicrob. Agents Chemother.* 39, 1647–1654. doi: 10.1128/AAC.39.8.1647

Gangadharam, P. R., Perumal, V. K., Parikh, K., Podapati, N. R., Taylor, R., Farhi, D. C., et al. (1989). Susceptibility of beige mice to *Mycobacterium avium* complex infections by different routes of challenge. *Am. Rev. Respir. Dis.* 139, 1098–1104. doi: 10.1164/ajrccm/139.5.1098

Glassroth, J. (2008). Pulmonary disease due to nontuberculous mycobacteria. *Chest* 133, 243–251. doi: 10.1378/chest.07-0358

Griffith, D. E., Aksamit, T., Brown-Elliott, B. A., Catanzaro, A., Daley, C., Gordin, F., et al. (2007). An official ATS/IDSA statement: diagnosis, treatment, and prevention of nontuberculous mycobacterial diseases. *Am. J. Respir. Crit. Care Med.* 175, 367–416. doi: 10.1164/rccm.200604-571ST

Haug, M., Awuh, J. A., Steigedal, M., Frengen Kojen, J., Marstad, A., Nordrum, I. S., et al. (2013). Dynamics of immune effector mechanisms during infection with *Mycobacterium avium* in C57BL/6 mice. *Immunology* 140, 232–243. doi: 10.1111/imm.12131

Henao-Tamayo, M., Obregón-Henao, A., Creissen, E., Shanley, C., Orme, I., and Ordway, D. J. (2015). Differential *Mycobacterium bovis* BCG vaccine-derived efficacy in C3Heb/FeJ and C3H/HeOuJ mice exposed to a clinical strain of *Mycobacterium tuberculosis*. *Clin. Vaccine Immunol.* 22, 91–98. doi: 10.1128/CVI.00466-14

Henao-Tamayo, M., Ordway, D. J., and Orme, I. M. (2014). Memory T cell subsets in tuberculosis: what should we be targeting? *Tuberculosis* 94, 455–461. doi: 10.1016/j.tube.2014.05.001

Hibiya, K., Tateyama, M., Teruya, K., Mochizuki, M., Nakamura, H., Tasato, D., et al. (2013). Depression of local cell-mediated immunity and histological characteristics of disseminated AIDS-related *Mycobacterium avium* infection after the initiation of antiretroviral therapy. *Intern. Med.* 52, 1793–1803. doi: 10.2169/internalmedicine.52.9311

Honda, J. R., Alper, S., Bai, X., and Chan, E. D. (2018). Acquired and genetic host susceptibility factors and microbial pathogenic factors that predispose to nontuberculous mycobacterial infections. *Curr. Opin. Immunol.* 54, 66–73. doi: 10.1016/j.coi.2018.06.001

Hussain, S., Zwilling, B. S., and Lafuse, W. P. (1999). *Mycobacterium avium* infection of mouse macrophages inhibits IFN-gamma Janus kinase-STAT signaling and gene induction by down-regulation of the IFN-gamma receptor. *J. Immunol.* 163, 2041–2048.

Ji, B., Lounis, N., Truffot-Pernot, C., and Grosset, J. (1994). Effectiveness of various antimicrobial agents against *Mycobacterium avium* complex in the beige mouse model. *Antimicrob. Agents Chemother.* 38, 2521–2529. doi: 10.1128/AAC.38.11.2521

Kartalija, M., Ovrutsky, A. R., Bryan, C. L., Pott, G. B., Fantuzzi, G., Thomas, J., et al. (2013). Patients with nontuberculous mycobacterial lung disease exhibit unique body and immune phenotypes. *Am. J. Respir. Crit. Care Med.* 187, 197–205. doi: 10.1164/rccm.201206-1035OC

Kitahara, Y., Harada, Y., Harada, S., Maruyama, M., Kajiki, A., Takamoto, M., et al. (1997). The distribution and the characteristics in computed tomography (CT) of the lungs in primary *Mycobacterium avium* complex (MAC) infection. *Kekkaku* 72, 173–180.

Kobashi, Y., Mouri, K., Obase, Y., Kato, S., Nakata, M., and Oka, M. (2013). Mucoid impaction of the bronchi caused by *Mycobacterium avium*. *Intern. Med.* 52, 1537–1540. doi: 10.2169/internalmedicine.52.0065

Kramnik, I., Dietrich, W. F., Demant, P., and Bloom, B. R. (2000). Genetic control of resistance to experimental infection with virulent *Mycobacterium tuberculosis*. *Proc. Natl. Acad. Sci. U.S.A.* 97, 8560–8565. doi: 10.1073/pnas.150227197

Moraski, G. C., Cheng, Y., Cho, S., Cramer, J. W., Godfrey, A., Masquelin, T., et al. (2016). Imidazo[1,2-a]Pyridine-3-carboxamides are active antimicrobial agents against *Mycobacterium avium* infection *in vivo*. *Antimicrob. Agents Chemother.* 60, 5018–5022. doi: 10.1128/AAC.00618-16

Obregon-Henao, A., Arnett, K. A., Henao-Tamayo, M., Massoudi, L., Creissen, E., Andries, K., et al. (2015). Susceptibility of *Mycobacterium abscessus* to antimycobacterial drugs in preclinical models. *Antimicrob. Agents Chemother.* 59, 6904–6912. doi: 10.1128/AAC.00459-15

Obregon-Henao, A., Henao-Tamayo, M., Orme, I. M., and Ordway, D. J. (2013). Gr1(int)CD11b+ myeloid-derived suppressor cells in *Mycobacterium tuberculosis* infection. *PLoS One* 8:e80669. doi: 10.1371/journal.pone.0080669

Okumura, M., Iwai, K., Ogata, H., Ueyama, M., Kubota, M., Aoki, M., et al. (2008). Clinical factors on cavitary and nodular bronchiectatic types in pulmonary *Mycobacterium avium* complex disease. *Intern. Med.* 47, 1465–1472. doi: 10.2169/internalmedicine.47.1114

Ordway, D., Henao-Tamayo, M., Harton, M., Palanisamy, G., Troudt, J., Shanley, C., et al. (2007). The hypervirulent *Mycobacterium tuberculosis* strain HN878 induces a potent TH1 response followed by rapid down-regulation. *J. Immunol.* 179, 522–531. doi: 10.4049/jimmunol.179.1.522

Ordway, D., Henao-Tamayo, M., Shanley, C., Smith, E. E., Palanisamy, G., Wang, B., et al. (2008a). Influence of *Mycobacterium bovis* BCG vaccination on cellular immune response of guinea pigs challenged with *Mycobacterium tuberculosis*. *Cell. Vaccine Immunol.* 15, 1248–1258. doi: 10.1128/CVI.00019-08

Ordway, D., Henao-Tamayo, M., Smith, E., Shanley, C., Harton, M., Troudt, J., et al. (2008b). Animal model of *Mycobacterium abscessus* lung infection. *J. Leukoc. Biol.* 83, 1502–1511. doi: 10.1189/jlb.1007696

Pedrosa, J., Florido, M., Kunze, Z. M., Castro, A. G., Portaels, F., McFadden, J., et al. (1994). Characterization of the virulence of *Mycobacterium avium* complex (MAC) isolates in mice. *Clin. Exp. Immunol.* 98, 210–216. doi: 10.1111/j.1365-2249.1994.tb06127.x

Pichugin, A. V., Yan, B.-S., Sloutsky, A., Kobzik, L., and Kramnik, I. (2009). Dominant role of the sst1 locus in pathogenesis of necrotizing lung granulomas during chronic tuberculosis infection and reactivation in genetically resistant hosts. *Am. J. Pathol.* 174, 2190–2201. doi: 10.2353/ajpath.2009.081075

Prevots, D. R., and Marras, T. K. (2015). Epidemiology of human pulmonary infection with nontuberculous mycobacteria: a review. *Clin. Chest Med.* 36, 13–34. doi: 10.1016/j.ccm.2014.10.002

Roger, P. M., and Bermudez, L. E. (2001). Infection of mice with *Mycobacterium avium* primes CD8+ lymphocytes for apoptosis upon exposure to macrophages. *Clin. Immunol.* 99, 378–386. doi: 10.1006/clim.2001.5037

Shang, S., Gibbs, S., Henao-Tamayo, M., Shanley, C. A., McDonnell, G., Duarte, R. S., et al. (2011). Increased virulence of an epidemic strain of Mycobacterium massiliense in mice. *PLoS One* 6:e24726. doi: 10.1371/journal.pone.0024726

Shin, M. K., Park, H., Shin, S. W., Jung, M., Lee, S. H., Kim, D. Y., et al. (2015). Host transcriptional profiles and immunopathologic response following *Mycobacterium avium* subsp. paratuberculosis infection in mice. *PLoS One* 10:e0138770. doi: 10.1371/journal.pone.0138770

Shu, C. C., Wang, J. Y., Wu, M. F., Wu, C. T., Lai, H. C., Lee, L. N., et al. (2017). Attenuation of lymphocyte immune responses during *Mycobacterium avium* complex-induced lung disease due to increasing expression of programmed death-1 on lymphocytes. *Sci. Rep.* 7:42004. doi: 10.1038/srep42004

Taylor-Robinson, A. W., Liew, F. Y., Severn, A., Xu, D., McSorley, S. J., Garside, P., et al. (1994). Regulation of the immune response by nitric oxide differentially produced by T helper type 1 and T helper type 2 cells. *Eur. J. Immunol.* 24, 980–984. doi: 10.1002/eji.1830240430

Torrelles, J. B., Ellis, D., Osborne, T., Hoefer, A., Orme, I. M., Chatterjee, D., et al. (2002). Characterization of virulence, colony morphotype and the glycopeptidolipid of *Mycobacterium avium* strain 104. *Tuberculosis* 82, 293–300. doi: 10.1054/tube.2002.0373

van Ingen, J., Ferro, B. E., Hoefsloot, W., Boeree, M. J., and van Soolingen, D. (2013). Drug treatment of pulmonary nontuberculous mycobacterial disease in HIV-negative patients: the evidence. *Expert Rev. Anti Infect. Ther.* 11, 1065–1077. doi: 10.1586/14787210.2013.830413

Young, L. S., and Bermudez, L. E. (2001). Perspective on animal models: chronic intracellular infections. *Clin. Infect. Dis.* 33(Suppl. 3), S221–S226. doi: 10.1086/321851

Conflict of Interest Statement: The authors declare that the research was conducted in the absence of any commercial or financial relationships that could be construed as a potential conflict of interest.

frontiers in Microbiology

PERSPECTIVE
published: 10 July 2018
doi: 10.3389/fmicb.2018.01547

MmpL3 as a Target for the Treatment of Drug-Resistant Nontuberculous Mycobacterial Infections

Wei Li[1†], *Amira Yazidi*[2,3†], *Amitkumar N. Pandya*[4†], *Pooja Hegde*[4], *Weiwei Tong*[1], *Vinicius Calado Nogueira de Moura*[1], *E. Jeffrey North*[4*], *Jurgen Sygusch*[2,3*] and *Mary Jackson*[1*]

[1] Mycobacteria Research Laboratories, Department of Microbiology, Immunology and Pathology, Colorado State University, Fort Collins, CO, United States, [2] Biochimie et Médecine Moléculaire, Université de Montréal, Montréal, QC, Canada, [3] Groupe d'Étude des Protéines Membranaires, Université de Montréal, Montréal, QC, Canada, [4] Department of Pharmacy Sciences, School of Pharmacy and Health Professions, Creighton University, Omaha, NE, United States

OPEN ACCESS

Edited by:
Thomas Dick, Rutgers, The State University of New Jersey, Newark, United States

Reviewed by:
Shashank Gupta, Brown University, United States
Kapil Tahlan, Memorial University of Newfoundland, Canada

***Correspondence:**
E. Jeffrey North
jeffreynorth@creighton.edu
Jurgen Sygusch
jurgen.sygusch@umontreal.ca
Mary Jackson
mary.jackson@colostate.edu

[†] *Co-first authors.*

Specialty section:
This article was submitted to Antimicrobials, Resistance and Chemotherapy, a section of the journal Frontiers in Microbiology

Received: *18 May 2018*
Accepted: *21 June 2018*
Published: *10 July 2018*

Citation:
Li W, Yazidi A, Pandya AN, Hegde P, Tong W, Calado Nogueira de Moura V, North EJ, Sygusch J and Jackson M (2018) MmpL3 as a Target for the Treatment of Drug-Resistant Nontuberculous Mycobacterial Infections. Front. Microbiol. 9:1547. doi: 10.3389/fmicb.2018.01547

Nontuberculous mycobacterial (NTM) pulmonary infections are emerging as a global health problem and pose a threat to susceptible individuals with structural or functional lung conditions such as cystic fibrosis, chronic obstructive pulmonary disease and bronchiectasis. *Mycobacterium avium* complex (MAC) and *Mycobacterium abscessus* complex (MABSC) species account for 70–95% of the pulmonary NTM infections worldwide. Treatment options for these pathogens are limited, involve lengthy multidrug regimens of 12–18 months with parenteral and oral drugs, and their outcome is often suboptimal. Development of new drugs and improved regimens to treat NTM infections are thus greatly needed. In the last 2 years, the screening of compound libraries against *M. abscessus* in culture has led to the discovery of a number of different chemotypes that target MmpL3, an essential inner membrane transporter involved in the export of the building blocks of the outer membrane of all mycobacteria known as the mycolic acids. This perspective reflects on the therapeutic potential of MmpL3 in *Mycobacterium tuberculosis* and NTM and the possible reasons underlying the outstanding promiscuity of this target. It further analyzes the physiological and structural factors that may account for the apparent looser structure-activity relationship of some of these compound series against *M. tuberculosis* compared to NTM.

Keywords: *Mycobacterium abscessus*, nontuberculous mycobacteria, MmpL3, mycolic acids, drug development

INTRODUCTION

The prevalence of pulmonary nontuberculous mycobacterial (NTM) infections caused by *Mycobacterium avium* complex (MAC) and *Mycobacterium abscessus* complex (MABSC) species is increasing worldwide and poses a particular threat to susceptible individuals with structural or functional lung conditions such as cystic fibrosis (CF), chronic obstructive pulmonary disease, and bronchiectasis (Park and Olivier, 2015; Parkins and Floto, 2015; Bryant et al., 2016; Floto et al., 2016; Martiniano et al., 2016). Treatment options for NTM pulmonary infections involve lengthy (12–18 months) combination regimens with antibiotics that lack bactericidal activity and are associated with significant toxicity. For pulmonary MAC, the recommended treatment includes

a macrolide, rifamycin, and ethambutol to which intravenous amikacin may be added. Treatment of pulmonary MABSC typically consists of an oral macrolide in conjunction with intravenous or inhaled amikacin, and one or more of the following drugs: intravenous cefoxitin, imipenem, or tigecycline, in addition to oral antibiotics (minocycline, clofazimine, moxifloxacin, linezolid; Floto et al., 2016). The impermeability of the cell envelopes of NTM to drugs and the high number of efflux systems and antibiotic inactivation mechanisms with which NTM are typically endowed confer upon these microorganisms high intrinsic protection against antibiotics (Brown-Elliott et al., 2012). There is clearly an urgent need for more active and better-tolerated drugs to improve therapeutic outcome (Jarand et al., 2011; Maurer et al., 2014; Park and Olivier, 2015; Martiniano et al., 2016).

In last 3 years, the phenotypic screening of compound libraries against NTM has yielded a number of hits with activity against MABSC, MAC, or both complexes. Interestingly, several of these compounds appear to kill NTM through the inhibition of MmpL3, an essential mycolic acid transporter present in all mycobacteria whose therapeutic potential in the treatment of *M. tuberculosis* infections was highlighted in a number of recent studies (Sacksteder et al., 2012; Kondreddi et al., 2013; Lun et al., 2013; Rao et al., 2013; Remuinan et al., 2013; Yokokawa et al., 2013; Li et al., 2016, 2017; Poce et al., 2016, 2018; Stec et al., 2016; Degiacomi et al., 2017). The availability of cidal inhibitors against this new target, some of which have already demonstrated activity in *in vivo* models of MABSC infection (Dupont et al., 2016; De Groote et al., in revision; Pandya et al., in revision), provides much-needed novel opportunities for the treatment of pulmonary NTM infections.

This perspective reflects on the therapeutic potential and promiscuity of MmpL3 in NTM, and discusses recent findings from our laboratories toward understanding the basis for the better activity and looser structure-activity relationship of MmpL3 inhibitors against *M. tuberculosis* compared to NTM.

THE PHENOTYPIC SCREENING OF COMPOUND LIBRARIES AGAINST NTM IDENTIFIES INHIBITORS OF MmpL3

In the last 3 years, the screening of compound libraries, including libraries of TB actives, against MABSC and MAC, has yielded a number of potent hits that appear to target the mycolic acid transporter MmpL3. These include indole-2-carboxamides (ICs) (Franz et al., 2017; Kozikowski et al., 2017; Low et al., 2017), benzothiazole amides (De Groote et al., in revision), and a piperidinol derivative (PIPD1) (Dupont et al., 2016; Low et al., 2017). Earlier work on analogs of the *M. tuberculosis* MmpL3 inhibitor BM212 had further highlighted the activity of pyrole derivatives against a variety of NTM including *M. avium*, *M. gordonae*, *M. smegmatis,* and *M. marinum* (Biava et al., 1999, 2007; Biava, 2002). A subset of these hits and their MIC against *M. tuberculosis*, *M. avium* and MABSC isolates (including *M. abscessus* subsp. *abscessus*, *M. abscessus* subsp. *Massiliense,* and *M. abscessus* subsp. *bolletti*) is presented in **Table 1** along with that of other chemotypes reported to inhibit MmpL3 activity in *M. tuberculosis* (i.e., the 1,2-ethylene diamine SQ109, the tetrahydropyrazolopyrimide carboxamide THPP1, and the adamantyl urea AU1235) (Grzegorzewicz et al., 2012; La Rosa et al., 2012; Tahlan et al., 2012; Remuinan et al., 2013).

ICs have previously been identified as a novel chemical scaffold showing promise in the treatment of tuberculosis (Kondreddi et al., 2013; Lun et al., 2013; Rao et al., 2013; Stec et al., 2016). Based on their high anti-MABSC potency, bactericidal activity on extracellularly- and intracellularly-grown bacilli and promising safe pharmacological profile (Franz et al., 2017; Kozikowski et al., 2017; Pandya et al., in revision), two lead molecules were advanced for efficacy studies in a mouse model of MABSC infection. Oral administration of the lead compounds showed a statistically significant reduction in bacterial load in the lungs, spleen and liver of MABSC-infected mice compared to an untreated control group, with one of the two compounds (compound # IC25; see **Table 1**) showing similar efficacy to amikacin (Pandya et al., in revision). The intrapulmonary delivery of a lead benzothiazole amide compound also demonstrated *in vivo* efficacy in a mouse model of chronic MABSC lung infection (De Groote et al., in revision), whereas the piperidinol-based compound PIPD1 was reported to restrict bacterial growth in a zebrafish model of MABSC infection (Dupont et al., 2016). An interesting property of MmpL3 inhibitors first revealed in *M. tuberculosis* is their ability to synergize with a number of other antimycobacterial drugs or drug candidates including rifampicin, bedaquiline, clofazimine, and β-lactams (Li et al., 2017). Our preliminary studies with IC25 (see **Table 1**) in MABSC similarly point to the existence of a synergistic interaction between this MmpL3 inhibitor and clofazimine in MABSC (Table S1).

Collectively, these results highlight the therapeutic potential of MmpL3 inhibitors in the treatment of NTM infections and provide a strong incentive to develop these compounds into new generation antimycobacterial drugs as their inclusion in anti-NTM drug regimens has the potential to lead to the faster and more efficient clearance of NTM from infected tissues.

MmpL3: A PROMISCUOUS MYCOBACTERIAL TARGET

The reason why so many chemical scaffolds kill *M. tuberculosis* and NTM through the inhibition of MmpL3 remains incompletely understood. MmpL3 belongs to the Resistance, Nodulation and Division (RND) superfamily of transporters that requires the transmembrane electrochemical proton gradient for activity. The observation that the most common resistance mutations identified in both *M. tuberculosis* and MABSC tend to map to a transmembrane region of MmpL3 overlapping with functional residues required for proton translocation or proton-driven conformational changes in the transporter has led to the hypothesis that inhibitors might target the proton relay site of MmpL3 (Belardinelli et al., 2016). MmpL3 inhibitors are typically lipophilic (logP ∼2.6–7.0) and many suffer from poor aqueous solubility which likely favors their concentration in

TABLE 1 | MICs of MmpL3 inhibitors against *M. tuberculosis* [*Mtb*], *M. abscessus* complex species (*M. abscessus* subsp. *abscessus* ATCC 19977 [*Mabs*]; *M. abscessus* subsp. *massiliense* CIP 108297 [*Mmas*]; *M. abscessus* subsp. *bolletii* ATCC 14472 [*Mbol*]), *M. avium* 104 [*Mav*], and *M. smegmatis* recombinant strains expressing different *mmpL3* orthologs.

Inhibitor	Structure	*Mtb*	*Msmg*	*Mav*	*Mabs*	*Mmas*	*Mbol*	*MsmgΔmmpL3*		
								mmpL3smg	*mmpL3abs*	*mmpL3tb*
PIPD1	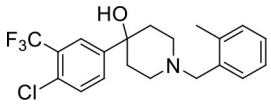	0.15[a]	<1	125[b]	0.125	0.125	nd	nd	nd	nd
AU1235	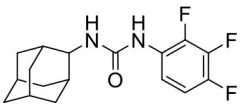	0.1–0.2	1.6–2.5	>32	0.5	1	0.5	2	2	0.3
BM212	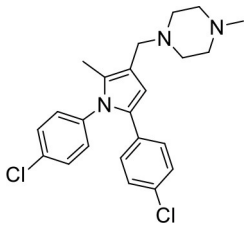	6	8–12	2	1–2	1–2	nd	8–12	8	4–6.2
SQ109	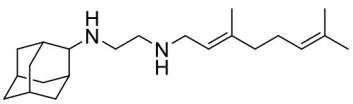	0.6-0.8	6.2–12.4	4	>32	>32	nd	8–12	16	0.4–0.8
THPP1	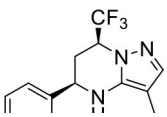	0.4-0.8	>25	>16	>16	>16	nd	>32	>32	0.8–2
NITD304	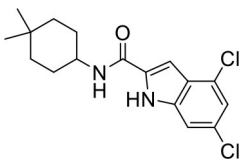	0.004	1	8	0.016	0.016	nd	1	0.12	0.06
NITD349	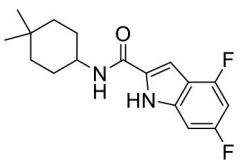	0.008	1	8	0.016	0.031	nd	0.25	0.25	0.06–0.12
IC5	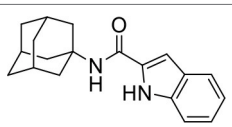	0.2	1.6–3.2	>32	0.25	0.5	0.25	1.6–3.2	3.2	0.2
IC6	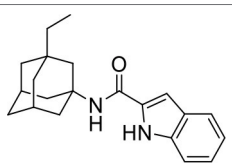	1.25	>20	>32	>32	>32	>32	>32	>32	1.25
IC9	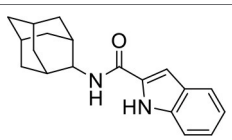	0.39	>25	>32	>32	>32	32	32	>32	0.25–0.39

(Continued)

TABLE 1 | Continued

Inhibitor	Structure	*Mtb*	*Msmg*	*Mav*	*Mabs*	*Mmas*	*Mbol*	*MsmgΔmmpL3*		
								mmpL3smg	*mmpL3abs*	*mmpL3tb*
IC10	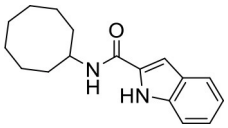	0.39	25	>32	>32	>32	32	25	>32	0.2
IC15	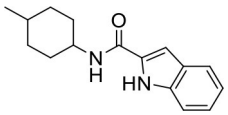	5	12.5	>32	>32	16	16	8–12.5	>32	3–4
IC16	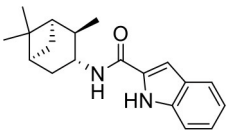	0.05	0.8	8	0.12	0.06	0.12	3–4	4	0.06
IC20	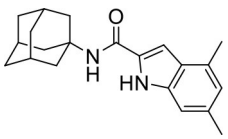	0.02	>20	>32	>32	>32	>32	>32	>32	0.16
IC21	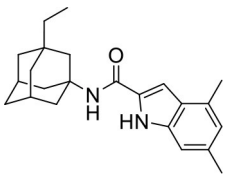	0.04	>20	>32	>32	> 32	>32	>32	>32	0.45
IC24	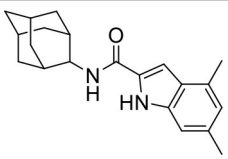	0.04	>20	>32	>32	>32	>32	>32	>32	0.16
IC25	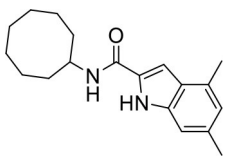	0.02	0.3–0.6	0.25–0.5	0.06	0.03	0.04	0.8–1	0.5	0.08
IC26	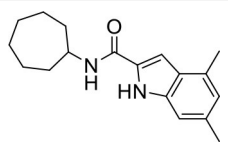	0.08	0.6	2	0.03	0.06	0.03	0.6–1	1	0.16–0.25
IC29	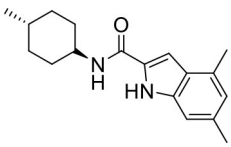	0.31	>20	>32	0.06	0.06	0.03	>32	1	0.62

(Continued)

TABLE 1 | Continued

Inhibitor	Structure	*Mtb*	*Msmg*	*Mav*	*Mabs*	*Mmas*	*Mbol*	*MsmgΔmmpL3*		
								mmpL3smg	*mmpL3abs*	*mmpL3tb*
IC30	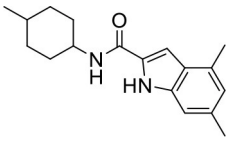	0.16	nd	>32	0.125	0.125	0.06	2	1	0.25–0.31
APRA	–	1	nd	2	2	4	nd	2	4	2
BDQ	–	0.5–1	nd	0.01	0.0625	nd	nd	<0.03	<0.03	<0.03
CFZ	–	0.5–1	nd	<0.125	0.125	nd	nd	1	1	0.5
CLA	–	<0.125		0.125	0.5-1	0.25	nd	0.5	1	0.5

MICs (in μg/mL) were determined were determined in 96-well microtiter plates at 37°C in 7H9-ADC-0.05% Tween 80 medium (M. smegmatis), 7H9-OADC-0.05% tyloxapol supplemented with 0.2% casaminoacids, 48 μg/ml pantothenate, and 50 μg/ml L-leucine (M. tuberculosis mc²6206), cation-adjusted Mueller-Hinton broth (M. abscessus complex) or in cation-adjusted Mueller-Hinton broth supplemented with 5% OADC (M. avium) using the resazurin blue test (Martin et al., 2003) and by visually scanning for growth. The orthologs of mmpL3 from M. abscessus (mmpL3abs), M. tuberculosis (mmpL3tb), and M. smegmatis (mmpL3smg) are expressed from the replicative plasmid pMVGH1 under control of the hsp60 promoter in the background of a M. smegmatis null mutant (MsmgΔmmpL3) of which the entire mmpL3 ORF was deleted and replaced with a kanamycin-resistance cassette. Control drugs: APRA, apramycin; BDQ, bedaquiline; CFZ, clofazimine; CLA, clarithromycin. nd, not determined. [a]MIC value against M. tuberculosis H37Rv ATCC 27294 (Low et al., 2017); [b]The precise M. avium strain used by Dupont et al. (2016) in the MIC determination of PIPD1 was not indicated and may be different from M. avium 104.

the inner membrane where MmpL3 is located. This property and the extreme vulnerability of MmpL3 (Li et al., 2016) that may allow inhibitors with relatively weak binding affinity to the transporter to still inhibit enough of its activity to cause growth arrest, could explain the bias of phenotypic screens toward small hydrophobic inhibitors of MmpL3. The exquisite vulnerability of MmpL3 may further mask potential secondary targets of the inhibitors as illustrated by THPP derivatives that were found to target another essential mycolic acid-related protein in *M. tuberculosis* (Cox et al., 2016) and compounds such as SQ109, BM212, and some THPPs that show activity against non-replicating *M. tuberculosis* bacilli, a property typically not shared by other MmpL3 inhibitors Li W. et al., 2014). The fact that the hydrophobicity of ICs, THPPs, SQ109 analogs and urea derivatives is a key driver of their efficacy provides further support to the notion that the concentration of MmpL3 inhibitors in the phospholipid bilayer plays a key role in their activity (Biava et al., 2005, 2007; Onajole et al., 2010, 2013; Brown et al., 2011; Scherman et al., 2012; Kondreddi et al., 2013; North et al., 2013; Li K. et al., 2014; Poce et al., 2016; Stec et al., 2016; Franz et al., 2017; Kozikowski et al., 2017).

A second mechanism through which high rates of apparent MmpL3 inhibitors may arise from phenotypic screens was proposed after it was found that unspecific uncouplers such as carbonyl cyanide *m*-chlorophenyl hydrazone (CCCP) or the K^+ ionophore, valinomycin, both abolished MmpL3 activity in *M. tuberculosis* and *M. smegmatis* (Li W. et al., 2014). This finding indicated that any compound with the ability to dissipate the proton motive force may indirectly inhibit MmpL3 activity with immediate consequences on mycobacterial growth and viability. Accordingly, and most likely explaining the relatively broad spectrum of activity of some of these compounds including against bacteria devoid of MmpL3 homolog, inhibitors such as the 1,2-ethylenediamine SQ109, the adamantyl urea AU1235 and the 1,5-diarylpyrrole derivative BM212 were found to impact to some degree the membrane potential, the electrochemical proton gradient or both components of the proton motive force of mycobacterial cells (Li K. et al., 2014; Li W. et al., 2014; Feng et al., 2015; Foss et al., 2016). This unspecific activity, however, was later disputed in the case of BM212 and this compound proposed to directly inhibit MmpL3 on the basis of its demonstrated binding to the purified MmpL3 protein from *M. smegmatis* (Xu et al., 2017).

In conclusion, both direct and indirect mechanisms can lead to MmpL3 inhibition in treated mycobacterial cells and contribute to the promiscuity of the target. While not mutually exclusive, a precise understanding of how these two mechanism(s) play out for each inhibitor to eventually abolish mycolic acid export will require a detailed analysis of how each of them interacts with the transporter and affects the energy metabolism of the bacterium.

NTM VS. *M. TUBERCULOSIS* EFFICACY

From the MIC data presented in **Table 1** and previous studies (Biava et al., 1999, 2007; Biava, 2002; Li K. et al., 2014; Franz et al., 2017; Kozikowski et al., 2017; Low et al., 2017; De Groote et al., in revision), it is obvious that the overall activity of MmpL3 inhibitors against NTM, particularly MAC, is less than that observed against *M. tuberculosis*. While the structural diversity of the chemotypes found to inhibit MmpL3 is very broad, spanning from compounds such as BM212 and THPP1, which are large (for MmpL3 inhibitors) multicyclic compounds, to SQ109 which is an ethylene diamine originally designed as an ethambutol analog, the majority of MmpL3 inhibitors reported to date have come from two other classes that contain the same pharmacophore which are the ureas (e.g., AU1235) and indole-2-carboxamides. The pharmacophore for these classes of MmpL3 inhibitors are two hydrogen bond

donors and one hydrogen bond acceptor in the center of the molecule and one bulky lipophilic aliphatic ring (adamantyl, cyclooctyl, cycloheptyl, or substituted cyclohexyl groups) and one aromatic ring on either side of the core. For structure activity relationships, generally, as lipophilicity is increased on either the bulky aliphatic ring (typically through ring expansion or addition of methylene or methyl groups) or aromatic ring (typically through addition of halogens or methyl groups), anti-NTM activity is improved.

Since a number of factors could account for the overall better activity of MmpL3 inhibitors against *M. tuberculosis* than NTM, including species-specific variations in the structure of MmpL3 orthologs, increased drug efflux/degradation/modification in NTM relative to *M. tuberculosis*, or reduced compound penetration in NTM, we first sought to compare the MIC of the inhibitors presented in **Table 1** against *M. smegmatis* recombinant strains expressing different MmpL3 orthologs. To this end, *mmpL3* from *M. tuberculosis*, *M. smegmatis* and *M. abscessus* subsp. *abscessus* were expressed from the same expression plasmid in the background of a *M. smegmatis* mutant whose endogenous *mmpL3* gene was deleted by allelic replacement (*Msmg*Δ*mmpL3*) (Belardinelli et al., 2016). Expressing all orthologs from the same promoter in the same *M. smegmatis* strain abolished any potential differences in compound uptake, modification and efflux allowing for a direct comparison of the effect of the inhibitors against the three MmpL3 proteins. Importantly, all three *mmpL3* orthologs were expressed at comparable levels in this recombinant system (Figure S1). The results of these comparative MIC studies clearly indicated that the MICs of the inhibitors against the different *M. smegmatis* strains generally reflected their MICs against the *Mycobacterium* species from which the rescue *mmpL3* ortholog originated (**Table 1**). The structure of MmpL3 thus appears to be the main driver of the susceptibility of each *Mycobacterium* species to these inhibitors.

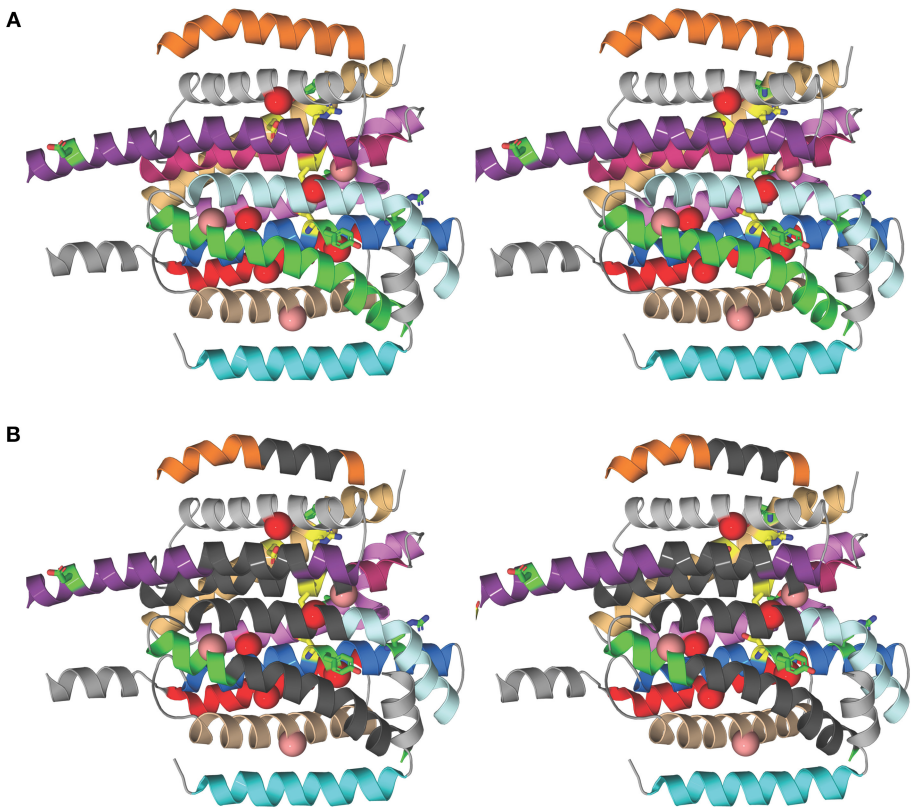

FIGURE 1 | Structural comparison of NTM and *M. tuberculosis* MmpL3 transporters. **(A)** Stereo model showing the transmembrane (TM) helices of the *M. tuberculosis* MmpL3 subunit structure as predicted by I-TASSER. The TM helices are color-coded to improve visibility. From top to bottom, TMS-7 (orange), TMS-9 (gray), TMS-8 (violet purple), TMS-10 (pink), TMS-12 (light orange), TMS-11 (violet), TMS-5 (pale cyan), TMS-4 (marine), TMS-6 (green), TMS-2 (red), TMS-3 (wheat), and TMS-1 (cyan). The TM helices encompass residues whose mutations resulted in significant reduction in transport activity, shown in green, and residues 251, 288, 640, 641, 710, and 715 whose mutation abolished transport activity, colored yellow (Belardinelli et al., 2016). The positions of frequently encountered resistance mutations to one or more MmpL3 inhibitor series are shown as red and salmon spheres centered on the Cα atom of the native MmpL3 residue (Belardinelli et al., 2016). These residues map to TM helices. Resistance mutations also producing a significant reduction in growth are shown in red and those that slightly attenuated growth are colored salmon. **(B)** Stereo model as in **(A)** showing regions of the TM helices where the majority of residues are not conserved between MmpL3 orthologs (dark gray). Most of the dissimilar residues represent semi-conservative and non-conservative mutations (see Figure S2). Several of these regions map vicinal to the functional residues and mutations that induce resistance.

MmpL3 MODELING

To investigate the structural basis for the different susceptibilities of MmpL3 orthologs to various classes of inhibitors, the I-TASSER server (Yang et al., 2015) was used for automated full-length 3D structure prediction of MmpL3 transporters from *M. tuberculosis* H37Rv, *M. abscessus* ATCC 19977, *M. smegmatis* mc^2155, and *M. avium* 104. The top predicted structure for each MmpL3 transporter corresponded to a C-score of >-1.5 suggesting a correct fold. All MmpL3 orthologs resemble each other (root mean square differences based C-alpha atoms < 0.4Å) and had as closest target the crystal structure of the *Burkholderia multivorans* hopanoid transporter HpnN (PDB 5khnB). Comparison of the predicted structures with that of HpnN yielded a high TM-score >0.8 and low RMSD <2.0 between residues that were structurally aligned by TM-align (Zhang, 2008). The superposition of all three NTM MmpL3 orthologs onto MmpL3 from *M. tuberculosis* H37Rv shows very similar spatial overlap of the C-alpha positions of essential residues identified in the reference MmpL3 transporter (Belardinelli et al., 2016) that can be seen in **Figure 1A**. Each of the predicted structures contained 12 TM helices.

We next aligned the amino acid sequences of the MmpL3 orthologs among each other using PSI/TM-Coffee (Chang et al., 2012; Figure S2). Essential functional residues identified in *M. tuberculosis* MmpL3 (namely, residues: 251, 288, 640, 641, 710, and 715; boxed in green in Figure S2; Belardinelli et al., 2016) are conserved and are all located in the central regions of the 12 TM helical bundle that is thought to be involved in proton translocation.

We then searched for sequence dissimilarities among the TM helices given the lipophilicity of the MmpL3 inhibitors. The stereo model in **Figure 1B** shows regions of the transmembrane helices in dark gray where the majority of amino acid residues are not conserved between MmpL3 orthologs and which span the central regions of the 12 TM helical bundle. Most of the dissimilar residues represent semi-conservative and non-conservative mutations that are shown as red boxes on the sequence alignment shown in Figure S2. Several of these regions map vicinal to the functional residues and mutations that induce resistance. The shape differences in the geometries of the hydrophobic and polar side chains alters the packing of the 12 TM helices and is likely to concomitantly modify their dynamical behavior important for transport activity and inhibitor binding. Given that the inhibitors are partitioned into the lipid bilayer, from a thermodynamic perspective, their propensity to interact with the TM helices will further depend on two factors: their ability to interact preferentially with the hydrophobic side chains of the TM helices and their ability to form polar interactions with either backbone or polar side chains. It follows that both the differential helical packing modifying the binding loci of the inhibitors and the nature of the side chains of the TM helices probably account for the ortholog-dependent activity of MmpL3 inhibitors.

FUTURE DIRECTIONS

There is an unmet medical need for the development of new bactericidal agents to treat pulmonary NTM infections. The novel classes of bactericidal MmpL3 inhibitors that have been reported in the last few years, some of which have demonstrated activity against *M. tuberculosis* and MABSC *in vivo*, highlight the therapeutic potential of this transporter in tuberculous and nontuberculous mycobacteria and provide much needed translational opportunities for the treatment of NTM infections. Future research is expected to gain further insight into the structure of MmpL3 and its variations across *Mycobacterium* species in order to leverage the emerging structure-activity relationship information now available for some of these compound series (Brown et al., 2011; Scherman et al., 2012; North et al., 2013; Li K. et al., 2014; Poce et al., 2016, 2018; Stec et al., 2016; Franz et al., 2017; Kozikowski et al., 2017). Also, critical to the further development of these inhibitors will be the availability of a simple, non-radioactive, and relatively high-throughput assay to screen optimized analogs with increased activity against MmpL3. Currently available cell-free and whole cell-based assays (e.g., Grzegorzewicz et al., 2012; Li W. et al., 2014; Li et al., 2016; Xu et al., 2017) indeed lack the simplicity of use and/or specificity required to rapidly screen such analogs. The development of such assays is currently the object of intense efforts in our laboratories.

AUTHOR CONTRIBUTIONS

EN, JS, and MJ conceived the project, analyzed the data, and wrote the manuscript. WL, PH, WT, and VC generated and characterized the *M. smegmatis* recombinant strains, and carried out the MIC determinations and checkerboard assays. AP synthesized inhibitors, contributed to the preparation of **Table 1** and analyzed SAR data. AY performed the MmpL3 modeling studies.

ACKNOWLEDGMENTS

This work was supported by a grant from the National Institutes of Health/National Institute of Allergy and Infectious Diseases (AI116525) (to MJ and EN) and a grant from the Bill and Melinda Gates Foundation (OPP1181207) (to MJ and JS). The content is solely the responsibility of the authors and does not necessarily represent the official views of the NIH. We are grateful to the Global Alliance for TB Drug Development for the provision of NITD-304 and NITD-349.

SUPPLEMENTARY MATERIAL

The Supplementary Material for this article can be found online at: https://www.frontiersin.org/articles/10.3389/fmicb.2018.01547/full#supplementary-material

REFERENCES

Belardinelli, J. M., Yazidi, A., Yang, L., Fabre, L., Li, W., Jacques, B., et al. (2016). Structure-Function profile of MmpL3, the essential mycolic acid transporter from *Mycobacterium tuberculosis*. *ACS Infect. Dis*. 2, 702–713. doi: 10.1021/acsinfecdis.6b00095

Biava, M. (2002). BM 212 and its derivatives as a new class of antimycobacterial active agents. *Curr. Med. Chem*. 9, 1859–1869. doi: 10.2174/0929867023368953

Biava, M., Fioravanti, R., Porretta, G. C., Deidda, D., Maullu, C., and Pompei, R. (1999). New pyrrole derivatives as antimycobacterial agents analogs of BM212. *Bioorg. Med. Chem. Lett*. 9, 2983–2988.

Biava, M., Porretta, G. C., and Manetti, F. (2007). New derivatives of BM212: A class of antimycobacterial compounds based on the pyrrole ring as a scaffold. *Mini-Rev. Med. Chem*. 7, 65–78. doi: 10.2174/138955707779317786

Biava, M., Porretta, G. C., Poce, G., Deidda, D., Pompei, R., Tafi, A., et al. (2005). Antimycobacterial compounds. Optimization of the BM 212 structure, the lead compound for a new pyrrole derivative class. *Bioorg. Med. Chem*. 13, 1221–1230. doi: 10.1016/j.bmc.2004.11.018

Brown, J. R., North, E. J., Hurdle, J. G., Morisseau, C., Scarborough, J. S., Sun, D., et al. (2011). The structure-activity relationship of urea derivatives as anti-tuberculosis agents. *Bioorg. Med. Chem*. 19, 5585–5595. doi: 10.1016/j.bmc.2011.07.034

Brown-Elliott, B. A., Nash, K. A., and Wallace, R. J. Jr. (2012). Antimicrobial susceptibility testing, drug resistance mechanisms, and therapy of infections with nontuberculous mycobacteria. *Clin. Microbiol. Rev*. 25, 545–582. doi: 10.1128/CMR.05030-11

Bryant, J. M., Grogono, D. M., Rodriguez-Rincon, D., Everall, I., Brown, K. P., Moreno, P., et al. (2016). Emergence and spread of a human-transmissible multidrug-resistant nontuberculous mycobacterium. *Science* 354, 751–757. doi: 10.1126/science.aaf8156

Chang, J. M., Di Tommaso, P., Taly, J. F., and Notredame, C. (2012). Accurate multiple sequence alignment of transmembrane proteins with PSI-Coffee. *BMC Bioinformatics* 13(Suppl. 4):S1. doi: 10.1186/1471-2105-13-S4-S1

Cox, J. A., Abrahams, K. A., Alemparte, C., Ghidelli-Disse, S., Rullas, J., Angulo-Barturen, I., et al. (2016). THPP target assignment reveals EchA6 as an essential fatty acid shuttle in mycobacteria. *Nat. Microbiol*. 1:15006. doi: 10.1038/nmicrobiol.2015.6

Degiacomi, G., Benjak, A., Madacki, J., Boldrin, F., Provvedi, R., Palu, G., et al. (2017). Essentiality of mmpL3 and impact of its silencing on *Mycobacterium tuberculosis* gene expression. *Sci. Rep*. 7:43495. doi: 10.1038/srep43495

Dupont, C., Viljoen, A., Dubar, F., Blaise, M., Bernut, A., Pawlik, A., et al. (2016). A new piperidinol derivative targeting mycolic acid transport in *Mycobacterium abscessus*. *Mol. Microbiol*. 101, 515–529. doi: 10.1111/mmi.13406

Feng, X., Zhu, W., Schurig-Briccio, L. A., Lindert, S., Shoen, C., Hitchings, R., et al. (2015). Antiinfectives targeting enzymes and the proton motive force. *Proc. Natl. Acad. Sci. U.S.A*. 112, E7073–E7082. doi: 10.1073/pnas.1521988112

Floto, R. A., Olivier, K. N., Saiman, L., Daley, C. L., Herrmann, J. L., Nick, J. A., et al. (2016). US Cystic fibrosis foundation and european cystic fibrosis society consensus recommendations for the management of non-tuberculous mycobacteria in individuals with cystic fibrosis: executive summary. *Thorax* 71, 88–90. doi: 10.1136/thoraxjnl-2015-207983

Foss, M. H., Pou, S., Davidson, P. M., Dunaj, J. L., Winter, R. W., Pou, S., et al. (2016). Diphenylether-Modified 1,2-Diamines with improved drug properties for development against *Mycobacterium tuberculosis*. *ACS Infect. Dis*. 2, 500–508. doi: 10.1021/acsinfecdis.6b00052

Franz, N. D., Belardinelli, J. M., Kaminski, M. A., Dunn, L. C., Calado Nogueira de Moura, V., Blaha, M. A., et al. (2017). Design, synthesis and evaluation of indole-2-carboxamides with pan anti-mycobacterial activity. *Bioorg. Med. Chem*. 25, 3746–3755. doi: 10.1016/j.bmc.2017.05.015

Grzegorzewicz, A. E., Pham, H., Gundi, V. A., Scherman, M. S., North, E. J., Hess, T., et al. (2012). Inhibition of mycolic acid transport across the *Mycobacterium tuberculosis* plasma membrane. *Nat. Chem. Biol*. 8, 334–341. doi: 10.1038/nchembio.794

Jarand, J., Levin, A., Zhang, L., Huitt, G., Mitchell, J. D., and Daley, C. L. (2011). Clinical and microbiologic outcomes in patients receiving treatment for *Mycobacterium abscessus* pulmonary disease. *Clin. Infect. Dis*. 52, 565–571. doi: 10.1093/cid/ciq237

Kondreddi, R. R., Jiricek, J., Rao, S. P., Lakshminarayana, S. B., Camacho, L. R., Rao, R., et al. (2013). Design, synthesis, and biological evaluation of Indole-2-carboxamides: a promising class of antituberculosis agents. *J. Med. Chem*. 56, 8849–8859. doi: 10.1021/jm4012774

Kozikowski, A. P., Onajole, O. K., Stec, J., Dupont, C., Viljoen, A., Richard, M., et al. (2017). Targeting mycolic acid transport by Indole-2-carboxamides for the treatment of *Mycobacterium abscessus* infections. *J. Med. Chem*. 60, 5876–5888. doi: 10.1021/acs.jmedchem.7b00582

La Rosa, V., Poce, G., Canseco, J. O., Buroni, S., Pasca, M. R., Biava, M., et al. (2012). MmpL3 is the cellular target of the antitubercular pyrrole derivative BM212. *Antimicrob. Agents Chemother*. 56, 324–331. doi: 10.1128/AAC.05270-11

Li, K., Schurig-Briccio, L. A., Feng, X., Upadhyay, A., Pujari, V., Lechartier, B., et al. (2014). Multi-target drug discovery for tuberculosis and other infectious diseases. *J. Med. Chem*. 57, 3126–3139. doi: 10.1021/jm500131s

Li, W., Obregon-Henao, A., Wallach, J. B., North, E. J., Lee, R. E., Gonzalez-Juarrero, M., et al. (2016). Therapeutic potential of the *Mycobacterium tuberculosis* mycolic acid transporter, MmpL3. *Antimicrob. Agents Chemother*. 60, 5198–5207. doi: 10.1128/AAC.00826-16

Li, W., Sanchez-Hidalgo, A., Jones, V., de Moura, V. C., North, E. J., and Jackson, M. (2017). Synergistic interactions of mmpl3 inhibitors with antitubercular compounds *in vitro*. *Antimicrob. Agents Chemother*. 61:e02399-e02316. doi: 10.1128/AAC.02399-16

Li, W., Upadhyay, A., Fontes, F. L., North, E. J., Wang, Y., Crans, D. C., et al. (2014). Novel insights into the mechanism of inhibition of MmpL3, a target of multiple pharmacophores in *Mycobacterium tuberculosis*. *Antimicrob. Agents Chemother*. 58, 6413–6423. doi: 10.1128/AAC.03229-14

Low, J. L., Wu, M. L., Aziz, D. B., Laleu, B., and Dick, T. (2017). Screening of TB actives for activity against nontuberculous mycobacteria delivers high hit rates. *Front. Microbiol*. 8:1539. doi: 10.3389/fmicb.2017.01539

Lun, S., Guo, H., Onajole, O. K., Pieroni, M., Gunosewoyo, H., Chen, G., et al. (2013). Indoleamides are active against drug-resistant *Mycobacterium tuberculosis*. *Nat. Commun*. 4:2907. doi: 10.1038/ncomms3907

Martin, A., Camacho, M., Portaels, F., and Palomino, J.-C. (2003). Resazurin microtiter assay plate testing of *Mycobacterium tuberculosis* susceptibilities to second-line drugs: rapid, simple, and inexpensive method. *Antimicrob. Agents Chemother*. 47, 3616–3619. doi: 10.1128/AAC.47.11.3616-3619.2003

Martiniano, S. L., Nick, J. A., and Daley, C. L. (2016). Nontuberculous mycobacterial infections in cystic fibrosis. *Clin. Chest. Med*. 37, 83–96. doi: 10.1016/j.ccm.2015.11.001

Maurer, F. P., Bruderer, V. L., Ritter, C., Castelberg, C., Bloemberg, G. V., and Bottger, E. C. (2014). Lack of antimicrobial bactericidal activity in *Mycobacterium abscessus*. *Antimicrob. Agents Chemother*. 58, 3828–3836. doi: 10.1128/AAC.02448-14

North, E. J., Scherman, M. S., Bruhn, D. F., Scarborough, J. S., Maddox, M. M., Jones, V., et al. (2013). Design, synthesis and anti-tuberculosis activity of 1-adamantyl-3-heteroaryl ureas with improved in vitro pharmacokinetic properties. *Bioorg. Med. Chem*. 21, 2587–2599. doi: 10.1016/j.bmc.2013.02.028

Onajole, O. K., Govender, P., van Helden, P. D., Kruger, H. G., Maguire, G. E., Wiid, I., et al. (2010). Synthesis and evaluation of SQ109 analogues as potential anti-tuberculosis candidates. *Eur. J. Med. Chem*. 45, 2075–2079. doi: 10.1016/j.ejmech.2010.01.046

Onajole, O. K., Pieroni, M., Tipparaju, S. K., Lun, S., Stec, J., Chen, G., et al. (2013). Preliminary structure-activity relationships and biological evaluation of novel antitubercular indolecarboxamide derivatives against drug-susceptible and drug-resistant *Mycobacterium tuberculosis* strains. *J. Med. Chem*. 56, 4093–4103 doi: 10.1021/jm4003878

Park, I. K., and Olivier, K. N. (2015). Nontuberculous mycobacteria in cystic fibrosis and non-cystic fibrosis bronchiectasis. *Semin. Respir. Crit. Care Med*. 36, 217–224. doi: 10.1055/s-0035-1546751

Parkins, M. D., and Floto, R. A. (2015). Emerging bacterial pathogens and changing concepts of bacterial pathogenesis in cystic fibrosis. *J. Cyst. Fibros* 14, 293–304. doi: 10.1016/j.jcf.2015.03.012

Poce, G., Cocozza, M., Alfonso, S., Consalvi, S., Venditti, G., Fernandez-Menendez, R., et al. (2018). *In vivo* potent BM635 analogue with improved drug-like properties. *Eur. J. Med. Chem*. 145, 539–550. doi: 10.1016/j.ejmech.2017.12.075

Poce, G., Consalvi, S., and Biava, M. (2016). MmpL3 inhibitors: diverse chemical scaffolds inhibit the same target. *Mini-Rev. Med. Chem.* 16, 1274–1283. doi: 10.2174/1389557516666160118105319

Rao, S. P., Lakshminarayana, S. B., Kondreddi, R. R., Herve, M., Camacho, L. R., Bifani, P., et al. (2013). Indolcarboxamide is a preclinical candidate for treating multidrug-resistant tuberculosis. *Sci. Transl. Med.* 5:214ra168. doi: 10.1126/scitranslmed.3007355

Remuinan, M. J., Perez-Herran, E., Rullas, J., Alemparte, C., Martinez-Hoyos, M., Dow, D. J., et al. (2013). Tetrahydropyrazolo[1,5-a]Pyrimidine-3-Carboxamide and N-Benzyl-6',7'-Dihydrospiro[Piperidine-4,4'-Thieno[3,2-c] Pyran] analogues with bactericidal efficacy against *Mycobacterium tuberculosis* targeting MmpL3. *PLoS ONE* 8:e60933. doi: 10.1371/journal.pone.0060933

Sacksteder, K. A., Protopopova, M., Barry, C. E. III, Andries, K., and Nacy, C. A. (2012). Discovery and development of SQ109: a new antitubercular drug with a novel mechanism of action. *Future Microbiol.* 7, 823–837. doi: 10.2217/fmb.12.56

Scherman, M. S., North, E. J., Jones, V., Hess, T. N., Grzegorzewicz, A. E., Kasagami, T., et al. (2012). Screening a library of 1600 adamantyl ureas for anti-*Mycobacterium tuberculosis* activity *in vitro* and for better physical chemical properties for bioavailability. *Bioorg. Med. Chem.* 20, 3255–3262. doi: 10.1016/j.bmc.2012.03.058

Stec, J., Onajole, O. K., Lun, S., Guo, H., Merenbloom, B., Vistoli, G., et al. (2016). Indole-2-carboxamide-based MmpL3 inhibitors show exceptional antitubercular activity in an animal model of tuberculosis infection. *J. Med. Chem.* 59, 6232–6247. doi: 10.1021/acs.jmedchem.6b00415

Tahlan, K., Wilson, R., Kastrinsky, D. B., Arora, K., Nair, V., Fischer, E., et al. (2012). SQ109 targets MmpL3, a membrane transporter of trehalose monomycolate involved in mycolic acid donation to the cell wall core of *Mycobacterium tuberculosis*. *Antimicrob. Agents Chemother.* 56, 1797–1809. doi: 10.1128/AAC.05708-11

Xu, Z., Meshcheryakov, V. A., Poce, G., and Chng, S. S. (2017). MmpL3 is the flippase or mycolic acids in mycobacteria. *Proc. Natl. Acad. Sci. U.S.A.* 114, 7993–7998. doi: 10.1073/pnas.1700062114

Yang, J., Yan, R., Roy, A., Xu, D., Poisson, J., and Zhang, Y. (2015). The I-TASSER suite: protein structure and function prediction. *Nat. Methods* 12, 7–8. doi: 10.1038/nmeth.3213

Yokokawa, F., Wang, G., Chan, W. L., Ang, S. H., Wong, J., Ma, I., et al. (2013). Discovery of tetrahydropyrazolopyrimidine carboxamide derivatives as potent and orally active antitubercular agents. *ACS Med. Chem. Lett.* 4, 451–455. doi: 10.1021/ml400071a

Zhang, Y. (2008). I-TASSER server for protein 3D structure prediction. *BMC Bioinformatics* 9:40. doi: 10.1186/1471-2105-9-40

Conflict of Interest Statement: The authors declare that the research was conducted in the absence of any commercial or financial relationships that could be construed as a potential conflict of interest.

frontiers in Microbiology

ORIGINAL RESEARCH
published: 30 April 2019
doi: 10.3389/fmicb.2019.00905

Lsr2 Is an Important Determinant of Intracellular Growth and Virulence in *Mycobacterium abscessus*

Vincent Le Moigne[1], Audrey Bernut[2†], Mélanie Cortès[3], Albertus Viljoen[2], Christian Dupont[2], Alexandre Pawlik[4], Jean-Louis Gaillard[1,5], Fabienne Misguich[1], Frédéric Crémazy[1], Laurent Kremer[2,6] and Jean-Louis Herrmann[1,5]**

[1] 2I, UVSQ, INSERM, Université Paris-Saclay, Versailles, France, [2] UMR 9004, Centre National de la Recherche Scientifique, Institut de Recherche en Infectiologie de Montpellier, Université de Montpellier, Montpellier, France, [3] VitamFero, Tours, France, [4] Unité de Pathogénomique Mycobactérienne, Institut Pasteur, Paris, France, [5] APHP, GHU PIFO, Hôpital Raymond-Poincaré – Hôpital Ambroise-Paré, Boulogne-Billancourt, France, [6] INSERM, Institut de Recherche en Infectiologie de Montpellier, Montpellier, France

OPEN ACCESS

Edited by:
Thomas Dick,
Center for Discovery and Innovation,
Hackensack Meridian Health,
United States

Reviewed by:
Thomas F. Byrd,
The University of New Mexico,
United States
Joseph Oliver Falkinham,
Virginia Tech, United States

***Correspondence:**
Frédéric Crémazy
frederic.cremazy@uvsq.fr
Jean-Louis Herrmann
jean-louis.herrmann@aphp.fr

†Present address:
Audrey Bernut,
Department of Infection, Immunity & Cardiovascular Disease, The Bateson Centre, The University of Sheffield, Sheffield, United Kingdom

Specialty section:
This article was submitted to Antimicrobials, Resistance and Chemotherapy, a section of the journal Frontiers in Microbiology

Received: 05 January 2019
Accepted: 09 April 2019
Published: 30 April 2019

Citation:
Le Moigne V, Bernut A, Cortès M, Viljoen A, Dupont C, Pawlik A, Gaillard J-L, Misguich F, Crémazy F, Kremer L and Herrmann J-L (2019) Lsr2 Is an Important Determinant of Intracellular Growth and Virulence in Mycobacterium abscessus. Front. Microbiol. 10:905. doi: 10.3389/fmicb.2019.00905

Mycobacterium abscessus, a pathogen responsible for severe lung infections in cystic fibrosis patients, exhibits either smooth (S) or rough (R) morphotypes. The S-to-R transition correlates with inhibition of the synthesis and/or transport of glycopeptidolipids (GPLs) and is associated with an increase of pathogenicity in animal and human hosts. Lsr2 is a small nucleoid-associated protein highly conserved in mycobacteria, including *M. abscessus,* and is a functional homolog of the heat-stable nucleoid-structuring protein (H-NS). It is essential in *Mycobacterium tuberculosis* but not in the non-pathogenic model organism *Mycobacterium smegmatis*. It acts as a master transcriptional regulator of multiple genes involved in virulence and immunogenicity through binding to AT-rich genomic regions. Previous transcriptomic studies, confirmed here by quantitative PCR, showed increased expression of *lsr2* (*MAB_0545*) in R morphotypes when compared to their S counterparts, suggesting a possible role of this protein in the virulence of the R form. This was addressed by generating *lsr2* knock-out mutants in both S (Δ*lsr2*-S) and R (Δ*lsr2*-R) variants, demonstrating that this gene is dispensable for *M. abscessus* growth. We show that the wild-type S variant, Δ*lsr2*-S and Δ*lsr2*-R strains were more sensitive to H_2O_2 as compared to the wild-type R variant of *M. abscessus*. Importantly, virulence of the Lsr2 mutants was considerably diminished in cellular models (macrophage and amoeba) as well as in infected animals (mouse and zebrafish). Collectively, these results emphasize the importance of Lsr2 in *M. abscessus* virulence.

Keywords: non-tuberculous mycobacteria, *Mycobacterium abscessus*, Lsr2, virulence, pathogenesis, zebrafish, mouse

INTRODUCTION

Mycobacterium abscessus is a rapidly growing mycobacterium (RGM) increasingly acknowledged as a serious non-tuberculous mycobacterial (NTM) pathogen (Mougari et al., 2016; Diel et al., 2017). Although it causes extrapulmonary infections (Jeong et al., 2017) and disseminated pulmonary diseases among otherwise healthy individuals (Varghese et al., 2012), it has become

notorious for the serious threat it poses to patients with cystic fibrosis (CF) and with other underlying lung disorders (Brown-Elliott and Wallace, 2002; Medjahed et al., 2010). *M. abscessus* infection correlates with a decline in pulmonary function and is an appreciable concern for CF patients requiring lung transplantation (Esther et al., 2010; Qvist et al., 2016; Smibert et al., 2016). *M. abscessus* has high intrinsic levels of resistance to many antibiotics, making infections with this mycobacterium hard to treat and eradicate (Brown-Elliott and Wallace, 2002; van Dorn, 2017).

Mycobacterium abscessus presents either smooth (S) or rough (R) colony morphotypes leading to different clinical outcomes (Howard et al., 2006; Catherinot et al., 2009; Medjahed and Reyrat, 2009; Ripoll et al., 2009; Roux et al., 2011). They also exhibit different morphological aspects (Howard et al., 2006; Sánchez-Chardi et al., 2011) and virulence phenotypes (Byrd and Lyons, 1999; Catherinot et al., 2007; Bernut et al., 2014a). These differences rely mainly on the presence (in S) or absence (in R) of surface-associated glycopeptidolipids (GPL) (Gutiérrez et al., 2018). The S variant is thought to be the colonizing form, capable of producing mature biofilms and exhibiting a significant motility on soft agar (Howard et al., 2006). The R variant, on the other hand, is impaired in these abilities and forms pronounced serpentine cords, a feature associated with hypervirulence (Byrd and Lyons, 1999; Catherinot et al., 2007; Bernut et al., 2014a; Halloum et al., 2016). Being the most pathogenic RGM, it is not surprising that both variants of *M. abscessus* resist phagocytosis by immune cells, a trait shared with pathogenic slow-growing mycobacterial (SGM) species, such as *M. tuberculosis* (Oberley-Deegan et al., 2010; Nessar et al., 2011; Roux et al., 2016). Therefore, the S-to-R transition, which occurs essentially *in vivo* and is responsible for a significant increase in pathogenicity (Jönsson et al., 2007; Rottman et al., 2007; Bernut et al., 2014b) likely represents an evolutionary adaptation mechanism to the host immune response (Pawlik et al., 2013; Roux et al., 2016).

Genome comparison of three distinct isogenic S/R couples of *M. abscessus* revealed the presence of genetic lesions in the R variant, such as single nucleotide polymorphisms and/or insertions/deletions, in genes belonging to the GPL biosynthesis and transport locus (Pawlik et al., 2013) and causing the S-to-R transition. Although these mutations can account for the change in colony morphology of *M. abscessus*, it is unlikely that they fully explain the virulence of the R variant observed in multiple cellular and animal models (Catherinot et al., 2007; Bernut et al., 2014b, 2017). This view is supported by transcriptomic studies performed in the same isogenic S/R pairs, which revealed differential expression for a large set of genes, including *lsr2* (Pawlik et al., 2013).

Lsr2 is a nucleoid-associated protein (NAP) and a functional analog of the heat-stable nucleoid-structuring proteins or H-NS (Chen et al., 2008; Gordon et al., 2008; Qu et al., 2013) that is conserved in all actinomycetes and mycobacteria (Chen et al., 2008; Gordon et al., 2008; Qu et al., 2013). Lsr2 was originally shown to be an immunodominant antigen of *Mycobacterium leprae* (Laal et al., 1991) and has since been reported to regulate a broad range of processes (Chen et al., 2008; Colangeli et al., 2009; Gordon et al., 2010). In *Mycobacterium smegmatis*, *lsr2* mutants show a different colony morphology and are defective in biofilm formation, a phenotype presumably resulting from an altered expression of key surface lipids, such as mycolyl-diacylglycerols (Chen et al., 2006; Arora et al., 2008; Kocíncová et al., 2008; Yang et al., 2017). Subsequent studies also demonstrated that Lsr2 is necessary for mycobacterial conjugal DNA transfer (Nguyen et al., 2010). In contrast to *M. smegmatis*, in which it is dispensable for planktonic growth, Lsr2 is considered essential in *M. tuberculosis* (Chen et al., 2006; Colangeli et al., 2007; Arora et al., 2008; Kocíncová et al., 2008; Yang et al., 2017). In addition, it has also been shown to contribute to antibiotic resistance (Colangeli et al., 2007) and to control the expression of a large panel of genes acquired by horizontal gene transfer in *M. tuberculosis* (Gordon et al., 2010). Like H-NS, Lsr2 preferentially binds to AT-rich sequences and can oligomerize through its protein-protein interaction domain to form filaments along the *M. tuberculosis* chromosome (Gordon et al., 2010, 2011). Moreover, it has the ability to bridge distant DNA segments, suggesting a role in the organization and compaction of the nucleoid (Chen et al., 2008).

Herein, we generated *lsr2* knock-out mutants in both S and R variants of *M. abscessus* to define the contribution of Lsr2 in major physiological processes that are relevant to the context of increased pathogenicity of the R variant.

MATERIALS AND METHODS

Strains and Culture Media

Mycobacterium abscessus subsp. *abscessus* S and R 19977-IP strains were used in this study and designated Mabs-S and Mabs-R, respectively. Mycobacterial strains were grown aerobically at 37°C in Middlebrook 7H9 broth or on Middlebrook 7H11 agar, supplemented with 0.2% glycerol and 1% glucose. When necessary; kanamycin, hygromycin, and zeocin were added to medium at 250 μg/ml, 500 μg/ml (or 1000 μg/ml for selection) and 25 μg/ml, respectively. After infection experiments, bacterial CFU were counted on agar plates (BioMérieux, France), either Columbia blood agar plates after infections in macrophages and amoeba, and H_2O_2 exposition, either VCAT (Vancomycin, Colistin sulfate, Amphotericin B, and Trimethoprim) chocolate agar plates after mice infections. The *Escherichia coli* TOP10 strain (Thermo Fisher) was grown in Lysogeny Broth (LB) medium with or without kanamycin (25 μg/ml).

Construction of *lsr2* Mutants in *M. abscessus*

The *lsr2* downstream and upstream regions were amplified by PCR using the primer pairs MC75/MC76 and MC80/MC81, respectively, then cloned with the zeocin resistance cassette yielding pMC34. Replacement of the endogenous *lsr2* gene by the zeocin resistance cassette was performed as described previously (van Kessel and Hatfull, 2007; Medjahed and Reyrat, 2009; Bakala N'Goma et al., 2015). *lsr2* knock-out mutants, designated Mabs-S-Δ*lsr2* and Mabs-R-Δ*lsr2* were confirmed by PCR (primer pairs lsr2-5/lsr2V and MC75/ZeoR) (**Supplementary Figure S1**) and Southern blotting (**Figure 2B**).

Complementation was achieved by PCR amplification of *lsr2* under the control of its endogenous promoter region (961 bp) using the primers Comp-MAB_0545+reg-AclI/Comp-MAB_0545-HpaI and insertion into the integrative vector pMV361. The resulting construct was then introduced into the Mabs-S-Δ*lsr2* strain. Mabs-R-Δ*lsr2* complementation was achieved by PCR amplification (primer pair Comp-MAB_0545-NdeI/ Comp-MAB_0545-HindIII) and cloning of *lsr2* under the control of the *hsp60* promoter in the replicative plasmid pVV16 (Grzegorzewicz et al., 2012) Expression of *lsr2* mRNA transcripts was checked by quantitative RT-PCR analysis. To generate the Mabs-S-Δ*lsr2-C**lsr2-FLAG* strain used for the ChIP-qPCR experiments, *lsr2* was fused to the FLAG tag by PCR amplification using the primer pair Comp-MAB_0545-reg-AclI/ Comp-MAB_0545-FLAG-HpaI and cloning with its endogenous promoter into the integrative plasmid pMVH361. All the primers used in this study are listed in **Supplementary Table S1**.

Quantitative RT-PCR Analysis

mRNA was reverse transcribed using the "iScript reverse transcription" kit (Bio-Rad). Quantitative PCR was performed with a MasterMix qPCR (Eurogentec) in a Chromo4 instrument (Bio-Rad), as described previously (Pawlik et al., 2013; Le Moigne et al., 2016).

ChIP-qPCR Analysis

For each ChIP library, 50 ml of Mabs-S-Δ*lsr2-C**lsr2-FLAG* was grown until an OD_{600} of 0.5 and fixed in 1% formaldehyde (Euromedex) and lysed using a Precellys grinder (3 cycles: 6,700 rpm −3 × 20 s ON/60 s OFF, Bertin Technologies) and VK05 beads. The bacterial chromatin was sheared in 100–300 bp fragments using a Bioruptor Pico (Diagenode). Chromatin Immunoprecipitation was performed as described previously (Grainger et al., 2006) using IgG M2 anti-FLAG (Sigma, F1804) and Anti-GFP (G6539, Sigma) mouse monoclonal antibodies attached to proteins A/G coupled to magnetic beads (Thermo fisher). The immunoprecipitated DNA and 1% of the total input were reverse-crosslinked and eluted using the iPure v2 kit (Diagenode). The quantitative PCR tests were performed using the SsoFast evergreen supermix (Bio-Rad). Enrichment of Lsr2 binding at the GPL operon operator was calculated using the "Percent Input" method using the primers MAB_4100c_qPCR1 and MAB_4100c_qPCR3 (**Supplementary Table S1**).

GPL Analysis

Apolar and polar lipid fractions were obtained from exponentially growing mycobacteria cultured as reported previously (Besra, 1998). The polar lipid fraction containing GPL was separated by TLC using silica gel 60 coated aluminum TLC plates (Merck) and chloroform/methanol (90:10; v/v) as solvent system, as previously described (Sondén et al., 2005; Pawlik et al., 2013). GPL were revealed by treating TLC plates with a mist of 0.2% (w/v) of Anthrone diluted in sulfuric acid, followed by charring.

Susceptibility Profile to H_2O_2

Exponential growth phase cultures (OD_{600} between 0.6 and 0.8) of *M. abscessus* were diluted to obtain an OD_{600} of 0.1 and transferred in two new tubes. One of the two cultures was exposed to 20 mM H_2O_2 and the other one to an equivalent volume of sterile water. CFUs were determined by plating aliquots at various time points after the addition of H_2O_2 (2, 4, 6, and 8 h) on blood agar plates. For each morphotype and mutant, three independent experiments were performed, and one experiment is shown.

Intracellular Survival in Macrophages and Amoeba After Infection

Murine J774.2 macrophages (MΦ) were grown at 37°C under 5% CO_2 in DMEM medium supplemented with 5% heat-inactivated Fetal Calf Serum (FBS), penicillin (100 IU/ml) and streptomycin (100 μg/ml). MΦ infections with the *M. abscessus* strains were carried out, as described previously (Bakala N'Goma et al., 2015; Roux et al., 2016). CFU were counted after 3 to 5 days of incubation at 37°C. Amoeba infections were done using *Acanthamoeba castellanii* (ATCC30010), as described earlier (Bakala N'Goma et al., 2015; Dubois et al., 2018a). At 1, 2, and 3 days of co-culture, the *A. castellanii* monolayer was disrupted with 0.1% SDS for 30 min at 32°C and CFU were counted.

Systemic Infection in Mice

Six to eight-week-old BALB/c mice were infected with *M. abscessus* strains, as described earlier (Catherinot et al., 2007; Rottman et al., 2007; Bakala N'Goma et al., 2015; Bernut et al., 2015). A Student *t*-test was carried out to test significance of differences between groups. All procedures were performed according to the institutional and national ethical guidelines and approved by the Comité d'éthique en experimentation animale N°047 with agreement A783223 under the reference APAFIS#11465.

Zebrafish Infections

All zebrafish experiments were done according to European Union guidelines for handling of laboratory animals[1] and approved by the Comité d'Ethique pour l'Expérimentation Animale de la région Languedoc Roussillon under the reference CEEALR36-1145. Experiments were performed using the *golden* mutant (Lamason et al., 2005). Zebrafish embryos were obtained, maintained and microinjected in the caudal vein of 30 hpf dechorionated embryos as described (Bernut et al., 2014a, 2015). Survival curves and statistics were carried out as described (Bernut et al., 2014a).

RESULTS

Transcription Levels of *lsr2* in *M. abscessus* R and S Strains

Our initial comparative genomic analyses performed on three isogenic *M. abscessus* S/R pairs identified several mutations in the GPL biosynthesis/transport locus that are responsible for the S-to-R transition (Pawlik et al., 2013). Microarray data obtained from RNAseq highlighted the differential expression

[1] http://ec.europa.eu/environment/chemicals/lab_animals/home_en.htm

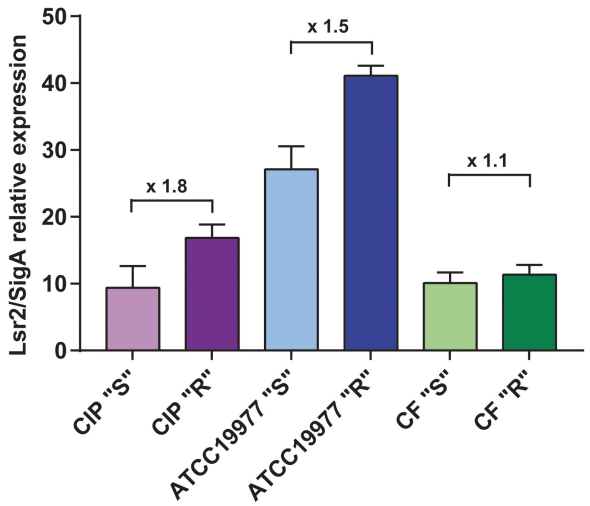

FIGURE 1 | Increased transcriptional expression of *lsr2* in *M. abscessus* R variants. qRT-PCR results of *lsr2* mRNA expression in the R and S variants of *M. abscessus* CIP104536 (Collection Institut Pasteur), ATCC19977 type strains and in the CF clinical isolate. Results are expressed as *lsr2/sigA* ratio as described in Pawlik et al. (2013). For each assay, $n = 3$ and error bars are SEM.

pattern of several genes, including *MAB_0545* (Pawlik et al., 2013; **Supplementary Table S2**). *MAB_0545*, encoding the Lsr2 protein, was found to be moderately more expressed in the R than in the S variants of the CIP104536 and ATCC19977 strains as well as in one clinical isolate, referred to as the CF R strain (Catherinot et al., 2009). To confirm these results, quantitative RT-PCR analysis was performed on *lsr2* using mRNA isolated from both the S and R variants of all three strains. **Figure 1** shows that transcription of *lsr2* is increased in the R strains relative to their S counterparts, particularly in the two type strains, thus validating the microarray data. Because Lsr2 appears to be involved in the virulence and the antibiotic resistance of *M. tuberculosis* (Colangeli et al., 2009; Gordon et al., 2010), we reasoned that induction of Lsr2 expression in the R strain may explain, at least in part, the increase of virulence in the R over the S variant.

Lsr2 Null Mutants Are Not Affected in Their Glycopeptidolipid Profile

To address the impact of Lsr2 on the *M. abscessus* morphotype, null mutants of *lsr2* were generated in both variants, designated Mabs-S-Δ*lsr2* and Mabs-R-Δ*lsr2*, using the recombineering method (van Kessel and Hatfull, 2007) that was adapted to *M. abscessus* (Bakala N'Goma et al., 2015; Halloum et al., 2016; Dubois et al., 2018b; Laencina et al., 2018). This was achieved by replacing *lsr2* with a zeocin resistance cassette using homologous recombination (**Figure 2A**). Proper allelic exchange was subsequently confirmed by PCR (**Supplementary Figure S1**) and Southern blotting (**Figure 2B**). qRT-PCR revealed that complementation with a functional *lsr2* gene was partial (**Supplementary Figure S2**).

The viability of the mutant indicates that *lsr2* is dispensable in *M. abscessus*, as previously reported in *M. smegmatis* (Chen et al., 2006; Arora et al., 2008; Cortes et al., 2011). However, Mabs-S-Δ*lsr2* and Mabs-R-Δ*lsr2* colonies were heterogenous in size with a tendency toward small colonies when compared to their wild-type progenitors (**Supplementary Figure S3A**). All strains exhibited a similar growth rate, suggesting that the reduced colony size did not affect *in vitro* growth in this liquid medium (**Supplementary Figures S3B,C**). Lsr2 has been reported to be a negative regulator of GPL expression

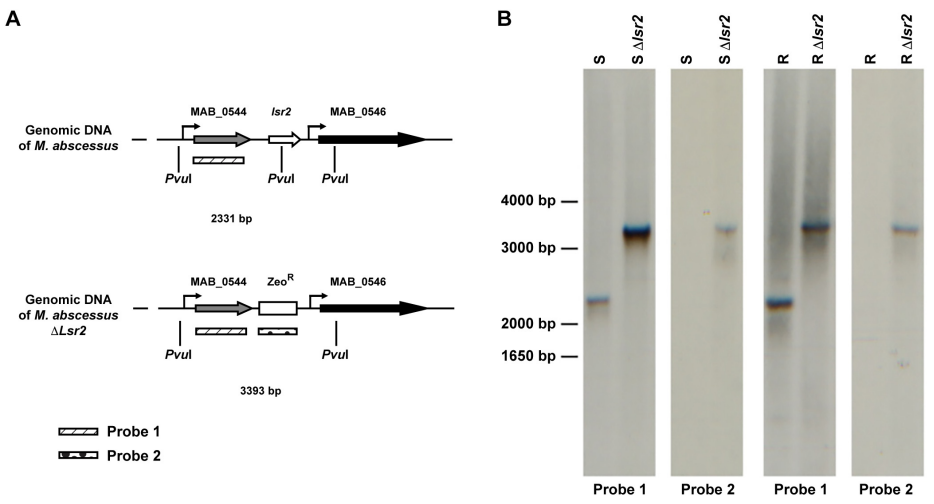

FIGURE 2 | Generation of *lsr2* null mutants. **(A)** Schematic representation of the genomic regions surrounding the *lsr2* gene in the WT and *lsr2* deletion mutant. **(B)** Southern blot of Mabs-S (S), Mabs-R (R), Mabs-S-Δ*lsr2* (S Δ*lsr2*) and Mabs-R-Δ*lsr2* (R Δ*lsr2*) using Probe 1 and Probe 2 depicted in panel **(A)**. Genomic DNA was digested with the restriction enzyme *Pvu*I, migrated on an agarose gel, transferred to a nitrocellulose membrane and hybridized with the two probes. Bands of the corresponding DNA fragments observed are of the expected size.

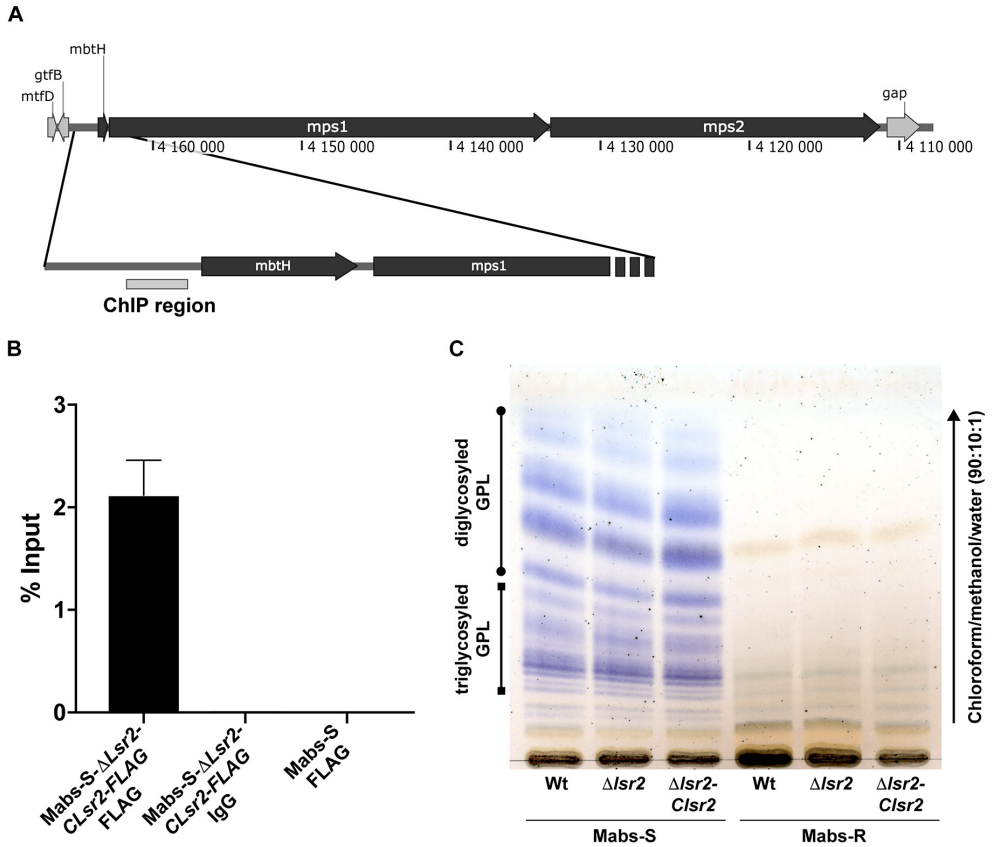

FIGURE 3 | Measurement of Lsr2 enrichment in the promoter region upstream of the *mbtH/mps1* genes. **(A)** Schematic representation of the GPL locus. The gray box upstream of the *mbtH* gene represents the region used to assay Lsr2 enrichment. **(B)** qPCR of ChIP performed using an anti-FLAG antibody. Enrichment of Lsr2 bound to the *mbtH/mps1* promoter region in Mabs-S-Δ*lsr2-Clsr2-FLAG* was calculated using the "percent input" method (% input = 1.894%). Negative controls included in ChIP assays using an unrelated IgG antibody on Mabs-S-Δ*lsr2-Clsr2-FLAG* (% input = 0.00274%) and the anti-FLAG antibody on Mabs-S (% input = 0.00049%) confirm the specificity of the results. For each assay, $n = 3$ and error bars are SEM. **(C)** GPL profile characterizing the WT and Δ*lsr2* and *lsr2* complemented strains in both S and R backgrounds. Following extraction, the GPL were separated by thin layer chromatography using chloroform/methanol (90:10, v/v) and revealed with a treatment of the TLC plate with a mist of 0.2% of Anthrone in concentrated sulfuric acid and charring.

through binding to an AT-rich element upstream of the coding region of *mbtH* and *mps1*, both known to be involved in GPL production in *M. smegmatis* ATCC607 (Kocíncová et al., 2008). However, two other independent studies reported an unaltered GPL profile in *lsr2* mutants generated from the *M. smegmatis* mc^2155 strain (Chen et al., 2006; Arora et al., 2008), which is the rough counterpart of the ATCC607 strain. We therefore addressed whether the inactivation of *lsr2* may affect the GPL profile in both S and R *M. abscessus* variants. First, chromatin immunoprecipitation was carried out on lysates of Mabs-S-Δ*lsr2* in which a *FLAG*-tagged *Lsr2* was introduced and Lsr2 enrichment in the AT-rich element within the promoter region of *mbtH/mps1* was then measured (**Figure 3A**). Binding of Lsr2 was found to be significantly enriched in this region (**Figure 3B**). However, GPL analysis by thin layer chromatography failed to show differences in the GPL profiles in Mabs-S-Δ*lsr2* and in its parental S strain (**Figure 3C**), suggesting that Lsr2 inactivation alone is not sufficient to alter the morphotype of the mutant. As expected, *Mabs-R-Δlsr2* also failed to produce GPL, which can be explained by the presence of severe genetic lesions that impair the transcription of genes such as *mps1* and *mmpL4b* (Pawlik et al., 2013).

Collectively, these data showed Lsr2 ability to bind the promoter region upstream of *mbtH/msp1*. However, loss of Lsr2 expression has no effect on production or composition of GPL in the S *M. abscessus* variant.

Lsr2 Promotes Resistance to Oxidative Species in the R Variant

An important function of Lsr2 resides in protecting the integrity of genomic DNA from the deleterious action of reactive oxygen species (ROS) during macrophage infection (Colangeli et al., 2009). We aimed at addressing the potential protective effect of the higher expression of *lsr2* in *M. abscessus* R cultures under H_2O_2 exposure. Exponential phase cultures, diluted 10 times, were exposed to 20 mM H_2O_2 and CFU were counted at various time points during treatment. When comparing WT *M. abscessus* S and R variants, a high proportion of the R population survived in the presence of H_2O_2 ($p < 0.001$) (**Figure 4A**). Whether

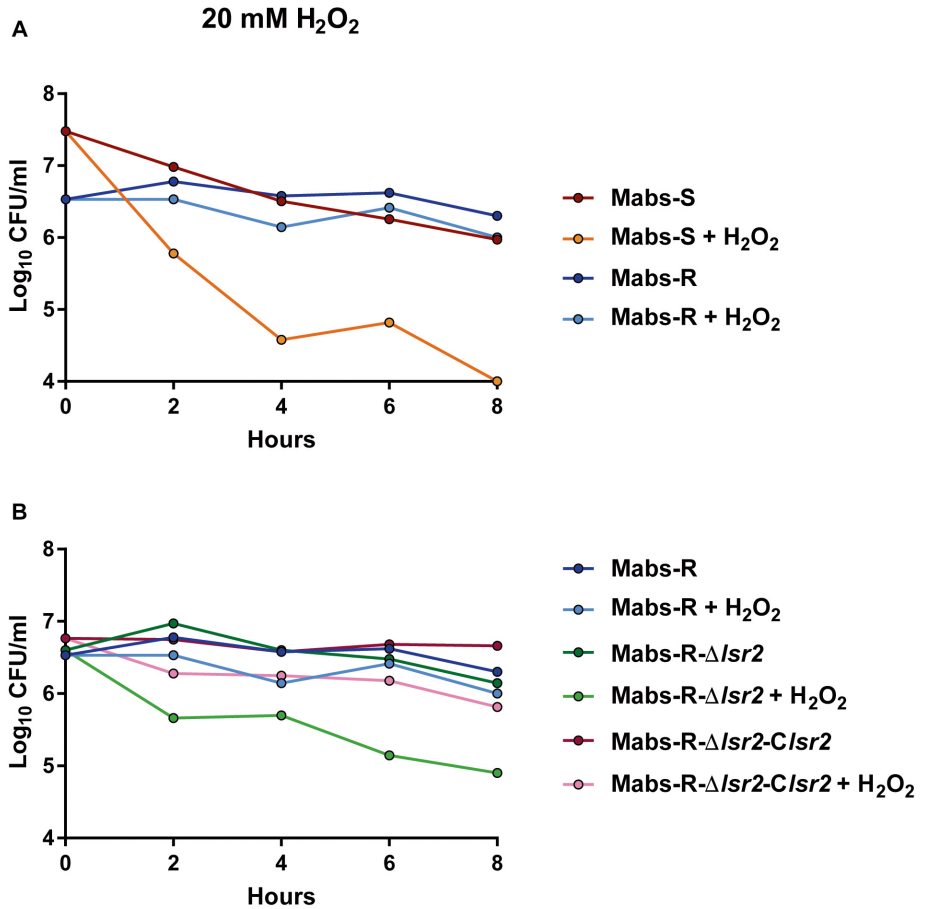

FIGURE 4 | Susceptibility profile of *M. abscessus* toward oxidative derivatives. Strains were grown in broth medium until exponential phase and exposed to 20 mM H_2O_2. Growth was monitored by CFU counting at 2, 4, 6, and 8 h. **(A)** Comparative response of *M. abscessus* S and R variants to the treatment. **(B)** Comparative response of Mabs-R-Δ*lsr2*, Mabs-R-Δ*lsr2* and Mabs-R Δ*lsr2-Clsr2*.

this advantage is conferred by a higher *lsr2* expression was next investigated. The growth defects of Mabs-S and Mabs-S-Δ*lsr2* in the presence of H_2O_2 were similar (**Supplementary Figure S4**). In contrast, Mabs-R-Δ*lsr2* was more sensitive than its WT R progenitor, while genetic complementation in the R *lsr2* mutant restored the WT R H_2O_2 resistance phenotype (**Figure 4B**). These results show a difference in the response of the *M. abscessus* S/R variants to H_2O_2, the R variant being less sensitive to oxidative stress than the S variant. However, the intrinsic resistance of the R variant was partially lost upon deletion of the *lsr2* gene.

The Intracellular Survival of *lsr2* Mutants Is Reduced in Amoebae and Macrophages

The role of Lsr2 in the resistance of *M. abscessus* to oxidative species suggests that it may also protect the bacilli from the microbicidal activity of macrophages (Roux et al., 2016) and/or amoebae (Bakala N'Goma et al., 2015). This prompted us to investigate and compare the impact of *lsr2* deletion on intracellular growth of the S and R mutants with their corresponding complemented strains (Mabs-S-Δ*lsr2*-C*lsr2* and Mabs-R-Δ*lsr2*-C*lsr2*) and wild-type progenitors. Mabs-S-Δ*lsr2* (**Figure 5A**) and Mabs-R-Δ*lsr2* (**Figure 5B**) exhibited a pronounced defect inside murine MΦ as compared to the WT and complemented strains. This survival defect was already significant at 1 dpi for the S strain ($p < 0.0001$) and at 5 dpi for the R strain ($p < 0.0001$). Inside *A. castellani*, a similar decrease in bacterial viability was observed for both Mabs-S-Δ*lsr2* and Mabs-R-Δ*lsr2* mutants (**Figures 5C,D**). At 3 dpi, both mutants showed a strong difference ($p < 0.0001$) in intra-amoebal multiplication compared to their respective WT and complemented strains.

Together, these results indicate that Lsr2 is required for intracellular survival of *M. abscessus* S/R forms in both macrophages and amoebae.

Lsr2 Plays a Key Role in *M. abscessus* Virulence *in vivo*

The impact of Lsr2 on mycobacterial virulence was originally suggested by demonstrating the preferential binding of Lsr2 to

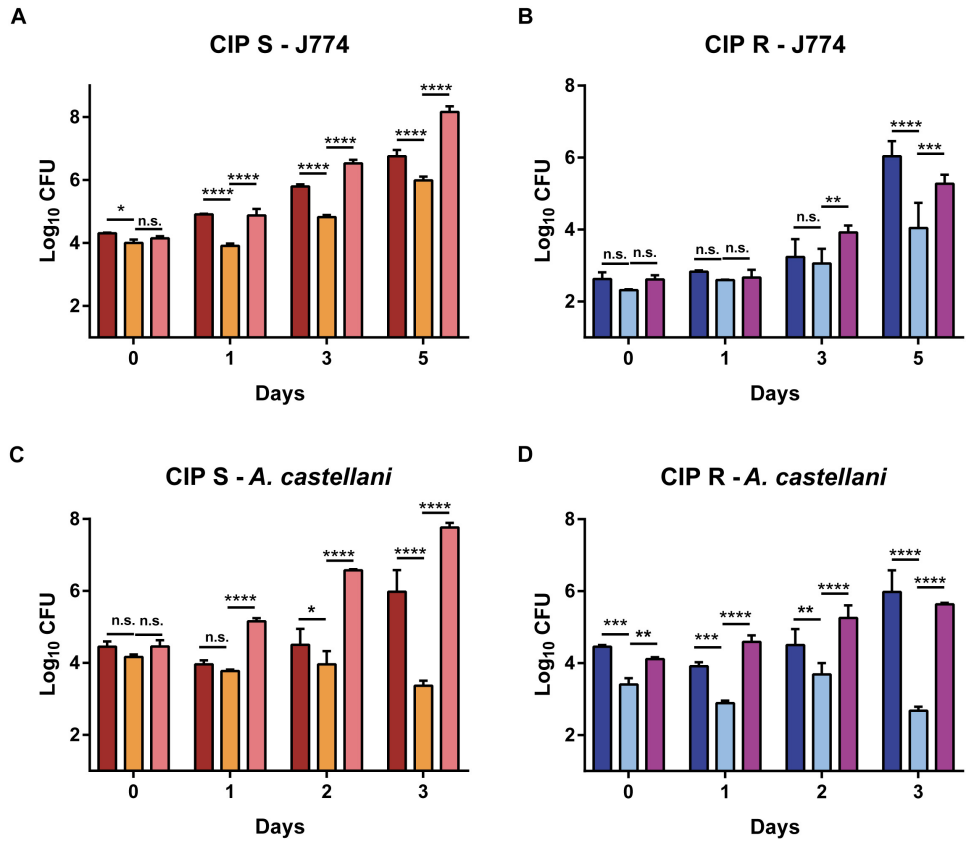

FIGURE 5 | Intracellular growth of Δ*lsr2* mutants in macrophages **(A,B)** and in amoebae **(C,D)**. Murine J774.2 macrophages were infected with CIP104536 (Collection Institut Pasteur) Mabs-S (in red) and Mabs-R (dark blue), Mabs-S-Δ*lsr2* (orange) and Mabs-R-Δ*lsr2* (light blue) and their respective complemented strains (C-Δ*lsr2*; pink for S and mauve for R) at a MOI 1 whereas *A. castellanii* cells were infected with the same strains at a MOI 10. Intracellular growth was assessed by CFU counting for 5 days in macrophages and 3 days in amoebae. CFU histograms with error bars represent means ± SD calculated using data from two independent experiments. Differences between means were analyzed by two-way ANOVA and the Tukey post-test, allowing multiple comparisons. ns, non-significant, $^{*}P < 0.05$, $^{**}P < 0.01$, $^{***}P < 0.001$, and $^{****}P < 0.0001$.

AT-rich regions in the *M. tuberculosis* genome, including several genomic islands acquired by horizontal gene transfer, encoding major virulence factors (Gordon et al., 2010). The behavior of the *lsr2* mutants was first addressed by infecting zebrafish larvae (Bernut et al., 2014a) with the wild-type R (Mabs-R) and Mabs-R-Δ*lsr2* strains. A significant reduction in the virulence of Mabs-R-Δ*lsr2* was observed when compared with Mabs-R (**Figure 6A**). Whereas only 10% of zebrafish were killed when infected with Mabs-R-Δ*lsr2* at 12 dpi, around 40% of the larvae died at 6 dpi with Mabs-R while nearly 70% died at 10 dpi (**Figure 6A**). Complementing with *lsr2* partially reversed the attenuated phenotype of Mabs-R-Δ*lsr2*.

To further evaluate the contribution of Lsr2 in pathogenesis of *M. abscessus* in a more complex animal host, BALB/c mice were intravenously infected with the wild-type S/R variants or Mabs-S/R-Δ*lsr2* strains (Catherinot et al., 2007; Rottman et al., 2007). Bacterial loads were monitored by measuring the CFU counts in the lung, spleen and liver homogenates from mice sacrificed at 1, 15, and 45 dpi. A significant reduction in the number of Mabs-S-Δ*lsr2* bacilli was observed in the lungs at 15 dpi when compared to the wild-type S progenitor ($p < 0.01$). This difference was further increased at 45 dpi, along with a complete clearance of Mabs-S-Δ*lsr2* ($p < 0.05$) (**Figure 6B**, upper panels). However, no significant differences in CFU counts in the spleen and the liver were observed between Mabs-S and Mabs-S-Δ*lsr2*. Monitoring the bacterial burden of Mabs-R-Δ*lsr2* revealed a significant reduction in all three organs at 45 dpi as compared to the WT parental strain ($p < 0.05$ in lungs and spleen; $p < 0.01$ in liver) (**Figure 6C**, lower panels).

Overall, these results indicate that Lsr2 plays a critical role in *M. abscessus* virulence in different animal hosts and highlight the requirement of Lsr2 for persistence in mice, particularly in the lungs, which represents the major targeted organ during infection in patients, especially in those with already underlying pulmonary diseases.

DISCUSSION

Lsr2, a unique nucleoid associated protein in the *Actinomyces* and *Mycobacterium* genera, has been extensively studied in *M. tuberculosis* (Colangeli et al., 2009; Gordon et al., 2010;

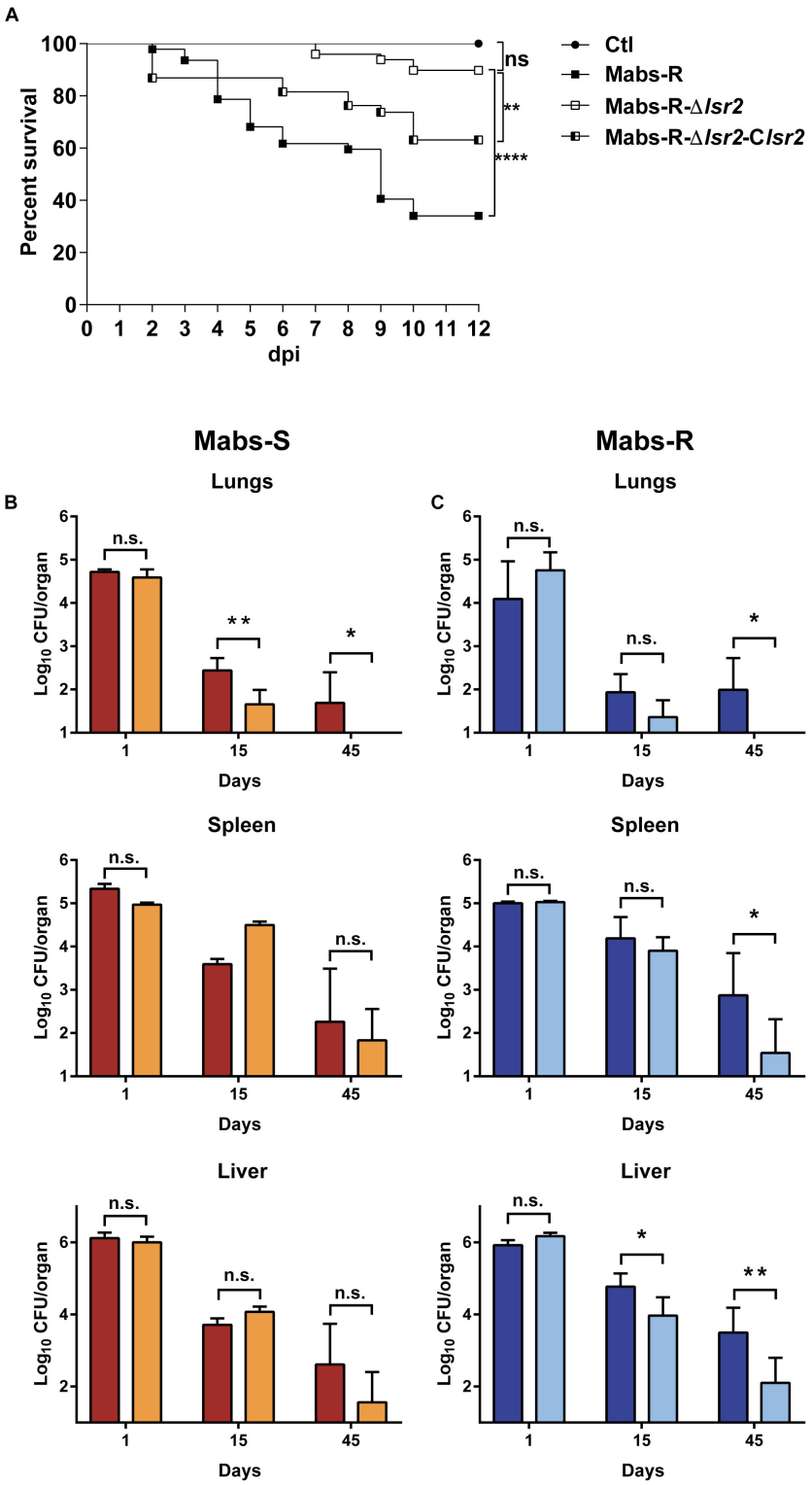

FIGURE 6 | Lsr2 is required for survival of *M. abscessus* in zebrafish and mice. **(A)** Survival curve of infected embryos with 50–164 CFU of Mabs-R (n = 47 embryos), 160–282 CFU of Mabs-R-Δ*lsr2* (n = 49 embryos) and 149–290 CFU of the complemented strain (n = 37 embryos). Experiments were done twice. Significant differences were obtained using the Log-rank (Mantel-Cox) statistical test; $^{**}P < 0.01$ and $^{****}P < 0.0001$. **(B,C)** Comparative analysis of bacterial burden in different organs after autopsy of BALB/c mice infected intravenously with 10^6 CFU of Mabs-S (in red) and Mabs-S-Δ*lsr2* (orange) **(B)** or Mabs-R (dark blue) and Mabs-R-Δ*lsr2* (light blue) **(C)** in the lungs, spleen and liver at 1, 15, and 45 dpi. Student's t-test and Fisher's exact test were used. A P-value of 0.05 was considered significant ($^{*}P < 0.05$ and $^{**}P < 0.01$).

Bartek et al., 2014). Like its ortholog H-NS, homodimers of Lsr2 can bind DNA cooperatively to form long oligomers on AT-rich sequences that can further interact to bridge distant DNA regions and contribute to loop formation (Chen et al., 2008; Liu and Gordon, 2012). At the genomic level, Lsr2 filaments are found at the promoters of 401 and 272 genes in *M. tuberculosis* and *M. smegmatis*, respectively, often extending into their coding regions (Gordon et al., 2010). This observation, as well as its known role as a negative regulator in several cellular functions, strongly suggest that like H-NS, Lsr2 represses transcription through promoter occlusion of RNA polymerase targets or by interfering with transcription elongation (Chen et al., 2008; Liu and Gordon, 2012; Landick et al., 2015). Lsr2 has been shown to be involved in *M. tuberculosis* virulence by binding to important genes, such as genes involved in the ESX secretion systems, the biosynthesis of the PDIM and PGL cell wall lipids or encoding antigenic proteins of the PE/PPE family (Gordon et al., 2010). Previous studies also demonstrated the implication of Lsr2 in multi-drug tolerance of *M. tuberculosis* (Colangeli et al., 2007) and in protection against reactive oxygen intermediates (Colangeli et al., 2009). All these phenotypes were investigated and confirmed in *M. abscessus*, except for the increased resistance to antibiotics (not shown), thus involving Lsr2 in increased resistance to oxidative species as well as in intracellular multiplication and survival of *M. abscessus* in zebrafish and mice.

The S-to-R transition of *M. abscessus* has only been found to occur during infection either in mice (Rottman et al., 2007) or in humans (Jönsson et al., 2007; Catherinot et al., 2009; Roux et al., 2009). In addition, the underlying genetic causes for this transition pointed to irreversible mechanisms, due to selective mutations such as indels that prevent the R form to reverse its morphotype to a S form (Pawlik et al., 2013). Thus, the S-to-R transition represents a clear advantage for *M. abscessus* during the course of the infection. When comparing pairs of isogenic S/R variants, it was found that *lsr2* was expressed at a higher level in the R morphotype (Pawlik et al., 2013). This was confirmed in the present study using qRT-PCR analysis. By inducing a higher expression of *lsr2*, the R variant becomes more resistant to reactive oxygen species. Interestingly, these conditions look similar to those prevailing in the CF airways, characterized by polymicrobial and chronic infections, which maintain a very harsh and oxidative environment in the lungs. Similarly, CF patients receive frequent cures involving large-spectrum antibiotics, such as inhaled tobramycin therapy. Herein, we show that the R form is more resistant to H_20_2 than the S form. But we were unable to confirm an increased resistance to antibiotics (not shown). This resistant phenotype was lost in the *lsr2* mutant but restored to wild-type levels following complementation with a functional copy of *lsr2*.

A major outcome of this work is to point out the role of Lsr2 in the intracellular behavior of *M. abscessus* and on its requirement for persistence in infected mice and zebrafish. It was previously shown that a deletion of *lsr2* in *M. smegmatis* has an impact on its survival in murine macrophages (Colangeli et al., 2009). *In vivo* studies of the role of *lsr2* in virulence in mice were also performed on *M. tuberculosis*, using an attenuated strain that was complemented by a replicative plasmid expressing Lsr2 under the control of an inducible promoter (Ehrt et al., 2005) to circumvent the absence of viability of the *lsr2 M. tuberculosis* deletion mutant (Colangeli et al., 2007). Using this strategy, it was shown that *lsr2* is important to protect *M. tuberculosis* against ROI during macrophage infection. The present study shows that despite being dispensable in *M. abscessus*, *lsr2* remains essential for optimal intracellular growth and virulence in different vertebrates.

Previous work in *M. smegmatis* emphasized the contribution of Lsr2 in defining the lipid profile, colony morphology, bacterial motility and biofilm formation by specifically repressing transcription at the GPL locus in the rough morphotypes (Chen et al., 2006; Arora et al., 2008; Kocíncová et al., 2008; Yang et al., 2017). However, this study clearly shows that *lsr2* mRNAs are detected in both *M. abscessus* S and R strains. Thanks to ChIP-qPCR, we also observed that Lsr2 is able to bind the promoter region of *mbtH* in *M. abscessus* S, despite the equivalent GPL profiles in the WT and the mutant strain. This suggests that binding of Lsr2 to this particular genomic region is not sufficient to regulate the biosynthetic *GPL* locus and that this process may involve other partners that remain to be identified. An alternative explanation is that the higher expression level of Lsr2 in *M. abscessus* R is needed to successfully reduce GPL production, eventually by increasing the formation of a DNA loop that can occlude RNA polymerase binding or inhibit transcription elongation, as proposed for H-NS in Gram-negative bacteria (Landick et al., 2015). One would have anticipated that increasing expression of Lsr2 in *M. abscessus* R would enhance the R phenotype by further repressing the genes of the GPL locus. However, deletion of *lsr2* in *M. abscessus* R did not restore GPL production as it was previously observed in *M. smegmatis* (Kocíncová et al., 2008). As mentioned above, the GPL locus in the *M. abscessus* R variant suffers from irreversible genetic lesions, adding a layer of complexity to the molecular mechanisms involved in the regulation of this locus. The pleiotropic nature of Lsr2 implies that its deletion has a broader impact on the fitness of *M. abscessus* as well as on the general compaction of its nucleoid. Thus, additional analysis using genome-wide methods will help to unravel the details of the molecular role of Lsr2 during S-to-R transition and its impact on pathogenicity.

Taken together, this work showed the impact of Lsr2 as a key virulence factor on the intracellular and *in vivo* survival of *M. abscessus*. These results also strongly suggest that Lsr2, like other NAPs, might represent a target of choice for the development of new antimicrobials. Indeed, compounds that would either silence expression of lsr2 or inhibit its function could therefore be considered as a new anti-virulence approach against *M. abscessus* (Liu and Gordon, 2012).

ETHICS STATEMENT

All procedures involving mice were performed according to the institutional and national ethical guidelines and approved by the comité d'éthique en experimentation animale N°047

with agreement A783223 under the reference APAFIS#11465. All zebrafish experiments were done according to European Union guidelines for handling of laboratory animals (http://ec.europa.eu/environment/chemicals/lab_animals/home_en.htm) and approved by the Comité d'Ethique pour l'Expérimentation Animale de la région Languedoc Roussillon under the reference CEEALR36-1145.

AUTHOR CONTRIBUTIONS

J-LH, LK, and FC designed the project and experiments. VLM, AB, MC, AV, CD, and AP performed the experiments. J-LG, FM, FC, LK, and J-LH wrote and corrected the manuscript.

FUNDING

This work was supported by the Vaincre la Mucoviscidose association (Post-doctoral fellowship to VLM #RF20110600446/1/3/130) and the ANR DIMYVIR Grant (ANR-13-BSV3-0007-01 to J-LH and LK) from the French National Research Agency Program.

SUPPLEMENTARY MATERIAL

The Supplementary Material for this article can be found online at: https://www.frontiersin.org/articles/10.3389/fmicb.2019.00905/full#supplementary-material

REFERENCES

Arora, K., Whiteford, D. C., Lau-Bonilla, D., Davitt, C. M., and Dahl, J. L. (2008). Inactivation of *lsr2* results in a hypermotile phenotype in *Mycobacterium smegmatis*. *J. Bacteriol.* 190, 4291–4300. doi: 10.1128/JB.00023-08

Bakala N'Goma, J. C., Le Moigne, V., Soismier, N., Laencina, L., Le Chevalier, F., et al. (2015). *Mycobacterium abscessus* phospholipase C expression is induced during coculture within amoebae and enhances *M. abscessus* virulence in mice. *Infect. Immun.* 83, 780–791. doi: 10.1128/IAI.02032-14

Bartek, I. L., Woolhiser, L. K., Baughn, A. D., Basaraba, R. J., Jacobs, W. R. Jr., Lenaerts, A. J., et al. (2014). *Mycobacterium tuberculosis* Lsr2 is a global transcriptional regulator required for adaptation to changing oxygen levels and virulence. *mBio* 5:e01106-14. doi: 10.1128/mBio.01106-14

Bernut, A., Dupont, C., Sahuquet, A., Herrmann, J.-L., Lutfalla, G., and Kremer, L. (2015). Deciphering and Imaging Pathogenesis and Cording of *Mycobacterium abscessus* in zebrafish embryos. *J. Vis. Exp.* 103:53130. doi: 10.3791/53130

Bernut, A., Herrmann, J.-L., Kissa, K., Dubremetz, J.-F., Gaillard, J.-L., Lutfalla, G., et al. (2014a). *Mycobacterium abscessus* cording prevents phagocytosis and promotes abscess formation. *Proc. Natl. Acad. Sci. U.S.A.* 111, E943–E952. doi: 10.1073/pnas.1321390111

Bernut, A., Le Moigne, V., Lesne, T., Lutfalla, G., Herrmann, J.-L., and Kremer, L. (2014b). In vivo assessment of drug efficacy against *Mycobacterium abscessus* using the embryonic zebrafish test system. *Antimicrob. Agents Chemother*. 58, 4054–4063. doi: 10.1128/AAC.00142-14

Bernut, A., Herrmann, J.-L., Ordway, D., and Kremer, L. (2017). The diverse cellular and animal models to decipher the physiopathological traits of *Mycobacterium abscessus* infection. *Front. Cell. Infect. Microbiol.* 7:100. doi: 10.3389/fcimb.2017.00100

Besra, G. S. (1998). Preparation of cell-wall fractions from mycobacteria. *Methods Mol. Biol.* 101, 91–107.

Brown-Elliott, B. A., and Wallace, R. J. (2002). Clinical and taxonomic status of pathogenic nonpigmented or late-pigmenting rapidly growing mycobacteria. *Clin. Microbiol. Rev.* 15, 716–746.

Byrd, T. F., and Lyons, C. R. (1999). Preliminary characterization of a *Mycobacterium abscessus* mutant in human and murine models of infection. *Infect. Immun.* 67, 4700–4707.

Catherinot, E., Clarissou, J., Etienne, G., Ripoll, F., Emile, J.-F., Daffé, M., et al. (2007). Hypervirulence of a rough variant of the *Mycobacterium abscessus* type strain. *Infect. Immun.* 75, 1055–1058.

Catherinot, E., Roux, A.-L., Macheras, E., Hubert, D., Matmar, M., Dannhoffer, L., et al. (2009). Acute respiratory failure involving an R variant of *Mycobacterium abscessus*. *J. Clin. Microbiol.* 47, 271–274. doi: 10.1128/JCM.01478-08

Chen, J. M., German, G. J., Alexander, D. C., Ren, H., Tan, T., and Liu, J. (2006). Roles of Lsr2 in colony morphology and biofilm formation of *Mycobacterium smegmatis*. *J. Bacteriol.* 188, 633–641.

Chen, J. M., Ren, H., Shaw, J. E., Wang, Y. J., Li, M., Leung, A. S., et al. (2008). Lsr2 of *Mycobacterium tuberculosis* is a DNA-bridging protein. *Nucleic Acids Res.* 36, 2123–2135. doi: 10.1093/nar/gkm1162

Colangeli, R., Haq, A., Arcus, V. L., Summers, E., Magliozzo, R. S., McBride, A., et al. (2009). The multifunctional histone-like protein Lsr2 protects mycobacteria against reactive oxygen intermediates. *Proc. Natl. Acad. Sci. U.S.A.* 106, 4414–4418. doi: 10.1073/pnas.0810126106

Colangeli, R., Helb, D., Vilchèze, C., Hazbon, M. H., Lee, C.-G., Safi, H., et al. (2007). Transcriptional regulation of multi-drug tolerance and antibiotic-induced responses by the histone-like protein Lsr2 in *M. tuberculosis*. *PLoS Pathog.* 3:e87. doi: 10.1371/journal.ppat.0030087

Cortes, M., Singh, A. K., Reyrat, J. M., Gaillard, J.-L., Nassif, X., and Herrmann, J.-L. (2011). Conditional gene expression in *Mycobacterium abscessus*. *PLoS One* 6:e29306. doi: 10.1371/journal.pone.0029306

Diel, R., Ringshausen, F., Richter, E., Welker, L., Schmitz, J., and Nienhaus, A. (2017). Microbiological and clinical outcomes of treating non-*Mycobacterium avium* complex nontuberculous mycobacterial pulmonary disease: a systematic review and meta-analysis. *Chest* 152, 120–142. doi: 10.1016/j.chest.2017.04.166

Dubois, V., Laencina, L., Bories, A., Le Moigne, V., Pawlik, A., Herrmann, J. L., et al. (2018a). Identification of virulence markers of *Mycobacterium abscessus* for intracellular replication in phagocytes. *J. Vis. Exp.* 139:e57766. doi: 10.3791/57766

Dubois, V., Viljoen, A., Laencina, L., Le Moigne, V., Bernut, A., Dubar, F., et al. (2018b). MmpL8MAB controls *Mycobacterium abscessus* virulence and production of a previously unknown glycolipid family. *Proc. Natl. Acad. Sci. U.S.A.* 115, E10147–E10156. doi: 10.1073/pnas.1812984115

Ehrt, S., Guo, X. V., Hickey, C. M., Ryou, M., Monteleone, M., Riley, L. W., et al. (2005). Controlling gene expression in mycobacteria with anhydrotetracycline and Tet repressor. *Nucleic Acids Res.* 33:e21. doi: 10.1093/nar/gni013

Esther, C. R., Esserman, D. A., Gilligan, P., Kerr, A., and Noone, P. G. (2010). Chronic *Mycobacterium abscessus* infection and lung function decline in cystic fibrosis. *J. Cyst. Fibros. Soc.* 9, 117–123. doi: 10.1016/j.jcf.2009.12.001

Gordon, B. R., Imperial, R., Wang, L., Navarre, W. W., and Liu, J. (2008). Lsr2 of *Mycobacterium* represents a novel class of H-NS like proteins. *J. Bacteriol.* 190, 7052–7059. doi: 10.1128/JB.00733-08

Gordon, B. R., Li, Y., Wang, L., Sintsova, A., van Bakel, H., Tian, S., et al. (2010). Lsr2 is a nucleoid-associated protein that targets AT-rich sequences and virulence genes in *Mycobacterium tuberculosis*. *Proc. Natl. Acad. Sci. U.S.A.* 107, 5154–5159. doi: 10.1073/pnas.0913551107

Gordon, B. R. G., Li, Y., Cote, A., Weirauch, M. T., Ding, P., Hughes, T. R., et al. (2011). Structural basis for recognition of AT-rich DNA by unrelated xenogeneic silencing proteins. *Proc. Natl. Acad. Sci. U.S.A.* 108, 10690–10695. doi: 10.1073/pnas.1102544108

Grainger, D. C., Hurd, D., Goldberg, M. D., and Busby, S. J. (2006). Association of nucleoid proteins with coding and non-coding segments of the *Escherichia coli* genome. *Nucleic Acids Res.* 34, 4642–4652. doi: 10.1093/nar/gkl542

Grzegorzewicz, A. E., Pham, H., Gundi, V. A. K. B., Scherman, M. S., North, E. J., Hess, T., et al. (2012). Inhibition of mycolic acid transport across the *Mycobacterium tuberculosis* plasma membrane. *Nat. Chem. Biol.* 8, 334–341. doi: 10.1038/nchembio.794

Gutiérrez, A. V., Viljoen, A., Ghigo, E., Herrmann, J.-L., and Kremer, L. (2018). Glycopeptidolipids, a double-edged sword of the *Mycobacterium abscessus* complex. *Front. Microbiol.* 9:1145. doi: 10.3389/fmicb.2018.01145

Halloum, I., Carrère-Kremer, S., Blaise, M., Viljoen, A., Bernut, A., Le Moigne, V., et al. (2016). Deletion of a dehydratase important for intracellular growth and cording renders rough *Mycobacterium abscessus* avirulent. *Proc. Natl. Acad. Sci. U.S.A.* 113, E4228–E4237. doi: 10.1073/pnas.1605477113

Howard, S. T., Rhoades, E., Recht, J., Pang, X., Alsup, A., Kolter, R., et al. (2006). Spontaneous reversion of *Mycobacterium abscessus* from a smooth to a rough morphotype is associated with reduced expression of glycopeptidolipid and reacquisition of an invasive phenotype. *Microbiology* 152, 1581–1590.

Jeong, S. H., Kim, S.-Y., Huh, H. J., Ki, C.-S., Lee, N. Y., Kang, C.-I., et al. (2017). Mycobacteriological characteristics and treatment outcomes in extrapulmonary *Mycobacterium abscessus* complex infections. *Int. J. Infect. Dis.* 60, 49–56. doi: 10.1016/j.ijid.2017.05.007

Jönsson, B. E., Gilljam, M., Lindblad, A., Ridell, M., Wold, A. E., and Welinder-Olsson, C. (2007). Molecular epidemiology of *Mycobacterium abscessus*, with focus on cystic fibrosis. *J. Clin. Microbiol.* 45, 497–504.

Kocíncová, D., Singh, A. K., Beretti, J. L., Ren, H., Euphrasie, D., Liu, J., et al. (2008). Spontaneous transposition of IS1096 or ISMsm3 leads to glycopeptidolipid overproduction and affects surface properties in *Mycobacterium smegmatis*. *Tuberculosis* 88, 390–398. doi: 10.1016/j.tube.2008.02.005

Laal, S., Sharma, Y. D., Prasad, H. K., Murtaza, A., Singh, S., Tangri, S., et al. (1991). Recombinant fusion protein identified by lepromatous sera mimics native *Mycobacterium leprae* in T-cell responses across the leprosy spectrum. *Proc. Natl. Acad. Sci. U.S.A.* 88, 1054–1058.

Laencina, L., Dubois, V., Le Moigne, V., Viljoen, A., Majlessi, L., Pritchard, J., et al. (2018). Identification of genes required for *Mycobacterium abscessus* growth in vivo with a prominent role of the ESX-4 locus. *Proc. Natl. Acad. Sci. U.S.A.* 115, E1002–E1011. doi: 10.1073/pnas.1713195115

Lamason, R. L., Mohideen, M. A., Mest, J. R., Wong, A. C., Norton, H. L., Aros, M. C., et al. (2005). SLC24A5, a putative cation exchanger, affects pigmentation in zebrafish and humans. *Science* 310, 1782–1786.

Landick, R., Wade, J. T., and Grainger, D. C. (2015). H-NS and RNA polymerase: a love–hate relationship? *Curr. Opin. Microbiol.* 24, 53–59. doi: 10.1016/j.mib.2015.01.009

Le Moigne, V., Belon, C., Goulard, C., Accard, G., Bernut, A., Pitard, B., et al. (2016). MgtC as a host-induced factor and vaccine candidate against *Mycobacterium abscessus* infection. *Infect. Immun.* 84, 2895–2903. doi: 10.1128/IAI.00359-16

Liu, J., and Gordon, B. R. (2012). Targeting the global regulator Lsr2 as a novel approach for anti-tuberculosis drug development. *Expert Rev. Anti. Infect. Ther.* 10, 1049–1053. doi: 10.1586/eri.12.86

Medjahed, H., Gaillard, J.-L., and Reyrat, J.-M. (2010). *Mycobacterium abscessus*: a new player in the mycobacterial field. *Trends Microbiol.* 18, 17–23. doi: 10.1016/j.tim.2009.12.007

Medjahed, H., and Reyrat, J.-M. (2009). Construction of *Mycobacterium abscessus* defined glycopeptidolipid mutants: comparison of genetic tools. *Appl. Environ. Microbiol.* 75, 1331–1338. doi: 10.1128/AEM.01914-08

Mougari, F., Guglielmetti, L., Raskine, L., Sermet-Gaudelus, I., Veziris, N., and Cambau, E. (2016). Infections caused by *Mycobacterium abscessus*: epidemiology, diagnostic tools and treatment. *Expert Rev. Anti. Infect. Ther.* 14, 1139–1154.

Nessar, R., Reyrat, J.-M., Davidson, L. B., and Byrd, T. F. (2011). Deletion of the mmpL4b gene in the *Mycobacterium abscessus* glycopeptidolipid biosynthetic pathway results in loss of surface colonization capability, but enhanced ability to replicate in human macrophages and stimulate their innate immune response. *Microbiology* 157, 1187–1195. doi: 10.1099/mic.0.046557-0

Nguyen, K. T., Piastro, K., Gray, T. A., and Derbyshire, K. M. (2010). Mycobacterial biofilms facilitate horizontal DNA transfer between strains of *Mycobacterium smegmatis*. *J. Bacteriol.* 192, 5134–5142. doi: 10.1128/JB.00650-10

Oberley-Deegan, R. E., Rebits, B. W., Weaver, M. R., Tollefson, A. K., Bai, X., McGibney, M., et al. (2010). An oxidative environment promotes growth of *Mycobacterium abscessus*. *Free Radic. Biol. Med.* 49, 1666–1673. doi: 10.1016/j.freeradbiomed.2010.08.026

Pawlik, A., Garnier, G., Orgeur, M., Tong, P., Lohan, A., Le Chevalier, F., et al. (2013). Identification and characterization of the genetic changes responsible for the characteristic smooth-to-rough morphotype alterations of clinically persistent *Mycobacterium abscessus*. *Mol. Microbiol.* 90, 612–629. doi: 10.1111/mmi.12387

Qu, Y., Lim, C. J., Whang, Y. R., Liu, J., and Yan, J. (2013). Mechanism of DNA organization by *Mycobacterium tuberculosis* protein Lsr2. *Nucleic Acids Res.* 41, 5263–5272. doi: 10.1093/nar/gkt249

Qvist, T., Taylor-Robinson, D., Waldmann, E., Olesen, H. V., Hansen, C. R., Mathiesen, I. H., et al. (2016). Comparing the harmful effects of nontuberculous mycobacteria and Gram negative bacteria on lung function in patients with cystic fibrosis. *J. Cyst. Fibros.* 15, 380–385. doi: 10.1016/j.jcf.2015.09.007

Ripoll, F., Pasek, S., Schenowitz, C., Dossat, C., Barbe, V., Rottman, M., et al. (2009). Non-mycobacterial virulence genes in the genome of the emerging pathogen *Mycobacterium abscessus*. *PLoS One* 4:e5660. doi: 10.1371/journal.pone.0005660

Rottman, M., Soudais, C., Vogt, G., Renia, L., Emile, J.-F., Decaluwe, H., et al. (2007). Importance of T cells, gamma interferon, and tumor necrosis factor in immune control of the rapid grower *Mycobacterium abscessus* in C57BL/6 mice. *Infect. Immun.* 75, 5898–5907.

Roux, A.-L., Catherinot, E., Ripoll, F., Soismier, N., Macheras, E., Ravilly, S., et al. (2009). Multicenter study of prevalence of nontuberculous mycobacteria in patients with cystic fibrosis in France. *J. Clin. Microbiol.* 47, 4124–4128.

Roux, A.-L., Ray, A., Pawlik, A., Medjahed, H., Etienne, G., Rottman, M., et al. (2011). Overexpression of proinflammatory TLR-2-signalling lipoproteins in hypervirulent mycobacterial variants. *Cell. Microbiol.* 13, 692–704. doi: 10.1111/j.1462-5822.2010.01565.x

Roux, A.-L., Viljoen, A., Bah, A., Simeone, R., Bernut, A., Laencina, L., et al. (2016). The distinct fate of smooth and rough *Mycobacterium abscessus* variants inside macrophages. *Open Biol.* 6:160185.

Sánchez-Chardi, A., Olivares, F., Byrd, T. F., Julián, E., Brambilla, C., and Luquin, M. (2011). Demonstration of cord formation by rough *Mycobacterium abscessus* variants: implications for the clinical microbiology laboratory. *J. Clin. Microbiol.* 49, 2293–2295. doi: 10.1128/JCM.02322-10

Smibert, O., Snell, G. I., Bills, H., Westall, G. P., and Morrissey, C. O. (2016). *Mycobacterium abscessus* complex - a particular challenge in the setting of lung transplantation. *Expert Rev. Anti. Infect. Ther.* 14, 325–333.

Sondén, B., Kocíncová, D., Deshayes, C., Euphrasie, D., Rhayat, L., Laval, F., et al. (2005). Gap, a mycobacterial specific integral membrane protein, is required for glycolipid transport to the cell surface. *Mol. Microbiol.* 58, 426–440.

van Dorn, A. (2017). Multidrug-resistant *Mycobacterium abscessus* threatens patients with cystic fibrosis. *Lancet Respir. Med.* 5:15.

van Kessel, J. C., and Hatfull, G. F. (2007). Recombineering in *Mycobacterium tuberculosis*. *Nat. Methods* 4, 147–152.

Varghese, B., Shajan, S. E., Al Saedi, M. O., and Al-Hajoj, S. A. (2012). First case report of chronic pulmonary lung disease caused by *Mycobacterium abscessus* in two immunocompetent patients in Saudi Arabia. *Ann. Saudi Med.* 32, 312–314. doi: 10.5144/0256-4947.2012.312

Yang, Y., Thomas, J., Li, Y., Vilchèze, C., Derbyshire, K. M., Jacobs, W. R., et al. (2017). Defining a temporal order of genetic requirements for development of mycobacterial biofilms. *Mol. Microbiol.* 105, 794–809. doi: 10.1111/mmi.13734

Conflict of Interest Statement: The authors declare that the research was conducted in the absence of any commercial or financial relationships that could be construed as a potential conflict of interest.

frontiers in Microbiology

MINI REVIEW
published: 05 June 2018
doi: 10.3389/fmicb.2018.01145

Glycopeptidolipids, a Double-Edged Sword of the *Mycobacterium abscessus* Complex

*Ana Victoria Gutiérrez[1,2], Albertus Viljoen[1], Eric Ghigo[3], Jean-Louis Herrmann[4] and Laurent Kremer[1,5]**

[1] Centre National de la Recherche Scientifique, Institut de Recherche en Infectiologie de Montpellier, UMR 9004, Université de Montpellier, Montpellier, France, [2] CNRS, IRD 198, INSERM U1095, APHM, Institut Hospitalo-Universitaire Méditerranée Infection, UMR 7278, Aix-Marseille Université, Marseille, France, [3] CNRS, Campus Joseph Aiguier, Marseille, France, [4] 2I, UVSQ, INSERM UMR 1173, Université Paris-Saclay, Versailles, France, [5] INSERM, IRIM, Montpellier, France

Mycobacterium abscessus is a rapidly-growing species causing a diverse panel of clinical manifestations, ranging from cutaneous infections to severe respiratory disease. Its unique cell wall, contributing largely to drug resistance and to pathogenicity, comprises a vast panoply of complex lipids, among which the glycopeptidolipids (GPLs) have been the focus of intense research. These lipids fulfill various important functions, from sliding motility or biofilm formation to interaction with host cells and intramacrophage trafficking. Being highly immunogenic, the induction of a strong humoral response is likely to select for rough low-GPL producers. These, in contrast to the smooth high-GPL producers, display aggregative properties, which strongly impacts upon intracellular survival. A propensity to grow as extracellular cords allows these low-GPL producing bacilli to escape the innate immune defenses. Transitioning from high-GPL to low-GPL producers implicates mutations within genes involved in biosynthesis or transport of GPL. This leads to induction of an intense pro-inflammatory response and robust and lethal infections in animal models, explaining the presence of rough isolates in patients with decreased pulmonary functions. Herein, we will discuss how, thanks to the generation of defined GPL mutants and the development of appropriate cellular and animal models to study pathogenesis, GPL contribute to *M. abscessus* biology and physiopathology.

Keywords: *Mycobacterium abscessus*, glycopeptidolipid, cell wall, pathogenesis, host/pathogen interactions

OPEN ACCESS

Edited by:
Thomas Dick,
Rutgers, The State University of New Jersey, Newark, United States

Reviewed by:
Anil Ojha,
Wadsworth Center, United States
Olivier Neyrolles,
Centre National de la Recherche Scientifique (CNRS), France

***Correspondence:**
Laurent Kremer
laurent.kremer@irim.cnrs.fr

Specialty section:
This article was submitted to Antimicrobials, Resistance and Chemotherapy, a section of the journal Frontiers in Microbiology

Received: *21 March 2018*
Accepted: *14 May 2018*
Published: *05 June 2018*

Citation:
Gutiérrez AV, Viljoen A, Ghigo E, Herrmann J-L and Kremer L (2018) Glycopeptidolipids, a Double-Edged Sword of the Mycobacterium abscessus Complex. Front. Microbiol. 9:1145. doi: 10.3389/fmicb.2018.01145

INTRODUCTION

Mycobacterium abscessus is a fast-growing non-tuberculous mycobacterium (NTM) and an emerging human pathogen that causes nosocomial skin and soft tissue infections (Brown-Elliott et al., 2012) but also pulmonary infections, especially in patients with cystic fibrosis (CF) and other lung disorders (Sermet-Gaudelus et al., 2003; Esther et al., 2010). Recent investigations reported mechanisms of virulence and physiopathological processes characterizing *M. abscessus* infection thanks to (i) genetic tools that allowed generation of defined mutants and transposon libraries, particularly useful to seek out genetic determinants of intracellular survival (Medjahed and Reyrat, 2009; Cortes et al., 2011; Gregoire et al., 2017; Laencina et al., 2018) and (ii) the development of various complementary cellular and animal models, which have allowed delineation of the early

stages of the infection and the role of important cell types participating in controlling the infection and/or in the formation of granulomas (Ordway et al., 2008; Bernut et al., 2014a, 2017; Laencina et al., 2018). Evidence exists that granulomas harbor persistent *M. abscessus* for extended periods of time (Tomashefski et al., 1996; Medjahed et al., 2010). Additionally, these models have been used successfully to test the *in vivo* therapeutic efficacy of compounds against *M. abscessus*, considered as one of the most drug-resistant mycobacterial species (Bernut et al., 2014b; Dubée et al., 2015; Obregón-Henao et al., 2015; Dupont et al., 2016).

Like other NTMs, *M. abscessus* displays smooth (S) or rough (R) colony morphotypes, associated with distinct *in vitro* and *in vivo* phenotypes. This colony-based distinction is dependent on the presence (in S) or absence (in R) of surface-associated glycopeptidolipids (GPLs) (Howard et al., 2006; Medjahed et al., 2010). The presence or lack of GPL considerably influences important physiological and physiopathological aspects, including sliding motility or biofilm formation, interaction with host cells, intracellular trafficking in macrophages and virulence, ultimately conditioning the clinical outcome of the infection. This review gathers some of the most recent findings related to biosynthesis and transport of GPL in *M. abscessus*, the mechanisms driving the S-to-R switch and how this transition influences the surface properties of the bacilli, interaction with host cells, virulence and potentially the mode of transmission of *M. abscessus*.

GENOMICS AND STRUCTURAL ASPECTS OF GPL IN *M. abscessus*

The mycobacterial envelope comprises three layers: a typical plasma membrane, a complex cell wall partly resembling a Gram-positive wall and an outer layer (Daffé and Draper, 1998). Particularly unusual, the cell wall consists of a thick peptidoglycan layer covalently-linked to arabinogalactan, itself esterified by mycolic acids, forming the inner leaflet of the mycomembrane. In addition, a large variety of extractible lipids form the outer leaflet of the mycomembrane. Among these are the GPL, found in many NTM (**Figure 1A**). GPL are subdivided into alkali-stable C-type GPL and alkali-labile serine-containing GPL. The C-type GPL are found in saprophytic mycobacteria such as *Mycobacterium smegmatis* or in opportunistic pathogens like *Mycobacterium avium*, *Mycobacterium chelonae,* or *Mycobacterium abscessus* (Schorey and Sweet, 2008), whereas the alkali-labile serine-containing GPL were found in *Mycobacterium xenopi* (Besra et al., 1993). C-type GPL share a common lipopeptidyl core consisting of a mixture of 3-hydroxy and 3-methoxy C28-30 fatty acids amidated by a tripeptide-amino-alcohol core of D-Phe-D-*allo*-Thr-D-Ala-L-alaninol. This lipopeptide core is glycosylated with the *allo*-Thr linked to a 6-deoxy-α-L-talose and the alaninol linked to an α-L-rhamnose. These di-glycosylated GPL make up the less polar species (**Figure 1A**). In the case of *M. avium*, the 6-deoxytalose is non-methylated or 3-*O*-methylated, and the rhamnose is either 3-*O*-methylated or 3,4-di-*O*-methylated. *M. avium* GPL can also be *O*-acetylated at various locations, depending on the strain. In contrast, *M. smegmatis*, *M. chelonae,* and *M. abscessus* produce di-glycosylated GPL that contain a 3,4-di-*O*-acetylated 6-deoxytalose and a 3,4-di-*O*-methylated or 2,3,4-tri-*O*-methylated rhamnose (Villeneuve et al., 2003; Ripoll et al., 2007; Whang et al., 2017). These species also produce more polar GPL by the addition of a 2,3,4-tri-hydroxylated rhamnose to the alaninol-linked 3,4-di-*O*-methyl rhamnose. Although being structurally identical, triglycosylated GPL are more abundant in *M. abscessus* than in *M. smegmatis* (Ripoll et al., 2007). GPL are heterogenous in structure and vary according to the fatty acyl chain length and the degree of hydroxylation or *O*-methylation of the glycosidic moieties (**Figure 1B**).

The *gpl* locus is highly conserved in *M. smegmatis*, *M. abscessus,* and *M. avium* (**Figure 1C**) but differences exist, like the presence of an IS1096 in *M. smegmatis.* The tripeptide-aminoalcohol moiety of GPL is assembled by the products of *mps1* and *mps2* (Billman-Jacobe et al., 1999). The genes *gtf1* and *gtf2* catalyze glycosylation of the lipopeptide core whereas *gtf3* adds the extra rhamnose defining triglycosylated GPL. The genes *rmt2*, *rmt3,* and *rmt4* participate in *O*-methylation of the rhamnose and *fmt*, absent in *M. avium*, in *O*-methylation of the lipid moiety. In contrast to *M. smegmatis* which possesses a single *atf* gene involved in acetylation of the two positions of the deoxytalose, two genes, *atf1* and *atf2*, transfer the acetyl residues in a sequential manner in *M. abscessus* (Ripoll et al., 2007). Separated by *gtf3*, *rmlA* and *rmlB* are responsible for monosaccharide activation and epimerization. On the proximal end of the *gpl* locus is found *mmpS4*, *mmpL4a* and *mmpL4b* in an operon and encoding membrane proteins required for the transport of GPL across the plasma membrane (Medjahed and Reyrat, 2009; Deshayes et al., 2010; Bernut et al., 2016b). MmpS4 has been proposed to mediate formation of the GPL biosynthesis/transport machinery megacomplex located at the bacterial pole (Deshayes et al., 2010). GPL transport requires also the integral membrane protein Gap in *M. smegmatis* (Sondén et al., 2005) (**Figure 1A**). How GPL are translocated from the periplasmic space to the outer membrane, however, remains unknown. Additionally, a block of eight genes [*MSMEG_0406* (*fadE5*) to *MSMEG_0413* (*gap-like*)] in *M. smegmatis*, originally proposed to catalyze the lipid synthesis and attachment to the tripeptide-aminoalcohol moiety of GPL (Ripoll et al., 2007) was recently reattributed to the synthesis of trehalose polyphleates (TPP) (Burbaud et al., 2016). In *M. abscessus*, this cluster is far away from the main *gpl* locus with *Rv0926* and *fadE5* being scattered in the *M. abscessus* chromosome (**Figure 1C**).

MOLECULAR MECHANISMS OF THE SMOOTH-TO-ROUGH TRANSITION AND ASSOCIATED PHENOTYPES

Comparative genomics to understand the molecular basis of the S and R phenotypes using isogenic S and R pairs revealed multiple indels or single nucleotide polymorphisms within the *gpl* locus (Pawlik et al., 2013). A single nucleotide deletion in *mmpL4b* and nucleotide insertions in *mps1* were identified in the R variants

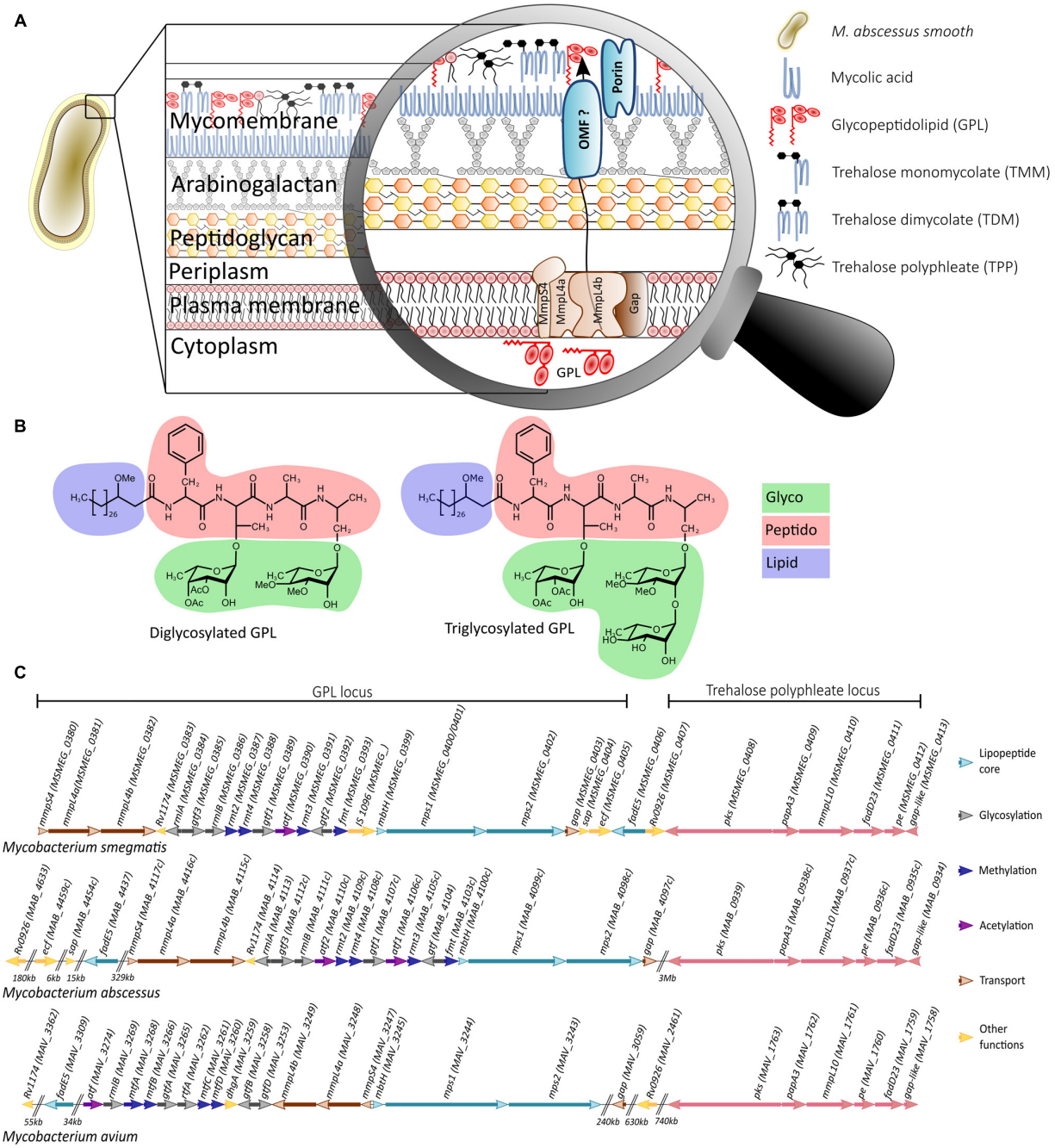

FIGURE 1 | Cell wall localization, structure, and genomics of GPL. **(A)** Schematic representation of the *Mycobacterium abscessus* envelope, with a special focus on the plasma membrane proteins participating in the transport of GPL and on the inner and outer leaflets of the mycomembrane impregnated with various extractible lipids such as GPL. **(B)** Structure of the diglycosylated (apolar) and triglycosylated (polar) GPL. As GPL represent a highly heterogenous population of lipids, only one structure is depicted. Modifications can occur in the lipid chain length or in the hydroxylation/*O*-methylation status of the various monosaccharides. **(C)** Genomic organization of the *gpl* and *tpp* loci in *Mycobacterium smegmatis, Mycobacterium abscessus,* and *Mycobacterium avium*. Arrows indicating the transcription orientation of the different genes are drawn to scale. A color code has been used to specify the participation of these genes in synthesis of the lipopeptide core, glycosylation, methylation, acetylation, transport and other biological functions, as indicated. Genes in the *tpp* locus are displayed in pink.

when compared to the S variants from the three different isogenic S/R couples. Moreover, RNA sequencing demonstrated that S and R isogenic strains differed considerably at the transcriptomic level, with the transcriptional extinction of *mps1*, *mps2,* and *gap* in the R strain caused by an insertion in the 5′-end of *mps1* (Pawlik et al., 2013). Additional mutations in *mps2*, *mmpL4a,* and *mmpS4* were subsequently identified in R strains isolated from later disease stages (Park et al., 2015). Disruption of *mmpL4b* in

M. abscessus S was initially reported to abrogate GPL production, leading to a rough colonial morphotype (Medjahed and Reyrat, 2009; Nessar et al., 2011) (**Figure 2A**). Point mutations in MmpL4a at Tyr842 or MmpL4b at Tyr854, corresponding to two critical residues presumably involved in the proton-motive force of the MmpL proteins, were also associated with loss of GPL production (Bernut et al., 2016b) (**Figure 2A**), suggesting that no functional redundancy exists between MmpL4a and MmpL4b.

Hydrophilic and hydrophobic properties of bacteria can influence surface adhesion and biofilm formation (Krasowska and Sigler, 2014). As shown in *M. smegmatis* (Recht and Kolter, 2001), *M. abscessus* (Howard et al., 2006) and *M. bolletii* (Bernut et al., 2016b) the presence of GPL in the S variants facilitates sliding across the surface of motility agar and biofilm formation on the liquid medium/air interface whereas lack of GPL promotes bacterial aggregation (Brambilla et al., 2016) and cording (Howard et al., 2006; Bernut et al., 2014a, 2016b). However, whether *M. abscessus* R fails at producing biofilms was recently readdressed and proposed that it can grow in biofilm-like structures, which, like S biofilms, are significantly more tolerant than planktonic cultures to acidic pH, hydrogen peroxide, and drugs (Clary et al., 2018). In *M. smegmatis,* the nucleoid-associated protein Lsr2 negatively regulates GPL production (Kocíncová et al., 2008) and plays a role during the initial stages of biofilm development (Yang et al., 2017). Despite the presence of an *lsr2* gene in *M. abscessus,* which is up-regulated in the R variant (Pawlik et al., 2013), the contribution of Lsr2 in regulating GPL expression, sliding motility and biofilm formation remains to be established.

External factors, such as sub-inhibitory antibiotic concentrations, can promote a transient S-to-R change with more aggregated cultures and a higher resistance to phagocytosis (Tsai et al., 2015). Strangely, these phenotypes were neither linked to a loss of GPL production nor to the differential expression of genes within the *gpl* cluster, but were rather mediated by *MAB_3508c*, homologous to *whiB7* and conferring extreme resistance to antibiotics in *M. abscessus* (Hurst-Hess et al., 2017). In contrast, another study reported that sub-inhibitory amikacin treatment, also leading to a S-to-R transition, was associated with decreased GPL, resulting from down-regulation of several *gpl* biosynthetic genes (Lee et al., 2017). Overall, these results suggest that exposure to sub-inhibitory amikacin doses may induce alterations in GPL content, increase virulence and influence the outcome of the infection as well as the therapeutic efficacy of drugs.

PRESENCE OR LOSS OF GPL CONDITIONS BACTERIAL SURFACE PROPERTIES AND INTERACTIONS WITH HOST CELLS

The S and R variants interact differently with host cells and exhibit different intracellular behaviors, as first reported in human monocytes with the R variant persisting longer in these cells (Byrd and Lyons, 1999) and then confirmed in other phagocytes (Howard et al., 2006; Roux et al., 2016). Macrophages encountering the aggregative R strain, are incapable of engulfing clumps of R bacteria, which remain embedded in phagocytic cups on the exterior of the cells (Roux et al., 2016). However, smaller clumps are phagocytosed, resulting in social phagosomes (containing numerous bacilli) that rapidly fuse with lysosomes. In addition, R variant-containing THP1 cells were more acidified, more autophagic and more apoptotic than those infected with the S variant. In contrast, in the majority of S variant-containing phagosomes, a continuous tight apposition is maintained between the phagosome membrane and the mycobacterial cell envelope, leading to phagosome maturation blockage and the absence of acidification in S-infected macrophages. Another conspicuous trait of the S-containing phagosomes is the occurrence of a large electron translucent zone (ETZ) enclosing the bacilli (**Figure 2B**). This ETZ is barely detected in R-containing phagosomes or in phagosomes containing S strains mutated in either *mmpL4a* or *mmpL4b*, indicating that the ETZ relies on the presence of cell surface GPL (Bernut et al., 2016b; Roux et al., 2016). Interestingly, infection with *M. abscessus* S, but not R, leads to phagosome membrane lesions, suggesting that, similarly to pathogenic slow-growing mycobacteria, this variant has the capacity to induce phagosome–cytosol communications (Simeone et al., 2012), through a mechanism that likely involves the type VII secretion system ESX-4 (Laencina et al., 2018).

The distinct mechanisms responsible for the S- and R-induced responses in macrophages are being delineated, highlighting a model whereby the loss of GPL at the surface unmasks underlying phosphatidyl-*myo*-inositol dimannoside (PIM_2) (Rhoades et al., 2009) and lipoproteins (Roux et al., 2011). These TLR-2 agonists stimulate the expression of TNF and intense inflammation. Exacerbation of this response can also lead to tissue lesions associated with R strains. In S strains, by covering underlying immunostimulatory cell wall components, GPL may delay the activation of the immune response during early infection stages and facilitate colonization by preventing TLR-2 signaling in the respiratory epithelial cells (Davidson et al., 2011).

Apoptosis represents an innate response of cells to restrict multiplication of intracellular pathogens (Lamkanfi and Dixit, 2010). *M. abscessus* R was found to be more apoptotic than *M. abscessus* S in different types of macrophages (Roux et al., 2016; Whang et al., 2017). Supporting these findings, purified GPL from *M. abscessus* S inhibits macrophage apoptosis, presumably by suppressing the production of radical oxygen species (ROS), the release of cytochrome c and by preserving the mitochondrial transmembrane potential (Whang et al., 2017) (**Figure 2B**). This mechanism appears to be mediated by targeting of acetylated GPL to the mitochondria where they interact with cyclophilin D, a component of the mitochondrial permeability transition pore (MPTP), inhibiting the MPTP that results in a block on cell death in similar fashion to cyclosporin A. That exogenous GPL-dependent apoptosis inhibition restricts intracellular growth and spreading of *M. abscessus* R, suggests also that GPL may limit *M. abscesssus* virulence (Whang et al., 2017).

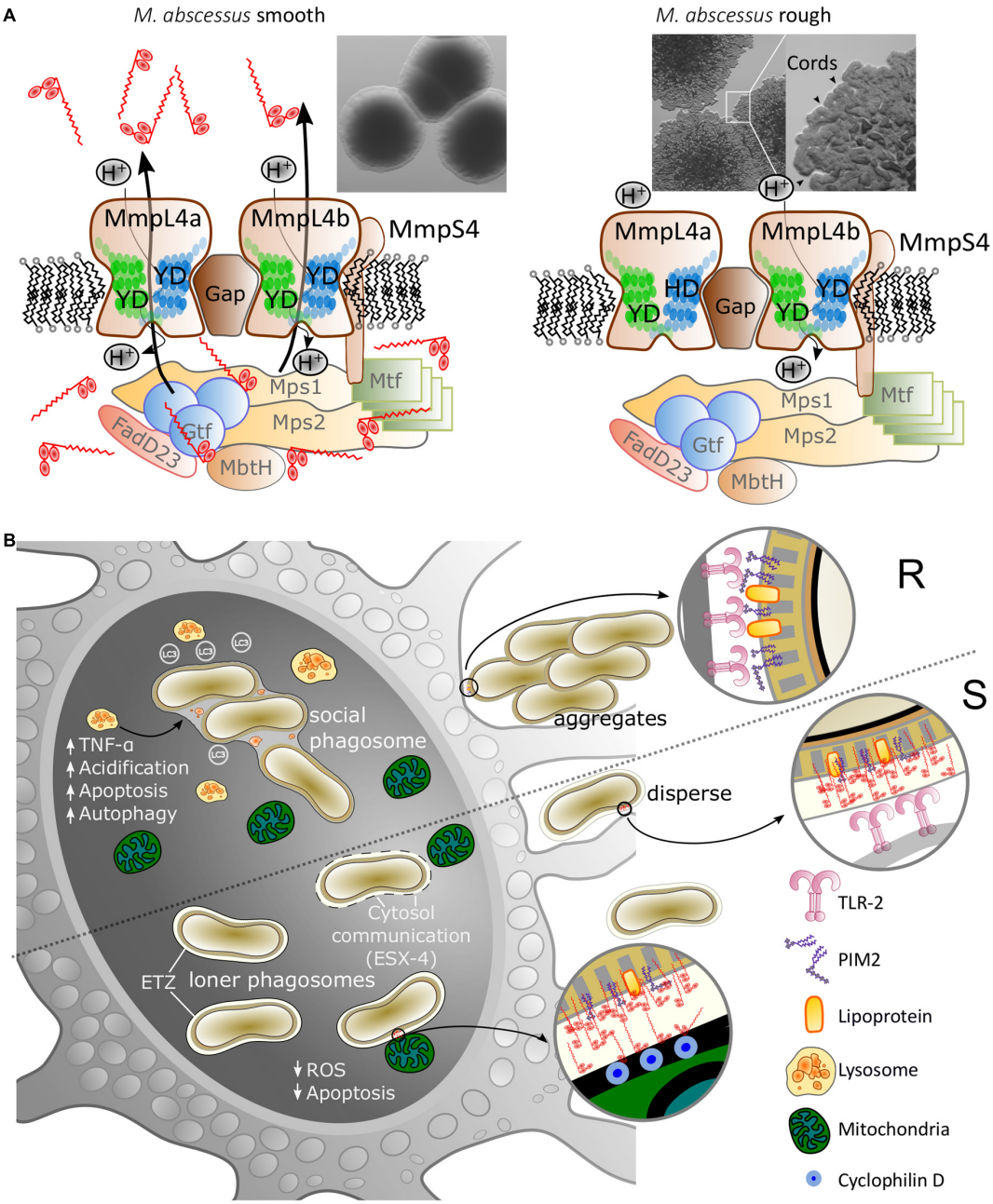

FIGURE 2 | Glycopeptidolipid (GPL) composition influences the colonial morphology and host cell interactions of *M. abscessus*. **(A)** Morphology of the high-GPL producing smooth (S) morphotype (left panel) and low-GPL producing rough (R) morphotype (right panel). The production and transport of GPL requires multiple cytosolic biosynthetic enzymes and transmembrane proteins. Mutations in genes involved in GPL production/transport occurring *in vivo* or introduction of point mutations of crucial Tyr/Asp (Y/D) couples in MmpL4a/MmpL4b participating in the proton relay lead to the arrest of lipid transport and a rough morphotype (right panel). R strains are typified by the production of serpentine cords (inset, arrowheads). **(B)** Inhibition of the macrophage apoptotic response by GPL covering *M. abscessus* S occurs through mitochondrial targeting and interaction with cyclophilin D, reduced production of radical oxygen species (ROS) and limitation of the spread of *M. abscessus* among macrophages. In contrast, the loss of GPL in *M. abscessus* R uncovers immunostimulatory TLR-2 agonists, such as PIM_2 and lipoproteins, leading to an exacerbated pro-inflammatory response that contributes to acute and severe infections.

Collectively, these observations emphasize the diversity of the infection programs orchestrated by S and R variants. While the S variant is promptly phagocytosed by macrophages without immediately affecting cell survival, phagocytosis of the R variant is more harmful to macrophage viability and, following apoptosis, the released bacteria replicate extracellularly in the form of serpentine cords (**Figure 2A**).

IMPACT OF THE GPL CONTENT ON VIRULENCE

Epidemiological surveys document the prominence of the R strain in patients with severe pulmonary infections (Catherinot et al., 2009) and with chronic colonization of the airways in CF patients (Jönsson et al., 2007), but the exact proportions of S and R forms in these populations remain largely unknown. This distinction is, however, of crucial importance considering that the cord-forming R variant causes much more aggressive and invasive pulmonary disease that ends in severe respiratory failure. Further alarm is raised by several studies using various cellular and animal models, confirming the increased virulence of the R over the S form (Bernut et al., 2017). Among these models, the zebrafish (*Danio rerio*) has been proposed as a relevant and genetically tractable host–pathogen conjugate for dissecting *M. abscessus* interactions with host cells (Bernut et al., 2015). This led to important breakthroughs regarding mechanisms of *M. abscessus* pathogenesis, involving cording and granuloma formation (Bernut et al., 2014a) or the importance of the TNF response in controlling the infection and establishment of protective granulomas (Bernut et al., 2016a). S-to-R transitioning is associated with exacerbation of the bacterial burden, the formation of massive serpentine cords, abscess formation, notably in the central nervous system, and increased larval killing (Bernut et al., 2014a). Deletion of *MAB_4780*, encoding a dehydratase required for cording, resulted in extreme attenuation in wild-type and immunocompromized larvae (Halloum et al., 2016), further incriminating cording as a major virulence determinant in strains lacking GPL. Replacing the endogenous *mmpS4-mmpL4a-mmpL4b* promoter with the leaky acetamidase promoter from *M. smegmatis* in *M. abscessus* S resulted in a strain with low-GPL levels, but still aggregating in culture with a rough appearance, similar to R strains. In zebrafish, this mutant exhibited an intermediate virulence phenotype with a delay in killing compared to the R strain. Moreover, the number and size of the abscesses in larvae infected with this low-GPL producing strain were significantly reduced compared to the R strain (Viljoen et al., 2018). This indicates that low-GPL levels impede the induction of the physiopathological signs and virulence of *M. abscessus* R, confirming the opposite relationship between the amount of GPL and virulence. In addition, the S variant is more hydrophilic than the R variant or the rough low-GPL producing strain. This suggests that lack of the hydrophilic GPL components is responsible for their increased hydrophobicity over the S strain and confirm a positive correlation between GPL production and hydrophilicity.

Supporting the theory of transmission *via* aerosols from the environment, *M. abscessus,* along with other NTM, was isolated from household water and shower aerosols in the homes of patients with pulmonary disease (Thomson et al., 2013). Importantly, a direct person-to-person transmission of *M. abscessus* by aerosol inhalation has been asserted in recent world-wide surveys, although the link between morphology/GPL profile and mode of transmission remains to be investigated (Bryant et al., 2013, 2016).

CONCLUSION AND PERSPECTIVES

Fundamental aspects of the *M. abscessus* lifecycle rely on the beneficial effects of GPL in promoting and facilitating the early stages of colonization of the S variant, presumably the major form existing in the environment. By covering the bacilli, the highly immunogenic GPL induce a strong humoral response in infected individuals and it is possible that this strong immune pressure leads to selection of GPL-deficient strains, allowing *M. abscessus* to escape the anti-GPL response and the emergence of R bacilli. The lack of GPL, in turn, leads to increased apoptosis, promoting extracellular replication and cording, acute infection and the most severe forms of the disease. This has also detrimental consequences for the host since, by unmasking other pro-inflammatory cell-surface components, the loss of GPL translates to severe inflammation and lung damage. Therefore, the double edged sword effect of GPL allows *M. abscessus* to efficiently transition between a colonizing environmental micro-organism to an invasive human pathogen. Given the importance of the GPL content in driving the interaction with host cells and in conditioning the issue of the infection, it appears important to pay more attention to the variant (S or R) selected for experimental infections and to systematically report the morphotype of the strains isolated in clinical studies.

Important unsolved questions remain on GPL in *M. abscessus*. Future investigations should describe the complete GPL export machinery since, while transfer of GPL across the plasma membrane has been addressed to some extent, additional unidentified outer-membrane proteins are likely to participate in this important physiological process. So far, the literature only reports the effects of near total loss of GPL in *M. abscessus*, portraying an incomplete picture of the functions of these lipids in the physiology of this pathogen. Polar GPL species in *M. smegmatis* are only produced under carbon starvation and induce smooth-colony formation (Ojha et al., 2002) opening up the possibility that in *M. abscessus* GPL composition is modulated in response to changing environments. Therefore, studies are required to address whether GPL composition affects *M. abscessus* persistence and/or host inflammation, as well as how the dynamics of GPL production, potentially mediated by yet unidentified factors, influences adaptation of *M. abscessus* to its host.

AUTHOR CONTRIBUTIONS

AG designed the figures. All authors contributed to writing the manuscript.

FUNDING

LK acknowledges the support by the Fondation pour la Recherche Médicale (FRM) (DEQ20150331719) and the Infectiopôle Sud Méditerranée for funding the Ph.D. Fellowship of AG.

REFERENCES

Bernut, A., Dupont, C., Sahuquet, A., Herrmann, J.-L., Lutfalla, G., and Kremer, L. (2015). Deciphering and imaging pathogenesis and cording of *Mycobacterium abscessus* in zebrafish embryos. *J. Vis. Exp.* 103:e53130. doi: 10.3791/53130

Bernut, A., Herrmann, J.-L., Kissa, K., Dubremetz, J.-F., Gaillard, J.-L., Lutfalla, G., et al. (2014a). *Mycobacterium abscessus* cording prevents phagocytosis and promotes abscess formation. *Proc. Natl. Acad. Sci. U.S.A.* 111, E943–E952. doi: 10.1073/pnas.1321390111

Bernut, A., Le Moigne, V., Lesne, T., Lutfalla, G., Herrmann, J.-L., and Kremer, L. (2014b). *In vivo* assessment of drug efficacy against *Mycobacterium abscessus* using the embryonic zebrafish test system. *Antimicrob. Agents Chemother.* 58, 4054–4063. doi: 10.1128/AAC.00142-14

Bernut, A., Herrmann, J.-L., Ordway, D., and Kremer, L. (2017). The diverse cellular and animal models to decipher the physiopathological traits of *Mycobacterium abscessus* infection. *Front. Cell. Infect. Microbiol.* 7:100. doi: 10.3389/fcimb.2017.00100

Bernut, A., Nguyen-Chi, M., Halloum, I., Herrmann, J.-L., Lutfalla, G., and Kremer, L. (2016a). *Mycobacterium abscessus*-induced granuloma formation is strictly dependent on TNF signaling and neutrophil trafficking. *PLoS Pathog.* 12:e1005986. doi: 10.1371/journal.ppat.1005986

Bernut, A., Viljoen, A., Dupont, C., Sapriel, G., Blaise, M., Bouchier, C., et al. (2016b). Insights into the smooth-to-rough transitioning in *Mycobacterium bolletii* unravels a functional Tyr residue conserved in all mycobacterial MmpL family members. *Mol. Microbiol.* 99, 866–883. doi: 10.1111/mmi.13283

Besra, G. S., McNeil, M. R., Rivoire, B., Khoo, K. H., Morris, H. R., Dell, A., et al. (1993). Further structural definition of a new family of glycopeptidolipids from *Mycobacterium xenopi*. *Biochemistry* 32, 347–355. doi: 10.1021/bi00052a043

Billman-Jacobe, H., McConville, M. J., Haites, R. E., Kovacevic, S., and Coppel, R. L. (1999). Identification of a peptide synthetase involved in the biosynthesis of glycopeptidolipids of *Mycobacterium smegmatis*. *Mol. Microbiol.* 33, 1244–1253. doi: 10.1046/j.1365-2958.1999.01572.x

Brambilla, C., Llorens-Fons, M., Julián, E., Noguera-Ortega, E., Tomàs-Martínez, C., Pérez-Trujillo, M., et al. (2016). Mycobacteria clumping increase their capacity to damage macrophages. *Front. Microbiol.* 7:1562. doi: 10.3389/fmicb.2016.01562

Brown-Elliott, B. A., Nash, K. A., and Wallace, R. J. (2012). Antimicrobial susceptibility testing, drug resistance mechanisms, and therapy of infections with nontuberculous mycobacteria. *Clin. Microbiol. Rev.* 25, 545–582. doi: 10.1128/CMR.05030-11

Bryant, J. M., Grogono, D. M., Greaves, D., Foweraker, J., Roddick, I., Inns, T., et al. (2013). Whole-genome sequencing to identify transmission of *Mycobacterium abscessus* between patients with cystic fibrosis: a retrospective cohort study. *Lancet* 381, 1551–1560. doi: 10.1016/S0140-6736(13)60632-7

Bryant, J. M., Grogono, D. M., Rodriguez-Rincon, D., Everall, I., Brown, K. P., Moreno, P., et al. (2016). Emergence and spread of a human-transmissible multidrug-resistant nontuberculous mycobacterium. *Science* 354, 751–757. doi: 10.1126/science.aaf8156

Burbaud, S., Laval, F., Lemassu, A., Daffé, M., Guilhot, C., and Chalut, C. (2016). Trehalose polyphleates are produced by a glycolipid biosynthetic pathway conserved across phylogenetically distant mycobacteria. *Cell Chem. Biol.* 23, 278–289. doi: 10.1016/j.chembiol.2015.11.013

Byrd, T. F., and Lyons, C. R. (1999). Preliminary characterization of a *Mycobacterium abscessus* mutant in human and murine models of infection. *Infect. Immun.* 67, 4700–4707.

Catherinot, E., Roux, A.-L., Macheras, E., Hubert, D., Matmar, M., Dannhoffer, L., et al. (2009). Acute respiratory failure involving an R variant of *Mycobacterium abscessus*. *J. Clin. Microbiol.* 47, 271–274. doi: 10.1128/JCM.01478-08

Clary, G., Sasindran, S. J., Nesbitt, N., Mason, L., Cole, S., Azad, A., et al. (2018). *Mycobacterium abscessus* smooth and rough morphotypes form antimicrobial-tolerant biofilm phenotypes but are killed by acetic acid. *Antimicrob. Agents Chemother.* 62, e1782-17. doi: 10.1128/AAC.01782-17

Cortes, M., Singh, A. K., Reyrat, J.-M., Gaillard, J.-L., Nassif, X., and Herrmann, J.-L. (2011). Conditional gene expression in *Mycobacterium abscessus*. *PLoS One* 6:e29306. doi: 10.1371/journal.pone.0029306

Daffé, M., and Draper, P. (1998). The envelope layers of mycobacteria with reference to their pathogenicity. *Adv. Microb. Physiol.* 39, 131–203. doi: 10.1016/S0065-2911(08)60016-8

Davidson, L. B., Nessar, R., Kempaiah, P., Perkins, D. J., and Byrd, T. F. (2011). *Mycobacterium abscessus* glycopeptidolipid prevents respiratory epithelial TLR2 signaling as measured by HβD2 gene expression and IL-8 release. *PLoS One* 6:e29148. doi: 10.1371/journal.pone.0029148

Deshayes, C., Bach, H., Euphrasie, D., Attarian, R., Coureuil, M., Sougakoff, W., et al. (2010). MmpS4 promotes glycopeptidolipids biosynthesis and export in *Mycobacterium smegmatis*. *Mol. Microbiol.* 78, 989–1003. doi: 10.1111/j.1365-2958.2010.07385.x

Dubée, V., Bernut, A., Cortes, M., Lesne, T., Dorchene, D., Lefebvre, A.-L., et al. (2015). β-Lactamase inhibition by avibactam in *Mycobacterium abscessus*. *J. Antimicrob. Chemother.* 70, 1051–1058. doi: 10.1093/jac/dku510

Dupont, C., Viljoen, A., Dubar, F., Blaise, M., Bernut, A., Pawlik, A., et al. (2016). A new piperidinol derivative targeting mycolic acid transport in *Mycobacterium abscessus*. *Mol. Microbiol.* 101, 515–529. doi: 10.1111/mmi.13406

Esther, C. R., Esserman, D. A., Gilligan, P., Kerr, A., and Noone, P. G. (2010). Chronic *Mycobacterium abscessus* infection and lung function decline in cystic fibrosis. *J. Cyst. Fibros.* 9, 117–123. doi: 10.1016/j.jcf.2009.12.001

Gregoire, S. A., Byam, J., and Pavelka, M. S. (2017). *galK*-based suicide vector mediated allelic exchange in *Mycobacterium abscessus*. *Microbiology* 163, 1399–1408. doi: 10.1099/mic.0.000528

Halloum, I., Carrère-Kremer, S., Blaise, M., Viljoen, A., Bernut, A., Le Moigne, V., et al. (2016). Deletion of a dehydratase important for intracellular growth and cording renders rough *Mycobacterium abscessus* avirulent. *Proc. Natl. Acad. Sci. U.S.A.* 113, E4228–E4237. doi: 10.1073/pnas.1605477113

Howard, S. T., Rhoades, E., Recht, J., Pang, X., Alsup, A., Kolter, R., et al. (2006). Spontaneous reversion of *Mycobacterium abscessus* from a smooth to a rough morphotype is associated with reduced expression of glycopeptidolipid and reacquisition of an invasive phenotype. *Microbiology* 152, 1581–1590. doi: 10.1099/mic.0.28625-0

Hurst-Hess, K., Rudra, P., and Ghosh, P. (2017). *Mycobacterium abscessus* WhiB7 regulates a species-specific repertoire of genes to confer extreme antibiotic resistance. *Antimicrob. Agents Chemother.* 61, e1347-17. doi: 10.1128/AAC.01347-17

Jönsson, B. E., Gilljam, M., Lindblad, A., Ridell, M., Wold, A. E., and Welinder-Olsson, C. (2007). Molecular epidemiology of *Mycobacterium abscessus*, with focus on cystic fibrosis. *J. Clin. Microbiol.* 45, 1497–1504. doi: 10.1128/JCM.02592-06

Kocíncová, D., Singh, A. K., Beretti, J.-L., Ren, H., Euphrasie, D., Liu, J., et al. (2008). Spontaneous transposition of IS1096 or ISMsm3 leads to glycopeptidolipid overproduction and affects surface properties in *Mycobacterium smegmatis*. *Tuberculosis* 88, 390–398. doi: 10.1016/j.tube.2008.02.005

Krasowska, A., and Sigler, K. (2014). How microorganisms use hydrophobicity and what does this mean for human needs? *Front. Cell. Infect. Microbiol.* 4:112. doi: 10.3389/fcimb.2014.00112

Laencina, L., Dubois, V., Le Moigne, V., Viljoen, A., Majlessi, L., Pritchard, J., et al. (2018). Identification of genes required for *Mycobacterium abscessus* growth *in vivo* with a prominent role of the ESX-4 locus. *Proc. Natl. Acad. Sci. U.S.A.* 115, E1002–E1011. doi: 10.1073/pnas.1713195115

Lamkanfi, M., and Dixit, V. M. (2010). Manipulation of host cell death pathways during microbial infections. *Cell Host Microbe* 8, 44–54. doi: 10.1016/j.chom.2010.06.007

Lee, S.-Y., Kim, H.-Y., Kim, B.-J., Kim, H., Seok, S.-H., Kim, B.-J., et al. (2017). Effect of amikacin on cell wall glycopeptidolipid synthesis in *Mycobacterium abscessus*. *J. Microbiol.* 55, 640–647. doi: 10.1007/s12275-017-6503-7

Medjahed, H., Gaillard, J.-L., and Reyrat, J.-M. (2010). *Mycobacterium abscessus*: a new player in the mycobacterial field. *Trends Microbiol.* 18, 117–123. doi: 10.1016/j.tim.2009.12.007

Medjahed, H., and Reyrat, J.-M. (2009). Construction of *Mycobacterium abscessus* defined glycopeptidolipid mutants: comparison of genetic tools. *Appl. Environ. Microbiol.* 75, 1331–1338. doi: 10.1128/AEM.01914-08

Nessar, R., Reyrat, J.-M., Davidson, L. B., and Byrd, T. F. (2011). Deletion of the *mmpL4b* gene in the *Mycobacterium abscessus* glycopeptidolipid biosynthetic pathway results in loss of surface colonization capability, but enhanced ability to replicate in human macrophages and stimulate their innate immune response. *Microbiology* 157, 1187–1195. doi: 10.1099/mic.0.046557-0

Obregón-Henao, A., Arnett, K. A., Henao-Tamayo, M., Massoudi, L., Creissen, E., Andries, K., et al. (2015). Susceptibility of *Mycobacterium abscessus* to

antimycobacterial drugs in preclinical models. *Antimicrob. Agents Chemother.* 59, 6904–6912. doi: 10.1128/AAC.00459-15

Ojha, A. K., Varma, S., and Chatterji, D. (2002). Synthesis of an unusual polar glycopeptidolipid in glucose-limited culture of *Mycobacterium smegmatis*. *Microbiology* 148, 3039–3048. doi: 10.1099/00221287-148-10-3039

Ordway, D., Henao-Tamayo, M., Smith, E., Shanley, C., Harton, M., Troudt, J., et al. (2008). Animal model of *Mycobacterium abscessus* lung infection. *J. Leukoc. Biol.* 83, 1502–1511. doi: 10.1189/jlb.1007696

Park, I. K., Hsu, A. P., Tettelin, H., Shallom, S. J., Drake, S. K., Ding, L., et al. (2015). Clonal diversification and changes in lipid traits and colony morphology in *Mycobacterium abscessus* clinical isolates. *J. Clin. Microbiol.* 53, 3438–3447. doi: 10.1128/JCM.02015-15

Pawlik, A., Garnier, G., Orgeur, M., Tong, P., Lohan, A., Le Chevalier, F., et al. (2013). Identification and characterization of the genetic changes responsible for the characteristic smooth-to-rough morphotype alterations of clinically persistent *Mycobacterium abscessus*. *Mol. Microbiol.* 90, 612–629. doi: 10.1111/mmi.12387

Recht, J., and Kolter, R. (2001). Glycopeptidolipid acetylation affects sliding motility and biofilm formation in *Mycobacterium smegmatis*. *J. Bacteriol.* 183, 5718–5724. doi: 10.1128/JB.183.19.5718-5724.2001

Rhoades, E. R., Archambault, A. S., Greendyke, R., Hsu, F.-F., Streeter, C., and Byrd, T. F. (2009). *Mycobacterium abscessus* glycopeptidolipids mask underlying cell wall phosphatidyl-myo-inositol mannosides blocking induction of human macrophage TNF-α by preventing interaction with TLR2. *J. Immunol.* 183, 1997–2007. doi: 10.4049/jimmunol.0802181

Ripoll, F., Deshayes, C., Pasek, S., Laval, F., Beretti, J.-L., Biet, F., et al. (2007). Genomics of glycopeptidolipid biosynthesis in *Mycobacterium abscessus* and *M. chelonae*. *BMC Genomics* 8:114. doi: 10.1186/1471-2164-8-114

Roux, A.-L., Ray, A., Pawlik, A., Medjahed, H., Etienne, G., Rottman, M., et al. (2011). Overexpression of proinflammatory TLR-2-signalling lipoproteins in hypervirulent mycobacterial variants. *Cell. Microbiol.* 13, 692–704. doi: 10.1111/j.1462-5822.2010.01565.x

Roux, A.-L., Viljoen, A., Bah, A., Simeone, R., Bernut, A., Laencina, L., et al. (2016). The distinct fate of smooth and rough *Mycobacterium abscessus* variants inside macrophages. *Open Biol.* 6:160185. doi: 10.1098/rsob.160185

Schorey, J. S., and Sweet, L. (2008). The mycobacterial glycopeptidolipids: structure, function, and their role in pathogenesis. *Glycobiology* 18, 832–841. doi: 10.1093/glycob/cwn076

Sermet-Gaudelus, I., Le Bourgeois, M., Pierre-Audigier, C., Offredo, C., Guillemot, D., Halley, S., et al. (2003). *Mycobacterium abscessus* and children with cystic fibrosis. *Emerg. Infect. Dis.* 9, 1587–1591. doi: 10.3201/eid0912.020774

Simeone, R., Bobard, A., Lippmann, J., Bitter, W., Majlessi, L., Brosch, R., et al. (2012). Phagosomal rupture by *Mycobacterium tuberculosis* results in toxicity and host cell death. *PLoS Pathog.* 8:e1002507. doi: 10.1371/journal.ppat.1002507

Sondén, B., Kocíncová, D., Deshayes, C., Euphrasie, D., Rhayat, L., Laval, F., et al. (2005). Gap, a mycobacterial specific integral membrane protein, is required for glycolipid transport to the cell surface. *Mol. Microbiol.* 58, 426–440. doi: 10.1111/j.1365-2958.2005.04847.x

Thomson, R., Tolson, C., Carter, R., Coulter, C., Huygens, F., and Hargreaves, M. (2013). Isolation of nontuberculous mycobacteria (NTM) from household water and shower aerosols in patients with pulmonary disease caused by NTM. *J. Clin. Microbiol.* 51, 3006–3011. doi: 10.1128/JCM.00899-13

Tomashefski, J. F., Stern, R. C., Demko, C. A., and Doershuk, C. F. (1996). Nontuberculous mycobacteria in cystic fibrosis. An autopsy study. *Am. J. Respir. Crit. Care Med.* 154, 523–528. doi: 10.1164/ajrccm.154.2.8756832

Tsai, S.-H., Lai, H.-C., and Hu, S.-T. (2015). Subinhibitory doses of aminoglycoside antibiotics induce changes in the phenotype of *Mycobacterium abscessus*. *Antimicrob. Agents Chemother.* 59, 6161–6169. doi: 10.1128/AAC.01132-15

Viljoen, A., Gutiérrez, A. V., Dupont, C., Ghigo, E., and Kremer, L. (2018). A simple and rapid gene disruption strategy in *Mycobacterium abscessus*: on the design and application of glycopeptidolipid mutants. *Front. Cell. Infect. Microbiol.* 8:69. doi: 10.3389/fcimb.2018.00069

Villeneuve, C., Etienne, G., Abadie, V., Montrozier, H., Bordier, C., Laval, F., et al. (2003). Surface-exposed glycopeptidolipids of *Mycobacterium smegmatis* specifically inhibit the phagocytosis of mycobacteria by human macrophages. Identification of a novel family of glycopeptidolipids. *J. Biol. Chem.* 278, 51291–51300. doi: 10.1074/jbc.M306554200

Whang, J., Back, Y. W., Lee, K.-I., Fujiwara, N., Paik, S., Choi, C. H., et al. (2017). *Mycobacterium abscessus* glycopeptidolipids inhibit macrophage apoptosis and bacterial spreading by targeting mitochondrial cyclophilin D. *Cell Death Dis.* 8:e3012. doi: 10.1038/cddis.2017.420

Yang, Y., Thomas, J., Li, Y., Vilchèze, C., Derbyshire, K. M., Jacobs, W. R., et al. (2017). Defining a temporal order of genetic requirements for development of mycobacterial biofilms. *Mol. Microbiol.* 105, 794–809. doi: 10.1111/mmi.13734

Conflict of Interest Statement: The authors declare that the research was conducted in the absence of any commercial or financial relationships that could be construed as a potential conflict of interest.

frontiers in Microbiology

ORIGINAL RESEARCH
published: 01 June 2018
doi: 10.3389/fmicb.2018.01072

Mycobacterium abscessus subsp. *massiliense mycma_0076* and *mycma_0077* Genes Code for Ferritins That Are Modulated by Iron Concentration

*Fábio M. Oliveira[1], Adeliane C. Da Costa[1], Victor O. Procopio[1], Wanius Garcia[2], Juscemácia N. Araújo[2], Roosevelt A. Da Silva[3], Ana Paula Junqueira-Kipnis[1] and André Kipnis[1]**

[1] Tropical Institute of Pathology and Public Health, Department of Microbiology, Immunology, Parasitology and Pathology, Federal University of Goiás, Goiânia, Brazil, [2] Centro de Ciências Naturais e Humanas, Federal University of ABC (UFABC), Santo André, Brazil, [3] Collaborative Center of Biosystems, Regional Jataí, Federal University of Goiás, Goiânia, Brazil

OPEN ACCESS

Edited by:
Thomas Dick,
Rutgers, The State University of New Jersey, Newark, United States

Reviewed by:
Divakar Sharma,
Aligarh Muslim University, India
Zeeshan Fatima,
Amity University, India

***Correspondence:**
André Kipnis
andre.kipnis@gmail.com

Specialty section:
This article was submitted to Antimicrobials, Resistance and Chemotherapy, a section of the journal Frontiers in Microbiology

Received: 27 February 2018
Accepted: 04 May 2018
Published: 01 June 2018

Citation:
Oliveira FM, Da Costa AC, Procopio VO, Garcia W, Araújo JN, Da Silva RA, Junqueira-Kipnis AP and Kipnis A (2018) Mycobacterium abscessus subsp. massiliense mycma_0076 and mycma_0077 Genes Code for Ferritins That Are Modulated by Iron Concentration. Front. Microbiol. 9:1072. doi: 10.3389/fmicb.2018.01072

Mycobacterium abscessus complex has been characterized in the last decade as part of a cluster of mycobacteria that evolved from an opportunistic to true human pathogen; however, the factors responsible for pathogenicity are still undefined. It appears that the success of mycobacterial infection is intrinsically related with the capacity of the bacteria to regulate intracellular iron levels, mostly using iron storage proteins. This study evaluated two potential *M. abscessus* subsp. *massiliense* genes involved in iron storage. Unlike other opportunist or pathogenic mycobacteria studied, *M. abscessus* complex has two genes similar to ferritins from *M. tuberculosis* (Rv3841), and in *M. abscessus* subsp. *massiliense,* those genes are annotated as *mycma_0076* and *mycma_0077*. Molecular dynamic analysis of the predicted expressed proteins showed that they have a ferroxidase center. The expressions of *mycma_0076* and *mycma_0077* genes were modulated by the iron levels in both *in vitro* cultures as well as infected macrophages. Structural studies using size-exclusion chromatography, circular dichroism spectroscopy and dynamic light scattering showed that r0076 protein has a structure similar to those observed in the ferritin family. The r0076 forms oligomers in solution most likely composed of 24 subunits. Functional studies with recombinant proteins, obtained from heterologous expression of *mycma_0076* and *mycma_0077* genes in *Escherichia coli*, showed that both proteins were capable of oxidizing Fe^{2+} into Fe^{3+}, demonstrating that these proteins have a functional ferroxidase center. In conclusion, two ferritins proteins were shown, for the first time, to be involved in iron storage in *M. abscessus* subsp. *massiliense* and their expressions were modulated by the iron levels.

Keywords: rapid growing mycobacteria, iron storage protein, pathogenic, ferritin, ferroxidase center, iron homeostasis

INTRODUCTION

The *Mycobacterium abscessus* complex, composed of *M. abscessus* subsp. *abscessus*, *M. abscessus* subsp. *massiliense,* and *M. abscessus* subsp. *bolletii* has emerged as human pathogens in the last few years (Petrini, 2006; Medjahed et al., 2010; Lee et al., 2015; Tortoli et al., 2016). Mycobacteria belonging to this complex cause several diseases in humans. These include severe lung, skin, post-traumatic, and post-surgical infections, especially in patients that have cystic fibrosis as well as in immunocompetent individuals (Medjahed et al., 2010). Due to its capacity to adapt and persist in the environment as well as to resist disinfection procedures, the infections caused by the *M. abscessus* group are usually due to cross contamination, through surgical equipment or other contaminated procedures (Cardoso et al., 2008). The transmission of *M. abscessus* has been already documented among cystic fibrosis individuals. Therefore, infections in humans can occur by both direct and indirect transmission (Bryant et al., 2013; Lee et al., 2015; Bryant et al., 2016).

Its capacity to infect and multiply within phagocytic cells indicates that *M. abscessus* can evade the defense mechanisms imposed by the host, resulting in successful infection (Martins de Sousa et al., 2010; Shang et al., 2011; Bernut et al., 2014; Abdalla et al., 2015a; Bakala et al., 2015; Caverly et al., 2015). One mechanism used by this bacillus to multiply within macrophages is the induction of Heme-Oxygenase-1 (HO-1), which reduces the toxic oxidative stress effects produced by the cell (Abdalla et al., 2015a). Part of the HO-1 action is accomplished by the reduction of free ferrous ion Fe^{2+} inside macrophages through the storage of this metal by ferritins, thus preventing the formation of free radicals by the Fenton reaction (Imlay et al., 1988; Vile and Tyrrell, 1993). Hence, mechanisms of extracellular iron level regulation are crucial for the bacilli to survive within macrophages. However, studies have shown that the intracellular levels of iron are also important for bacilli to establish infection, because both absence and excess of iron are deleterious (De Voss et al., 2000; Pandey and Rodriguez, 2012). Consequently, in order to survive within macrophages, the bacilli must be able to obtain, store, and regulate the iron levels during entire infection (Gold et al., 2001; Pandey and Rodriguez, 2014; Pandey et al., 2014).

The main protein family involved in regulating intracellular iron levels and reducing its toxic effects are the ferritins. The proteins within this family may be divided into three sub-classes: ferritin (non-heme binding), bacterioferritin (heme bound) and Dps (DNA-binding protein from starved cells) (Andrews et al., 2003). Bacterial ferritins and bacterioferritins have similar structures, and they are composed of 24 identical subunits arranged in an octahedral form, with a ferroxidase catalytic site at its center. At this catalytic site, Fe^{2+} is oxidized to Fe^{3+} and stored within its hollow interior, where it can store up to 4,500 atoms of this metal ion (Andrews, 1998; Bou-Abdallah, 2010). Consequently, iron is stored in its non-reactive form (Fe^{3+}), avoiding its toxic effects on the cell, and can be released when needed (Andrews, 1998).

Despite similar structure between baterial ferritins and bacterioferritins, their amino acid sequences present low identity and bacterioferritins have a heme group suggesting different origins for these proteins (Andrews, 1998; Carrondo, 2003). *M. tuberculosis* (Mtb) has two types of ferritin-like molecules, bacterioferritin (BfrA) and ferritin (BfrB), coded by the genes Rv1876 and Rv3841, respectively (Cole et al., 1998). Crystallographic studies showed that these proteins are organized similar to the ferritin superfamily, which is an oligomer in the form of a shell with a catalytic center of ferroxidase (Gupta et al., 2009; Khare et al., 2011). Studies using Mtb mutants, which had their *bfrA* and *bfrB* genes deleted solely or together, demonstrated the importance of both in iron homeostasis, as well as in the virulence and pathogenicity of this bacillus in different infection models (Pandey and Rodriguez, 2012, 2014; Reddy et al., 2012; Khare et al., 2017).

In addition, ferritins appear to be involved in drug resistance of Mtb, because it was shown that the lack of ferritin in this bacillus increased the susceptibility to antimicrobials used to treat tuberculosis (Pandey and Rodriguez, 2012). Proteomic analysis indicated that both BfrA and BfrB were overexpressed in aminoglycosides resistant as compared to sensitive clinical isolates of Mtb (Kumar et al., 2013; Sharma et al., 2015). Additionally, overexpression of Rv3841 (*bfrB*) by recombinant *Escherichia coli* resulted in increased kanamycin and amikacin resistance (Sharma et al., 2016). Taken together, BfrA and BfrB proteins, could be promising drug targets against mycobacteria infection.

Recent studies with drugs that act in the iron metabolism of *M. abscessus* confirm that this metal is crucial for the development of this bacillus (Abdalla et al., 2015b). However, the genes and proteins involved in the iron homeostasis and their importance for establishing infection remain unclear. The present study demonstrates for the first time that *M. abscessus* subsp. *massiliense* has two ferritin (non-heme binding) proteins involved in iron storage and related in the iron homeostasis both *in vitro* and in infected macrophages.

MATERIALS AND METHODS

M. abscessus subsp. *massiliense* GO06 Genome Annotation

The complete genome sequences of *M. abscessus* subsp. *massiliense* GO06 (Mycma GO06, taxid: 1198627) and the pathogen reference strain of *M. tuberculosis* H37Rv (taxid: 83332) used in this study were obtained from NCBI[1]. The BLAST tool from NCBI[2] was used for genome and proteome annotations of the Mycma GO06 strain as well as other mycobacteria species genomes.

Bacterial Strains and Growth Conditions

Escherichia coli XL1-Blue and BL21 (DE3) pLysS were used for cloning and expression of the recombinant proteins, respectively. *E. coli* strains were cultured in Luria Bertani (LB) broth (Himedia) and *M. abscessus* subsp. *massiliense*

[1]http://www.ncbi.nlm.nih.gov/genome/

[2]http://blast.ncbi.nlm.nih.gov/Blast.cgi

(Cardoso et al., 2008) was cultured in Mueller Hinton broth or agar at 37°C under 180 rpm shaking. For growth in different iron concentrations, the minimal medium contained 3.6 mM of KH_2PO_4, 2.0 mM of $MgSO_4$ $7H_2O$, 6% (v/v) of glycerol, 30 mM of L-asparagine, 0.006 mM of $ZnSO_4$, and 0.05% (v/v) of Tween 80, pH 6.8 in iron free conditions. For low iron conditions, media was supplemented with 1.25 mM of deferoxamine mesylate (DFO). In high iron conditions, media was supplemented with 50, 150, 300, or 450 μM of $FeCl_3$. Minimal media without supplementation (iron or DFO) contains enough iron concentration to sustain *M. abscessus* subsp. *massiliense* growth, and thus this condition was used as normalizer. *E. coli* transformants were selected in medium supplemented with the antibiotics kanamycin (KAN) and chloramphenicol (CAM) at 20 μg/ml.

Homology Models

The predicted 0076 and 0077 amino acid sequences were initially submitted to I-TASSER (Zhang, 2008) and an initial model was obtained for each sequence. I-TASSER strategy starts from the structure templates identified by LOMETS (Wu and Zhang, 2007) in the PDB library. I-TASSER only uses the templates of the highest significance in the threading alignments, which are measured by the *Z*-score. The *C*-score for each model was verified to evaluate the quality of the predictions from I-TASSER. *C*-score values are related to the expected TM-score (Zhang and Skolnick, 2004, 2005) between the model and native structure (structural similarity of two proteins).

Molecular Dynamics Simulations

To explore the stability and conformational variability of the initial models in its native environment, molecular dynamics (MD) simulations were performed with Gromacs 5.1.3 (Berendsen et al., 1995; Yu, 2012) using force field AMBER99SB-ILDN (Yildirim et al., 2010). The proteins were solvated with a box cubic wall distance of 10 Å using water model TIP3P (Mahoney and Jorgensen, 2000). The system was neutralized by adding the required number of counter ions according of each protein. The system was initially minimized using the steepest descent energy. The simulations were complete when the tolerance no longer exceeded 1000 kJ/mol. In the next three steps consisted of 50 picoseconds MD simulations in NVT and NPT ensemble at 300 K with a restraint of 50 kcal/mol/Å on the protein atoms and 0.5 ns without restraint in NPT ensemble at 300 K. Finally, the simulations were performed for 100 ns for all proteins with a constant temperature of 300 K, 1 atm pressure, time-set of 2 fs, and without any restriction of protein conformations. All information concerning the trajectory of these times were collected every 50 ps. The equilibration of the trajectory was evaluated by monitoring the equilibration of quantities, such as the root-mean-square deviation (RMSD) (Coutsias et al., 2004) of the non-hydrogen atoms, total energy, potential energy, and kinetic energy. The conformations that best represented the structures of the entire trajectory were selected following the algorithm described by Daura et al. (1999). A cutoff of 0.2 nm for the clusters was used considering the profile of the RMSD observed for each protein. The clusters were determined using the non-hydrogen atom RMSD values. The quality of the predicted structure was assessed using the MolProbity server (Chen et al., 2010).

Gene Expression Evaluation of *M. abscessus* subsp. *massiliense*

Mycobacterium abscessus subsp. *massiliense* cultures grown in minimal media with different iron concentrations were harvested by centrifugation at 3,200 × *g* for 10 min. The pellet was suspended with 1 ml of nuclease-free water (Ambio Life Technologies) and 0.25 ml of glass beads (0.1 mm in diameter, Glass Glass Disruptor Beads; USA Scientific, Inc.) was added. The suspension was maintained in ice and vortexed five times for 2 min with 30 s intervals. The Lysate was centrifuged at 12,000 × *g* for 10 min at 4°C, and the aqueous phase was transferred to a new tube for addition of 215 μl of ethanol (J.T. Baker) for each 400 μl of recovered solution. The solution was then applied to an RNA purification column (Phenol-Free Total RNA Purification, Amresco) for purification according manufacture's instructions. The obtained RNA was treated with RNAse free DNAse (Sigma-Aldrich) and stored at −80°C until further use.

The Reverse Transcriptase M-MLV kit (Sigma-Aldrich) was used for cDNA synthesis. The reaction consisted of 200 ηg of total RNA, 0.5 mM of dNTPS and 0.63 μM of random hexamer primers (Gibco/Thermo Fisher Scientific) and was incubated for 5 min at 65°C. Next, the system was transferred to ice and reverse transcriptase buffer, 200 U of M-MLV reverse transcriptase, and 40 U of RNAse OUT (Invitrogen) were added. The reaction was incubated at 37°C for 1.5 h. Then the synthesized cDNA was stored at −20°C until its use for Real Time PCR (RT-PCR). RT-PCR was set up in a 0.2 ml tube, using 10 μl of SYBR Green mix (Bio-Rad), 0.5 μM of each primer (**Supplementary Table S2**) and 5 μl of cDNA in a final volume of 20 μl. The reaction was run on a IQ5 thermocycler (Bio-Rad). RT-PCR conditions were as follows: 95°C (5 min), 40 cycles of 95°C (15 s), 58°C (30 s), and 72°C (1 min), and at the end a melting temperature curve ranging from 70 to 99°C (ramp rate of 0.5°C per cycle and 30 s in each temperature) was performed and the detected fluorescence emission recorded. Positive samples were considered when the fluorescence surpassed the threshold baseline. The cycle of threshold crossing corresponded to the Ct value. Ct values greater than 35 were considered negative. Ct values were tabulated on an Excel 2011 spreadsheet, and the relative expression was determined with the Delta Delta Ct ($2^{-\Delta\Delta Ct}$) method using the expression of the *16s* rRNA gene as normalizer. The calibrator condition in this study was bacteria grown in minimal media without DFO and $FeCl_3$, as these conditions contain sufficient iron levels to support mycobacteria growth. The relative gene expression levels were analyzed on GraphPad Prism 7 (version Prism 7a, Graph Pad) for statistical analysis and graphic representations.

Infection of Bone Marrow-Derived Macrophages (BMDM)

To evaluate the *ex vivo* gene expression of *M. abscessus* subsp. *massiliense,* bone marrow from C57BL/6 mice were collected

(Becker et al., 2012) and submitted to differentiation as previously described da Costa et al. (2017). BMDM (1×10^6/ml) were infected with *M. abscessus* subsp. *massiliense* at a MOI of 10 in a 24 well plate with or without coverslip. Three hours after infection, extracellular bacteria were removed by washing the wells twice with RPMI with 10 μg/ml of kanamycin and then adding RPMI media supplemented with 10% fetal bovine serum (FBS). The CFU determination and expression profile of the genes *mycma_0076* and *mycma_0077* during infection was assessed by recovering the bacilli at three different times: 3, 24, 48, and 72 h post infection and additionally the wells with coverslip 24 and 72 h were randomly selected to stained with Instant-Prov (NewPRQV) according to the manufactured instruction's. At these times, the wells were randomly selected and from them the supernatant was removed and substituted with nuclease free water (Ambion) to lyse macrophages. The lysate was transferred to 1.5 ml nuclease free tubes, centrifuged at 16,000 × *g* for 10 min at 4°C and the pellet was processed for RNA extraction. The relative gene expression was determined by the delta delta Ct ($2^{-\Delta\Delta Ct}$) method using the expression of the *16s* rRNA gene as normalizer. The bacilli, obtained from culture supernatant after 3 h of macrophage infection, was used as calibrator.

Cloning and Expression of *mycma_0076* and *mycma_0077* Genes

The *mycma_0076* and *mycma_0077* genes were amplified by PCR using *M. abscessus* subsp. *massiliense* GO06 (Raiol et al., 2012) genomic DNA as template. The primers were designed using NCBI Primer designing tool[3]. The following primers were used to amplify the *mycma_0076* gene include: forward 5′ CATATGACCGCGACCGACACCCCGA 3′ that incorporates an *Nde*I restriction site (underlined) and reverse 5′ GGATCCTCTTGTTGACGTGCTTAGAGCG 3′ that incorporates a *Bam*HI restriction site (underlined). Similarly, the primers for the *mycma_0077* gene amplification were: forward 5′ CATATGGTGGCTACCACCGATCTCCATG 3′ and reverse 5′ CTCGAGCGCAAAATTATCAGAGCGCGC 3′ that incorporate an *Nde*I and an *Xho*I restriction sites, respectively. The PCR products of each gene were cloned into pET28a (Novagen) vector using their respective flanking sites. Recombinant plasmids were confirmed by sequencing. Recombinant protein expression was performed by transforming the recombinant plasmids into *E. coli* BL21 (DE3) pLysS cells.

Recombinant Protein Purification

Escherichia coli BL21 (DE3) pLysS containing the recombinant plasmids were grown in LB containing kanamycin (20 μg/ml) and chloramphenicol (20 μg/ml) until $OD_{550\ nm}$ reached 0.5. Then the culture was induced with 1 mM of isopropyl-1-thio-β-D-galactopyranoside (IPTG) at 37°C, 180 rpm for 4 h. Cells were then harvested by centrifugation at 4,000 × *g* for 20 min at 4°C. The pellet was used for protein extraction using the commercial protein purification QIAexpress-Ni_NTA Fast Start kit (Qiagen) according to the manufacturer's instructions. Proteins eluted from the nickel column were further purified on a gel filtration Superdex 200 10/300 GL chromatographic column (GE Healthcare). The column was previously equilibrated with 50 mM NaH_2PO_4 buffer adjusted at pH 8.0 containing 300 mM NaCl (pH 8.0) buffer. The column was calibrated with molecular weight standards (GE Healthcare), and chromatography was performed at a 1 ml/min rate with 5 MPa pressure and detection at 280 nm on an AKTA purifier system (GE Healthcare). Eight microliters from each collected fraction were analyzed on 12% SDS-PAGE. Protein concentration was determined by using Bradford's reagent with bovine serum albumin as the standard.

[3]http://www.ncbi.nlm.nih.gov/tools/primer-blast

Mouse Anti-r0076 Antibody Production

Three C57BL/6 mice were immunized by the subcutaneous route with purified r0076 protein. In the first immunization, a formulation consisting of 50 μg of r0076 protein and 50% (v/v) of complete Freund adjuvant was administered. Fourteen days later the same amount of protein was used mixed with incomplete Freund adjuvant. The third immunization was performed 14 days after the second with the same formulation as the second. Ten days after the last immunization, total blood was collected and incubated for 30 min at room temperature. The blood was centrifuged at 3,000 × *g* for 10 min and the sera was aliquoted in 50 μl volumes and stored at −20°C until their use. The antiserum was titrated and used in western blotting experiments.

Culture Filtrate Proteins (CFP) and Cell Lysate Obtention

Mycobacteria cultures at logarithmic growth were harvested at 6,000 × *g* for 10 min. The supernatant and pellet were processed for CFP and cell lysate preparations, respectively. The supernatant was filtered through a 0.22 μm filter and then concentrated by centrifugation using a 10 kDa (Amicon) centricon filter at 7,000 × *g* for 30 min at 4°C. Glycerol was added to the obtained CFP to a final concentration of 20% and CFP was stored at −20°C until use. The culture pellet was resuspended in PBS buffer and sonicated in an ice bath twice for 1 min to obtain cell lysate. The cell lysate was adjusted to 20% glycerol and stored at −20°C.

Western Blotting

After electrophoresis of the proteins by PAGE, under denaturing or non-denaturing conditions, the separated proteins were electrotransferred to a nitrocellulose membrane. The membrane was blocked with an incubation of 2 h with PBS containing 5% skimmed milk at room temperature. Then the membranes were incubated overnight at 4°C with the mouse serum against r0076 diluted 1:500 in PBS containing 2% skimmed milk. The membrane was then washed three times with PBS buffer and incubated with 4 μg of secondary anti-Mouse-F (ab') 2-xx-biotin (Molecular Probes) for 2 h at 37°C. Then, horse anti-mouse antibody conjugated with avidin-peroxidase (Sigma-Aldrich) was added and incubated for 1 h. The reaction was developed by adding 0.05% diaminobenzidine (DAB, Roche) in 10 ml of H_2O_2. The image was acquired with the help of Gel documentation system (Bio-Rad) and analyzed with Quantity One 4.5.6 software (Bio-Rad).

Circular Dichroism (CD) Spectroscopy

Circular dichroism spectrum was collected using a Jasco-815 spectropolarimeter equipped with a temperature control device. The r0076 concentration was 5 μM in 50 mM NaH_2PO_4 buffer adjusted at pH 8.0 containing 50 mM NaCl. All data were collected using 1 mm quartz cuvette. The spectrum was recorded over the wavelength range from 195 to 260 nm. A total of eight accumulations were averaged to form the CD spectrum, using a scanning speed of 100 nm/min, a spectral bandwidth of 1 nm, and a response time of 0.5 s. The buffer contribution was subtracted in each experiment. Thermal denaturation of r0076 at pH 8.0 was characterized by measuring the ellipticity changes at 222 nm induced by a temperature increase from 20 to 90°C. The fraction of denatured protein (α) was calculated from the relationship: $\alpha = (\theta_n - \theta_{obs})/(\theta_n - \theta_d)$ and $\alpha + \beta = 1$, in which θ_{obs} is the ellipticity obtained at a particular temperature, and θ_d and θ_n are the values of the ellipticity characteristic of the denatured and native states, respectively.

Dynamic Light Scattering (DLS)

The size of r0076 was examined by means of the Nano-ZS dynamic light scattering system (Malvern Instruments Ltd., Malvern, United Kingdom). This system employs a $\lambda = 633$ nm laser and a fixed scattering angle of 173°. The r0076 solution (1 mg/ml), in buffer 50 mM NaH_2PO_4 buffer adjusted at pH 8.0 containing 50 mM NaCl, was centrifuged at 16,000 × *g* for 10 min at room temperature, and subsequently loaded into a quartz cuvette prior to measurement. The temperature was raised from 20 to 90°C and the sample was allowed to equilibrate for 2 min in each temperature prior to DLS measurements. The hydrodynamic radius (R_H) was determined from a second-order cumulant fit to the intensity auto-correlation function (size distribution by volume). The determined R_H was converted to molecular mass (kDa) based on the assumption of a spherical particle and using the Zetasizer software.

Iron Oxidation Assays

Oxidation reactions were performed according to Khare et al. (2011) using a fresh solution of 0.1 M of HEPES, pH 6.5 containing 125 μM of ammonium ferrous sulfate. The recombinant protein was added to the buffer containing ferrous sulfate for a final concentration of 0.25 μM, and the optical density was monitored at 310 nm for 18 min at 37°C. At this wavelength, the Fe^{3+} is detected, and consequently, the amount of oxidation can be monitored. To determine the amount of oxidized iron, additional replicate reactions were performed, but ferrozine iron reagent was also added to the reaction. Ferrozine makes a complex with free ferrous iron in solution, resulting in a violet color solution that can be detected at 570 nm. Ferrozine was added at 3-min intervals to individual wells and the 570 nm was recorded. A ferrous iron concentration curve was generated by adding ferrozine to different Fe^{2+} concentrations and recording the optical density (O.D.) at 570 nm. The experimental readings were converted to concentration based on the generated curve. The concentration at time zero was considered 100%, and the remaining concentrations were transformed in percentages relative to time zero. In all oxidation reactions, the 50 mM NaH_2PO_4 buffer adjusted to pH 8.0 containing 50 mM NaCl was used as negative control.

Ethical Committee

The study was approved by the Ethics Committee for Animal use (CEUA: Comite de Ética no uso de animais; #229/11) of the Universidade Federal de Goiás (UFG), Goiânia, Brazil.

Statistical Analysis

Comparison between means was assayed for variance (ANOVA) and non-paired *t*-test using Prism software version 6.0c (GraphPad). Values of $p < 0.05$ were considered statistically significant.

RESULTS

Mycobacteria Belonging to the *Mycobacterium abscessus* Complex Have Two Genes Possibly Coding for Ferritin Proteins

To identify possible genes coding for bacterioferritin and ferritin in the *M. abscessus* subsp. *massiliense* genome, a BLAST using the genes *bfrA* (Rv1876) and *bfrB* (Rv3841) from *M. tuberculosis* H37Rv performed against *M. abscessus* genomes and *M. abscessus* subsp. *massiliense* did not present any gene with significant similarity to the Rv1876 gene (**Supplementary Table S1**). However, *M. abscessus* subsp. *massiliense* has two genes with similarities higher than 70% to the Rv3841 gene (**Table 1**). Both *mycma_0076* and *mycma_0077* genes (**Figure 1A**) are located in tandem in the genome. Similar results were seen for other *M. abscessus* subspecies and other non-tuberculosis mycobacteria (NTM). A phylogenetic tree with the bacterioferritin and ferritin protein sequences from different mycobacteria species was constructed (**Figure 1B**). This shows that mycobacteria species closest to the group of *M. abscessus* may have two ferritins, while *M. tuberculosis* and other mycobacteria have one of both ferritin and bacterioferritin proteins. Thus, *M. abscessus* subsp. *massiliense* and other closely related genetic mycobacterial species do not have genes that are similar to the bacterioferritin gene *bfrA* (Rv1876) from *M. tuberculosis,* which suggests for the first time that mycobacteria from the *M. abscessus* complex and their closely related species have two genes possibly coding for ferritin.

Molecular Dynamics Evaluation of 0076 and 0077 Proteins Demonstrate a Ferritin Like Protein

To correlate the genes *mycma_0076* and *mycma_0077* with ferritin, their hypothetic structures were modeled and analyzed by molecular dynamics (MD). Initial models of 0076 and 0077 proteins were built from I-Tasser server using as

principal templates (PDB files) 3qd8A (Crystal structure of *M. tuberculosis* BfrB), 1vlgA (Crystal structure of Ferritin from *Thermotoga maritima*), 3unoA (*M. tuberculosis* ferritin homolog, BfrB), and 1z6oA (Crystal Structure of *Trichoplusia ni* secreted ferritin). The information from each template compared to 0076 and 0077 proteins are shown in (**Table 2**). The best model (model 1) for 0076 and 0077 structures had a *C*-score of 1.13 and 0.92, respectively. These values provide an estimate for TM-score above 0.84 and an RMSD below 3.5 Å for both models. These predicted values indicate that the models determined by ITASSER have a great chance of representing the expected native structures for the 0076 and 0077 proteins.

The MD simulations from theses initial models were performed to achieve stability and/or improve the structure quality of them. In **Figure 2**, the RMSD evolution from initial models is shown for 0076 and 0077. For both proteins, after 60 ns, a transient stability could be verified for them. Just one simulation from 0077 protein had high fluctuations after 60 ns, which is mainly associated to moves from the residues located at the N and C-terminal (**Figure 2**).

From the trajectory of each simulation, cluster analysis of the conformations with a cutoff of 2 Å helped identify multiple conformations that could represent their flexibility. We selected only the center structure of the cluster most common during the simulations to represent each protein. **Figure 3** shows the clusters obtained for structures over time. For 0076 simulations (**Figure 3A**), cluster number one (most frequent structure) appeared only after about 60 ns, which remained stable until the end of the simulations. The same feature was observed for 0077 simulations (**Figure 3B**). In MD1 simulation of 0077 protein, the number of clusters observed between 60 ns and 80 ns fell from 70 to less than 20 (**Figure 3B**). Outside this interval, more intense structural fluctuations occur around N terminal region. The quality of the selected structures was measured by molprobity score, which indicates a better quality for the structure when its value tends to zero. **Table 3** shows that the quality of the models (model 1) had comparable molprobity scores from high-resolution structures. The highest value was 1.65 for 0077 (DM2) model, which is still a very common value in high resolution structures. The structural alignment of the likely active site of the *Helicobacter pylori* ferritin structure (PDB id 3bvi – chain C) and proteins 0076 and 0077 is shown in **Figure 4**.

Evaluation of *mycma_0076* and *mycma_0077* Genes Expression

Bacteria require a mechanism for iron storage for efficient homeostasis of this ion and to avoid the deleterious effects of iron excess (Pandey and Rodriguez, 2012; Reddy et al., 2012). *M. abscessus* subsp. *massiliense* growth did not alter in different iron concentrations, ranging from minimal concentrations to excess conditions, such as 450 μM $FeCl_3$ (**Figure 5A**). However, when iron was completely removed from the media, the mycobacteria growth was seriously compromised (**Figure 5A**). Thus, *M. abscessus* subsp. *massiliense* has mechanisms for iron homeostasis that allows this bacterium to grow in conditions of iron overload.

As *mycma_0076* and *mycma_0077* genes possibly correspond to ferritin genes, their expression was evaluated during *M. abscessus* subsp. *massiliense* growth in different iron concentrations. Surprisingly, the *mycma_0076* gene had its expression up regulated 50 times in high iron concentrations, while *mycma_0077* gene was not induced under those conditions (**Figure 5B**). Thus, only *mycma_0076* gene seemed to have a positive correlation between iron levels and expression (**Figure 5B**).

The Expression of *mycma_0076* and *mycma_0077* Genes Is Modulated During Macrophage Infection

In order to understand if the differential expression observed *in vitro* was also used by *M. abscessus* subsp. *massiliense* to overcome the infection, the expression of *mycma_0076* and *mycma_0077* genes were evaluated during macrophage infection.

TABLE 1 | BLAST results from similarity search for *Mycobacterium tuberculosis* H37Rv Rv3841 gene.

Strain	Gene	Query cover	Identity	Location in genome
M. abscessus subsp. *massiliense* GO 06	*mycma_0076*	86%	71%	4557641 – 4558110
	mycma_0077	83%	70%	4556946 – 4557395
M. abscessus subsp. *abscessus*	A3O03_00650	86%	71%	129762 – 130307
	A3O03_00655	83%	70%	130479 – 131036
M. abscessus subsp. *bolletii*	MMASJCM_0130	86%	70%	127112 – 127581
	MMASJCM_0131	83%	69%	127827 – 128276
M. chelonae	BB28_00635	86%	70%	124938 – 125483
	BB28_00640	79%	70%	125655 – 126212
M. immunogenum	BAB75_00915	86%	69%	184826 – 185371
	BAB75_00920	89%	69%	185543 – 186100
M. fortuitum	XA26_58160	95%	76%	5966689 – 5967212
M. smegmatis mc^2 155	LJ00_31750	95%	76%	6492666 – 6493211
M. bovis	LH58_20775	100%	99%	4272259 – 4272804

Alignments were performed with Basic Local Alignment Search Tool (BLAST) program at http://blast.ncbi.nlm.nih.gov, using the nucleotide BLAST algorithm.

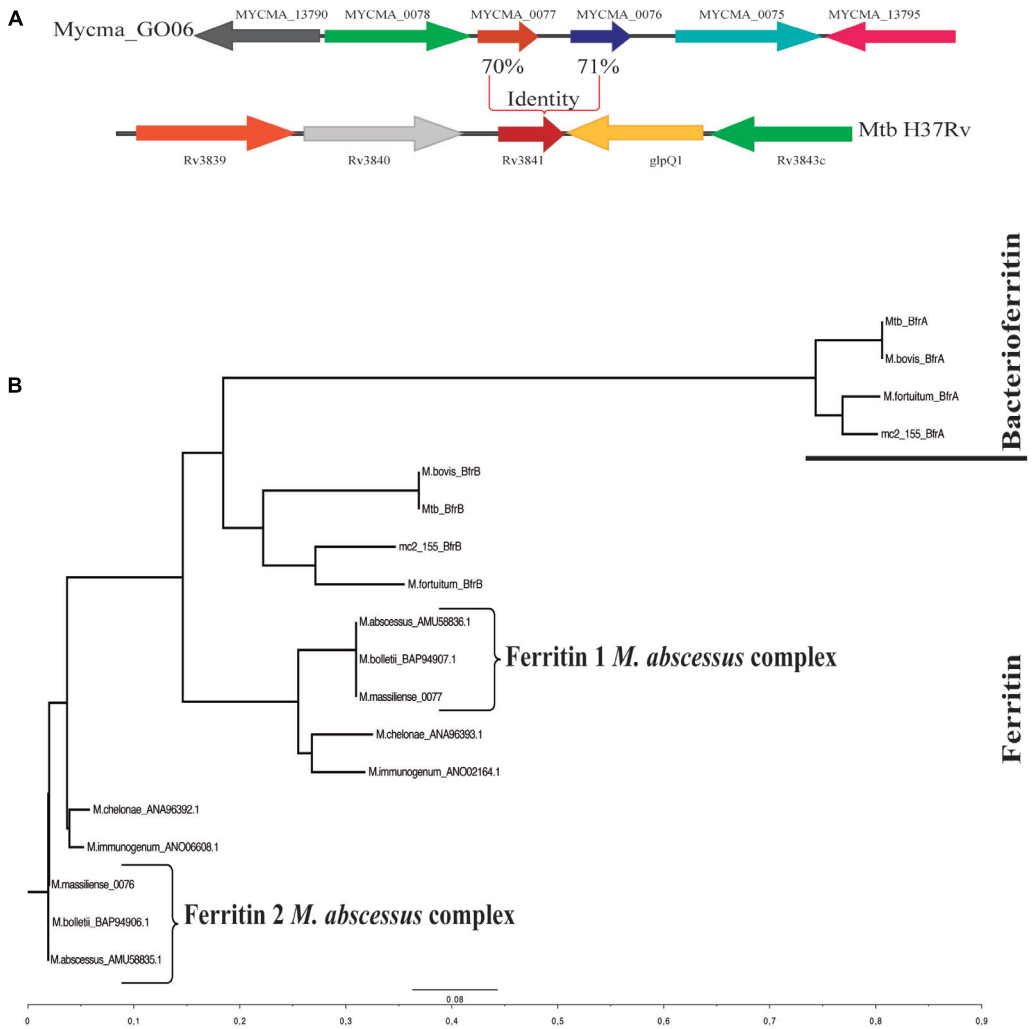

FIGURE 1 | Genomic organization of the *Mycobacterium abscessus* subsp. *massiliense* genes *mycma_0076* and *mycma_0077* and phylogenetic tree obtained from alignments of ferritin and bacterioferritin protein sequences. **(A)** Genomic organization of the *M. abscessus* subsp. *massiliense* genes similar to *M. tuberculosis* H37Rv Rv3841. **(B)** Phylogenetic tree constructed from ferritin (BfrB) and bacterioferritin (BfrA) mycobacterial protein sequences performed on ClustalX. The protein sequences were obtained from NCBI BLAST searches for proteins with similarity to ferritin and bacterioferritin from *M. tuberculosis* H37Rv.

TABLE 2 | Accuracy of models and threading templates information.

Proteins Mycma	Accuracy of the model 1			Identity* (coverage#) from threading templates			
	C-score	TM-score (estimated)	RMSD (estimated)	3qd8A	1vlgA	3unoA	1z6oA
0076	1.13	0.87 ± 0.07	2.9 ± 2.1 Å	0.63 (0.95)	0.26 (0.91)	0.64 (0.96)	0.20 (0.93)
0077	0.92	0.84 ± 0.08	3.4 ± 2.3 Å	0.58 (0.93)	0.22 (0.89)	0.58 (0.93)	0.20 (0.92)

**Identity is the percentage sequence identity of the whole template chains with query sequence.* # *Coverage represents the coverage of the threading alignment and is equal to the number of aligned residues divided by the length of query protein.*

In contrast to the *in vitro* observations, expression of both genes was induced during macrophage infection, but these genes were differently modulated (**Figures 6A,B**). While the expression of *mycma_0076* gene was reduced 3 h after macrophage infection (**Figure 6A**), the *mycma_0077* had its expression up regulated 80 times (**Figure 6B**). At 24 h of infection both genes had similar levels of expression, however, after 48 h the expression of gene *mycma_0076* was reduced again, while the expression of *mycma_0077* remained highly expressed (**Figures 6A,B**). After 72 h of infection, both genes were expressed at lower levels compared to 48 h (**Figures 6A,B**). These results suggested that the expression of *mycma_0076* and *mycma_0077* genes could be related to the establishment of infection, but their possible role in this process is not redundant. Moreover, it was observed

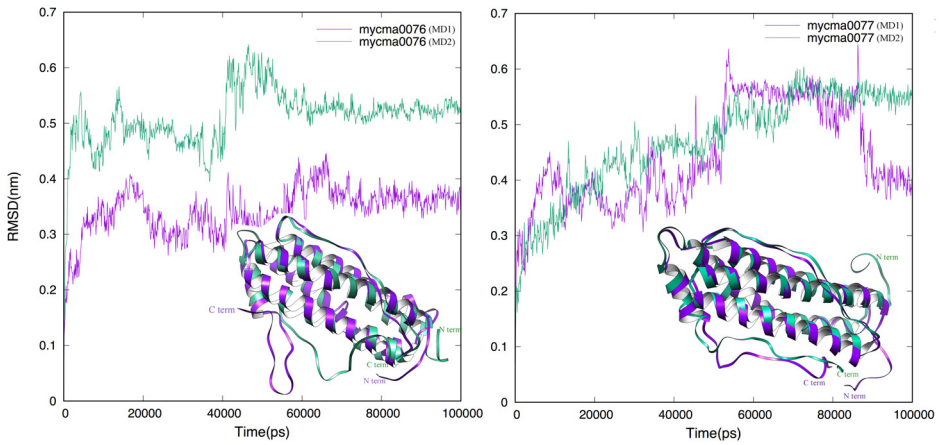

FIGURE 2 | Root-mean-square deviation (RMSD) dynamic profiles obtained for the MD simulations of 0076 and 0077 protein structures over 100 ns. The MD1 (purple) and MD2 (green) are superimposed in the ribbon mode in insert figure.

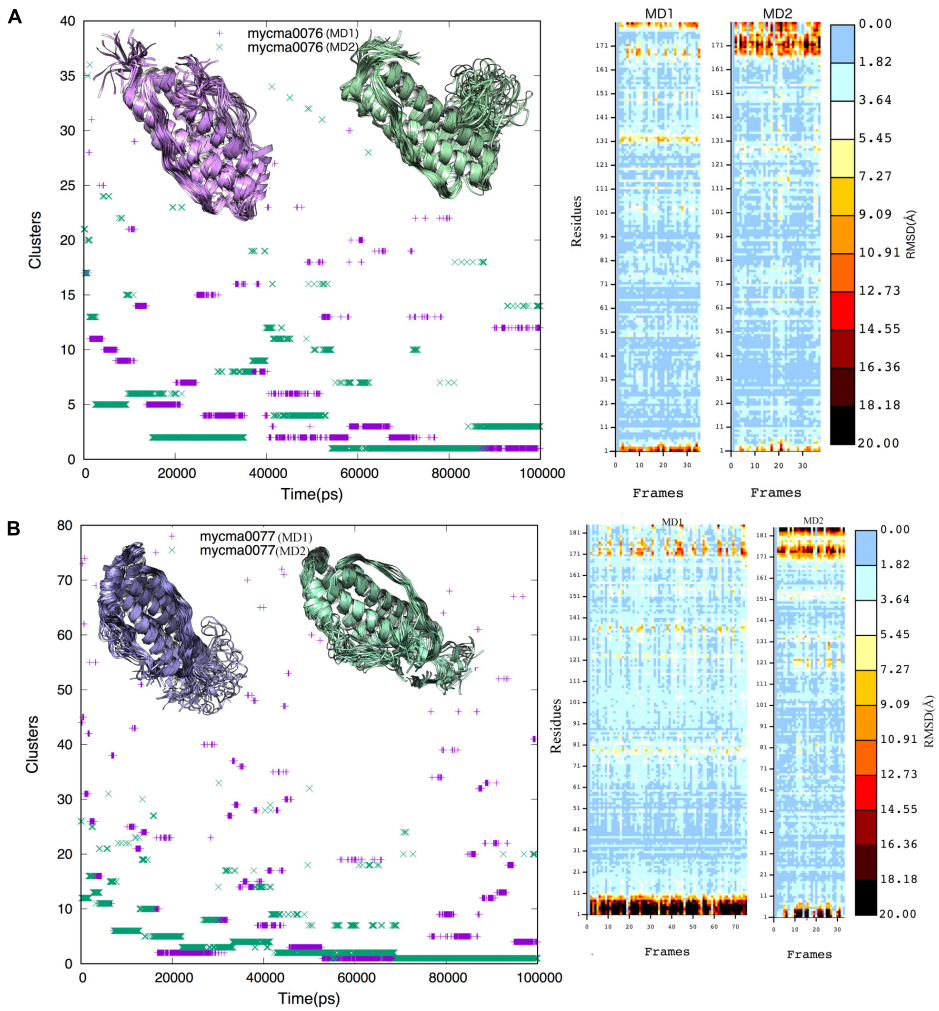

FIGURE 3 | Cluster analysis of the 0076 **(A)** and 0077 **(B)** protein trajectories obtained over 100 ns. A cutoff of 0.2 nm was selected to include the main structures during the simulations. The cluster structures were determined using the non-hydrogen-atom RMSD values. Insert figures represent the cluster structures from MD1 (purple) and MD2 (green) independent simulations.

TABLE 3 | Molprobity score and ferritin active site key residues for proteins 0076 and 0077.

Proteins	Clashscore[$]	MolProbity score* (&)	% secondary structures			Key residues to ferritin active site
			Helix	Sheet	Others	
0076 (MD1)	0.0 (100th)	1.33 (98th)	65.20	0	34.8	GLU22, GLU55, HIS58, GLU99, GLN132, GLU135
0076 (MD2)	0.36 (99th)	1.11 (100th)	61.30	2.2	36.5	
0077 (MD1)	1.06 (99th)	1.46 (96th)	61.60	0	38.4	GLU25, GLU58, HIS61, GLU102, GLN135, GLU138
0077 (MD2)	2.47 (99th)	1.65 (91st)	58.40	0	41.6	
3bvi_C	1.43 (100th)	0.96 (100th)	71.70	0	28.3	GLU17, GLU50, HIS53, GLU94, GLN 127, GLU130

[$]*Clashscore measured from molprobity program.* **Molprobity scores after molecular dynamics simulations.* [&]*Percent scores observed in high resolution structures.*

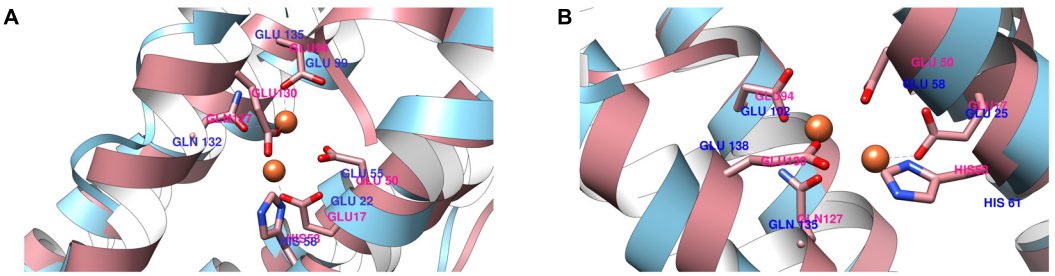

FIGURE 4 | Structural alignment of the ferritin active site (pink) between 0076 **(A)** and 0077 **(B)** proteins against *Helicobacter pylori* ferritin.

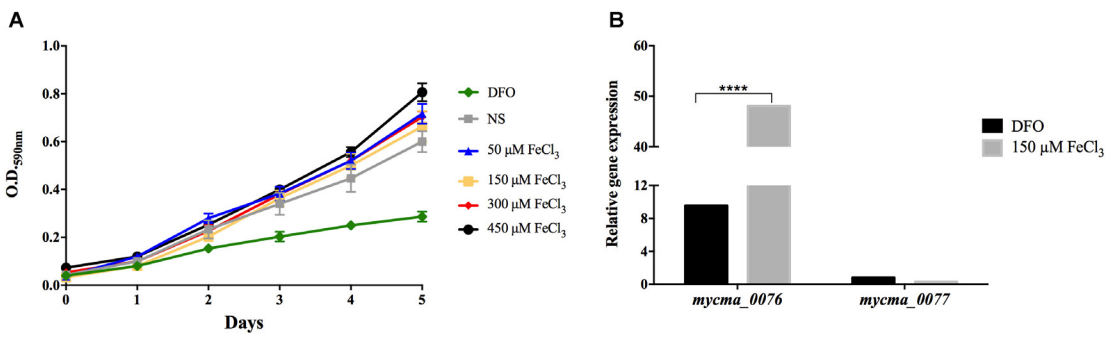

FIGURE 5 | *Mycobacterium abscessus* subsp. *massiliense* growth **(A)** and relative gene expression of the genes *mycma_0076* and *mycma_0077* **(B)** in different iron concentrations. *M. abscessus* subsp. *massiliense* was grown in minimal media containing different iron concentrations at 37°C under agitation for 5 days. During this period, the growth was monitored by OD 590 nm readings. After incubation, total RNA was extracted and the expression of *mycma_0076* and *mycma_0077* was analyzed by quantitative RT-PCR with SYBR green under high (150 μM $FeCl_3$) and low (DFO) iron conditions. The relative gene expression was determined by the Delta Delta Ct ($2^{-\Delta\Delta Ct}$) method using the expression of the *16s* rRNA gene as normalizer and the growth under non-supplemented (NS) condition as calibrator. ****$p < 0.0001$ indicate statistically significant difference between groups.

that expression of *mycma_0076* and *mycma_0077* increased accompanied by the growth of bacilli inside of macrophages (24 h) (**Figures 6A–C**). However, the bacterial number within macrophage culture reduced after 72 h (**Figure 6C**), as did the expression both genes were (**Figures 6A,B**). It is of important notice that the observed decrease in intracellular bacteria was accompanied by increase in extracellular bacilli (**Figure 6D**) and macrophage death (data not shown). These data suggest that the expression of both genes are important for bacilli growth inside of macrophages, differently to extracellular growth as in RPMI when the *mycma_0076* gene was predominantly expressed (**Figures 6A,B**).

Protein 0076 Cytolocalization in *M. abscessus* subsp. *massiliense*

Both *mycma_0076* and *mycma_0077* genes from *M. abscessus* subsp. *massiliense* were separately cloned in pET28a(+) plasmid, expressed in *E. coli* and the recombinant proteins were purified (**Figures 7A** and **Supplementary Figure S2**). While recombinant 0076 (r0076) protein was easily obtained in its soluble form, r0077 had very low solubility and yield. Consequently, some experiments for ferritin characterization was performed only for r0076. The protein 0076 was detected by specific polyclonal antibodies only in the cellular fraction of *M. abscessus* subsp. *massiliense* (**Figure 7B**).

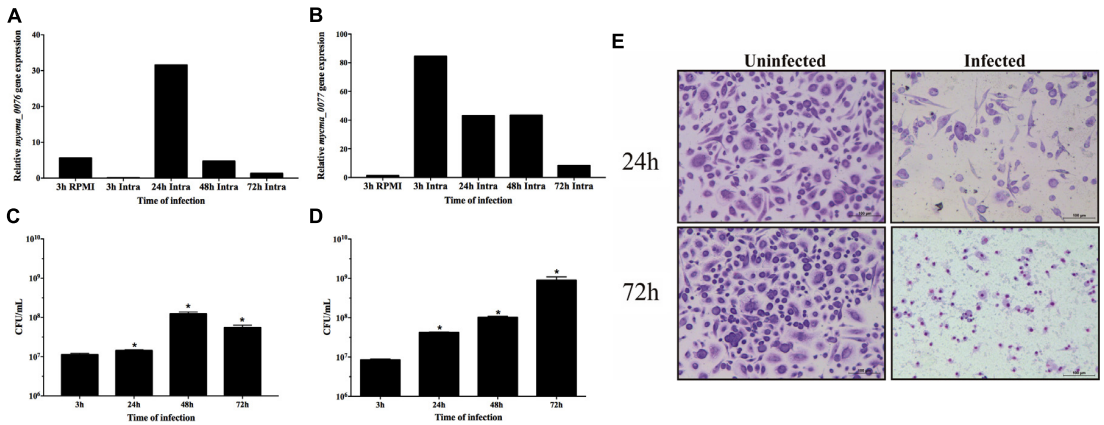

FIGURE 6 | Relative gene expression of *mycma_0076* **(A)** and *mycma_0077* **(B)** genes and growth of *M. abscessus* subsp. *massiliense* during infection of BMDM. **(A,B)** Macrophages were infected at a multiplicity of infection of 1:10 with *M. abscessus* subsp. *massiliense,* and total RNA was extracted at 3, 24, 48, and 72 h after infection. Expression of *mycma_0076* and *mycma_0077* was analyzed by quantitative RT-PCR with SYBR green. The relative gene expression was determined by the delta delta Ct ($2^{-\Delta\Delta Ct}$) method using the expression of the *16s* rRNA gene as normalizer and the bacilli obtained from supernatant of macrophage infection after 3 h as calibrator. **(C)** After 3, 24, 48, and 72 h of macrophage infection the macrophages were washed, lysed with water and plated on MH agar for CFU determination. **(D)** After 3, 24, 48, and 72 h of macrophage infection, the supernatant was collected for CFU quantification of extracellular bacilli. **p*-value < 0.05 indicate statistically significant difference between groups as compared with 3 h post infection. **(E)** After 24 and 72 h of incubation, uninfected and infected cells were stained and analyzed by light microscopy (Leica Application Suite v.4.4.0) to observe cell damage.

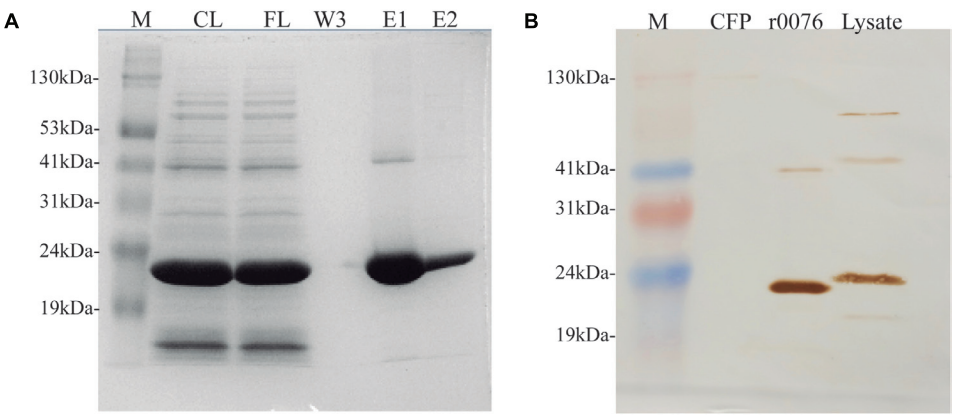

FIGURE 7 | *Mycobacterium abscessus* subsp. *massiliense* recombinant protein r0076 expression, purification, and localization. **(A)** SDS-PAGE analysis of different purification fractions of r0076. M, prism protein marker (Amresco); CL, cell lysate; FL, flow-through fraction; W, third wash fraction; E1 and E2, elution fractions. **(B)** *M. abscessus* subsp. *massiliense* grown for 5 days in MH at 37°C was harvested and its supernatant culture filtrate (CFP) and cell pellet (Lysate) where analyzed on a western blotting using polyclonal antibodies raised against r0076. The purified recombinant protein was used as control (r0076). M, prism protein marker (Amresco); CFP, culture filtrate protein.

Recombinant 0076 Protein Complex Formation

The results presented above support the function of the protein 0076 as a ferritin. Several studies have shown that ferritin proteins require the formation of an oligomeric structure to perform iron oxidation and storage (Levi et al., 1988; Khare et al., 2011, 2013). We could show that this was the case for r0076 by performing western blotting of the protein under native polyacrylamide gel conditions. As shown in **Figure 8A**, r0076 forms a high molecular mass protein. Upon gel filtration analysis, r0076 elutes as single peak of apparent molecular mass of 480 kDa (**Figure 8B**) similar to ferritins.

Recombinant Ferritin From *M. abscessus* subsp. *massiliense* (r0076) Forms Stable Oligomers in Solution

Circular dichroism spectroscopy was used to analyze the secondary structure of the r0076 in solution at pH 8.0 (**Figure 9A**). The CD spectrum of r0076 is characterized by two minima at 210 ± 1 nm and 222 ± 1 nm, a maximum near 200 ± 1 nm, and a negative to positive crossover at 201 ± 1 nm. The negative minimum was around 210 and 222 nm, which strongly indicate the presence of α helices, comparable to the secondary structure of other ferritins (Khare et al., 2011, 2013). As a next step, the quaternary structure of r0076 was analyzed in

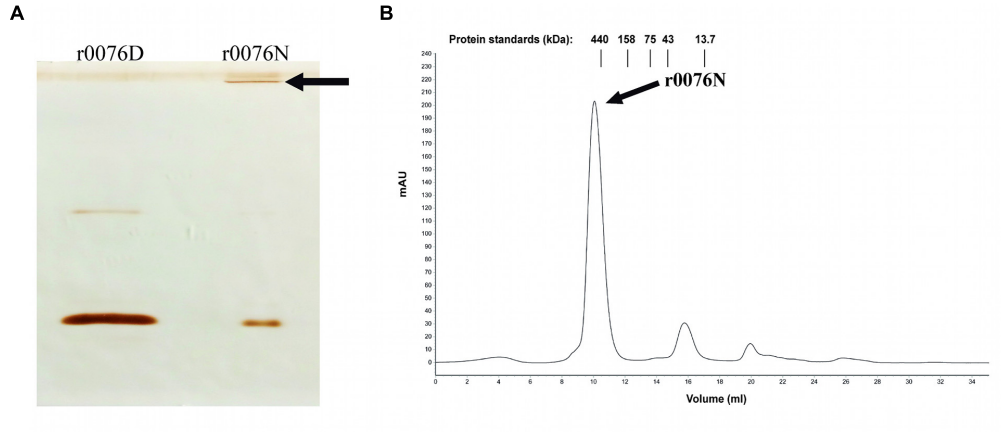

FIGURE 8 | Recombinant protein r0076 forms a high molecular mass complex. **(A)** Western blotting of non-denaturing gel using polyclonal antibodies against r0076. The r0076 protein was boiled in denaturing buffer (r0076D) or only resuspended in non-denaturing buffer (r0076N). **(B)** Gel filtration chromatographic profile of native r0076 elution on a Superdex 200 10/300 GL column.

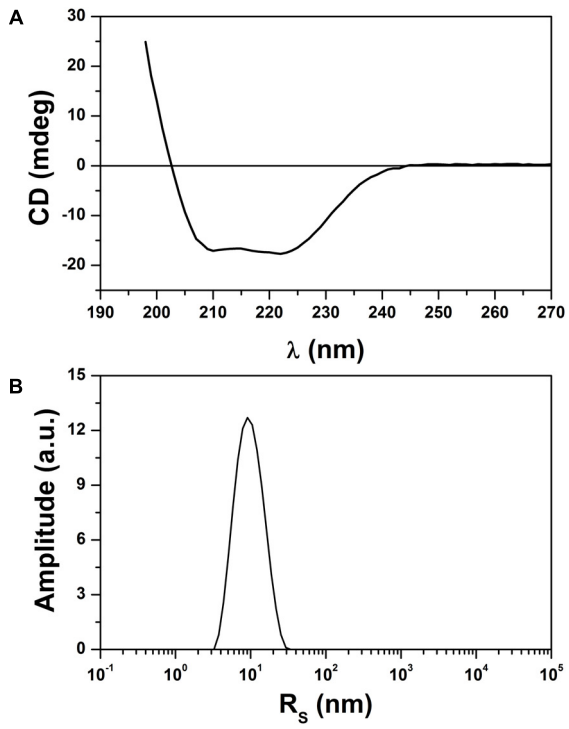

FIGURE 9 | Analysis of secondary and quaternary structures. **(A)** Circular dichroism (CD) spectrum of the recombinant 0076 at pH 8. **(B)** Size distribution by intensity for recombinant 0076 where DLS runs were conducted at pH 8.

solution at pH 8.0 by dynamic light scattering (DLS). When r0076 was analyzed by DLS the observed profile was characteristic of a monodisperse solution (**Figure 9B**). The value of hydrodynamic radius (R_H) determined for r0076 was 8.0 ± 0.5 nm, certainly corresponding to an oligomeric form of the protein in solution. This result is consistent with the size-exclusion chromatography profile obtained for r0076 (**Figure 8B**).

Influence of Temperature on r0076 Stability and Compactness

The thermostability of the r0076 at pH 8.0 was monitored following changes in the ellipticity at 222 nm (**Figure 10A**). The spectrum remained constant at temperatures below 55°C. However, the spectrum was progressively altered when the temperature was increased above 55°C, which indicates loss of the regular secondary structure. The melting temperature (T_m), value determined by CD spectroscopy for r0076, was 57 ± 1°C (**Figure 10A**). The structural alteration observed by CD spectroscopy was accompanied by DLS analyses. **Figure 10B** shows the variation of R_H as a function of temperature for r0076 at pH 8.0. The R_H of r0076 exhibited minimal temperature dependence between the ranges of 20 to 55°C. However, when r0076 was incubated at temperature values above 55°C, the R_H increased significantly, suggesting the formation of aggregates as a consequence of the denaturation process. The thermal denaturation process was essentially irreversible in the conditions described in this study (data not shown).

Recombinant r0076 and r0077 Proteins Promote Oxidation of Fe^{2+} Into Fe^{3+}

The capacity of the recombinant proteins to promote the oxidation of ferrous iron was evaluated by incubating them with Fe^{2+} and observing the increase in optical density at 310 nm. Both r0076 and r0077 proteins were capable to oxidize ferrous iron (**Figure 11A**), but the activity of r0076 was much greater than r0077. The r0076 protein oxidized 25% of the available Fe^{2+} (**Figure 11B**) after 3 min, while r0077 protein oxidized only 16% during the same time (**Figure 11B**). After 18 min, the r0076 protein oxidized more than 80% of the available Fe^{2+} while, r0077 oxidized 55%. These results demonstrate that both

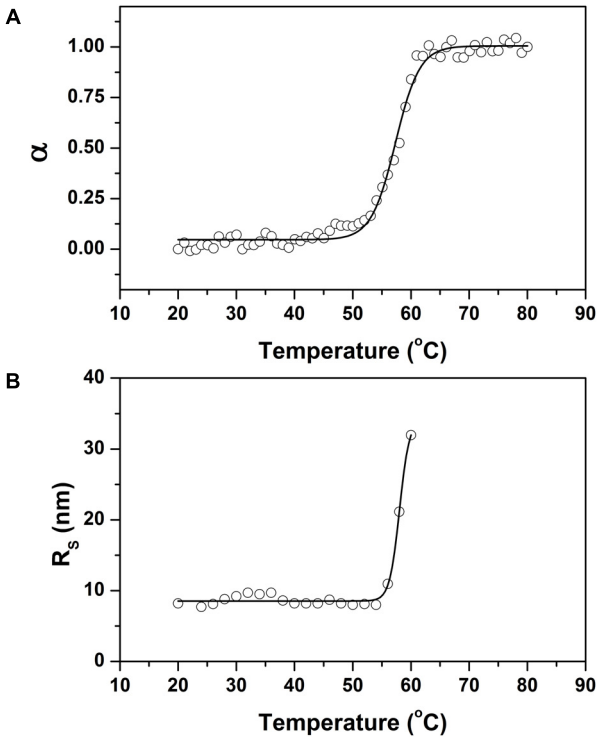

FIGURE 10 | Thermal stability of recombinant 0076. **(A)** Thermal denaturation of recombinant 0076 at pH 8 was monitored by measuring the ellipticity at 222 nm as a function of temperature. **(B)** The hydrodynamic radius (R_H) of r0076 at pH 8 as a function of temperature.

r0076 and r0077 proteins are capable of oxidizing Fe^{2+} into Fe^{3+}, evidencing their activities as ferritins.

DISCUSSION

In the last decades, the *M. abscessus* complex has emerged as a human pathogen (Petrini, 2006; Medjahed et al., 2010). Its ability to infect and persist inside phagocytic cells and in the extracellular environment indicates that this bacterium has evolved to adapt and establish infection in humans (Bernut et al., 2014; Helguera-Repetto et al., 2014; Brambilla et al., 2016). In this study, we showed that *M. abscessus* subsp. *massiliense* has two ferritins similar to the Mtb ferritin that might be important for intracellular iron homeostasis, which in turn is crucial for successful infection.

It has been shown that *E. coli* and *Haemophilus influenza* have more than one gene coding for ferritin, while *M. tuberculosis* and *M. smegmatis* have only one (Andrews, 1998; Bou-Abdallah et al., 2014). Here, we showed for the first time that bacteria from the *M. abscessus* complex have two genes coding for ferritins and none for bacterioferritin (**Figure 1**, **Table 1**, and **Supplementary Table S1**). It was observed that the proteins-coded by *mycma_0076* and *mycma_0077* genes do not have the methionine (Met) residue at position 52 as observed in bacterioferritin from *M. tuberculosis* (data not shown). The absence of Met-52 may render these proteins unable to bind heme (Gupta et al., 2009; Yasmin et al., 2011) as shown in Met-52 *M. tuberculosis* mutants (Gupta et al., 2009; Khare et al., 2017). Absence of the gene with similarity to Rv1867 gene (**Supplementary Table S1**) and lack of Met-52 raise the possibility that *M. abscessus* subsp. *massiliense* do not have bacterioferritin homolog.

To confirm if the proteins 0076 and 0077 might support ferritin functions, structural and molecular dynamic analyzes were performed. Considering model-1 structures from MD1 and MD2 simulations, the RMSD (CA atoms) between them is 7.03 Å and 6.24 Å for 0076 and 0077 proteins, respectively. The 0076 and 0077 proteins have about 60% of α helix secondary structures and low content of β-sheet secondary structures (see **Table 2**). When residues involved in segments other than the helices are removed from the RMSD estimates, RMSD values fall to 1.20 Å (113 CA atoms) and 1.23 Å (111 CA atoms). This becomes clear in the RMSD fluctuations for residues shown in **Figures 2**, **3** from all clusters. RMSD above 5.0 Å occurred mainly in the segments involved in the N and C terminus, except around residues 130–135, where sensitive structural fluctuations were observed. This may have provided instability in this region and even partial loss of the helix structure, such as illustrated in **Supplementary Figure S1**. The slight fluctuation of the residues involved in segment 130–135 may be due to the templates used to construct the model (3d8A) whose irons were present in the structure and not included in the simulations. On the other hand, it may also be associated with the flexibility expected to assist in the conformational rearrangement of this region to accommodate iron ions and make them more stable. Above all, irrespective of the presence of iron, the conformations of the proteins were stable at their sites, as expected for the positions of the key residues of a ferritin (**Figure 4**). This reinforces the idea that these structures are not dependent on iron for their stability and formation (Stookey, 1970; Waldo and Theil, 1993; Theil et al., 2000).

Although the main crystal structure used to construct the models was not solved with the presence of iron in this region (3qd8A), the MD simulations showed the importance of these ions for the stability of this site. **Table 2** shows that the main residues from *Helicobacter pylori* ferritin structure (GLU17, HIS53, GLU50 GLU94, GLN 127, GLU 130) are conserved in 0076 and 0077 proteins (Cho et al., 2009). Additionally, we observed that the residues involved in the self-assembly and stability are the same as those recently reported by Khare et al. (2013). The 3D position of theses residues for both structures are highly correlated with that observed for *Helicobacter pylori* ferritin structure (**Figure 4**), which strongly supports the ferritin activity and the same iron binding mechanism of these two proteins.

The expression of the *mycma_0076* and *mycma_0077* genes, evaluated *in vitro* with different iron concentrations was found to be differently regulated, suggesting different roles in iron homeostasis for this *Mycobacterium*. Furthermore, *M. abscessus* subsp. *massiliense* was able to grow in highly toxic iron concentrations (450 μM $FeCl_3$), which indicates the presence of a homeostasis mechanism (**Figure 5A**). A recent transcriptomic

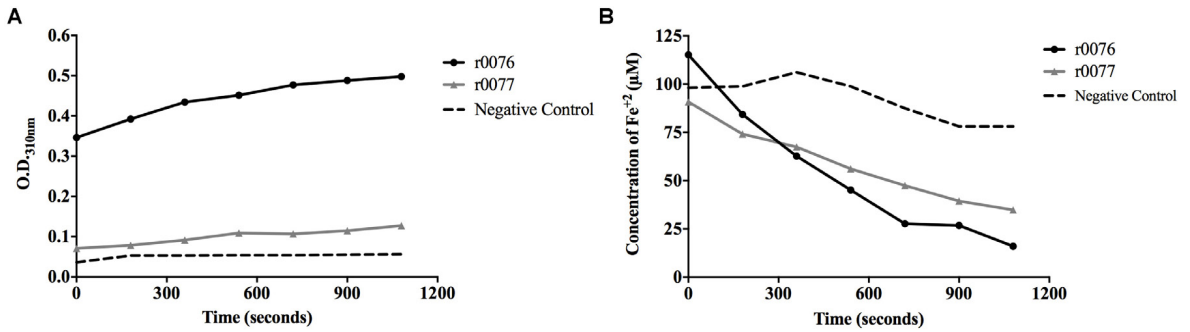

FIGURE 11 | Recombinant proteins r0076 and r0077 have iron oxidizing activity. **(A)** The oxidation of Fe^{2+} into Fe^{3+} was monitored by the increase in absorbance at 310 nm. **(B)** Oxidation of Fe^{2+} into Fe^{3+} rates through the decrease of absorbance by the ferrozin-Fe^{2+} complex at 570 nm wavelength. The negative control was buffer 50 mM NaH_2PO_4 buffer adjusted at pH 8.0 containing 50 mM NaCl.

analysis study of *M. abscessus* subsp. *abscessus* grown in the presence of cystic fibrosis patient sputum listed the different expression of the genes similar to *mycma_0076 (MAB_0126c)* and *mycma_0077 (MAB_0127c*), although that study did not investigate ferritins specifically (Miranda-CasoLuengo et al., 2016). In this previous study, the gene *MAB_0126c* was induced when grown with patient sputum as the stress condition. We found that the gene *mycma_0076* was also induced under *in vitro* conditions with high stressing concentration of iron (**Figure 5B**). Similarly, the requirement of ferritin expression to reduce the effects of oxidative damage was observed in Mtb (Pandey and Rodriguez, 2012, 2014). Thus, among other functions, ferritins play an important role in the resistances against stress conditions (Khare et al., 2017).

The different expression profiles of both *mycma_0076* and *mycma_0077* genes under different iron concentrations (**Figure 5B**), suggests that the proteins coded by theses genes have different roles in iron homeostasis. Recent studies have shown that Mtb ferritin and bacterioferritin have different roles in the cellular homeostasis, suggesting that the presence of two classes of ferritins is non-redundant and important for virulence (Khare et al., 2017). The interesting question is why does *M. abscessus* subsp. *massiliense* have two similar proteins of the same ferritin group? The overexpression of 0076 in high iron concentrations suggests that this protein may be involved in the storage of the ion providing protection to the bacilli from iron-mediated toxicity (**Figure 5B**).

Nonetheless, both *mycma_0076* and *mycma_0077* genes were expressed during macrophage infection, but they were differentially regulated according to the time of infection, which indicates that inside of macrophages, *M. abscessus* subsp. *massiliense* find a different microenvironment as compared with the medium, requiring different expression of those genes. It was observed during macrophage infection that the *mycma_0077* gene was expressed at higher levels, when compared with the levels of expression the *mycma_0076* (**Figures 6A,B**). That difference suggested that the expressions of *mycma_0076* and *mycma_0077* genes and their respective involvement in iron homeostasis are largely dictated by the microenvironment surrounding the cell, and they may play different or redundant but independent roles in iron management. Additionally, during macrophage infection, the *M. abscessus* find a more oxidizing environment compared to an uninfected cell, but the bacilli grow better in this condition (Oberley-Deegan et al., 2010). Moreover, it was demonstrated that an enhanced oxidative stress happens at 24 h post infection of macrophages when the bacilli growth increase (Oberley-Deegan et al., 2010). Our results demonstrated that the *mycma_0076* and *mycma_0077* genes were induced at the same time during macrophage infection (**Figure 6**). Furthermore, we have previously shown that the infection of *M. abscessus* subsp. *massiliense* induced high levels production of NO by spleen and liver cells (Martins de Sousa et al., 2010). Our findings raise the possibility that induction of the *mycma_0076* and *mycma_0077* genes expression during macrophage infection could be related to the resistance of these mycobacteria from oxidative stress caused by the macrophage. Besides, it was demonstrated in *M. tuberculosis* that the ferritin provide protection against oxidative stress and the deletion of this protein increased the sensibility to oxidative damage (Pandey and Rodriguez, 2012; Khare et al., 2017).

After 72 h post infection the burden of bacilli inside macrophages reduced significantly as compared with 48 h (**Figure 6C**) and in the same time of infection, the expression of the *mycma_0076* and *mycma_0077* genes also were reduced (**Figures 6A,B**). An initial interpretation of this observation could be related to the control of infection by macrophages, however, it was observed that the mycobacteria was extravasating to the extracellular milieu (**Figure 6D**). It has been reported that the *M. abscessus* can induce apoptosis of macrophages as a mode of mycobacterial escape for release and growth at the extracellular milieu (Sohn et al., 2009; Bernut et al., 2014; Brambilla et al., 2016; Whang et al., 2017). To confirm that this was the case, infected and uninfected cells were stained and analyzed 24 and 72 h post incubation. Damaged macrophages were observed after 24 h of *M. abscessus* subsp. *massiliense* infection and increased as the infection progressed (**Figure 6E**) concomitant to the increase of extracellular bacteria (**Figure 6D**). This result indicates that *M. abscessus* subsp. *massiliense* can induce damage on macrophages and consequently be released to the extracellular environment when the expression of the

mycma_0076 and *mycma_0077* genes would not be as much necessary as within the intracellular environment.

To confirm the iron storage characteristics of the protein encoded by the *mycma_0076* and *mycma_0077* genes, the recombinant proteins were expressed in *E. coli*. While r0076 was obtained in the soluble form, r0077 remained mostly in insoluble form despite different attempts to obtain it in a soluble form. The CD spectrum obtained for r0076 is typical of proteins with high content of α-helical secondary structure (**Figure 9A**). Moreover, the formation of oligomers in solution (**Figure 9B**), together with the presence of bound iron ions, indicates that r0076 folded correctly. As seen in **Figure 8**, r0076 eluted as a major peak (**Figure 8B**) with an apparent molecular mass of 480 kDa. This result is broadly consistent with an oligomer composed of 24 subunits, whose theoretical expected mass for each subunit is 20 kDa. When r0076 was analyzed by DLS, a R_H of 8.0 ± 0.5 was determined. Assuming a spherical particle, the value determined for R_H correspond to a molecular mass of 437 ± 63 kDa, which would also be consistent with an oligomer composed of 24 subunits. The quaternary structures of several ferritins were found to be strikingly similar (Khare et al., 2011, 2013). The ferritin from *M. tuberculosis* exhibits a quaternary structure where 24 subunits assemble in octahedral 432-symmetric arrangements to form a roughly spherical protein shell (Khare et al., 2011).

The CD spectrum of r0076 was constant below 55°C; however, above this temperature there was a progressive loss of regular secondary structure (**Figure 10A**). Concomitantly, the R_H of r0076 exhibited minimal temperature dependence in the range of 20–55°C, while the R_H increased significantly when the protein was incubated at temperatures above 55°C (**Figure 10B**). Taken together, these results indicate that the increase in temperature does not induce r0076 dissociation prior to denaturation.

The main function of ferritin is to detoxify and store free cellular iron, which is accomplished by oxidation reaction at the ferroxidase center (Andrews, 1998). Molecular dynamics of both models obtained from the amino acid sequences of 0076 and 0077 proteins found conserved amino acid residues involved in the ferroxidase active site as shown for *H. pylori* crystallographic resolved ferritin protein (**Figure 4**) (Cho et al., 2009). We showed here that both proteins r0076 and r0077 are capable of oxidizing Fe^{2+} into Fe^{3+}, confirming their ferritin function similarly to Mtb ferritin (**Figure 11**) (Khare et al., 2011, 2013).

Although the essentiality of the ferritin genes reported here can only be demonstrated by silencing their expression (knockdown them out for example), we have clearly shown for the first time that *mycma_0076* and *mycma_0077* genes codes for a ferritin.

CONCLUSION

The genes *mycma_0076* and *mycma_0077* from *M. abscessus* subsp. *massiliense* code for bacterial ferritins, homologous to Mtb ferritin gene (Rv3841), that are differently modulated by iron concentration both *in vitro* and *in vivo*. Additionally, both proteins r0076 and r0077 were capable to oxidize Fe^{2+} into Fe^{3+} supporting an active ferroxidase center. The implications that *M. abscessus* complex has only ferritins and no bacterioferritins should be further explored.

AUTHOR CONTRIBUTIONS

FO, ADC, and VP carried out most of the experiments. RS performed the MD experiments and wrote the pertinent data of these experiments. WG and JA performed the CD and DLS experiments and wrote the results and discussion regarding this data. AJ-K and AK designed the experiments and supervised all work. FO, AJ-K, and AK wrote the manuscript. All authors revised the manuscript and approved the final version.

FUNDING

This study had financial support from CNPq (307186/2013-0 and 303675/2015-2) and FAPEG (2012/0267000-48 and 2013/10267000-46).

ACKNOWLEDGMENTS

The authors are thankful to Dr. Cirano Jose Ulhoa and Dr. Fabrícia Paula de Faria from Universidade Federal de Goiás for their laboratory support with the experimental procedures for the purification of the recombinant proteins. This manuscript is part of the Ph.D. thesis of FO.

SUPPLEMENTARY MATERIAL

The Supplementary Material for this article can be found online at: https://www.frontiersin.org/articles/10.3389/fmicb.2018.01072/full#supplementary-material

FIGURE S1 | Secondary fluctuations structures over 100 ns from 0076 to 0077 proteins. **(A)** Secondary structures of 0076 MD1. **(B)** Secondary structures of 0076 MD2. **(C)** Secondary structures of 0077 MD1. **(D)** Secondary structures of 0077 MD2.

FIGURE S2 | Solubilization of r0077 protein from inclusion bodies using sarkosyl and purification. **(A)** SDS-PAGE gel showing lysis of bacterial cells induced or not with 1 mM IPTG for 4 h. **(B,C)** SDS-PAGE gel showing solubilization of r0077 protein with various concentration of sarkosyl. **(D)** Purification of r0077 using His tag from soluble fraction obtained with 2.5% sarkosyl. **(E)** SDS-PAGE gel showing r0077 protein purified concentrated.

TABLE S1 | BLAST results from similarity search for the Rv1876 gene from *M. tuberculosis* H37Rv.

TABLE S2 | Primer sequences used to evaluate the expression of *M. abscessus* subsp. *massiliense* genes.

REFERENCES

Abdalla, M. Y., Ahmad, I. M., Switzer, B., and Britigan, B. E. (2015a). Induction of heme oxygenase-1 contributes to survival of *Mycobacterium abscessus* in human macrophages-like THP-1 cells. *Redox Biol.* 4, 328–339. doi: 10.1016/j.redox.2015.01.012

Abdalla, M. Y., Switzer, B. L., Goss, C. H., Aitken, M. L., Singh, P. K., and Britigan, B. E. (2015b). Gallium compounds exhibit potential as new therapeutic agents against *Mycobacterium abscessus*. *Antimicrob. Agents Chemother.* 59, 4826–4834. doi: 10.1128/aac.00331-15

Andrews, S. C. (1998). Iron storage in bacteria. *Adv. Microb. Physiol.* 40, 281–351.

Andrews, S. C., Robinson, A. K., and Rodriguez-Quinones, F. (2003). Bacterial iron homeostasis. *FEMS Microbiol. Rev.* 27, 215–237.

Bakala, N., Goma, J. C., Le Moigne, V., Soismier, N., Laencina, L., Le Chevalier, F., et al. (2015). *Mycobacterium abscessus* phospholipase C expression is induced during coculture within amoebae and enhances *M. abscessus* virulence in mice. *Infect. Immun.* 83, 780–791. doi: 10.1128/iai.02032-14

Becker, L., Liu, N. C., Averill, M. M., Yuan, W., Pamir, N., Peng, Y., et al. (2012). Unique proteomic signatures distinguish macrophages and dendritic cells. *PLoS One* 7:e33297. doi: 10.1371/journal.pone.0033297

Berendsen, H. J. C., van der Spoel, D., and van Drunen, R. (1995). Gromacs: a message-passing parallel molecular dynamics implementation. *Comput. Phys. Commun.* 91, 43–56.

Bernut, A., Herrmann, J. L., Kissa, K., Dubremetz, J. F., Gaillard, J. L., Lutfalla, G., et al. (2014). *Mycobacterium abscessus* cording prevents phagocytosis and promotes abscess formation. *Proc. Natl. Acad. Sci. U.S.A.* 111, E943–E952. doi: 10.1073/pnas.1321390111

Bou-Abdallah, F. (2010). The iron redox and hydrolysis chemistry of the ferritins. *Biochim. Biophys. Acta* 1800, 719–731. doi: 10.1016/j.bbagen.2010.03.021

Bou-Abdallah, F., Yang, H., Awomolo, A., Cooper, B., Woodhall, M. R., Andrews, S. C., et al. (2014). Functionality of the three-site ferroxidase center of *Escherichia coli* bacterial ferritin (EcFtnA). *Biochemistry* 53, 483–495. doi: 10.1021/bi401517f

Brambilla, C., Llorens-Fons, M., Julian, E., Noguera-Ortega, E., Tomas-Martinez, C., Perez-Trujillo, M., et al. (2016). Mycobacteria clumping increase their capacity to damage macrophages. *Front. Microbiol.* 7:1562. doi: 10.3389/fmicb.2016.01562

Bryant, J. M., Grogono, D. M., Greaves, D., Foweraker, J., Roddick, I., Inns, T., et al. (2013). Whole-genome sequencing to identify transmission of *Mycobacterium abscessus* between patients with cystic fibrosis: a retrospective cohort study. *Lancet* 381, 1551–1560. doi: 10.1016/s0140-6736(13)60632-7

Bryant, J. M., Grogono, D. M., Rodriguez-Rincon, D., Everall, I., Brown, K. P., Moreno, P., et al. (2016). Emergence and spread of a human-transmissible multidrug-resistant nontuberculous *mycobacterium*. *Science* 354, 751–757. doi: 10.1126/science.aaf8156

Cardoso, A. M., Martins de Sousa, E., Viana-Niero, C., Bonfim de Bortoli, F., Pereira das Neves, Z. C., Leao, S. C., et al. (2008). Emergence of nosocomial *Mycobacterium massiliense* infection in Goias. Brazil. *Microbes Infect.* 10, 1552–1557. doi: 10.1016/j.micinf.2008.09.008

Carrondo, M. A. (2003). Ferritins, iron uptake and storage from the bacterioferritin viewpoint. *EMBO J.* 22, 1959–1968. doi: 10.1093/emboj/cdg215

Caverly, L. J., Caceres, S. M., Fratelli, C., Happoldt, C., Kidwell, K. M., Malcolm, K. C., et al. (2015). *Mycobacterium abscessus* morphotype comparison in a murine model. *PLoS One* 10:e0117657. doi: 10.1371/journal.pone.0117657

Chen, V. B., Arendall, W. B. III, Headd, J. J., Keedy, D. A., Immormino, R. M., Kapral, G. J., et al. (2010). MolProbity: all-atom structure validation for macromolecular crystallography. *Acta Crystallogr. D Biol. Crystallogr.* 66(Pt 1), 12–21. doi: 10.1107/S0907444909042073

Cho, K. J., Shin, H. J., Lee, J. H., Kim, K. J., Park, S. S., Lee, Y., et al. (2009). The crystal structure of ferritin from *Helicobacter pylori* reveals unusual conformational changes for iron uptake. *J. Mol. Biol.* 390, 83–98. doi: 10.1016/j.jmb.2009.04.078

Cole, S. T., Brosch, R., Parkhill, J., Garnier, T., Churcher, C., Harris, D., et al. (1998). Deciphering the biology of *Mycobacterium tuberculosis* from the complete genome sequence. *Nature* 393, 537–544. doi: 10.1038/31159

Coutsias, E. A., Seok, C., and Dill, K. A. (2004). Using quaternions to calculate RMSD. *J. Comput. Chem.* 25, 1849–1857. doi: 10.1002/jcc.20110

da Costa, A. C., de Resende, D. P., Santos, B. P. O., Zoccal, K. F., Faccioli, L. H., Kipnis, A., et al. (2017). Modulation of macrophage responses by CMX, a fusion protein composed of Ag85c, MPT51, and HspX from *Mycobacterium tuberculosis*. *Front. Microbiol.* 8:623. doi: 10.3389/fmicb.2017.00623

Daura, X., Gademann, K., Jaun, B., Seebach, D., van Gunsteren, W. F., and Mark, A. E. (1999). Peptide folding: when simulation meets experiment. *Angew. Chemie Int. Ed.* 38, 236–240. doi: 10.1039/c0cp01773f

De Voss, J. J., Rutter, K., Schroeder, B. G., Su, H., Zhu, Y., and Barry, C. E. I. I. I. (2000). The salicylate-derived mycobactin siderophores of *Mycobacterium tuberculosis* are essential for growth in macrophages. *Proc. Natl. Acad. Sci. U.S.A.* 97, 1252–1257.

Gold, B., Rodriguez, G. M., Marras, S. A., Pentecost, M., and Smith, I. (2001). The *Mycobacterium tuberculosis* IdeR is a dual functional regulator that controls transcription of genes involved in iron acquisition, iron storage and survival in macrophages. *Mol. Microbiol.* 42, 851–865.

Gupta, V., Gupta, R. K., Khare, G., Salunke, D. M., and Tyagi, A. K. (2009). Crystal structure of Bfr A from *Mycobacterium tuberculosis*: incorporation of selenomethionine results in cleavage and demetallation of haem. *PLoS One* 4:e8028. doi: 10.1371/journal.pone.0008028

Helguera-Repetto, A. C., Chacon-Salinas, R., Cerna-Cortes, J. F., Rivera-Gutierrez, S., Ortiz-Navarrete, V., Estrada-Garcia, I., et al. (2014). Differential macrophage response to slow- and fast-growing pathogenic mycobacteria. *Biomed Res. Int.* 2014:916521. doi: 10.1155/2014/916521

Imlay, J. A., Chin, S. M., and Linn, S. (1988). Toxic DNA damage by hydrogen peroxide through the Fenton reaction in vivo and in vitro. *Science* 240, 640–642.

Khare, G., Gupta, V., Nangpal, P., Gupta, R. K., Sauter, N. K., and Tyagi, A. K. (2011). Ferritin structure from *Mycobacterium tuberculosis*: comparative study with homologues identifies extended C-terminus involved in ferroxidase activity. *PLoS One* 6:e18570. doi: 10.1371/journal.pone.0018570

Khare, G., Nangpal, P., and Tyagi, A. K. (2013). Unique residues at the 3-fold and 4-fold axis of mycobacterial ferritin are involved in oligomer switching. *Biochemistry* 52, 1694–1704. doi: 10.1021/bi301189t

Khare, G., Nangpal, P., and Tyagi, A. K. (2017). Differential roles of iron storage proteins in maintaining the iron homeostasis in *Mycobacterium tuberculosis*. *PLoS One* 12:e0169545. doi: 10.1371/journal.pone.0169545

Kumar, B., Sharma, D., Sharma, P., Katoch, V. M., Venkatesan, K., and Bisht, D. (2013). Proteomic analysis of *Mycobacterium tuberculosis* isolates resistant to kanamycin and amikacin. *J. Proteom.* 94, 68–77. doi: 10.1016/j.jprot.2013.08.025

Lee, M. R., Sheng, W. H., Hung, C. C., Yu, C. J., Lee, L. N., and Hsueh, P. R. (2015). *Mycobacterium abscessus* complex infections in humans. *Emerg. Infect. Dis.* 21, 1638–1646. doi: 10.3201/2109.141634

Levi, S., Luzzago, A., Cesareni, G., Cozzi, A., Franceschinelli, F., Albertini, A., et al. (1988). Mechanism of ferritin iron uptake: activity of the H-chain and deletion mapping of the ferro-oxidase site. A study of iron uptake and ferro-oxidase activity of human liver, recombinant H-chain ferritins, and of two H-chain deletion mutants. *J. Biol. Chem.* 263, 18086–18092.

Mahoney, M. W., and Jorgensen, W. L. (2000). A five-site model for liquid water and the reproduction of the density anomaly by rigid, nonpolarizable potential functions. *J. Chem. Phys.* 112:8910. doi: 10.1063/1.481505

Martins de Sousa, E., Bonfim de Bortoli, F., Amaral, E. P., Batista, A. C., Liberman Kipnis, T., Marques Cardoso, A., et al. (2010). Acute immune response to *Mycobacterium massiliense* in C57BL/6 and BALB/c mice. *Infect. Immun.* 78, 1571–1581. doi: 10.1128/iai.00731-09

Medjahed, H., Gaillard, J. L., and Reyrat, J. M. (2010). *Mycobacterium abscessus*: a new player in the mycobacterial field. *Trends Microbiol.* 18, 117–123. doi: 10.1016/j.tim.2009.12.007

Miranda-CasoLuengo, A. A., Staunton, P. M., Dinan, A. M., Lohan, A. J., and Loftus, B. J. (2016). Functional characterization of the *Mycobacterium abscessus* genome coupled with condition specific transcriptomics reveals conserved molecular strategies for host adaptation and persistence. *BMC Genomics* 17:553. doi: 10.1186/s12864-016-2868-y

Oberley-Deegan, R. E., Rebits, B. W., Weaver, M. R., Tollefson, A. K., Bai, X., McGibney, M., et al. (2010). An oxidative environment promotes growth of

Mycobacterium abscessus. *Free Radic. Biol. Med.* 49, 1666–1673. doi: 10.1016/j.freeradbiomed.2010.08.026

Pandey, R., and Rodriguez, G. M. (2012). A ferritin mutant of *Mycobacterium tuberculosis* is highly susceptible to killing by antibiotics and is unable to establish a chronic infection in mice. *Infect. Immun.* 80, 3650–3659. doi: 10.1128/IAI.00229-12

Pandey, R., and Rodriguez, G. M. (2014). IdeR is required for iron homeostasis and virulence in *Mycobacterium tuberculosis*. *Mol. Microbiol.* 91, 98–109. doi: 10.1111/mmi.12441

Pandey, S. D., Choudhury, M., Yousuf, S., Wheeler, P. R., Gordon, S. V., Ranjan, A., et al. (2014). Iron-regulated protein HupB of *Mycobacterium tuberculosis* positively regulates siderophore biosynthesis and is essential for growth in macrophages. *J. Bacteriol.* 196, 1853–1865. doi: 10.1128/JB.01483-13

Petrini, B. (2006). *Mycobacterium abscessus*: an emerging rapid-growing potential pathogen. *APMIS* 114, 319–328. doi: 10.1111/j.1600-0463.2006.apm_390.x

Raiol, T., Ribeiro, G. M., Maranhao, A. Q., Bocca, A. L., Silva-Pereira, I., Junqueira-Kipnis, A. P., et al. (2012). Complete genome sequence of *Mycobacterium massiliense*. *J. Bacteriol.* 194:5455. doi: 10.1128/JB.01219-12

Reddy, P. V., Puri, R. V., Khera, A., and Tyagi, A. K. (2012). Iron storage proteins are essential for the survival and pathogenesis of *Mycobacterium tuberculosis* in THP-1 macrophages and the guinea pig model of infection. *J. Bacteriol.* 194, 567–575. doi: 10.1128/JB.05553-11

Shang, S., Gibbs, S., Henao-Tamayo, M., Shanley, C. A., McDonnell, G., Duarte, R. S., et al. (2011). Increased virulence of an epidemic strain of *Mycobacterium massiliense* in mice. *PLoS One* 6:e24726. doi: 10.1371/journal.pone.0024726

Sharma, D., Kumar, B., Lata, M., Joshi, B., Venkatesan, K., Shukla, S., et al. (2015). Comparative proteomic analysis of aminoglycosides resistant and susceptible *Mycobacterium tuberculosis* clinical isolates for exploring potential drug targets. *PLoS One* 10:e0139414. doi: 10.1371/journal.pone.0139414

Sharma, D., Lata, M., Faheem, M., Khan, A. U., Joshi, B., Venkatesan, K., et al. (2016). *M. tuberculosis* ferritin (Rv3841): potential involvement in Amikacin (AK) & Kanamycin (KM) resistance. *Biochem. Biophys. Res. Commun.* 478, 908–912. doi: 10.1016/j.bbrc.2016.08.049

Sohn, H., Kim, H. J., Kim, J. M., Jung Kwon, O., Koh, W. J., and Shin, S. J. (2009). High virulent clinical isolates of *Mycobacterium abscessus* from patients with the upper lobe fibrocavitary form of pulmonary disease. *Microb. Pathog.* 47, 321–328. doi: 10.1016/j.micpath.2009.09.010

Stookey, L. L. (1970). Ferrozine - a new spectrophotometric reagent for iron. *Anal. Chem.* 42, 779–781.

Theil, E. C., Takagi, H., Small, G. W., He, L., Tipton, A. R., and Danger, D. (2000). The ferritin iron entry and exit problem. *Inorganica Chim. Acta* 297, 242–251. doi: 10.1021/ar500469e

Tortoli, E., Kohl, T. A., Brown-Elliott, B. A., Trovato, A., Leao, S. C., Garcia, M. J., et al. (2016). Emended description of *Mycobacterium abscessus*, *Mycobacterium abscessus* subsp. *abscessus* and *Mycobacterium abscessus* subsp. *bolletii* and designation of *Mycobacterium abscessus* subsp. *massiliense* comb. nov. *Int. J. Syst. Evol. Microbiol.* 66, 4471–4479. doi: 10.1099/ijsem.0.001376

Vile, G. F., and Tyrrell, R. M. (1993). Oxidative stress resulting from ultraviolet A irradiation of human skin fibroblasts leads to a heme oxygenase-dependent increase in ferritin. *J. Biol. Chem.* 268, 14678–14681.

Waldo, G. S., and Theil, E. C. (1993). Formation of iron(III)-tyrosinate is the fastest reaction observed in ferritin. *Biochemistry* 32, 13262–13269.

Whang, J., Back, Y. W., Lee, K. I., Fujiwara, N., Paik, S., Choi, C. H., et al. (2017). *Mycobacterium abscessus* glycopeptidolipids inhibit macrophage apoptosis and bacterial spreading by targeting mitochondrial cyclophilin D. *Cell Death Dis.* 8:e3012. doi: 10.1038/cddis.2017.420

Wu, S., and Zhang, Y. (2007). LOMETS: a local meta-threading-server for protein structure prediction. *Nucleic Acids Res.* 35, 3375–3382. doi: 10.1093/nar/gkm251

Yasmin, S., Andrews, S. C., Moore, G. R., and Le Brun, N. E. (2011). A new role for heme, facilitating release of iron from the bacterioferritin iron biomineral. *J. Biol. Chem.* 286, 3473–3483. doi: 10.1074/jbc.M110.175034

Yildirim, I., Stern, H. A., Kennedy, S. D., Tubbs, J. D., and Turner, D. H. (2010). Reparameterization of RNA chi torsion parameters for the AMBER force field and comparison to NMR spectra for cytidine and uridine. *J. Chem. Theory Comput.* 6, 1520–1531. doi: 10.1021/ct900604a

Yu, M. (2012). *Computational Modeling of Protein Dynamics with GROMACS and Java*. San Jose, CA: San Jose State University.

Zhang, Y. (2008). I-TASSER server for protein 3D structure prediction. *BMC Bioinformatics* 9:40. doi: 10.1186/1471-2105-9-40

Zhang, Y., and Skolnick, J. (2004). Scoring function for automated assessment of protein structure template quality. *Proteins* 57, 702–710. doi: 10.1002/prot.20264

Zhang, Y., and Skolnick, J. (2005). TM-align: a protein structure alignment algorithm based on the TM-score. *Nucleic Acids Res.* 33, 2302–2309. doi: 10.1093/nar/gki524

Conflict of Interest Statement: The authors declare that the research was conducted in the absence of any commercial or financial relationships that could be construed as a potential conflict of interest.

frontiers in Microbiology

ORIGINAL RESEARCH
published: 18 December 2018
doi: 10.3389/fmicb.2018.03140

Evaluation of a Novel MALDI Biotyper Algorithm to Distinguish *Mycobacterium intracellulare* From *Mycobacterium chimaera*

*L. Elaine Epperson[1], Markus Timke[2], Nabeeh A. Hasan[1], Paul Godo[3], David Durbin[3], Niels K. Helstrom[3], Gongyi Shi[4], Markus Kostrzewa[2], Michael Strong[1] and Max Salfinger[3,5,6]**

[1] Center for Genes, Environment and Health, National Jewish Health, Denver, CO, United States, [2] Bruker Daltonik GmbH, Bremen, Germany, [3] Mycobacteriology Laboratory, National Jewish Health, Denver, CO, United States, [4] Bruker Daltonics, Billerica, MA, United States, [5] Department of Medicine, National Jewish Health, Denver, CO, United States, [6] College of Public Health, University of South Florida, Tampa, FL, United States

OPEN ACCESS

Edited by:
Thomas Dick, Rutgers, The State University of New Jersey, United States

Reviewed by:
Jeanette Teo, National University Hospital, Singapore
Maurizio Sanguinetti, Catholic University of the Sacred Heart, Italy

***Correspondence:**
Max Salfinger
salfingerm@njhealth.org

Specialty section:
This article was submitted to Antimicrobials, Resistance and Chemotherapy, a section of the journal Frontiers in Microbiology

Received: *31 August 2018*
Accepted: *04 December 2018*
Published: *18 December 2018*

Citation:
Epperson LE, Timke M, Hasan NA, Godo P, Durbin D, Helstrom NK, Shi G, Kostrzewa M, Strong M and Salfinger M (2018) Evaluation of a Novel MALDI Biotyper Algorithm to Distinguish Mycobacterium intracellulare From Mycobacterium chimaera. Front. Microbiol. 9:3140. doi: 10.3389/fmicb.2018.03140

Accurate and timely mycobacterial species identification is imperative for successful diagnosis, treatment, and management of disease caused by nontuberculous mycobacteria (NTM). The current most widely utilized method for NTM species identification is Sanger sequencing of one or more genomic loci, followed by BLAST sequence analysis. MALDI-TOF MS offers a less expensive and increasingly accurate alternative to sequencing, but the commercially available assays used in clinical mycobacteriology cannot differentiate between *Mycobacterium intracellulare* and *Mycobacterium chimaera*, two closely related potentially pathogenic species of NTM that are members of the *Mycobacterium avium* complex (MAC). Because this differentiation of MAC species is challenging in a diagnostic setting, Bruker has developed an improved spectral interpretation algorithm to differentiate *M. chimaera* and *M. intracellulare* based on differential spectral peak signatures. Here, we utilize a set of 185 MAC isolates that have been characterized using *rpoB* locus sequencing followed by whole genome sequencing in some cases, to test the accuracy of the Bruker subtyper software to identify *M. chimaera* (n = 49) and *M. intracellulare* (n = 55). 100% of the *M. intracellulare* and 82% of the *M. chimaera* isolates were accurately identified using the MALDI Biotyper algorithm. This subtyper module is available with the MALDI Biotyper Compass software and offers a promising mechanism for rapid and inexpensive species determination for *M. chimaera* and *M. intracellulare*.

Keywords: nontuberculous mycobacteria, diagnostics, MALDI, *Mycobacterium chimaera*, *Mycobacterium intracellulare*, species identification, MAC, NTM

INTRODUCTION

The use of Matrix Assisted Laser Desorption Ionization-Time of Flight Mass Spectrometry (MALDI-TOF MS) for identification of microbial specimens has scaled up dramatically over the past decade due to the continual improvement of available tools, including expanded spectral peak databases [reviewed in Doern and Butler-Wu (2016); Rahi et al. (2016); and Alcaide et al. (2018)].

Species identification of bacteria is now honed to strain-specific and subspecies distinctions in many cases (Neville et al., 2011; Huang et al., 2018) as well as the characterization of non-bacterial organisms such as fungi (Chalupova et al., 2014; Levesque et al., 2015). These approaches are relatively rapid, inexpensive, and accurate for use in clinical diagnostics (Neville et al., 2011), environmental sample analysis, food safety, and other applications (Carbonnelle et al., 2011; Florio et al., 2018). MALDI-TOF MS is increasingly utilized to distinguish clinically relevant nontuberculous mycobacteria (NTM) (Levesque et al., 2015; Costa-Alcalde et al., 2018).

The *Mycobacterium avium* complex (MAC) comprises several clinically important mycobacterial species including *M. avium* (subsp. *hominissuis*), *M. intracellulare*, and *M. chimaera* (Diel et al., 2018; Forbes et al., 2018), among others [e.g., *M. colombiense* (Murcia et al., 2006) and *M. yongonense* (Castejon et al., 2018)]. Although *M. avium* and *M. intracellulare* species are more frequently observed in clinical cases, a recent series of *M. chimaera* infections originating in cardiac surgery suites (van Ingen et al., 2017) illuminates the importance of identifying members of the MAC complex at the species level in a rapid and accurate manner. While the spectrum of *M. avium* is relatively distinct from the other two species, *M. intracellulare* and *M. chimaera* are highly similar to each other (van Ingen et al., 2012), and not readily distinguished using the standard approaches of most MALDI-TOF peak interpretation algorithms (Boyle et al., 2015a; Leyer et al., 2017). Pulmonary infections caused by the different MAC species are distinct in their virulence and clinical features, indicating that species-level identification is important for effective prognostics (Boyle et al., 2015b; Kim et al., 2017). Bruker Daltonik (Bremen, Germany) developed a commercially available algorithm to differentiate *M. chimaera* and *M. intracellulare* from each other using only MALDI-TOF peak data. This algorithm was found to perform well against 59 bacterial isolates of European origin using the internal transcribed spacer (ITS) sequence to identify species (Pranada et al., 2017). Here we set out to evaluate the same MALDI algorithm against 111 isolates of United States origin. Sequence from the *rpoB* locus was used to determine species, but in 16 discrepant cases, the isolates were whole genome sequenced and species identity was determined using phylogenomics.

MATERIALS AND METHODS

NTM Species Determination Using Sanger Sequencing

All samples were of clinical origin within the United States, either bronchoalveolar lavage, sputum, or tissue. Isolates were sent to National Jewish Health for NTM species identification and/or antimicrobial susceptibility testing. DNA from these isolated cultures of 300 acid-fast bacilli were analyzed using a targeted 711 base pair region of the *rpoB* locus that was Sanger sequenced using ABI 3730xL and queried against the National Center for Biotechnology Information (NCBI) Basic Local Alignment Search Tool (BLAST) database. The *rpoB* target is one of several recommended for NTM species determination according to current national clinical microbiology guidelines (Forbes et al., 2018); other targets that are utilized for this purpose are 16S rRNA, secA, ITS, and hsp65 (Lecorche et al., 2018). From this collection, a subset (185) were identified as one of the MAC species according to rpoB sequence, i.e., *M. avium* ($n = 74$), *M. intracellulare* ($n = 55$), or *M. chimaera* ($n = 56$).

MALDI-TOF MS

MAC strains were subcultured onto Middlebrook 7H11 agar media and incubated for 7–10 days to obtain sufficient biomass for MALDI-TOF MS identification. Colonies from the 7H11 plates were harvested and heat-killed in high performance liquid chromatography (HPLC) grade water, followed by acetonitrile/formic acid extraction procedure according to the manufacturer protocol. The MALDI-TOF target was spotted with 1 μL of extract supernatant and overlaid with 1 μL of α-Cyano-4-hydroxycinnamic acid (HCCA) matrix prior to data capture using the Bruker MALDI-TOF Biotyper system (software v4.0). A minimum score of 1.8 was required. A complete MALDI spectrum dataset was sent to Germany for MALDI spectrum analysis in parallel at Bruker Daltonik in Bremen, Germany.

For samples identified by MALDI-TOF MS as *M. chimaera-intracellulare* group, a second-tier analysis was performed using a recently developed research subtyping software from Bruker Daltonik [(Pranada et al., 2017) herein referred to as MBT Subtyping Module]. One sample, NTM-184, was eliminated from the sensitivity and specificity calculations because the MALDI results placed it in the *M. chimaera-intracellulare* group, but the *rpoB* result was *M. avium*, and this sample did not have whole genome sequence (WGS) information (see below.) An additional seven samples, six of which were identified as *M. chimaera* using *rpoB*, were also eliminated from these calculations because the MBT Subtyping Module did not yield a result. These strains are listed in **Table 1** under the MBT Subtyper as "*M. chim/M. int.*" It should be noted that the MBT Subtyping Module returned a high score on these seven samples but because it was unable to distinguish the two species, it does not make a call in these cases.

Phylogenomic Analysis of Ambiguous NTM Strains

For almost all samples, the *rpoB* species identification was considered to be the actual species of that strain. In a few cases, samples yielded discrepant results, and for these samples, WGS was used to assign a species identification to a given mycobacterial strain. Genomic DNA was isolated according to a protocol adapted from Käser et al. (2010), employing a column DNA clean in lieu of a phenol chloroform extraction and alcohol precipitation. Genomic libraries were constructed using Nextera XT and sequenced using Illumina chemistry (Illumina, Inc., San Diego, CA).

Illumina reads were trimmed of adapters and low quality bases (< Q20) using Skewer (Jiang et al., 2014). Trimmed reads were assembled into scaffolds using Unicycler (Wick et al., 2017), and genome assemblies were compared against a selection of reference genomes to calculate average nucleotide identities (ANI, chjp/ANI on GitHub.com, **Supplementary Table S1**)

and to assign a species call to each isolate (Goris et al., 2007; Richter and Rossello-Mora, 2009). Trimmed reads and background reference genomes were mapped to the *M. chimaera* CDC 2015-22-71 genome (Hasan et al., 2017) using Bowtie2 software (Langmead and Salzberg, 2012). Single nucleotide polymorphisms (SNPs) were called using SAMtools mpileup program (Li et al., 2009), and a multi-fasta sequence alignment was created from concatenated basecalls from all strains (Davidson et al., 2014; Page et al., 2016). Resulting sequences were used to make a maximum likelihood (ML) phylogenetic tree using RAxML-NG with a GTR+G substitution model (Kozlov et al., 2018) and 1,000 bootstrap replicates. The tree was annotated and visualized with ggtree (Yu et al., 2017). Reference genomes for the tree are, for *M. chimaera*, listing genome name, accession number: AH16, CP012885.2; CDC 2015-22-71,CP019221.1; DSM 44623, CP015278.1; SJ42, CP022223.1; ZUERICH-2, CP015267.1; LJHL01, LJHL00000000.1; LJHM01, LJHM00000000.1; LJHN01, LJHN00000000.1; 1956, CP009499.1; ATCC 13950, NC_016946.1; MOTT-02, NC_016947.1; MOTT-64, NC_016948.1; and for *M. intracellulare*: 1956, CP009499.1; ATCC 13950, NC_016946.1; MOTT-02, NC_016947.1; MOTT-64, NC_016948.1.

The whole genome sequence data are available at NCBI in Bioproject number PRJNA506060[1] with the following accession numbers: NTM-006, SAMN10441865; NTM-019, SAMN10441945; NTM-035, SAMN10441946; NTM-054, SAMN10441947; NTM-105, SAMN10441948; NTM-107, SAMN10441949; NTM-168, SAMN10441950; NTM-178, SAMN10441951; NTM-203, SAMN10441952; NTM-204, SAMN10441953; NTM-206, SAMN10441954; NTM-208, SAMN10441955; NTM-223, SAMN10441956; NTM-224, SAMN10441957; NTM-230, SAMN10441958; NTM-232, SAMN10441959.

[1]https://www.ncbi.nlm.nih.gov/bioproject/PRJNA506060/

Comparison of WGS to Single Locus Species Determination

Using primer sequences of known targets, three regions were extracted from the WGS data. These were previously targeted regions from the following loci: 16S rDNA (Springer et al., 1996; van Ingen et al., 2012), the 16S–23S internal transcribed spacer (ITS) (Schweickert et al., 2008), and *rpoB* (Adekambi et al., 2003; Ben Salah et al., 2008). These sequences were used to BLAST against the non-redundant NCBI database and the top species call or calls are reported in **Table 1**.

RESULTS

From the initial strain collection, 185 isolates were identified by *rpoB* amplicon sequencing as one of the three prominent clinical MAC species, specifically 74 *M. avium*, 55 *M. intracellulare*, and 56 *M. chimaera*. These 185 strains were then analyzed using MALDI-TOF MS at National Jewish Health, in Denver, Colorado, United States and the data were re-analyzed in Bremen, Germany, yielding identical results according to the Biotyper 4.0 software. Of the 74 *M. avium* isolates, 73 were identified as *M. avium*. A single *M. avium* sample (as identified by *rpoB*) and the remaining 111 samples were all identified as being in the *M. chimaera-intracellulare* group.

These 112 strains were then subjected to a second tier of analysis wherein their MALDI-TOF MS spectra were evaluated

TABLE 1 | Comparison of single locus sequencing results to whole genome sequencing results for sixteen MAC strains for each sample that was whole genome sequenced, three loci were extracted and analyzed by BLAST to the non-redundant NCBI database giving the results listed.

	Region extracted from WGS data					
Sample	**16S (1026bp)**	**16S 403***	**ITS (335-336bp)**	**rpoB (752bp)**	**MBT subtyper**	**WGS**
NTM-006	*M. chim/M.int*	*M. int*	*M. chim/M.int*	*M. chim*	*M. int*	*M. int*
NTM-168	MAC	*M. int*	*M. chim/M.int*	*M. int*	*M. chim/M.int*	*M. int*
NTM-224	*M. mars/M.int*	*M. chim*	*M. int*	*M. chim*	*M. chim/M.int*	*M. chim*
NTM-105	MAC	*M. int*	*M. chim/M.int*	*M. chim*	*M. int*	*M. chim*
NTM-206	MAC	*M. int*	*M. chim/M.int*	*M. chim*	*M. int*	*M. chim*
NTM-035	MAC	*M. int*	missing data	*M. chim*	*M. int*	*M. chim*
NTM-232	MAC	*M. int*	*M. chim/M.int*	*M. chim*	*M. int*	*M. chim*
NTM-019	*M. chim/M.int*	*M. int*	*M. chim/M.int*	*M. chim*	*M. int*	*M. chim*
NTM-178	MAC	*M. int*	*M. chim/M.int*	*M. chim*	*M. int*	*M. chim*
NTM-107	MAC	*M. int*	*M. chim/M.int*	*M. chim*	*M. int*	*M. chim*
NTM-054	*M. mars/M.int*	*M. chim*	*M. int/M.int yong*	*M. chim*	*M. int*	*M. chim*
NTM-223	MAC	*M. int*	*M. int*	*M. chim*	*M. chim/M.int*	*M. chim*
NTM-203	MAC	*M. int*	*M. int*	*M. chim*	*M. chim/M.int*	*M. chim*
NTM-208	MAC	*M. int*	*M. int*	*M. chim*	*M. chim/M.int*	*M. chim*
NTM-204	MAC	*M. int*	*M. int*	*M. chim*	*M. chim/M.int*	*M. chim*
NTM-230	*M. chim*	*M. chim*	*M. chim*	*M. chim*	*M. chim/M.int*	*M. chim*

Also listed are the species as determined using only the 403 SNP from 16S, assuming a strain was previously identified as belonging to the chimaera/intracellulare group. MBT Subtyper result and the WGS species call based on phylogenomic tree. M. chim = M. chimaera, M. int = M. intracellulare, M. yong = M. yongonense, M. mars = M. marseillense.

using the recently developed MBT Subtyping Module software; see Methods (Pranada et al., 2017). One sample, NTM-006, was identified as *M. chimaera* by *rpoB* but as *M. intracellulare* by WGS, thus the sample was categorized as *M. intracellulare*. This was the only sample for which WGS yielded a result that differed from *rpoB*. In this case, the WGS result was considered to be the actual species for calculations. After removing the eight samples that were unconfirmed (see Methods), the samples numbered 55 *M. intracellulare* and 49 *M. chimaera* that were suitable to evaluate the MBT Subtyping Module algorithm for its ability to distinguish these two species.

Sixteen isolates were selected for WGS. These strains were investigated in greater depth using extracted sequences of specific loci (**Table 1**) in addition to phylogenomic tree analysis using the WGS data (**Figure 1**). The specific loci were selected to reflect the regions that are most commonly used for mycobacterial species identification. For most Mycobacteria spp., these loci are useful for identifying to the NTM species level. But the close relationship of *M. chimaera* and *M. intracellulare* is apparent in these genes since the two species' sequences over these regions are largely interchangeable, consistent with the initial confounding observations that led to the naming of *M. chimaera* (Tortoli et al., 2004). Based on these extracted sequences, the *rpoB* fragment was most reflective of the WGS result (**Table 1**).

For the 49 samples identified by sequencing as *M. chimaera*, the MBT Subtyping Module identified 40 as *M. chimaera* and 9 as *M. intracellulare* for a sensitivity of 81.6%. However, because all of the Subtyper *M. chimaera* calls were in fact *M. chimaera* according to whole genome sequencing, the positive predictive value for a call of *M. chimaera* is 100%. The *M. intracellulare* (n = 55) data differed in that all 55 samples were identified as *M. intracellulare* for a sensitivity of 100%, but nine of the *M. chimaera* samples were called *M. intracellulare* by the Subtyping software, reducing the specificity, and the positive predictive value is 86% or 55/(55+9). This indicates that a minority (∼18%, or 9/49) of the true *M. chimaera* samples would be recognized as *M. intracellulare* using the MALDI Biotyper Compass software.

DISCUSSION

The recent outbreak of *M. chimaera*-contaminated heater-cooler devices used in cardiac surgery has increased the clinical urgency for differentiating *M. chimaera* from *M. intracellulare*. The MALDI-TOF MS approach to species identification is less expensive and more rapid than sequencing methods, but until now has been unable to distinguish these two closely related MAC species. Our findings indicate that a call of *M. chimaera* by the Bruker subtyping algorithm tested here is correct every time for a positive predictive value of 100%. We also found that a call of *M. intracellulare* is correct 86% of the time, that is, 14% of our samples that were recognized as *M. intracellulare* by MALDI are actually more closely related to *M. chimaera* than to *M. intracellulare*. Given the regional diversity of NTM species, it is possible that these strains were not available in

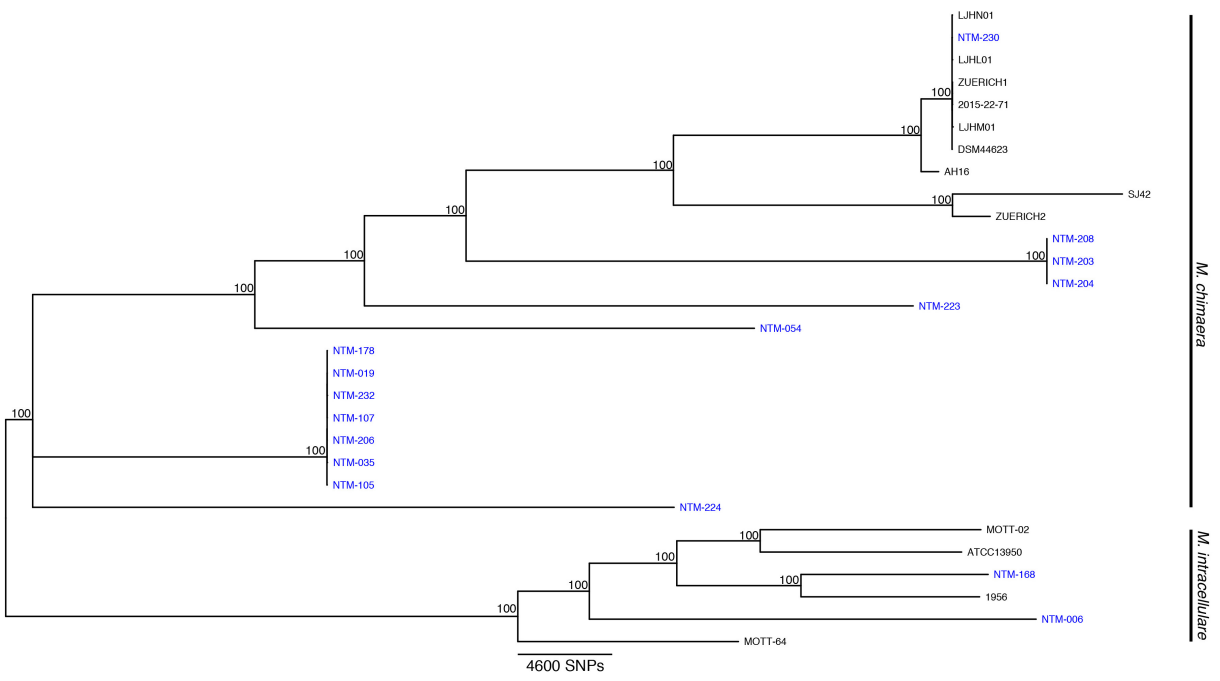

FIGURE 1 | *Mycobacterium chimaera and Mycobacterium intracellulare* whole genome phylogenomic tree. Available whole genome data from *M. chimaera* and *M. intracellulare* were used to visualize the relationships of 16 strains for this study (in blue) and 13 reference strains in comparison to the reference genome of *M. chimaera* CDC 2015-22-71. Bootstrap support values are given at nodes, scale bar for SNP distances is at bottom of figure.

the initial European sample set during test design. A number of these strains cluster more closely with the *M. chimaera* reference strains (samples 178, 019, 232, etc.), although they are arguably relatively distant from any available reference. The dynamic nature of bacterial phylogenomics requires us to integrate currently available references and whole genome approaches with an understanding that species nomenclature is always evolving as new branches and clades become apparent.

With increasing numbers of *M. chimaera* and *M. intracellulare* isolates requiring species identification in diagnostic reference laboratories, it is clear that improved tools are needed to quickly and accurately identify and distinguish these close mycobacterial species, in most cases inseparable using average nucleotide identity measures (**Supplementary Table S1**). We observe a qualitative difference in genome size for these two species and performed a statistical comparison of available complete reference genomes from *M. chimaera* (mean ± 1s.d., 6.24 ± 0.29Mb, $n = 8$) and *M. intracellulare* (5.52 ± 0.12Mb, $n = 6$), and found that *M. chimaera* was consistently larger by ∼700,000 bases ($p < 0.001$, Mann-Whitney U test.) This information may provide a path to discovering markers that can distinguish the two species, but the standard and reliable tools used to distinguish most NTM from one another often fail to discriminate between these very closely related strains. The discerning capability of the Bruker Subtyper module with MALDI spectral data offers an available and notable advance in MAC species identification.

AUTHOR CONTRIBUTIONS

MT, MK, GS, and MaS designed the study. LEE wrote the manuscript and performed whole genome sequencing. NKH, PG, and DD performed *rpoB* sequencing and MALDI-TOF analysis. MT, MK, and GS performed parallel MALDI-TOF spectral analysis and developed and implemented the subtyping software. NAH analyzed whole genome sequencing data, extracted loci of interest, and created visualizations. All authors contributed to writing, editing, and overall presentation of the manuscript.

ACKNOWLEDGMENTS

We thank Sara Kammlade and Rebecca Davidson for providing genomic ANIs. LEE, NAH, MiS, and MaS thank the Cystic Fibrosis Foundation, NICK15R0.

SUPPLEMENTARY MATERIAL

The Supplementary Material for this article can be found online at: https://www.frontiersin.org/articles/10.3389/fmicb.2018.03140/full#supplementary-material

REFERENCES

Adekambi, T., Colson, P., and Drancourt, M. (2003). rpoB-based identification of nonpigmented and late-pigmenting rapidly growing mycobacteria. *J. Clin. Microbiol.* 41, 5699–5708. doi: 10.1128/JCM.41.12.5699-5708.2003

Alcaide, F., Amlerova, J., Bou, G., Ceyssens, P. J., Coll, P., Corcoran, D., et al. (2018). Genomics European Study Group on, and Diagnosis Molecular. How to: identify non-tuberculous Mycobacterium species using MALDI-TOF mass spectrometry. *Clin. Microbiol. Infect.* 24, 599–603. doi: 10.1016/j.cmi.2017.11.012

Ben Salah, I., Adekambi, T., Raoult, D., and Drancourt, M. (2008). rpoB sequence-based identification of *Mycobacterium avium* complex species. *Microbiology* 154, 3715–3723. doi: 10.1099/mic.0.2008/020164-0

Boyle, D. P., Zembower, T. R., and Qi, C. (2015a). Evaluation of Vitek MS for rapid classification of clinical isolates belonging to *Mycobacterium avium* complex. *Diagn. Microbiol. Infect. Dis.* 81, 41–43. doi: 10.1016/j.diagmicrobio.2014.09.026

Boyle, D. P., Zembower, T. R., Reddy, S., and Qi, C. (2015b). Comparison of clinical features, virulence, and relapse among *Mycobacterium avium* complex species. *Am. J. Respir. Crit. Care Med.* 191, 1310–1317. doi: 10.1164/rccm.201501-0067OC

Carbonnelle, E., Mesquita, C., Bille, E., Day, N., Dauphin, B., Beretti, J. L., et al. (2011). MALDI-TOF mass spectrometry tools for bacterial identification in clinical microbiology laboratory. *Clin. Biochem.* 44, 104–109. doi: 10.1016/j.clinbiochem.2010.06.017

Castejon, M., Menendez, M. C., Comas, I., Vicente, A., and Garcia, M. J. (2018). Whole-genome sequence analysis of the *Mycobacterium avium* complex and proposal of the transfer of *Mycobacterium yongonense* to *Mycobacterium intracellulare* subsp. *yongonense* subsp. nov. *Int. J. Syst. Evol. Microbiol.* 68, 1998–2005. doi: 10.1099/ijsem.0.002767

Chalupova, J., Raus, M., Sedlarova, M., and Sebela, M. (2014). Identification of fungal microorganisms by MALDI-TOF mass spectrometry. *Biotechnol. Adv.* 32, 230–241. doi: 10.1016/j.biotechadv.2013.11.002

Costa-Alcalde, J. J., Barbeito-Castineiras, G., Gonzalez-Alba, J. M., Aguilera, A., Galan, J. C., and Perez-Del-Molino, M. L. (2018). Comparative evaluation of the identification of rapidly growing non-tuberculous mycobacteria by mass spectrometry (MALDI-TOF MS), GenoType Mycobacterium CM/AS assay and partial sequencing of the rpobeta gene with phylogenetic analysis as a reference method. *Enferm. Infect. Microbiol. Clin.* doi: 10.1016/j.eimc.2018.04.012 [Epub ahead of print].

Davidson, R. M., Hasan, N. A., Reynolds, P. R., Totten, S., Garcia, B., Levin, A., et al. (2014). Genome sequencing of *Mycobacterium abscessus* isolates from patients in the United States and comparisons to globally diverse clinical strains. *J. Clin. Microbiol.* 52, 3573–3582. doi: 10.1128/JCM.01144-14

Diel, R., Nienhaus, A., Ringshausen, F. C., Richter, E., Welte, T., Rabe, K. F., et al. (2018). Microbiologic outcome of interventions against *Mycobacterium avium* complex pulmonary disease: a systematic review. *Chest* 153, 888–921. doi: 10.1016/j.chest.2018.01.024

Doern, C. D., and Butler-Wu, S. M. (2016). Emerging and future applications of matrix-assisted laser desorption ionization Time-of-flight (MALDI-TOF) mass spectrometry in the clinical microbiology laboratory: a report of the association for molecular pathology. *J. Mol. Diagn.* 18, 789–802. doi: 10.1016/j.jmoldx.2016.07.007

Florio, W., Tavanti, A., Barnini, S., Ghelardi, E., and Lupetti, A. (2018). Recent advances and ongoing challenges in the diagnosis of microbial infections by MALDI-TOF mass spectrometry. *Front. Microbiol.* 9:1097. doi: 10.3389/fmicb.2018.01097

Forbes, B. A., Hall, G. S., Miller, M. B., Novak, S. M., Rowlinson, M. C., Salfinger, M., et al. (2018). Practice guidelines for clinical microbiology laboratories: mycobacteria. *Clin. Microbiol. Rev.* 31:e00038-17. doi: 10.1128/CMR.00038-17

Goris, J., Konstantinidis, K. T., Klappenbach, J. A., Coenye, T., Vandamme, P., and Tiedje, J. M. (2007). DNA-DNA hybridization values and their relationship to

whole-genome sequence similarities. *Int. J. Syst. Evol. Microbiol.* 57, 81–91. doi: 10.1099/ijs.0.64483-0

Hasan, N. A., Lawsin, A., Perry, K. A., Alyanak, E., Toney, N. C., Malecha, A., et al. (2017). Complete genome sequence of *Mycobacterium chimaera* strain CDC2015-22-71. *Genome Announc.* 5:e00693-17. doi: 10.1128/genomeA.00693-17

Huang, T. S., Lee, C. C., Tu, H. Z., and Lee, S. S. (2018). Rapid identification of mycobacteria from positive MGIT broths of primary cultures by MALDI-TOF mass spectrometry. *PLoS One* 13:e0192291. doi: 10.1371/journal.pone.0192291

Jiang, H., Lei, R., Ding, S. W., and Zhu, S. (2014). Skewer: a fast and accurate adapter trimmer for next-generation sequencing paired-end reads. *BMC Bioinformatics* 15:182. doi: 10.1186/1471-2105-15-182

Käser, M., Ruf, M. T., Hauser, J., and Pluschke, G. (2010). Optimized DNA preparation from mycobacteria. *Cold Spring Harb. Protoc.* 2010:pdb.prot5408. doi: 10.1101/pdb.prot5408

Kim, S. Y., Shin, S. H., Moon, S. M., Yang, B., Kim, H., Kwon, O. J., et al. (2017). Distribution and clinical significance of *Mycobacterium avium* complex species isolated from respiratory specimens. *Diagn. Microbiol. Infect. Dis.* 88, 125–137. doi: 10.1016/j.diagmicrobio.2017.02.017

Kozlov, A., Diego, D., Tomas, F., Benoit, M., and Alexandros, S. (2018). RAxML-NG: a fast, scalable, and user-friendly tool for maximum likelihood phylogenetic inference. *bioRxiv* [Preprint]. doi: 10.1101/447110

Langmead, B., and Salzberg, S. L. (2012). Fast gapped-read alignment with Bowtie 2. *Nat. Methods* 9, 357–359. doi: 10.1038/nmeth.1923

Lecorche, E., Haenn, S., Mougari, F., Kumanski, S., Veziris, N., Benmansour, H., et al. (2018). Comparison of methods available for identification of *Mycobacterium chimaera*. *Clin. Microbiol. Infect.* 24, 409–413. doi: 10.1016/j.cmi.2017.07.031

Levesque, S., Dufresne, P. J., Soualhine, H., Domingo, M. C., Bekal, S., Lefebvre, B., et al. (2015). A side by side comparison of bruker biotyper and VITEK MS: utility of MALDI-TOF MS technology for microorganism identification in a public health reference laboratory. *PLoS One* 10:e0144878. doi: 10.1371/journal.pone.0144878

Leyer, C., Gregorowicz, G., Mougari, F., Raskine, L., Cambau, E., and de Briel, D. (2017). Comparison of Saramis 4.12 and IVD 3.0 Vitek MS matrix-assisted laser desorption ionization-time of flight mass spectrometry for identification of mycobacteria from solid and liquid culture media. *J. Clin. Microbiol.* 55, 2045–2054. doi: 10.1128/JCM.00006-17

Li, H., Handsaker, B., Wysoker, A., Fennell, T., Ruan, J., Homer, N., et al. (2009). Genome project data processing subgroup. 2009. The sequence alignment/map format and SAMtools. *Bioinformatics* 25, 2078–2079. doi: 10.1093/bioinformatics/btp352

Murcia, M. I., Tortoli, E., Menendez, M. C., Palenque, E., and Garcia, M. J. (2006). *Mycobacterium colombiense* sp. nov., a novel member of the *Mycobacterium avium* complex and description of MAC-X as a new ITS genetic variant. *Int. J. Syst. Evol. Microbiol.* 56, 2049–2054. doi: 10.1099/ijs.0.64190-0

Neville, S. A., Lecordier, A., Ziochos, H., Chater, M. J., Gosbell, I. B., Maley, M. W., et al. (2011). Utility of matrix-assisted laser desorption ionization-time of flight mass spectrometry following introduction for routine laboratory bacterial identification. *J. Clin. Microbiol.* 49, 2980–2984. doi: 10.1128/JCM.00431-11

Page, A. J., Taylor, B., Delaney, A. J., Soares, J., Seemann, T., Keane, J. A., et al. (2016). SNP-sites: rapid efficient extraction of SNPs from multi-FASTA alignments. *Microb. Genom.* 2:e000056. doi: 10.1099/mgen.0.000056

Pranada, A. B., Witt, E., Bienia, M., Kostrzewa, M., and Timke, M. (2017). Accurate differentiation of *Mycobacterium chimaera* from *Mycobacterium intracellulare* by MALDI-TOF MS analysis. *J. Med. Microbiol.* 66, 670–677. doi: 10.1099/jmm.0.000469

Rahi, P., Prakash, O., and Shouche, Y. S. (2016). Matrix-assisted laser desorption/ionization time-of-flight mass-spectrometry (MALDI-TOF MS) based microbial identifications: challenges and scopes for microbial ecologists. *Front. Microbiol.* 7:1359. doi: 10.3389/fmicb.2016.01359

Richter, M., and Rossello-Mora, R. (2009). Shifting the genomic gold standard for the prokaryotic species definition. *Proc. Natl. Acad. Sci. U.S.A.* 106, 19126–19131. doi: 10.1073/pnas.0906412106

Schweickert, B., Goldenberg, O., Richter, E., Gobel, U. B., Petrich, A., Buchholz, P., et al. (2008). Occurrence and clinical relevance of *Mycobacterium chimaera* sp. nov., Germany. *Emerg. Infect. Dis.* 14, 1443–1446. doi: 10.3201/eid1409.071032

Springer, B., Stockman, L., Teschner, K., Roberts, G. D., and Bottger, E. C. (1996). Two-laboratory collaborative study on identification of mycobacteria: molecular versus phenotypic methods. *J. Clin. Microbiol.* 34, 296–303.

Tortoli, E., Rindi, L., Garcia, M. J., Chiaradonna, P., Dei, R., Garzelli, C., et al. (2004). Proposal to elevate the genetic variant MAC-A, included in the *Mycobacterium avium* complex, to species rank as *Mycobacterium chimaera* sp. nov. *Int. J. Syst. Evol. Microbiol.* 54, 1277–1285. doi: 10.1099/ijs.0.02777-0

van Ingen, J., Hoefsloot, W., Buijtels, P. C., Tortoli, E., Supply, P., Dekhuijzen, P. N., et al. (2012). Characterization of a novel variant of *Mycobacterium chimaera*. *J. Med. Microbiol.* 61, 1234–1239. doi: 10.1099/jmm.0.045070-0

van Ingen, J., Kohl, T. A., Kranzer, K., Hasse, B., Keller, P. M., and Katarzyna, A. (2017). Global outbreak of severe *Mycobacterium chimaera* disease after cardiac surgery: a molecular epidemiological study. *Lancet Infect. Dis.* 17, 1033–1041. doi: 10.1016/S1473-3099(17)30324-9

Wick, R. R., Judd, L. M., Gorrie, C. L., and Holt, K. E. (2017). Unicycler: resolving bacterial genome assemblies from short and long sequencing reads. *PLoS Comput. Biol.* 13:e1005595. doi: 10.1371/journal.pcbi.1005595

Yu, G., Smith, D. K., Zhu, H., Guan, Y., and Lam, T. T.-Y. (2017). ggtree: an R package for visualization and annotation of phylogenetic trees with their covariates and other associated data. *Methods Ecol. Evol.* 8, 28–36. doi: 10.1111/2041-210X.12628

Conflict of Interest Statement: MT and MK are employed by Bruker Daltoniks and GS by Bruker Daltonics.

The remaining authors declare that the research was conducted in the absence of any commercial or financial relationships that could be construed as a potential conflict of interest.

frontiers in Microbiology

ORIGINAL RESEARCH
published: 03 April 2018
doi: 10.3389/fmicb.2018.00587

MALDI Spectra Database for Rapid Discrimination and Subtyping of *Mycobacterium kansasii*

Jayaseelan Murugaiyan[1], Astrid Lewin[2], Elisabeth Kamal[2], Zofia Bakuła[3], Jakko van Ingen[4], Vit Ulmann[5], Miren J. Unzaga Barañano[6], Joanna Humięcka[7], Aleksandra Safianowska[8], Uwe H. Roesler[1] and Tomasz Jagielski[3]**

[1] Centre for Infectious Medicine, Institute of Animal Hygiene and Environmental Health, Freie Universität Berlin, Berlin, Germany, [2] Division 16, Mycotic and Parasitic Agents and Mycobacteria, Robert Koch Institute, Berlin, Germany, [3] Department of Applied Microbiology, Faculty of Biology, Institute of Microbiology, University of Warsaw, Warsaw, Poland, [4] Department of Medical Microbiology, Radboud University Medical Center, Nijmegen, Netherlands, [5] Institute of Public Health, Ostrava, Czechia, [6] Clinical Microbiology and Infection Control, Basurto Hospital, Bilbao, Spain, [7] Hospital for Infectious Diseases in Warsaw, Medical University of Warsaw, Warsaw, Poland, [8] Department of Internal Medicine, Pulmonology, and Allergology, Medical University of Warsaw, Warsaw, Poland

OPEN ACCESS

Edited by:
Veronique Anne Dartois, Rutgers University–Newark, United States

Reviewed by:
An Van Den Bossche, Institut Scientifique de Santé Publique, Belgium
Haiqing Chu, Shanghai Pulmonary Hospital, China

***Correspondence:**
Jayaseelan Murugaiyan
jayaseelan.murugaiyan@fu-berlin.de
Tomasz Jagielski
t.jagielski@biol.uw.edu.pl

Specialty section:
This article was submitted to Antimicrobials, Resistance and Chemotherapy, a section of the journal Frontiers in Microbiology

Received: *10 January 2018*
Accepted: *14 March 2018*
Published: *03 April 2018*

Citation:
Murugaiyan J, Lewin A, Kamal E, Bakuła Z, van Ingen J, Ulmann V, Unzaga Barañano MJ, Humięcka J, Safianowska A, Roesler UH and Jagielski T (2018) MALDI Spectra Database for Rapid Discrimination and Subtyping of Mycobacterium kansasii. Front. Microbiol. 9:587. doi: 10.3389/fmicb.2018.00587

Mycobacterium kansasii is an emerging non-tuberculous mycobacterial (NTM) pathogen capable of causing severe lung disease. Of the seven currently recognized *M. kansasii* genotypes (I-VII), genotypes I and II are most prevalent and have been associated with human disease, whereas the other five (III-VII) genotypes are predominantly of environmental origin and are believed to be non-pathogenic. Subtyping of *M. kansasii* serves as a valuable tool to guide clinicians in pursuing diagnosis and to initiate the proper timely treatment. Most of the previous rapid diagnostic tests for mycobacteria employing the matrix-assisted laser desorption/ionization time-of-flight mass spectrometry (MALDI-TOF MS) technology focused on species-level identification. The purpose of this study was to establish MALDI-TOF MS reference spectra database for discrimination of *M. kansasii* at the genotype level. A panel of 32 strains, representatives of *M. kansasii* genotypes I-VI were selected, whole cell proteins extracted and measured with MALDI-TOF MS. A unique main spectra (MSP) library was created using MALDI Biotyper Compass Explorer software. The spectra reproducibility was assessed by computing composite correlation index and MSPs cross-matching. One hundred clinical *M. kansasii* isolates used for testing of the database resulted in 90% identification at genus-level, 7% identification at species-level and 2% identification was below the threshold of log score value 1.7, of which all were correct at genotype level. One strain could not be identified. On the other hand, 37% of strains were identified at species level, 40% at genus level and 23% was not identified with the manufacturer's database. The MALDI-TOF MS was proven a rapid and robust tool to detect and differentiate between *M. kansasii* genotypes. It is concluded that MALDI-TOF MS has a potential to be incorporated into the routine diagnostic workflow of *M. kansasii* and possibly other NTM species.

Keywords: Biotyper, matrix-assisted laser desorption ionization—time of flight mass spectrometry, microflex, *Mycobacterium kansasii*, genotypes

INTRODUCTION

Mycobacterium kansasii is one of the leading causative agents of pulmonary and extrapulmonary infections due to non-tuberculous mycobacteria (NTM). It is also among the top six most frequently isolated NTM species across the world. The isolation rate of this pathogen is exceptionally high in Slovakia, Poland, and the UK, that is 36, 35, and 11% respectively, compared to a mean isolation rate of 5% in Europe and 4% globally (Hoefsloot et al., 2013).

The major clinical manifestations attributable to *M. kansasii* include fibro-cavitary or nodular-bronchiectatic lung disease, lymphadenitis, skin, and soft-tissue infections, and disseminated disease (van Ingen and Kuijper, 2014).

Pulmonary diseases caused by *M. kansasii* tend to cluster in specific geographical areas, such as central Europe or metropolitan centers of London, Brasilia, and Johannesburg (Hoefsloot et al., 2013). In most of the countries there is no obligation of registration of such cases, thus the true incidence of *M. kansasii* disease is largely unknown. The estimated incidence of infections due to this pathogen, reported in the general population, fall within the range of 0.3–1.5 cases per 100,000 (Santin et al., 2004; Moore et al., 2010; Namkoong et al., 2016).

As with other NTM, *M. kansasii* infections are believed to be acquired from environmental exposures rather than by person-to-person transmission. Rarely has *M. kansasii* been isolated from soil, natural water systems or animals. Instead, the pathogen has commonly been recovered from municipal tap water, which is considered to be its major environmental reservoir (Thomson et al., 2014).

The existence of five (I–V) distinct *M. kansasii* types was initially evidenced by unique DNA profiles they produced upon hybridization with the major polymorphic tandem repeat (MPTR) probe, pulsed-field gel electrophoresis (PFGE), amplified fragment length polymorphism (AFLP) analysis, and PCR restriction enzyme analysis (PCR-REA) of the *hsp65* gene (Alcaide et al., 1997; Picardeau et al., 1997). In somewhat later studies two novel types (VI and VII) have been described, with similar methods (Taillard et al., 2003). This intra-species polymorphism has important clinical and epidemiological implications. Genotypes I and II have been involved in human disease, with the former being the most prevalent, whereas the remaining genotypes have usually been non-pathogenic. Therefore, recovery of *M. kansasii* type I and II isolates from clinical specimens should raise a clinical suspicion of *M. kansasii* disease. Furthermore, *M. kansasii* type I has been found more likely to be recovered from immunocompetent individuals, whereas type II has been linked to patients with some form of immunosuppression (Taillard et al., 2003). Furthermore, despite a paucity of studies, there seems to be some genotype-specific differences in drug susceptibility profiles. For instance, clarithromycin resistance appears to be associated with *M. kansasii* type I (Li et al., 2016), while *M. kansasii* type V, contrary to all other types, shows susceptibility to ethambutol (Bakuła et al., 2018). Currently, identification of *M. kansasii* genotypes is performed by PCR-sequencing or PCR-REA of the *hsp65*, *rpoB*, and *tuf* genes (Telenti et al., 1993; Kim et al., 2001; Bakuła et al., 2016). These methods, though accurate and reproducible, require post-PCR manipulations, which are time-consuming and laborious. A fast, reliable and automated screening method for *M. kansasii* genotype determination is needed.

In the past two decades, MALDI-TOF MS-based species identification has been integrated into the routine diagnostic workflow in microbiology laboratories due to its rapidness, reliability, cost-effectiveness, and high throughput. A prerequisite for MALDI-TOF MS profiling is a robustly established reference spectra database. The growing accessibility of MALDI-TOF MS instruments along with spectra pattern matching software databases made that the interest in this technology and its applications across research and diagnosis has exponentially increased (Wattal et al., 2017).

In this study, a commercially available software package, MALDI Biotyper (Bruker Daltonics) was used for creation of genotype-specific reference database of *M. kansasii*.

MATERIALS AND METHODS

Mycobacteria Strains and Isolates

A total of 32 strains, representing I-VI genotypes of *Mycobacterium kansasii* were used to establish a MALDI-TOF MS spectra reference database (**Table 1**). In addition, 100 clinical *M. kansasii* isolates were used for evaluation of the database. The species identity of these isolates was confirmed with the high-pressure liquid chromatography (HPLC). Genomic DNA was extracted with the AMPLICOR Respiratory Specimen Preparation Kit (Roche, Basel, Switzerland). Genotyping was performed upon PCR-REA of *hsp65* and *tuf* genes, as previously described (Telenti et al., 1993; Bakuła et al., 2016).

Culture and Protein Extraction

A single bacterial colony was picked from Löwenstein-Jensen (L-J) slant and used for inoculation of 10 mL of Middlebrook 7H9 medium supplemented with glycerol and OADC (10%) (Becton-Dickinson, Franklin Lakes, USA). The bacteria were cultured at 37°C with shaking for 7 days. Each strain/isolate was cultured independently for three independent replicates. The cells were harvested by brief centrifugation (4,500 rpm, 2 min) and killed by suspending in 300 µL of deionized water and 900 µL of absolute ethanol. After centrifugation (12,000 rpm, 2 min) at room temperature (RT), excessive ethanol was discarded and the samples were air-dried completely. The cell pellet was dissolved in 50 µL of 70% formic acid and 50 µL acetonitril. The samples were then subjected to sonication on ice for 1 min (cycle, 1.0; amplitude, 100%) using a sonicator (UP100H, Hielscher Ultrasound Technology, Teltow, Germany). The suspension was centrifuged at 12,000 rpm for 2 min at RT, and 1.0 µL of the clear supernatant was spotted in triplicate onto the MALDI target (MSP 96 target polished steel (MicroScout Target) plate, Bruker Daltonik, Bremen, Germany). Following

Abbreviations: MALDI-TOF MS, Matrix-assisted laser desorption ionization-time-of-flight mass spectrometry; MSP, main spectra libraries.

TABLE 1 | *M. kansasii* strains and their genotypes utilized for generation of reference spectra.

S. No	Strain designation	Genotype	Source	NTM disease	Country
1	*M. kansasii* ATCC12478^T	I	No data	Yes	USA
2	*M. kansasii* ATCC25221^T		Sputum	Yes	Germany
3	*M. kansasii* NLA001000449		Sputum	Yes	Netherlands
4	*M. kansasii* NLA001000521		Bronchoalveolar lavage fluid	Yes	Netherlands
5	*M. kansasii* 1502/11		Bronchoalveolar lavage fluid	Yes	Poland
6	*M. kansasii* 803/13		Bronchial washing	Yes	Poland
7	*M. kansasii* 5482/08		Bronchial washing	Yes	Poland
8	*M. kansasii* 305/01		Sputum	No	Poland
9	*M. kansasii* 1010001495^E		Water	–	Czech Republic
10	*M. kansasii* 10130/12		No data	Yes	Germany
11	*M. kansasii* 4911/16		Sputum	Yes	Germany
12	*M. kansasii* 8034/16		Bronchoalveolar lavage fluid	Yes	Germany
13	*M. kansasii* 8050/16		No data	Yes	Germany
14	*M. kansasii* 8091/16		No data	Yes	Germany
15	*M. kansasii* 8112/16		Bronchoalveolar lavage fluid	Yes	Germany
16	*M. kansasii* 8617/16		Sputum	Yes	Germany
17	*M. kansasii* B11063838	II	Bronchoalveolar lavage fluid	No	Netherlands
18	*M. kansasii* B11073207		Sputum	No	Netherlands
19	*M. kansasii* NLA001001128		Bronchoalveolar lavage fluid	No	Netherlands
20	*M. kansasii* 2193/11		Bronchial washing	No	Poland
21	*M. kansasii* 1010001469^E		Water	–	Italy
22	*M. kansasii* 8190/16		Tracheal secretion	Yes	Germany
23	*M. kansasii* 8709/16		Bronchial secretion	Yes	Germany
24	*M. kansasii* 1010001468^E	III	Soil	–	Belgium
25	*M. kansasii* 8197/16		No data	Yes	Germany
26	*M. kansasii* 101		No data	Yes	Germany
27	*M. kansasii* 1010001458^E	IV	Tap water	–	Germany
28	*M. kansasii* 1010001454^E	V	Tap water	–	Germany
29	*M. kansasii* 1010001493^E		Water	–	Netherlands
30	*M. kansasii* 6097/16		Bronchial secretion	Yes	Germany
31	*M. kansasii* NLA001001166	VI	Sputum	No	Netherlands
32	*M. kansasii* NTM G7 Lu1		Gundi, lung tissue	Yes	Germany

^{T}*Type strain,* ^{E}*Environmental isolate.*

air drying each sample was overlaid with 1.0 μL of saturated α-cyano-4-hydroxycinnamic acid matrix solution and allowed to dry completely prior to MALDI-TOF measurement.

MALDI Measurements

Bruker MALDI Microflex LT (Bruker Daltonics, Bremen, Germany) with a linear positive mode of spectra acquisition, at a laser frequency of 20 Hz was used for the measurements. A broad m/z range (2,000–20,000 kDa) of spectra was automatically acquired using the AutoXecute acquisition control software (Flex control 3.0, Bruker Daltonics, Leipzig, Germany) with the following instrument settings: ion source 1 at 20 kV, ion source 2 at 16.7 kV, lens at 6 kV, extraction delay time of 150 ns, 240 laser shots/spot in 40 shot steps (random walk movement), initial laser power of 45%, maximal laser power of 55%, laser attenuation Offset of 46% and at the range 30%). The bacterial test standard (BTS) mixture covering the mass range between 2,000 and 20,000 Da (BTS, Bruker Daltonics, Bremen, Germany), was used for external calibration.

MSP Library Construction

The spectra quality and reproducibility were assessed by using Flex analysis 3.0 software (Bruker Daltonics, Bremen, Germany). For every strain/isolate, 27 spectra representing three independent culturing and three technical replicates and 3 measurements per replicate were collected. The raw spectra were loaded in the MALDI Biotyper Compass Explorer 4.1 and matched against the commercial BDAL database—updated

version 6.0.0.0 with 6,903 Main Spectra (MSP) entries (including 75 for mycobacteria with seven genotype undefined *M. kansasii* entries)—plus the in-house entries of *Staphylococcus intermedius* group of microorganisms (60 entries) (Murugaiyan et al., 2014) and microalgae *Prototheca* species (23 entries) (Murugaiyan et al., 2012). The spectra preprocessing parameters included mass adjustment (lower bound- 3,000, upper bound- 15,000; resolution-1 and spectra compressing factor- 10), smoothing (Savitzky-Golay algorithm with a frame size of 25 Da), baseline correction (multipolygon with search window 5 Da and number of runs 2), normalization (maximum norm), and peak detection (spectra differentiation with maximum peaks of 100, signal-to-noise ratio 3 and threshold of 0.001). Main spectrum profiles (MSPs) were created for each strain using the following parameters: maximum mass error for each single spectrum 2,000, mass error for the MSP 100, peak frequency minimum 70%, and maximum peak number 70. The details of the newly created reference spectra will be listed at the MALDI-UP, an online platform for the MALDI-TOF mass spectra (Rau et al., 2016) to facilitate exchange of the reference spectra as btmsp files with users from other laboratories.

Statistical Evaluations

To evaluate the spectral variation (similarity) between the spectra sets acquired from strains of all genotypes, the Composite Correlation Index (CCI) was calculated with MALDI Biotyper Compass Explorer 4.1. All measured spectra were loaded and CCI was computed using the following settings, mass lower bound 3,000, mass upper bound 12,000, resolution 4, and CCI parameter interval of 8. CCI value nearing 1.0 indicates the complete congruence and 0.0 – complete deviation within the spectra sets.

Following the creation of spectral reference database, the genotype discrimination limits were assessed by crosswise comparison by matching the newly created *M. kansasii* genotype-specific MSPs with an augmented BDAL commercial database described earlier. The resulted log score values of the first hits were imported into MS excel and conditional formatting, in accordance to the manufacturer's recommended cutoff log score values, was applied to generate a heat-map. The score-oriented MSP dendrogram (distance level: correlation and linkage: average) was also calculated using the MALDI Biotyper Compass Explorer 4.1 software to explore the closeness of the genotypes in terms of arbitrary distance level.

Blind Coded Sample Testing

For validation purposes, 100 clinical *M. kansasii* isolates and single reference strains of *M. conspicuum*, *M. marinum*, *M. szulgai*, and *M. gastri* were subjected to MALDI-TOF MS identification, by comparing with the database before and after addition of genotype-specific MSPs (**Supplementary Table 1**). The isolates used for validation, had previously been identified, as specified above and blind coded. The log score values for species discrimination, recommended by the manufacturer, were applied i.e., 0–1.699 indicating "no reliable identification", 1.7–1.999 indicating a "probable genus identification", 2.0–2.299 indicating a "secure genus identification and probable species identification" (PSI), and 2.300–3.000 indicating a "highly probable species identification."

RESULTS

A total of 32 strains representing genotypes I-VI of *M. kansasii* were used to establish *M. kansasii* genotype-specific reference spectra library. The choice of the strains was based on the availability of strains representing a given genotype and strains of genotype VII were not available in any of the culture collections. Each strain was cultured independently three times, each culture-derived extract was spotted three times, and each spot was measured three times on MALDI-TOF MS to generate 27 spectra in total per strain. Altogether, 864 spectra within the mass range of 2,000–20,000 Da were acquired. The spectra quality in terms of peak presence and intensity were assessed using Flex analysis software. The flat line spectra and low-intensity spectra were replaced by new measurement of the same spots or fresh spotting of the same protein extract.

As shown in **Figure 1**, different genotypes displayed distinct peak patterns and the spectral sets of each strain were fully reproducible and comparable.

The spectra of the same strains showed a high level of similarity, with the CCI value ranging from 0.78 to 0.94 (**Figure 2**). Genotype I displayed CCI within the range of 0.78 to 0.99 while it was between 0.82 and 0.91 for genotype II, 0.80 to 0.94 for genotype III, 0.83 for a single genotype IV strain, 0.83 to 0.94 for genotype V, and 0.88 to 0.91 for genotype VI. The resulted CCI values reflected the similarities of the measured spectra sets. The CCIs between different genotypes displayed lower values indicating the possibility for spectra fingerprinting of genotype level discrimination.

The created *M. kansasii* genotype MSPs were then matched to the augmented BDAL database described earlier to generate the cross-matching result. Then, the first hits log score values were imported in MS excel and a heat map was generated using MS excel conditional color formatting option following the manufacturer's cut-off values (**Supplementary Figure 1**). The MSPs of any given strain matched 100% with themselves, as indicated by the log score of 3.0, and had high matching scores with the other strains within a genotype. The seven strains without any genotype information included in the original version of the manufacturer's database, displayed higher score values among each other, although the MSPs had been configured upon a much lower number of spectra. The manufacturer's MSPs displayed log score values of >2.0 with several strains of newly added genotype I and borderline or genus-level matching was observed with genotype III, IV, and V strains. One of the manufacturer's MSP (S.No. 37) did not match any of the newly introduced genotype-specific MSPs.

In addition, the individual spectra used for MSP creation were matched first with the manufacturer's database (BDAL database-plus in-house entries of *Staphylococcus intermedius* group and microalgae *Prototheca* species) and then after introduction of our genotype-specific MSPs. This enhanced considerably the overall identification confidence and identification at the genotype level with first hits always being the same strain (**Figure 3**).

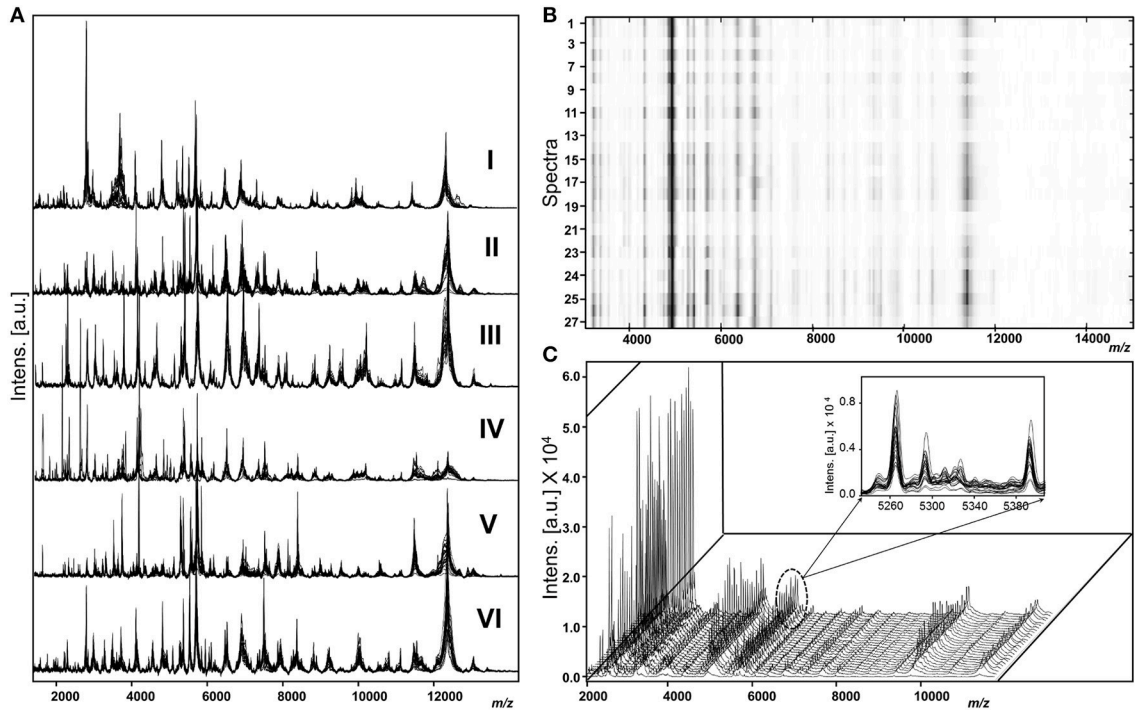

FIGURE 1 | Representative raw spectra of *M. kansasii* genotypes **(A)** overlaid view of spectra sets ($n = 27$) of genotype I (strain 1010001495), genotype II (Strain 2193/11), genotype III (strain1010001468), genotype IV (strain 1010001458), genotype V (strain 6097/16), and genotype VI (strain NLA 001001166). **(B)** Heat map view of spectra acquired from a single strain (genotype I strain 1010001495). **(C)** Stacked view indicating the uniformity among spectra acquired from a genotype I strain 1010001495 and highlighted overlaid view as an inserted figure.

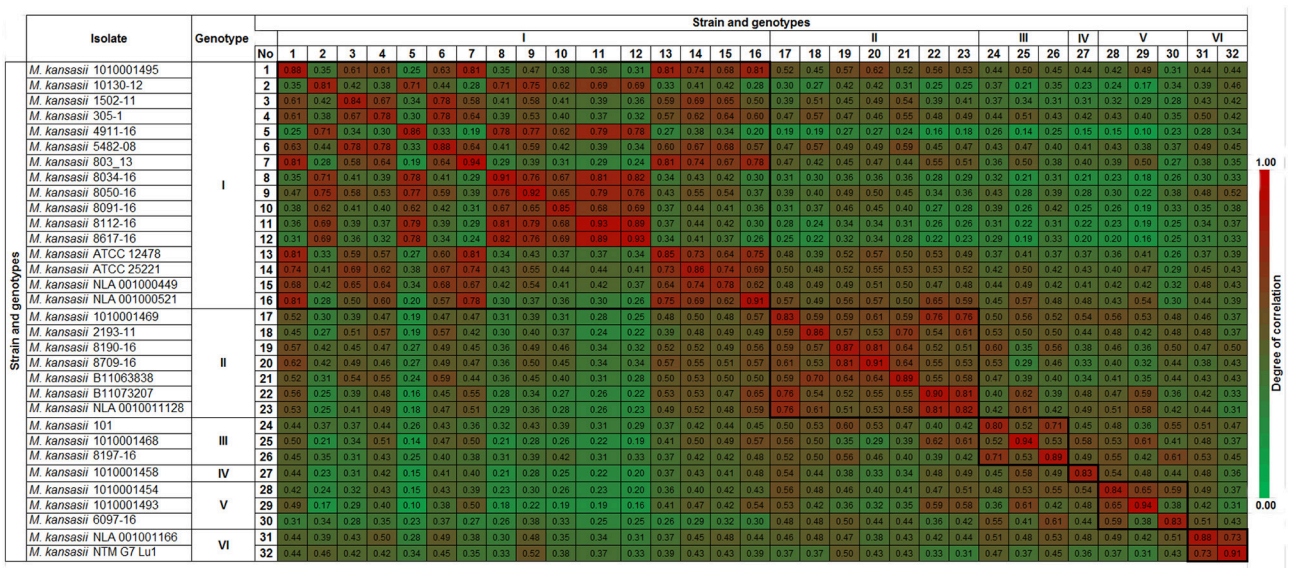

FIGURE 2 | Composite Correlation Index (CCI) matrix as calculated using Biotyper RTC software with the following parameter settings: 3,000 lower bound, 15,000 upper bound, mass range resolution of 4 and number of interval set at 4. The CCI values were extracted and the displayed image was redrawn using conditional formatting option in MS Excel. The CC value nearing 1.0 indicates the congruence among the measured spectra sets and 0 represents completely different spectra.

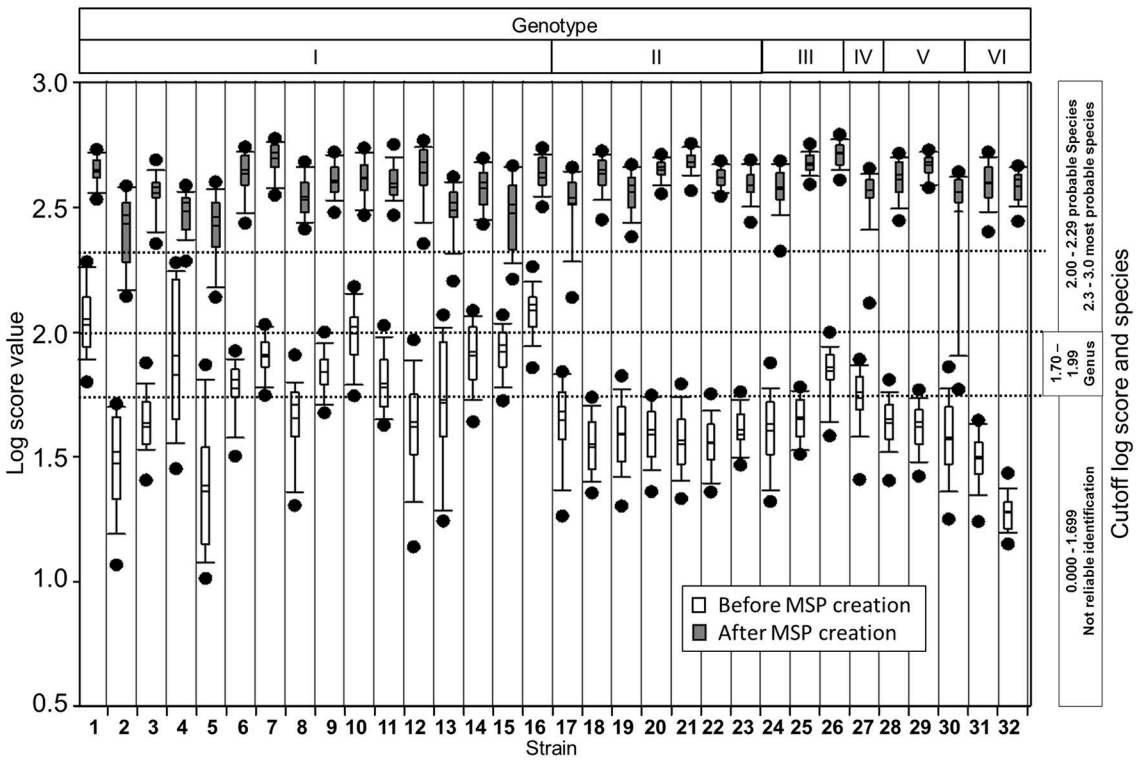

FIGURE 3 | Box plot of log score values before and after creation of in-house database for *M. kansasii* genotypes. Plots show mean and median (horizontal lines within each boxes), 5th and 95th percentiles (whiskers) and outliers (black dots) for each set of the measured spectra. Log score values compared to the database before (white boxes) and after (gray) creation of genotype-specific reference spectra indicate improvement in the identification confidence.

As shown in **Figure 4**, a score-oriented dendrogram demonstrated two major clusters. The first cluster contained all genotype I strains and two genotype VI strains. The second cluster accommodated all type II, III, IV, and V strains.

The augmented genotype-specific reference database was tested with 104 blind-coded samples, representing clinical isolates of *M. kansasii* ($n = 100$) and single strains of *M. conspicuum, M. gastri*, *M. marimum*, and *M. szulgai*, to find any cross-matching with *M. kansasii* database. The identification rates were significantly higher for the expanded MALDI Biotyper database when compared with the original library (**Table 2**). In **Figure 5**, a shift of identification confidence is shown for all 100 blind-coded *M. kansasii* samples (**Supplementary Table 1**). The augmented database resulted in an overall identification success rate of 97% isolates identified at the species/genotype level, among which 7 isolates, representatives of genotype I, were identified at the genus level. Two genotype I isolates could not be identified despite the first hit as the correct genotype but with log score value <1.7. One isolate (*M. kansasii* 17.14) did not display any improvement in the log score value despite the database augmentation. The results also indicated that, 89 strains belonged to genotype I (19-SI, 63-PSI, and 7-PGI), 4 – to genotype II, and 2 – to genotype III. Single isolates were recognized as representing genotypes IV and V. Whereas the MALDI Biotyper using the manufacture's BDAL database displayed "Not reliable identification" for 15% isolates of genotype I and six other genotype isolates. Two genotype II isolates were identified only as *Mycobacterium* sp.

DISCUSSION

MALDI-TOF MS profiling has been successfully employed in various commercial software packages allowing the identification of a wide array of *Mycobacterium* species, including *M. kansasii*. The discrimination of different *M. kansasii* genotypes is useful for the clinical categorization of *M. kansasii* infection, however, it has never been attempted by MALDI-TOF analysis (Pignone et al., 2006; El Khechine et al., 2011; Saleeb et al., 2011; Balada-Llasat et al., 2013; Chen et al., 2013; Machen et al., 2013; Mather et al., 2014; Mediavilla-Gradolph et al., 2015; Rodriguez-Sanchez et al., 2015; Wilen et al., 2015; Ceyssens et al., 2017; Leyer et al., 2017). *M. kansasii* genotype level information is still not included in the commercial reference database package, MBT Mycobacteria library. Previously, identification of *M. kansasii* with low spectral scores was linked to the intra-species heterogeneity, and supplementation of the database with additional strains of *M. kansasii* was proposed to remedy this problem (El Khechine et al., 2011; Saleeb et al., 2011). Responding to this necessity, this study established MSPs for all *M. kansasii* genotypes (I–VI), except for the genotype VII (Taillard et al., 2003), for which strains could not be retrieved in any of the culture collection, which could not be retrieved from any culture

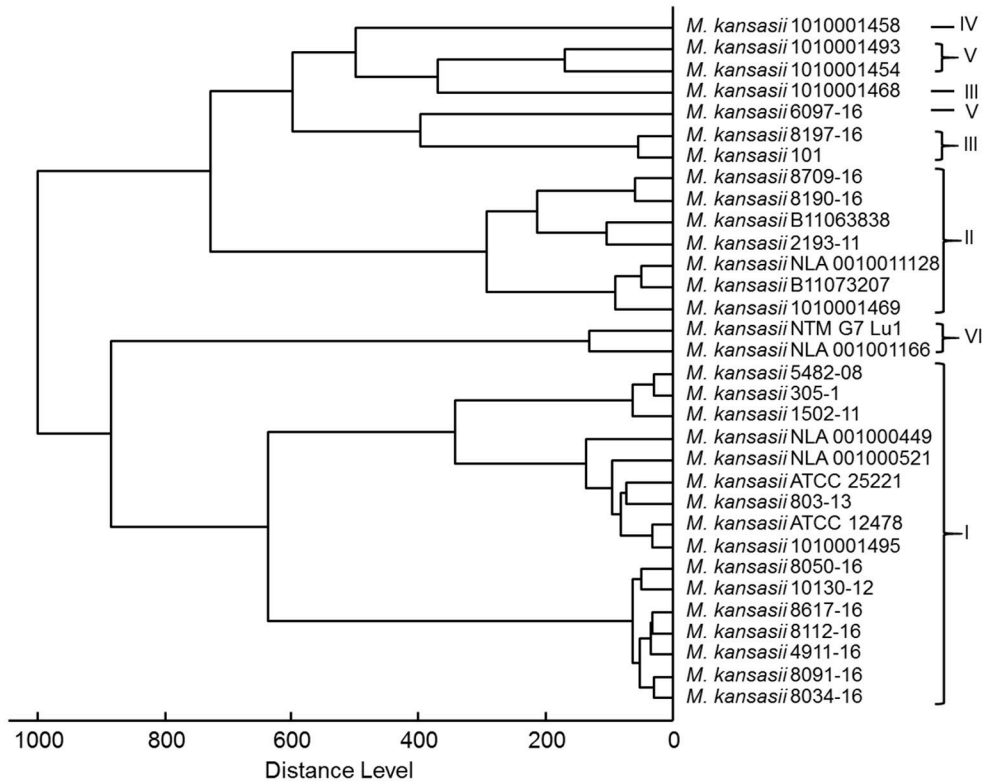

FIGURE 4 | Score-oriented dendrogram of genotype-specific MSPs (distance measure was set at correlation and linkage was set at complete).

collections. It has to be noted, however, that given the paucity of genotype II-VI strains, differentiation of these types may still pose certain difficulties, and much more strains would be needed to verify the genotype-specificity of the MALDI-TOF profiles established.

Inspection with Flex analysis software, the spectral profiles of the *M. kansasii* genotypes clearly showed their disparateness. At the same time, a high intra-genotype reproducibility of the spectra was demonstrated. The spectra sets acquired from the same strains and from strains representing the same genotypes were highly consistent, as evidenced with the computed CCI values.

The cross identification of the established MSPs together with seven MSPs originally deposited in the manufacturer's database resulted in a log score value of 3.0 indicating matching of the 70 most frequently encountered peaks of the species or genotypes. When compared against the manufacturer's database, with exception of genotypes I and II, whose spectra matched those of *M. kansasii*, all other genotypes produced spectra ascribable to merely *Mycobacterium* genus level. It clearly proved that the existing database is not sufficient for genotype-level discrimination of *M. kansasii*. Special mycobacteria library with lowered threshold log score values of 1.6 and 1.8 was implemented for genus and species identification. It was later reported that the log score values for *M. kansasii* were unchanged with the improved mycobacteria library (Rodríguez-Sánchez et al., 2016). In the present study, augmentation of genotype-specific MSPs resulted in an enhanced log score value, which indicates that the identification confidence improvement can be mainly achieved through inclusion of genotypically well-defined strains.

The grouping, as shown on score-oriented dendrogram, of genotypes I, II, and VI in three distinct clusters supports the potential of MALDI-TOF to easily differentiate between these three types. Whereas identification of genotypes III, IV, and V may pose certain difficulties, since they all belonged to a single cluster. Inclusion of additional strains of these genotypes may produce better identification scores.

The blind coded *M. kansasii* samples tested with augmented genotype specific MSPs resulted in an overall identification success rate of 97%. Eighty-eight (98%) out of 91 blinded coded samples of genotype I gave a genotype match, despite the fact that log score values for seven strains were within the genus level cutoff (1.7–1.99). Four strains of genotype II, two of genotype III, and single strains of genotype IV and V were used for blind coded study, which resulted in successful identification of all strains at the species level, otherwise, except one genotype II strain, all these strains resulted in log score value <1.7 before the MSP augmentation. Despite an exhaustive search through culture collections of *M. kansasii* strains, genotype II–IV strains were seriously underrepresented. According to previous studies, *M. kansasii* involved in human disease belong almost exclusively to genotypes I and II, with the former accounting for 42–100%

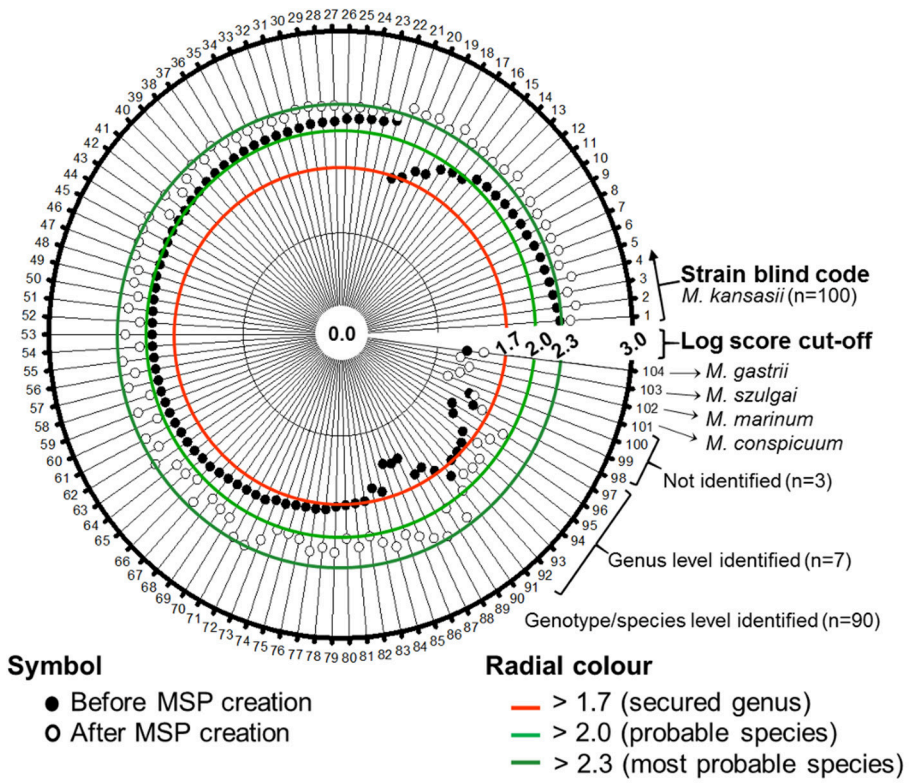

FIGURE 5 | Polar plot was constructed to show the enhancement of log score values of blind-coded *M. kansasii* isolates ($n = 100$). No difference in the log score values were observed for the four non-*M. kansasii* species included in the database evaluation.

TABLE 2 | Identification results of 100 blind-coded *M. kansasii* and one each of *M. conspicuum, M. marinum*, *M. szulgai*, and *M. gastri* strains using MALDI Biotyper Explorer Compass 4.1 reference database and after augmentation of genotype-specific reference database.

Identification result	Score	MALDI Biotyper explorer compass 4.1	Augmented genotype-specific database
Not reliable identification (NRI)	<1.7	23 (23%)	3 (3%)
Probable genus identification' (PGI)	1.7–2.0	40 (40%)	7 (7%)
Secure genus identification and probable species identification (PSI)	2.0–2.3	37 (37%)	69 (69%)
Highly probable species identification(SI)	>2.3	0	21 (21%)

of the clinical isolations (Alcaide et al., 1997; Bakuła et al., 2013). The other types (III-VII), only sporadically recovered, are predominantly of environmental origin (Alcaide et al., 1997; Santin et al., 2004). The reason why seven isolates could be identified at the genus level only, and three isolates unidentifiable at all can hardly be found. We propose that the addition of spectra from genotype II-VI from various geographical regions could enable accurate and rapid differentiation of these genotypes.

In conclusion, unique, reproducible spectra for six genotypes of *M. kansasii* were established. The expansion of the database with reference spectra resulted in successful species- and genotype-level identification despite the limited number of genotype II–VI strains. Overall, we believe that MALDI-TOF MS can easily be employed for efficient genotype-level discrimination of *M. kansasii* and that further augmentation of spectral patterns might enable fast and accurate diagnosis in future.

AUTHOR CONTRIBUTIONS

JM, TJ conceived and designed the work, acquired the data and wrote the manuscript. AL, EK, VU, MU, JH, and AS collected the strains and performed species-level identification. ZB performed species confirmation and genotype-level identification. JI and UR critically revised the manuscript. All authors had read and approved the submission version of the manuscript.

ACKNOWLEDGMENTS

The study was in part financed by the National Centre for Research and Development LIDER Programme [LIDER/044/457/L-4/12/NCBR/2013]. We are grateful to Elvira Richter (Labor Limbach, Heidelberg, Germany) and Katharina Kranzer, and Doris Hillemann (NRC for Mycobacteria, Borstel, Germany) for patient isolates of *M. kansasii*. We would like to

thank Michael Kühl (Freie Universitaet Berlin, Germany) for excellent technical assistance.

SUPPLEMENTARY MATERIAL

The Supplementary Material for this article can be found online at: https://www.frontiersin.org/articles/10.3389/fmicb.2018.00587/full#supplementary-material

Supplementary Figure 1 | MSP matching matrix was created by matching with *M. kansasii* genotype-specific MSPs augmented BDAL database. Color coded as per the manufacturer's recommendation on log score cutoff values.

Supplementary Table 1 | Blind coded isolates testing. Manufacturers recommended interpretation of score values were followed: from 0 to 1.699 indicates "no reliable identification" (Red); 1.7 to 1.999 indicate a "probable genus identification" (yellow); 2.0 to 2.299 indicate a "secure genus identification and probable species identification" (light green), and values from 2.300 to 3.000 indicate a "highly probable species identification" (intensive green).

REFERENCES

Alcaide, F., Richter, I., Bernasconi, C., Springer, B., Hagenau, C., Schulzerobbecke, R., et al. (1997). Heterogeneity and clonality among isolates of *Mycobacterium kansasii*: implications for epidemiological and pathogenicity studies. *J. Clin. Microbiol.* 35, 1959–1964.

Bakuła, Z., Modrzejewska, M., Pennings, L., Proboszcz, M., Safianowska, A., Bielecki, J., et al. (2018). Drug susceptibility profiling and genetic determinants of drug resistance in *Mycobacterium kansasii*. *Antimicrob. Agents Chemother.* doi: 10.1128/AAC.01788-17. [Epub ahead of print].

Bakuła, Z., Modrzejewska, M., Safianowska, A., van Ingen, J., Proboszcz, M., Bielecki, J., et al. (2016). Proposal of a new method for subtyping of *Mycobacterium kansasii* based upon PCR restriction enzyme analysis of the tuf gene. *Diagn. Microbiol. Infect. Dis.* 84, 318–321. doi: 10.1016/j.diagmicrobio.2015.12.009

Bakuła, Z., Safianowska, A., Nowacka-Mazurek, M., Bielecki, J., and Jagielski, T. (2013). Short communication: subtyping of *Mycobacterium kansasii* by PCR-restriction enzyme analysis of the hsp65 gene. *Biomed Res. Int.* 2013:178725. doi: 10.1155/2013/178725

Balada-Llasat, J. M., Kamboj, K., and Pancholi, P. (2013). Identification of mycobacteria from solid and liquid media by matrix-assisted laser desorption ionization-time of flight mass spectrometry in the clinical laboratory. *J. Clin. Microbiol.* 51, 2875–2879. doi: 10.1128/JCM.00819-13

Ceyssens, P. J., Soetaert, K., Timke, M., Van Den Bossche, A., Sparbier, K., De Cremer, K., et al. (2017). Matrix-assisted laser desorption ionization-time of flight mass spectrometry for combined species identification and drug sensitivity testing in Mycobacteria. *J. Clin. Microbiol.* 55, 624–634. doi: 10.1128/JCM.02089-16

Chen, J. H., Yam, W. C., Ngan, A. H., Fung, A. M., Woo, W. L., Yan, M. K., et al. (2013). Advantages of using matrix-assisted laser desorption ionization-time of flight mass spectrometry as a rapid diagnostic tool for identification of yeasts and mycobacteria in the clinical microbiological laboratory. *J. Clin. Microbiol.* 51, 3981–3987. doi: 10.1128/JCM.01437-13

El Khechine, A., Couderc, C., Flaudrops, C., Raoult, D., and Drancourt, M. (2011). Matrix-assisted laser desorption/ionization time-of-flight mass spectrometry identification of Mycobacteria in routine clinical practice. *PLoS ONE* 6:e24720. doi: 10.1371/journal.pone.0024720

Hoefsloot, W., van Ingen, J., Andrejak, C., Angeby, K., Bauriaud, R., Bemer, P., et al. (2013). The geographic diversity of nontuberculous mycobacteria isolated from pulmonary samples: an NTM-NET collaborative study. *Eur. Respir. J.* 42, 1604–1613. doi: 10.1183/09031936.00149212

Kim, B. J., Lee, K. H., Park, B. N., Kim, S. J., Bai, G. H., Kim, S. J., et al. (2001). Differentiation of mycobacterial species by PCR-restriction analysis of DNA (342 base pairs) of the RNA polymerase gene (rpoB). *J. Clin. Microbiol.* 39, 2102–2109. doi: 10.1128/JCM.39.6.2102-2109.2001

Leyer, C., Gregorowicz, G., Mougari, F., Raskine, L., Cambau, E., and De Briel, D. (2017). Comparison of Saramis 4.12 and IVD 3.0 Vitek Ms Matrix-assisted laser desorption ionization-time of flight mass spectrometry for identification of Mycobacteria from solid and liquid culture media. *J. Clin. Microbiol.* 55, 2045–2054. doi: 10.1128/JCM.00006-17

Li, Y., Pang, Y., Tong, X., Zheng, H., Zhao, Y., and Wang, C. (2016). *Mycobacterium kansasii* subtype I is associated with clarithromycin resistance in China. *Front. Microbiol.* 7:2097. doi: 10.3389/fmicb.2016.02097

Machen, A., Kobayashi, M., Connelly, M. R., and Wang, Y. F. (2013). Comparison of heat inactivation and cell disruption protocols for identification of Mycobacteria from solid culture media by use of vitek matrix-assisted laser desorption ionization-time of flight mass spectrometry. *J. Clin. Microbiol.* 51, 4226–4229. doi: 10.1128/JCM.02612-13

Mather, C. A., Rivera, S. F., and Butler-Wu, S. M. (2014). Comparison of the Bruker Biotyper and Vitek MS matrix-assisted laser desorption ionization-time of flight mass spectrometry systems for identification of mycobacteria using simplified protein extraction protocols. *J. Clin. Microbiol.* 52, 130–138. doi: 10.1128/JCM.01996-13

Mediavilla-Gradolph, M. C., De Toro-Peinado, I., Bermudez-Ruiz, M. P., Garcia-Martinez, M. D., Ortega-Torres, M., Quezel-Guerraz, N. M., et al. (2015). Use of MALDI-TOF MS for identification of nontuberculous Mycobacterium species isolated from clinical specimens. *BioMed Res. Int.* 2015:854078 doi: 10.1155/2015/854078

Moore, J. E., Kruijshaar, M. E., Ormerod, L. P., Dobroniewski, F., and Abubakar, I. (2010). Increasing reports of non-tuberculous mycobacteria in England, Wales and Northern Ireland, 1995–2006. *BMC Public Health* 10:612. doi: 10.1186/1471-2458-10-612

Murugaiyan, J., Ahrholdt, J., Kowbel, V., and Roesler, U. (2012). Establishment of a matrix-assisted laser desorption ionization time-of-flight mass spectrometry database for rapid identification of infectious achlorophyllous green micro-algae of the genus Prototheca. *Clin. Microbiol. Infect.* 18, 461–467. doi: 10.1111/j.1469-0691.2011.03593.x

Murugaiyan, J., Walther, B., Stamm, I., Abou-Elnaga, Y., Brueggemann-Schwarze, S., Vincze, S., et al. (2014). Species differentiation within the *Staphylococcus intermedius* group using a refined MALDI-TOF MS database. *Clin. Microbiol. Infect.* 20, 1007–1015. doi: 10.1111/1469-0691.12662

Namkoong, H., Kurashima, A., Morimoto, K., Hoshino, Y., Hasegawa, N., Ato, M., et al. (2016). Epidemiology of pulmonary nontuberculous mycobacterial disease. *Emerging Infect. Dis.* 22, 1116–1117. doi: 10.3201/eid2206.151086

Picardeau, M., Prod'hom, G., Raskine, L., Lepennec, M. P., and Vincent, V. (1997). Genotypic characterization of five subspecies of *Mycobacterium kansasii*. *J. Clin. Microbiol.* 35, 25–32.

Pignone, M., Greth, K. M., Cooper, J., Emerson, D., and Tang, J. (2006). Identification of mycobacteria by matrix-assisted laser desorption ionization-time-of-flight mass spectrometry. *J. Clin. Microbiol.* 44, 1963–1970. doi: 10.1128/JCM.01959-05

Rau, J., Eisenberg, T., Male, A., Wind, C., Lasch, P., and Sting, R. (2016). *MALDI-UP - An Internet Platform for the MALDI-TOF Mass Spectra.* Aspects of Food Control and Animal Health 01, 2016. Available online at http://maldi-up.ua-bw.de/

Rodriguez-Sanchez, B., Ruiz-Serrano, M. J., Marin, M., Lopez Roa, P., Rodriguez-Creixems, M., and Bouza, E. (2015). Evaluation of matrix-assisted laser desorption ionization-time of flight mass spectrometry for identification of nontuberculous mycobacteria from clinical isolates. *J. Clin. Microbiol.* 53, 2737–2740. doi: 10.1128/JCM.01380-15

Rodríguez-Sánchez, B., Ruiz-Serrano, M., Ruiz, A., Timke, M., Kostrzewa, M., and Bouza, E. (2016). Evaluation of MALDI biotyper Mycobacteria Library v3.0 for identification of nontuberculous mycobacteria. *J. Clin. Microbiol.* 54, 1144–1147. doi: 10.1128/JCM.02760-15

Saleeb, P. G., Drake, S. K., Murray, P. R., and Zelazny, A. M. (2011). Identification of mycobacteria in solid-culture media by matrix-assisted laser desorption ionization-time of flight mass spectrometry. *J. Clin. Microbiol.* 49, 1790–1794. doi: 10.1128/JCM.02135-10

Santin, M., Alcaide, F., Benitez, M. A., Salazar, A., Ardanuy, C., Podzamczer, D., et al. (2004). Incidence and molecular typing of *Mycobacterium kansasii* in a

defined geographical area in Catalonia, Spain. *Epidemiol. Infect*. 132, 425–432. doi: 10.1017/S095026880300150X

Taillard, C., Greub, G., Weber, R., Pfyffer, G. E., Bodmer, T., Zimmerli, S., et al. (2003). Clinical implications of *Mycobacterium kansasii* species heterogeneity: Swiss national survey. *J. Clin. Microbiol*. 41, 1240–1244. doi: 10.1128/JCM.41.3.1240-1244.2003

Telenti, A., Marchesi, F., Balz, M., Bally, F., Bottger, E. C., and Bodmer, T. (1993). Rapid identification of mycobacteria to the species level by polymerase chain-reaction and restriction enzyme analysis. *J. Clin. Microbiol*. 31, 175–178.

Thomson, R., Tolson, C., Huygens, F., and Hargreaves, M. (2014). Strain variation amongst clinical and potable water isolates of *M. kansasii* using automated repetitive unit PCR. *Int. J. Med. Microbiol*. 304, 484–489. doi: 10.1016/j.ijmm.2014.02.004

van Ingen, J., and Kuijper, E. J. (2014). Drug susceptibility testing of nontuberculous mycobacteria. *Future Microbiol*. 9, 1095–1110. doi: 10.2217/fmb.14.60

Wattal, C., Oberoi, J. K., Goel, N., Raveendran, R., and Khanna, S. (2017). Matrix-assisted laser desorption ionization time of flight mass spectrometry (MALDI-TOF MS) for rapid identification of micro-organisms in the routine clinical microbiology laboratory. *Eur. J. Clin. Microbiol. Infect. Dis*. 36, 807–812. doi: 10.1007/s10096-016-2864-9

Wilen, C. B., McMullen, A. R., and Burnham, C. A. (2015). Comparison of sample preparation methods, instrumentation platforms, and contemporary commercial databases for identification of clinically relevant mycobacteria by matrix-assisted laser desorption ionization-time of flight mass spectrometry. *J. Clin. Microbiol*. 53, 2308–2315. doi: 10.1128/JCM.00567-15

Conflict of Interest Statement: The authors declare that the research was conducted in the absence of any commercial or financial relationships that could be construed as a potential conflict of interest.

The reviewer AVDB declared a past co-authorship with one of the authors JI to the handling Editor.

Advantages of publishing in Frontiers

OPEN ACCESS
Articles are free to read for greatest visibility and readership

FAST PUBLICATION
Around 90 days from submission to decision

HIGH QUALITY PEER-REVIEW
Rigorous, collaborative, and constructive peer-review

TRANSPARENT PEER-REVIEW
Editors and reviewers acknowledged by name on published articles

Frontiers
Avenue du Tribunal-Fédéral 34
1005 Lausanne | Switzerland

Visit us: www.frontiersin.org
Contact us: info@frontiersin.org | +41 21 510 17 00

REPRODUCIBILITY OF RESEARCH
Support open data and methods to enhance research reproducibility

DIGITAL PUBLISHING
Articles designed for optimal readership across devices

FOLLOW US
@frontiersin

IMPACT METRICS
Advanced article metrics track visibility across digital media

EXTENSIVE PROMOTION
Marketing and promotion of impactful research

LOOP RESEARCH NETWORK
Our network increases your article's readership